Role of RORγt+ Innate Lymphoid Tissue Inducer Cells within breast cancer microenvironments

Kanth, Sheeba Irshad

Awarding institution:
King's College London

Role of RORγt^{+} Innate Lymphoid Tissue Inducer Cells within breast cancer microenvironments.

A thesis submitted to the Kings College London for the degree of Doctor of Philosophy

By

Dr Sheeba Irshad Kanth

Breakthrough Breast Cancer Research Unit, Department of Research Oncology, Guy's Hospital King's College London School of Medicine, London, SE1 9RT.

Dedication of this thesis is split three ways:

To my silent inspiration - Dad.

"And ever has it been known that love knows not its own depth until the hour of separation". *Khalil Gibran*

To my hero - Mum.

I am in awe of your strength and love you for the person YOU are.

To my happiness - Aadil.

My world is a brighter place with you at my side.

Acknowledgements

A research project like this is never the work of anyone alone. The contributions of many different people, in their different ways, have made this possible.

This project has been funded by a generous grant from the Sarah Greene Fellowship, and I would like to thank Sarah Greene's family for providing me with such an opportunity.

I express my deepest gratitude to Professor Tony Ng and Professor Andrew Tutt for their unflinching support and encouragement, not only for this project but also with my on-going career development. They have been both supervisors and role models from the outset. I thank Tony for giving me the freedom to pursue various aspects of this project without too much objection. I also wish to thank our collaborators, Professor Peter Lane and his team, without whom the identification of lymphoid tissue inducer cells in human tissues would not have been possible in such a short time.

I offer my enduring gratitude to Gilbert Fruhwirth, Fabian Flores, James Monypenny, Rachel Evans for making my transition from the clinic to the laboratory seamless. I owe an added thanks to Fabian Flores for making the time to proof read this thesis, and Dr Katherine Lawler for her endless bio-informatic expertise. I would like to extend my thanks to the staff of the Biological Services Unit (BSU) for looking after the animals and always being available to help when required, and Natalie Woodman for spending hours cutting tissue sections for me. Lastly, I would like to thank many members of Tony's ("the dimblebees") and Andy's breakthrough breast cancer lab: Anthony Cheung and Anjalika Mallick

for reminding me what it was like to be 18 years of age, Gargi Patel for her contagious energy; Gilbert Fruhwirth for making sure my pipetting skills were flawless, Fabian Flores for putting up with my colour coordinated labelling; Rachel Evans for putting up with my frequent use of her bench, Appitha Arulappu for sneaking her little pink radio into the lab, Michel Eissenblaetter for his red socks and being the best dressed man in the lab, Hanna Milewicz for being a good friend and part of the North London massive, James Monypenny for being a friend, mentor and of course for being the "king of sarcasm", although Simon Poland, Gregory Weitsmann and Oana Coben may have tried to take his crown on a few occasions. I wish the newest recruit to the swarm of dimblebees, Ruhe Choudhury, the best of luck with her PhD. In short, you have all given me memories I will cherish forever – thank you.

Thanks to my friends outside the lab, especially Una Sheerin, Sharmistha Ghosh, Deborah Enting and Debra Josephs. Thank you for putting up with my endless chats about my beloved LTi cells, paper submissions and the dreaded reviewers.

Lastly, but by no means least, I need to thank the Buchh, Mufti and Khan families for everything. I can't name you all here, but in your own ways you taught me to be independent, to walk my own path, and above all, be true to myself. Without your love and acceptance, I would never have achieved any of this. Thank you to my Dad, Mum and my beautiful family in Wales for all you have given me, taught me and sacrificed for me. Of course this wouldn't be complete without a special mention to my big sis Shaz, little bro Fas and all the cousins that make up the "Mufti mafia". Finally, my husband, thank you for being amazing, understanding and sharing me with my laptop for the past four years!

Abstract

Within invasive breast cancers, lymphatic invasion is thought to be the first step tumour cells undertake when metastasizing through the lymphatic vasculature. The presence of lymphatic metastasis has been shown to stratify breast cancer phenotypes into distinct prognostic groups. The exact molecular mechanisms mediating tumour cell entry and dissemination within the lymphatic system remain unclear. We report the first identification of RORγt^{+}-innate lymphoid tissue inducer (LTi) cells within the human breast cancer tumour microenvironment and the enrichment of lymphoid chemokines/chemokine receptor gene signature within an aggressive breast cancer subtype. The presence of these cells within the tumour microenvironment was shown to correlate with both an increased lymphatic vessel density (LVD) and tumour invasion into lymphatic vessels. We demonstrate the CCL21-dependent recruitment of LTi cells into breast tumours, the CXCL13-dependent interaction between the tumoural LTi and stromal cells and the downstream effect of the CXCL13 positive feedback loop in promoting lymphatic tumour cell motility via the RANK-RANKL axis. These data suggest a novel role for LTi cells in enhancing lymphatic invasion of tumour cells through modulation of the local lymphoid chemokine profile.

Table of Contents

List of Figures

List of Tables

List of Abbreviations

B

BLBC	Basal-like breast cancer
BSA	Bovine serum albumin
BVI	Blood vessel invasion

C

CKR	Chemokine receptors
CM	Conditioned media

D

DAPI	4,6-diamidino-2-phenylindole
DC	Dendritic cells
DLN	Draining lymph node

E

EATI	European Academy of Tumour Immunology
ECM	Extracellular matrix
EGF	Epidermal growth factor
ELISA	Enzyme-linked immunosorbent assay
EMT	Epithelial mesenchymal transition
ER	Oestrogen

F

FBS	Foetal bovine serum
FDC	Follicular dendritic cells
FGF	Fibroblast growth factor

H

HER2	Human epidermal factor receptor 2
HEV	High endothelial venules
HGF	Hepatocyte growth factor
HSC	Haematopoietic stem cells

I

ICAM	Intercellular adhesion molecule
Id2	Inhibitor of DNA binding 2
IF	Immunofluorescence
IFN	Interferon
IHC	Immunohistochemistry
IL	Interleukin
ILC	Innate lymphoid cell

L

LECs	Lymphatic endothelial cells
$LT\alpha_1\beta_2$	Lymphotoxin
LTβR	Lymphotoxin beta-receptor
LTi	Lymphoid tissue inducer cell
LTo	Lymphoid tissue organiser cell
LVD	Lymphatic vessel density
LVI	Lymphatic vessel invasion
LYVE-1	Lymphatic vessel endothelial hyaluronan receptor-1

M

MADCAM	Mucosal addressin cell adhesion molecule
MDSC	Myeloid derived suppressor cells
MIW	Mammary imaging window
METABRIC	Molecular Taxonomy of Breast Cancer International Consortium

MSC	Mesenchymal stromal cells

N

NDLN	Non draining lymph node
NK	Natural Killer cell
NCR	Natural cytotoxicity triggering receptor

P

PFA	Paraformaldehyde
Prox 1	Homeobox prospero-like protein
PgR	Progesterone receptoor

R

RA	Retinoic acid
RANK	Receptor activator of NF-κB
RANKL	Receptor activator of NF-κB ligand
RFU	Relative fluorescent units
RORγT	Retinoid-related-orphan receptor-γ
RT	Room temperature

S

SDF-1	Stromal cell derived factor -1
SLO	Secondary lymphoid organs
SITC	Society of Immunotherapy of Cancer
siRNA	Short interfering RNA

T

TLS	Tertiary lymphoid structures
TME	Tumour microenvironment
TNF	Tumour necrosis family
TNM	Tumour, nodes, metastasis
Treg	T-regulatory cell

V

VCAM	Vascular cell adhesion molecule
VEGF	Vascular endothelial growth factor
VEGFR	Vascular endothelial growth factor receptor

List of Publications

The following is the list of work published during the course of this doctorate. Some of this work is cited in the text and appears in the full in Appendix 1.

Original Research

2014**:** **Irshad S,** et al. Assessment of microtubule associated protein (MAP)-Tau expression as a predictive and prognostic marker in TACT; a trial assessing substitution of sequential docetaxel for FEC as adjuvant chemotherapy for early breast cancer. Breast Cancer Res Treat. 2014 Apr;144(2):331-41.

Book Chapters

2014: **Irshad S** & Tutt A. Single agent PARPi clinical trials for "PARP Inhibitors for Cancer Therapy" to be published by Springer. 2014

2013: **Irshad S,** Tutt A and Ellis P. Chapter 8: Antiangiogenic therapy: patient selection & clinical outcomes for breast cancer. Ebook chapter, Publisher: Future Science Group. 2013

Editorial

2013: Ng T, **Irshad S,** Stebbing J. BRCA1 mutations and luminal-basal transformation. Oncogene. 2013 May 30;32(22):2712-4.

Reviews

2014: **Irshad S*,** Chowdhury R*, Balaji* et al. The use of molecular imaging combined with genomic techniques to understand the heterogeneity in cancer metastasis. Br J Radiol. 2014 Jun;87(1038):20140065.

2014: Johnathan A Watkins, **Sheeba Irshad,** Anita Grigoriadis and Andrew Tutt. Genomic scars as biomarkers of homologous recombination deficiency and drug response in breast and ovarian cancers. Breast Cancer Research 2014, 16:211 (3 June 2014)

2012: **Irshad, S.** et al. Profiling the Immune Stromal Interface in Breast Cancer and Its Potential for Clinical Impact. Breast Care 2012;7:273-280

2012: Glenndening J, **Irshad S**, Tutt A and O'Shaughnessy. Treatment of Triple negative breast Cancer. Current Breast Cancer Reports. 2012; 4 (1):10-21

2011: **Irshad S,** Ellis P, and Tutt A. Molecular Heterogeneity of triple negative breast cancer and its clinical implications. Current Opinions in Oncology 2011 Nov;23(6):566-77.

2011: **Irshad S**, Ashworth A and Tutt A. The Therapeutic Potential of PARP inhibitors for Metastatic Breast Cancer. Expert Rev Anticancer Ther. 2011 Aug;11(8):1243-51.

Peer-reviewed Conference Abstracts

2014: **Sheeba Irshad** et al. Lymphoid tissue inducer cells promote lymphatic tumor cell invasion via activation of the RANKL/RANK axis within triple negative breast cancers. *Journal of Clinical Oncology, 2014 ASCO Annual Meeting Abstracts*. ***Awarded ASCO Merit award 2014.***

2013: **Sheeba Irshad** et al. *Lymphoid tissue inducer cells:* Identification of a novel immune cell within the tumour microenvironment and its role in promoting tumour cell invasion. *Cancer Research* SABCS13- P5-01-01

2012: **Irshad S,** et al. Time dependent breast cancer metastasis prediction using novel biological imaging, clinico-pathological and genomic data combined with Bayesian modeling to reduce over-fitting and improve on inter-cohort reproducibility. *Cancer Research*: December 15, 2012; Volume 72, Issue 24, Supplement 3 doi: 10.1158/0008-5472.SABCS12-P2-10-29

International Oral Presentation

2013: ***IMPAKT 2013, Brussels, Belgium, May 2013***

Sheeba Irshad: Use of *in vivo* lymphatic imaging techniques to study the effects of immune cell interactions in mouse models of breast cancer.

Awarded Best Abstract Oral Presentation

Chapter 1: Introduction

Breast cancer is the most common malignancy in women, with an estimated lifetime risk of developing breast cancer of 1 in 8 for women in the UK [1]. An estimated 1 million cases are diagnosed annually worldwide and approximately 400 000 patients die due to the disease every year [2]. Although the survival rates from breast cancer have improved within the last three decades owing to significant improvements in oncological management, the global burden of breast cancer exceeds all other cancers [3]. Majority of cancer-related deaths are caused by the development and continuous growth of metastases that are resistant to conventional therapies. Approximately 5-10% of women with breast cancer have metastatic disease at diagnosis and an additional 20% to 30% of patients with early breast cancers will experience relapse with distant metastatic disease within 3 years of diagnosis [4]. Median survival in women with metastatic breast cancer is about 18-24 months [5].

1.1 Breast cancer subtypes

It has become increasingly clear that rather than constituting a monolithic entity, breast cancer is a heterogeneous disease with subgroups that exhibit substantial differences in terms of presentation, morphology and response to therapy. A clinical shorthand classification divides breast cancer into three major subtypes based on the expression of oestrogen (ER), progesterone (PgR) hormone receptors, human epidermal factor receptor 2 (HER2): luminal (ER/ PgR-positive disease) divided into low (A) and high proliferation (B) forms, HER2-amplified

tumours and triple-negative breast cancers (TNBCs). However in recent years, various molecular techniques, particularly gene expression profiling, have been used increasingly to help refine breast cancer classification. Parker et al. [6] developed an efficient classifier, called PAM50, to distinguish breast cancers into five biologically intrinsic subtypes using the expression of 50 "classifier genes". These include luminal A, luminal B, HER2-enriched (HER2+), basal-like, and normal-like [6,7], and more recently the breast cancer genomic analysis of a large breast cancer cohort (including approximately 2000 patients) produced a novel classification of breast cancers into 10 subgroups [8].

The overall prognosis of women with TNBC, characterized by tumours that do not express ER, PgR, or HER-2 genes is significantly poorer compared to that of women with other subtypes of breast cancer; with upto 70% of women developing metastatic disease at 3 years. It is characterized by its unique molecular profile, aggressive nature, increased incidence in younger women, distinct metastatic patterns and lack of effective targeted therapies, thus representing an important clinical challenge. The poor prognosis of TNBC is derived largely from the fraction of patients with chemo-resistant disease, unfortunately representing >50% of TNBCs. While those who achieve a pathological complete response (pCR) at surgery following neoadjuvant (preoperative) chemotherapy have an excellent long-term outcome, the majority of patients with TNBC do not achieve pCR and suffer a much poorer prognosis compared to those with other breast cancer subtypes [9,10]. Tumour cells remaining after neoadjuvant chemotherapy are likely to represent the cancer cell population intrinsically resistant to chemotherapy, eventually reflecting metastatic disease.

In patients with early stage breast cancer, presence of tumour cells within the regional lymph nodes is one of the most important prognostic factors for survival independent of tumour size, histological grade and other clinico-pathological parameters [11-14]. When compared with node-negative breast cancer, those patients with four or more involved axillary lymph nodes have a significantly worse outcome [15,16]. Presence or absence of lymph node metastases remains central to staging and prognosis as well as guidance of treatment decisions. While this clinical significance of lymphatic metastasis in breast cancer is well recognized, the exact molecular mechanisms mediating tumour cell entry and persistence within the lymphatic system remain under considerable debate [17].

Central to this thesis is the discussion surrounding: **what tumour and or host cell factors regulate tumour cell trafficking in and out of lymphatic vessels?** A mechanistic understanding into the regulation of tumour cell trafficking in and out of lymphatic vessels could provide important insights into the metastatic process and allow identification of targets for development of anti-metastatic therapies.

1.2 Tumour metastasis model

For most cancer cell types, the acquisition of metastatic ability leads to clinically incurable disease. Appropriately the words “cancer” (Latin for “crab”) and metastasis (Greek for “change in position”) refer to the slow co-ordinated migration of tumour cells from the primary to a distant site. Traditionally, development of metastases is believed to be a late event that occurs only after primary tumours reach a certain critical mass (the linear-progression model).

However, recent evidence indicates that tumour cells disseminate at a relatively early stage of the natural history of tumour growth [18].

Metastasis formation is a multi-step process that require tumour cells to separate from the primary site, invade through the surrounding tissues and basement membranes, intravasate into the haematic or lymphatic circulation, migrate, extravasate and ultimately result in colonization and growth at distant sites (Figure 1-1) [19,20].

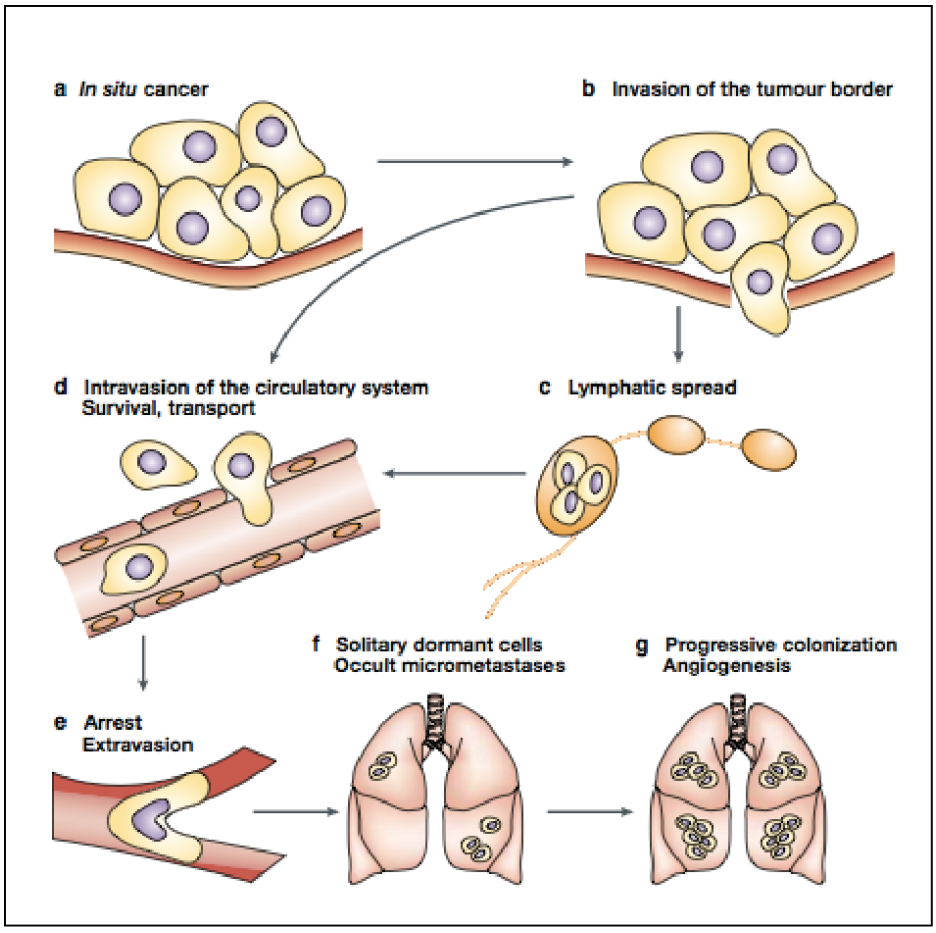

Figure 1-1: Tumour metastasis model [21].

a) *in situ* tumour - defined by the absence of invasive cells. b) Local invasion of the surrounding extracellular matrix (ECM) and stroma. Metastasizing cells can then c) enter lymphatics, or d) directly enter the circulation. e) Survival and arrest of tumour cells, and extravasation into the parenchyma of distant tissue f) Metastatic colonization of the distant site progresses to form occult micrometastases and g) re-initiate their proliferative pathways to generate macroscopic, clinically relevant metastatic tumours.

This metastatic cascade is an exceedingly complex process, and an exhaustive discussion of each stage is not pertinent to this introduction. Suffice to say, that the metastatic process is highly selective with each step demanding from the tumour cells survival skills to overcome the challenges imposed by the surrounding stroma. As a result metastasis formation is an extremely inefficient process, with 1% or fewer circulating tumour cells eventually able to thrive to form clinically relevant metastases [22,23]. Despite this relative metastatic inefficiency, the burden of metastatic disease on cancer morbidity and mortality remains high. Identification of mechanisms that regulate tumour cell trafficking in and out of vasculature is crucial to control the metastatic process.

1.2.1 Lymphatic vascular invasion

While invasion of tumour cells into both the blood and the lymphatic vascular systems have been implicated, a vast number of clinical studies support the notion that the most common pathway for breast tumours to metastasize is through the lymphatic system [24,25]. Tumour cell emboli in lymphatic or blood vessels surrounding the tumour are often considered to be the morphological correlate of breast cancer cells metastasising to loco-regional lymph nodes and distant haematogenous sites, respectively.

Several independent studies have investigated the prevalence and prognostic significance of lymphatic vessel invasion (LVI) compared to blood vessel invasion (BVI) in both lymph node negative and positive breast cancer patients (briefly summarised in Table 1-1). Of these a large retrospective clinical study of 1408 primary breast cancer cases reported a much higher prevalence rate of LVI

compared to BVI (34.2% vs 4.2%; p<0.0001) [26]. Given that breast cancers are now being increasingly recognised as heterogeneous, characterised by distinct molecular 'intrinsic subtypes' relating to tumour biology and behaviour; [8] whether the differences seen in these studies are skewed by a subtype-specific effect has not been studied. However, a more recent study reported that within basal-like breast cancer subtype (an aggressive form of triple negative breast cancer) the vascular invasion is almost entirely lymphatics [27].

Table 1-1: LVI and BVI in breast cancer

Study size	% Invasion		Associated with lymphatic metastasis		Prognostic for disease outcome (DFS or OS)*		Ref.
	LVI	BVI	LVI	BVI	LVI	BVI	
1408	34.2	4.2	-	-	Yes	No	[26]
177	96.4	3.5	Yes	No	Yes	No	[27]
1258	27.6	-	-	-	Yes	-	[28]
378	28	-	-	-	Yes	-	[29]
123	28.5	15.4	-	-	Yes	No	[30]
95	69.6	37.9	Yes	No	-	-	[31]
850	-	-	Yes	-	-	-	[32]
4351	-	-	Yes	-	-	-	[33]
2606	22.6		Yes		Yes		[34]
	Peri-tumoural vascular invasion (LVI + BVI) assessed						

* DFS = disease free survival; OS = overall survival; "-" = not determined.

LVI have also been shown to correlate with increased metastatic lymph node involvement, as well as with poor prognosis within breast cancer patients [27,31-34]. Although these studies do not rule out the role that haematogenous metastasis

play in mortality from breast cancer, they do highlight the strong independent contribution that local invasion into the lymphatic vessels play for long term survival of patients with breast cancer. Indeed, LVI has been included in the guidelines developed by the International Consensus Panel during the St Gallen Conference, 2005, as a novel adverse prognostic factor for postoperative adjuvant systemic therapies of early breast cancer [35].

The lymphatic vessels themselves offer several advantages over blood vessels for invasion and transport of pre-metastatic cells. The lymphatic system is physiologically equipped to transport cells throughout the body while ensuring cell survival remains optimal. The lymphatic capillaries are thin walled with discontinuous basement membrane and loose cell–cell junctions, rendering them highly permeable [36]. They also contain intraluminal valves, ensuring unidirectional flow to the thoracic duct in order to reach the systemic blood circulation. Importantly, the primary source of pressure within the lymphatic is created by local skeletal muscle contractions resulting in a low flow rate, minimizing the shear stress on the cells inside the lymph [37]. Lymphoid tissue includes structurally well-organized lymph nodes located at intervals along the lymphatic vascular tree, representing a preferred site for lodgement of pre-metastatic cells [38].

Alongside these passive properties of the lymphatic system, mounting clinical and experimental data highlight the more complex, active role for the lymphatic system in metastatic tumour spread. Tumour lymphangiogenesis, a process by which tumours actively induce the formation of new lymphatic vessels - quantified as lymphatic vessel density (LVD) - is a novel prognostic parameter for

the metastatic risk of human cancers and it has been shown to correlate with lymph node metastasis in a breast cancer model [36,39-44]. Similarly, overexpression of lymphangiogenic growth factors such as vascular endothelial growth factor (VEGF)-A, VEGF-C or VEGF-D have now been detected in a range of human tumour types, such as melanoma, breast [39], cervical [45], non-small-cell lung [46], prostate [47], colorectal [48] and gastric cancers [49]. In a breast cancer mouse model, the increased VEGF-C secretion by transplanted tumours induced proliferation of the lymphatic endothelium and a fourfold increase in peritumoural and intratumoural lymphangiogenesis but had no effect on blood vessels. These manipulations resulted in a 50% increase in lymph node and lung metastases [39].

Although it is clear that tumour-induced lymphangiogenesis is controlled by the stimulation of various lymphatic growth factors secreted by the tumour cells, stromal cells, and inflammatory cells within the tumour microenvironment, the exact molecular and cellular processes that underpin lymphatic invasion and tumour lymphangiogenesis remain poorly understood.

1.3 Immune cell trafficking

One of the key physiological elements of immune surveillance and homeostasis is the continuous migration of immune cells such as dendritic cells (DCs) and T-cells into the secondary lymphoid organs and then back into the blood (lymphocyte recirculation). This continuous recirculation of immune cells from the blood to the lymphoid organs and back occurs as often as one or two times a day [50]. By being almost continually on the move, immune cells are able in a matter of days to survey many of the secondary lymphoid organs in hunt for

specific antigen. An important structural characteristic of lymph nodes allowing for this continuous recirculation is the existence of specialized vascular and lymphatic systems (Figure 1-2). The steps that regulate the trafficking of immune cells in lymph nodes include: 1) entry of the immune cells into specialized blood vessels termed (HEVs), as well as via afferent lymphatics; 2) intra-nodal migration and positioning; and 3) egress via efferent lymphatics.

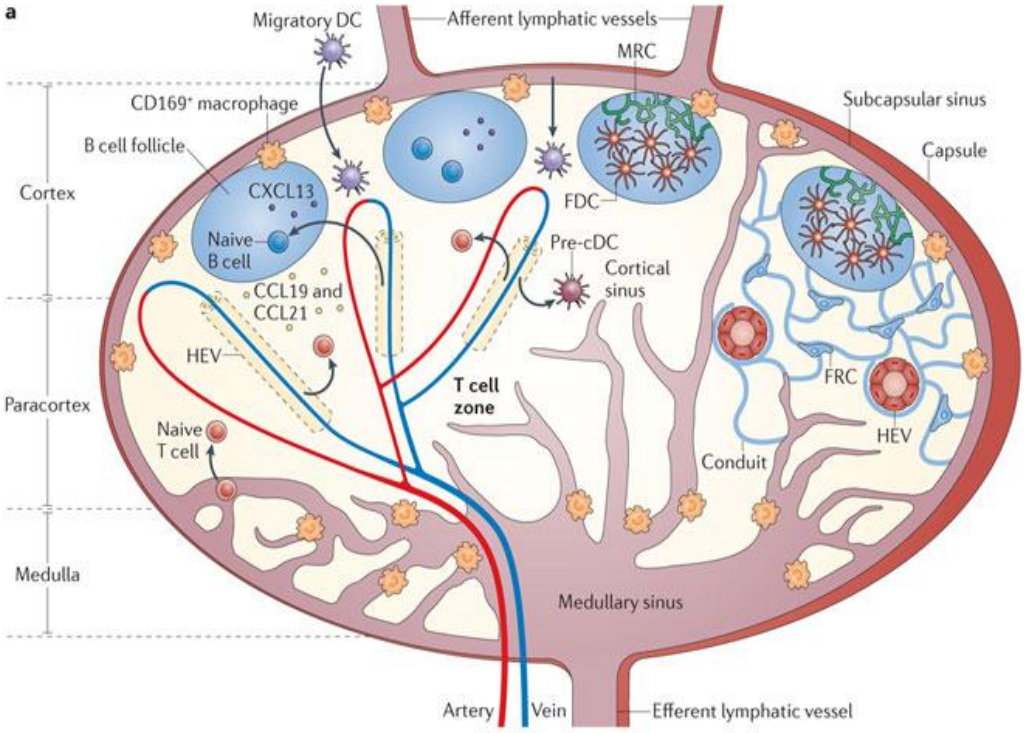

Figure 1-2: Organisation of the lymph node and entry of immune cells *(Adapted from [51])*.

Within peripheral tissues, DCs constitutively sample their environment for antigens and eventually entry the lymph node via afferent lymphatic vessels into a large subcapsular sinus (SCS). The bottom of the SCS, being the roof of the lymphoid compartment and is formed by sinus-lining cells which form a basement membrane that can be actively crossed by cells that enter the sinus with the afferent lymph but is otherwise impermeable for fluids. This way a closed

lymphoid compartment is created that is shielded from afferent and efferent lymph [52]. Following enter into the SCS, DCs settle onto the sinus floor, actively migrate through the sinus-lobule membrane and home in the vicinity of HEVs in the paracortex where they present the antigen to cognate T-cells; a process that can either mount to a protective immune response or contribute to peripheral tolerance [51,53,54], a process that is actively orchestrated and controlled by a family of secreted proteins called chemokines (see section 1.3.1). During this journey in the lymph node, DCs lose their ability to collect antigen and gain the ability to present antigen to T cells [55]. DCs are thought to be short-lived, dying in the lymph nodes after they have presented antigen to lymphocytes [56].

The main bulk of the naïve lymphocytes enter the lymph node via the HEVs which are anatomically distinct post-capillary venules characterised by their cuboidal morphology, discontinuous junctions between adjacent cells, and also by their luminal presentation of various adhesion molecules [51]. HEVs are found only in lymphoid organs, but they can develop in non-lymphoid tissues during chronic inflammatory conditions and cancer, where they are associated with high levels of lymphocyte infiltration (see also section 1.5.2). During this "homing" process B cells and T cells migrate to separate compartments within the secondary lymphoid organ, called B cell follicles and T cell areas respectively, staying there for several hours. Naïve immune cells that do not encounter their specific antigen exit from the lymphoid tissue via the efferent lymphatics, and continue recirculating. As with DC migration into lymphatics, this process is also under the control of chemokines.

1.3.1 Chemokines and immune cell trafficking

The original model of immune cell extravasation proposed three main stages: 1) selectin-mediated rolling; 2) chemokine-triggered activation and 3) integrin-dependent arrest for a free flowing cell to move from the blood into the tissue [57-59]. However, recent evidence suggests that additional steps are involved [60], which include slow rolling, adhesion strengthening, intraluminal crawling, paracellular and transcellular migration, and migration through the basement membrane (Figure 1-3). Pertinent to this introduction is the role that chemokine and their receptors play in immune cell trafficking into lymph nodes via the lymphatics and the HEVs.

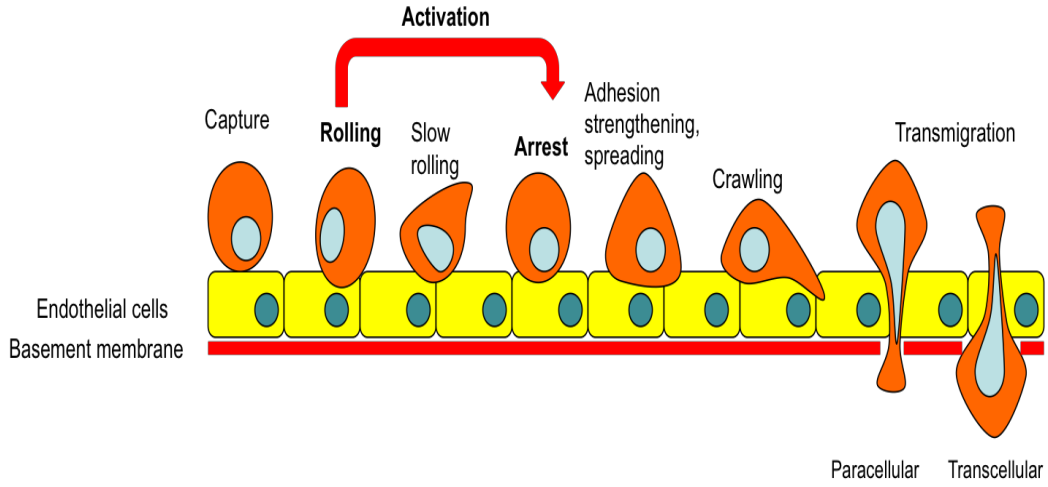

Figure 1-3: Leukocyte adhesion cascade (adapted from [60]).

The initial capture of lymphocytes occurs through integrin-mediated interactions with adhesion molecules. During the activation phase, lymphocyte G-coupled chemokine receptors respond to chemokine signals on endothelial cells, leading to a conformational change in lymphocyte-associated integrins.

Chemokines constitute a large family of small (8–12kDa), structurally related polypeptides, and exert their functions by binding specific $G\alpha_i$-protein coupled chemokine receptors (CKR) on the cell surface [61]. To date, more than 40 human chemokines have been described. The most widely used nomenclature subdivides chemokines into four subfamilies (CC, CXC, CX3C and XC) according to the position of one or two conserved cysteine residues in their amino acid sequence. In CC chemokines, the two N-terminal cysteines are next to each other, while as in CXC chemokines, they are separated by a single amino acid. In CX3C chemokines three amino acids separate both cysteines, while as in XC chemokines, these lack two of the four mentioned cysteines [62]. Another classification system broadly separates chemokines functionally into an "inflammatory" and a "lymphoid/homeostatic" subset.

Lymphoid chemokines (CXCL12, CXCL13, CCL19, CCL21) are constitutively expressed in discrete microenvironments within lymphoid (bone marrow, thymus and secondary lymphoid organs) or non-lymphoid tissue like the skin or mucosa. Although traditionally thought to activate only one or two chemokine receptors, more recent studies also report that they can mediate signaling through a small family of atypical chemokine receptors (ACKRs), (Table 1-2) [63]. These chemokines are key regulators of leukocyte trafficking during homeostasis [64].

Table 1-2: Lymphoid chemokines and their corresponding receptors

Chemokine	Chemokine Receptor
CXCL12	CXCR4 ACKR3 *(also known as CXCR7)*
CXCL13	CXCR5
CCL19 **CCL21**	CCR7
	ACKR4 *(also known as CCRL1)*

Entry of DCs to activated lymphatic vessels is a highly complex multi-step process involving numerous chemokines and adhesion molecules. The lymphatic endothelial-derived chemokine CCL21 plays a well-characterized role in directing migration of CCR7+ DC in both resting and acute inflammatory conditions. It has been suggested that hot spots of high CCL21 concentrations are formed at the basement membranes of initial lymphatics, and that migrating DCs contact these CCL21 "puncta" before actually transmigrating into the lymph vessel lumen from these points [65,66]. These CCL21 gradients have been shown to attract DCs from a distance of upto 90micrometers [67]. An elegant study by Weber et al, demonstrated that the main source of CCL21 production is the lymphatic endothelium, which harbors intracellular depots of this chemokine [67]. In the presence of such a chemokine gradient, DCs respond to chemokines by haptotaxis (rather than chemotaxis), which is defined as migration along a gradient of molecules that are bound to the extracellular matrix. The degree to which the selectins and integrins participate in this process remains under debate. On entry into the lumen, DCs crawl along the inner surface of the lymphatic endothelium, and by sensing lymph flow thereby undergoing directed migration downstream until they reach the

collecting afferent lymphatics which together with rhythmical contractions and one-way valves facilitate the active pumping of lymph and DCs towards the SCS of the draining LNs [68].

Similar to DCs trafficking into afferent lymphatics, there is now a growing body of evidence supporting that chemokines produced in and around HEVs have a crucial role in the lymphocyte trafficking into lymphoid organs. In particular, the CCR7 ligands, CCL21 and to a minor extent, CCL19 are the principal integrin activating chemokines for T-cell entry into the lymph nodes [69]. CCL21 is produced by the endothelial cells of HEVs [70], while as CCL19 is thought to be produced by stomal cells in the area surrounding HEVs and seems to be transported to the luminal surface of HEVs [71]. These chemokines activate the integrins on the T-cells causing an interaction between the endothelial cell molecules, intercellular adhesion molecule 1 (ICAM1) and ICAM2, and the activated integrin lymphocyte function-associated antigen 1 (LFA1) resulting ultimately in lymphocyte arrest (sticking) to the HEV endothelium. The T-cells can then proceed to migrate across HEVs. CXCL12 also participate to a small extent during T-cell adhesion to venules and particularly in the transmigration process [72]. In vivo studies have showed that the transmigration of T cells through cultured HEV cells was strongly inhibited by a CXCR4 antagonist or by the CXCL12-mediated desensitization of T cells [73]. In contrast, B cells rely principally on CXCR5 and its ligand CXCL13 to carry out its LFA-1-dependent cell adhesion and transmigration [74]. Similar to CCL19 and CXCL12, CXCL13 is produced mainly by non-HEV cells and might be transported to the HEV area through the fibroblastic reticular cell (FRC) network or ‘conduit’, which acts as a special delivery system for the transit of soluble factors to HEVs from the SCS [75].

Interestingly, when high-molecular-weight molecules were injected into the draining areas of the LN, they were excluded from the cortical parenchyma, indicating that the conduit functions as a molecular sizing column, allowing only low-molecular-weight molecules (e.g. chemokines) to reach the HEVs [76].

Despite the continuously changing cellular composition of the lymph node, once inside the lymphoid tissues naïve lymphocytes, with remarkable precision, are restricted to specialized sub-compartments: T-cells migrate to the T-zones and naïve B cells migrate towards the B-cell zones. This compartmentalization is achieved through expression of the chemokine CXCL13 by follicular DCs, which directs CXCR5-expressing B cells to migrate to and stay within the cortical B-zone [77]. By contrast, expression of CCL19 and CCL21 by fibroblastic reticular cells is largely restricted to the paracortex, attracting T cells as well as DCs that both express high surface levels of CCR7 [78]. Within the T cell zone, T cells randomly migrate along the fibroblastic reticular cell network decorated with immobilized CCR7 ligands to search for cognate antigen presented by surrounding DCs [79]. Antigen stimulation of the naïve B-cells has been shown to upregulate its CCR7 expression, and the altered balance of chemokine responsiveness (i.e. between CXCL13 and CCL21) drives the migration of antigen-stimulated B cells into the T-cell zone [80].

Other than being strong chemo-attractants of T-, B- and DCs [54,81,82], the lymphoid chemokines play a key role in lymphoid organogenesis (discussed in further detail in section 1.3.3), and have also been implicated in numerous pathological processes such as autoimmune conditions, infections, tissue injury, allergy, cardiovascular diseases and cancers.

1.3.2 Lymphoid chemokines in cancers

Tumour cells, through the expression of lymphoid chemokine receptors, may exploit the physiological lymphatic trafficking system to mediate invasion into the lymphatic vasculature [83]. Within the last decade there have been numerous publications reporting on the expression of chemokine receptors on malignant cells and their utilisation for promoting tumour growth and metastasis. Chemokine receptors can potentially facilitate tumour dissemination at numerous stages of the metastatic cascade, including adherence of tumour cells to endothelium, vascular extravasation, metastatic colonization, angiogenesis, proliferation, and protection from the host [83-86]. To date the most recognised receptor/ligand pairs in these phenomena include CXCR4/CXCL12 and CCR7/CCL21.

1.3.2.1 CXCR4/CXCL12

In the context of cancers, CXCL12 (also known as stromal cell derived factor -1 (SDF-1)) and its receptor CXCR4, is the most widely studied. CXCL12 is expressed constitutively in a number of tissues including liver, lung, lymph nodes, adrenal glands and bone marrow, which may explain why this chemokine axis might be exploited by the tumours to promote distant metastasis. CXCR4 is expressed by tumour types of epithelial, mesenchymal and haematopoietic origins [87]. Interestingly, although CXCR4 expression is absent from normal breast, prostate and ovarian tissue, it is characteristically expressed on malignant tissues from these sites [87]. A large study (*n=600*) reported significantly higher CXCR4

and CXCL12 protein expression in localised and metastatic prostate cancer compared to normal or benign prostate tissue [85].

The spread of breast cancer follows a distinct metastatic pattern typically involving spread of tumour to regional lymph nodes, lung, liver, and/or marrow, highlighting the fact that the process of metastasis formation is not random. An elegant experiment by Muller et al; demonstrated that breast cancer cells migrate towards lymph node tissue extracts expressing high levels of CXCL12 and chemotaxis can be inhibited by neutralising antibodies for CXCR4 [88]. These data formed the basis of the hypothesis that malignant cells may employ chemokine receptors to migrate toward chemokine ligands expressed at common metastatic sites, such as the lungs, bone marrow, and lymph nodes. A high CXCL12 concentration in the lymph node has been shown to ensure a chemotactic gradient within the lymphatic vessels, facilitating metastasis to the lymph nodes. Compared to normal lymphatic vessels, peritumoural or intratumoural lymphatics have been reported to express higher levels of CXCL12 [89].

It is noteworthy that only a sub-population of tumour cells have been reported to express CXCR4 (1-2%), raising the intriguing possibility that CXCR4 may be a marker of cancer stem cells and represent those cells that migrate and survive to form metastatic deposits [90]. In support of this, Fusi and colleagues reported that circulating tumour cells (possibly representing the metastasis-initiating cells) from patients with various types of solid tumours were positive for CXCR4 expression [91].

Soon after the CXCL12/CXCR4 axis was proposed to regulate the trafficking of cancer cells, it was also implicated in other aspects of tumour progression. For example, an interaction between CXCL12 and CXCR4 has been shown to stimulate proliferation of tumour cells [85,86]. Similarly, studies demonstrate CXCL12 can mobilize and recruit CXCR4 expressing endothelial precursor cells to support revascularisation of ischaemic tissue within the tumour [92]. In short, it would seem that CXCR4 expression in tumours provides a selective advantage to the tumour cells at several levels; it is therefore not surprising to find numerous clinical studies in literature reporting a correlation between high CXCR4 expression and poor prognosis in lung cancer [93], melanoma [94], pancreatic [95], ovarian [96], colorectal [97], and breast cancer [98].

Targeting the CXCR4/CXCL12 axis is now regarded as a novel and efficient strategy for treating cancer metastases and their antagonists have shown some utility as potential therapeutics agents in pre-clinical models. CXCR4 inhibition has been shown to reduce metastasis formation in breast [88] and non-small cell lung [99] cancer mouse models. These studies highlight the functional significance of CXCL12 for effective metastatic tumour spread.

1.3.2.2 CCR7/CCL21

While overexpression of CXCR4/CXCL12 is related with homing of cancer cells to lung, liver, lymph nodes and bone marrow, the overexpression of CCR7/CCL21 has mainly been related with lymph node metastasis. Several studies have reported that overexpression of the CCR7/CCL21 axis is associated with lymph node metastases and poor prognosis in gastric [100], head and neck [101],

lung [102], oesophageal [103], cervical [104], tonsillar [105], colorectal [106] and prostate cancers [107]. Within gastric cancers, CCR7 expression in the primary was reported as the most important factor determining lymph node metastasis [100]. There is also preclinical evidence that CCR7 expression is a rate limiting step for mediating the lymphatic spread of pancreatic ductal adenocarcinoma [108].

Pre-clinical studies have demonstrated that CCL19/CCL21 producing lymphatic endothelial cells can actively guide the chemotactic migration of CCR7 expressing tumour cells [109]. The lymphatic flow to draining lymph nodes is know to be higher compared to non-tumour-bearing controls [110]; and this increased lymphatic flow has been reported to increase the expression of CCL21 by the lymphatic endothelium, thereby enhancing invasion of the lymphatics by the tumours cells [111]. Another elegant mechanism by which CCL19/CCL21/CCR7 chemokine axis can promote tumour cell homing to lymphatics has been proposed based on the effect of interstitial fluid flow resulting from lymphatic drainage — a phenomena known as autologous chemotaxis [112]. CCL21/CCL19 secreting tumour cells of various types were shown to generate autologous gradients of these ligands under the influence of slow interstitial flow rate, which then allow CCR7 expressing tumour cells to migrate along the chemokine gradient.

Additionally, CCL21 has been shown to promote generation of new lymphoid-like structures within the tumour microenvironment, which are characterized by infiltration of immune-suppressive T-regulatory cells and myeloid derived suppressor cells [113]. However, unlike CXC12 the role of CCL21 during tumour progression remains rather controversial, with tumour-suppressive properties also having been reported. CCL21 is a strong chemoattractant for tumour infiltrating

lymphocytes, which can exert a strong anti-tumour immune response especially during early stages of tumour progression [114]. A recent clinical study reported improved outcome associated with increased infiltration of CCR7 positive T-cells within advanced colorectal carcinoma [115]. The interaction between CCR7-CCL21 has been shown to improve the immunogenicity of CCR7 expressing breast cancer cells [116]. Similarly, studies report that intratumoural injection of recombinant CCL21 significantly delayed tumour progression and stimulated cytotoxic immune responses [117-119]. In summary, the dual roles of CCR7/CCL21 axis in protective immunity and tumour promotion suggest that its targeted therapies must be carefully evaluated.

1.3.3 Lymphoid chemokines and lymphoid organogenesis

Since the migrational cues employed during tumour progression share many characteristics with lymphoid tissue embryogenesis, it is important to dissect the molecular and cellular mechanisms that govern organogenesis of lymphoid organs. The development of secondary lymphoid organs (SLOs) such as lymph nodes begins prenatally around embryonic day (E) 15 and requires the interaction of two specialised cell populations: haematopoietic lymphoid tissue inducer (LTi) cells, belonging to the family of innate lymphoid cells and mesenchymal lymphoid organiser cell (LTo), whose origin remains under investigation. Mesenteric lymph nodes are thought to develop first, followed by the rest of these organs along the anterior-posterior body axis [120].

Production of CXCL13 by the mesenchymal lymphoid organiser cell is essential for the attraction of the first CXCR5-expressing LTi cell to the site of the lymph

node formation [121]. Notably nerve fibres adjacent to the lymph node anlagen secrete retinoic acid (RA), a metabolite of vitamin A, which induce the initial production CXCL13 by the LTo cells (Figure 1-4). Knockout mice for $CXCR5^{-/-}$, $CXCL13^{-/-}$ or RA-synthesizing enzyme $RALDH2^{-/-}$ have all demonstrated an absolute lack of peripheral lymph nodes, indicating an important role for both retinoic acid and CXCL13-CXCR5 interaction for lymphoid organogenesis [121]. Interestingly, the origin or the mechanisms that induce the specification of mesenchymal progenitor cells prior to the arrival of LTi cells remain largely unknown.

After LTi cells collect in the areas designated for lymph node development they express lymphotoxin ($LT\alpha_1\beta_2$) and a set of tumour necrosis factor (TNF) family members. $LT\alpha_1\beta_2$ activate the LTo cells through lymphotoxin-β-receptor (LTβR), resulting in the activation of the NF-κB family of transcription factors through the classical/canonical (NF-κB1 p50/RelA) and the alternative/non-canonical pathways (NF-κB2 p52/RelB) [122]. This coincides with the differentiation of mesenchymal cells into vascular cell adhesion $molecule^{high}$, intercellular adhesion $molecule^{high}$, and mucosal addressin cell adhesion molecule 1^{+} ($VCAM^{high}ICAM^{high}MAdCAM\text{-}1^{+}$) LTo cells [123]; and an increased production by these LTo cells of "lymphoid" chemokines (CXCL13, CCL19, and CCL21) and lymphangiogenic factors such as VEGF-C, VEGF-D, fibroblast growth factor (FGF)-2 and hepatocyte growth factor (HGF), leading eventually to formation of Lyve-1^{+} lymphatic vessels [124 ,125-127]. The production of lymphoid chemokines initiates an important positive feedback loop for a second wave of LTi cell clusters formation and for the proliferation and homeostasis of LTo cells.

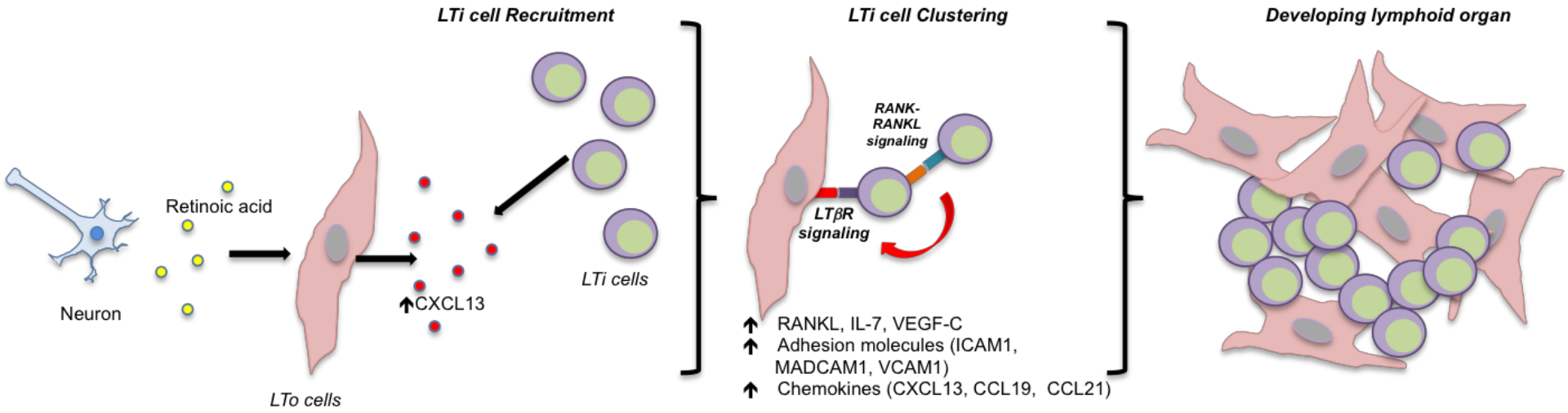

Figure 1-4: Schematic overview of the early phases of lymphoid tissue development.

Neuronal stimulation by retinoic acid induces CXCL13 expression in the organizer cells, which determine the site for first LTi recruitment. Clustering of LTi cells initiates RANK-RANKL and LTβR signaling, leading eventually to a fully formed lymphoid organ.

Receptor activator of NF-κB ligand (RANKL, also called TRANCE, TNFSF11) signaling has also been shown to contribute to LTα1β2 expression in LTi cells [128]. RANK and RANKL-knockout mice display a complete absence of peripheral lymph nodes, defects in Peyer's patches and cryptopatches along with abnormalities of the spleen [128-130]. In fact, the clustering itself enhances the interaction between the membrane bound RANKL and RANK receptor on LTi cells. However, the LTβR-dependent interaction between the LTi cells and the mesenchymal LTo cells also induces a positive feedback on RANKL production by the stromal cells with resultant increase in the expression of $LT\alpha_1\beta_2$ on the LTi cells. In support of this feedback loop, RANKL expression has been shown to be up to 10-times higher in LTo cells than in LTi cells [131].

Albeit controversial, sufficient clustering of LTi cells and production of lymphoid chemokines eventually leads to the differentiation of LTo cells to give rise to the various stromal cell lineages that are present in the mature lymph nodes, including follicular dendritic cells, fibroblastic reticular cells, lymphatic and vascular endothelium [132]. The subsequent organization of lymphocytes into B and T cell zones of the lymph nodes is mediated by the lymphoid chemokines, with CCL21 guiding T-cells into the T-zone and CXCL13 guiding the B-cells into the B-zones. The exact mechanisms that ensure subsequent organisation of lymphoid tissues remain unclear (see section 1.4.1.2).

1.4 Innate lymphoid cells

Lymphoid tissue inducer cells are members of an emerging family of developmentally related innate lymphoid cells (ILCs). A major setback for the

ILC field has been the confusing number of different names that have been used to characterize the subsets of ILCs. For example, IL-22-producing ILCs have also been called NK22 cells [133], NKR-LTi cells, NCR22 cells and ILC22s [134]. However, recent moves to propose a uniform nomenclature to denote these cells have divided them into three groups based on their ability to produce type 1, type 2 and T_H17-cell associated cytokines (Table 1-3) [135]. These various ILCs have been implicated in protection against infectious organisms, organogenesis of lymphoid tissue, tissue remodeling during wound healing and homeostasis in tissue stromal cells.

Table 1-3: Innate lymphoid cell family classification

Family	Subgroup	Signature cytokine	Function
Group1 ILCs	ILC1s	IFN-γ	Innate immunity against viral infections, tumour surveillance
	NK cells		
Group 2 ILCs	ILC2s	IL-5 & IL-13	Innate immunity against parasites
Group 3 ILCs (*RORγt*$^+$ *ILCs*)	LTi cells	IL-17 & IL-22	Lymphoid tissue formation and repair; innate immunity against bacteria
	ILC3s*	IL-17 & IL-22	

ILC = Innate lymphoid cell; NK= Natural killer; IFN = Interferon; IL=interleukin; LTi= lymphoid tissue inducer; NCR = natural cytotoxicity triggering receptor; *also referred to as NKp46 positive LTi-like cells.

Development of ILCs depends on the transcription factor inhibitor of DNA binding 2 (Id2), suggesting that the innate lymphocyte lineages share a common transcriptional and developmental program [136]. Early expression of Id2 protein has been show to act as a developmental block for the common lymphoid

progenitor cells against differentiation down the T cell and B cell pathway [137]. Commitment towards the group 3 ILCs (including LTi cells) – in the fetal liver or the adult bone marrow - has been shown to be dependent primarily on retinoid-related orphan receptor (RORγt) and interleukin-7 receptor α (IL-7R α) signaling [138].

The retinoic acid receptor-related orphan receptors (Rorα, Rorβ, and Rorγ) are a family of DNA-binding transcription factors which are nuclear receptors. Rorγt is a short Rorγ isoform that is specifically expressed in cells of the immune system and studies demonstrate that mice deficient in the expression of the RORγt completely lacked LTi cells and this correlates with a total absence of lymph nodes [139]. IL-7 has been implicated in maintaining RORγt expression, maintaining the pool of LTi cells *in vivo* [140,141]. Mice with a defect in the IL-7 signaling pathway have severe defects in peripheral lymph node development [125]. Similarly, over-expression of IL-7 *in vivo* has been shown to significantly increase LTi cells numbers causing de novo formation of multiple organized ectopic lymph nodes. However, mice overexpressing IL-7 but lacking either RORγ, or $LT\alpha_1\beta_2$ were unable to develop ectopic lymph nodes [141].

1.4.1 RORγt$^+$ ILCs – Lymphoid tissue inducer cells

1.4.1.1 LTi phenotype

LTi cells represent the prototypic cell type of the "group 3" RORγt$^+$ family of ILCs and broadly speaking are CD45$^+$ haematopoietic cells distinguished by the

expression of the nuclear RORγt receptor and membranous IL-7Rα in the absence of lineage markers (e.g. CD3, CD19, B220, CD11c) [141,142]. These LTi cells are innate cells in that they do not develop in the thymus and lack antigen-specific receptors; instead they respond to cytokines or receptor ligands.

Within the last decade the shared expression of RORγt by Th17 cells and LTi-like cells which express NK cell receptors (such as NKp46) have promoted various hypotheses speculating a lineage or functional relationship between the cell types; inadvertently sparking an interest in LTi cells themselves. Both mouse and human LTi cells have now been well characterized (Table 1-4).

LTi cells can be readily visualized in and isolated from mice in which a GFP reporter has been inserted at the start site of the RORγt gene [139]. Approximately, 50% of the LTi cells in mice are $CD4^+$ while the other 50% are $CD4^-$, possibly indicating the diversity in the LTi cell phenotypes. Adult LTi cells differ from their fetal counterpart due to expression of the T cell costimulatory molecule ligand (OX40-L) and CD30L [143]. It is noteworthy that $NKp46^+$ LTi-like cells have not been detected in the embryo, and therefore unlikely to be involved in lymphoid organogenesis.

Table 1-4: Phenotypic comparison of mouse and human LTi cells

Marker		Mouse LTi	Human LTi
Surface marker	CD4	50%	-
	CD117 (c-KIT)	+	+
	CD127 (IL-7Rα)	+	+
	CD90 (Thy-1.2)	+	ND
	Nkp44	+	+
	Nkp46	-	ND
	CD56	-	10%
	CD161 (NK1.1)	+	+
	OX40L*	+	+
	CD30L*	+	+
Transcriptional factors	RORγ□	+	+
	Id2	+	+
Chemokine receptors	CXCR5	+	+
	CCR7	+	+
	CXCR6	+	+
TNF family members	RANK	+	+
	RANKL	+	+
	Lymphotoxin αβ	+	+
Secretory molecules	IL-22	+	-
	IL-17	+	+

*Found in adult LTi cells only. "+" = Positive; "-" = Negative.

1.4.1.2 LTi function

As discussed earlier in section 1.3.3, LTi cells are indispensable for embryonic lymphoid tissue organogenesis with studies demonstrating that mice deficient in the expression of the RORγt completely lacked LTi cells and this correlated with a total absence of lymph nodes [139]. Identification of LTi cells in adults, albeit in far less abundance than fetal tissue have provided the impetus for exploring the role of LTi cells for adult organogenesis. Fate mapping experiments have established that the half-life of LTi cells is 3 weeks, indicating that fetal LTi cells do not account for the pool of adult LTi cells [144]. One of the most frequently documented examples of adult organogenesis driven by LTi cells is found in the intestine, where LTi numbers are found in much larger numbers than other adult tissues [145] . Gut-associated lymphoid tissue (e.g. cryptopatches) formation occurs after birth around 1– 2 weeks of age in mice; consisting of numerous small and randomly distributed clusters of LTi cells, with a few DCs but almost no T or B cells [146]. These structures are absent in RORγt-deficient mice. Following bacterial gastro-intestinal infections, these cryptopatches have been shown to transform into isolated lymphoid follicles (ILFs), which are important anatomical sites for the generation of IgA-producing plasma cells [147]. In the mouse, these structures are not observed until the colonization of the intestine by microflora around weaning time (3–4 weeks). This transformation is regulated by interactions between RORγt$^+$ LTi cells and stromal cells through LTβR signaling [148].

In addition to organogenesis of lymphoid tissue, evidence indicates that postnatal LTi cells also help repair damaged lymphoid structure after viral infections, which

is crucial for an effective immune response [149]. For example, an elegant study by Scandella et al, reported that during an acute infection with lymphocytic choriomeningitis virus, the splenic architecture was disrupted with a consequent failure in the ability of mice to mount protective antibody responses to secondary infections. However, the accumulation of proliferative LTi cells and the crosstalk between the LTi and stromal cells via the LTβR signaling restored the lymphoid lymphoid microanatomy, as well as the ability to form high-affinity antibodies, a process that is severely delayed in mice lacking LTi cells [150].

Adult LTi cells have recently been implicated to influence T-cell adaptive immune responses. Within lymphoid tissues, LTi cells are often located at the edge of the B cell follicles, where interactions between T cells and B cells commonly occur in primary and secondary immune responses [151]. Adult LTi cells express costimulatory molecules, OX40L and CD30L and interactions between LTi and T cells via these co-stimulatory molecules have been shown to induce survival of Th2 cells [152]. These interactions have also been implicated in establishing microenvironments within which $CD4^+$ T cells provide help for effector immune responses and then sustain primed $CD4^+$ T cells for memory responses [149,152-154]. Within the intestinal LN anlagen, LTi cells have also been reported to produce pro-inflammatory cytokines interleukin 17 (IL-17) and/ IL-22 in response to IL-23 both inducing the production of anti-microbial peptides by epithelial cells, providing support for their role in tissue remodelling and mucosal immunity [155]. However, whether IL-17 or IL-22 producing LTi cells represent three distinct subpopulations of group 3 ILCs or activation stages of a single plastic lineage modulated by environmental cues remains under debate [156].

1.5 RORγt$^+$ LTi cells and Cancers

Collectively, referred to as the tumour microenvironment (TME), tumours are complex tissues that comprise of malignant cells and a multitude of stromal cells [157]. These include e.g. the extracellular matrix (ECM), activated fibroblasts, mesenchymal stem cells, immune cells, pericytes, adipocytes, epithelial cells, vascular and lymphatic endothelial cells (see Figure 1-5). Recently RORγt$^+$ ILCs have been added to the list of immune cells that may contribute to the TME within mouse melanoma models [113,158].

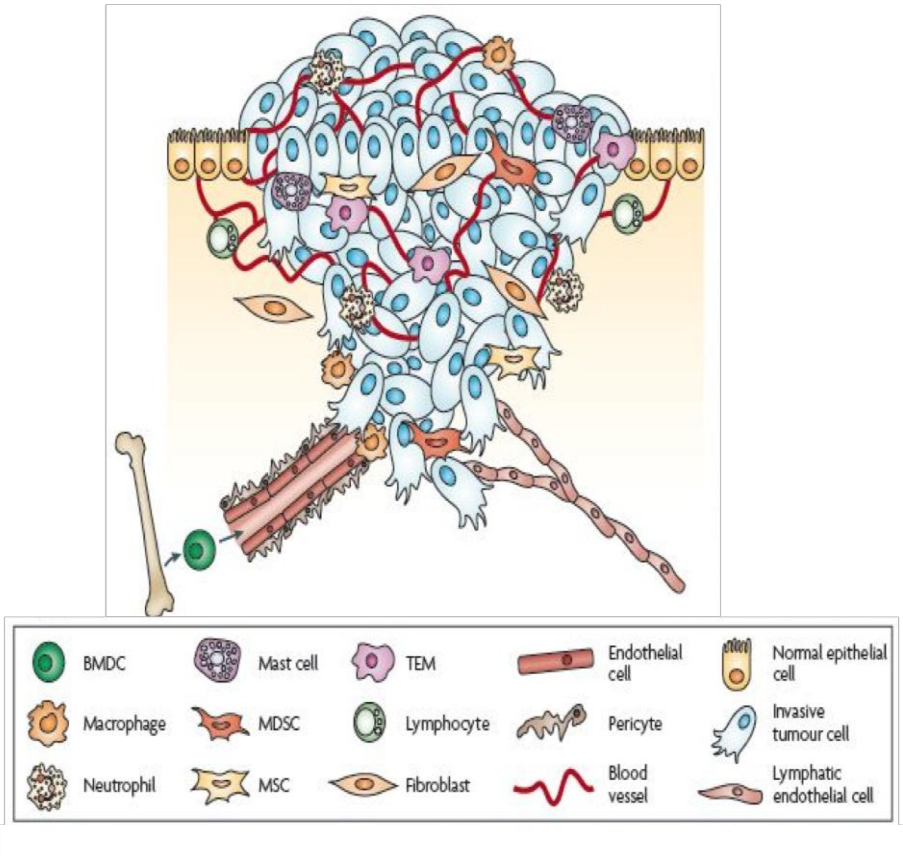

Figure 1-5: Schematic representation of the tumour microenvironment [159].

TME comprises of malignant and stromal cells. Stromal components include vascular or lymphatic endothelial cells, supporting pericytes, fibroblasts, and both innate and adaptive infiltrating immune cells.

Components within the TME have been shown, from experimental models and clinical studies to either provide host protection leading to tumour regression or tumour-promotion by providing an immunosuppressive milieu. The role that RORγt^{+} ILCs play within the TME remains to be established with the two aforementioned studies reporting conflicting findings. Whilst Shields et al [113], reported that tumours with a higher LTi count (CCL21^{high} expressing tumours) were associated with an increased tumour growth/survival, Eisenring et al [158], reported that even a small number of LTi cells were able to potently inhibit tumour growth by initiating an intense leukocyte invasion into the tumour microenvironment. The authors speculated that IL-12 converts a subpopulation of LTi cells in the tumour into innate NKp46^{+} LTi-like cells, which in turn changes the tumour microenvironment from anti-inflammatory to pro-inflammatory [158]. The study by Shields et al [113] also reported that CCL21^{high} melanoma tumours induced lymphoid-like stromal networks resembling those of the lymph node paracortex within a tumour microenvironment. Whether the induced lymphoid-like stoma within the tumour promoted immune escape/immune tolerance via neo-lymphangiogenesis remains unclear but this study does highlight the potential for the lymphatic stroma as a key modulator of tumour-immune responses. The presence or role of RORγt^{+} LTi cells has not been explored in human tumours and requires further investigation.

1.5.1 Cancer Immunoediting

Recent years have seen a growing appreciation of the term, "*cancer immunoediting"* as an academic framework integrating the immune system's dual

host-protective and tumour-promoting roles and consists of three successive steps: elimination, equilibrium and escape [160,161] (see Figure 1-6).

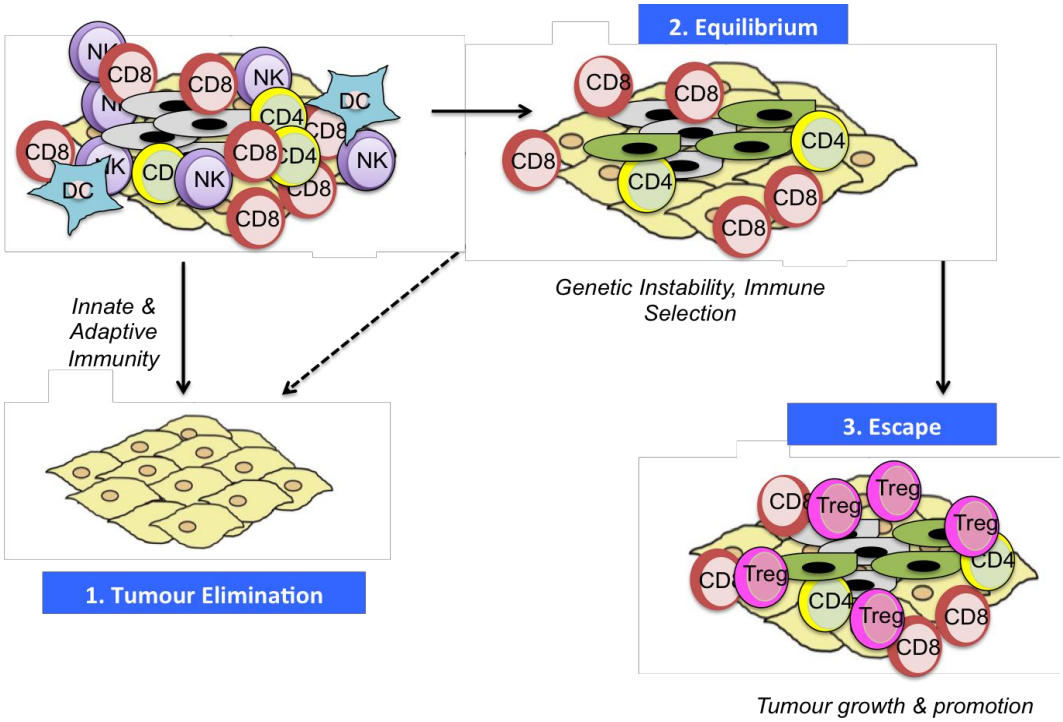

Figure 1-6: Phases of "cancer immunoediting."

1): Elimination/immunosurveillance: Functional innate and adaptive immune cells and molecules recognise a transformed cancer cell and function to destroy the tumour cell or prevent its outgrowth. This can sometimes represent the end of immunoediting process. **2): Equilibrium:** However, the inability of the antitumour immunity to completely eliminate transformed cells results in the surviving tumour variants to enter into a state of equilibrium, where the tumour cells become dormant and clinically unapparent. **3): Escape**: Tumour variants may eventually acquire further mutations that result in the evasion of tumour cell recognition, killing, or increase cancer-induced immunosuppression to promote tumour growth and survival.

In the elimination phase, various components of the immune response work together to destroy developing tumours long before they become clinically apparent. The role of an effective innate immune system during the elimination phase is well recognized [162-164]. During the 'equilibrium' phase, a balance is established between the tumour and the immune system, shaping each other reciprocally [165,166]. Finally, the immune system contributes to the selection of

tumour variants that enter the escape phase, in which their outgrowth is no longer blocked by immunity resulting in clinically apparent disease [166,167].

Data collected from large cohorts of human cancers demonstrate that the immune contexture of primary tumours hold prognostic information that may be superior to the AJCC/UICC TNM-classification of tumours, particularly in early stage cancers [168,169]. A strong lymphocytic infiltration has been reported to be associated with good clinical outcome in many different tumour types, including melanoma, head and neck, breast, bladder, ovarian, colorectal, renal, prostatic and lung cancer [170]. Within colon cancers, an immune score that quantifies the intra-tumoural density and location of CD8+T cells and memory CD45RO+T cells has been proposed as a useful approach both for predicting the impact of the tumour microenvironment on clinical outcome in colon cancer patients, and for selecting therapy for patients [169]. Loi et al [171], recently reported on the prognostic role for tumour-associated lymphocytes in breast cancer in a large prospective clinical trial, evaluating more than 2,000 tumour samples from patients with node-positive breast cancer. Within specific subtypes of breast cancer, patients with an increased lymphocytic infiltrate had reduced relapse rates and improved survival. Moving forward, implementation of the “Immunoscore” as a new component for the classification of cancer, designated TNM-Immune (TNM-I) have already began [170]; and international immunological consortia (the Society for Immunotherapy of Cancer (SITC), the European Academy of Tumour Immunology (EATI), the Cancer and Inflammation Program, the National Cancer Institute, National Institutes of Health, USA and "La Fondazione Melanoma Onlus) recently addressed the issue of immune assay harmonization across

laboratories with the objective of accelerating immune biomarker identification and drug development [172].

Although, the exact mechanisms that underpin immunoediting remain poorly understood, an increasing body of evidence suggests that antigen presentation can take place in ectopic lymph node-like structures named "tertiary lymphoid structures" (TLS) within the tumour microenvironment. Given the well-recognised link between LTi cells and lymphoid organogenesis, these innate lymphoid cells may play a role in immunoediting by inducing TLS neogenesis.

1.5.2 Tertiary Lymphoid Structures

Several pieces of evidence suggest that the development of 'tertiary' or 'ectopic' lymphoid tissues in areas of chronic inflammatory stimulation (e.g. in autoimmune diseases or viral and bacterial infections) represent a compensatory mechanism for the increased demand for a localized immune reaction. Malignant tumours resemble chronic inflammatory conditions in that they host a persistent immune infiltration that fails to clear the antigenic insult - often referred to as "*a wound that never heals*".

TLS are structurally reminiscent to SLOs (e.g. lymph nodes, spleen), in that they have organized immune cell infiltrates containing anatomically distinct yet adjacent T and B cell compartments and, in most cases, they contain high endothelial venules through which lymphocytes can enter from the blood. Although, in theory the immunosuppressive nature of the tumour microenvironment would represent a challenge for the induction or the

functioning of TLSs, the presence of organised intratumoural lymphoid aggregates have been described in a range of tumour types (See Table 1-5).

Table 1-5: Clinical studies reporting on the presence of lymphoid aggregates

Tumour	Composition	Ref.
Breast Cancer	T- cells, mature DCs	173
	T- cells, B-cells, FDCs	174
	Lymphocytes (Haemotoxylin counterstaining)	175
	T-cells, B-cells, HEVs	176
	T-cells (TfH, CD4+ & CD8+ cells), B-cells, FDCs	177
	T-cells, B-cells, mature DCs, HEVs	178
Colorectal Cancer	T-cells, B-cells, mature DCs	179
	T-cells, mature DCs	180
	T-cells, B-cells, FDCs	181
	T-cells, B-cells, mature DCs	182
Lung Cancer	T-cells, B-cells, mature DCs, FDCs	183
	T-cells, B-cells, mature DCs, HEVs	184
Melanoma	T-cells (CD4+, CD8+, Foxp3+ Tregs), B-cells, mature DCs	185
	T-cells, B-cells, mature DCS, FDCs, HEV	186
Ovarian Cancer	T-cells, B-cells, HEVs	176
Renal Cell Cancer	T-cells, B-cells, mature DCs	182

Abbreviations: DC: dendritic cell, FDC: follicular DC, HEV: high endothelial venules. Bold text represent studies describing distinct TLSs. *Adapted from* [187]

Although most experts agree that LTα1β2 is necessary for TLS induction, the role of LTi cells in the process remains controversial. LTi cells have been identified within TLS and the injection of LTi cells into normal skin has been shown to be sufficient to induce them [188], but mice lacking in LTi cells (e.g. $Id2^{-/-}$ or $Rorc^{-/-}$ mice) have also been shown to develop TLS in response to influenza viral infection [189,190]. Pathological lymphoid neogenesis is therefore likely to involve additional players that can substitute for LTi cells [190,191].

While evidence suggests that the presence of HEVs around the TLS represent an ideal gateway for the entry of circulating lymphocytes into the tumour microenvironment providing per se a survival benefit for cancer patients [187], cancer-associated TLSs may also provide a niche for the differentiation of functional suppressive immune cell populations (e.g. T regulatory (Treg) or myeloid-derived suppressor cells (MDSC)). These immunological alterations may act to enhance tumour metastasis to the draining lymph nodes. A deeper comprehension of the molecular and cellular interactions of cancer-associated LTi cells may provide an insight into the mechanisms involved in the phases of "immunoediting" by cancers, and allow for further exploration of the concept of the chemokines and/chemokine receptors associated lymphangiogenesis with an opportunity for identification of targets for anti-lymphangiogenenic strategies for breast cancer patients.

1.6 Summary

Within invasive breast cancers, trans-endothelial migration through existing or new lymphatic vessels is thought to be the first step for tumour cells to undertake when disseminating through the lymphatic vasculature; and has been shown to stratify breast cancer phenotypes into distinct prognostic groups [192]. The exact molecular mechanisms mediating tumour cell entry and persistence within the lymphatic system remain unclear. Genetic and functional studies have established an important role for the "lymphatic-based migratory" chemokines (CXCL13, CCL19 and CCL21) in the trafficking of LTi, DC, T- and B-cells to the secondary lymphoid organs (reviewed in [62]).

Tumour cells may manipulate normal processes that govern chemokine-dependent trans-lymphatic migration of immune cells. RORγt^{+} ILCs, which include LTi cells are a family of immune cells that are heterogeneous in their cytokine production, tissue location and effector functions (reviewed in [134,156]). Despite studies reporting on the presence of LTi cells within the tumour microenvironment of a melanoma xenograft [113,158], the presence or role of these cells has not been explored in human tumours. Thus, the relevance of these findings to human cancers requires further investigation.

Chapter 2: Hypothesis and Aims

2.1 Hypothesis

The null hypothesis of this thesis is that lymphoid tissue inducer (LTi) cells do not have a role in the tumourogenesis of breast cancers.

2.2 Aims

Investigating the relationship between LTi cells, stromal and breast cancer cells within the tumour microenvironment (TME) will further our insight into the mechanisms involved in lymphangiogenesis and lymphatic invasion of breast tumours.

2.2.1 Experimental plan

- Identification of LTi cells within human breast cancer tissue
- Analyse the expression of lymphoid chemokine and/chemokine receptors within human breast cancer datasets and relate this to the presence or absence of LTi cells
- Explore any correlation between LTi cells and lymphatic invasion, neolymphangiogenesis and lymph node tumour burden.
- Explore the interactions between LTi, stromal and tumour cells *in vitro and in vivo*

Chapter 3: Materials and Methods

This project received the approval of the NHS Research Ethics Committee (REC No: 07/40874/131) for use of tissue from the King's Health Partners Cancer Biobank at Guy's Hospital, London. All *in vivo* experiments were performed in accordance with the local ethical review panel, the UK Home Office Animals Scientific Procedures Act, 1986 and the UKCCCR guidelines [193].

3.1 Reagents & Materials

3.1.1 Cell lines

The mouse breast cancer cell line 4T1.2 (derived from a spontaneous mammary carcinoma in a BALB/c mouse[194] was procured from Professor Robin Anderson's group (Peter MacCallum Cancer Centre, Australia).

Bone marrow derived mesenchymal stromal cells (HS-5) were a kind gift from Professor Lythgoe's laboratory (Centre for Advanced Biomedical Imaging, University College London). Two further fluorescently labelled cell lines (GFP and DsRed) were generated from the human bone-marrow-derived mesenchymal stromal cell line (Courtesy of Dr Gilbert Fruhwirth).

3.1.2 Cell culture

Dulbecco's Modified Eagle Media - DMEM (Life Technologies Ltd)

RPMI Media 1640 (Life Technologies Ltd)

"Complete media" contains 10% Penicillin/ Streptomycin (10,000IU Penicillin and 10mg/ml Streptomycin) (Life Technologies Ltd, UK) 2mM L-Glutamine (Life Technologies Ltd, UK), and 10% heat inactivated Foetal Bovine Serum (Sera Laboratories International Ltd)

Trypsin/EDTA (0.25% trypsin, 0.02% ethylenediaminetetraacetic acid, EDTA) (PAA Laboratories, Germany)

3.1.3 Immunofluorescence staining

4% (w/v) paraformaldehyde (PFA; Sigma-Aldrich) in PBS

99.5% acetone (PFA; Sigma-Aldrich) - ice cold

Blocking solution: 10% goat serum in 1% BSA in PBS or 1% BSA in PBS alone

Sodium borohydride (Sigma-Aldrich)

Triton X-100 (polyethylene glycol p-(1,1,3,3-tetramethylbutyl)-phenyl ether) (Fischer)

Heat inactivated human serum (Invitrogen): 10% in 1% BSA in PBS

Heat inactivated goat serum (Invitrogen): 10% in 1% BSA in PBS

TBS: Tris-buffered saline (25mM Tris, 100mM NaCl, pH 7.5)

Hoechst 33342 (Invitrogen)

Mowiol: 10% (w/v) Mowiol 4-88, 25% glycerol, 100mM Tris-HCl pH 8.5 (Calbiochem)

DABCO: 2.5% (w/v) 1,4-diazabicyclooctane (Sigma-Aldrich)

Immersol 510 Immersion oil (Zeiss)

3.1.4 Immunohistochemical staining

3% hydrogen peroxidise (Sigma-Aldrich) in PBS

Xylene (Solmedia)

100% and 70% ethanol (Tennants)

Haematoxylin (VMR)

Eukit mounting media: contains 45% acrylic resin and 55% xylene (Sigma-Aldrich

DAKO primary antibody diluent: (Tris-HCI buffer containing stabilizing protein and 0.015 mol/L sodium azide).

Bond primary antibody diluent: (Tris-buffered saline, surfactant, protein stabilizer and 0.35% ProClin 950 (active ingredient is the biocide, 2-methyl-4-isothiazolin-3-one)

Leica BOND refine polymer detection kit (DS9800).

3.1.5 FACS sorting and staining

RPMI Media 1640 (Life Technologies Ltd)

Collagenase-dispase (100mg/ml stock, Roche)

DNase (10mg/ml stock, Sigma-Aldrich).

Red Blood Cell Lysis Solution: contains 8.3 g/L ammonium chloride in 0.01 M Tris-HCl buffer (Sigma-Aldrich)

Cell strainer (70µm mesh size)

FACS buffer solution: 0.5% BSA in PBS, 2mM EDTA

Foxp3 staining buffer kit: contains Fix/perm diluents, fix/perm concentrate and 10x permeabilisation buffer (ebioscience)

4% (w/v) paraformaldehyde (PFA; Sigma-Aldrich) in PBS

CD11c MACS beads (Miltenyi Biotec)

PeakFlow blue flow cytometry reference bead (Life technologies Ltd)

3.1.6 Western blotting

Lysis buffer: 50mM Tris/Hcl pH7.4, 150mM NaCl, 2.5mM EDTA, 2.67mM EGTA (ethylene glycol tetraacetic acid),10% Glycerol, 1% Triton X- 100

Freshly added: 0.2mM sodium orthovanadate, 0.01μM Calyculin A (in EtOH), 1:100 P8340 Protease inhibitor cocktail (Calbiochem USA) (aprotinin 0.8μM, leupeptin 20μM, AEBSF 1040μM, E-64 protease inhibitor 14μM, pepstatin-A 15μM, bestatin 40μM)

Sample buffer: after protein determination in the sample, 100mM Dithiothreitol (DTT) and 0.4% w/v Serva blue dye were added

Gels: pre-made Novex Nupage 12% or 4-12% Bris Tris gel (Invitrogen)

Standard: Precision Plus protein dual colour standard (BioRad)

Nupage MES SDS Running Buffer (20X) (Invitrogen). This buffer was diluted to 1X with distilled H_2O for electrophoresis

Transfer buffer: 7.2g glycine, 1.7g Trisma base, 200ml methanol, made up to a final volume of 1L in distilled H_2O

Wash buffer: Tris-buffered saline (TBS): 0.02mM Tris, 0.05M NaCl, 0.01M KCl, pH 7.4

TBS-Tween (TBST): TBS containing 0.1% Tween-20

Blocking solution: 4% Bovine Serum Albumin (BSA) (BioSera) made up in TBS-Tween or 5% nonfat dry *milk* in TBS-Tween

PVDF transfer membrane (Immobillon)

Pierce ECL Western Blotting substrate (ThermoScientific)

3.1.7 ELISA

Human CXCL13/BLC/BCA-1 Quantikine ELISA Kit (Cat no: DCX 130, R&D systems)

Mouse CXCL13/BLC/BCA-1 Quantikine ELISA Kit (Cat no: MCX 130, R&D systems)

Human CCL21/6Ckine DuoSet (Cat no: DY366, R&D systems)

Mouse CCL21/6Ckine DuoSet (Cat no: DY457, R&D systems)

Human TRANCE/RANK L/TNFSF11 DuoSet (Cat no: DY462, R&D systems)

Mouse TRANCE/RANK L/TNFSF11 DuoSet (Cat no: DY462, R&D systems)

Wash Buffer - 0.05% Tween 20 in PBS, pH 7.4

Reagent diluents: 0.1% BSA, 0.05% Tween 20 in Tris-buffered saline (20nM Trizma base, 150nM Nacl), pH 7.2-7.4, 0.2μM filtered).

Streptavidin-HRP (R&D Systems)

1-Step Ultra TMB (3,3′,5,5′-tetramentylbenzidine) ELISA (Thermo Scientific)

2mM sulphuric acid stop solution (Fisher chemicals)

3.1.8 Elispot cytokine antibody array

RayBio human cytokine antibody array 5 kit (Cat# AAH-CYT-5-8)

10% bovine serum albumin in Tris-buffered saline

Biotinylated antibody cocktail mixed with 2ml of blocking buffer

1X HRP streptavidin

3.1.9 Invasion assay

QCM ECMatrix Cell Invasion Assay, 96-well (8 μm), fluorime (Millipore, UK)

Staining solution: contains 0.5 g Crystal Violet (0.05% w/v), 27 ml 37% Formaldehyde (1%), 100 mL 10X PBS (1X), 10 mL methanol (1%), 863 dH_20 to 1L

3.1.10 Migration assay

8-well μ-Slide (chambered coverslip) (Ibidi)

0.5M 4-(2-Hydroxyethyl)piperazine-1-ethanesulfonic acid (Hepes) buffer (PAA Laboratories, Germany)

3.1.11 Cell stimulation

Recombinant Mouse CXCL13/BLC/BCA-1 stock 25μg/ml (R&D systems)

Recombinant Mouse CCL21/6Ckine stock 25μg/ml (R&D systems)

Recombinant Mouse TRANCE/RANK L/TNFSF11 stock 10μg/ml (R&D systems)

Recombinant human epidermal growth factor, stock 100μg/ml (PeproTech, USA)

3.1.12 Cell inhibition

70mg/ml denusumab (Xgeva, Amgen) was a kind gift from the London Oncology Clinic; diluted to the required concentration in PBS

3.1.13 Multi-photon imaging

Custom-made titanium mammary imaging window (In collaboration with Professor Boris Vojnovic, Advanced Technology Development Group, Oxford, UK)

CellTracker™ Orange CMTMR

(5-(and-6)-(((4-Chloromethyl)Benzoyl)Amino)Tetramethylrhodamine)

(invitrogen)

CellTracker™ Green CMFDA (5-Chloromethylfluorescein Diacetate) (invitrogen)

Soft silk wax coated braided suture (Covidian)

Isoflurane-Vet 100% w/w Inhalation Vapour, Liquid (Merial Animal Health Ltd.)

3.1.14 Fresh frozen tissue storage of animal tissue

2-Methylbutane (*ReagentPlus*®, ≥99%) (Ispopentane, Sigma-Aldrich)

OCT Mounting media (VMR)

3.1.15 siRNA transfection

OPTi-MEM-1 (Gibco)

Lipofectamine™ RNAiMAX (Invitrogen)

Table 3-1: Sequence of siRNA oligonucleotides

Gene	siRNA ID	Target Sequence (5' → 3')
CXCL13	S20727	CAAGCUGAAUGGAUACAAA
CXCL13	S20726	UGAUGGAAGUAUUGAGAAA
CXCL13	S20725	AUCGAAUUCAAAUCUUGGU
CCL21	S12606	CCAUCCCAGUAUCCUGUU
CCL21	S12605	CAGCUACCGAAGCAGGAA
CCL21	S12607	GCTATCCTGTTCTTGCCCCG
Scrambled	#10300934	Non-targeting siRNA pool from Thermo Scientific Dharmacon

3.1.16 Antibodies

Table 3-2: List of antibodies used

Name	Clone	Dilution	Company	Application	Cross-reactivity to MS	Cross-reactivity to Hu
Primary antibodies						
Rat anti-human RORγt	AFKJ5-9	1:25	ebioscience	IF	Yes	Yes
Mouse anti-human CD127 Biotin	ebioRDR5	1:25	ebioscience	IF	No	Yes
Mouse anti-human CD3 APC	UCHT1	1:30	ebioscience	IF	No	Yes
Mouse Anti-human gp36/podoplanin	18H5	1:1500	Abcam	IHC	No	Yes
Goat anti-mouse Pancytokeratin	-	1:500	Santa Cruz	IHC	Yes	Yes
Rat anti-mouse e-cadherin PerCP-efluor 710	DECMA-1	1:100	ebioscience	FACS	Yes	Yes
Rat anti-mouse CD11c PE	N418	1:100	ebioscience	FACS	Yes	No
Rat anti-mouse B220R PE	RA3-6B2	1:100	ebiosciene	FACS	Yes	Yes
Rat anti-mouse CD3e-PE-Cy7	145-2C11	1:100	ebioscience	FACS	Yes	Yes
Rat anti-mouse CD127 (IL-7Ra)-PerCP/Cy5.5	A7R34	1:50	Biolegend®	FACS	Yes	No
Rat anti-mouse CD90.2-APC/Cy7	30-H12	1:50	Biolegend®	FACS	Yes	No
Rat anti-mouse CD335 (NKp46) eFluor® 450	29A1.4	1:100	ebioscience	FACS	Yes	No

Rat anti-mouse CD19 FITC	1D3	1:200	BD Pharmingen	FACS	Yes	No
Armenian Hamster anti-mouse CD3e-PE	145-2C11	1:200	Ebioscience	FACS	Yes	No
Armenian Hamster anti-mouse CD11c-FITC	N418	1:100	Miltenyi Biotec	FACS	Yes	No
Rat anti-mouse B220/CD45R- Alexa Flour® 646	RA3-6B2	1:150	Biolegend®	FACS	Yes	No
Multi-potent mesenchymal Stromal Cell Marker Antibody Panel Kit	Cat No. SC017	-	R&D systems	IF	No	Yes
Rabbit anti-human LT□R	AA11-60	1:100	LifeSpan BioSciences	IF	Yes	Yes
Mouse anti-mouse Vimentin	V1-10	1:100 (IF) 1:1000 (WB)	Abcam	IF, WB	Yes	Yes
Rabbit anti-human/mouse RANK	-	1:1000	Cell Signaling	IF/WB	Yes	Yes
Goat anti-mouse RANKL	-	1:500	R&D systems	IF/WB	Yes	No
Secondary antibodies						
Dnk anti-Rat-IgG-FITC	-	1: 100	Jackson ImmunoResearch	IF	Minimal	Minimal
Rabbit anti-rat IgG-FITC	-	1:200	Invitrogen	IF	No	No
Goat anti-Rabbit-FITC	-	1:100	Southern Biotech	IF	No	No
Streptavidin Alexa 555	-	1:500	Invitrogen	IF	No	No

Dnk anti-rabbit Cy3	-	1:200	Jackson ImmunoResearch	IF	No	No
Neutralising antibodies						
Mouse CXCL13/BLC/BCA-1 Affinity Purified Polyclonal Ab, Goat IgG	-	0.5mg	R&D systems	B/N	Yes	No
Mouse CCL21/6Ckine Affinity Purified Polyclonal Ab, Goat IgG	-	0.5mg	R&D systems	B/N	Yes	No
Mouse TRANCE/RANK L/TNFSF11 Affinity Purifed Polyclonal Ab, Goat IgG	-	0.5mg	R&D systems	B/N	Yes	No
Normal Goat IgG Control		0.5mg	R&D systems	Control	-	-

3.2 Methods

3.2.1 METABRIC cohort/dataset

The METABRIC (Molecular Taxonomy of Breast Cancer International Consortium) project represents a cohort of patients who were recruited from 1989 and 2002 from 5 different hospitals/research centres across Canada and the UK: Guy's & St Thomas' NHS Trust Hospitals, Cambridge Breast Unit, Addenbrooke's Hospital, Nottingham University City Hospital in the UK and the Tumour Bank of British Columbia, Vancouver and the Manitoba Tumour Bank in Canada [195]. The cohort selection criteria entailed female patients with primary breast cancer, who had not had neoadjuvant treatment and had been followed-up for more than 5 years. METABRIC has been approved by the 'NHS National Research Ethics Service, Cambridgeshire 4 Research Ethics Committee' with reference number: 07/MRE05/35.

This project aimed to analyse 2000 tumours by using a combination of high-resolution array-CGH, expression profiling, sequencing and tissue microarray analysis, and correlate the molecular profiles obtained with the clinical outcome of the tumours. The clinical data collected included survival data, date and cause of death, treatment information and hormone receptor status, e.g. ER, PR and HER2 status.

The data used in Chapter 4:, relates to the subset of patients which were recruited at Guy's and St. Thomas' Hospital, for whom tumour samples were stored in the

King's Health Partners Cancer Biobank at Guy's Hospital, London. The KHP Breast Tissue and Data Bank (GSTT/KCL BTDB) is a Human Tissue Authority licensed tissue bank, which has been banking breast tissue and clinical data on patients over the last 30 years. The Tissue Bank maintains over 7200 FFPE primary tumours, 2500 fresh frozen tumours and 900 matched tumour and blood DNA samples, all of which are associated with prospectively acquired pathological and clinical data.

3.2.1.1 Gene expression dataset

The King's Health Partners Cancer Biobank at Guy's Hospital subset of the METABRIC data set was profiled using the Illumina HT12 platform [8]. The frozen tissue sections from which nucleic acids were isolated were subject to expert histopathological review to assess the presence of invasive tumour, pre-malignant or benign changes, tumour cellularity, and lymphocytic infiltration in specific subgroups and only samples with >70% tumour DNA were included. Samples were filtered for array intensity, quantile normalised, and a ComBat BeadChip correction applied (n=234; 176 ER^+ samples, 58 ER^- samples based on *ESR1* gene expression). PAM50 subtype was assigned as in [196] using re-sampling to reflect the hormone receptor statuses of the PAM50 discovery cohort [6,197]. Dr Katherine Lawler kindly carried out the analysis of gene expression data.

3.2.2 Immunohistochemical (IHC) staining

3.2.2.1 IHC staining in fresh frozen tissue

5μm thick sections were cut from frozen archival primary breast cancer tissue. Depending on the antibody tissues were either fixed in acetone for 20 minutes at 4^{o}C, then stored at -80^{o}C at the time of sectioning or 4% PFA fixation immediately at the time of staining. At the time of staining, tissue sections taken out from -80^{o}C were left to dry for 30 minutes. They were then rehydrated with PBS for 5 minutes. Slides were then incubated for 5 minutes at room temperature (RT) with 3% hydrogen peroxide in order to inactivate endogenous peroxidase. Following 5 minute washing steps with PBS, slides were incubated with the primary antibody of interest, diluted in DAKO Primary Antibody Diluent, which contains Tris-HCI buffer containing stabilizing protein and 0.015 mol/L sodium azide), for 1 hour. Apart from when using an HRP conjugated antibody, antigen binding was detected using an enzyme-conjugated secondary antibody diluted to the optimised concentration. 3-3′-diaminobenzidine (DAB) chromogen technique was used to perform the immune histochemical reaction. A light haematoxylin counterstain was applied and sections dehydrated, cleared and mounted using Eukitt mounting medium. Stained sections were photographed using a Hamamatsu NanoZoomer-XR C12000 digital slide scanner (Hamamatsu Photonics; Japan).

3.2.2.2 IHC staining in formalin fixed paraffin embedded tissues samples

Immunohistochemistry of 2μm thick formalin-fixed, paraffin-embedded wax sections were stained with no antigen retrieval step, using protocol F, on the Leica BOND-Max automated IHC platform (Leica Microsystems Inc, Wetzlar, Germany). Slides were incubated with the primary antibody of interest, diluted in Bond Primary Antibody Diluent, which contains Tris-buffered saline, surfactant, protein stabilizer and 0.35% ProClin 950 (active ingredient is the biocide, 2-methyl-4-isothiazolin-3-one), for 30-40 minutes; and antigen binding detected using the Leica BOND refine polymer detection kit (DS9800). A light haematoxylin counterstain was applied and sections dehydrated, cleared and mounted using Eukitt mounting medium. Stained sections were photographed using a Hamamatsu NanoZoomer-XR C12000 digital slide scanner (Hamamatsu Photonics; Japan).

The mean number of stained lymphatic vessels was collected through Chalkley count, where a 25-point grid was placed onto the scanned image and all points coinciding with the marked vessels counted (see Figure 3-1). Three to five images were used and the mean value was obtained with the number of vessels in each image. This method is thought to abolish the observer-dependent step of measuring LVD since the Chalkley count is a relative area estimate rather than a true vessel count.

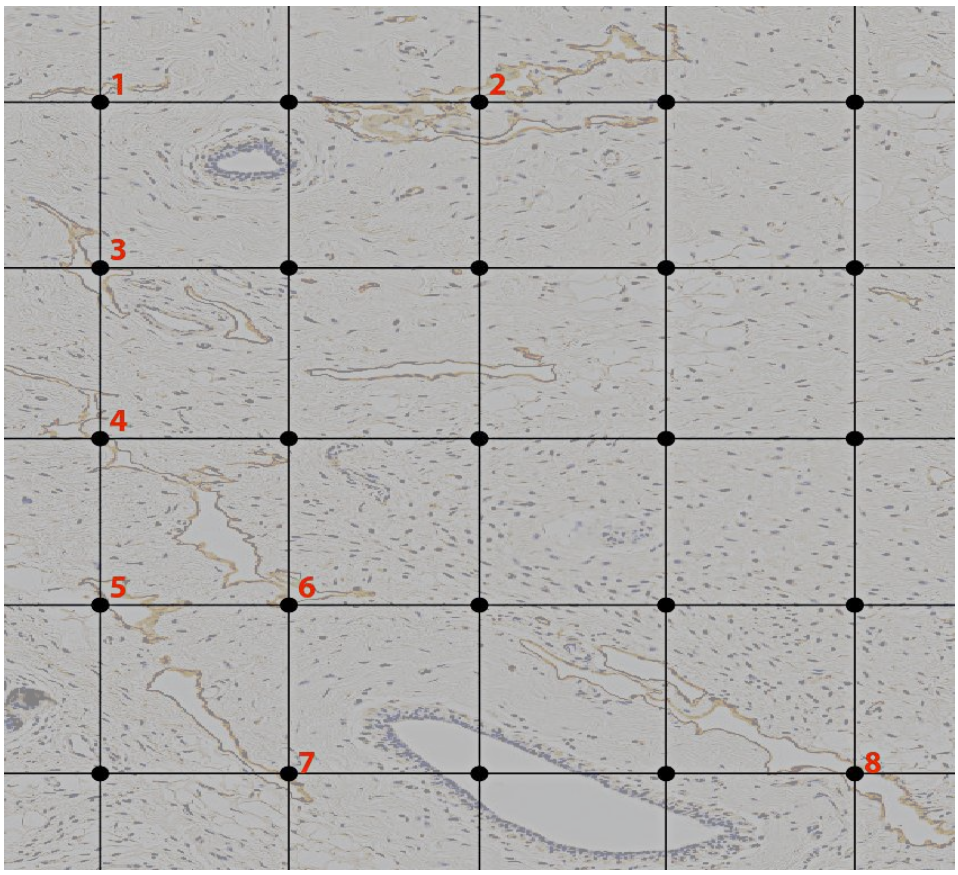

Figure 3-1: Chalkley point counting. Following identification of a "hotspot" at low magnification, a 25-point grid was placed onto the scanned image and all points coinciding with the marked vessels counted. In the current example, 8 points were scored as positive. Three to five images were used and the mean value was obtained with the number of vessels in each image.

3.2.3 Immunofluorescence (IF) staining

3.2.3.1 IF staining for LTi cells in human fresh frozen breast cancer tissues.

All the antibodies used were optimized for use in fresh frozen human tissue samples, initially by IHC. 5μm thick sections were cut from frozen archival primary breast cancer tissue and fixed in acetone for 20 minutes at 4^{o}C, then stored at -80^{o}C. This fixation method was superior to 4% PFA or fixation immediately at the time of staining (data not shown). At the time of staining, tissue sections taken out from -80^{o}C were left to dry for 30 minutes. They were

then rehydrated with PBS for 5 minutes. Tissues were then blocked with 10% goat serum in 1% BSA in PBS for 15 minutes. Samples were incubated with three primary antibodies (e.g. rat anti-human/mouse ROR-γt, mouse anti-human CD3e-APC, mouse anti-human CD127-biotin) for one hour. Biotinylated antibody was detected with Steptavidin-Alexa Fluor®555. In order to amplify the nuclear RORγt staining, the sections were incubated with fluorescently labelled donkey anti-rat IgG-FITC (AbD Serotec), then rabbit anti-FITC- Alexa Fluor 488 (Invitrogen), then goat anti-rabbit IgG FITC (Southern Biotech) for 30 minutes each, with 10 minute washing steps in between. Sections were counterstained with Hoechst 33342 (Invitrogen) and mounted with mowiol mounting medium mixed with 2.5% DABCO as an antifading agent, and dried overnight at room temperature.

Confocal tile scan images were obtained using an LSM 510 Metamicroscope (Carl Zeiss, Welwyn Garden City, UK) equipped with 405, 488, 543 and 633nm lasers and image analysis for LTi quantification was carried out using MacBiophototonics Image J software.

3.2.3.2 IF staining of cells in vitro

For cellular imaging experiments, cells that were seeded on glass coverslips overnight. The cells were washed in PBS and treated and fixed with 4% paraformaldehyde (PFA) in PBS for 15 minutes then rinsed thrice with PBS over a five-minute interval. Samples were then incubated with 0.25% Triton X-100 in PBS for 12 minutes at RT to permeabilize cells. The cells were rinsed once with PBS and treated with fresh 0.1% sodium borohydride/PBS (1mg/ml) for 5

minutes to reduce background autofluorescence, washed 3 times in PBS and then blocked with 1% BSA solution for 30 minutes followed by a incubation step at RT with the primary antibody of interest along with an unstained control. The coverslips were rinsed once with PBS and then incubated with a secondary antibody for upto 45 minutes. The cells were then washed 3 times in PBS and nuclei were stained with Hochst33342 at a concentration of 0.1µg/ml. Following a further washing step, coverslips were mounted on slides with Mowiol/DABCO (antifade) mounting medium, and dried overnight at room temperature.

3.2.4 Cell culture

HS-5 cells and 4T1/4T1.2 were cultured in DMEM and RPMI Medium 164 respectively. All media were supplemented with 10% foetal bovine serum (FBS), 2mM L-glutamine and penicillin/streptomycin antibiotics. The cell cultures were kept at 37°C in humidified air containing 5% CO_2. Media were changed frequently to remove dead cells and to refresh nutrients. 4T1 and 4T1.2 cells were split once they became 80-90% confluent. HS-5 cells were split once they became 50-60% confluent.

3.2.5 4T1.2 triple negative mouse model

Female BALB/c immune-competent mice were purchased from Charles River Laboratories (Wilmington, MA). The animals were 6–8 weeks of age, maintained under sterile conditions in filter top cages on sterile bedding, and fed an irradiated diet of standard mouse chow. 1 X 10^6 cells were suspended in 50µl sterile PBS and were injected subcutaneously into the mammary fat pads of the animals.

Tumour volume was calculated using the formula v = l x (w) ^{2}/2, where v = volume, l = length and w = width of tumour.

3.2.5.1 Preservation of fresh frozen tissue

Tissues (e.g. primary tumours or lymph nodes) were dissected out and embedded in the optimal cutting temperature (OCT) compound. The tissue was then immersed into isopentane which had been cooled by suspension in liquid nitrogen. Tissue was not removed from the isopentane until freezing is complete (5 seconds or less depending on size). We then transferred the snap frozen sample from the isopentane to a pre-chilled storage container for transfer to a -80^{o}C freezer until further use. Frozen tumours were cut into 4-5µm sections with a cryostat for immunostaining.

3.2.5.2 In vivo neutralization experiments

In neutralization experiments, 1 day after the subcutaneous inoculation of the 4T1.2 cells into the mammary fat pads of female BALB/c mice, groups of mice were treated with a neutralizing antibody for CXCL13, CCL21, RANKL or isotype control antibodies (0.5mg each antibody) via tail-vein injections. This was repeated every 3 days until either day 14 or day 21. Mice were monitored continuously for external symptoms of toxicity and health status.

3.2.5.3 *In vivo serum collection*

500µl of peripheral blood was obtained from tumour-bearing mice via intracardiac puncture at the termination of the experiment and transferred into a micro-container serum separator tube (Becton Dickinson). The blood samples were centrifuged at 6000rpm for 5 minutes and the separated serum was stored in −80°C until usage.

3.2.6 Flow cytometry

3.2.6.1 *LTi cell sorting*

For LTi cell sorting experiments, spleens were harvested from BALB/c immune-competent mice. Spleens were minced by scalpel and passed through a 40-µm nylon mesh to produce a single-cell suspension. Cells were then stained for CD3, CD11c, B220R, CD127, CD90.2 and NKp46 and sorted into populations by using a FACSAria. Purity was confirmed by flow cytometry and confirmed at > 90% (n = 3). For multi-photon experiments, 5-6x10^4 sorted LTi cells were injected intravenously into tumour bearing mice on the same day.

3.2.6.2 *Flow cytometric analysis of immune cell components within tumours and lymph nodes*

Tissues were weighed and dissociated mechanically to obtain a single-cell suspension. Tumours were minced by scalpel and incubated in RPMI media

mixed with collagenase/hyaluronidase at 37°C for 60 min. Lymph nodes did not require this digestion step. The tissues were further dissociated by pipette trituration and then passed through a 40-µm nylon mesh to produce a single-cell suspension. Total numbers of live cells were determined by staining with Trypan blue and counting under a microscope or by using the Casy® cell counter and analysis system. Cells were then stained for immune cell components e.g. LTi (CD3, CD11c, B220, CD127, CD90.2 and NKp46). Flow cytometry reference beads (PeakFlow blue; Invitrogen) were added to the samples before analysis for quantification of cells in each tumour. Flow cytometric analysis was performed by using BD FACSCanto II or Fortessa, employing FACSDiva Software (BD Biosciences). Data were analyzed by using FlowJo software (TreeStar Inc., Ashland, OR, USA). The absolute number of a subset of cells per milligram of tumour was calculated using the formula: Density of x cells = (number of beads added to each sample multiplied by count of x cells/count of beads)/tumour weight. Further details and list of antibodies used are included in Table 3-2.

3.2.7 Protein quantification assays

3.2.7.1 Enzyme linked immunosorbent assay (ELISA)

We have used commercial kits (R&D systems) as part of the "sandwich ELISA" technique as advised by the manufacturer. In principle, as antigen the kits contain E. coli-expressed recombinant protein (e.g. CXCL13, CCL21 or RANKL). Results of the test show linear curves that are parallel to natural protein in serum, saliva and cell- culture supernatants, and can therefore be used for determination of relative mass values for natural protein.

Briefly, monoclonal antibody directed against the antigen of interest was allowed to adsorb to a 96-well plate overnight. After three washes in PBS containing 0.05% Tween-20 (PBS-T), wells were incubated for 1 h at RT with PBS containing 1% bovine serum albumin (BSA) (Sigma) to block non-specific binding. 50µl of standard or sample supernatant were added to the wells and incubated for 2 hours at RT. Tests were loaded in triplicates. Unbound antigen was removed by washing with PBS-T and the plate was incubated with biotinylated monoclonal antibody against the antigen of interest for 2 hours at RT. After the wells have been washed a second time to remove any unbound antibody-enzyme reagent, 200µl substrate solution (streptavidin-conjugated HRP (1:200)) is pipetted into the wells and left in the dark for 30 minutes for incubation. During this time, colouring occurs in relation to the amount of protein bound in the first step. The reaction was stopped by adding 100µL sulfuric acid to the wells and the optical density at 450 nm and 540 nm was determined using a microplate reader.

3.2.7.2 Elispot cytokine antibody array

Conditioned media from various human breast cancer cell lines were analysed with a semiquantitative human cytokine antibody array that detects upto 80 chemokine/cytokines in one experiment (RayBio Human Cytokine Antibody Array V). The assay was performed as per the manufacturers guidelines. Briefly, antibody membranes were blocked with 10% bovine serum albumin in Tris-buffered saline for 30minutes. 1ml of 2-fold diluted supernatants were added into each separate well and shaken at 90 rpm at RT for 2hours. Thereafter the array membrane was washed and incubated with a biotin-conjugated antibody cocktail for a further 2 hours at RT. After the membranes have been washed a second

time, 2ml of 1X HRP-Streptavidin is pipetted into each well and left in the dark for 2 hours for incubation. Following a thorough wash, the membranes were placed in an X-ray cassette, covered in a chemiluminescent substrate for 2 minutes as per manufacturer instructions. The blots were then exposed on Hyperfilm and developed using Imaging Systems Xograph compact X4 developer. HRP-conjugated antibody served as a positive substrate control at six spots and was also used to identify membrane orientation.

3.2.7.3 Western blotting

Cells were cultured until 80% confluent in 6 well or 12 well tissue culture dishes. Cells were stimulated or inhibited as described elsewhere. Cells were then washed twice in ice-cold PBS and lysed on ice by scraping into 100-350µl of 1.5 fold sample buffer, heated to 75^{o}C. The lysates were centrifuged at 4^{o}C at 16,000g for 5 minutes to clear debris. The total protein content of the samples was measured by the BCA protein assay kit (Pierce) using known concentrations of BSA protein as standards.

For immunoblot, cell lysates were heated at 95˚C for 15minutes in 100mM DTT reducing agent (to break disulfide bonds) and loaded on to pre-made Novex Nupage 12% or 4-12% Bris Tris gels immersed in MES-SDS running buffer. One lane was reserved for a standard molecular weight marker ladder. Gels were run on an Invitrogen X-Cell mini-gel system, which were subjected to constant voltage electrophoresis at 200V until the blue loading dye reached the bottom of the gel. After separation, proteins were electrophoretically transferred onto PVDF transfer membrane using the Invitrogen XCell IITM transfer apparatus

(arrangement: sponge, two filter papers, gel, membrane, two filter papers, sponge). The gels were subjected to constant voltage at 38V for 45mins for the transfer to occur.

Membranes were blocked in the relevant blocking buffer as per the antibody's manufacturers instructions for 45min at RT with shaking and then incubated with specific primary antibody overnight at 4^{o}C. Blots were rinsed once and washed two times with TBS-Tween for 5 minutes each on a roller, prior to incubation with the appropriate secondary antibody for 45min at room temperature. Following a second washing step, the blots membranes were placed in an X-ray cassette, covered in enhanced chemiluminescent (ECL) substrate for one minute as per manufacturer instructions. The blots were then exposed on Hyperfilm and developed using Imaging Systems Xograph compact X4 developer.

It was possible to re-use the transfer membrane for incubation with second primary antibody. The protein bound to the transfer membrane were stripped off with Re-BLOT Plus Strong solution, diluted 1:10 with TBS-Tween, for 15minutes at 37^{o}C, followed by blocking and antibody incubation steps as above. Western blot results were analysed and normalised with Quantity One software (Bio-Rad Ltd).

3.2.8 siRNA Knockdown

siRNA knockdown of was achieved by treating cells with three different predesigned sequences targeting the sequence of interest (see Table 3-1). In the control group, cells were treated with scrambled non-targeting siRNA. Cells

were transfected following the manufacturer's instructions. Briefly, mesenchymal stromal cells (MSC) were seeded in 6-well plates 1 day before transfection in DMEM media that was supplemented with 2% fetal calf serum without antibiotics. Targeting or non-targeting siRNA was mixed with Lipofectamine RNAiMAX (Invitrogen) in Opti-MEM medium (Invitrogen) for 20 min at room temperature and then added to the cell culture medium at a final concentration of 20 nmol/liter. The cells were incubated at 37 °C for 24-72 hours. At the end of this incubation, protein expression was determined by ELISA analysis to assess knockdown efficiency.

3.2.9 Invasion Assay

The ability of cells to invade through ECM was assessed using the CM ECMatrix 96-well Cell Invasion Assay Kit (ECM555, CHEMICON, International, CA, USA). The assay was performed as per the manufacturers instructions. Briefly, 4×10^4 cells were seeded on to the Transwell® insert and allowed to attach at 37°C with 5% CO_2 for 2 h. Inserts were then placed in serum-free DMEM and DMEM containing 10% FBS or media containing increasing concentration of the recombinant stimulant (e.g. CCL21, CXCL13, EGF or RANK) acting as a chemoattractant. Cells were left to invade for 24 hours at 37°C with 5% CO_2. The invasive cells, which migrated through the ECM layer and attached to the bottom of the polycarbonate membrane, were dissociated from the membrane after incubation with the Cell Detachment Solution for 30 minutes at 37 °C. Next, 50 µL of lysis buffer/CyQuant GR Dye Solution (1:75) was added to each well and incubated for 15 min at room temperature. Finally, 150 µL of the mixture was transferred to a new 96-well plate, and the fluorescence value was detected with a

fluorescence plate reader using 480nm/520nm filter set. As a negative control, Cell Detachment Solution in the absence of cells was used.

3.2.10 Migration assay

For LTi-MSC co culture cell migration experiments, MSCs were grown in 9.4 x 10.7 mm ibidi^{TM} 8-well μ-slide chambers and allowed to attach at 37°C with 5% CO_2 for 24 hours. Prior to imaging sorted splenic LTi cells in RPMI complete medium supplemented with 25 mM HEPES were added to the MSC plated chambers.

For the 4T1.2 cell stimulation migration experiments, cells were plated in 6-well plates and allowed to incubate at 37°C with 5% CO_2 for 24hours. Six hours before to imaging, cells were stimulated with either control media or recombinant proteins. The media was supplemented with 25 mM HEPES just prior to imaging for 10 hours.

3.2.11 Microscopy

3.2.11.1 Confocal Microscopy

Confocal fluorescence images were acquired on a confocal fluorescence laser-scanning microscope (model LSM 510; Carl Zeiss Inc.) equipped with 40X/1.3Plan-Neofluar and 63X/1.4Plan-APOCHROMAT oil immersion objectives, or a Leica DMIRE2 (Leica Microsystems, Germany). Confocal

aperture was set to one Airy unit for the longest wavelength. The various colour filters that were used for detecting the different fluorophores are as follow (excitation wavelength): DAPI (405- 450nm), FITC (488- 510nm), Cy3 (543- 573nm) and Cy5 (633- 738nm). Images were analysed using the LSM Image Brower software.

3.2.11.2 Time-lapse microscopy and image analysis

For time-lapse microscopy experiments cells were cultured in DMEM/RPMI complete medium supplemented with 25 mM HEPES. Image acquisition was performed using an Olympus IX71 inverted microscope fitted with an automated xy stage (Ludl), a CCD camera (Andor), and shutter controller (Ludl). The microscope body was housed within an environment chamber accurately maintained at 37°C. The automated XY stage enabled imaging of multiple fields across multiple wells over the course of time-lapse experiments. Sequential phase contrast images were captured at 10-minute intervals for a total of 10 hours. Automated image acquisition was under the control of Andor iQ imaging software. Sequential images were assembled into video files in ImageJ for subsequent image processing and cell tracking.

3.2.11.3 Surgical window and Multi-photon Imaging In vivo

The Mammary Imaging Window (MIW) was placed on D10 after injection of $1x10^6$ 4T1.2 cells into the mammary fat-pad. All surgical procedures were performed under 2% isoflurane inhalation anaesthesia and under aseptic conditions. Before surgery, the tumour area was shaved and the skin was

disinfected using 70% ethanol. An incision was made through the skin, where the imaging window was inserted (for details see [198]). After surgery the mice were kept at 32°C until fully recovered from anaesthesia.

For multi-photon experiments, $1x10^6$ MSCs followed 24 hours later by $5X10^4$ sorted LTi cells were injected (intravenously) into tumour-bearing mice treated with an IgG control antibody or neutralising CXCL13 antibody respectively. Twenty-four hours later the mice were sedated using isoflurane inhalation anaesthesia (1.5% to 2% isoflurane/O_2 mixture) and placed with their head in a facemask within a custom designed imaging box. The imaging box and microscope were kept at 32°C using a climate chamber surrounding the complete microscope stage, including the objectives. Mice were imaged for a maximum period of 3 hours per day.

All post-hoc image processing and image reconstructions were done using MacBiophototonics Image J software. At the end of the experiments, tumours, lymph nodes and tissues with suspected metastatic foci were surgically removed.

3.2.12 Analytical Methods

3.2.12.1 ImajeJ clustering

To measure the LTi clustering around stromal cells, series of image processing functions in ImageJ were performed to measure the area of the frame occupied by the cells. AVI videos were recorded in an RGB format and then converted to 8-bit grey-scale. Each frame of the video was treated independently and a 2-D rolling

ball algorithm (aka grey-scale morphology) was run using the "Subtract Background" function with a ball radius of 10 pixels to remove interfering background variations. The Otsu algorithm ("Auto Threshold", "method=Otsu white"), was used to segment the foreground cells from the background by thresholding. On the resulting binary image the "Measure" function reports the average image intensity. This value divided by 255 equals the area proportion of foreground in the frame, for a binary image, and this was used to quantify the clustering. This algorithm has been implemented as an ImageJ macro running in batch mode, with a processing time of about 7 minutes for one 300-frame video. The macro is available from:
(http://users.ox.ac.uk/~atdgroup/software/ForegroundArea_batch.ijm).

3.2.12.2 Cell tracking

In order to generate trajectory data for the analysis of cell migration interactive tracking of cells from time-lapse videos was performed using the ImageJ Manual Tracking plugin
(http://imagej.nih.gov/ij/plugins/track/track.html). Resulting trajectory data was used to analyse cell speed and to generate trackplots for the visual representation of migration data.

3.2.12.3 Statistical analysis

Permutation tests for small samples with multiple ties were performed using the "coin" package in R-2.13.0 [199,200]. Prism software (GraphPad) was used for other

data analysis. P values less than 0.05 were considered significant. In figures, asterisks were used as follows: * $p \leq 0.05$; ** $p \leq 0.01$; *** $p \leq 0.001$; **** $p \leq 10^{-4}$.

Chapter 4: Lymphoid tissue inducer cells within human breast cancers

In this chapter I will discuss the novel identification of RORγt^{+} LTi cells within the breast cancer tumour microenvironments and their possible role in providing signals for lymphatic tumour cell invasion and lymphangiogenesis within specific subtypes of breast cancer.

4.1 Identification of RORγt^{+} LTi cells within the human breast cancer tumour microenvironment.

As described in section 1.5, the presence or role of LTi cells has not been explored in human tumours. In collaboration with Professor Peter Lane's group at the MRC Centre for Immune Regulation, University of Birmingham; we stained fresh frozen primary tumour sections of patients with breast cancer for markers discriminatory for LTi cells (defined as positive for a nuclear transcription factor RORγt and membrane receptor CD127 (IL-7Rα) but negative for CD3 as previously described [201,202]. Given that postnatal LTi numbers are found in much larger numbers in the intestines and the tonsils [145], we first optimised our protocol for LTi staining using small bowel lymph node fresh frozen sections (Figure 4-1) .

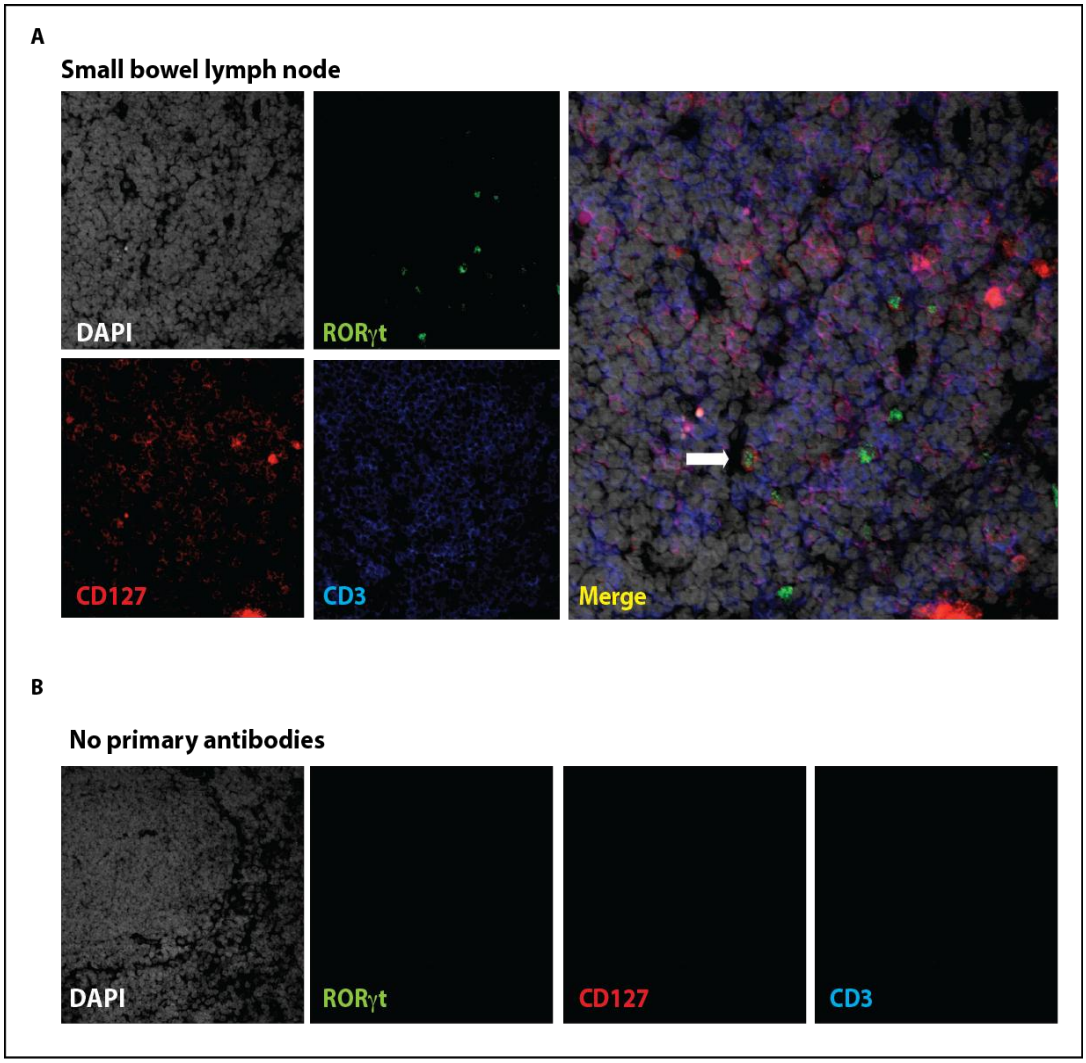

Figure 4-1: LTi cell identification within small bowel lymph node sections

A: Low-power (x25 oil immersion optic) confocal image is shown. LTi cells (white arrow in merged image) are identified as positive for CD127 (red perinuclear staining), negative for CD3 (blue membrane and cytoplasmic staining) and positive for RORγt (green nuclear staining). Grey corresponds to 4,6-diamidino-2-phenylindole (DAPI) staining of the cell nuclei. **B:** Negative controls with no primary antibody to identify non-specific binding are shown (i.e. only secondary antibodies were used).

Having optimised the protocol, we then stained fresh frozen primary breast cancer tumour sections for LTi cells. We identified within the breast cancer microenvironment RORγt^{+}CD127^{+}CD3^{-} cells that were comparable in phenotype to the LTi cells (Figure 4-2A-C). The staining of RORγt^{+}, which is a class of DNA-binding transcription factors with hitherto unknown gene target (hence also known as nuclear orphan receptors) has a characteristic nuclear "speckled" or punctate appearance (Figure 4-2D).

Within 2 out of the 60 cases (approximately 3.3%), we noticed that tumour-infiltrating lymphocytes were not only scattered throughout the stroma and interspersed between tumour cells; but they also cluster in aggregates resembling tertiary lymphoid structures (TLS) with distinct compartmentalization between a T and a B cell zone (Figure 4-3). B-zones represent the unstained centres within the lymphocyte aggregate. RORγt^{+}CD127^{+}CD3^{-} cells were in close proximity to CD3 positive cells within the stromal component of tumours and were also seen within TLS.

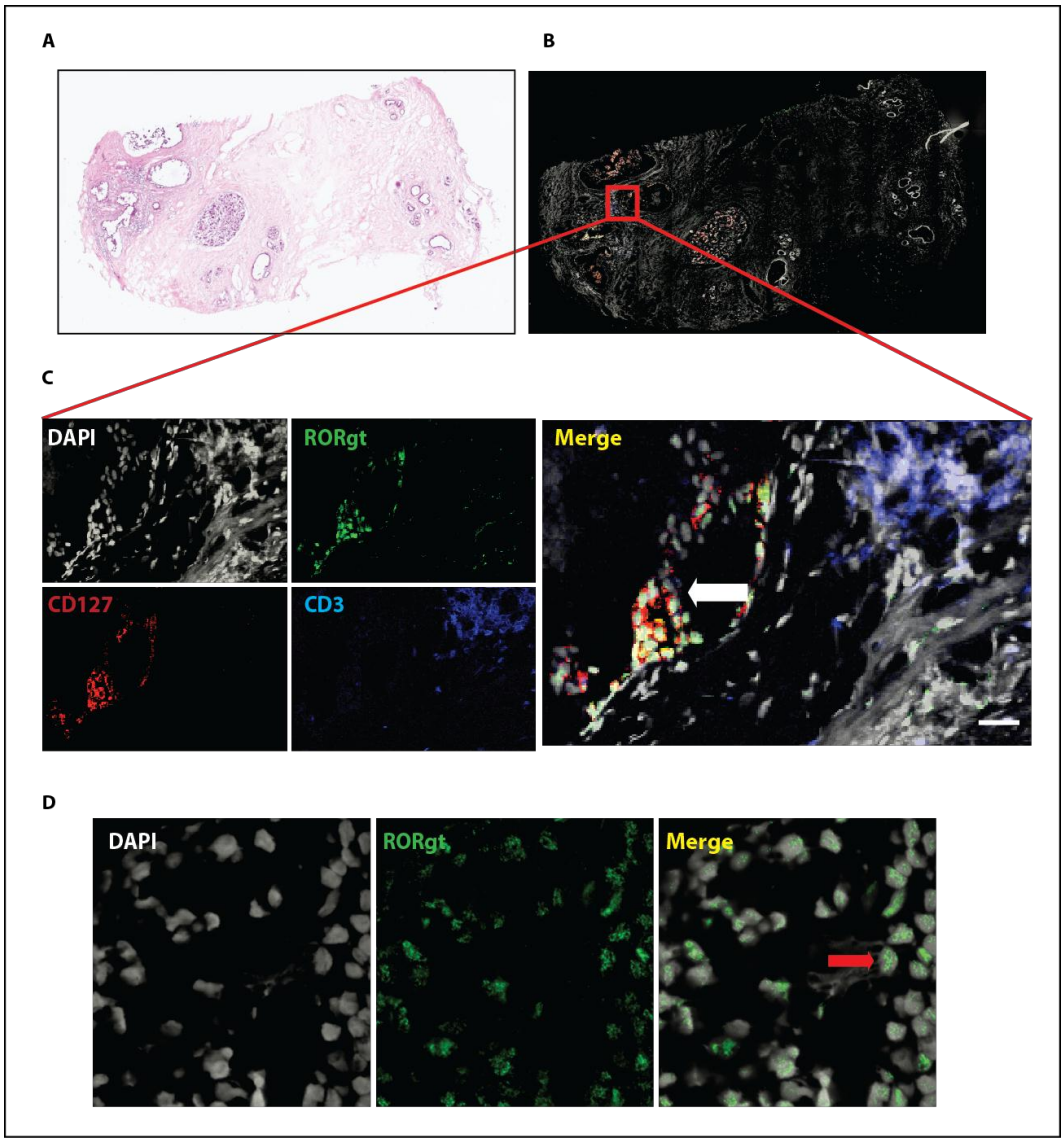

Figure 4-2: LTi cell identification within the breast cancer microenvironment.

A: Haematoxylin-eosin (H&E) staining of fresh frozen section of a primary human breast cancer. **B:** Immunofluorescence detection of LTi cells in a low-power (x25) 15x15 confocal tile scan is shown. **C:** Zoomed images show confocal micrographs of LTi cells (white arrow) are identified as positive for RORγt (green nuclear staining) and CD127 (red perinuclear staining) and negative for CD3 (blue membrane and cytoplasmic staining). Grey corresponds to 4,6-diamidino-2-phenylindole (DAPI) staining of the cell nuclei. (Scale bar = 15μm). *(Sample No: GU_801098)*. **D:** The characteristic speckled appearance of RORγt staining (green) within the nucleus (grey) is shown. *(Sample No: 461649080-C)*.

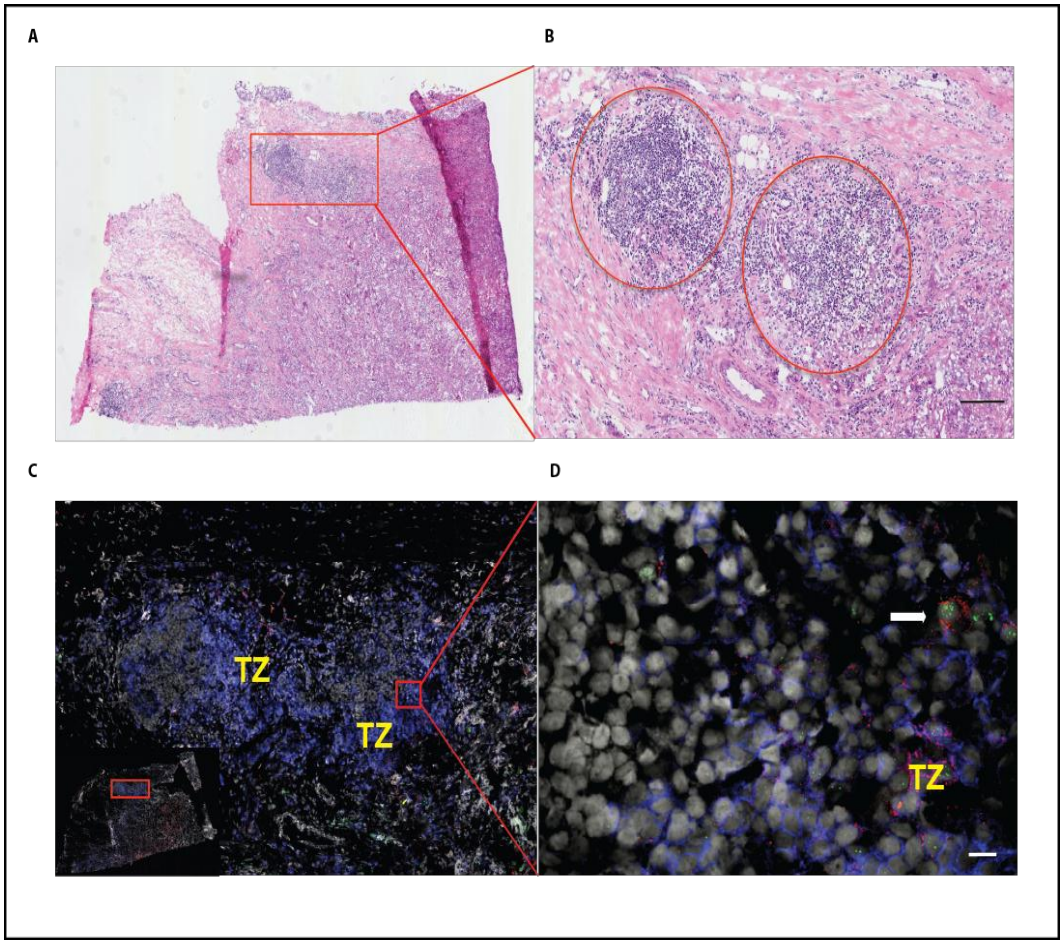

Figure 4-3: Breast cancer tissue with prominent tertiary lymphoid follicle formation.

H&E histopathological images show (**A):** Low power view of a breast cancer tumour section and **(B):** High power view allows identification of dense areas of lymphoid cell aggregates within the human breast cancer microenvironment (red circles). **C**: Immunofluorescence for CD3 (membrane or cytoplasmic blue staining) identifies the outer T-zone of these lymphoid structures. **D:** Identification of a RORγt^{+}CD127^{+}CD3^{-} LTi cells (white arrow) (RORγt^{+}, green nuclear; CD127^{+}, red perinuclear) within the TLS. TZ=T zone. Red squares represent areas of interest. *(Sample No: GU_1027)*.

4.2 Breast cancer datasets confirm differential expression of the lymphoid chemokines between tumours.

4.2.1 The King's Health Partners Cancer METABRIC Biobank

The breast cancer genomic analysis performed by METABRIC (Molecular Taxonomy of Breast Cancer International Consortium) recently produced a novel classification of breast cancers into 10 subgroups [8]; one of the subgroups (IntClust4) represents a common breast cancer subtype in which the antigen presentation pathway, OX40 signalling, and cytotoxic T-lymphocyte-mediated immune response is prominent and has very few DNA aberrations (such as acquired somatic copy number aberrations (CNA)) compared with those in other subgroups [8]. In collaboration with Dr Katherine Lawler (Bioinformatics, Institute for Mathematical and Molecular Biomedicine, King's College London), we further analysed the gene expression of lymphoid chemokines (CXCL13, CCL19, and CCL21) [62,78,203] and their corresponding receptors (CXCR5 and CCR7) within the METABRIC samples originating from Guys & St Thomas' Breast Tissue and Data Bank.

An unsupervised hierarchical cluster analysis of the transcriptional profile of the Guy's & St Thomas' Breast Tissue and Data Bank subset of METABRIC tumour samples (*n=234*) revealed that this breast cancer cohort could be categorized based on the expression of lymphoid chemokines and their receptors. Interestingly, the group of tumours exhibiting relatively high expression of these genes was found to be enriched for the aggressive form of breast cancer -"basal-like" breast cancers - according to PAM50 intrinsic subtype assignments (see

section 1.1) [204,205] (31/53 basal-like tumours lie in the top-branch cluster, n=89; p=0.0007, two-tailed Fisher's exact test) (Figure 4-4). Lymphoid chemokine and receptor genes showed highly significant internal pair-wise correlations. Specificity was demonstrated by virtue of a lack of correlation of these lymphoid chemokine and receptor genes with other lymphoid chemokine genes such as the ligand-receptor pair CCL20-CCR6 that is known to chemoattract immature DC, effector/memory T-cells and B-cells [206] (Figure 4-4).

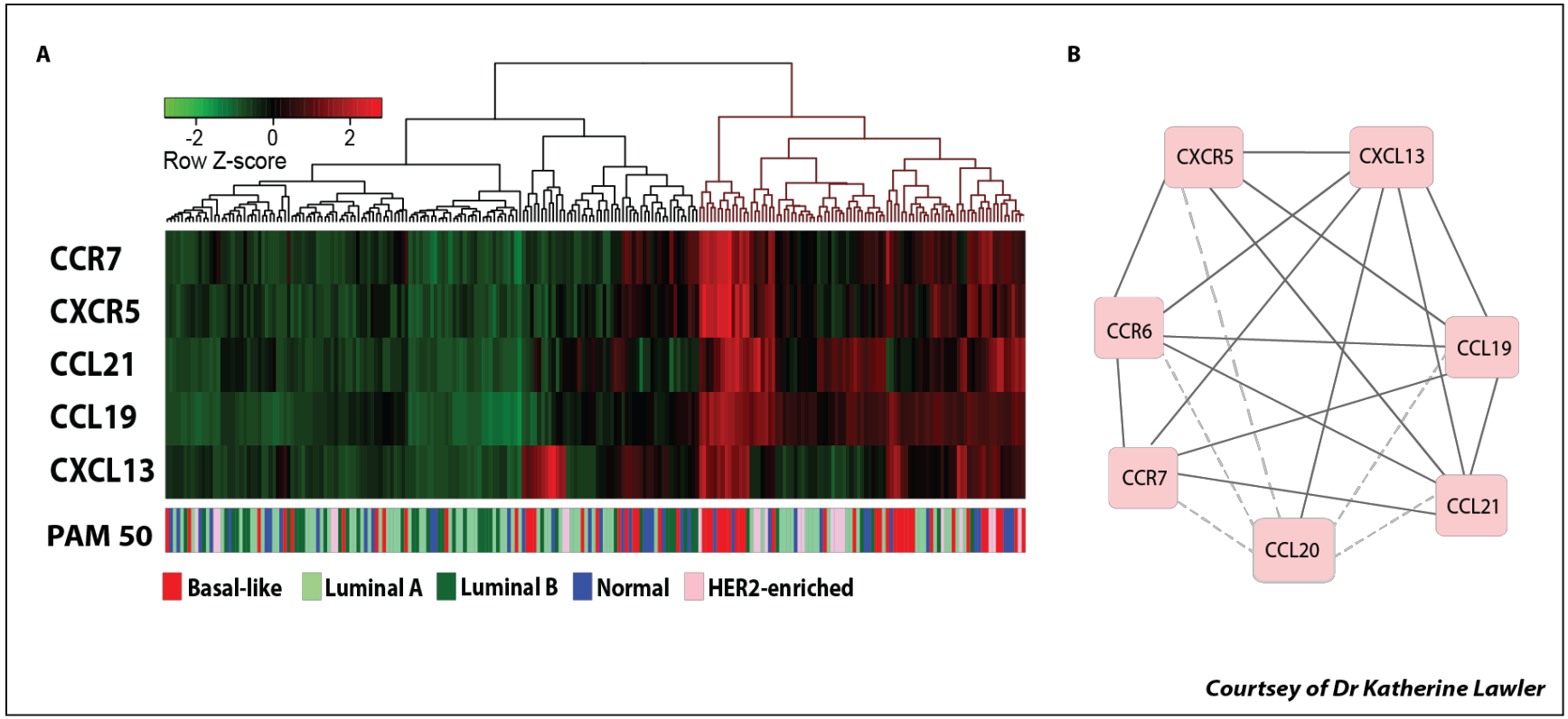

Figure 4-4: LTi cells and associated chemokine gene signature within breast cancer microenvironment.

A: Hierarchical clustering of the expression of genes encoding lymphoid-associated chemokines and receptors in the Guy's METABRIC data set (*n=234*). Columns represent patient samples, with dendrogram colored according to the top-level cut-point (black/red). PAM50 intrinsic subtype assignments are displayed below. **B:** Significance of pair-wise gene expression correlations for genes encoding lymphoid-associated chemokines and receptors (solid line: $p < 10^{-4}$; dashed otherwise). The significance of each gene-gene correlation was assessed using a background distribution estimated from 1000 randomisations of each gene probe across samples.

4.2.2 Cross validation of lymphoid chemokine signature using other breast cancer gene expression datasets

An additional six independent breast cancer datasets were used to evaluate further the correlation of the co-expression of lymphoid chemokines and their receptors with subtypes of primary breast tumour tissue. These data sets originated from multiple platforms and different patient cohorts. The BREAKTHROUGH dataset (n=196; 18 oestrogen positive (ER^+) and 178 ER negative (ER^-) tumours by unified ER gene expression and immunohistochemical evaluation) [207] is a triple-negative-enriched data set performed on Affymetrix Exon arrays. Due to the enrichment for triple-negative samples in the BREAKTHROUGH data-set, PAM50 intrinsic subtypes were assigned based on resampling to reflect the hormone receptor status of the PAM50 training cohort [207]. The remaining five breast cancer data-sets were retrieved as pre-processed data sets from Bioconductor.org and filtered for samples with known ER status [208-213]: TRANSBIG (n=198; 134 ER+, 64 ER-) [214], MAINZ (n=200; 162 ER+, 38 ER-) [215], UPP (n=247; 213 ER+, 34 ER-) [216], VDX (n=344; 209 ER+, 135 ER-) [217,218], UNT (n=126; 86 ER+, 40 ER-) [219]. Probes corresponding to the lymphoid chemokine and receptor genes were matched using gene symbols; where multiple probes match a single gene symbol, the probe with the highest standard deviation across samples is displayed. PAM50 intrinsic subtypes were assigned according to Weitgel et al., [196] using gene-standardised data and "Gene.symbol" to match features.

All six datasets indicated that breast cancer cohorts could be categorized based on the expression of lymphoid chemokines and their receptors. Four out of the six

datasets (BREAKTHROUGH, TRANSBIG, UPP, VDX) confirmed the association seen between basal-like breast cancer (BLBC) subtype and relatively high expression of genes encoding -associated chemokines and their receptors (Figure 4-5). Apart from the MAINZ and UNT datasets, the red bars (representing BLBCs) were higher amongst the 5th quintile (representing the high expressers within the dataset).

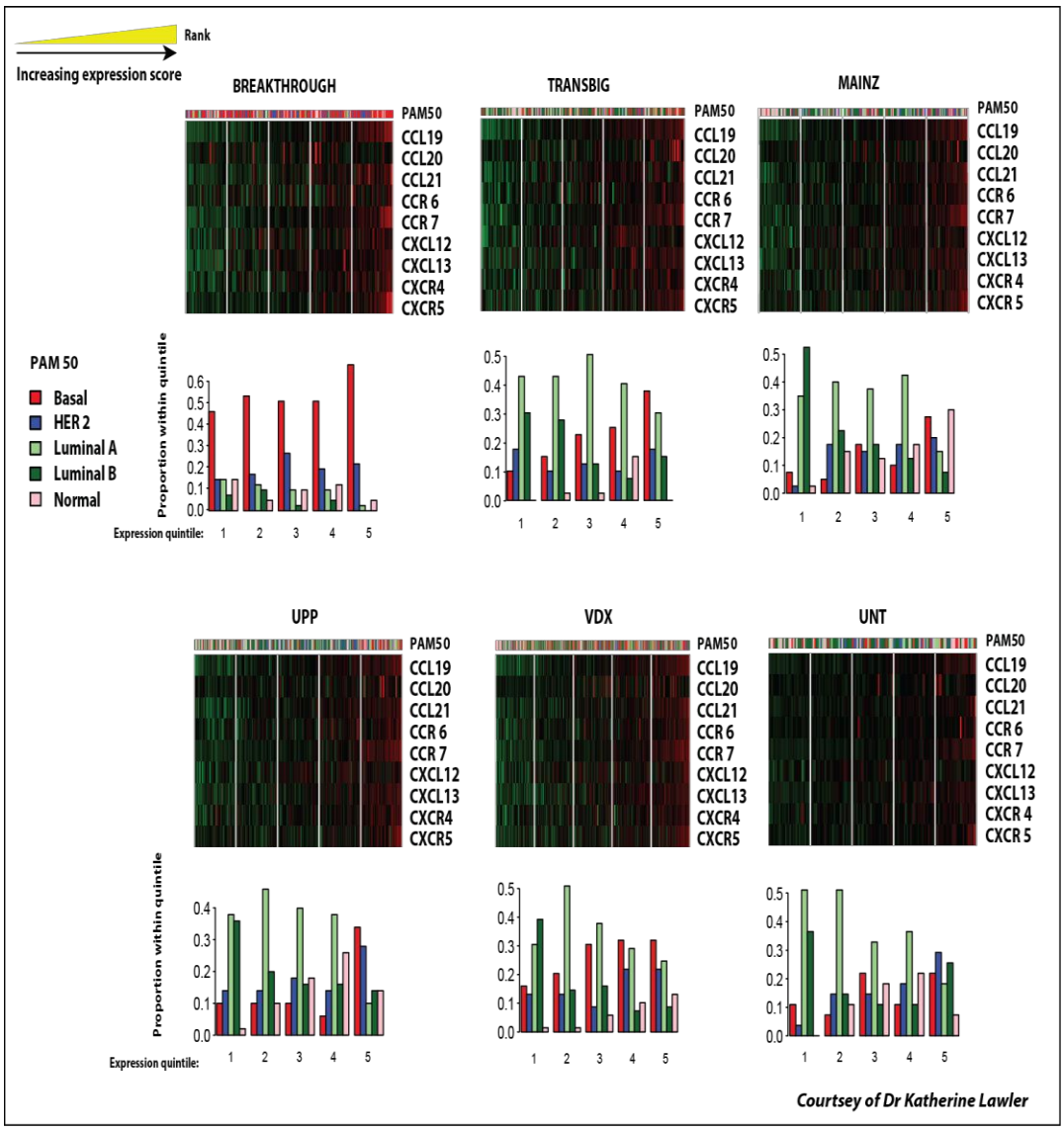

Figure 4-5: Expression of lymphoid chemokine and chemokine receptor genes in breast cancer datasets.

Heat maps display gene-standardised expression for each breast cancer data set. Columns (samples) are ordered by increasing expression score (mean of gene-standardised expression values of the listed genes) and displayed in blocks representing score quintiles (left-right, lowest to highest expression score). PAM50 assignments are depicted above. Bar plots show the distribution of intrinsic subtype assignments within each expression quintile. Relative enrichment for the basal-like subtype (red) amongst samples with higher expression scores is observed in multiple independent data sets.

4.3 Tumoural LTi cell density correlation with lymphoid gene signature

We hypothesised that tumours with high levels of lymphoid chemokines would have a higher number of LTi cells present within the tumour microenvironment. We therefore performed a blinded study to investigate how the selected gene expression levels for lymphoid chemokines correlated with the presence of $ROR\gamma t^{+}CD127^{+}CD3^{-}$ LTi cells in primary breast cancer sections.

A total of 60 tumour sections from the METABRIC Guy's and St Thomas' Tissue bank were selected at random for LTi staining. I was blinded to the information relating to the lymphoid chemokine gene expression levels of the tumours. These tumours were stained following the protocol described in section 3.2.3.1 and confocal tile scan (15x15 using a X25/1.8 objective) images obtained. The total number of $CD3^{+}$ lymphocytes and LTi cells/mm^2 within each section were recorded. An example of the analysis for LTi quantification of a breast cancer sample is shown in Figure 4-6.

Patient characteristics for the cohort stained for LTi density in comparison to the Guys' METABRIC data set are depicted in Table 4-1. The dataset was relatively well balanced for ER expression with 54% of cases being ER-positive and 46% being ER-negative. This is important as majority of the BLBCs and therefore higher expressers for the lymphoid chemokine gene signature are ER-negative (75%) as compared the ER-positive cases, the majority of which would fall in the group representing the "low" expressers of the lymphoid gene signature. Any difference between the two is therefore more likely to be seen.

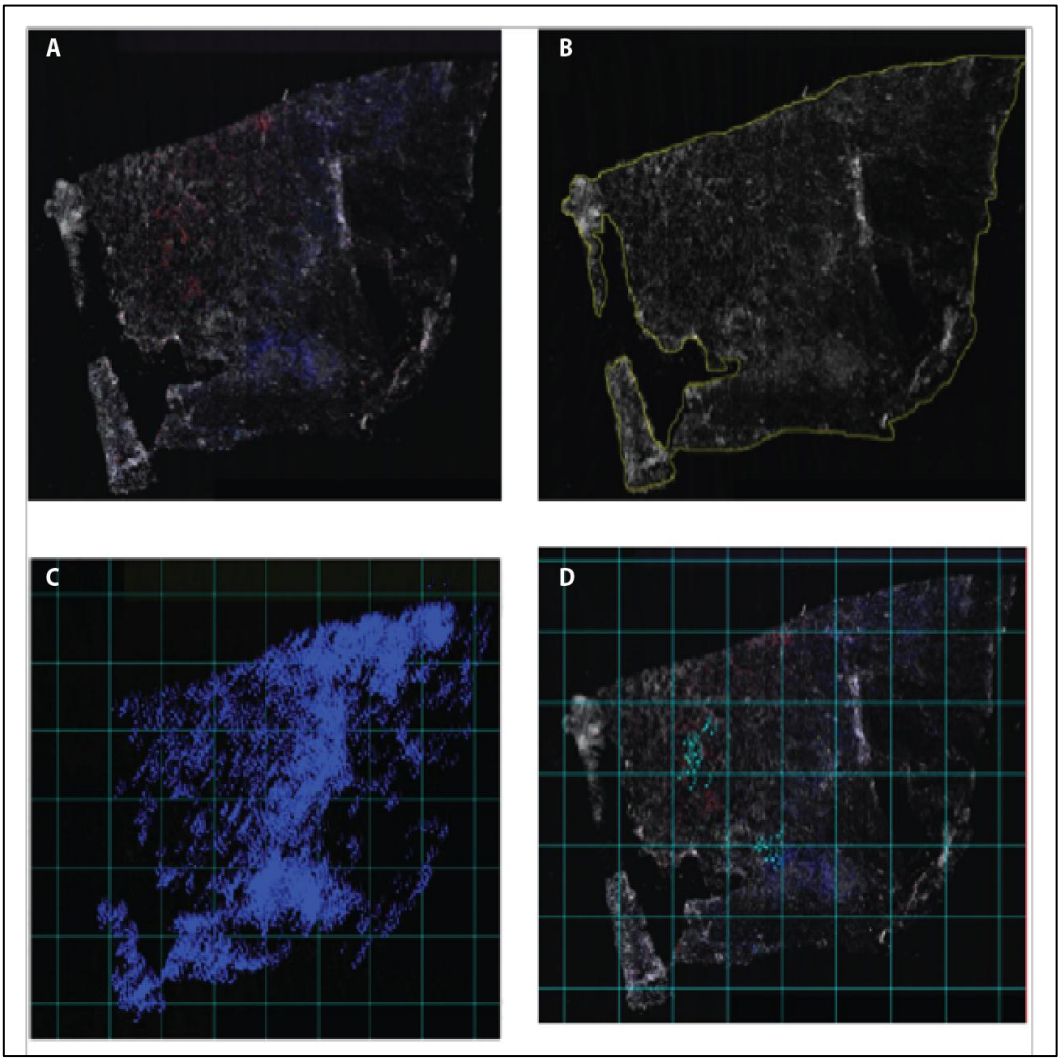

Figure 4-6: Strategy for LTi cell density quantification in primary breast tumour sections.

A: A15x15 tile scan obtained at low power (x25/1.4 oil immersion optic) of a fresh frozen breast cancer tumour section stained for CD127, CD3, and RORγt. **B:** Further analysis was carried out using the MacBiophototonics Image J software to obtain the total surface area of the tissue. The total numbers of $CD3^+$ (**C**) and $CD127^+CD3^-ROR\gamma t^+$ LTi (**D**) cells were recorded using an Image J manual cell counter.

Table 4-1: Clinico-pathological characteristics for the METABRIC data set

Guy's METABRIC									
	(i) Gene expression data set		**(ii) Gene expression & LTi assay dataset**		**(iii) By PAM 50 subtype**				
					Basal	**Luminal A**	**Luminal B**	**HER2**	**Normal**
	N = 234		*N = 59*		*N =53*	*N =75*	*N =44*	*N =40*	*N =22*
	Number	(%)	Number	(%)	*Numbers*				
Age									
Median (y)	60.8		59.3		56.8	62.9	65.5	57.2	59.5
Grade									
1	29	(12%)	3	(5%)	-	23	3	1	2
2	84	(36%)	12	(20%)	5	36	22	10	11
3	112	(48%)	42	(71%)	48	9	19	29	7
Unknown	9	(4%)	2	(3%)	-	7	-	-	2
ER status (*ESR1* expression)									
Positive	176	(75%)	32	(54%)	13	75	44	25	19
Negative	58	(25%)	27	(46%)	40	-	-	15	3

Lymph nodes, No. positive									
0	95	(41%)	15	(25%)	19	34	16	17	9
1-3	93	(40%)	27	(46%)	25	29	16	14	9
4+	45	(19%)	17	(29%)	9	12	11	9	4
Unknown	1	(0.4%)	-	-	-	-	1	-	-
Invasive tumour size									
<= 2cm	100	(43%)	21	(36%)	20	41	15	15	9
> 2cm	134	(57%)	38	(64%)	33	34	29	25	13
Hormone treatment									
Yes	188	(80%)	39	(66%)	28	69	40	32	19
No	46	(20%)	20	(34%)	25	6	4	8	3
Chemotherapy									
Yes	49	(21%)	28	(47%)	29	6	2	9	3
No	184	(79%)	31	(53%)	24	69	42	31	19

We observed that the number of RORγt^{+}CD127^{+}CD3^{-} LTi cells/mm^{2} (of the total surface area) varied considerably from case to case (range 0-56/mm^{2}). Within the study group, patients with high LTi counts within the tumour microenvironment were also likely to have a gene expression profile corresponding to a high gene expression score for the LTi- associated chemokines ($p < 10^{-3}$, Spearman's correlation permutation test) (Figure 4-7). Similarly the numbers of CD3^{+}cells/mm^{2} also varied considerably from case to case (range 0-1065/mm^{2}). Again patients belonging to the high gene expressing group for the lymphoid-associated chemokines correlated with higher CD3^{+} cell counts within the tumour microenvironment ($p < 10^{-3}$, Spearman's correlation permutation test).

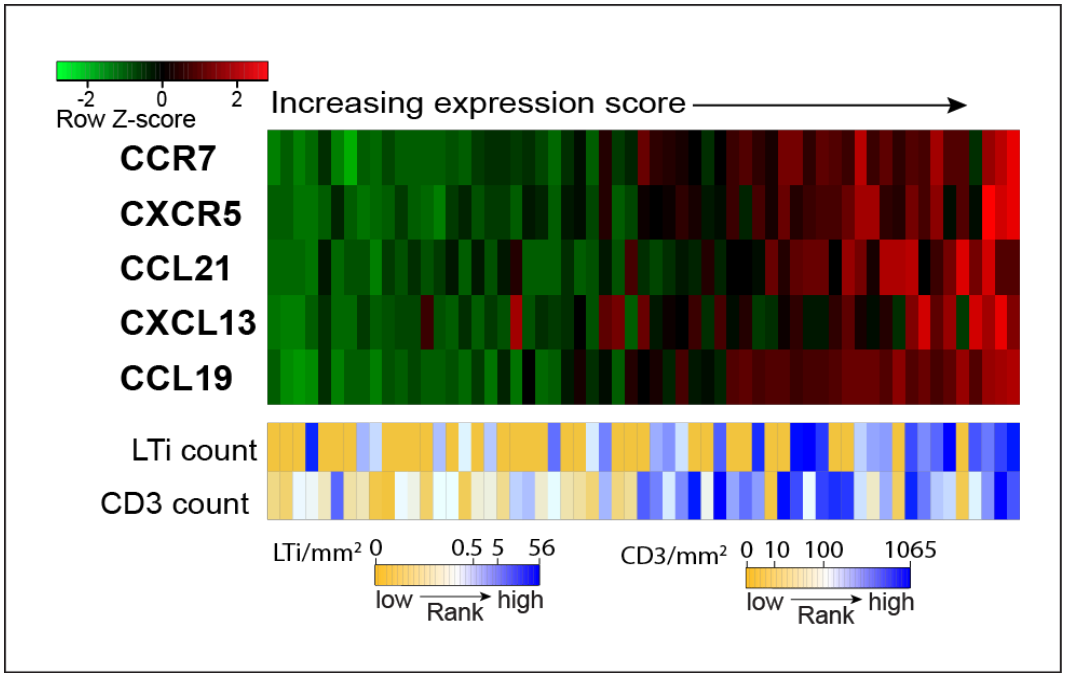

Figure 4-7: Comparison of gene expression profiles and presence of LTi cells in primary breast tumours.

The heat map illustrates relative expression of genes encoding lymphoid chemokines and receptors. Columns (samples, n = 59) are ordered by increasing expression score and rows by hierarchical clustering. The ranks of LTi and CD3 counts (cells per mm^{2}) are depicted below and are ordered from lowest to highest (range 0-56 cells/mm^{2}) and (range 0-1065 cells/mm^{2}).

4.4 Tumoural LTi cell density correlation with lymphatic invasion and lymphangiogenesis

As discussed in section 1.2.1, information about lymphatic invasion (LI) and lymphatic vessel density (LVD) have been shown to be promising and important prognostic factors for various tumour types. Given the known effect of LTi cells in enhancing the production of lymphangiogeneic factors such as VEGF-C/D by the mesenchymal lymphoid tissue organiser (LTo, stromal) cells [127], immunohistochemistry for the lymphatic endothelial marker, podoplanin was performed on tumour sections of the patient cases that had been analysed for LTi cell counts with the aim of investigating their role in lymphatic vessel invasion or in promoting lymphangiogenesis within breast cancers.

4.4.1 Podoplanin staining

In order to avoid false data from low specificity of staining, selection of the optimal marker of the lymphatic endothelium was a critical step in the assessment of LI or LVD for our study. Within the last decade, major research efforts have lead to the discovery of a large spectrum of candidate lymphatic markers. In 2006, Van der Auwera et al, published the first international consensus on the methodology and criteria of the evaluation of lymphatic vessels within solid tumours [220]. Commonly used markers include vascular endothelial growth factor receptor 3 (VEGFR-3/Flt4), homeobox prospero-like protein (Prox1), lymphatic vessel endothelial hyaluronan receptor-1 (LYVE-1) and podoplanin (*E11 antigen, gp38, D2-40*).

Podoplanin (*E11 antigen, gp38, D2-40*) is a ~38-kD surface glycoprotein that is expressed by lymphatic endothelial cells (LECs) and is not expressed by blood vessels [221]. It is expressed by both developing and mature LECs as compared to LYVE-1 which is detected in only a subset of cultured podoplanin positive endothelial cells [222]. Podoplanin is not an exclusive marker of the lymphatic endothelium; it is also expressed in podocytes, osteoblastic cells, osteocytes, basal keratinocytes, choroid plexus epithelial cells, alveolar type I cells, osteoblasts, peritoneal mesothelial cells, dendritic cells and a subset of macrophages [223].

Comparative studies between podoplanin and other lymphatic markers have proved it to be the most sensitive and specific marker for lymphatic vessel endothelium in sections of both frozen and formalin-fixed paraffin-embedded normal and neoplastic tissues [224,225]. Extremely high specificity of 99.7% and high sensitivity of 92.6% has been reported for podoplanin antibodies [224]. We therefore chose this lymphatic marker for further work within this study.

4.4.2 Lymphatic invasion

Conventional H&E immunohistochemical staining of the 60 selected cases with known LTi density score were first evaluated for lympho-vascular invasion by Professor Sarah Pinder (Lead Professor in Histopathology, Kings College London) in order to select the most appropriate specimen block for immunohistochemical staining. This also allowed for each case to have a LVI positive/negative status, representing a measure of tumour cell invasion within both the blood and the lymphatic vessels (Figure 4-8A). Although we did not

find a significant correlation between the LTi and LVI statuses within the tumour microenvironment, a non-significant trend in favour of the presence of LTi cells with associated LVI and vice versa was seen (Figure 4-8B).

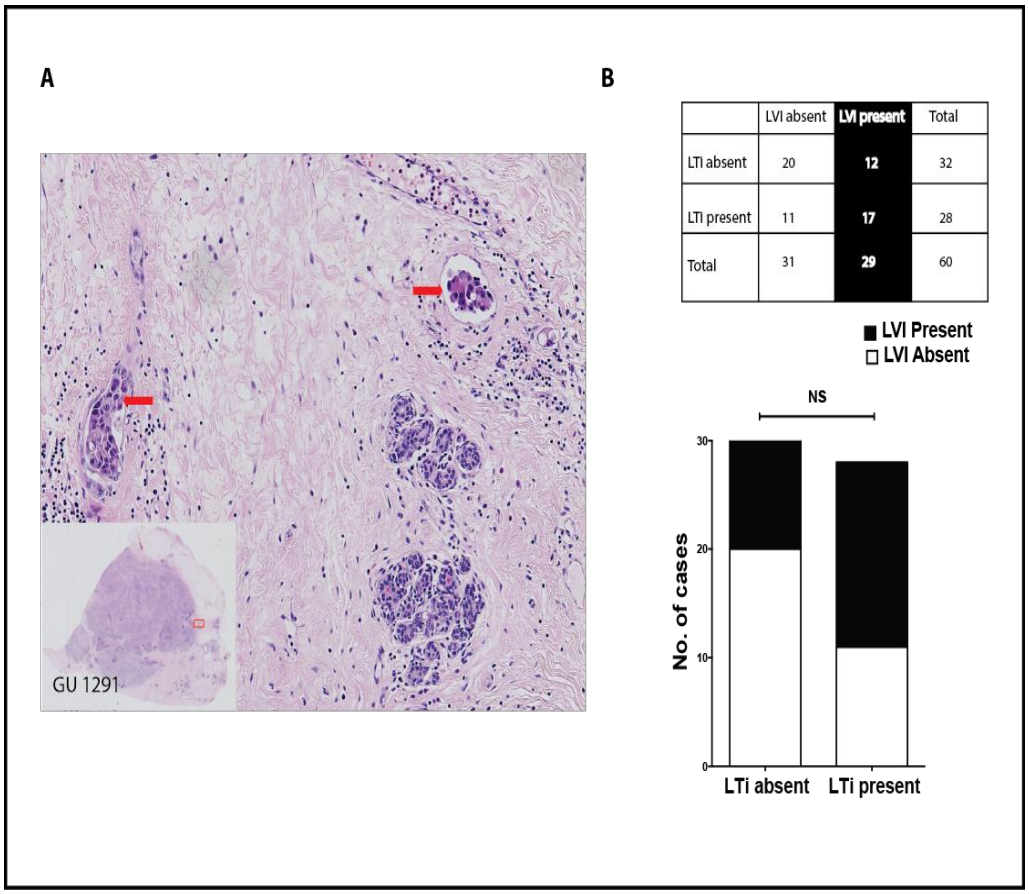

Figure 4-8: The presence of LVI within breast tumour sections as determined by pathological review.

A: H&E section of breast tissue with lympho-vascular invasion (red arrows) is shown. **B:** Correlations between LTi counts within the breast cancer tumour microenvironment and LVI is shown (NS=non significant; Fisher's exact test).

Without knowledge of the LVI status based on the H&E slide, I evaluated the cases for tumour cell lymphatic invasion by reviewing the podoplanin immunohistochemical stained paraffin embedded tumour sections of the selected 60 cases. Presence or absence of tumour cell invasion into the lymphatics was recorded and used to derive a lymphatic invasion score (LI). LI was considered

evident if at least one tumour cell cluster was clearly visible in the lymphatic vascular space (red arrows in Figure 4-9). Samples showing inappropriate staining in internal negative or positive controls were considered non-informative and were excluded from the analysis.

Seventy eight percent (47/60) of the cases were evaluable for analysis. We found that 82% (14/17) of patients with lymphatic tumour cell invasion had LTi cells present within the microenvironment; whilst the patients without lymphatic tumour cell invasion only 27% (8/30) had LTi cells present in the primary tumours. Similarly, 73% (22/30) of patients without lymphatic tumour cell invasion did not have any LTi cells present within the microenvironment, whereas only 17% (3/17) of patients without LTi cells were seen to have LI present (Figure 4-9C; p <0.001, Fisher's exact test).

We concluded that patients with tumour cell invasion into lymphatics were more likely to have a higher LTi score, compared to patients without lymphatic invasion. This correlation did not hold true for association between LI and $CD3^+$ cells counts, strengthening the specificity of our LTi – LI correlation.

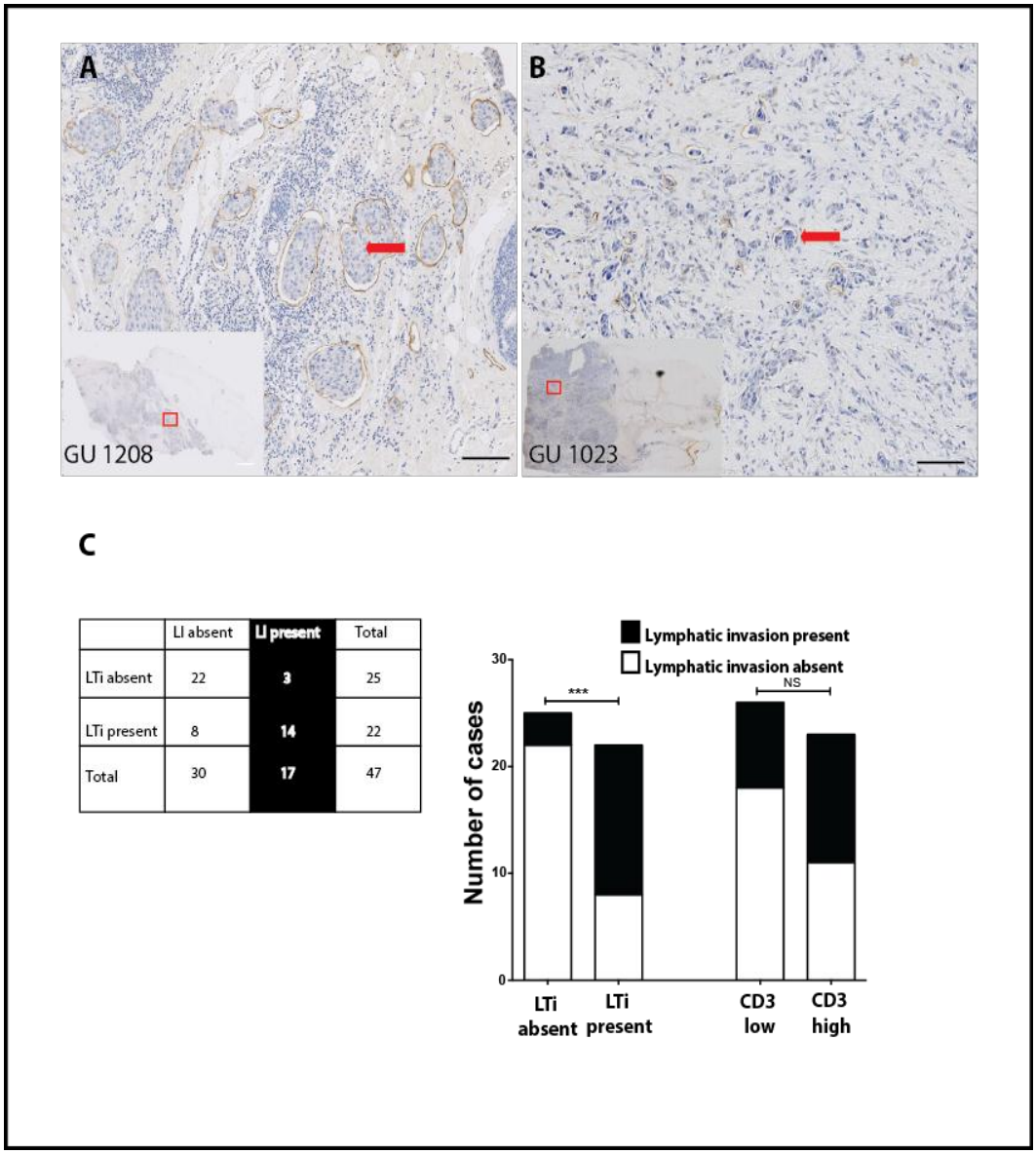

Figure 4-9: Podoplanin staining of primary breast tumour tissue shows tumour cell invasion into lymphatics is associated with increased number of LTi cells

Podoplanin staining is shown in brown and cell nuclei are stained blue. **A:** Staining in *sample No. GU 1208* shows large tumour emboli present within dilated lymphatics. **B:** Staining in *sample No. GU 1023* shows the presence of small tumour cell clusters within small lymphatics. Scale bar = 100µm. **C:** Correlations between LTi and CD3 cell counts within the breast cancer tumour microenvironment and LI is demonstrated. $CD3_{low}$ = <100cells/mm^2. $CD3_{high}$ = >100cells/mm^2. Asterisks represent the p-values (Fisher's exact test: *** $p \leq 0.001$; NS = not significant).

4.4.3 Lymphatic vessel density

Immunohistochemical application of podoplanin has been used as a tool to measure lymphatic vessel density (LVD), a surrogate marker for tumour-associated lymphangiogenesis. Its quantification has been proven valuable to assess metastatic involvment within regional lymph nodes. We therefore went on to determine the LVD according to the previously described "hotspot" method by Weidener et al [226]; whereby LVD is determined by counting the number of podoplanin-positive vessels in the selected 'hot-spot' areas. 'Hot spots' are defined as areas visualised at low magnification of containing numerous microvessels (Figure 4-10A). Traditionally, vascular 'hot spots' are thought to represent localised areas of biological importance [220].

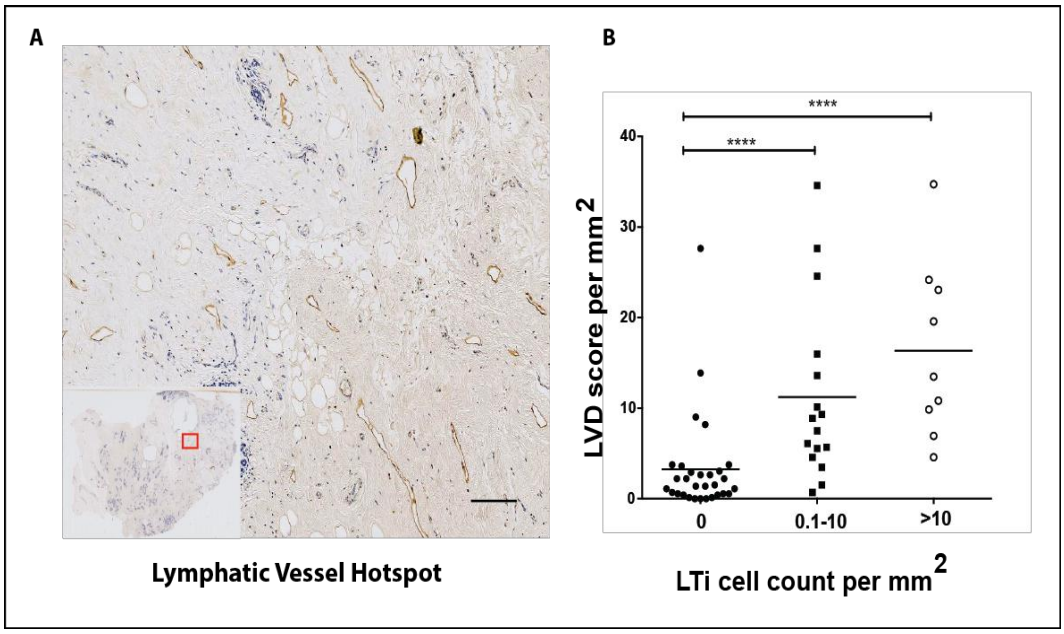

Figure 4-10: Positive correlation between increased LVD and LTi cell density within human breast cancers.

A: Podoplanin staining is shown in brown and cell nuclei are stained blue. Intra- and peritumour lymphatic vessel densities (LVD) were determined using the "hot-spot" method. Scale bar = 100μm. **B:** Correlations between LTi cell count and LVD. Asterisks represent the p-values (****$p<10^{-4}$, Mann-Whitney test).

Lymphatic vessels were considered countable only when podoplanin stained microvessels showed visible lumen. The mean LVD was collected through a Chalkey count, where a grid was placed onto the scanned image and all points coinciding with the stained lymphatic vessels counted [220]. Three to five images were used and the mean value obtained with the number of counted vessels in each image (see Figure 3-1).

Of the 47 evaluable cases, the average LVD was approximately 9 vessels/mm$^{2.}$ We found a statistically significant correlation between increasing numbers of LTi cell counts within the tumour microenvironment and increased LVD (Figure 4-10B; $p < 10^{-4}$, Mann-Whitney test). These findings provide evidence for a possible role of LTi cells in lymphangiogenesis within tumours.

4.4.4 Lymph node burden

Axillary lymph node positive breast cancers have a significantly worse prognosis than node-negative disease. The number of involved nodes (rather than simply the absence or presence of nodal involvement) is a key determinant of prognosis after relapse. For example studies report that, when compared with node-negative patients, those with four or more involved lymph nodes have a significantly worse outcome after relapse. However, for patients with only one to three involved nodes, the outcome is not significantly different from that of the node-negative patients [15]. Our data supported the role of lymphoid-associated chemokines and LTi cells in promoting lymphatic invasion and or lymphangiogenesis within tumours. We therefore went on to test if this translated to an association with an increased risk of lymph node metastasis.

We returned to our selected patient cohort within the METABRIC dataset to investigate any relationship between the tumoural LTi density and lymph node tumour burden. As shown in Figure 4-11, we observed that within the BLBC – a poor outcome breast cancer subtype, the majority of which are triple negative breast cancers – a high lymph node tumour burden (4 or more metastatic lymph nodes at surgical resection) was associated with significantly increased levels of LTi cell counts (p=0.02; permutation-based Mann-Whitney). These correlations were not seen within other breast cancer subtypes ($HER2^+$ and Luminal A/B), strongly suggesting that the proposed roles/associations may be subtype specific, although limited numbers within these groups may account for the non-significance in the $HER2^+$ cases.

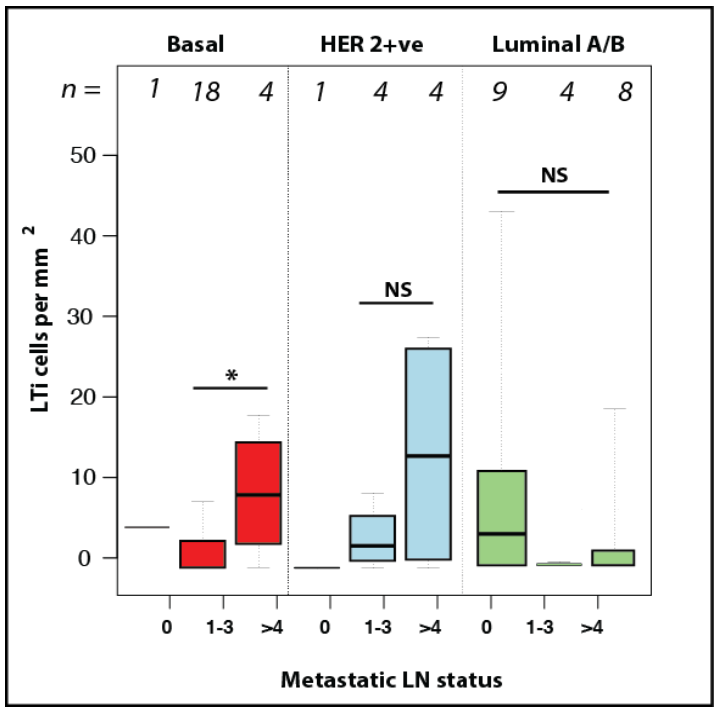

Figure 4-11: Correlation between LTi cell count and lymph node tumour burden.

A positive correlation between the higher LTi counts and tumour burden within draining lymph nodes with BLBCs is shown. Asterisks represent the p-values when comparing the >4 LN status to 1-3 LN status (Permutation-based Mann-Whitney Fisher's exact test: * p≤0.05; NS = non significant).

Additionally, we examined how the metastatic burden within the lymph nodes was related to gene expression of the key lymphoid--associated chemokines CCL21 and CXCL13 in the primary tumours within the METABRIC dataset. We observed a significant association of high lymph node tumour burden with increased levels of CCL21 (Figure 4-12; $p \leq 0.01$; lymph nodes positive, 4+ vs. 0; two-tailed Mann-Whitney) in BLBCs but not in human epidermal receptor 2^{+} ($HER2^{+}$) or Luminal A/B tumours (Figure 4-12A). Although not statistically significant, a trend in increased CXCL13 expression and high lymph node burden was observed amongst the BLBC subgroup (Figure 12B).

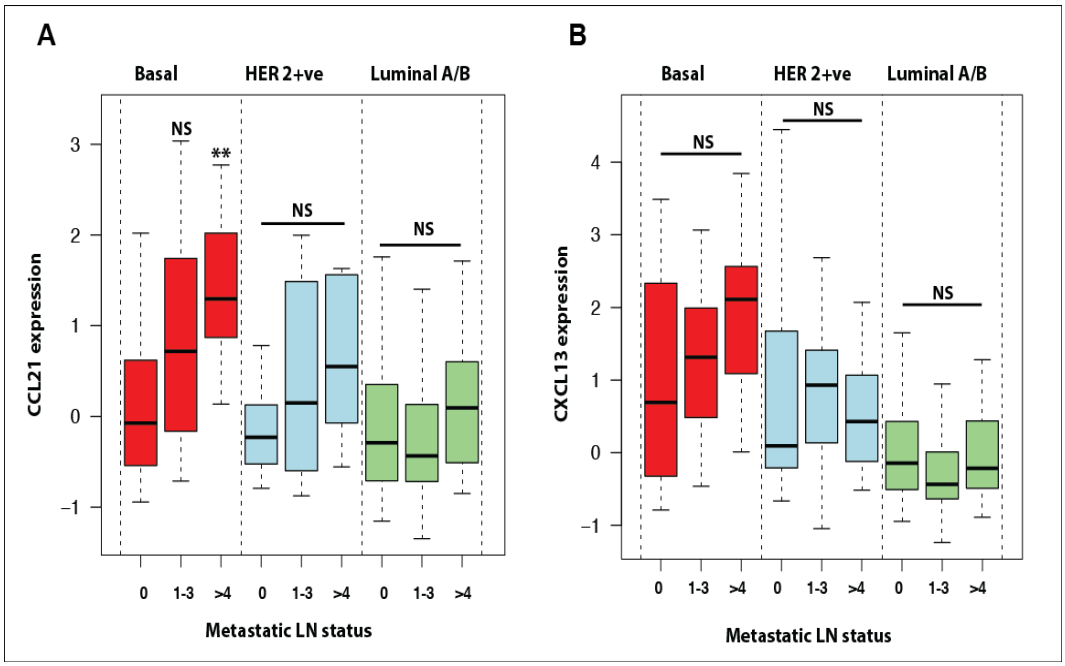

Figure 4-12: Clinical relevance of lymphoid-associated chemokine gene expression in the context of lymph node metastasis.

Correlation of CCL21 (**A**) and CXCL13 (**B**) chemokines gene expression with lymphatic tumour burden within our subset of the METABRIC dataset. Asterisks represent the p-values when comparing to the LN negative cases (Two-tailed Mann-Whitney: ** $p \leq 0.01$, NS = non significant).

4.5 Discussion

The previously unappreciated family of RORγt^{+} innate lymphoid cells (ILCs), which include LTi cells have been shown to be key components for the construction of lymphoid structures underlying key immune response (see section 1.4.1.2). The aims of the experiments presented in this chapter were to explore the possible relevance of LTi cells in human breast cancers, which are summarised here in Figure 4-13. A model system I hope to build upon in the subsequent chapters.

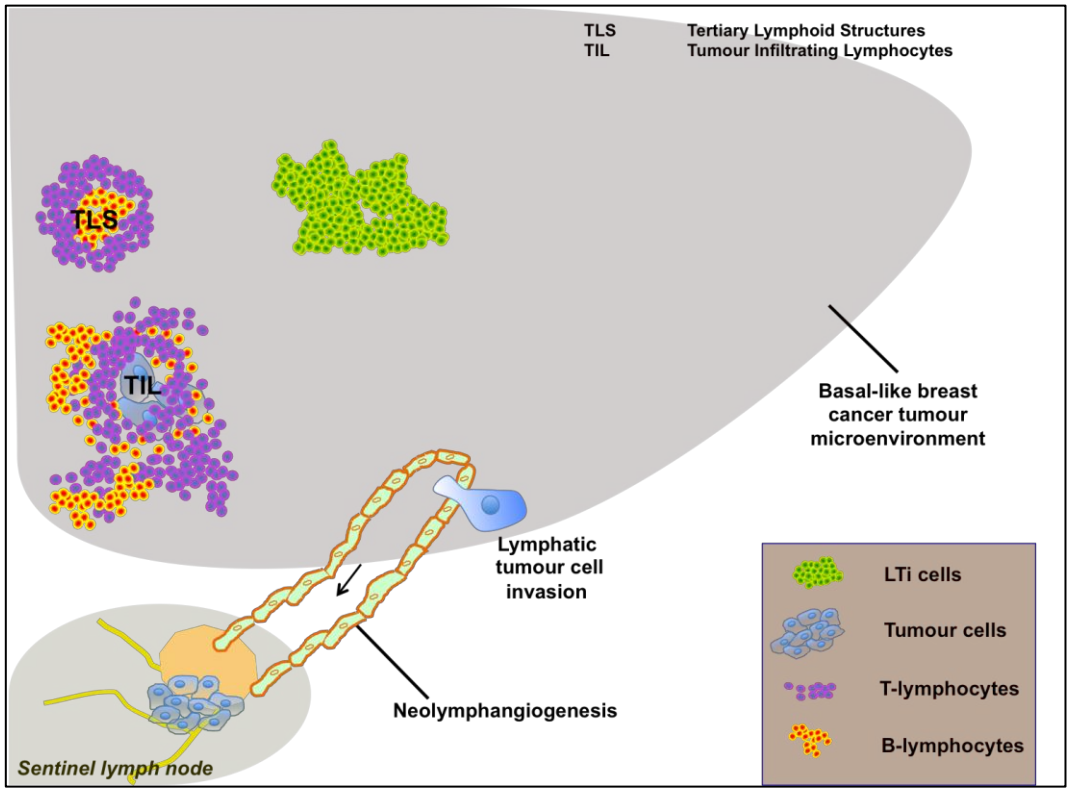

Figure 4-13: Schematic illustration of correlations between LTi cells and chemokines, tertiary lymphoid structures and markers of tumour invasion observed in human basal-like breast cancer datasets.

Increased LTi cells within the primary tumours were associated with increased lymphatic tumour cell invasion, lymphatic vessel density and increased tumour load in the draining lymph nodes. Consistent with previous studies, we observed tumour-infiltrating lymphocytes (CD3^{+}) and TLS were present within the tumour microenvironment.

From the data presented in this chapter I report, for the first time, on the identification of RORγt^{+}CD127^{+}CD3^{-} LTi cells within the human breast tumour microenvironments. The CD3 negativity distinguishes these cells from the RORγt^{+} Th17 cells. However, it is important to note that although there is published data using these three markers to identify LTi cells within tissue sections [202], recent moves proposing a uniform nomenclature for ILCs would denote RORγt^{+}CD127^{+}CD3^{-} as group 3 ILC, which include both the LTi cells and the NK-like LTi cells. To further investigate the role of LTi cells in cancers for our *in vivo* and *in vitro* studies, we have therefore included the marker NKp46 to make a clear distinction between the two cell types. Nonetheless, to the best of our knowledge, the presence or absence of these RORγt^{+}CD127^{+}CD3^{-} ILCs has not been explored in any human cancers to date. Although tumour periphery is often thought of as the place of greatest immunological importance (allowing sufficient immune tumour cell interaction) we did not observe a specific pattern for distribution of LTi cells within tumours. For example not only were the LTi cells scattered throughout the stroma and interspersed between tumour cells; they were also seen in aggregates resembling tertiary lymphoid tissue structures. Identification of these cells within the tumour microenvironment provides strong clinical support for the two previously published pre-clinical studies reporting on the presence of LTi cells within melanoma xenograft models [113,158].

Subsequently, we went on to explore the relevance of the presence of these cells within the tumour microenvironment. Our results support two main hypotheses. Firstly, LTi cells promote intratumoural lymphangiogenesis. Corroborative evidence is provided by a direct correlation between intratumoural LVD and a higher LTi count within human breast cancer samples, suggesting an association

between LTi cells and neo-lymphangiogenesis in tumours. In line with this, previous studies reporting on the initiation of fetal lymphoid tissue organogenesis have shown that LTi cells activate LTo cells by ligating LTβR on these stromal cells. Once activated, stromal cells secrete lymphoid chemokines, increase expression of adhesion molecules, as well as secrete lymphangiogeneic factors such a VEGF-C and VEGF-D [120,123,227]. Interpretation of our results have an inherent limitation in that the sections selected for podoplanin staining were chosen from tissue blocks which were first evaluated by our senior pathologist for lymphovascular invasion, thereby introducing a potential selection bias to the analysis. Ideally scoring for LVD from a number of sections from different blocks for each patient sample would provide a more representative picture of lymphangiogenesis within each tumour sample. However, given the limitations of having access to precious human tissue, we did not receive ethical approval for this to be done from the Guy's and ST Thomas Tissue Bank. Nonetheless, the possible influence of the infiltrating LTi cells on the expression of these lymphangiogenic factors within tumours [228], at the transcriptional and post-transcriptional levels is interesting and requires further investigation.

Secondly, our data suggests that LTi cells may provide signals for lymphatic invasion by the tumours cells. We showed that patients with tumour cell invasion into lymphatics were more likely to have a higher LTi score compared to patients without lymphatic vessel invasion; and within the BLBC subtype the higher LTi density translated to a greater risk of increased tumour burden within the lymph nodes. In support of this subtype specific relationship between LTi cells and BLBC subtypes, we also report on the discovery of a novel lymphoid chemokine gene expression signature within seven independent datasets that correlates with

1) LTi infiltration of human breast tumour and 2) relatively higher expression of the lymphoid chemokines and receptor genes within BLBCs. Additionally, we observed that within the BLBC a high lymph node tumour burden was associated with significantly increased levels of CCL21 and an associated trend in CXCL13.

Given the recent advances in microarray-based gene expression studies that have helped classify breast cancer as a highly heterogeneous disease with distinct molecular 'intrinsic subtypes' relating to tumour biology and behaviour [8,205,229], the subtype specific link between LTi cells and BLBCs is not particularly surprising. Similarly, it is noteworthy that within our dataset not all the BLBCs fall in the group characterised as having a high expression of the chemokine/chemokine receptors, possibly reflecting limitations of the PAM50 classification of breast cancer into only 5 main subtypes. As discussed, the breast cancer genomic analysis performed by METABRIC recently produced a novel classification of breast cancers into 10 subgroups [8]; and this is further complicated by the recently published study by Lehmann et al. [230] demonstrating that even within triple negative breast cancers (representing the BLBCs of the PAM50 classification) the group can be further sub-divided into six distinct subtypes [230]. These include: two basal like (BL1 and BL2), an immunomodulatory, a mesenchymal (M), a mesenchymal stem like (MSL), and a luminal androgen receptor (LAR) subtype; each representing subgroup exhibiting unique tumour biology.

Among the molecular subtypes of breast cancer identified, none has generated as much interest or controversy as the basal-like group. BLBCs account for 15% of all breast cancers and are more prevalent amongst young African, African-

American and Latino women. They are known to be associated with an aggressive clinical course and a generally poorer prognosis [231-233]. BLBCs show a specific pattern of distant metastasis with an increased propensity for visceral metastases to the brain and lung and are less likely to metastasize to the bone and liver, suggesting that such tumours might also possess a distinct mechanism of metastatic spread from non-basal-like tumours [232]. A recent study reported that within BLBCs the vascular invasion is almost entirely via lymphatics [27]. My own view is that LTi cells play a role in this lymphatic tumour cell invasion within the BLBCs. However, bearing in mind that studies have reported abnormal multidirectional flow within tumour associated lymphatic vessels (perhaps due to insufficient or dysfunctional valves) [234], it is also possible that the increased number of lymphatic vessels within these tumours results in an increased infiltration of immune (including LTi) cells into the microenvironment.

Histologically, majority of BLBCs are of high histological grade, and characterized by exceptionally high mitotic indices, the presence of central necrotic or fibrotic zones and conspicuous lymphocytic infiltrate. Several lines of evidence suggest that clinical outcomes in this molecular subtype are particularly influenced by the host immune response [171,235]. Given our pathological findings, the lymphoid chemokine gene signature is likely to contribute additional prognostic information within the BLBCs. It is possible that the correlation between the chemokine gene signature and LTi infiltration reflects the known physiological chemotactic functions of the lymphoid chemokines for lymphocytes (see section 1.3); supported by our observed higher CD3 infiltration within the relatively higher expressers for the lymphoid gene signature.

In summary, identification of LTi cells and their relevance particularly in the lymphatic invasion of basal-like breast cancers requires further investigation.

Chapter 5: Lymphoid tissue inducer cells within a murine breast cancer microenvironment

The aim of this chapter was to further investigate the mechanisms that underlie the correlations observed in Chapter 4: between the presence of tumoural LTi cells in human basal-like breast cancers (BLBCs) and increased tumour cell invasion within a breast cancer mouse model.

5.1 Syngeneic murine model of triple negative breast cancer

A clinical shorthand classification divides breast cancer into three major subtypes based on the expression of oestrogen (ER), progesterone (PgR) hormone receptors, human epidermal factor receptor 2 (HER2) and grade or Ki67 staining: luminal (ER/ PgR-positive disease) divided into low (A) and high proliferation (B) forms, HER2-amplified tumours and triple negative breast cancer (TNBC). TNBC describes a subset of breast cancers that lack expression of oestrogen and PgR as defined by immunohistochemistry (IHC), as well as HER2 overexpression or gene amplification of HER2 by IHC or in-situ hybridization, respectively [232]. BLBCs are dominated by the TNBC phenotype and some investigators have suggested that the TNBC and basal-like phenotypes are effectively synonymous [236].

A clinically relevant animal model of spontaneous triple negative breast cancer metastasis to multiple sites is now available [194,237,238]. Several tumour lines with a

spectrum of metastatic phenotypes have been derived from a spontaneously arising mammary tumour in a BALB/cfC3H mouse, offering the advantage of being able to be transplanted into immune competent recipients[239]. Of these the highly metastatic 4T1 and its variant 4T1.2 cell lines are thought to most closely mimic the tumour growth and metastatic spread of human breast cancers [194,237]. These cell lines have been shown to not express the ER, PgR or the gene for HER2 [238]. In particular mice bearing 4T1.2 are thought to develop metastatic disease via a lymphatic route as compared to a haematogenous route and occasionally these mice have been shown to develop hind limb paralysis and have elevated plasma levels of calcium and parathyroid hormone-related protein (PTHrP), two pathologic hallmarks of the human disease[240].

We first confirmed the lymphotropic metastatic capacity of the 4T1.2 cell line in BALB/c mice. We observed that following subcutaneous inoculation of $1x10^6$ cells of either the 4T1 or its daughter clone 4T1.2 cell lines into the mammary fat pad of BALB/c mice, the growth of the primary tumour did not differ significantly between the two cell lines (Figure 5-1A). However, the size of the draining lymph nodes at day 21 was significantly larger within the 4T1.2 tumour-bearing mice (Figure 5-1B). There was no significant difference between the lymph nodes from the 4T1 tumour-bearing mice and non-tumour-bearing mice. Consistent with previous studies, analysis of tumour load with the lymph nodes, by staining for E-cadherin and pan-cytokeratin for FACS analysis and immunohistochemistry respectively indicated that 4T1.2 metastasize preferentially via the lymphatics compared to 4T1 tumours, at least until day 21 of the tumour development (Figure 5-1C &D).

The lymphotropic nature of this 4T1.2 triple negative breast adenocarcinoma cell line made it an attractive model system for us to understand the mechanistic basis for the association between BLBCs and LTi cells *in vivo*.

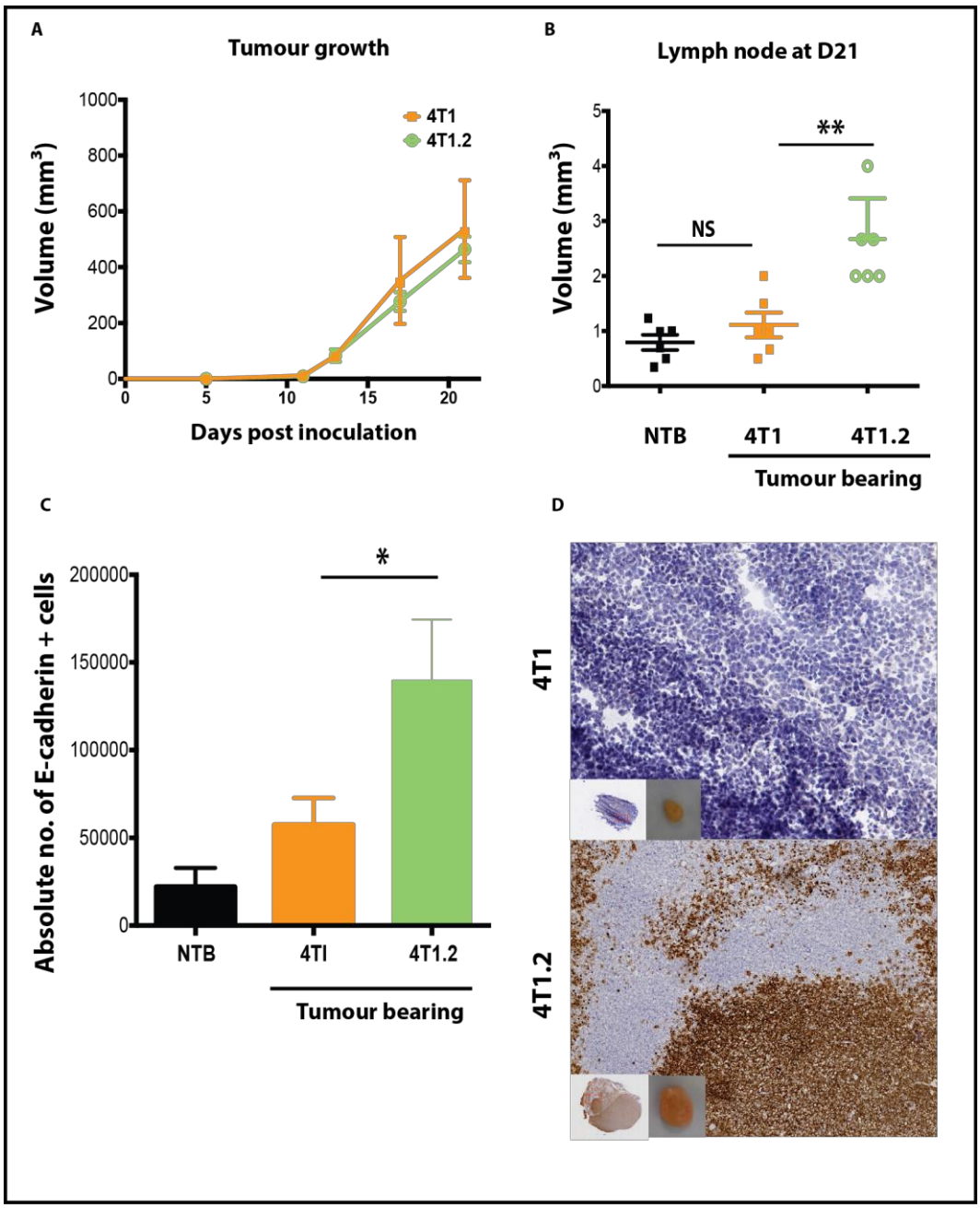

Figure 5-1: 4T1.2 cell line as a syngeneic model of murine triple-negative breast cancer.

A: Tumour size was evaluated two-three times per week by caliper measurements using the following formula: tumour volume = [length × width^2] / 2. The change in tumour volume after inoculation of tumour cells is shown. **B:** The average volume of draining inguinal lymph node from mice sacrificed at the end of the *in vivo* experiment at Day 21 is shown. Lymph node size was evaluated at the end of the experiment at Day 21 using the following formula: volume = [length × width^2] / 2. **C**: Flow cytometry analysis of E-cadherin positive cells obtained from the draining lymph nodes of non-tumour-bearing (NTB) and 4T1/4T1.2 tumour-bearing mice. **D:** Immunohistochemical staining of the draining lymph nodes of tumour-bearing mice using a pancytokeratin (*brown*) to assess for tumour load between the treatment groups. Cell nuclei are stained blue. The inserts represent low magnification images and a photograph of the dissected lymph node. Data represent means ± SEM. Asterisks represent the p-values when comparing to the groups to 4T1 tumour bearing cohort (one-way ANOVA: * $p \leq 0.05$, ** $p \leq 0.01$, NS= Non significant).

5.2 Analysis of tumour infiltration by LTi cells in a mouse model of triple negative breast cancer

To further investigate the relationship between TNBCs and LTi cells *in vivo*, we first set about to identify LTi cells within the 4T1.2 mouse breast cancer microenvironment. Groups of BALB/c mice (*n=18*) were inoculated subcutaneously with 1 x 10^6 4T1.2 cells on day 0. Following tumour inoculation, groups of tumour-bearing mice (*n=3*) were culled on days 10, 12, 14, 18, 20, 24. We performed flow cytometric analysis to determine the absolute numbers of LTi cells ($CD3^-$,$CD11c^-$,$B220^-$,$CD127^+$,$CD90.2^+$,$NKp46^-$) at different stages of tumour growth within the tumours, draining lymph nodes and non-draining lymph nodes [241]. The gating strategy used for identification of LTi cells is shown in Figure 5-2A. Absolute cell numbers in tumours were calculated using the reference fluorescent beads method (see Methods & Material section 3.2.6.2).

Infiltration of LTi cells into the tumours was seen to peak at day14 (D10 vs D14 p=0.0019 unpaired t-test); followed by a later transient peak at day18 within the draining lymph nodes (D10 vs D18 p=0.0041 unpaired t-test) (Figure 5-2B). Importantly, LTi density within the non-draining lymph nodes did not change significantly, acting as an internal control. These experiments confirmed the presence of LTi cells within our triple negative 4T1.2 breast cancer mouse model, demonstrating also a temporal pattern of LTi infiltration into the tumours and the draining lymph nodes.

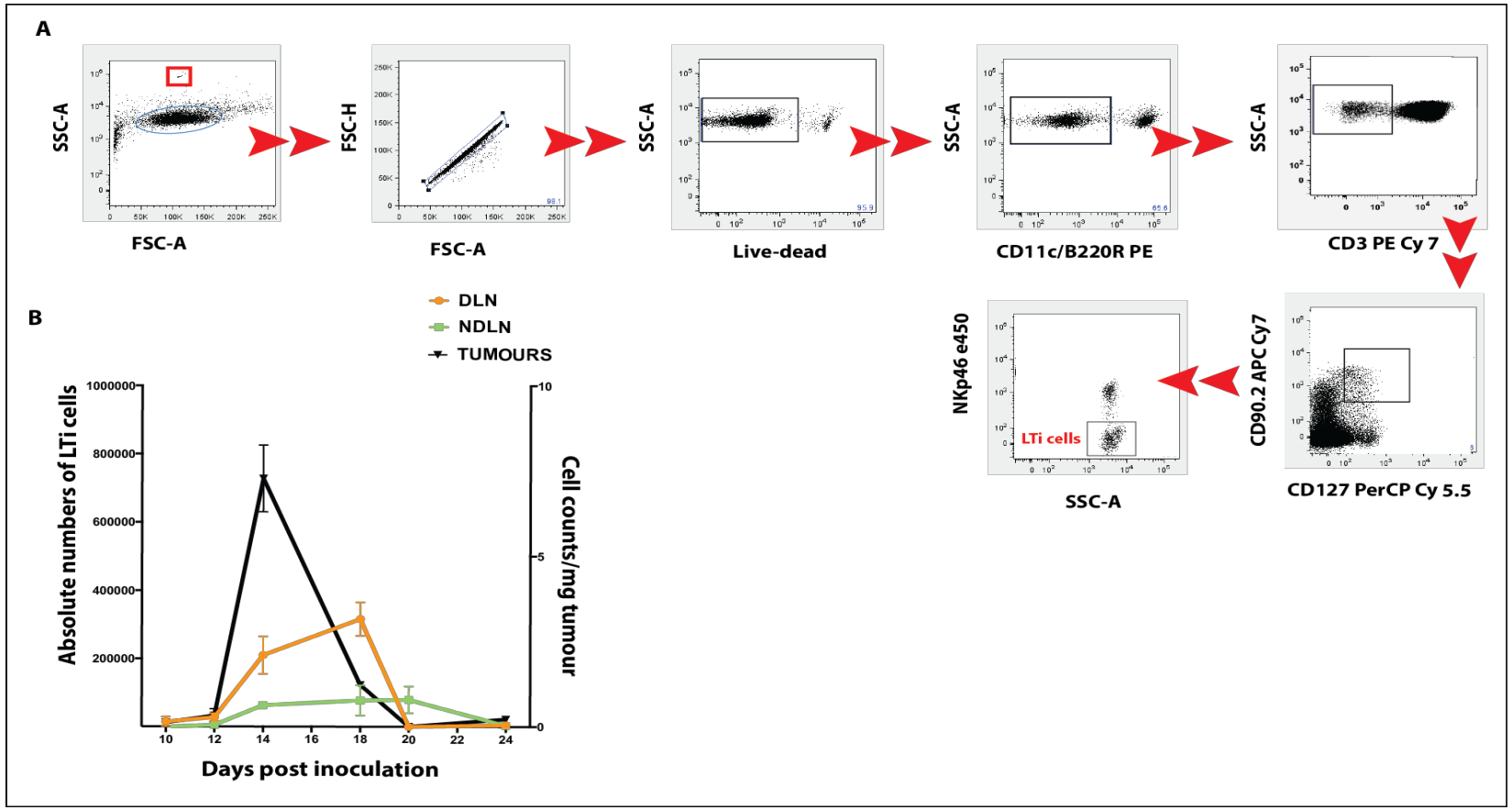

Figure 5-2: Tumour infiltration of LTi cells in the 4T1.2 tumour-bearing mice

A: Gating strategy for flow cytometry analysis for LTi cells: In this sample gating, cells were first gated for lymphocytes (SSC-A vs FSC-A) and then for singlets (FSC-H vs. FSC-A). The gate for the reference beads (red gate) used to obtain the absolute cell count is shown. The singlets are further analyzed for their uptake of the Live/Dead stain to determine live versus dead cells and taking only the live cells. Cells expressing CD11c, B220R and CD3 were then gated out and from this lineage negative population, cells identified as $CD127^{+}$ $CD90.2^{+}$ $NKp46^{-}$ were recognised as the LTi cells. **B**: Absolute number of LTi cells in draining (orange line) and non-draining (green line) lymph nodes and cell counts per milligram of tumour in tumours (black line) is shown (n=3). A temporal pattern of LTi infiltration into the tumours and the draining lymph nodes is seen. Data represent means ± SEM. DLN, draining lymph nodes, NDLN, non draining lymph nodes.

5.3 Tumour infiltrating lymphocytes within 4T1.2 breast cancer mouse model

Given the correlations seen between the chemokine gene signature, LTi and CD3 cell infiltration into tumours, (Figure 4-7) and to look for any relationship between the tumour infiltrating lymphocytes and LTi cells; we investigated the pattern of infiltration of the T- and B-lymphocytes (defined as $CD3^+$ or $CD19^+$ cells) at different stages of tumour growth within the tumours, draining and non-draining lymph nodes (between days 10-24). The gating strategy used for identification of T- and B-cells is shown in Figure 5-3A.

In contrast to the temporal pattern of tumour infiltration by LTi cells observed in Figure 5-2B, the infiltration of $CD3^+$(Figure 5-3B) and $CD19^+$ (Figure 5-3C) cells decreased over time; whilst the recruitment of $CD3^+$ and $CD19^+$ lymphocytes into the draining lymph nodes continued up to day 24. The density of the lymphocytes did not change significantly within the non-draining lymph nodes. These data suggested an independent mechanism for the lymphocyte *c.f.* LTi infiltration into the tumours or the draining lymph nodes.

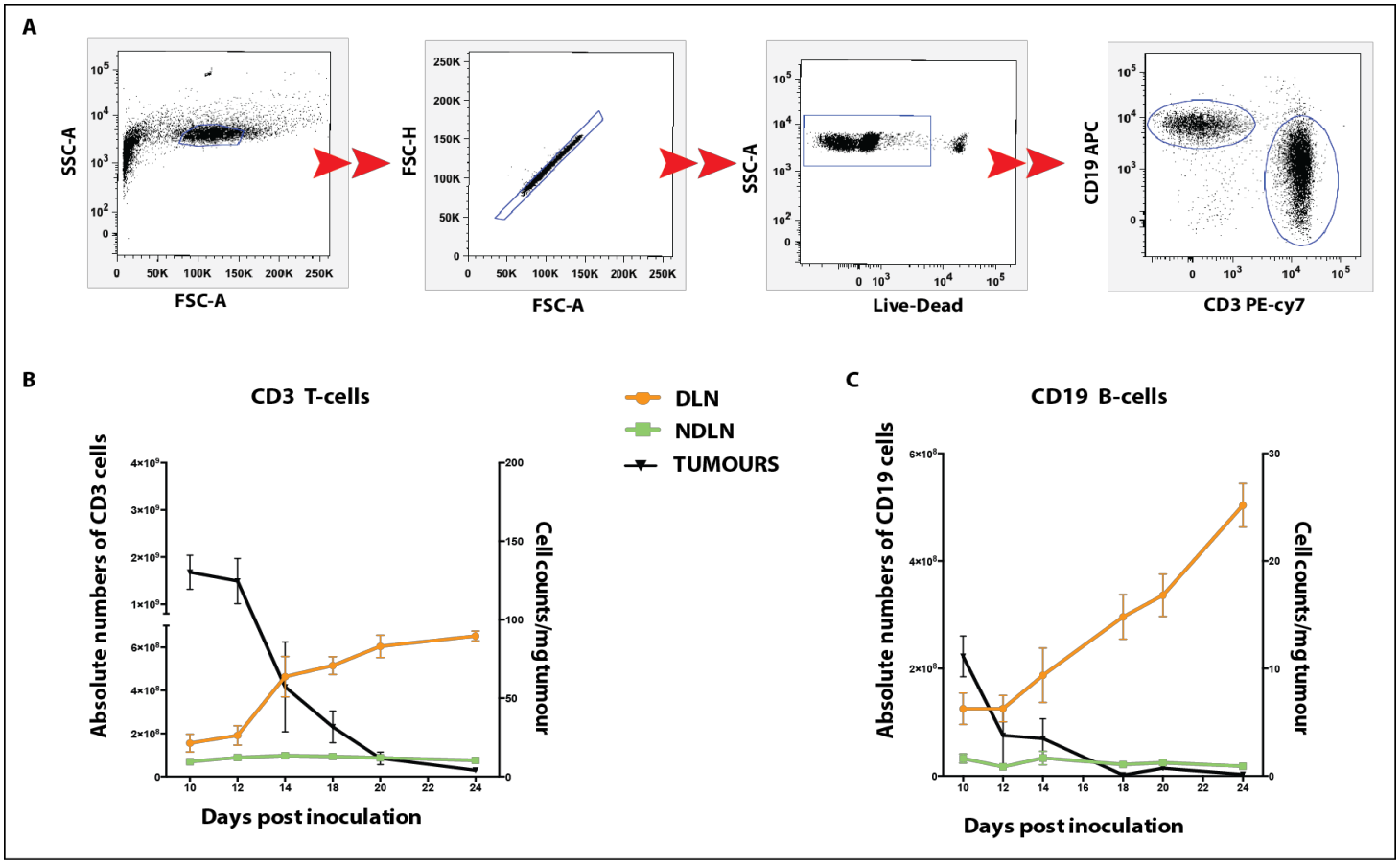

Figure 5-3: Kinetics of lymphocyte infiltration within the 4T1.2 tumour-bearing mice.

A: Gating strategy for flow cytometry analysis for $CD3^+$ and $CD19^+$cells: In this sample cells were first gated for lymphocytes (SSC-A vs FSC-A) and then for singlets (FSC-H vs. FSC-A). The singlets are further analyzed for their uptake of the Live/Dead stain to exclude dead cells. Cells expressing either CD3 or CD19 were recognised as the T- or B-cells, respectively. **B** & **C**: Tissues collected at different time points following tumour induction were analysed for absolute number of $CD3^+$ T-cells and $CD19^+$ B-cells in draining (orange line) and non-draining (green line) lymph nodes (n=3). Cell counts per milligram of tumour tissue are indicated by the black line). Data represent means ± SEM. DLN: draining lymph nodes. NDLN: non-draining lymph nodes.

5.4 Variations in the levels of lymphoid chemokines during tumour development in the 4T1.2 breast cancer mouse model

Given the essential role of CXCL13 in LTi cell function [121] and the correlation between CCL21 expression and induction of lymphoid-like stroma (reminiscent of lymph node paracortex) within primary tumours [113]; we analysed the serum CXCL13 and CCL21 responses following inoculation of 4T1.2 tumour cells into the mammary fat pad. 500μl of peripheral blood was obtained from 4T1.2 tumour-bearing mice via intracardiac puncture at the termination of the experiment at each time-point between days 10-24. Separated serum was analysed by enzyme-linked immunosorbent assay (ELISA) (see Materials & Methods; Section 3.2.7.1).

An early peak in serum CCL21 levels was observed at day 12, with a mean increase in concentration from 112pg/ml at day 10 to 1631pg/ml at day 12 ($p<10^{-4}$ unpaired t-test) (Figure 5-4; green line). In contrast, levels of serum CXCL13 peaked later at day 14, with a mean increase in concentration from 538pg/ml at day 10 to 1399pg/ml at day 14 ($p<10^{-4}$ unpaired t-test). Levels of CXCL13 appeared to oscillate with a second peak in concentration at day 24 (1615pg/ml) (Figure 5-4; orange line).

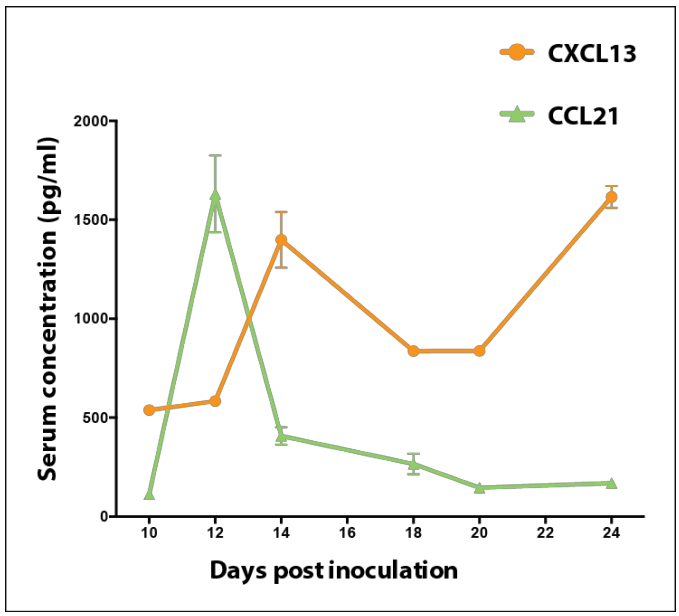

Figure 5-4: The levels of chemokines CXCL13 and CCL21 vary during tumour development.

Chemokine CCL21 and CXCL13 serum concentrations after inoculation of 4T1.2 cells into the mammary fat pad were determined at the indicated time points by ELISA. 3 animals were analysed per time point. Data represent means ± SEM.

5.5 Analysis of the effect of *in vivo* blocking of chemokines CXCL13 and CCL21 in a triple negative breast cancer mouse model

5.5.1 Chemokine-dependent lymphatic metastasis and LTi cell recruitment

In order to examine if there was any relationship between the LTi recruitment and changes in the chemokine levels within the serum, we investigated the effect of CCL21 or CXCL13 blockade on LTi recruitment within tumours *in vivo*. Tumour-bearing mice were treated with a neutralizing antibody for CXCL13, CCL21 or isotype control antibodies (0.5mg each via tail-vein injections) started one day after tumour cell implantation and repeated every 3 days. Two time points, day 14 and day 21 were tested. As discussed in section 5.1, day 14

represents an early stage within our 4T1.2 mouse breast cancer model as lymphatic metastases were not present at this time-point; compared to day 21 when lymphatic metastasis (seen by pancytokeratin IHC and E-cadherin positive cells on FACS) were present.

We observed from our antibody blockade *in vivo* experiments that neither anti-CXCL13 nor anti-CCL21 treatments significantly affected the growth of the primary tumour when compared with isotype control antibody at both time-points (day 14 and day 21) (Figure 5-5A-C); suggesting no effect on the proliferation of 4T1.2 cells *in vivo*. We observed no statistically significant difference in the weight of the draining lymph nodes at day 14 within either cohorts (Figure 5-5D). However, when compared with the isotype control antibody the weight of the draining inguinal lymph nodes at day 21 were significantly reduced in both cohorts (anti-CXCL13 and anti-CCL21), when compared with isotype control (anti-CXCL13 $p \leq 0.05$; anti-CCL21 $p \leq 0.01$; Figure 5-5E). No side effects, or severe toxicity, of anti-CXCL13 or anti-CCL21 treatments were observed during the whole course of treatment.

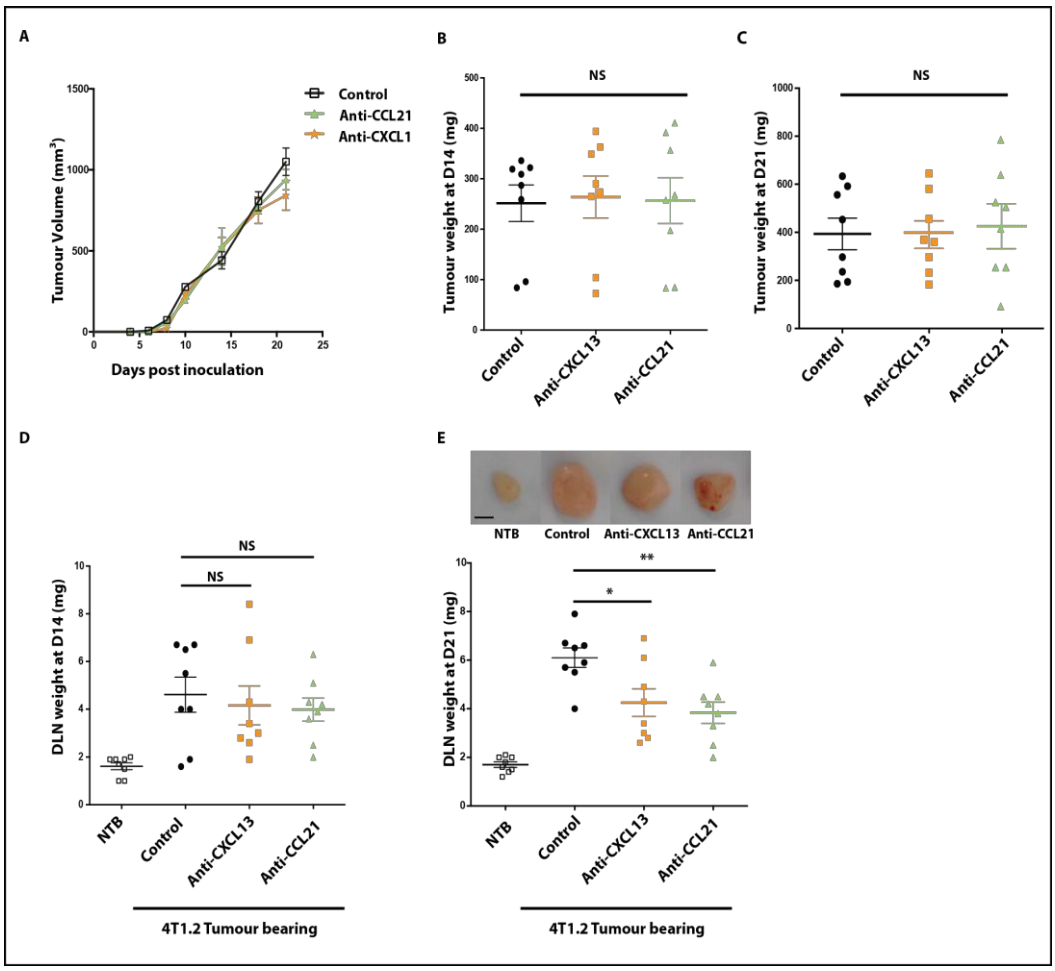

Figure 5-5: Effect of chemokine neutralization (CXCL13/CCL21) within the 4T1.2 tumour model *in vivo*.

BALB/c mice were injected s.c. with 1×10^6 4T1.2 breast cancer cells. Mice were treated with either an anti-murine anti-CXCL13 antibody, anti-CCL21 or goat IgG isotype control antibody injected intravenously every other day for a total of 21 days. **A**: Subcutaneous tumour growth curves of the 4T1.2 cells within each cohort are demonstrated. **B**: The average weight of primary tumours collected from mice sacrificed at the end of *in vivo* experiments at day 14. **C**: The average weight of primary tumours collected from mice sacrificed at the end of *in vivo* experiments at day 21. **D**: The average weight of draining inguinal lymph node (DLN) from non tumour bearing (NTB) and tumour bearing mice sacrificed at the end of *in vivo* experiments at day 14. **E**: The average weight of draining lymph nodes collected from mice sacrificed at the end of *in vivo* experiments at day 21. Photographic example of the lymph nodes within each cohort is shown (Scale Bar = 1mm). The results are expressed as mean +/- SEM. Asterisks represent the p-values when comparing to the control (Mann Whitney test: * $p\leq0.05$, ** $p\leq0.01$, NS= Non significant)

Tumours and draining lymph nodes were analysed for LTi ($CD3^-$, $CD11c^-$, $B220^-$, $CD127^+$, $CD90.2^+$, $NKp46^-$) cell numbers by flow cytometry (as per the gating strategy in Figure 5-2A) at day 14, a time-point by which maximum number of LTi cells had been recruited into the tumours (demonstrated in Figure 5-2B) and at day 21, a time-point when lymphatic metastasis are present within the lymph nodes (demonstrated in Figure 5-1D-E).

At day 14, when compared with the isotype control antibody, antibody blockade using an anti-CCL21, but not an anti-CXCL13 neutralising antibody, was able to reduce significantly LTi recruitment into the primary tumours (control vs anti-CCL21 $p \leq 0.01$, one-way ANOVA; Figure 5-6A), supporting the earlier findings by Shields *et al*. that CCL21 chemokine is involved in the recruitment of LTi cells into the primary tumour. Within the draining lymph nodes, the numbers of LTi cells were significantly lower in both cohorts (control vs anti-CCL21 & control vs anti-CXCL13 $p \leq 0.05$, one-way ANOVA; Figure 5-6A).

At day 21, when compared with the control group, the numbers of intratumoural LTi cells were higher amongst the anti-CXCL13 treated cohort (control vs anti-CXCL13 $p \leq 0.05$, one-way ANOVA; Figure 5-6B). Although, a similar trend for an increase in the numbers of LTi cell counts within the anti-CXCL13 cohort at day 14 was also noted, this was not statistically significant. In keeping with the findings at day 14, we confirmed again that antibody blockade using an anti-CCL21 neutralizing antibody was able to reduce significantly the numbers of intratumoural LTi cells control vs anti-CCL21 ($p \leq 0.001$, one-way ANOVA, Figure 5-6B). Within the draining lymph nodes, the numbers of LTi cells were again lower amongst both the anti-CXCL13 and anti-CCL21 treated cohorts when

compared to the control cohort (control vs anti-CCL21 $p \leq 10^{-4}$; control vs anti-CXCL13 $p \leq 0.01$, one-way ANOVA; Figure 5-6B).

These data propose a key role for CCL21 in the recruitment of LTi cells into the primary tumour.

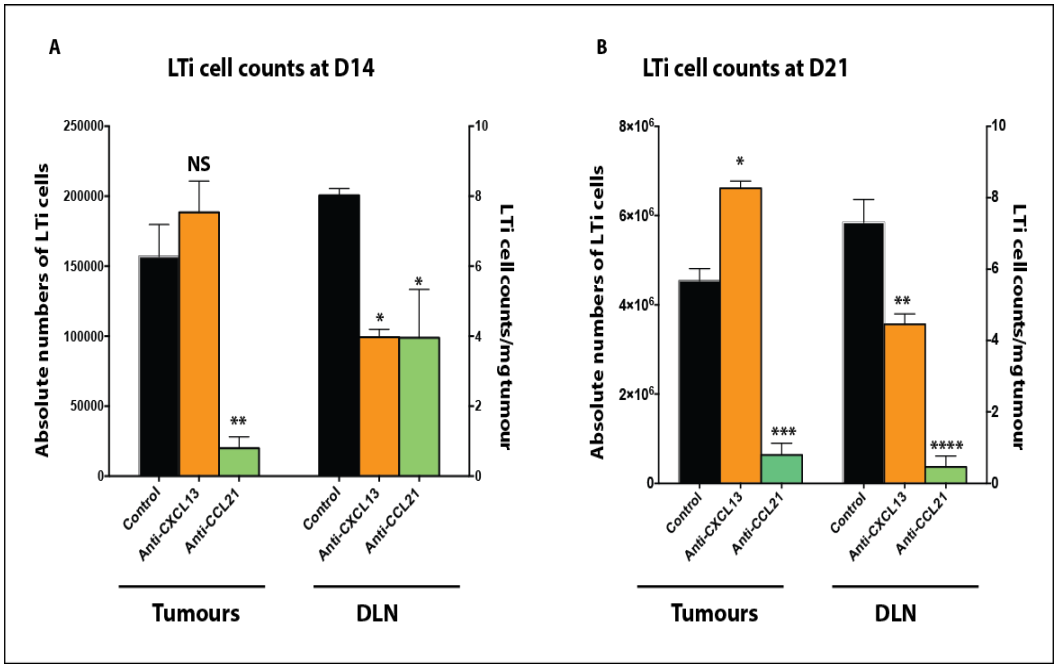

Figure 5-6: Effect on LTi recruitment following chemokine (CXCL13/CCL21) neutralization within the 4T1.2 tumour model in vivo.

Absolute cell counts of LTi cells per milligram of tumour detected in tumours (right-axis) and absolute numbers within the draining lymph nodes from 4T1.2 tumour-bearing BALB/c mice treated with anti-CXCL13, anti-CCL21 or isotype control antibody at day 14 (A) or day 21 (B) are shown, ($n \geq 3$). Data represent means ± SEM. Asterisks represent the p-values when comparing to the control group (One way ANOVA: * $p \leq 0.05$, ** $p \leq 0.01$, *** $p \leq 0.001$, **** $p \leq 10^{-4}$, NS= Non significant).

5.5.2 Effect of chemokine blockade on lymphocyte blockade

Given the known chemotactic roles of CCL21 and CXCL13 on T- and B-cells respectively, we also examined for the anti-inflammatory effect of our chemokine blockade within the 4T1.2 breast cancer mouse model. We analysed by flow cytometry the total B/T-cell counts, defined as $CD3^+$ or $CD19^+$ cells respectively (as per the gating strategy in Figure 5-3) within the tumours and the draining lymph nodes at day 14 and day 21.

Irrespective of the time-point, our analysis demonstrated a statistically significant decrease in the number of $CD3^+$ T-cells within the primary tumours and the draining lymph nodes amongst both the anti-CCL21 and anti-CXCL13 treated cohorts compared to the cohort group (Figure 5-7A &B). Similarly, the number of $CD19^+$ cells within the primary tumours and the draining lymph nodes (Figure 5-7C & D) was significantly decreased at day 14 and day 21 amongst both the anti-CCL21 and anti-CXCL13 treated cohorts (see figure legend for the p-values). It was reassuring to note that the greatest effect on T-cell and B-cell recruitment was observed amongst the anti-CCL21 or anti-CXCL13 treated cohort respectively.

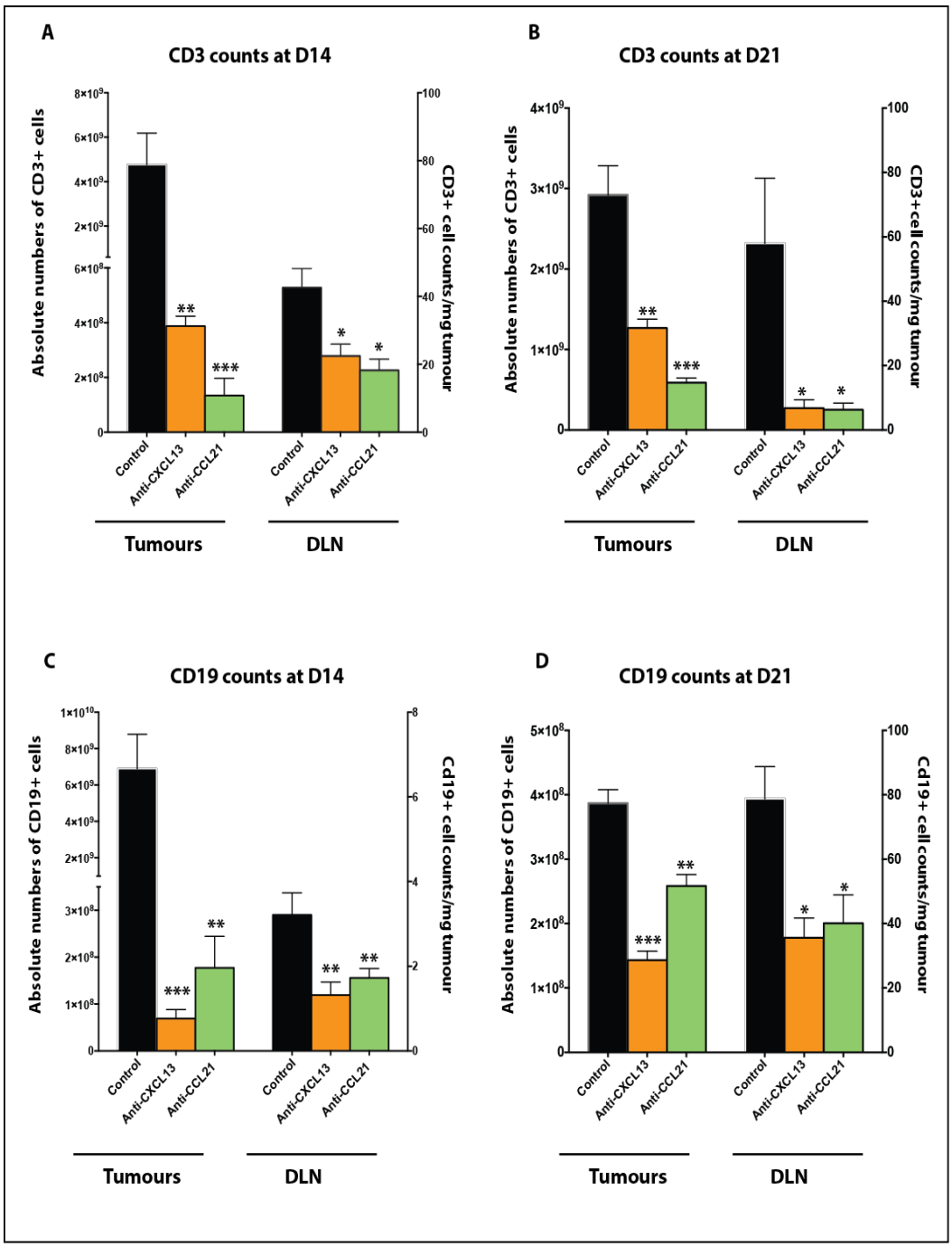

Figure 5-7: Effect on T-/B-cell recruitment following *in vivo* chemokine (CXCL13/CCL21) neutralization within the 4T1.2 tumour model.

Absolute cell counts of $CD3^+$ (**A** and **B**) or $CD19^+$ (**C** and **D**) cells per milligram of tumour detected in tumours (right-axis) and absolute numbers within the draining lymph nodes from 4T1.2 tumour-bearing BALB/c mice treated with anti-CXCL13, anti-CCL21 or isotype control antibody at day 14 (**A** and **C**) or day 21 (**B** and **D**) are shown, ($n \geq 3$). Data represent means ± SEM. Asterisks represent the p-values when comparing to the control groups (one-way ANOVA: * $p \leq 0.05$; ** $p \leq 0.01$; *** $p \leq 0.001$).

5.5.3 Effect on tumour burden within the lymph nodes

From our earlier studies day 21 represents a time-point when lymphatic metastases are present within the lymph nodes. Although the decreased size of the lymph nodes at day 21 (Figure 5-5E) was in part due to effects of chemokine blockade on the lymphocyte recruitment into the primary tumours and the draining lymph nodes (Figure 5-7), we further examined for a difference in the tumour load within the lymph nodes by staining for pancytokeratin.

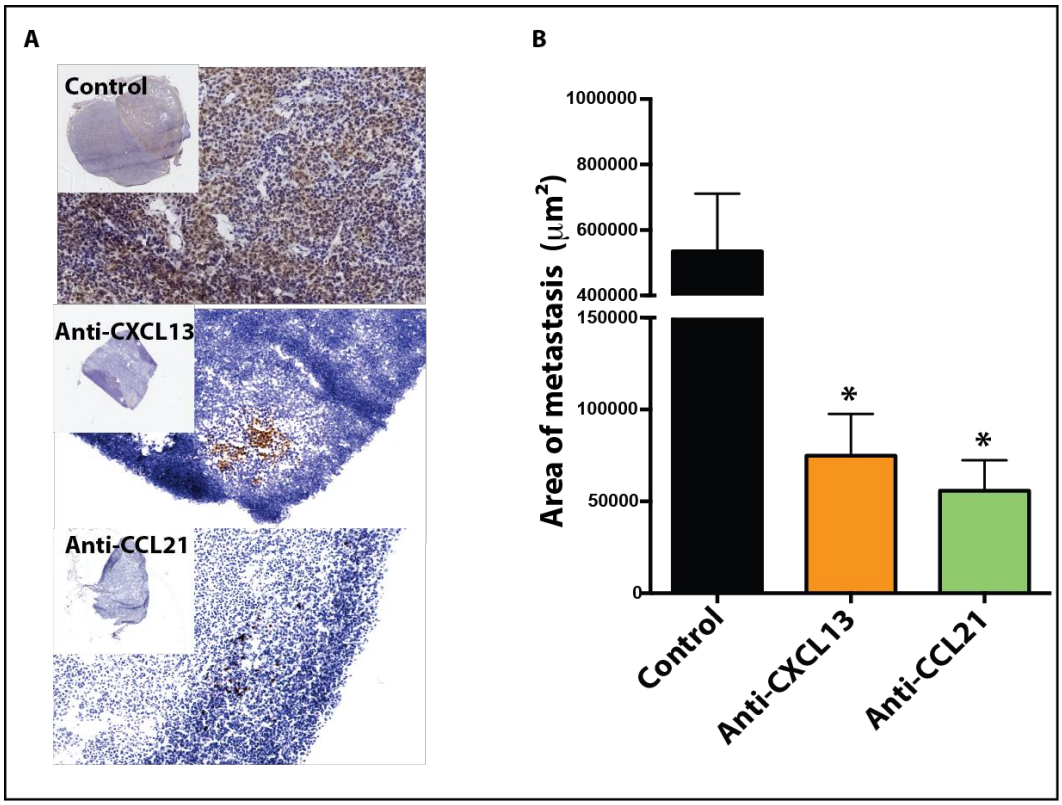

Figure 5-8: Tumour load in draining lymph nodes is decreased by *in vivo* CXCL13 or CCL21 neutralization within the 4T1.2 tumour model

A: Immunohistochemical staining of the draining lymph nodes of tumour-bearing mice using a pancytokeratin (*brown*) to assess for tumour load between the treatment groups. Cell nuclei are stained blue. B: Quantification of the total area of metastasis per mm^2 of sectional area within lymph nodes. Data represent means ± SEM. Asterisks represent the p-values when comparing to the control groups (one-way ANOVA: * $p \leq 0.05$).

Immunohistochemical analysis of tumour load with a pancytokeratin antibody revealed noticeably fewer tumour foci within the lymph nodes in mice treated with anti-CXCL13 or anti-CCL21 treatment compared with those treated with isotype control antibody (Figure 5-8A). Measurements of the total surface area of tumour foci (μm^2) demonstrated a significant decrease in the tumour load within the lymph nodes of mice treatment with anti-CXCL13 or anti-CCL21 ($p \leq 0.05$ one-way ANOVA; Figure 5-8B), suggesting an inhibitory effect of chemokine blockade on 4T1.2 tumour cell migration into the draining lymph nodes.

5.6 Chemokine dependent LTi cell interactions within the breast cancer microenvironment

Sufficient clustering of LTi cells and production of lymphoid chemokines by activated LTo cells (stromal cells of mesenchymal origin) during lymphoid tissue embryogenesis is dependent on CXCL13, which is responsible for initiating an important positive feedback loop on further LTi cell recruitment (after the initial LTi-stromal cell contact) and subsequent amplification of lymphotoxin (LT)β receptor signaling [242]. Given that within our 4T1.2 breast cancer mouse model, the circulating CXCL13 level was upregulated after that of CCL21 (Figure 5-4) we investigated whether there is a non-redundant function of CXCL13, as a consequence of the initial CCL21-mediated recruitment of LTi cells (Figure 5-6) into the primary tumour.

There is a lineage relationship between mesenchymal stromal cells (MSCs), which exhibit a marked tropism for tumours [243-247], and LTo cells that are known to interact with LTi cells. MSCs are adult multi-potent non-hematopoietic stem

cells capable of self-renewal and generation of different cell lines. Recent evidence suggests that the bone-marrow-derived MSCs are recruited in large numbers to the stroma of developing tumours and are capable of suppressing the immune response for example by inhibiting the maturation of dendritic cells and suppressing the function of T-lymphocytes, B-lymphocytes and NK cells [248-252]. We therefore hypothesized that LTi cells may interact with bone marrow derived MSCs, thereby modulating the chemokine profile of the tumour microenvironment.

5.6.1 Characterization of the mesenchymal stromal cells

We obtained a parental bone marrow derived MSC cell line (HS-5) from Professor Lythgoe's laboratory at UCL. Morphologically, cells grew with a fibroblast like format (fusiform) and were plastic-adherent when maintained in standard culture conditions using tissue culture flasks. *In vitro*, the MSC cell lines could be efficiently expanded reaching 50-60% confluency within 3-4 days. Cells generally appeared to have a limited *in vitro* lifespan of up to 8-9 passages, a phenomenon which is well documented in literature and is thought to occur due to a lack of activity of immortalizing enzyme telomerase ("replicative senescence") [253,254].

5.6.1.1 Mesenchymal Stromal Cell Marker Panel Immunofluorescence

In accordance with the Mesenchymal and Tissue Stem Cell Committee guidelines for the characterization of MSCs [255], immunofluorescence staining showed that

our cell line was as expected positive for Stro-1, CD90, CD106, CD105, CD146, CD166, and CD44 and negative for CD19 and CD45 (Figure 5-9).

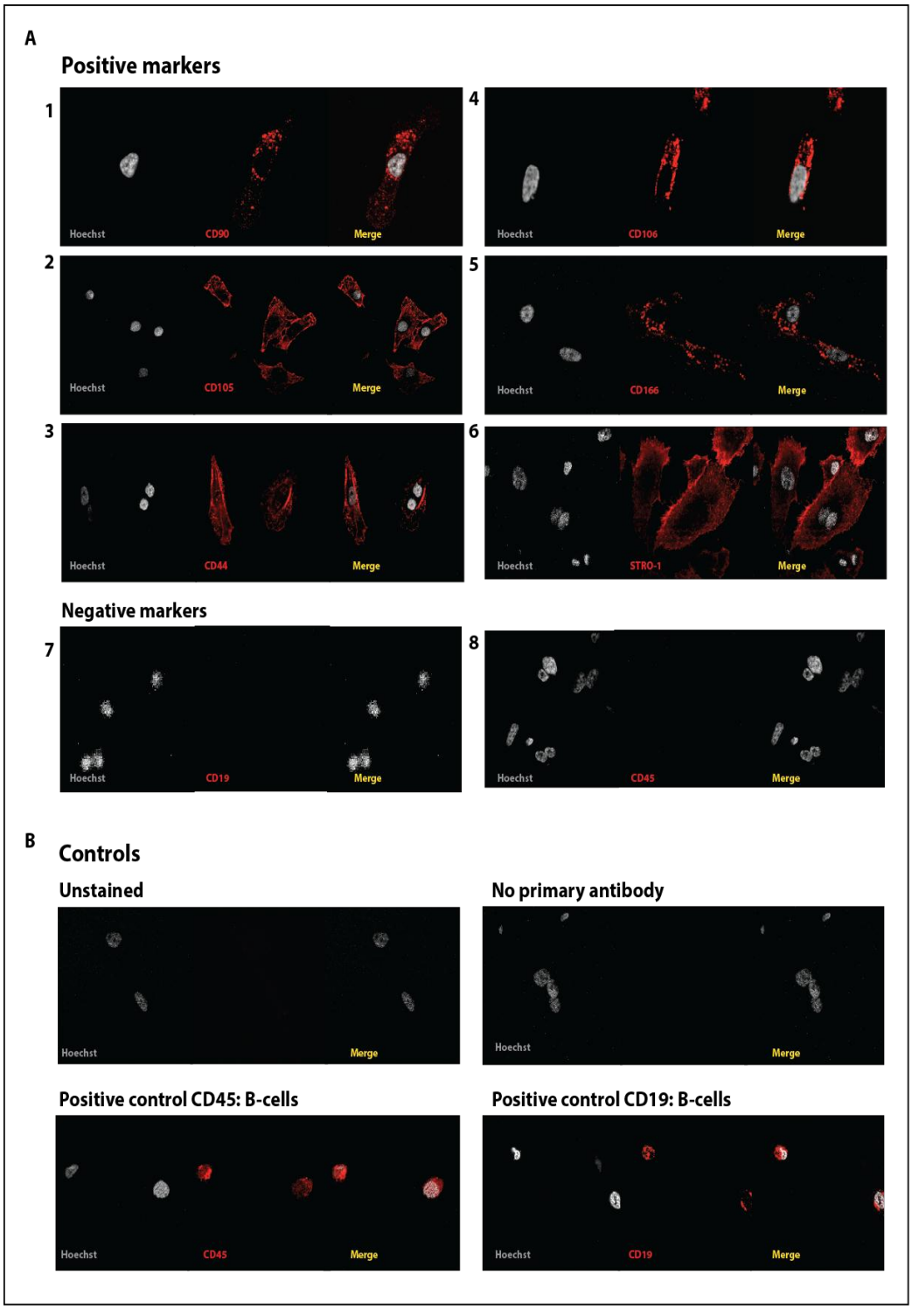

Figure 5-9: Phenotypic characterization of mesenchymal stem cell line.

A: Immunofluorescence images of staining for stem cell markers (red) in the bone marrow derived MSC cell line HS-5 using a x63 oil immersion objective. (1-6: positive markers and 7-8: negative markers). **B:** Negative and positive controls are shown. Hoechst stained nuclei are shown in grey.

5.6.1.2 LTβR receptor expression on MSCs

An interaction between LTαβ on LTi cells and LTβR, expressed on mesenchymal LTo cells, is an absolute requirement for effective lymphoid tissue development [256,257]. We therefore confirmed the expression of LTβR on the MSCs by immunofluorescence; providing support to the theory that the recruited MSCs within the tumour microenvironment could interact with LTi cells (Figure 5-10).

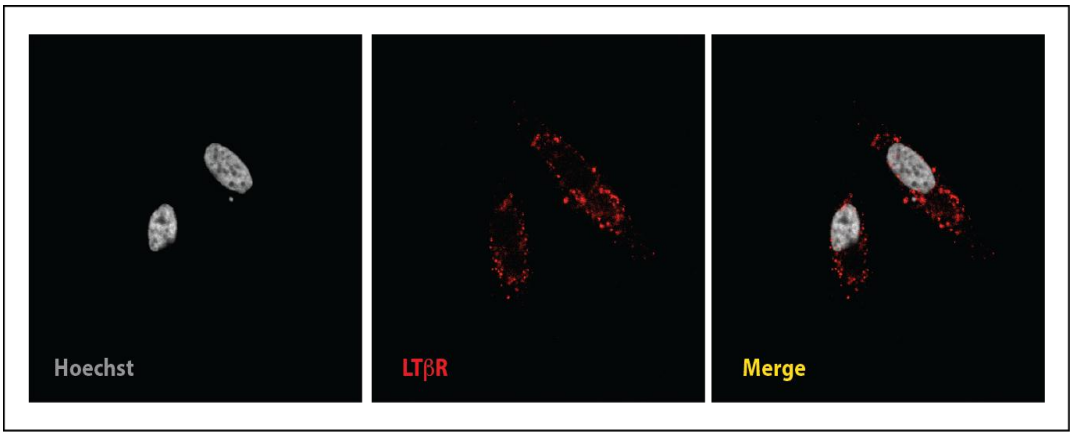

Figure 5-10: LTβR expression in MSCs

Immunofluorescence staining showing the LTβR staining (red) using a x63 oil immersion objective. Hoechst stained nuclei are shown in grey.

5.6.1.3 Lymphoid chemokine secretion by MSCs.

As discussed in Chapter 1 section 1.3.3, during organogenesis mesenchymal LTo cells are the main source of lymphoid chemokines which function to first attract the LTi cells into the lymph anlagen and then act as strong chemo-attractant for lymphoid cells within the secondary lymphoid organs. We next measured the protein levels of CXCL13 and CCL21 in conditioned media (CM) obtained from the bone marrow derived MSC cell line (HS-5) compared to non-conditioned

media by ELISA. MSC cells were seeded at a density of either $6x10^3$ or $12x10^3$ cells per well and kept in culture for 48 hours. We confirmed that within 48 hours $12x10^3$ MSCs were able to secrete significantly high concentrations of CCL21 (>2000pg/ml) and CXCL13 (>1000pg/ml) (Figure 5-11). These data provided additional support for exploring the interactions of MSCs and LTi cells within the tumour microenvironment.

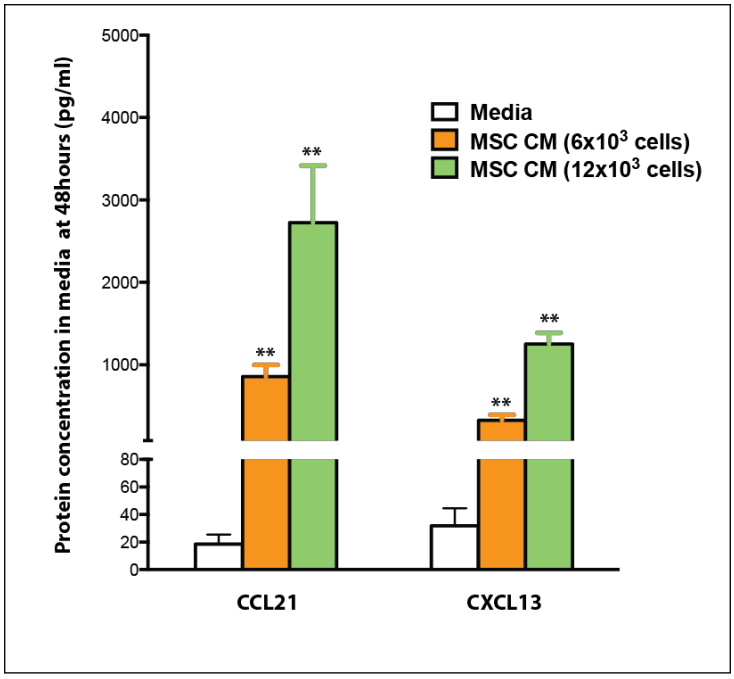

Figure 5-11: ELISA based quantification of CCL21 and CXCL13 secretion by MSCs.

CCL21 and CXCL13 concentrations were measured by ELISA. MSC cells seeded at densities of either $6x10^3$ or $12x10^3$ cells per well are labelled in orange and green, respectively. The levels were compared to media alone. Data represent means of three independent experiments ± SEM. Asterisks represent the p-values when comparing to the control groups (one-way ANOVA; ** $p \leq 0.01$).

5.6.2 CXCL13 dependent, CCL21-independent interactions between LTi and stromal cells

To further investigate the interaction of LTi cells with MSCs, we first sought to optimise our protocol for isolating LTi cells. Freshly isolated splenocytes from BALB/c mice were FACS sorted into $CD3^-$, $CD11c^-$, $B220^-$, $CD335^-$, $CD127^+$, $CD90.2^+$, $NKp46^-$LTi cells (as per the gating strategy in Figure 5-2A). We found that the yield for LTi cells was relatively low (approximately 7000 cells/spleen). Our protocol required an enrichment step by depleting for $CD11c^+$ cells using microbeads. This improved the yield to 20,000 LTi cells per spleen. The purity of the LTi cells isolated by flow cytometry was confirmed by RORγt expression using confocal immunofluorescence analysis (Figure 5-12).

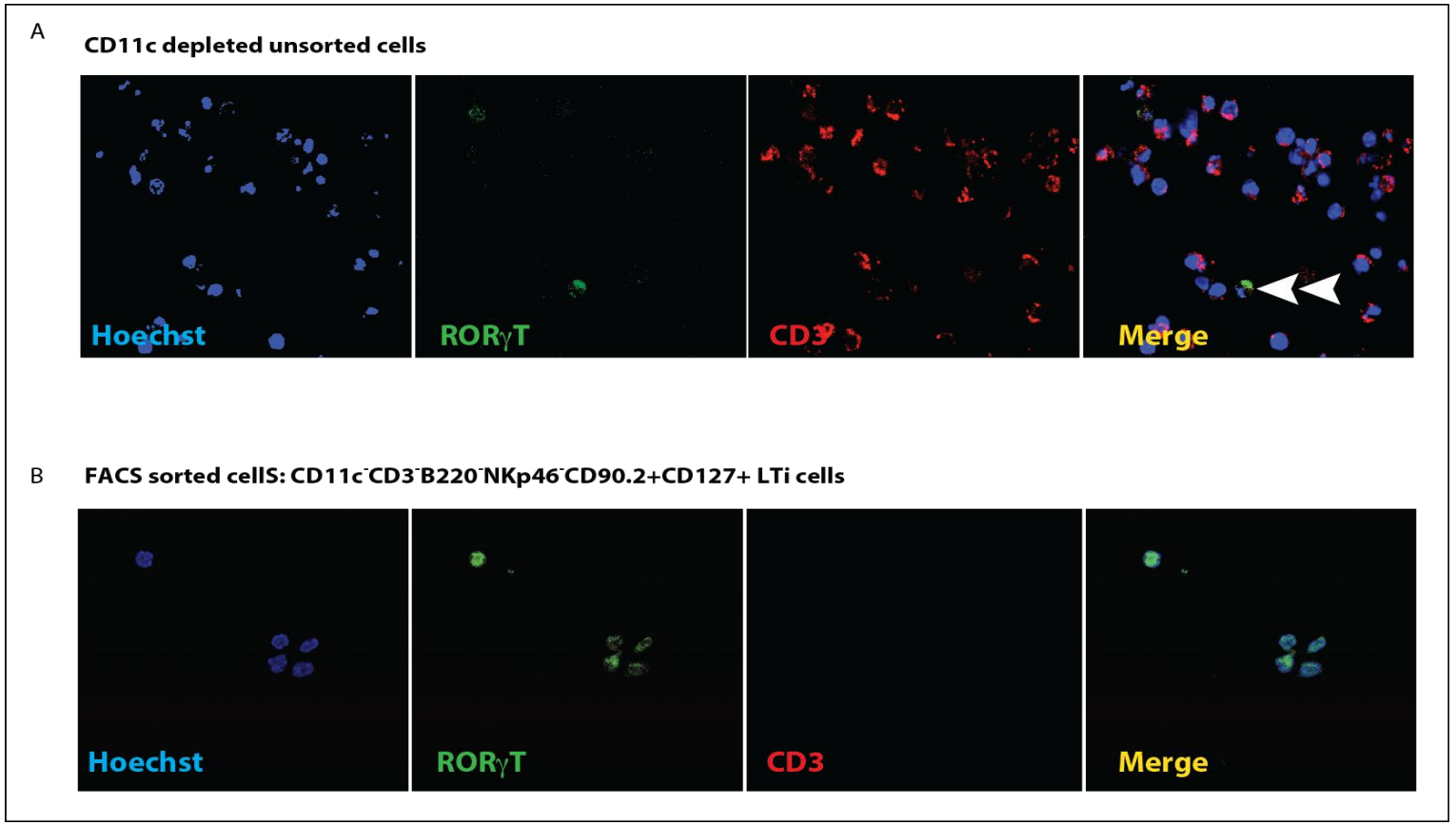

Figure 5-12: Flow cytometric sorting of $CD3^-$, $CD11c^-$, $B220^-$, $CD127^+$, $CD90.2^+$, $NKp46^-$ LTi cells

A: Immunofluorescence of unsorted CD11c-depleted splenocytes. An LTi cell (white arrow) is seen amongst $CD3^+$ cells. Bottom panel demonstrated that majority (if not all) of the sorted cells express the nuclear transcription factor RORγt.

5.6.2.1 LTi cell clustering around MSCs

Owing to the sparsity of the LTi cell population, various migration assays to study MSC and LTi cells interactions were difficult to interpret. However, an interaction between the two cells was observed when freshly isolated splenic LTi cells ($CD3^-$, $CD11c^-$, $B220^-$, $CD127^+$, $CD90.2^+$, $NKp46^-$ cells) were co-cultured with MSCs growing in 9.4 x 10.7 mm ibidi^{TM} 8-well μ-Slide chambers and monitored by time-lapse microscopy with images captured at regular intervals for 10 hours. LTi cells were observed to cluster around MSCs (Figure 5-13A, upper panel), remaining closely associated for as long as 7 hours (Figure 5-13A, red arrow in lower panel). We observed that this clustering was not evident with a co-culture of $CD11c^+$ cells (collected following the CD11c depletion step) and MSC cells (Figure 5-13B). The clustering of LTi cells around MSCs was quantified by measuring the area of the frame occupied by the MSC and or LTi cells (Figure 5-13C) (see Methods & Material section 3.2.11.2). The mean value (area occupied by cells) was found to reduce with increased incubation time, as LTi-MSC clustering occurred (Figure 5-13D). The extent of LTi-MSC clustering was then measured as the rate of reduction in the area occupied by cells during the time-lapse series.

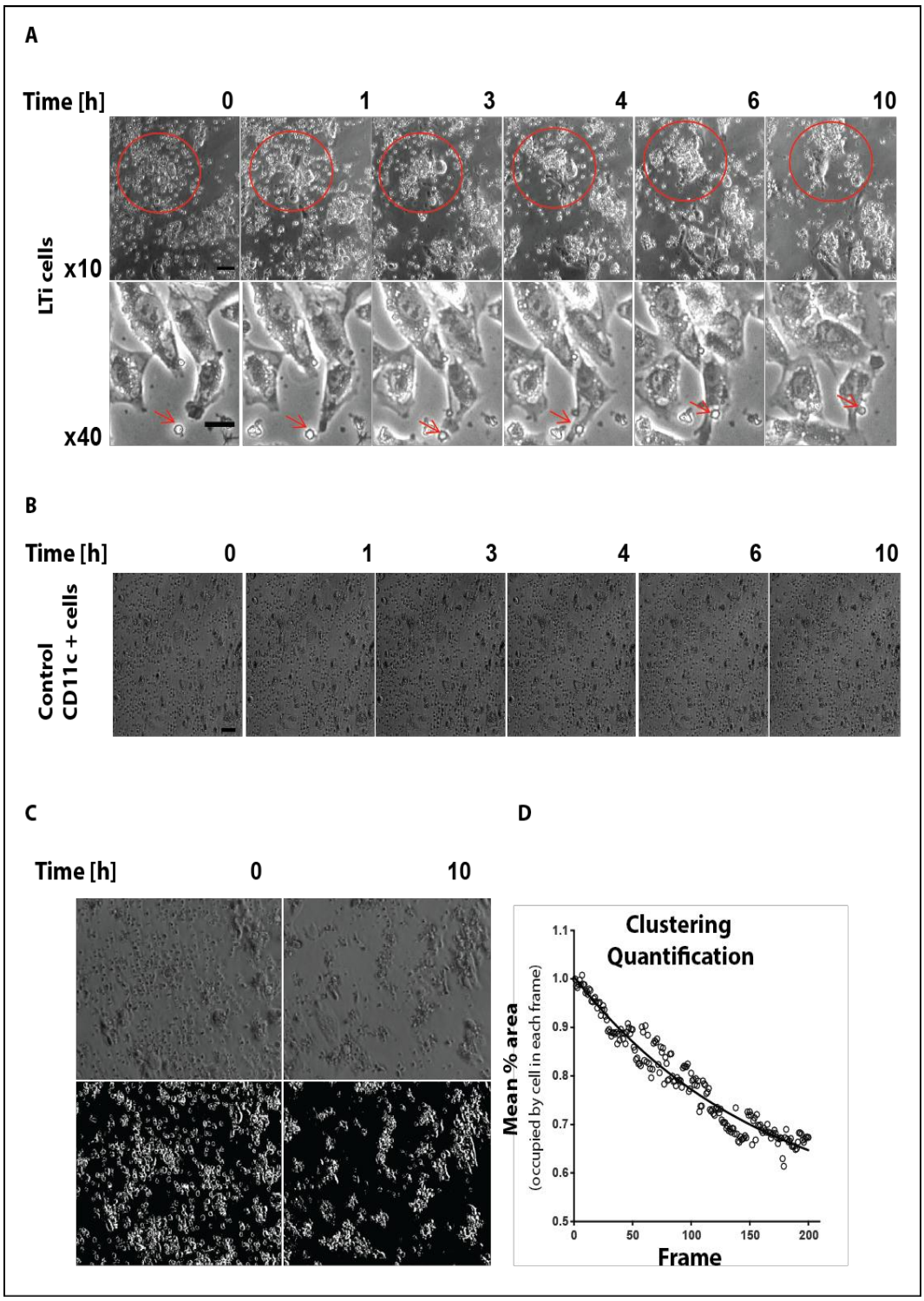

Figure 5-13: CXCL13-dependent interactions between LTi cells and stromal cells *in vitro*.

A: Time-lapse microscopy of sorted splenic LTi cells ($CD3^-$, $CD11c^-$, $B220^-$, $NKp46^-$, $CD127^+$, $CD90.2^+$) co-cultured with MSC cells over a 10h period. Scale bar: upper panel = 50□m; lower panel = 20□m. B: Representative phase contrast images (upper panel) from co-culture time-lapse experiments and associated binary images (lower panel) used for the quantification of cell clustering. C: The graph summarises the change in mean area of the image field occupied by cells over the course of time-lapse experiments and was generated from binary image data. The area occupied by cells falls as clustering increases.

At the end of these experiments, we also assessed the effect of MSC-LTi cells interaction on the secretion of CCL21 and CXCL13 by the stromal cells by measuring the protein levels of the chemokine in the cell culture supernatants at 48 hours by ELISA. CXCL13 secretion by the stromal cells was enhanced significantly when co-cultured with LTi cells at 48 hours (~ 4-fold increase, $p \leq 0.05$, paired t-test; Figure 4A). Although a similar trend was seen in the CCL21 secretion, this was not statistically significant.

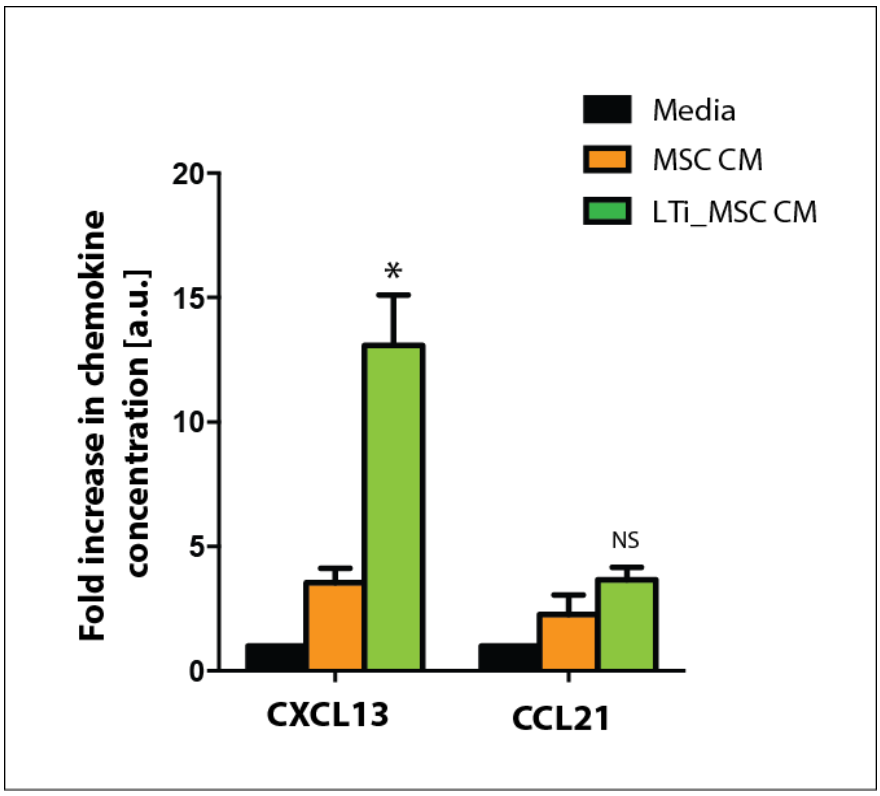

Figure 5-14: Effect on MSC-LTi cells interactions on lymphoid chemokine secretion by stromal cells

Cell culture supernatants from co-culture experiments of MSC and LTi cells were analysed after 48h to determine levels of CXCL13 and CCL21 by ELISA (*p=0.04, paired t-test; NS= non significant, paired t-test). Data represent means ± SEM. Asterisks represent the p-values when comparing to MSC CM (paired t-test: * $p \leq 0.05$, NS= Non significant).

5.6.2.2 Effect of chemokine knockdown on LTi clustering in vitro

We then investigated how short interfering RNA (siRNA) knockdown of CXCL13 and CCL21 in MSCs would affect the extent of LTi clustering around MSCs. Three siRNAs for either chemokines were evaluated. MSC cells cultured in 6-well plates to 30% confluency were transiently transfected with one of three different siRNAs against either CXCL13 (Figure 5-15A), CCL21 (Figure 5-15B) or with a control non-targeting scrambled siRNA. Chemokines levels in the cell supernatants were measured by ELISA 24 hours after transfection. Protein expression of both CXCL13 and CCL21 by the MSCs was downregulated significantly by all targeting siRNAs (Figure 5-15). However, siRNA-2 for CXCL13 and and siRNA-1 for CCL21 provided the maximum gene knockdown achieving >90% reduction in the chemokine levels. We therefore used these siRNAs for subsequent experiments.

We observed in the co-culture experiments of MSCs and LTi cells, that knockdown of CXCL13 resulted in a decrease of LTi clustering around MSCs (Figure 5-15C & D, $p<1x10^{-4}$). In contrast knockdown of CCL21 did not affect LTi clustering. These data suggested a non-redundant role for CXCL13 (i.e. promotion of clustering of LTi around MSCs), which may be synergistic with the initial CCL21-mediated recruitment of LTi cells into the primary tumour (Figure 5-6).

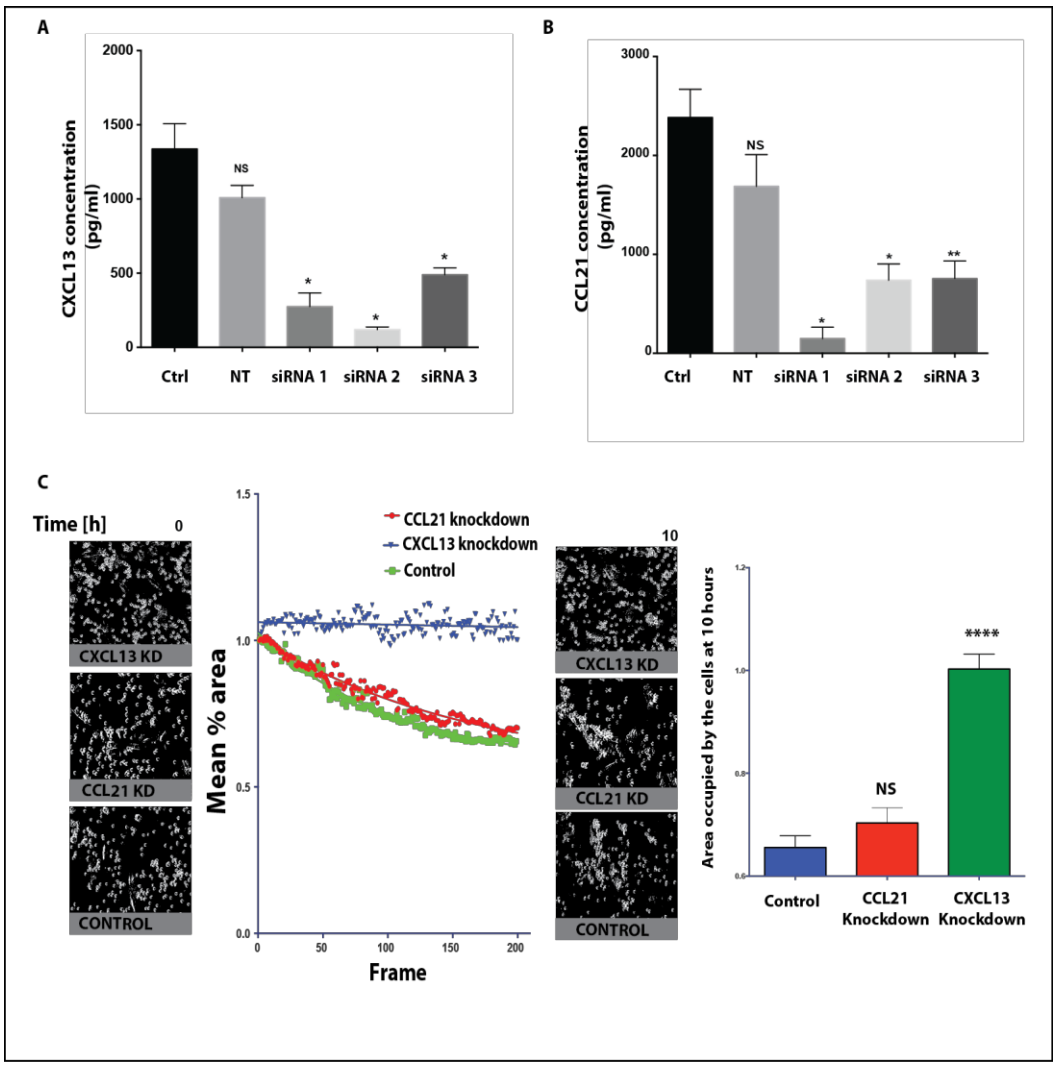

Figure 5-15: Effect on LTi clustering from chemokine knockdown in MSCs.

A, **B**: MSC cells were transfected with non targeting (NT) control or siRNAs specific for CXCL13 or CCL21 (CXCL13 siRNA: si-20725, si-20726, si-20727 or CCL21 siRNA: si-12605, si-12606, si-12607 respectively). Cell culture supernatants were analysed by ELISA at 48 hours (* $p \leq 0.05$, ** $p \leq 0.01$, paired t-test). Data represent means ± SEM. Asterisks represent the p-values when comparing to the control group (paired t-test: * $p \leq 0.05$, ** $p \leq 0.01$, NS= Non significant) **C:** Summary of time-lapse microscopy cell clustering experiments showing co-cultures of sorted splenic LTi cells and siRNA-transfected MSCs (with either non-targeting siRNAs or siRNAs specific for CCL21 or CXCL13). One independent experiment, representative of three (n=3 fields for each group) is shown. **D:** Quantification data reporting on the area occupied by the cells in the last frame (i.e. at 10 hours). Asterisks represent the p-values when comparing to the control group (one-way AVONA ****$p<10^{-4}$, NS = non significant).

5.6.2.3 Effect of chemokine knockdown on LTi function within the 4T1.2 breast cancer tumour model

The use of high-resolution multi-photon imaging of tumours *in vivo* is now an established and powerful technique to assess cell-cell behaviour at single cell resolution. To assess the interaction between LTi and MSC cells intravitally within our syngeneic mouse model of triple negative breast cancer, we utilized the recently reported mammary imaging window (MIW) technique [258] with multi-photon imaging. The MIW consists of a titanium ring which forms a mount for a glass coverslip. The mount has holes which facilitate suturing into the skin, whereas the glass coverslip assures the optimal working distance and refraction index for high resolution imaging. Studies have shown that tumours with MIW implants do not show inflammation, or a change in growth and microenvironments scored at 1–9 days after the implantation procedure [258].

4T1.2 tumour cells were injected into the mammary fat pad subcutaneously and a MIW was surgically placed over the mammary tumour 10 days after tumour establishment (Figure 5-16A). Treatment with either a neutralizing antibody for CXCL13 or isotype control antibody was initiated one day after cell implantation, given every three days. Fluorescently labelled MSC cells (cell tracker orange CMTMR) were injected via the tail-vein at day 22, 48 hours prior to multi-photon imaging. Twenty four hours later freshly isolated splenic LTi cells (labelled with cell tracker green CMFDA) were injected via the tail-vein (Figure 5-16B).

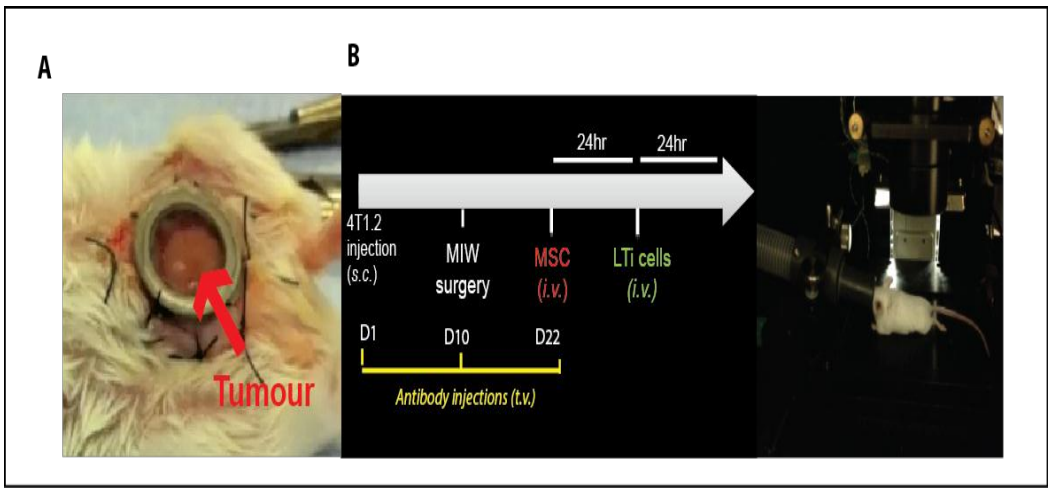

Figure 5-16: Multi-photon imaging of using mammary imaging window within the 4T1.2 tumour model

A: Mammary imaging window (MIW) consisting of a coverslip mounted on top of a titanium ring was surgically implanted on top of the developing mammary tumour. **B**: Representation of the experimental set up: 48hours prior to imaging $1x10^6$ labelled MSC cells (*red cell tracker orange CMTMR dye*) were injected intravenously. into all tumour-bearing mice; followed 24hours later by injecting $1x10^5$ sorted splenic LTi cells (*green cell tracker dye*). The MSC-LTi cell interaction was then imaged under the MIW using a multi-photon microscope over 3 consecutive days.

Within the experimental cohort of mice injected with a neutralizing anti-CXCL13 antibody, LTi and MSC cells were seen within the primary tumour but not in direct contact with each other; this was in contrast to the cohort injected with the control antibody, where LTi cells (likely to be clusters i.e. not single cells, similar in size to that detected in the human tissues stained in Chapter 3 Figure 4-2) and MSC cells were seen in close proximity within the primary tumour (Figure 5-17; $p<10^{-4}$ unpaired t-test).

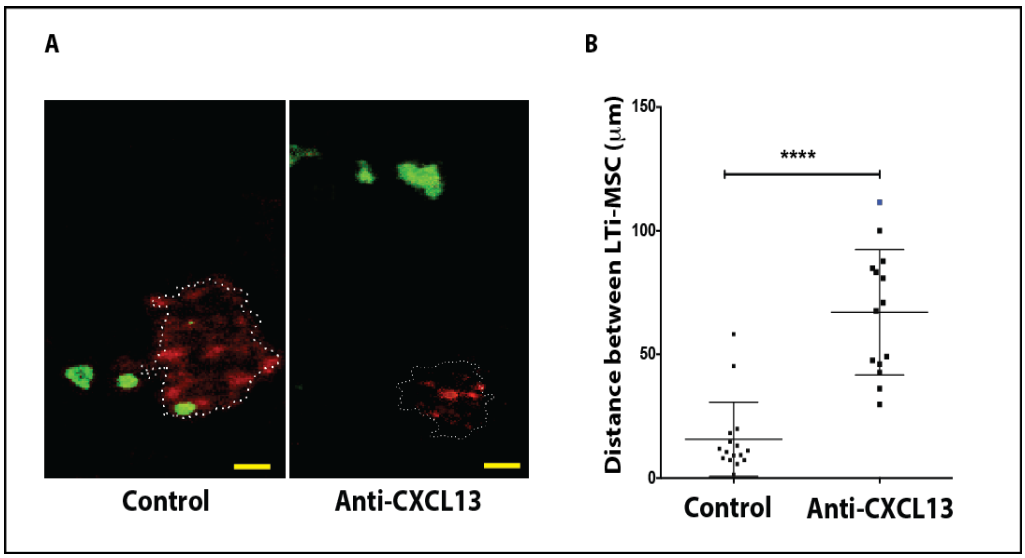

Figure 5-17: Multi-photon imaging of LTi-MSC cell interactions *in vivo* within the 4T1.2 tumour model.

BALB/C mice were injected s.c. with 1×10^6 4T1.2 breast cancer cells. Mice (*n=6*) were treated with an anti-murine anti-CXCL13 antibody (30µg/ml in PBS; R&D systems) or goat IgG antibody via t.v. every other day for 22 days. **A**: Representative combined multi-photon images from the green and red channels using an imageJ function are shown from both experimental groups (IgG control and anti-CXCL13 treatment). **B**: The average distance between the centre of imaged MSC and LTi cells is demonstrated. Data represent means ± SEM. Asterisks represent the p-values when comparing to the control (unpaired t-test: ****$p\leq10^{-4}$).

These in vivo imaging results, obtained from within the primary tumour, further support the *in vitro* observation of a CXCL13-dependent clustering of LTi cells around the mesenchymal stromal cells. This CXCL13-dependent LTi-MSC interaction can then initiate a positive feedback loop whereby further CXCL13 secretion by the stromal cells is stimulated.

5.7 Discussion

Following on from the results presented in chapter 4, the aims of the experiments presented in this chapter were to explore the relevance of LTi cells in murine triple negative breast cancers, a type of breast cancer that has been described to be more aggressive than other kinds of breast cancers. We confirmed the lymphotropic metastatic capacity of the 4T1.2 cell line within a syngeneic mouse model; thereby providing an attractive model system to further investigate the mechanistic relationship between TNBCs and LTi cells *in vivo*.

Our data confirm that effective recruitment of LTi cells into the primary tumours was primarily dependent on the chemokine CCL21 (Figure 5-6); in addition to the observation that the peak in serum CCL21 levels (Figure 5-4) was closely followed by a peak in the number of LTi cells within tumours (Figure 5-2C). It was interesting to note that this CCL21 dependence was present from an early stage of tumour progression – i.e. before lymph node metastases developed within our 4T1.2 mouse model. The CCL21/CCR7 axis has been shown to play a key role in the progression of a number of different malignancies [88,100,259]. Work by Shields et al described, in a murine model of melanoma, a novel mechanism by which CCL21-expressing tumours transform their microenvironment into that of a lymphoid-like tissue to create a tolerant milieu that promotes immune evasion [113]. Consistent with our data, the authors found that higher expression of CCL21 within tumours was correlated with LTi cell recruitment.

Given the lineage relationship between MSC, which are known to infiltrate tumours in large numbers [243-247], and LTo cells that are known to interact with LTi

cells, we hypothesized that LTi cells recruited into the tumours may interact with bone marrow derived MSCs. In support of this we confirmed that our MSC cells express the LTβR and secrete high levels of the lymphoid chemokines, CXCL13 and CCL21. In line with this, previous studies reporting on the initiation of foetal lymphoid tissue organogenesis have shown that LTi cells activate LTo cells by ligating LTβR on these stromal cells. Once activated, stromal cells secrete chemokines (e.g., CXCL13, CCL21, and CCL19), increase expression of adhesion molecules such as VCAM-1, ICAM-1, and MAdCAM-1, as well as secrete lymphangiogeneic factors such a VEGF-C [120,123,227]. The co-clustering between these innate lymphoid cells and stromal cells is induced in a CXCL13-dependent fashion, shown *in vitro* by our time-lapse microscopy analysis (Figure 5-15), and *in vivo* by multi-photon imaging through the mammary window chamber –i.e. within the tumour microenvironment (Figure 5-17). We therefore concluded that there is a non-redundant function of CXCL13, produced as a consequence of the initial CCL21-mediated recruitment of LTi cells into the primary tumour. Although our results demonstrate that LTi interaction with the surrounding stromal cells is dependent on CXCL13, it is important to highlight here that but I do not propose that the secretion of CXCL13 within tumours is a function exclusive to MSC cells. For example, a recent study proposed that CXCL13-producing $CD4^+$ follicular helper T-cells infiltrating breast tumours were involved in promoting TLS within tumours [177]. Further research into the relationship between the LTi and follicular helper T-cells may provide important information to understand the complex and potential interactions between innate and adaptive components of the immune response to tumours.

The co-clustering itself further amplifies, in a positive feedback fashion, the production of CXCL13 within the mesenchymal stromal cells (Figure 3A) and may provide an explanation for the second peak in serum CXCL13 levels seen during tumour progression in vivo (Figure 5-4). Interestingly our *in vivo* data also showed that although anti-CXCL13 treatment did not affect LTi recruitment/migration at an early time point (i.e. day 14); the numbers of intratumoural LTi cells were much higher amongst this cohort compared to the control groups at day 21, with concomitant reduction in lymph node metastases (Figure 5-6). Although speculative, these results may provide some evidence for the role of CXCL13 on LTi migration – i.e. within the anti-CXCL13 treated cohort despite an effective CCL21-dependent recruitment of LTi cells into the primary, there is defective migration of LTi cells out of the tumour into the draining lymph nodes. To me, this observation also raises the fascinating "pied piper" hypothesis, whereby CXCL13-dependent LTi cell migration into the lymph nodes subsequently results in tumours cells following. Using the MIW technique in transgenic mice with fluorescent RORγt^{+} LTi cells may allow for this hypothesis to be investigated.

Both the CCL21-CCR7 and CXCL13-CXCR5 axes are reported as being highly expressed in clinical samples from numerous tumour types [88,100,259-261]; but there is conflicting evidence on how they affect tumour progression. For example, whilst high CXCL13-CXCR5 expression has been reported to positively correlate with classical determinants of poor prognosis, such as high grade, hormone receptor negativity and axillary node involvement [260,262], it appears to serve, counter-intuitively, as a good prognostic marker within this subgroup of high risk breast cancer patients [262]. In the context of the tumour microenvironment, the role of

immune cells and/or chemokines is particularly complex (reviewed by [263,264]), as a prime example of CCL2 being able to promote tumour metastasis [265] as well as immune-mediated tumour rejection [266]. Genomic profiling studies have verified the role of CXCL13 as a good prognostic marker for patients with triple negative breast cancer [267,268]. However we found that although not affecting tumour growth itself, CXCL13 and for that matter CCL21 promoted lymph node metastases within our triple negative mouse model (Figure 5-8).

However, there are a few important additional factors to consider, given the multivariate factors that influence the heterogeneous clinical outcome in patients. Firstly, these chemokines can influence anti-tumour immunity by acting as powerful chemoattractants for lymphocytes[177]. As discussed in chapter 4.5, basal-like breast cancers/TNBCs frequently bear a prominent associated tumoural lymphocytic infiltrate. The presence of TILs has been described as key prognostic and predictive marker for specific breast cancer subtypes [171,177,235,269]. This is in line with our own *in vivo* data demonstrating a significant decrease in the number of infiltrating $CD3^+$ and $CD19^+$ lymphocytes within the primary carcinoma in mice treated with a neutralizing antibody for CCL21 or CXCL13 (Figure 5-7). Additionally, the possibility that early tumour cell lymphatic vessel invasion in response to an increase in CXCL13 levels within the cancer microenvironment may effectively cross-present tumour antigens in the draining lymph nodes thus acting as a powerful mitogen for responding T-cells requires further investigation.

There are some limitations to the data presented in this chapter that necessitate some caution in the interpretation of the findings. Firstly, it is important to point out the caveat of assuming that the changes in the serum chemokine levels

represent also the changes occurring more locally within the tumour microenvironment. While a number of studies have reported overexpression of chemokine receptors and ligands within the tumour stroma being associated with progression of various cancer types (see section 1.3.2), few studies of serum levels have yielded significant links to the prognosis of cancer or been translated into clinically meaningful biomarkers. It would seem that studies analysing differences in local expression of chemokines, compared to those measuring chemokine levels in the serum, offer a stronger, more consistent association between cancer prognosis and changes in patterns of chemokines ligands and receptors in the primary tumor and metastatic lesions.

Secondly, although embryonic and adult splenic LTi cells have been reported to co-express both CXCR5 and CCR7 [241], our results could have been further supported by investigating the expression of these receptors on tumoural LTi cells themselves; or comparing the expression of LTi cells from tumour bearing with non tumour bearing mice. Fetal LTi and adult LTi cells are known to differ and similarly within our own group we have seen differences in the expression of some co-stimulatory molecules on splenic LTi from tumour bearing compared to splenic LTi cells from non-tumour bearing mice (discussed in further detail in Chapter 7:); highlighting the need for a more in-depth phenotyping of tumoural LTi cells themselves.

In summary, from the data presented in this chapter, our model system introduced in chapter 4.5 can be further illustrated to show the CCL21-dependent recruitment of LTi cells into tumours with a subsequent CXCL13-dependent interaction between the tumoural LTi and stromal cells.

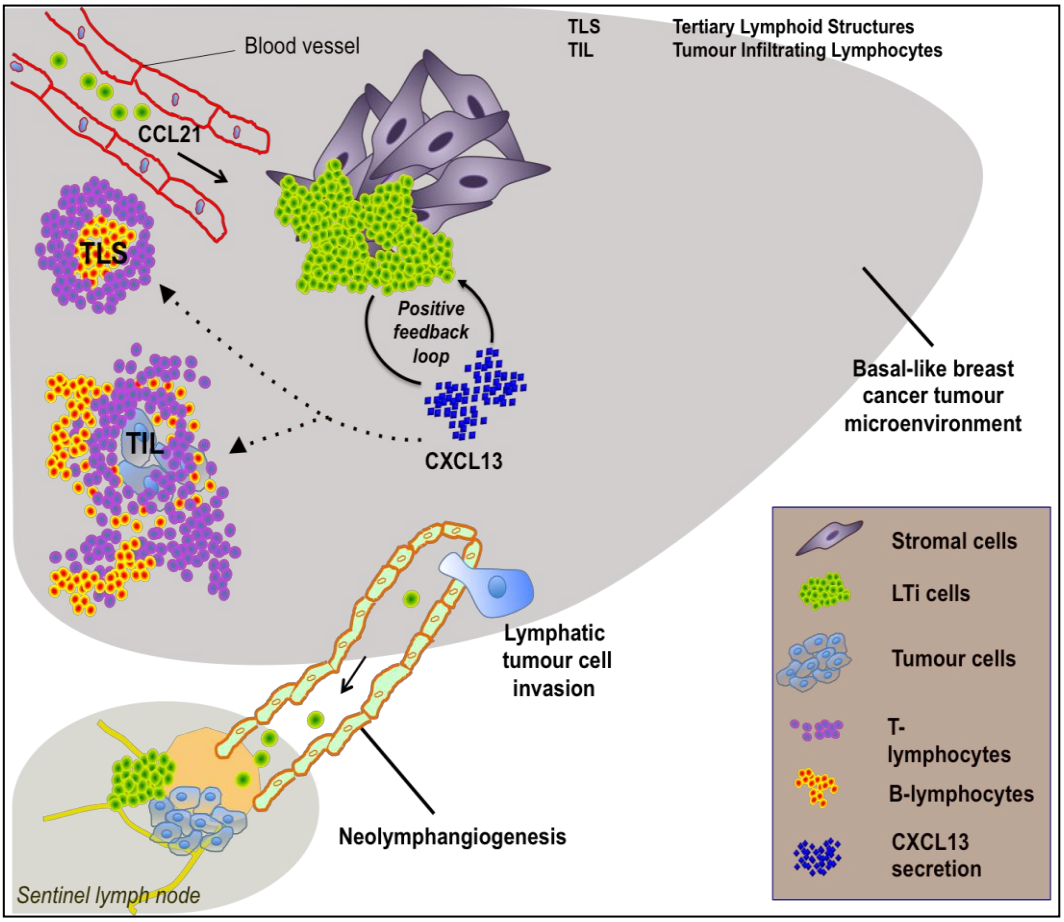

Figure 5-18: Schematic illustration of our proposed model for the role of LTi cells within triple negative breast cancers.

Recruitment of LTi cells into the primary tumours is primarily dependent on CCL21. Following a CXCL13-dependent LTi-stromal cell interaction a positive feedback loop develops which helps promote lymph tumour cell invasion and alongside CCL21 also acts as a strong chemoattractant for tumour infiltrating lymphocytes.

Chapter 6: Lymphoid tissue inducer cells promote lymphatic invasion of breast cancer cells via a CXCL13- dependent RANK-RANKL axis

The aim of this chapter was to further investigate the downstream mechanisms that underlie the relationship between chemokine-dependent lymphatic metastasis and LTi cell recruitment.

6.1 Tumour cells are not the source of CXCL13 and CCL21

To test the relationship between CXCL13, CCL21 and tumour cell invasion *in vitro*, we first screened a panel of human breast cancer cell lines using a cytokine antibody array that simultaneously detects 80 cytokines and chemokines. We confirmed that cancer cells were not the source of CXCL13 and CCL21 chemokines (Figure 6-1). To validate our mouse model of breast cancer, we quantified by ELISA the levels of CXCL13 and CCL21 within the conditioned media from our murine breast cancer cell line (4T1.2). For our positive control, we obtained a murine bone marrow derived stromal cell line (ST2s), from Professor Agi Grigoriadis, Craniofacial Development& Stem Cell Biology, KCL. Although high levels of CCL21 and CXCL13 were seen in the conditioned media from the stromal cell line, no significant increase compared to the negative control (media alone) was seen in the conditioned media from the 4T1.2 cell line. These findings confirmed that the source of CXCL13 and CCL21 was likely to be stromal cells within tumours.

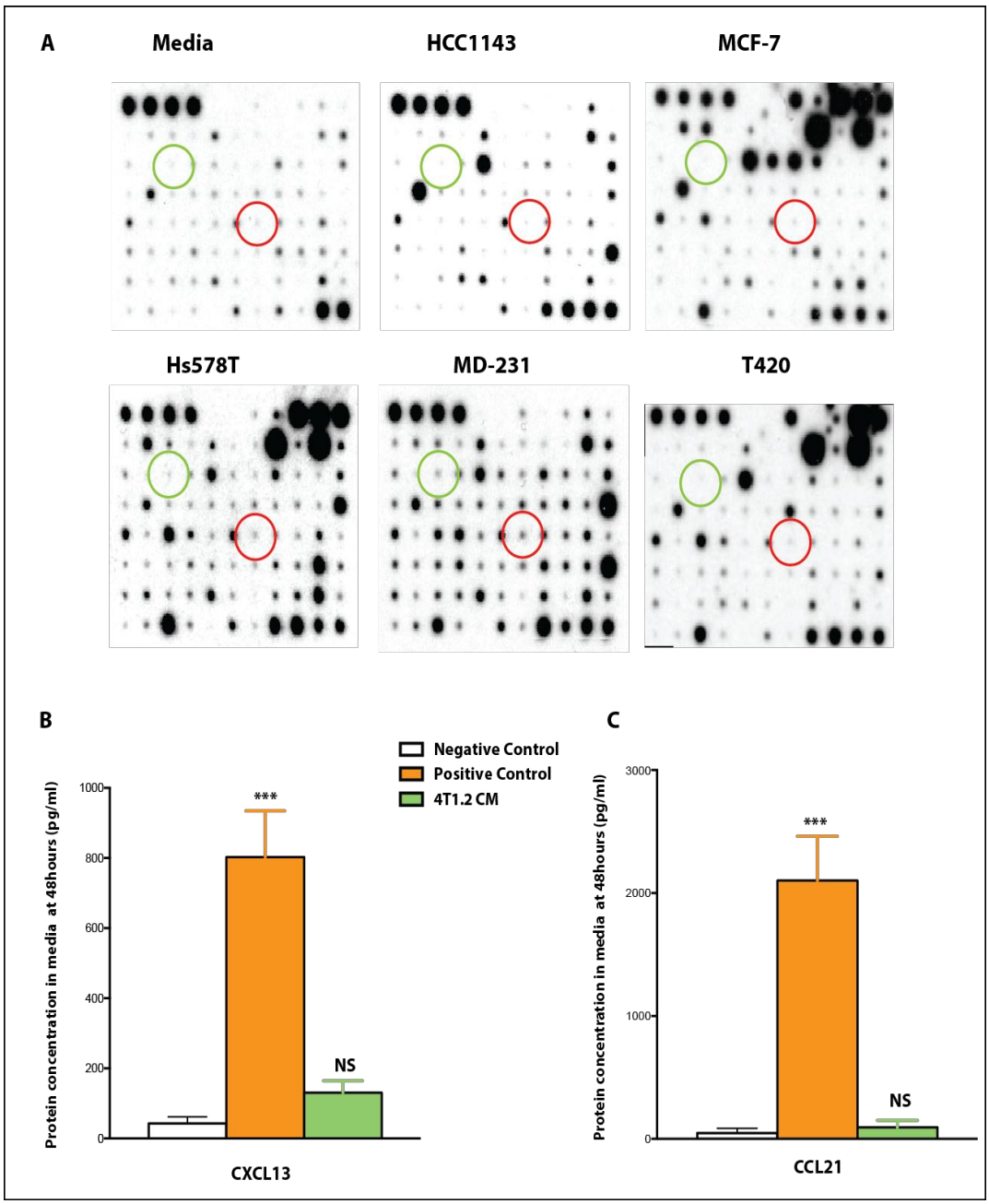

Figure 6-1: Analysis of cytokines secretion by human and murine breast cancer cell lines

Conditioned medium was collected from various human breast cancer cell lines at 48 hours after plating 50,000 cells in 6 well plates. Cytokine array membranes were incubated with 1 ml conditioned medium. Non-conditioned media represents the negative control. **A:** Representative array readouts are shown. Upper left four spots and lower right two spots serve as positive controls on each membrane. The 80 human inflammatory cytokines examined included CXCL13 (red circles) and CCL21 (green circles). **B & C:** ELISA quantification of CXCL13 and CCL21 chemokine levels in the conditioned media from the 4T1.2 cell line. Positive control = murine stromal cell line (ST2s); Negative control = media alone**.** Data represent means of three independent experiments ± SEM. Asterisks represent the p-values when comparing to the negative control (one-way ANOVA: *** $p \leq 0.001$, NS – non significant).

6.2 Effect of CXCL13 and CCL21 on tumour cell invasion

Considering that invasion across the basement membrane by cancer cells is a critical process in tumour metastasis and our in vivo results in Chapter 4 section 5.5.3 suggested an inhibitory effect of CXCL13 or CCL21 chemokine blockade on 4T1.2 tumour cell invasion into the draining lymph node, we used an extracellular matrix invasion assay, to directly investigate the effects of CXCL13 and CCL21 on 4T1.2 cancer cell invasion (see Chapter 2 section 3.2.9).

4T1.2 tumour cells were incubated with increasing concentrations of CCL21, CXCL13 or epidermal growth factor (EGF) (positive control for 4T1.2 invasion). A mouse embryonic fibroblast cell line, NIH3T3 served as a non-invasive control. The invasion assay used was based on the Boyden chamber principal, as demonstrated in Figure 6-2A. Each insert contains an 8μm pore size polycarbonate membrane coated with a thin layer of extracellular matrix (ECM). The ECM layer occludes the membrane pores, blocking non-invasive cells from migrating through. Invasive cells, on the other hand, migrate through the ECM layer and cling to the bottom of the polycarbonate membrane. Invading cells on the bottom of the insert membrane are then dissociated from the membrane when incubated with cell detachment buffer and subsequently lysed and detected by a green fluorescent dye, which exhibits strong fluorescence enhancement when bound to cellular nucleic acids. As expected, EGF-dependent invasion was detected with 4T1.2 cell line at all concentrations between 10-100ng/ml. In contrast, addition of recombinant CXCL13 or CCL21 did not significantly increase the invasion of 4T1.2 cells at any concentrations between 10-100ng/ml (Figure 6-2B). At the end of the experiment, the invading cells were stained with

1% crystal violet in PBS, further confirming that CXCL13 or CCL21 did not affect the migration of 4T1.2 cells across the ECM membrane (Figure 6-2C).

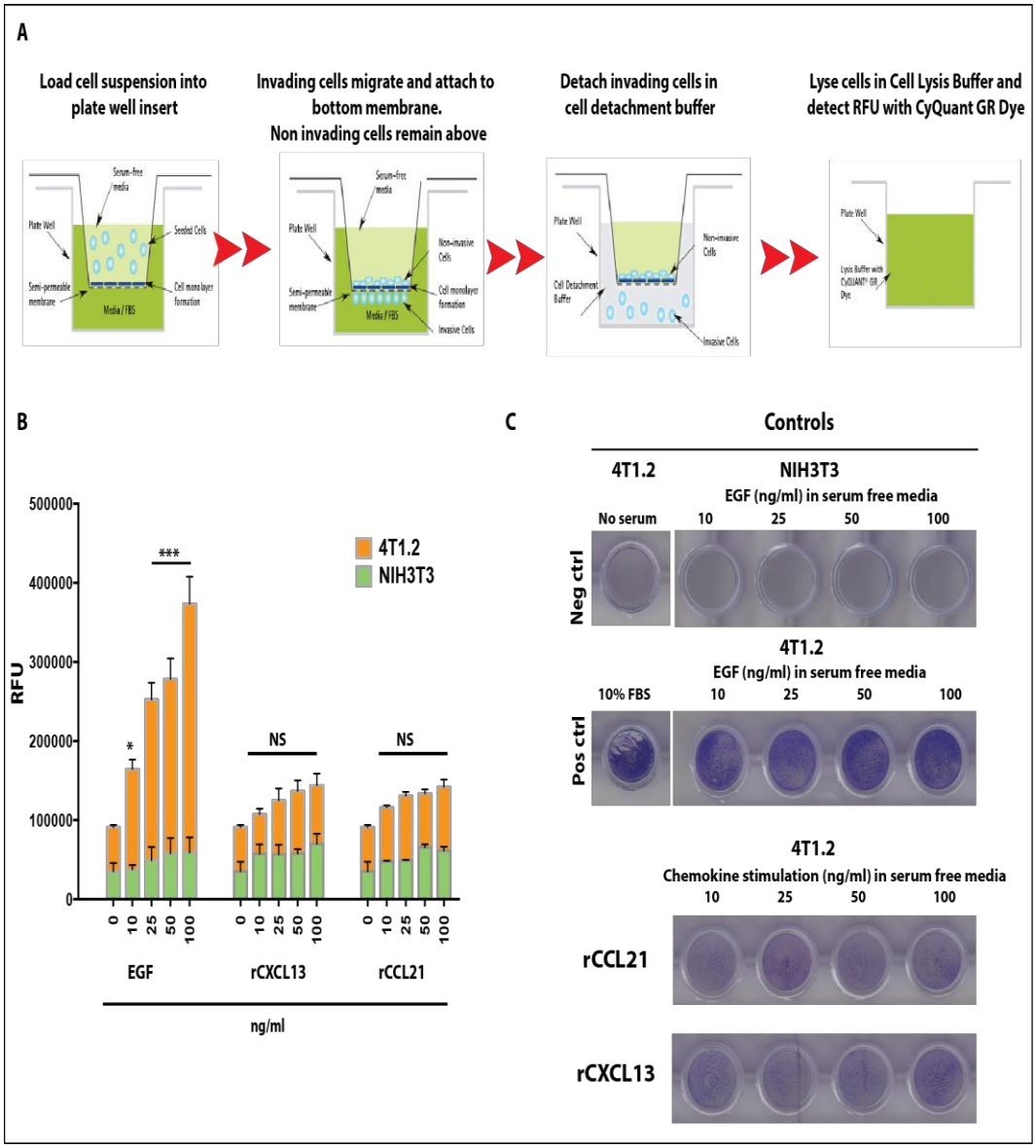

Figure 6-2: Effect of CXCL13 and CCL21 on tumour cell invasion.

A: Schematic presentation of the ECMatrix cell invasion chamber composed of a ECM coated transwell insert containing an 8µm pore size membrane. Cells were seeded at high density into the upper chamber. Cells were allowed to invade through membrane for 24 hours at 37ºC in a 5% CO_2 incubator. After 24 hours the cell migration was measured using a fluorescence reader after labeling the lysed cells with a green fluorescent dye. **B**: Cell invasion assay results are shown. An increase in the relative fluorescent units (RFU) indicates more invasion of cells through the extracellular matrix membrane. NIH3T3 cells (green bars) were used as a non-invasive control. Data represent means ± SEM. **C**: Invading cells were visualized by crystal violet staining. Asterisks represent the p-values when comparing to the control groups (one-way ANOVA: *** $p \leq 0.001$, NS – non significant).

6.3 Effect of CXCL13 and CCL21 on tumour cell migration

We had observed that stimulation of 4T1.2 cells with conditioned media from MSC cells resulted in tumour cells developing an elongated morphology which was accompanied by membrane ruffling, giving rise to the formation of lamellipodia and filapodia; visualised by phase contrast microscopy (Figure 6-3A). This change in morphology was quantified by measuring the circularity of cells, calculated using the formula: $4\pi \times (\text{area}/\text{perimeter}^2)$. This derives a value between 0 - 1 with values that tend towards one representing highly circular shapes and those that tend towards zero representing highly elongated shapes. A significant decrease in the circularity of the 4T1.2 tumour cells was seen following stimulation with MSC-CM as compared to unstimulated control tumour cells ($p<10^{-4}$, unpaired t-test; Figure 6-3B).

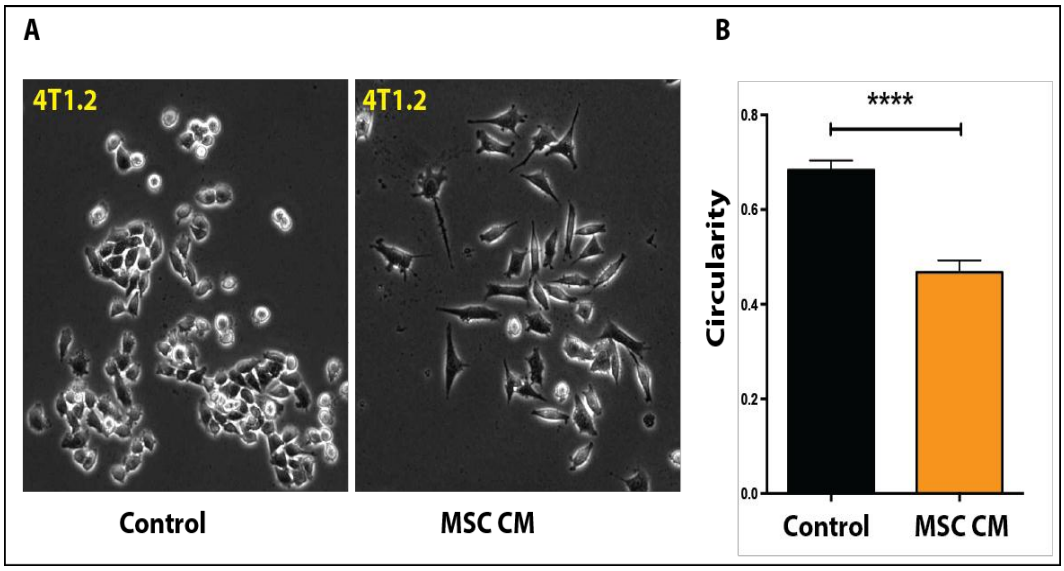

Figure 6-3: Stimulation with MSC CM induces changes in 4T1.2 cell morphology

A: Phase contrast micrograph images taken 6 hours after stimulation of 4T1.2 cells with control media or MSC-CM. **B**: Quantification of the circularity of 4T1.2 cells (defined by $4\pi \times (\text{area}/\text{perimeter}^2)$) within each group. Data represent means ± SEM Asterisks represent the p-values when comparing to the control (unpaired t-test: **** $p\leq10^{-4}$). CM = conditioned media.

An epithelial-mesenchymal transition (EMT) is a physiological process that allows a non-migratory epithelial cell to undergo profound morphological transformation into highly migratory, invasive mesenchymal-like cells. EMT involves a cascade of genetic programs in epithelial cells which eventually leads to loss of expression of the epithelial markers, including E-cadherin and cytokeratins; with concomitantly, gain in expression of mesenchymal-associated proteins, such as fibronectin and vimentin[270]. We observed by confocal microscopy and western blotting that the change in morphology of 4T1.2 cells was associated with an increase in the expression of vimentin, a classical marker of EMT (Figure 6-4A &B). Vimentin expression was significantly increased in cells cultured with MSC-CM at 4hours (< 6-fold increase, Figure 6-4C).

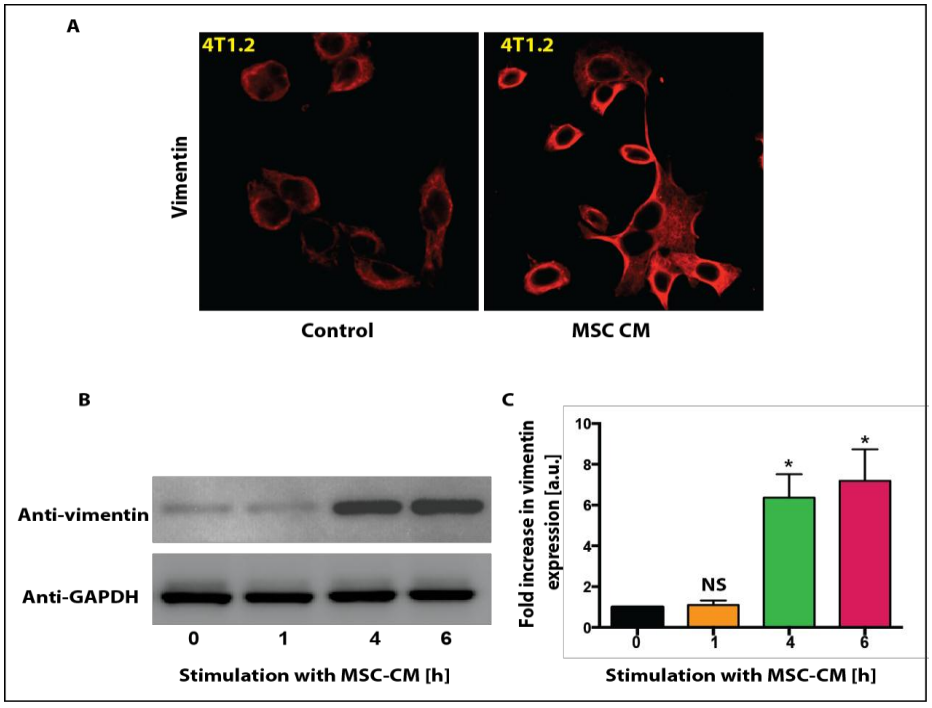

Figure 6-4: Stimulation of 4T1.2 cells with MSC CM induces upregulation of vimentin expression

A: Confocal micrograph for vimentin expression of 4T1.2 cells cultured with control media or MSC CM for at least 6 hours. **B:** Representative immunoblot illustrating the effect of MSC CM on vimentin expression on 4T1.2 cells. **C:** Quantification of the vimentin expression shown as a fold increase compared to time 0. Data represent means ± SEM Asterisks represent the p-values when comparing to 0h (paired t-test: *p<0.05; Ns= non significant). GAPDH served as a loading control.

To test if CXCL13 or CCL21 chemokines within the MSC CM directly affected tumour cell migration within our 4T1.2 breast cancer model, we performed time-lapse microscopy experiments. The conditioned media for these stimulation experiments was taken from MSC cells seeded at a density of 12 $x10^3$ and incubated for 48 hours. The protein concentration of CCL21 and CXCL13 within this media was approximately 3ng/ml and 1ng/ml respectively (see Figure 5-11). 4T1.2 tumour cells were plated in 6-well plates and stimulated with control media, MSC CM (positive control), rCXCL13 (1ng/ml or 25ng/ml) or rCCL21 (3ng/ml or 25 ng/ml) 6 hours prior to time-lapse microscopy. Interactive tracking of cells from time-lapse videos was performed using the ImageJ Manual Tracking plugin in order to generate trajectory data for the analysis of cell migration (Figure 6-5).

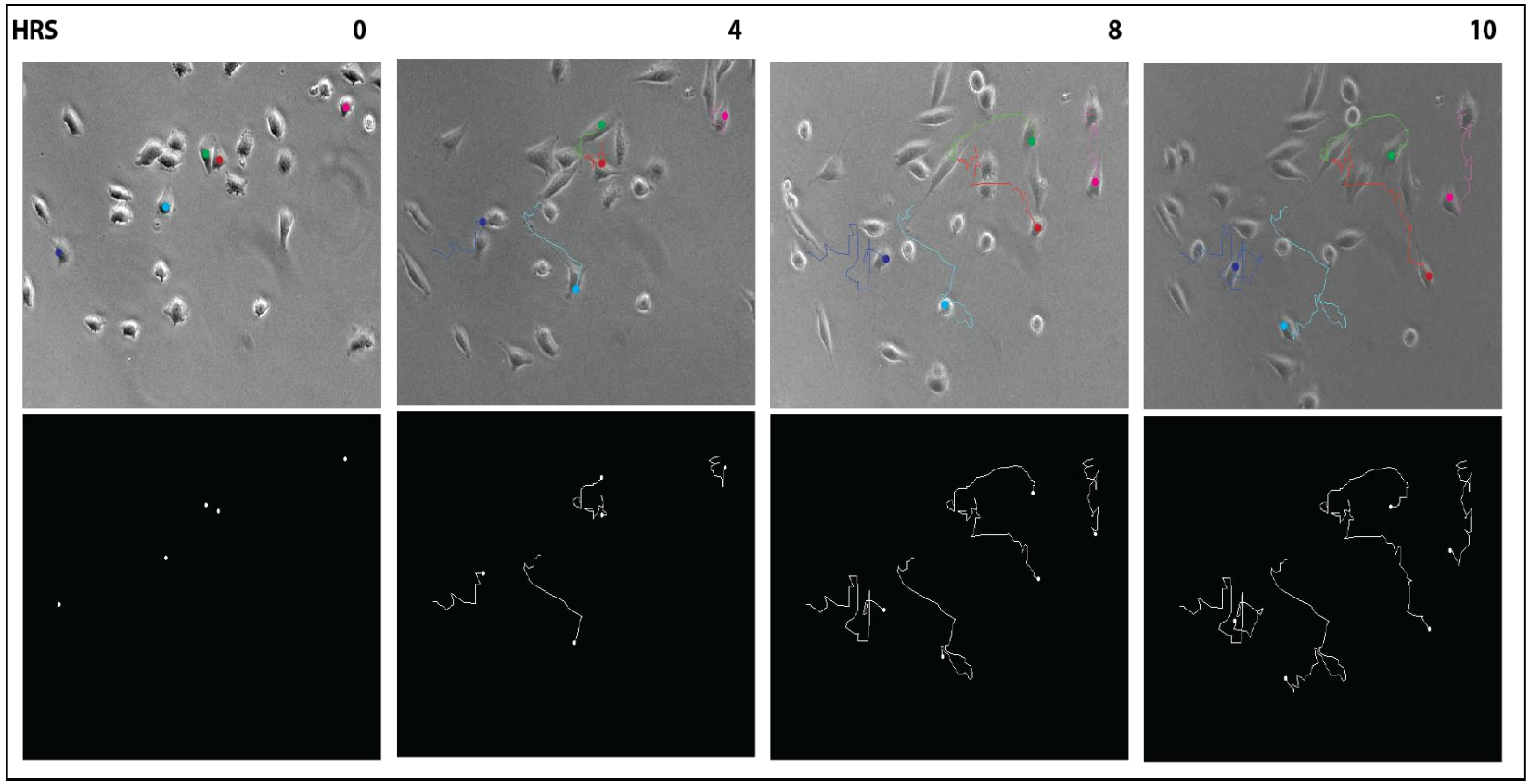

Figure 6-5: Cell tracking of time-lapse microscopy videos

Time-lapse frame image sequence of 4T1.2 cells observed for 10 hours is shown (upper panel). The time difference in hours to the first image of the sequence is given in the top right hand corner of each frame. Using ImageJ, each cell is tracked over 60 frames (10 minutes apart), generating a trajectory for each cell (lower panel).

Resulting trajectory data was used to generate trackplots for the visual representation of migration data and to analyse cell speed. Trackplots (Figure 6-6) represent pooled cell trajectories, shifted to a common origin, for all cells from a given treatment group and were generated using purpose-written software developed in-house by Dr James Monypenny, KCL, London. The circular horizon associated with each trackplot represents the maximum displacement from the origin achieved by at least 50% of the cell population and provides a visual indication of the overall propensity for cells to migrate within each treatment group. We observed that stimulation of 4T1.2 tumour cells with low (1ng/ml – comparable to the concentration of CXCL13 in the MSC CM) and high (25ng/ml) concentrations of rCXCL13 did not significantly increase the motility of the cells (Figure 6-6A & B). Similarly, stimulation of 4T1.2 with low (3ng/ml) and high (25ng/ml) concentration of rCCL21 did not significantly increase the motility of the cells (Figure 6-6A &B). We noticed that the 4T1.2 cells did not look healthy at concentration of higher than 25ng/ml of rCCL21 *in vitro*.

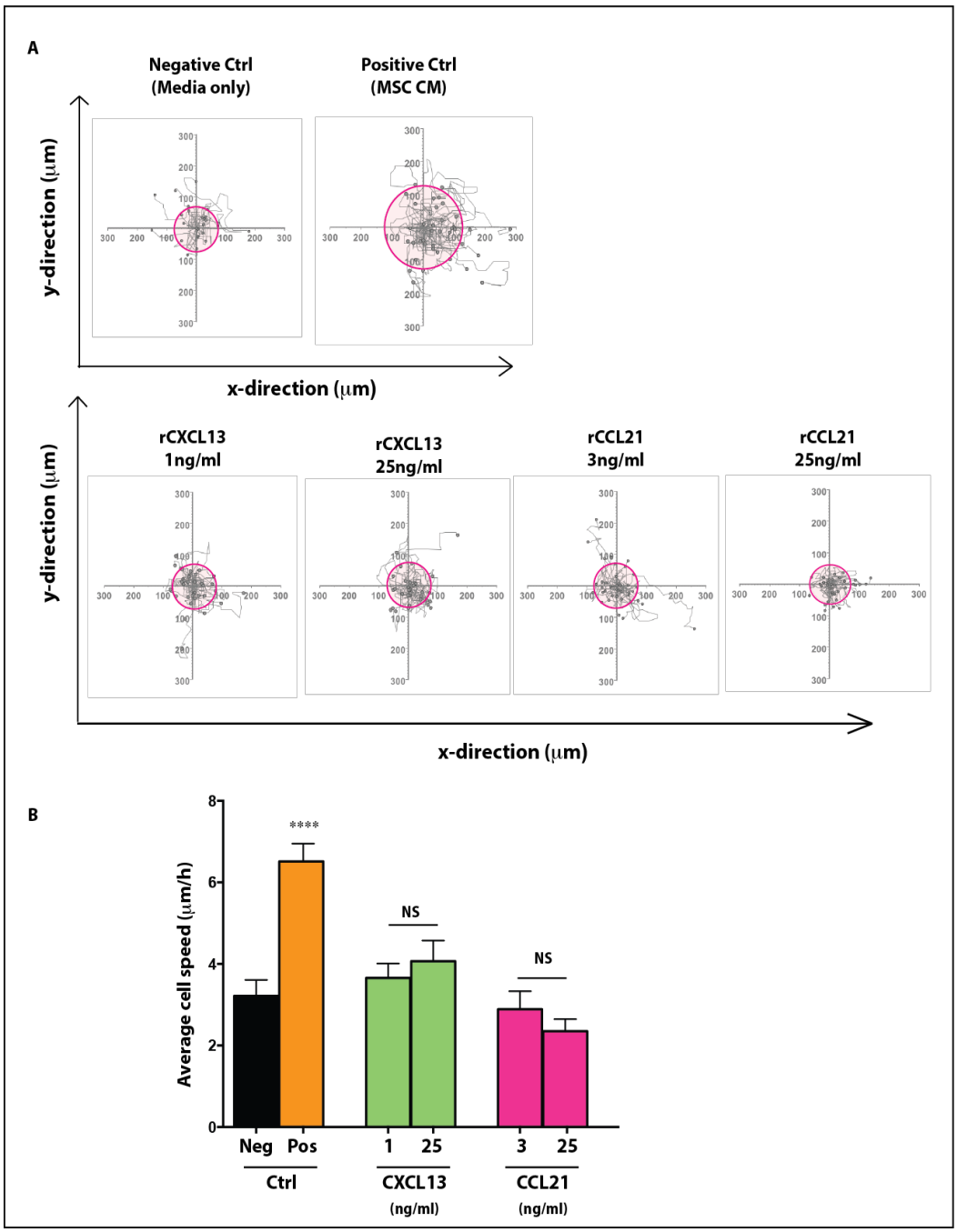

Figure 6-6: Effect of rCXCL13 and rCCL21 on 4T1.2 migration

A: 4T1.2 tumour cells were plated in 6-well plates and stimulated with control media, MSC CM, recombinant CXCL13 or CCL21 6 hours prior to time-lapse microscopy. Track plots illustrate the trajectories, shifted to a common origin, of individual 4T1.2 cells from time-lapse experiments (n=3 independent experiments per treatment. The circular boundary for each plot (pink shaded circle) represents the maximum displacement from the origin achieved by at least 50% of the cells. **B:** Mean speed (measured in microns/hour) of 4T1.2 cells within each group. Data represent means ± SEM. Asterisks represent the p-values when comparing to the media alone group (unpaired t-test; ****$p<10^{-4}$; NS, not significant).

6.4 CXCL13-dependent RANK-RANKL signaling

The physiological role of the TNF receptor (TNFR) family member, RANK (Receptor activator of NF-κB), for downstream LTi signaling during lymph node development is well established (discussed in Chapter 1 section 1.3.3). In development (embryonic lymphangiogenesis), the interaction of LTi cells with LTo (akin to the LTi-MSC interaction/co-clustering we have observed, both *in vitro* and *in vivo*, in chapter 4 section 5.6.2) is thought to establish a positive feedback loop for stimulating RANKL production by the stromal cells, via RANKL/RANK- and $LT\alpha_1\beta_2$/LTβR-dependent amplification (reviewed in [271]). Although LTi cells are known to secrete RANKL, RANKL expression is up to 10-fold higher in LTo than in LTi cells [131].

More recently, the RANK receptor has been shown to be expressed by several human breast cancer cell lines and its signaling has been reported to induce an epithelial-mesenchymal transition in various tumour types [272]. Reciprocally, pharmacologic inhibition of RANKL or genetic ablation of RANK attenuates mammary tumour development [273]. Additionally, CXCL13-CXCR5 signaling axis has been shown to induce RANKL expression in stromal cells within oral squamous cell carcinomas [274]. Given that CXCL13 and CCl21 chemokine did not stimulate tumour cell invasion *in vitro*, we hypothesised that following the CCL21-dependent LTi cell recruitment into the primary tumours *in vivo* (Figure 5-6), CXCL13-dependent LTi interaction with the surrounding stromal cells (Figure 5-13) establishes a positive feedback loop for CXCL13 amplification, which in turns triggers RANKL production, thus promoting increased tumour cell motility into the draining lymph nodes.

6.4.1 RANK-RANKL expression within 4T1.2 cell line

To test the relationship between CXCL13 and RANK signaling within our murine breast cancer model, we first analysed the RANK and RANKL expression in our 4T1.2 cell line. We observed by confocal microscopy that 4T1.2 cancer cells expressed the RANK receptor *in vitro* (Figure 6-7A). The concentrations of RANKL secreted into the culture media after 48 hours were determined by ELISA quantification. Recombinant RANKL (100pg/ml) and media alone served as positive and negative controls respectively. In keeping with previous findings by Sambandam et al [274], we found that 4T1.2 tumour cells did not secrete any RANKL Figure 6-7B). In contrast, levels over 200pg/ml of RANKL were observed in the MSC CM, supporting the hypothesis that the source of RANKL within the tumour is also likely to be stromal.

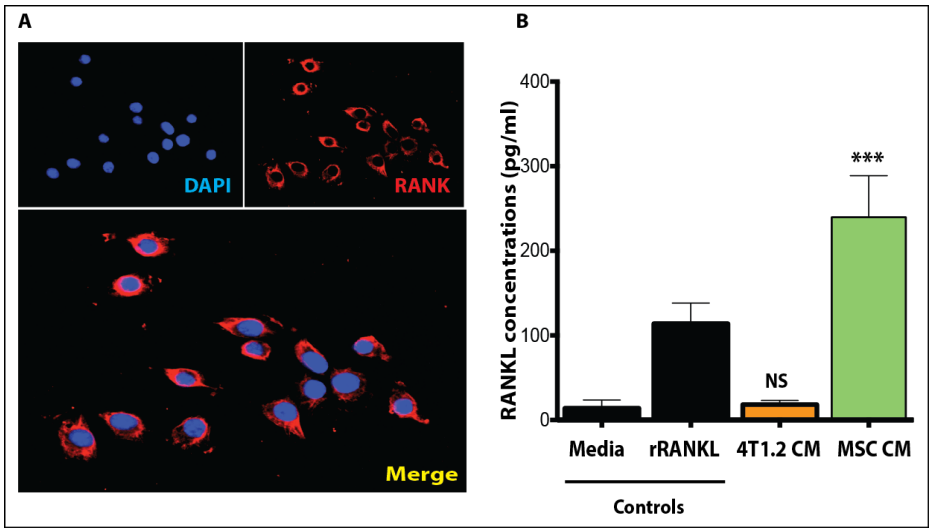

Figure 6-7: RANK-RANKL expression within 4T1.2 triple negative breast cancer cell line

A: Confocal micrograph showing cytoplasmic and membranous staining of RANK (red) in 4T1.2 breast cancer cells. Dapi-stained nuclei are shown in blue. **B:** Cell culture supernatants from culture experiments of 4T1.2 cells and MSCs were analysed after 48h to determine the level of RANKL by ELISA. Data represent means ± SEM. Asterisks represent the p-values when comparing to the media alone group (one-way ANOVA: *** $p \leq 0.001$; NS, non significant).

6.4.2 Effect on RANKL expression following chemokine stimulation in stromal cells

We then tested the effect on RANKL levels in the MSC conditioned media following stimulation with increasing concentrations of recombinant CXCL13 or CCL21. We observed by ELISA that stimulation of the MSCs by rCXCL13 at concentrations between 25-100ng/ml significantly increased the expression of RANKL by the MSC cells (Figure 6-8B). In contrast, stimulation of the MSCs by rCCL21 at any concentration between 5-100ng/ml had no significant effect on the expression of RANKL by the MSC cells (Figure 6-8A). RANKL is synthesized as a membrane-bound protein, which is then cleaved by metalloproteases into a soluble form by ectodomain shedding [275]. We therefore also stained for membrane-bound RANKL on the MSC following stimulation with increasing concentrations of recombinant CXCL13. Consistent with our ELISA findings, we observed that stimulation of MSCs by CXCL13 resulted in an increase in the intensity of staining for RANKL (Figure 6-8B).

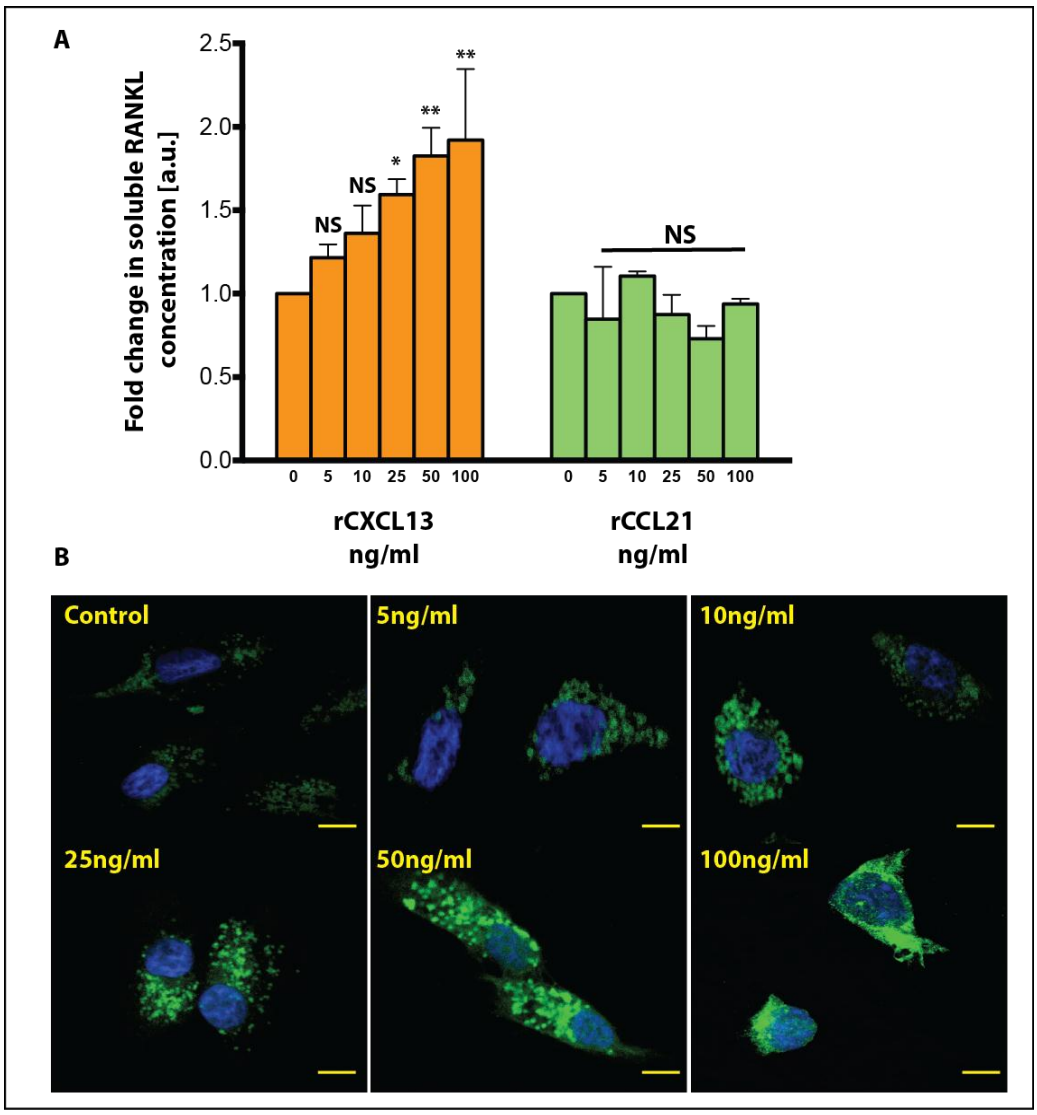

Figure 6-8: CXCL13, but not CCL21, induces the expression of RANKL in MSCs.

A: ELISA-based quantification of soluble RANKL concentrations in the supernatants of MSC cell cultures after 48h of stimulation with the indicated concentrations of rCXCL13 or rCCL21. Data represent means ± SEM. Asterisks represent the p-values when comparing to the non-stimulated control (one-way ANOVA: * $p \leq 0.05$; ** $p \leq 0.01$; NS, non significant). **B:** Increased expression of membrane-associated RANKL (green) in MSCs following stimulation by rCXCL13. Scale bar = 50µm.

6.4.3 Effect of RANKL on tumour cell invasion

We then investigated if increasing concentrations of recombinant RANKL would increase tumour cell invasion within our ECM based invasion assay. Again EGF stimulation of 4T1.2 and NIH3T3 cell lines served as positive and negative control respectively. In contrast to the results in Figure 6-2, addition of recombinant RANKL to 4T1.2 cells at any concentration between 10-100ng/ml significantly increased the ability of the tumour cells to invade through the matrix (Figure 6-9).

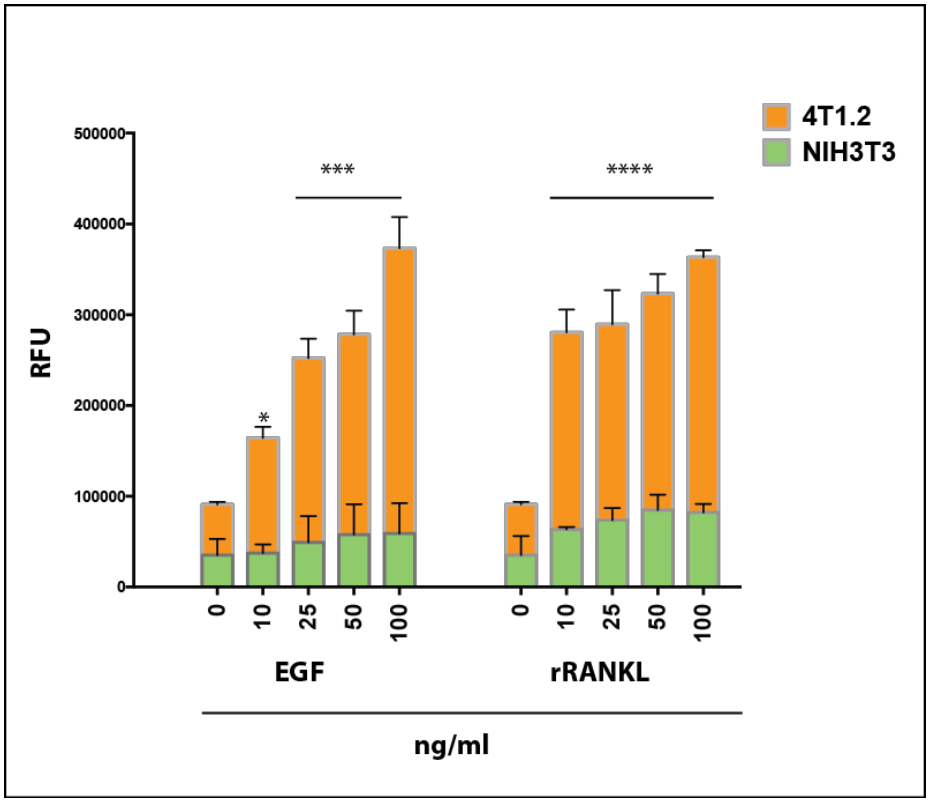

Figure 6-9: Effect of RANKL on 4T1.2 tumour cells invasion in vitro.

Cell invasion assay results are shown. An increase in the RFU indicates more invasion of cells through an extracellular matrix membrane. NIH3T3 cells (green bars) were used as a non-invasive control. EGF stimulation was used as the positive control. Data represent means ± SEM. Asterisks represent the p-values when comparing to the non-stimulated control group (one-way ANOVA: *** $p \leq 0.01$, **** $p \leq 0.001$).

6.4.4 Effect of RANKL on tumour cell migration

Given the effect of RANKL on tumour cell invasion, we went on to test if increasing concentration of recombinant RANKL would promote the migration of 4T1.2 cells *in vitro*. 4T1.2 tumour cells were stimulated with control media or recombinant RANKL (5ng/ml and 25ng/ml) 6 hours prior to time-lapse microscopy and imaged for a total of 10 hours. Contrary to our hypothesis, we observed that stimulation with rRANKL did not significantly increase the motility of the 4T1.2 cells in culture (Figure 6-10A & B). However, MSC-CM-induced migration of 4T1.2 cells (observed in Figure 6-6A) was inhibited significantly by the addition of a RANKL blocking antibody (Figure 6-10C & D). This decrease in migration was associated with a decrease (< 2-fold) in the expression of vimentin, providing support for the role of RANKL in promoting a more migratory phenotype of tumour cells (Figure 6-10E &F).

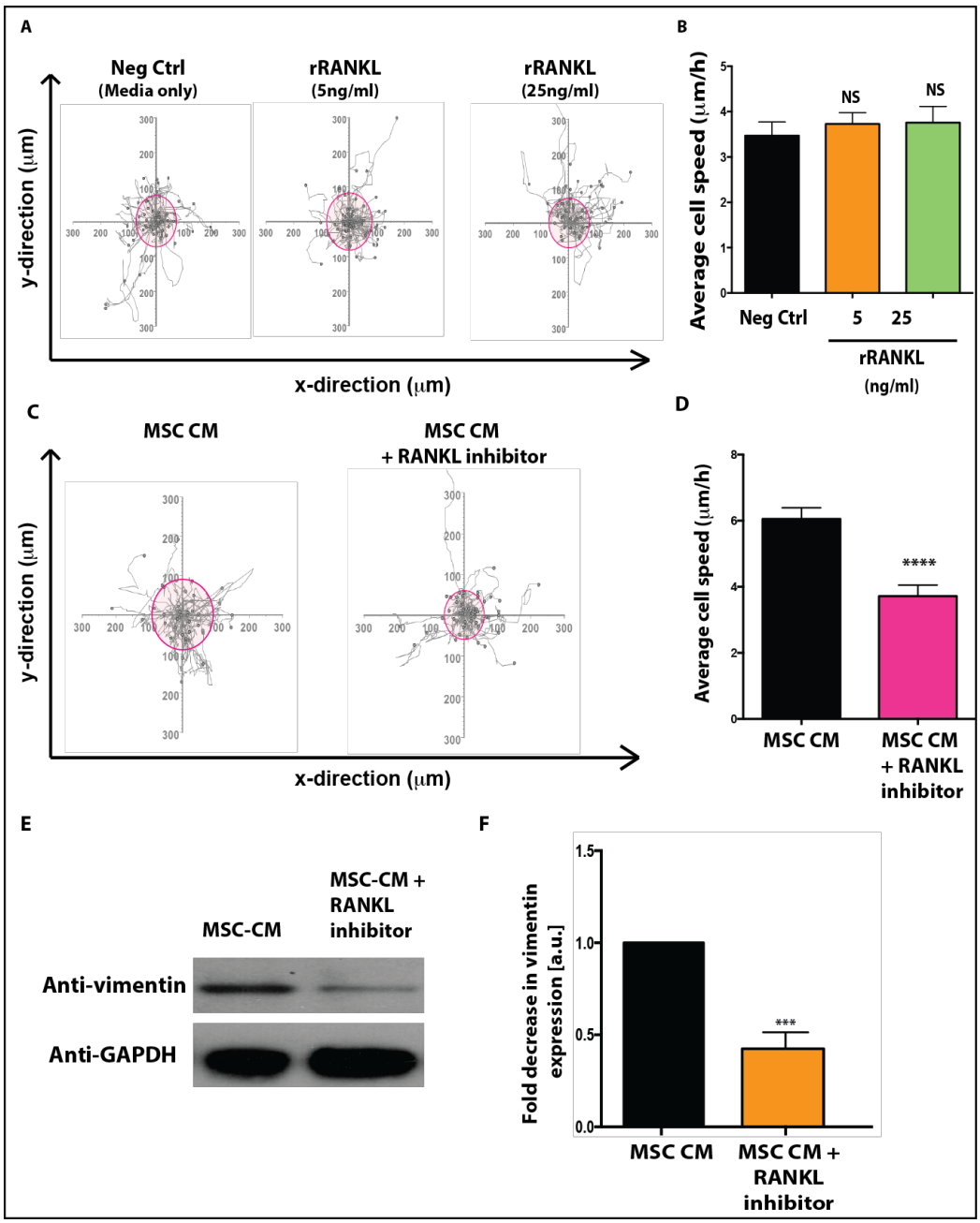

Figure 6-10: Effect of RANKL on 4T1.2 tumour cells migration *in vitro*

4T1.2 tumour cells were plated in 6-well plates and kept in media only or stimulated with different concentrations of rRANKL (**A**), or MSC CM with or without RANKL-blocking antibody (**B**) for 6 hours prior to time-lapse microscopy. Track plots illustrate the trajectories, shifted to a common origin (n=3 independent experiments per treatment). **C** and **D** show the mean speed (measured in microns/hour) of 4T1.2 cells within each group. **E/F:** Immunoblot analysis of vimentin expression by 4T1.2 cells following stimulation with MSC CM or MSC-CM + RANKL blocking antibody. GAPDH served as a loading control. Data represent means ± SEM. Asterisks represent the p-values when comparing to the control group.

6.4.5 Kinetics of serum RANKL during tumourigenesis within the 4T1.2 breast cancer mouse model

Complimentary to the kinetics of lymphoid chemokine changes observed in Figure 5-4, we analysed the serum RANKL response following inoculation of 4T1.2 tumour cells into the mammary fat pad. 500µl of peripheral blood was obtained from 4T1.2 tumour-bearing mice via intracardiac puncture at the termination of the experiment at each time-point between days 10-24. Separated serum was analysed by ELISA (see Method & Material Chapter 2 section 3.2.5.3). RANKL levels were seen to peak (up to 3000pg/ml) at day 18 ($p \leq 10^{-4}$, unpaired t-test). This peak is seen approximately 4 days after the peak in CXCL13 levels as observed in Figure 5-4.

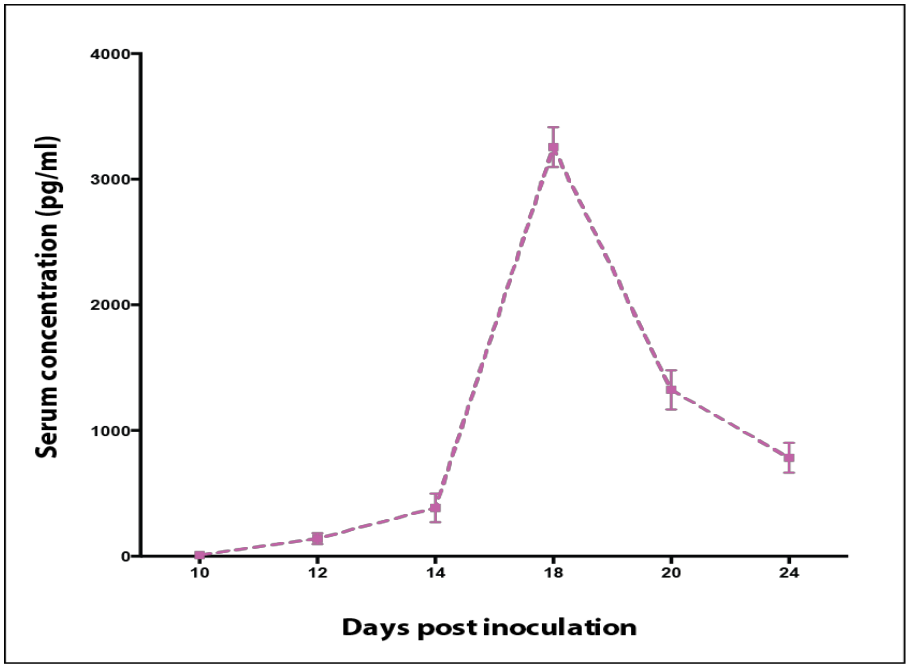

Figure 6-11: Kinetics of circulating RANKL following tumour induction.

RANKL serum concentrations after inoculation of 4T1.2 cells into the mammary fat pad were determined at the indicated time points by ELISA. 3 animals were analysed per time-point. Data represent means ± SEM.

6.4.6 RANKL blockade within our triple negative breast cancer mouse model

In order to examine further the relationship between the CXCL13, RANKL and LTi cells within our TNBC mouse model, we investigated the effect of RANKL blockade on LTi recruitment within tumours *in vivo*. 4T1.2 tumour-bearing mice were treated with a neutralizing antibody for RANKL or isotype control antibodies (0.5mg each antibody via tail-vein injections) started one day after tumour cell implantation and repeated every 3 days. Again two time-points, day 14 and day 21 were tested; whereby day 14 represents an early stage within our 4T1.2 mouse breast cancer model, and day 21, a time-point when lymphatic metastasis are present within the lymph nodes.

We observed from our antibody blockade *in vivo* experiments that anti-RANKL treatment did not significantly affected the growth of the primary tumour when compared with isotype control antibody at both time-points (day 14 and day 21); suggesting no effect on the proliferation of 4T1.2 cells *in vivo* (Figure 6-12A-C) - similar to results from anti-CXCL13 and anti-CCL21 treatments.

We observed that the weight of the draining inguinal lymph nodes at both time-points (day 14 & 21) was significantly reduced in the anti-RANKL cohort, when compared with isotype control (Figure 6-12D &E). We noticed also that the size and the weight of the spleens within tumour-bearing mice treated with anti-RANKL blocking antibody were much significantly lower as compared to the weight of the spleens within the control isotype, anti-CXCL3 or anti-CCL21 treatment cohorts (Figure 6-12F &G). It was noteworthy that in the cohort treated with anti-RANKL majority of the mice developed toxic symptoms of lethargy,

ruffled fur, and body weight loss by day 14 and one mouse died within 10 days of treatment.

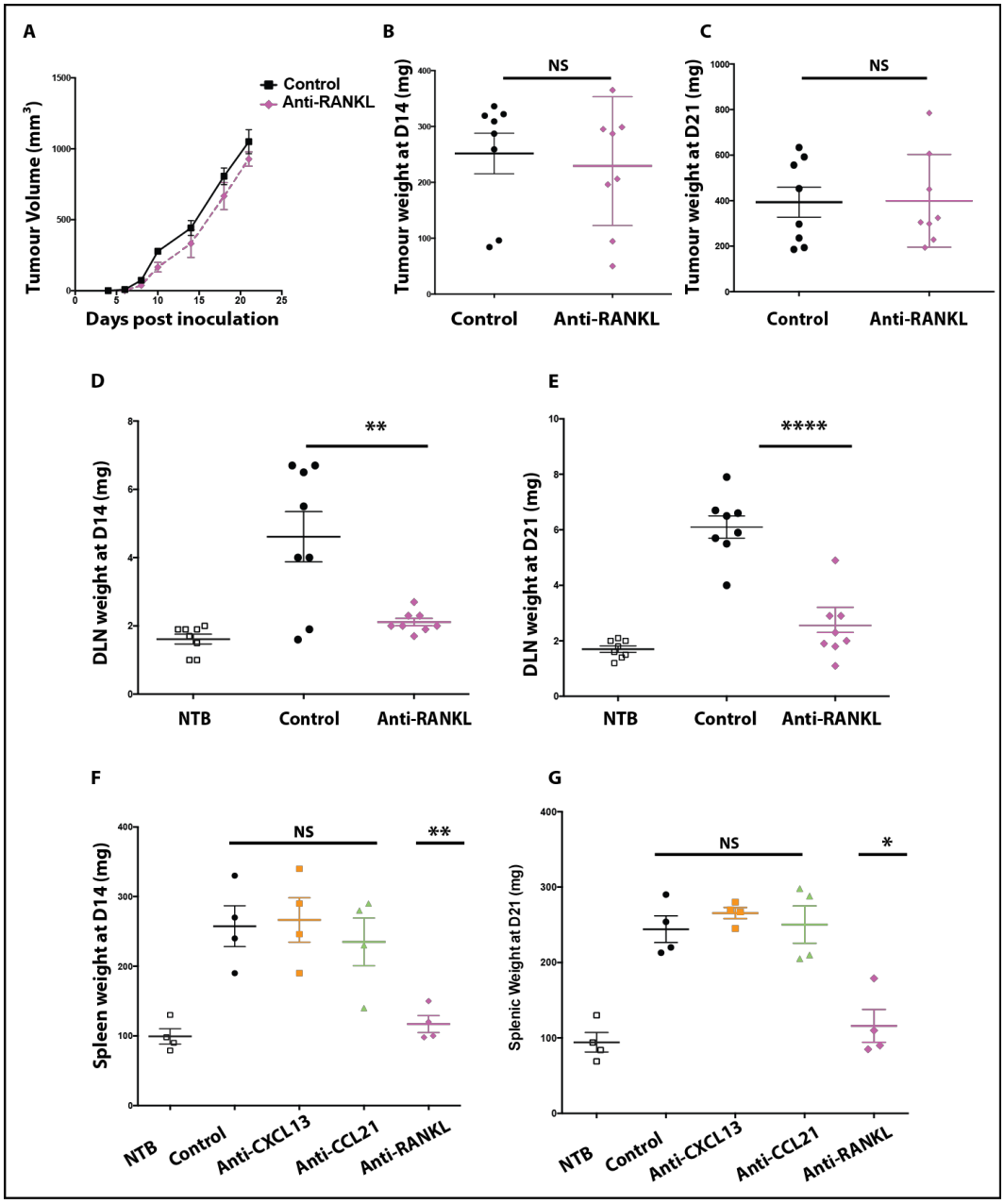

Figure 6-12. Effect of RANKL *in vivo* neutralization on primary tumour and secondary lymphoid organs size within the 4T1.2 tumour model.

BALB/c mice were injected s.c. with 1×10^6 4T1.2 breast cancer cells. Mice were treated with either an anti-murine RANKL antibody or goat IgG isotype control antibody injected intravenously every other day for a total of 21 days. **A:** Subcutaneous 4T1.2 tumour growth curves within each cohort is demonstrated. The average weight of primary tumours (**B & C**), draining inguinal lymph node (DLN) (**D & E**), and spleens (**F & G**) from mice sacrificed at the end of in vivo experiments at day 14 and day 21 respectively. The results are expressed as mean +/- SEM. Asterisks represent the p-values when comparing to the control group (* $p\leq0.05$, ** $p\leq0.01$, ** $p\leq10^{-4}$ NS= Non significant). NTB=non-tumour-bearing.

6.4.7 Effect on LTi recruitment into lymph nodes

Tumours and draining lymph nodes were analysed for LTi ($CD3^-$,$CD11c^-$,$B220^-$, $CD127^+$,$CD90.2^+$,$NKp46^-$) cell numbers by flow cytometry (as per the gating strategy in Figure 5-2A) at day 14, a time-point by which maximum number of LTi cells had been recruited into the tumours (demonstrated in Figure 5-2B) and at day 21, a time-point when lymphatic metastasis are present within the lymph nodes. It is noteworthy that whilst the increased tumour cells at D21 represents partly an increase in tumour burden within these lymph nodes, the increase in lymph node size at day 14 was not due to the presence of metastatic disease within these nodes.

Within tumours, when compared with the isotype control antibody, antibody blockade using an anti-RANKL neutralising antibody, did not significantly affect the recruitment of LTi cells into the primary tumours (Figure 6-13). Within the draining lymph nodes, despite a trend for lower LTi numbers within the anti-RANKL treated cohort at day 14, this did not reach statistically significance (Figure 6-13A). In contrast, at day 21, when compared with the control group, the numbers of LTi cells within the draining lymph nodes were significantly lower amongst the anti-RANKL treated cohort (Figure 6-13B).

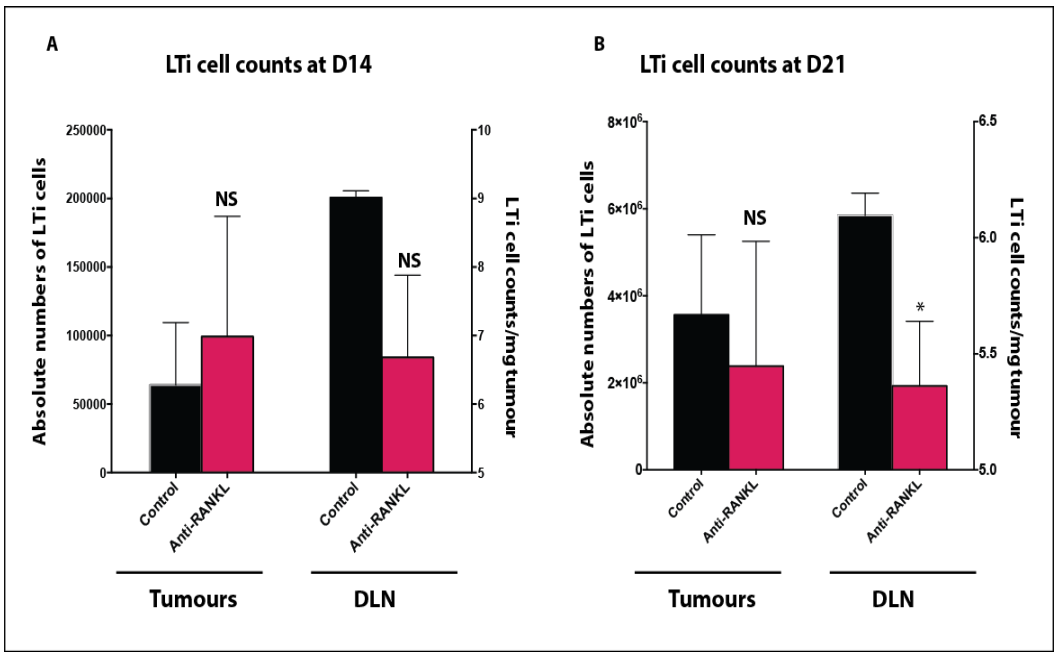

Figure 6-13: Effect of *in vivo* RANKL neutralisation on LTi recruitment to primary tumour and draining lymph nodes in the 4T1.2 tumour model.

A: Absolute cell counts of LTi cells per milligram of tissue detected in tumours (right-axis), and absolute numbers within the draining lymph nodes (left axis) derived from 4T1.2 tumour-bearing mice. Mice ($n \geq 3$) were treated with anti-RANKL blocking antibody or isotype control antibody until day 14 (**A**) or day 21 (**B**). Data represent means ± SEM. Asterisks represent the p-values when comparing to the control group (* $p \leq 0.05$, NS= Non significant).

6.4.8 Anti-inflammatory effect of RANKL blockade

We also examined for the anti-inflammatory effect of RANKL blockade within the 4T1.2 breast cancer mouse model. As in chapter 4 section 5.5.2, we analysed by FACS analysis the total B/T-cell counts, defined as CD3- or CD19-positive cells respectively (as per the gating strategy in Figure 5-3A) within the tumours and the draining lymph nodes at day 14 and day 21.

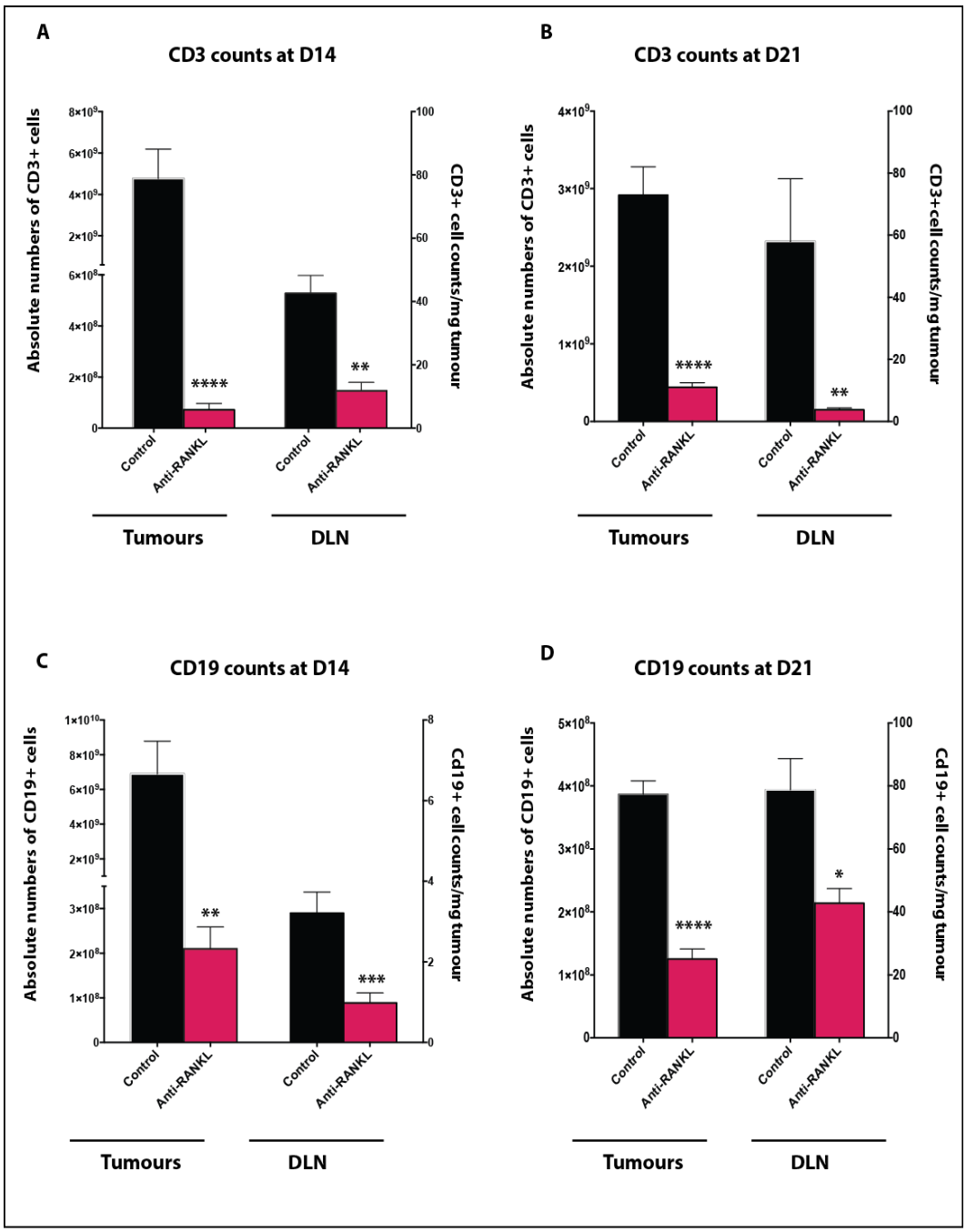

Figure 6-14: Effect on T and B cells recruitment following RANKL neutralization within the 4T1.2 tumour model *in vivo*.

A & B: Analyses of absolute cell counts of $CD3^+$ cells per milligram of tumour detected in tumours (right-axis) and absolute numbers within the draining lymph nodes (left axis) from 4T1.2 tumour-bearing mice treated with anti-RANKL or isotype control antibody at (**A**) day 14 or (**B**) day 21 are shown. **C & D:** Analyses of absolute cell counts of $CD19^+$ cells per milligram of tumour detected in tumours (right-axis) and absolute numbers within the draining lymph nodes from 4T1.2 tumour bearing BALB/c mice treated with anti-RANKL or isotype control antibody at (**C**) day 14 or (**D**) day 21 are shown ($n \geq 3$). Data represent means ± SEM. Asterisks represent the p-values when comparing to the control groups (one-way ANOVA: * $p \leq 0.05$; ** $p \leq 0.01$; *** $p \leq 0.001$; **** $p \leq 0.0001$).

Irrespective of the time-point, analysis of the CD3-positive cells (Figure 6-14A &B) demonstrated a statistically significant decrease in the number of T-cells within the primary tumours and the draining lymph nodes amongst both the anti-RANKL treated cohort compared to the cohort group (similar to results from anti-CXCL13 and anti-CCL21 treatments (Chapter 4 section 5.5.2)). Similarly, analysis of the CD19 positive cells (Figure 6-14C & D) within the primary tumours and the draining lymph nodes at day 14 and day 21 demonstrated a statistically significant decrease in the number of B-cells amongst anti-RANKL treated cohort (see figure legend for the p-values).

6.4.9 Effect on tumour burden within the lymph nodes

To confirm if the decreased size of the lymph nodes at day 21 was also due to any differences in the tumour load within the lymph node, we performed immunohistochemical analysis of tumour load with a pancytokeratin antibody. We observed absence of metastasis within the draining lymph nodes in majority of the cases (n=5/7) (Figure 6-15); suggesting an inhibitory effect of RANKL blockade on 4T1.2 tumour cell migration into the draining lymph node.

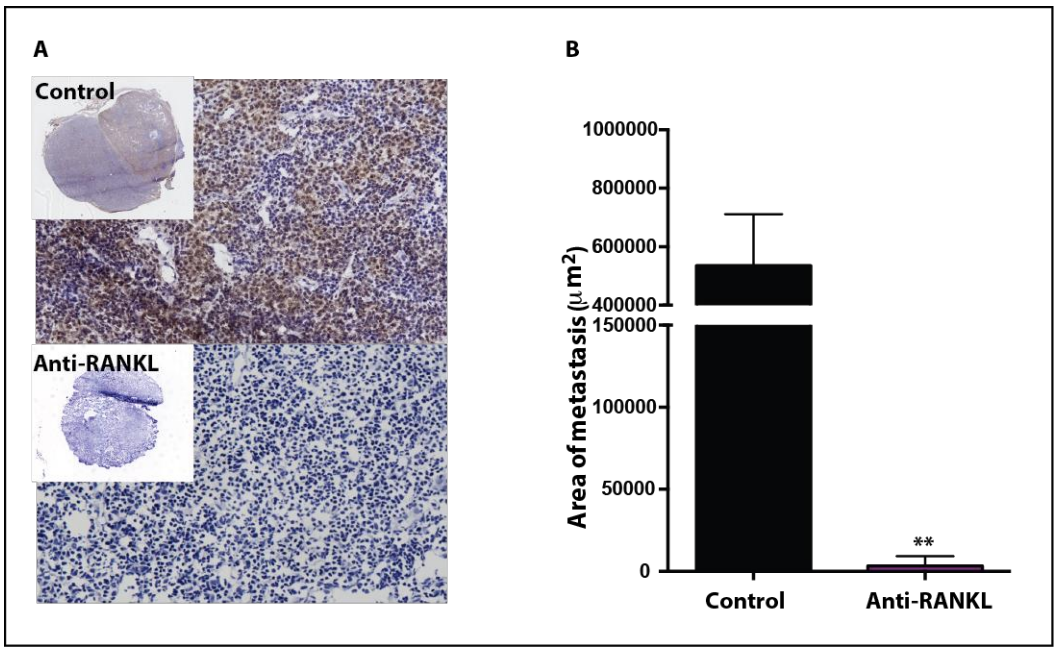

Figure 6-15: In vivo neutralisation of RANKL inhibits the migration of 4T1.2 tumour cells into draining lymph nodes.

A: Immunohistochemical staining of the draining lymph nodes of tumour-bearing mice using a pancytokeratin (*brown*) to assess for tumour load between the treatment groups. Cell nuclei are stained blue. **B:** Quantification of the total area of metastasis per μm^2 of sectional area within lymph nodes. Data represent means ± SEM. Asterisks represent the p-values when comparing to the control groups (one-way ANOVA: ** $p \leq 0.01$).

6.4.10 Effect of chemokine and RANKL blockade on the CXCL13 and CCL21 serum levels

Next we examined the relationship between CCL21, CXCL13 and RANKL within our 4T1.2 tumour bearing mouse model. We quantified by ELISA the serum concentrations of CCL21, CXCL13 and RANKL at day 14 in mice treated with a neutralizing antibody for CXCL13, CCL21, RANKL or isotype control antibodies. We observed that in mice treated with anti-CXCL13 and anti-RANKL treatments, the serum levels of CCL21 were seen significantly reduced in both cohorts (Figure 6-16A). Similarly, the serum concentration levels of CXCL13 were significantly reduced in mice treated with anti-CCL21 or anti-RANKL neutralising antibodies (Figure 6-16B). Finally, in mice treated with

anti-CCL21 and anti-CXCL13 treatments, the serum levels of RANKL were seen significantly reduced in both cohorts (Figure 6-16). These data provide evidence of the complex mechanisms involved in regulating the chemokine profiles within tumour bearing mice.

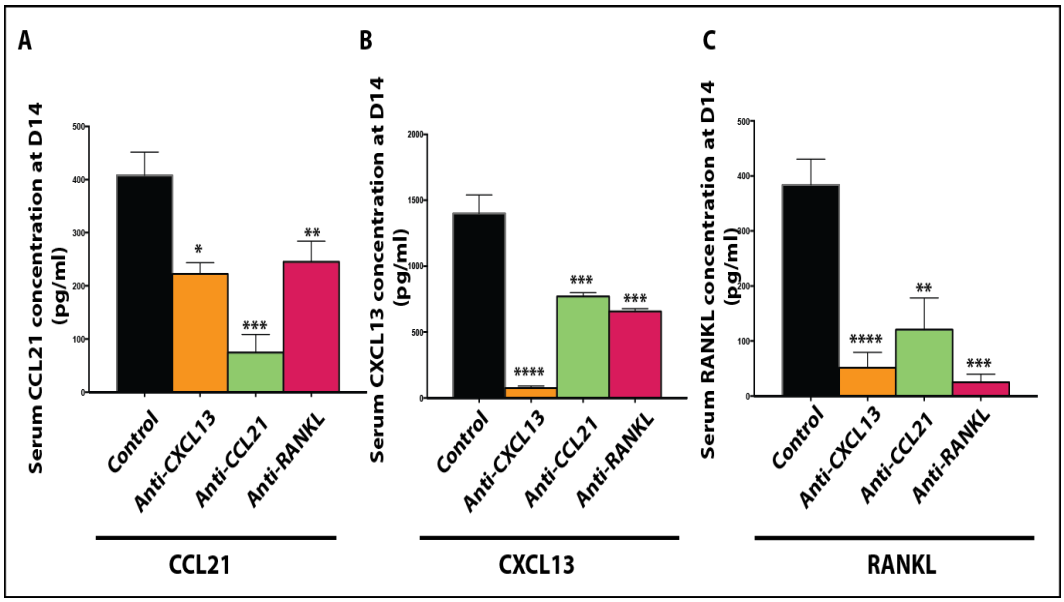

Figure 6-16: Relationship between serum concentrations of CCL21, CXCL13 and RANKL

Serum concentrations of CCL21 (**A**), CXCL13 (**B**) and RANKL (**C**) at day 14 were analysed by ELISA within each treatment cohort respectively. Data represent means ± SEM. Asterisks represent the p-values when comparing to the control groups (one-way ANOVA: * $p \leq 0.05$; ** $p \leq 0.01$; *** $p \leq 0.001$; **** $p \leq 0.0001$).

6.5 Discussion

Following on from the results presented in chapter 4, the aims of the experiments presented in this chapter were to investigate the downstream mechanisms that underlie the relationship between CXCL13 and CCL21-dependent lymphatic metastasis and LTi cell recruitment.

Our data suggest that a CXCL13-dependent autocrine feedback loop promotes RANKL upregulation in the mesenchymal stromal cells, which causes the tumour cells to become more invasive. Although we did not directly observe increasing concentrations of recombinant RANKL promoting tumour cell migration, inhibition of RANKL by a RANKL blocking antibody did inhibit the induction of EMT (hallmark for a migratory phenotype) in the tumour cells. The complexity that exists between the regulation of CCL21, CXCL13 and RANKL within our in vivo model was evident by analysis of serum chemokine and RANKL levels in mice treated with either anti-CCL21, anti-CXCL13 or anti-RANKL treatments. We observed a reduction in the serum levels of RANKL by both anti-CCL21 and anti-CXCL13 treatments; hence it would seem that the action of CXCL13 on RANKL production *in vivo* depends on LTi recruitment by CCL21. Our observations are in keeping with studies reporting that RANKL can increase the migration of tumour cells by activating the c-Src/Akt and c-Src/ ERK signaling pathways [261,276,277]. Additionally, these recent studies provide further support for our findings that RANKL expression is sensitive to CXCR5-CXCL13 signalling.

Although the functions of RANKL and its receptor RANK in bone remodeling and mammary gland development have long been recognized; more recently

activation of the RANK pathway has also been shown to promote tumourigenesis in both human and murine studies [272]. For example, Tan *et al*. demonstrated that RANK signaling in mammary carcinomas enhances lung metastases in mice [278]. Similarly, overexpression of RANK or RANKL in the mammary gland leads to increased proliferation of the mammary epithelia [279], increased expression of breast cancer stem cell markers and EMT contributing to tumour cell invasion and metastasis [272]. Yamada *et al*. show that RANKL promotes EMT and induces angiogenesis independently of VEGF in a human head and neck squamous carcinoma [280]. This is in keeping with our own *in vitro* and *in vivo* findings showing that following stimulation by MSC CM, acquisition of a motile phenotype (via EMT) contributing to increased tumour cell migration is primarily dependent on the RANK pathway; and that RANKL blockade inhibits tumour cell invasion into the lymph nodes within our triple negative breast cancer mouse model.

An association of RANK/RANKL levels in tumours with patient outcome also support the pro-metastatic role of this pathway. Interestingly, in primary breast cancer, RANK expression is more commonly observed in the more aggressive triple negative tumours (50%) than ER/PR positive tumours (18%) [272]. RANK-RANKL signaling has been shown to specifically promote the tumourigenesis of TNBCs by enriching cancer stem cells[281]. Furthermore, RANK/RANKL mRNA expression levels (determined by reverse transcription (RT)-PCR) were able to discriminate between node-negative and lymph node-positive patients [282]. Numerous studies demonstrate that higher RANK expression in primary tumours correlates with shorter overall survival [283,284]. Therefore, it would seem that RANK-RANKL pathway manipulation may not only provide benefit in patients

with bone metastases but inhibiting RANKL may offer a therapeutic advantage for reducing the risk of lymph node and or distant metastasis, especially in the aggressive triple negative breast cancer subtype.

Given this context, complementary gain- or loss-of-function approaches (RANK transgenic and knock-out mouse models and pharmacological RANKL inhibition) have been of great interest. Interestingly, treatment of mice in our experiments with anti-RANKL caused majority of the mice to develop profound toxicity on subsequent intravenous injections. These findings may be consistent with the diverse functions of the RANK-L/RANK interactions within the immune system. Recent work has demonstrated that RANKL/RANK signaling is important in lymph-node development, lymphocyte differentiation, dendritic cell survival, T-cell activation, and tolerance induction. These considerations do give rise to some questions as to the immunological safety of RANKL inhibition for human use. RANKL and RANK knockout mice have been shown to result in disruptions in the microarchitecture of the spleen [285]. Of note is that whilst patients with mutations in the *RANKL* gene do not present with any immunological defects[286], patients with mutations in the *RANK* gene present with significantly decreased mature B-cells and failure to mount an antibody response [287]. In comparison, both RANK/RANKL knockout mice exhibit marked reduction in the splenic and marrow mature B-cell numbers [129,288]. It may be RANKL/RANK signaling pathway may be more crucial to murine than human B cell maturation.

Following on from the pre-clinical and clinical data establishing that RANKL inhibition delays the formation of *de novo* bone metastases, and inhibits the progression of established bone metastases [289]; denosumab (Xgeva® injection,

Amgen Inc.), a fully human monoclonal antibody against RANKL, was approved by the Food and Drug Administration (FDA) for the treatment of bone metastasis in patient with solid tumours in June 2013. The studies that led to this approval were designed to address the skeletal effects and not designed to test an anti-tumour effect of denosumab. For example, meta-analyses of three randomized double-blind phase 3 trials reported that denosumab was superior to the prior standard of care zoledronic acid, for the prevention or delay of skeletal complications in patients with advanced cancer and bone metastases [290]. Patients enrolled within the trial tolerated denosumab well with no related serious adverse events. A recent post hoc analysis of the above mentioned trials has indicated that treatment with denosumab was also associated with improved overall survival compared with zoledronic acid in a subgroup of patients with lung cancer [291]. These findings are particularly exciting and the results of an ongoing phase III trial studying the effect of denosumab in preventing disease recurrence, when given as an adjuvant therapy for women with early-stage breast cancer, who are at high risk of disease recurrence (NCT01077154) are eagerly awaited. One of the major issues in the development of anti-metastatic therapies is the extremely long time periods required to achieve the study endpoints, e.g. disease free survival. This is particularly the case with ER-positive breast cancers. However, within triple negative breast cancer (TNBC) patients the clinical pattern of developing metastases differs: approximately 50% of TNBC patients do not achieve pathological complete response (pCR) following neoadjuvant chemotherapy, and 70% of this pCR-negative group go on to develop metastatic disease within the first three years following diagnosis, making it very feasible to test anti-metastatic therapies such as denosumab within this clinical trials setting. Additionally, a shift towards innovative study designs, such as pre-surgical “window of opportunity”

early phase trials in patients prior to surgery provide an opportunity to prospectively answer key biological hypotheses within breast cancer patients.

In summary, from the data presented in this chapter, we found that downstream of CCL21-mediated recruitment of intra-tumoural LTi cells, CXCL13 promotes lymphatic invasion of tumour cells via a chemokine dependent RANK-RANKL axis through the aforementioned positive feedback loops (illustrated in Figure 6-17 below). Investigations into how the CXCL13, CCL21 chemokine and RANKL axes, in a coordinated way, establish a network of interactions between the tumour cells and their microenvironment; may provide new avenues for possible anti-cancer treatments.

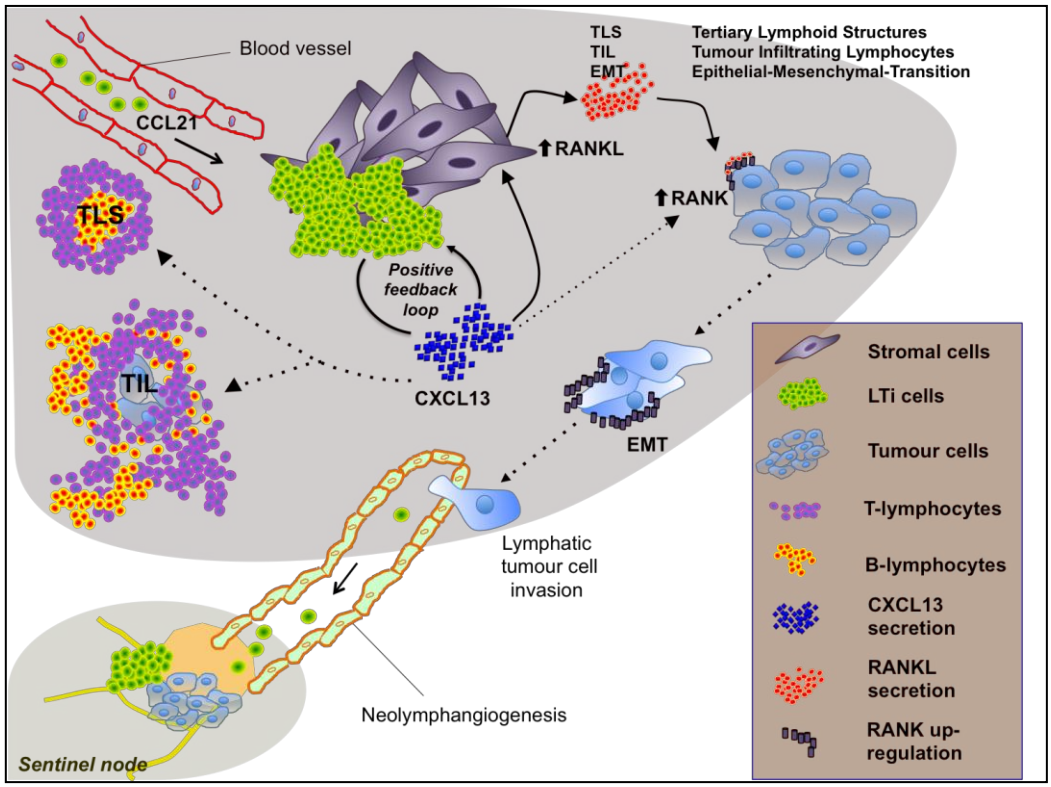

Figure 6-17: Schematic illustration of our proposed model for the role of LTi cells within triple negative breast cancers.

Recruitment of LTi cells into the primary tumours is primarily dependent on CCL21. Following a CXCL13-dependent LTi-stromal cell interaction a positive feedback loop develops which helps promote lymph tumour cell invasion via the RANK-RANKL axis by promoting EMT within the tumour cells.

Chapter 7: Summary & Future Directions

7.1 Summary

Breast remains the most common cancer in females. Although early breast cancer is not fatal, majority of cancer-related deaths are caused by the metastatic spread of the disease. Within invasive breast cancers, lymphatic invasion is thought to be the first step tumour cells undertake when disseminating through the lymphatic vasculature. Emerging evidence supports the strong contribution of stromal influences on tumour progression to help sustain growth, invasion and metastasis [292]. The components and the relevance of the bi-directional (host-protection vs. tumour promotion) nature of these complex interactions of tumour cells with their adjacent microenvironment (tumour stroma) remain to be fully elucidated.

Research over the past few years has revealed a previously unappreciated family of innate lymphoid cells (including LTi cells) with diverse physiological roles, ranging from immune protection to wound repair and homeostasis [156,293]. In this thesis, we report, for the first time, the identification of LTi ($ROR\gamma t^{+}CD127^{+}CD3^{-}$) cells within the human breast TME and the enrichment of lymphoid chemokines/chemokine receptors gene signature within an aggressive triple negative breast cancer subtype. LTi cells and the lymphoid chemokines were seen to provide signals for lymphatic tumour cell invasion and lymphangiogenesis in tumours. Our *in vitro* and *in vivo* work demonstrate the

CCL21-dependent recruitment of LTi cells into tumours, the CXCL13-dependent interaction between the tumoural LTi and stromal cells and the downstream effect of the CXCL13 positive feedback loop in promoting lymphatic tumour cell motility via the RANK-RANKL axis. These results suggest a pivotal role for LTi cells and the associated chemokines in facilitating lymphatic vessel invasion of tumour cells particularly in the poor outcome triple negative breast cancer subtype. Our work is likely to represent a significant advance for understanding tumour-immune-stromal interactions within tumours.

7.2 Future directions

Our novel identification of LTi cells within human breast cancer microenvironments has laid a foundation for exploring the role of these cells within human cancers. Specifically, a number of interesting data presented in this thesis open several avenues for future work in order to understand the implications of this crosstalk for breast cancer patients.

As discussed in Chapter 3, we observed that higher LTi numbers within human primary tumours correlate with higher intratumoural LVD, suggesting an association between LTi's cells and neo-lymphangiogenesis in tumours. Studies indicate that lymphangiogenic factors such as VEGF-C and VEGF-D induce hyperplasia of peritumoural lymphatics, as well as formation of intratumoural lymphatics, and that these lymphatics facilitate metastatic spread to lymph nodes [39-41]. The known mechanism by which LTi cells activate VEGF-C and VEGF-D expression via the LTβR signaling on the stromal organiser cells during fetal lymphangiogenesis[127], requires further investigation in the context of LTi

recruitment in tumours. The hypothesis that LTi cells promote neo-lymphangiogenesis within tumours is now being tested within our group. In collaboration with Dr Matt Smalley (European Cancer Stem Cell Research Institute, Cardiff) and Dr Taija MaKinen, (Department of Immunology, Genetics and Pathology, Cancer and Vascular Biology, Uppsala), we are in the process of developing a triple negative mouse model in Prox1-CreERT2;R26-mTmG transgenic mice. This animal model expresses the green fluorescent protein under the promoter of Prox1, a master control gene in lymphatic development and therefore providing a great tool for further lymphatic research. Using the MIW technique discussed in Figure 5-16, we will investigate further the LTi-associated lymphangiogenesis within breast tumours.

Secondly, our group has already begun to explore further the role that LTi cells play in the immunoediting/immune surveillance mechanisms within tumours. In particular, despite high CXCL13-CXCR5 expression acting as a good prognostic marker within high-risk breast cancer patients [262]; results presented in this thesis reported that downstream of CCL21-mediated recruitment of intra-tumoural LTi cells, CXCL13 promotes lymphatic invasion of tumour cells via a chemokine dependent RANK-RANKL axis. The possibility that early tumour cell lymphatic vessel invasion in response to an increase in CXCL13 levels within the cancer microenvironment may effectively enhance the cross-presentation of tumour antigens in the draining lymph nodes thus acting as a powerful mitogen for responding T-cells requires further investigation. It was interesting to note that as well as blocking lymph node metastases, anti-RANKL treatment within our mouse demonstrated a significant decrease in the numbers of LTi cells within the draining lymph nodes. Recent studies have indicated that LTi cells influence the

adaptive immune responses within lymphoid tissues. For example, LTi cells have been shown to be located at the edge of the B cell follicles, where T and B cell zones intersect [152,293,294]; specifically where intranodal lymphatics drain lymph to the efferent lymphatics – a point of entry for the incoming lymphocytes. Despite the low numbers of LTi cells present in adult life, this location puts them in position to interact with immune cells as they recirculate between blood and lymph [294]. Strikingly, LTi cells in fetal and neonatal lymphoid tissues, before the need for adaptive immune responses, do not express co-stimulatory molecules; in contrast to adult LTi cells which have been shown to express high levels of co-stimulatory molecules such as: OX40 ligand (OX40L; TNFSF4) and CD30 ligand (CD30L; TNFSF8)[143]. We therefore hypothesize that studying the molecular and cellular interactions of LTi cells with the surrounding immune cells within tumour models may provide an insight into some of the mechanisms involved in the phases of "immunoediting" by cancers.

In support of this, we have recently analysed the expression levels of a panel of co-stimulatory molecules on splenic LTi cells from non-tumour bearing mice compared with splenic LTi cells from tumour bearing mice (data not shown). We found that the **I**nducible T-cell **COS**timulatory (CD278/ICOS) molecule was expressed at much higher levels on LTi cells from tumour bearing compared to non-tumour bearing mice. ICOS and its ligand (ICOS-L) belongs to the CD28/CTLA-4/B7 immunoglobulin superfamily and have been shown to play diverse roles in T-cell responses such as mediating autoimmunity as well as enhancing the development/activity of regulatory T cells [295]. These findings require further investigation within both *in vitro* and *in vivo* settings.

Chapter 8: References

1. Cardoso, F., *et al.* Locally recurrent or metastatic breast cancer: ESMO Clinical Practice Guidelines for diagnosis, treatment and follow-up. *Annals of oncology : official journal of the European Society for Medical Oncology / ESMO* **23 Suppl 7**, vii11-19 (2012).
2. Malvezzi, M., *et al.* European cancer mortality predictions for the year 2011. *Annals of oncology : official journal of the European Society for Medical Oncology / ESMO* **22**, 947-956 (2011).
3. Jemal, A., Siegel, R., Xu, J. & Ward, E. Cancer statistics, 2010. *CA: a cancer journal for clinicians* **60**, 277-300 (2010).
4. Early Breast Cancer Trialists' Collaborative, G. Effects of chemotherapy and hormonal therapy for early breast cancer on recurrence and 15-year survival: an overview of the randomised trials. *Lancet* **365**, 1687-1717 (2005).
5. Honig, S. Hormonal therapy and chemotherapy. In Diseases of the Breast. . *Edited by Harris JR, Lippman ME, Morrow M, Osborne CK. Philadelphia: Lippincott-Raven Publishers;* **669-734.**(1996).
6. Parker, J.S., *et al.* Supervised risk predictor of breast cancer based on intrinsic subtypes. *Journal of clinical oncology : official journal of the American Society of Clinical Oncology* **27**, 1160-1167 (2009).
7. Sorlie, T., *et al.* Repeated observation of breast tumor subtypes in independent gene expression data sets. *Proceedings of the National Academy of Sciences of the United States of America* **100**, 8418-8423 (2003).
8. Curtis, C., *et al.* The genomic and transcriptomic architecture of 2,000 breast tumours reveals novel subgroups. *Nature* **486**, 346-352 (2012).
9. von Minckwitz, G., *et al.* Definition and impact of pathologic complete response on prognosis after neoadjuvant chemotherapy in various intrinsic breast cancer subtypes. *Journal of clinical oncology : official journal of the American Society of Clinical Oncology* **30**, 1796-1804 (2012).
10. Liedtke, C., *et al.* Response to neoadjuvant therapy and long-term survival in patients with triple-negative breast cancer. *Journal of clinical oncology : official journal of the American Society of Clinical Oncology* **26**, 1275-1281 (2008).
11. Grabau, D., Jensen, M.B., Rank, F. & Blichert-Toft, M. Axillary lymph node micrometastases in invasive breast cancer: national figures on incidence and overall survival. *APMIS : acta pathologica, microbiologica, et immunologica Scandinavica* **115**, 828-837 (2007).
12. Sivridis, E., Giatromanolaki, A., Galazios, G. & Koukourakis, M.I. Node-related factors and survival in node-positive breast carcinomas. *Breast* **15**, 382-389 (2006).
13. Fisher, B., *et al.* Relation of number of positive axillary nodes to the prognosis of patients with primary breast cancer. An NSABP update. *Cancer* **52**, 1551-1557 (1983).
14. Carter, C.L., Allen, C. & Henson, D.E. Relation of tumor size, lymph node status, and survival in 24,740 breast cancer cases. *Cancer* **63**, 181-187 (1989).

15. Jatoi, I., Hilsenbeck, S.G., Clark, G.M. & Osborne, C.K. Significance of axillary lymph node metastasis in primary breast cancer. *Journal of clinical oncology : official journal of the American Society of Clinical Oncology* **17**, 2334-2340 (1999).
16. Smeets, A.*, et al.* Impact of tumor chronology and tumor biology on lymph node metastasis in breast cancer. *SpringerPlus* **2**, 480 (2013).
17. Das, S. & Skobe, M. Lymphatic vessel activation in cancer. *Annals of the New York Academy of Sciences* **1131**, 235-241 (2008).
18. Klein, C.A. Parallel progression of primary tumours and metastases. *Nature reviews. Cancer* **9**, 302-312 (2009).
19. Christofori, G. New signals from the invasive front. *Nature* **441**, 444-450 (2006).
20. Steeg, P.S. Tumor metastasis: mechanistic insights and clinical challenges. *Nature medicine* **12**, 895-904 (2006).
21. Steeg, P.S. Metastasis suppressors alter the signal transduction of cancer cells. *Nature reviews. Cancer* **3**, 55-63 (2003).
22. Hynes, R.O. Metastatic potential: generic predisposition of the primary tumor or rare, metastatic variants-or both? *Cell* **113**, 821-823 (2003).
23. Luzzi, K.J.*, et al.* Multistep nature of metastatic inefficiency: dormancy of solitary cells after successful extravasation and limited survival of early micrometastases. *The American journal of pathology* **153**, 865-873 (1998).
24. Stacker, S.A., Baldwin, M.E. & Achen, M.G. The role of tumor lymphangiogenesis in metastatic spread. *FASEB journal : official publication of the Federation of American Societies for Experimental Biology* **16**, 922-934 (2002).
25. Sleeman, J.P. & Thiele, W. Tumor metastasis and the lymphatic vasculature. *International journal of cancer. Journal international du cancer* **125**, 2747-2756 (2009).
26. Lauria, R.*, et al.* The prognostic value of lymphatic and blood vessel invasion in operable breast cancer. *Cancer* **76**, 1772-1778 (1995).
27. Mohammed, R.A.*, et al.* Improved methods of detection of lymphovascular invasion demonstrate that it is the predominant method of vascular invasion in breast cancer and has important clinical consequences. *The American journal of surgical pathology* **31**, 1825-1833 (2007).
28. Woo, C.S.*, et al.* Lymph node status combined with lymphovascular invasion creates a more powerful tool for predicting outcome in patients with invasive breast cancer. *American journal of surgery* **184**, 337-340 (2002).
29. Schoppmann, S.F.*, et al.* Prognostic value of lymphangiogenesis and lymphovascular invasion in invasive breast cancer. *Annals of surgery* **240**, 306-312 (2004).
30. Marinho, V.F., Metze, K., Sanches, F.S., Rocha, G.F. & Gobbi, H. Lymph vascular invasion in invasive mammary carcinomas identified by the endothelial lymphatic marker D2-40 is associated with other indicators of poor prognosis. *BMC cancer* **8**, 64 (2008).
31. Van den Eynden, G.G.*, et al.* Distinguishing blood and lymph vessel invasion in breast cancer: a prospective immunohistochemical study. *British journal of cancer* **94**, 1643-1649 (2006).

32. Ozmen, V.*, et al.* Factors predicting the sentinel and non-sentinel lymph node metastases in breast cancer. *Breast cancer research and treatment* **95**, 1-6 (2006).
33. Viale, G.*, et al.* Predicting the status of axillary sentinel lymph nodes in 4351 patients with invasive breast carcinoma treated in a single institution. *Cancer* **103**, 492-500 (2005).
34. Colleoni, M.*, et al.* Prognostic role of the extent of peritumoral vascular invasion in operable breast cancer. *Annals of oncology : official journal of the European Society for Medical Oncology / ESMO* **18**, 1632-1640 (2007).
35. Goldhirsch, A.*, et al.* Meeting highlights: international expert consensus on the primary therapy of early breast cancer 2005. *Annals of oncology : official journal of the European Society for Medical Oncology / ESMO* **16**, 1569-1583 (2005).
36. Baluk, P.*, et al.* Functionally specialized junctions between endothelial cells of lymphatic vessels. *The Journal of experimental medicine* **204**, 2349-2362 (2007).
37. Ran, S., Volk, L., Hall, K. & Flister, M.J. Lymphangiogenesis and lymphatic metastasis in breast cancer. *Pathophysiology : the official journal of the International Society for Pathophysiology / ISP* **17**, 229-251 (2010).
38. Cao, Y. Opinion: emerging mechanisms of tumour lymphangiogenesis and lymphatic metastasis. *Nature reviews. Cancer* **5**, 735-743 (2005).
39. Skobe, M.*, et al.* Induction of tumor lymphangiogenesis by VEGF-C promotes breast cancer metastasis. *Nature medicine* **7**, 192-198 (2001).
40. Mandriota, S.J.*, et al.* Vascular endothelial growth factor-C-mediated lymphangiogenesis promotes tumour metastasis. *The EMBO journal* **20**, 672-682 (2001).
41. Stacker, S.A.*, et al.* VEGF-D promotes the metastatic spread of tumor cells via the lymphatics. *Nature medicine* **7**, 186-191 (2001).
42. Hirakawa, S.*, et al.* VEGF-A induces tumor and sentinel lymph node lymphangiogenesis and promotes lymphatic metastasis. *The Journal of experimental medicine* **201**, 1089-1099 (2005).
43. Hirakawa, S.*, et al.* VEGF-C-induced lymphangiogenesis in sentinel lymph nodes promotes tumor metastasis to distant sites. *Blood* **109**, 1010-1017 (2007).
44. Dadras, S.S.*, et al.* Tumor lymphangiogenesis: a novel prognostic indicator for cutaneous melanoma metastasis and survival. *The American journal of pathology* **162**, 1951-1960 (2003).
45. Ueda, M.*, et al.* Correlation between vascular endothelial growth factor-C expression and invasion phenotype in cervical carcinomas. *International journal of cancer. Journal international du cancer* **98**, 335-343 (2002).
46. Kajita, T.*, et al.* The expression of vascular endothelial growth factor C and its receptors in non-small cell lung cancer. *British journal of cancer* **85**, 255-260 (2001).
47. Tsurusaki, T.*, et al.* Vascular endothelial growth factor-C expression in human prostatic carcinoma and its relationship to lymph node metastasis. *British journal of cancer* **80**, 309-313 (1999).

48. Akagi, K.*, et al.* Vascular endothelial growth factor-C (VEGF-C) expression in human colorectal cancer tissues. *British journal of cancer* **83**, 887-891 (2000).
49. Yonemura, Y.*, et al.* Role of vascular endothelial growth factor C expression in the development of lymph node metastasis in gastric cancer. *Clinical cancer research : an official journal of the American Association for Cancer Research* **5**, 1823-1829 (1999).
50. Gowans, J.L. The recirculation of lymphocytes from blood to lymph in the rat. *The Journal of physiology* **146**, 54-69 (1959).
51. Girard, J.P., Moussion, C. & Forster, R. HEVs, lymphatics and homeostatic immune cell trafficking in lymph nodes. *Nature reviews. Immunology* **12**, 762-773 (2012).
52. Roozendaal, R., Mebius, R.E. & Kraal, G. The conduit system of the lymph node. *International immunology* **20**, 1483-1487 (2008).
53. Steinman, R.M. Decisions about dendritic cells: past, present, and future. *Annual review of immunology* **30**, 1-22 (2012).
54. Cyster, J.G. Chemokines and cell migration in secondary lymphoid organs. *Science* **286**, 2098-2102 (1999).
55. Willard-Mack, C.L. Normal structure, function, and histology of lymph nodes. *Toxicologic pathology* **34**, 409-424 (2006).
56. Miyasaka, M. & Tanaka, T. Lymphocyte trafficking across high endothelial venules: dogmas and enigmas. *Nature reviews. Immunology* **4**, 360-370 (2004).
57. Butcher, E.C. Leukocyte-endothelial cell recognition: three (or more) steps to specificity and diversity. *Cell* **67**, 1033-1036 (1991).
58. Ager, A. & Humphries, M.J. Use of synthetic peptides to probe lymphocyte--high endothelial cell interactions. Lymphocytes recognize a ligand on the endothelial surface which contains the CS1 adhesion motif. *International immunology* **2**, 921-928 (1990).
59. Ivetic, A., Deka, J., Ridley, A. & Ager, A. The cytoplasmic tail of L-selectin interacts with members of the Ezrin-Radixin-Moesin (ERM) family of proteins: cell activation-dependent binding of Moesin but not Ezrin. *The Journal of biological chemistry* **277**, 2321-2329 (2002).
60. Ley, K., Laudanna, C., Cybulsky, M.I. & Nourshargh, S. Getting to the site of inflammation: the leukocyte adhesion cascade updated. *Nature reviews. Immunology* **7**, 678-689 (2007).
61. Rossi, D. & Zlotnik, A. The biology of chemokines and their receptors. *Annual review of immunology* **18**, 217-242 (2000).
62. Stein, J.V. & Nombela-Arrieta, C. Chemokine control of lymphocyte trafficking: a general overview. *Immunology* **116**, 1-12 (2005).
63. Nibbs, R.J. & Graham, G.J. Immune regulation by atypical chemokine receptors. *Nature reviews. Immunology* **13**, 815-829 (2013).
64. Rot, A. & von Andrian, U.H. Chemokines in innate and adaptive host defense: basic chemokinese grammar for immune cells. *Annual review of immunology* **22**, 891-928 (2004).
65. Tal, O.*, et al.* DC mobilization from the skin requires docking to immobilized CCL21 on lymphatic endothelium and intralymphatic crawling. *The Journal of experimental medicine* **208**, 2141-2153 (2011).

66. Ohl, L.*, et al.* CCR7 governs skin dendritic cell migration under inflammatory and steady-state conditions. *Immunity* **21**, 279-288 (2004).
67. Weber, M.*, et al.* Interstitial dendritic cell guidance by haptotactic chemokine gradients. *Science* **339**, 328-332 (2013).
68. Forster, R., Braun, A. & Worbs, T. Lymph node homing of T cells and dendritic cells via afferent lymphatics. *Trends in immunology* **33**, 271-280 (2012).
69. von Andrian, U.H. & Mackay, C.R. T-cell function and migration. Two sides of the same coin. *The New England journal of medicine* **343**, 1020-1034 (2000).
70. Gunn, M.D.*, et al.* A chemokine expressed in lymphoid high endothelial venules promotes the adhesion and chemotaxis of naive T lymphocytes. *Proceedings of the National Academy of Sciences of the United States of America* **95**, 258-263 (1998).
71. Baekkevold, E.S.*, et al.* The CCR7 ligand elc (CCL19) is transcytosed in high endothelial venules and mediates T cell recruitment. *The Journal of experimental medicine* **193**, 1105-1112 (2001).
72. Scimone, M.L.*, et al.* CXCL12 mediates CCR7-independent homing of central memory cells, but not naive T cells, in peripheral lymph nodes. *The Journal of experimental medicine* **199**, 1113-1120 (2004).
73. Phillips, R. & Ager, A. Activation of pertussis toxin-sensitive CXCL12 (SDF-1) receptors mediates transendothelial migration of T lymphocytes across lymph node high endothelial cells. *European journal of immunology* **32**, 837-847 (2002).
74. Okada, T.*, et al.* Chemokine requirements for B cell entry to lymph nodes and Peyer's patches. *The Journal of experimental medicine* **196**, 65-75 (2002).
75. Ebisuno, Y.*, et al.* Cutting edge: the B cell chemokine CXC chemokine ligand 13/B lymphocyte chemoattractant is expressed in the high endothelial venules of lymph nodes and Peyer's patches and affects B cell trafficking across high endothelial venules. *Journal of immunology* **171**, 1642-1646 (2003).
76. Gretz, J.E., Norbury, C.C., Anderson, A.O., Proudfoot, A.E. & Shaw, S. Lymph-borne chemokines and other low molecular weight molecules reach high endothelial venules via specialized conduits while a functional barrier limits access to the lymphocyte microenvironments in lymph node cortex. *The Journal of experimental medicine* **192**, 1425-1440 (2000).
77. Hardtke, S., Ohl, L. & Forster, R. Balanced expression of CXCR5 and CCR7 on follicular T helper cells determines their transient positioning to lymph node follicles and is essential for efficient B-cell help. *Blood* **106**, 1924-1931 (2005).
78. Forster, R., Davalos-Misslitz, A.C. & Rot, A. CCR7 and its ligands: balancing immunity and tolerance. *Nature reviews. Immunology* **8**, 362-371 (2008).
79. Bajenoff, M.*, et al.* Stromal cell networks regulate lymphocyte entry, migration, and territoriality in lymph nodes. *Immunity* **25**, 989-1001 (2006).

80. Reif, K.*, et al.* Balanced responsiveness to chemoattractants from adjacent zones determines B-cell position. *Nature* **416**, 94-99 (2002).
81. Ogata, M.*, et al.* Chemotactic response toward chemokines and its regulation by transforming growth factor-beta1 of murine bone marrow hematopoietic progenitor cell-derived different subset of dendritic cells. *Blood* **93**, 3225-3232 (1999).
82. Nagira, M.*, et al.* A lymphocyte-specific CC chemokine, secondary lymphoid tissue chemokine (SLC), is a highly efficient chemoattractant for B cells and activated T cells. *European journal of immunology* **28**, 1516-1523 (1998).
83. Lazennec, G. & Richmond, A. Chemokines and chemokine receptors: new insights into cancer-related inflammation. *Trends in molecular medicine* **16**, 133-144 (2010).
84. Kruizinga, R.C.*, et al.* Role of chemokines and their receptors in cancer. *Current pharmaceutical design* **15**, 3396-3416 (2009).
85. Sun, Y.X.*, et al.* Expression of CXCR4 and CXCL12 (SDF-1) in human prostate cancers (PCa) in vivo. *Journal of cellular biochemistry* **89**, 462-473 (2003).
86. Scotton, C.J.*, et al.* Multiple actions of the chemokine CXCL12 on epithelial tumor cells in human ovarian cancer. *Cancer research* **62**, 5930-5938 (2002).
87. Balkwill, F. The significance of cancer cell expression of the chemokine receptor CXCR4. *Seminars in cancer biology* **14**, 171-179 (2004).
88. Muller, A.*, et al.* Involvement of chemokine receptors in breast cancer metastasis. *Nature* **410**, 50-56 (2001).
89. Hirakawa, S.*, et al.* Nodal lymphangiogenesis and metastasis: Role of tumor-induced lymphatic vessel activation in extramammary Paget's disease. *The American journal of pathology* **175**, 2235-2248 (2009).
90. Scotton, C.J., Wilson, J.L., Milliken, D., Stamp, G. & Balkwill, F.R. Epithelial cancer cell migration: a role for chemokine receptors? *Cancer research* **61**, 4961-4965 (2001).
91. Fusi, A.*, et al.* Expression of chemokine receptors on circulating tumor cells in patients with solid tumors. *Journal of translational medicine* **10**, 52 (2012).
92. Petit, I., Jin, D. & Rafii, S. The SDF-1-CXCR4 signaling pathway: a molecular hub modulating neo-angiogenesis. *Trends in immunology* **28**, 299-307 (2007).
93. Spano, J.P.*, et al.* Chemokine receptor CXCR4 and early-stage non-small cell lung cancer: pattern of expression and correlation with outcome. *Annals of oncology : official journal of the European Society for Medical Oncology / ESMO* **15**, 613-617 (2004).
94. Scala, S.*, et al.* Expression of CXCR4 predicts poor prognosis in patients with malignant melanoma. *Clinical cancer research : an official journal of the American Association for Cancer Research* **11**, 1835-1841 (2005).
95. Koshiba, T.*, et al.* Expression of stromal cell-derived factor 1 and CXCR4 ligand receptor system in pancreatic cancer: a possible role for tumor progression. *Clinical cancer research : an official journal*

of the American Association for Cancer Research **6**, 3530-3535 (2000).

96. Jiang, Y.P., Wu, X.H., Shi, B., Wu, W.X. & Yin, G.R. Expression of chemokine CXCL12 and its receptor CXCR4 in human epithelial ovarian cancer: an independent prognostic factor for tumor progression. *Gynecologic oncology* **103**, 226-233 (2006).
97. Kim, J.*, et al.* Chemokine receptor CXCR4 expression in colorectal cancer patients increases the risk for recurrence and for poor survival. *Journal of clinical oncology : official journal of the American Society of Clinical Oncology* **23**, 2744-2753 (2005).
98. Li, Y.M.*, et al.* Upregulation of CXCR4 is essential for HER2-mediated tumor metastasis. *Cancer cell* **6**, 459-469 (2004).
99. Phillips, R.J.*, et al.* The stromal derived factor-1/CXCL12-CXC chemokine receptor 4 biological axis in non-small cell lung cancer metastases. *American journal of respiratory and critical care medicine* **167**, 1676-1686 (2003).
100. Mashino, K.*, et al.* Expression of chemokine receptor CCR7 is associated with lymph node metastasis of gastric carcinoma. *Cancer research* **62**, 2937-2941 (2002).
101. Wang, J.*, et al.* Chemokine receptor 7 activates phosphoinositide-3 kinase-mediated invasive and prosurvival pathways in head and neck cancer cells independent of EGFR. *Oncogene* **24**, 5897-5904 (2005).
102. Koizumi, K.*, et al.* CCL21 promotes the migration and adhesion of highly lymph node metastatic human non-small cell lung cancer Lu-99 in vitro. *Oncology reports* **17**, 1511-1516 (2007).
103. Ishida, K.*, et al.* High CCR7 mRNA expression of cancer cells is associated with lymph node involvement in patients with esophageal squamous cell carcinoma. *International journal of oncology* **34**, 915-922 (2009).
104. Kodama, J.*, et al.* Association of CXCR4 and CCR7 chemokine receptor expression and lymph node metastasis in human cervical cancer. *Annals of oncology : official journal of the European Society for Medical Oncology / ESMO* **18**, 70-76 (2007).
105. Pitkin, L.*, et al.* Expression of CC chemokine receptor 7 in tonsillar cancer predicts cervical nodal metastasis, systemic relapse and survival. *British journal of cancer* **97**, 670-677 (2007).
106. Mumtaz, M.*, et al.* Decreased expression of the chemokine CCL21 in human colorectal adenocarcinomas. *Oncology reports* **21**, 153-158 (2009).
107. Yousefieh, N., Hahto, S.M., Stephens, A.L. & Ciavarra, R.P. Regulated expression of CCL21 in the prostate tumor microenvironment inhibits tumor growth and metastasis in an orthotopic model of prostate cancer. *Cancer microenvironment : official journal of the International Cancer Microenvironment Society* **2**, 59-67 (2009).
108. Sperveslage, J.*, et al.* Lack of CCR7 expression is rate limiting for lymphatic spread of pancreatic ductal adenocarcinoma. *International journal of cancer. Journal international du cancer* **131**, E371-381 (2012).

109. Shields, J.D.*, et al.* Chemokine-mediated migration of melanoma cells towards lymphatics--a mechanism contributing to metastasis. *Oncogene* **26**, 2997-3005 (2007).
110. Harrell, M.I., Iritani, B.M. & Ruddell, A. Tumor-induced sentinel lymph node lymphangiogenesis and increased lymph flow precede melanoma metastasis. *The American journal of pathology* **170**, 774-786 (2007).
111. Miteva, D.O.*, et al.* Transmural flow modulates cell and fluid transport functions of lymphatic endothelium. *Circulation research* **106**, 920-931 (2010).
112. Shields, J.D.*, et al.* Autologous chemotaxis as a mechanism of tumor cell homing to lymphatics via interstitial flow and autocrine CCR7 signaling. *Cancer cell* **11**, 526-538 (2007).
113. Shields, J.D., Kourtis, I.C., Tomei, A.A., Roberts, J.M. & Swartz, M.A. Induction of lymphoidlike stroma and immune escape by tumors that express the chemokine CCL21. *Science* **328**, 749-752 (2010).
114. Raman, D., Baugher, P.J., Thu, Y.M. & Richmond, A. Role of chemokines in tumor growth. *Cancer letters* **256**, 137-165 (2007).
115. Correale, P.*, et al.* Tumor infiltration by chemokine receptor 7 (CCR7)(+) T-lymphocytes is a favorable prognostic factor in metastatic colorectal cancer. *Oncoimmunology* **1**, 531-532 (2012).
116. Wu, S.*, et al.* CC chemokine ligand 21 enhances the immunogenicity of the breast cancer cell line MCF-7 upon assistance of TLR2. *Carcinogenesis* **32**, 296-304 (2011).
117. Sharma, S.*, et al.* Secondary lymphoid tissue chemokine mediates T cell-dependent antitumor responses in vivo. *Journal of immunology* **164**, 4558-4563 (2000).
118. Kirk, C.J.*, et al.* T cell-dependent antitumor immunity mediated by secondary lymphoid tissue chemokine: augmentation of dendritic cell-based immunotherapy. *Cancer research* **61**, 2062-2070 (2001).
119. Yang, S.C.*, et al.* Intratumoral administration of dendritic cells overexpressing CCL21 generates systemic antitumor responses and confers tumor immunity. *Clinical cancer research : an official journal of the American Association for Cancer Research* **10**, 2891-2901 (2004).
120. Mebius, R.E. Organogenesis of lymphoid tissues. *Nature reviews. Immunology* **3**, 292-303 (2003).
121. van de Pavert, S.A.*, et al.* Chemokine CXCL13 is essential for lymph node initiation and is induced by retinoic acid and neuronal stimulation. *Nature immunology* **10**, 1193-1199 (2009).
122. Dejardin, E.*, et al.* The lymphotoxin-beta receptor induces different patterns of gene expression via two NF-kappaB pathways. *Immunity* **17**, 525-535 (2002).
123. Benezech, C.*, et al.* Ontogeny of stromal organizer cells during lymph node development. *Journal of immunology* **184**, 4521-4530 (2010).
124. Mebius, R.E., Rennert, P. & Weissman, I.L. Developing lymph nodes collect CD4+CD3- LTbeta+ cells that can differentiate to APC, NK cells, and follicular cells but not T or B cells. *Immunity* **7**, 493-504 (1997).

125. Luther, S.A., Ansel, K.M. & Cyster, J.G. Overlapping roles of CXCL13, interleukin 7 receptor alpha, and CCR7 ligands in lymph node development. *The Journal of experimental medicine* **197**, 1191-1198 (2003).
126. Honda, K.*, et al.* Molecular basis for hematopoietic/mesenchymal interaction during initiation of Peyer's patch organogenesis. *The Journal of experimental medicine* **193**, 621-630 (2001).
127. Vondenhoff, M.F.*, et al.* LTbetaR signaling induces cytokine expression and up-regulates lymphangiogenic factors in lymph node anlagen. *Journal of immunology* **182**, 5439-5445 (2009).
128. Kim, D.*, et al.* Regulation of peripheral lymph node genesis by the tumor necrosis factor family member TRANCE. *The Journal of experimental medicine* **192**, 1467-1478 (2000).
129. Dougall, W.C.*, et al.* RANK is essential for osteoclast and lymph node development. *Genes & development* **13**, 2412-2424 (1999).
130. Knoop, K.A., Butler, B.R., Kumar, N., Newberry, R.D. & Williams, I.R. Distinct developmental requirements for isolated lymphoid follicle formation in the small and large intestine: RANKL is essential only in the small intestine. *The American journal of pathology* **179**, 1861-1871 (2011).
131. Sugiyama, M.*, et al.* Expression pattern changes and function of RANKL during mouse lymph node microarchitecture development. *International immunology* **24**, 369-378 (2012).
132. van de Pavert, S.A. & Mebius, R.E. New insights into the development of lymphoid tissues. *Nature reviews. Immunology* **10**, 664-674 (2010).
133. Cella, M.*, et al.* A human natural killer cell subset provides an innate source of IL-22 for mucosal immunity. *Nature* **457**, 722-725 (2009).
134. Spits, H. & Di Santo, J.P. The expanding family of innate lymphoid cells: regulators and effectors of immunity and tissue remodeling. *Nature immunology* **12**, 21-27 (2011).
135. Spits, H.*, et al.* Innate lymphoid cells--a proposal for uniform nomenclature. *Nature reviews. Immunology* **13**, 145-149 (2013).
136. Yokota, Y.*, et al.* Development of peripheral lymphoid organs and natural killer cells depends on the helix-loop-helix inhibitor Id2. *Nature* **397**, 702-706 (1999).
137. Engel, I. & Murre, C. The function of E- and Id proteins in lymphocyte development. *Nature reviews. Immunology* **1**, 193-199 (2001).
138. Mebius, R.E.*, et al.* The fetal liver counterpart of adult common lymphoid progenitors gives rise to all lymphoid lineages, CD45+CD4+CD3- cells, as well as macrophages. *Journal of immunology* **166**, 6593-6601 (2001).
139. Eberl, G.*, et al.* An essential function for the nuclear receptor RORgamma(t) in the generation of fetal lymphoid tissue inducer cells. *Nature immunology* **5**, 64-73 (2004).
140. Vonarbourg, C.*, et al.* Regulated expression of nuclear receptor RORgammat confers distinct functional fates to NK cell receptor-expressing RORgammat(+) innate lymphocytes. *Immunity* **33**, 736-751 (2010).

141. Meier, D.*, et al.* Ectopic lymphoid-organ development occurs through interleukin 7-mediated enhanced survival of lymphoid-tissue-inducer cells. *Immunity* **26**, 643-654 (2007).
142. Sun, Z.*, et al.* Requirement for RORgamma in thymocyte survival and lymphoid organ development. *Science* **288**, 2369-2373 (2000).
143. Kim, M.Y.*, et al.* OX40 ligand and CD30 ligand are expressed on adult but not neonatal CD4+CD3- inducer cells: evidence that IL-7 signals regulate CD30 ligand but not OX40 ligand expression. *Journal of immunology* **174**, 6686-6691 (2005).
144. Sawa, S.*, et al.* Lineage relationship analysis of RORgammat+ innate lymphoid cells. *Science* **330**, 665-669 (2010).
145. Colonna, M. Interleukin-22-producing natural killer cells and lymphoid tissue inducer-like cells in mucosal immunity. *Immunity* **31**, 15-23 (2009).
146. Kanamori, Y.*, et al.* Identification of novel lymphoid tissues in murine intestinal mucosa where clusters of c-kit+ IL-7R+ Thy1+ lympho-hemopoietic progenitors develop. *The Journal of experimental medicine* **184**, 1449-1459 (1996).
147. Hamada, H.*, et al.* Identification of multiple isolated lymphoid follicles on the antimesenteric wall of the mouse small intestine. *Journal of immunology* **168**, 57-64 (2002).
148. Tsuji, M.*, et al.* Requirement for lymphoid tissue-inducer cells in isolated follicle formation and T cell-independent immunoglobulin A generation in the gut. *Immunity* **29**, 261-271 (2008).
149. Kim, M.Y.*, et al.* Function of CD4+CD3- cells in relation to B- and T-zone stroma in spleen. *Blood* **109**, 1602-1610 (2007).
150. Scandella, E.*, et al.* Restoration of lymphoid organ integrity through the interaction of lymphoid tissue-inducer cells with stroma of the T cell zone. *Nature immunology* **9**, 667-675 (2008).
151. Lane, P.J., Gaspal, F.M. & Kim, M.Y. Two sides of a cellular coin: CD4(+)CD3- cells regulate memory responses and lymph-node organization. *Nature reviews. Immunology* **5**, 655-660 (2005).
152. Kim, M.Y.*, et al.* CD4(+)CD3(-) accessory cells costimulate primed CD4 T cells through OX40 and CD30 at sites where T cells collaborate with B cells. *Immunity* **18**, 643-654 (2003).
153. Gaspal, F.*, et al.* Critical synergy of CD30 and OX40 signals in CD4 T cell homeostasis and Th1 immunity to Salmonella. *Journal of immunology* **180**, 2824-2829 (2008).
154. Gaspal, F.M.*, et al.* Mice deficient in OX40 and CD30 signals lack memory antibody responses because of deficient CD4 T cell memory. *Journal of immunology* **174**, 3891-3896 (2005).
155. Takatori, H.*, et al.* Lymphoid tissue inducer-like cells are an innate source of IL-17 and IL-22. *The Journal of experimental medicine* **206**, 35-41 (2009).
156. Spits, H. & Cupedo, T. Innate lymphoid cells: emerging insights in development, lineage relationships, and function. *Annual review of immunology* **30**, 647-675 (2012).
157. Tlsty, T.D. & Coussens, L.M. Tumor stroma and regulation of cancer development. *Annual review of pathology* **1**, 119-150 (2006).
158. Eisenring, M., vom Berg, J., Kristiansen, G., Saller, E. & Becher, B. IL-12 initiates tumor rejection via lymphoid tissue-inducer cells

bearing the natural cytotoxicity receptor NKp46. *Nature immunology* **11**, 1030-1038 (2010).
159. Joyce, J.A. & Pollard, J.W. Microenvironmental regulation of metastasis. *Nature reviews. Cancer* **9**, 239-252 (2009).
160. Dunn, G.P., Bruce, A.T., Ikeda, H., Old, L.J. & Schreiber, R.D. Cancer immunoediting: from immunosurveillance to tumor escape. *Nature immunology* **3**, 991-998 (2002).
161. Ikeda, H., Old, L.J. & Schreiber, R.D. The roles of IFN gamma in protection against tumor development and cancer immunoediting. *Cytokine & growth factor reviews* **13**, 95-109 (2002).
162. Smyth, M.J.*, et al.* Differential tumor surveillance by natural killer (NK) and NKT cells. *The Journal of experimental medicine* **191**, 661-668 (2000).
163. Swann, J.B. & Smyth, M.J. Immune surveillance of tumors. *The Journal of clinical investigation* **117**, 1137-1146 (2007).
164. Smyth, M.J., Crowe, N.Y. & Godfrey, D.I. NK cells and NKT cells collaborate in host protection from methylcholanthrene-induced fibrosarcoma. *International immunology* **13**, 459-463 (2001).
165. Disis, M.L. Immune regulation of cancer. *Journal of clinical oncology : official journal of the American Society of Clinical Oncology* **28**, 4531-4538 (2010).
166. Koebel, C.M.*, et al.* Adaptive immunity maintains occult cancer in an equilibrium state. *Nature* **450**, 903-907 (2007).
167. Mantovani, A., Allavena, P., Sica, A. & Balkwill, F. Cancer-related inflammation. *Nature* **454**, 436-444 (2008).
168. Galon, J., Fridman, W.H. & Pages, F. The adaptive immunologic microenvironment in colorectal cancer: a novel perspective. *Cancer research* **67**, 1883-1886 (2007).
169. Mlecnik, B.*, et al.* Histopathologic-based prognostic factors of colorectal cancers are associated with the state of the local immune reaction. *Journal of clinical oncology : official journal of the American Society of Clinical Oncology* **29**, 610-618 (2011).
170. Fridman, W.H., Pages, F., Sautes-Fridman, C. & Galon, J. The immune contexture in human tumours: impact on clinical outcome. *Nature reviews. Cancer* **12**, 298-306 (2012).
171. Loi, S.*, et al.* Prognostic and predictive value of tumor-infiltrating lymphocytes in a phase III randomized adjuvant breast cancer trial in node-positive breast cancer comparing the addition of docetaxel to doxorubicin with doxorubicin-based chemotherapy: BIG 02-98. *Journal of clinical oncology : official journal of the American Society of Clinical Oncology* **31**, 860-867 (2013).
172. van der Burg, S.H.*, et al.* Harmonization of immune biomarker assays for clinical studies. *Science translational medicine* **3**, 108ps144 (2011).
173. Bell, D.*, et al.* In breast carcinoma tissue, immature dendritic cells reside within the tumor, whereas mature dendritic cells are located in peritumoral areas. *The Journal of experimental medicine* **190**, 1417-1426 (1999).
174. Coronella, J.A.*, et al.* Antigen-driven oligoclonal expansion of tumor-infiltrating B cells in infiltrating ductal carcinoma of the breast. *Journal of immunology* **169**, 1829-1836 (2002).

175. Gobert, M.*, et al.* Regulatory T cells recruited through CCL22/CCR4 are selectively activated in lymphoid infiltrates surrounding primary breast tumors and lead to an adverse clinical outcome. *Cancer research* **69**, 2000-2009 (2009).
176. Martinet, L.*, et al.* Human solid tumors contain high endothelial venules: association with T- and B-lymphocyte infiltration and favorable prognosis in breast cancer. *Cancer research* **71**, 5678-5687 (2011).
177. Gu-Trantien, C.*, et al.* CD4(+) follicular helper T cell infiltration predicts breast cancer survival. *The Journal of clinical investigation* **123**, 2873-2892 (2013).
178. Martinet, L.*, et al.* High endothelial venule blood vessels for tumor-infiltrating lymphocytes are associated with lymphotoxin beta-producing dendritic cells in human breast cancer. *Journal of immunology* **191**, 2001-2008 (2013).
179. Suzuki, A.*, et al.* Mature dendritic cells make clusters with T cells in the invasive margin of colorectal carcinoma. *The Journal of pathology* **196**, 37-43 (2002).
180. McMullen, T.P., Lai, R., Dabbagh, L., Wallace, T.M. & de Gara, C.J. Survival in rectal cancer is predicted by T cell infiltration of tumour-associated lymphoid nodules. *Clinical and experimental immunology* **161**, 81-88 (2010).
181. Coppola, D.*, et al.* Unique ectopic lymph node-like structures present in human primary colorectal carcinoma are identified by immune gene array profiling. *The American journal of pathology* **179**, 37-45 (2011).
182. Remark, R.*, et al.* Characteristics and clinical impacts of the immune environments in colorectal and renal cell carcinoma lung metastases: influence of tumor origin. *Clinical cancer research : an official journal of the American Association for Cancer Research* **19**, 4079-4091 (2013).
183. Dieu-Nosjean, M.C.*, et al.* Long-term survival for patients with non-small-cell lung cancer with intratumoral lymphoid structures. *Journal of clinical oncology : official journal of the American Society of Clinical Oncology* **26**, 4410-4417 (2008).
184. de Chaisemartin, L.*, et al.* Characterization of chemokines and adhesion molecules associated with T cell presence in tertiary lymphoid structures in human lung cancer. *Cancer research* **71**, 6391-6399 (2011).
185. Messina, J.L.*, et al.* 12-Chemokine gene signature identifies lymph node-like structures in melanoma: potential for patient selection for immunotherapy? *Scientific reports* **2**, 765 (2012).
186. Martinet, L.*, et al.* High endothelial venules (HEVs) in human melanoma lesions: Major gateways for tumor-infiltrating lymphocytes. *Oncoimmunology* **1**, 829-839 (2012).
187. Goc, J., Fridman, W.H., Sautes-Fridman, C. & Dieu-Nosjean, M.C. Characteristics of tertiary lymphoid structures in primary cancers. *Oncoimmunology* **2**, e26836 (2013).
188. Cupedo, T., Jansen, W., Kraal, G. & Mebius, R.E. Induction of secondary and tertiary lymphoid structures in the skin. *Immunity* **21**, 655-667 (2004).

189. Moyron-Quiroz, J.E.*, et al.* Role of inducible bronchus associated lymphoid tissue (iBALT) in respiratory immunity. *Nature medicine* **10**, 927-934 (2004).
190. Lochner, M.*, et al.* Microbiota-induced tertiary lymphoid tissues aggravate inflammatory disease in the absence of RORgamma t and LTi cells. *The Journal of experimental medicine* **208**, 125-134 (2011).
191. Endres, R.*, et al.* Mature follicular dendritic cell networks depend on expression of lymphotoxin beta receptor by radioresistant stromal cells and of lymphotoxin beta and tumor necrosis factor by B cells. *The Journal of experimental medicine* **189**, 159-168 (1999).
192. Mohammed, R.A.*, et al.* Lymphatic and blood vessels in basal and triple-negative breast cancers: characteristics and prognostic significance. *Modern pathology : an official journal of the United States and Canadian Academy of Pathology, Inc* **24**, 774-785 (2011).
193. Workman, P.*, et al.* Guidelines for the welfare and use of animals in cancer research. *British journal of cancer* **102**, 1555-1577 (2010).
194. Lelekakis, M.*, et al.* A novel orthotopic model of breast cancer metastasis to bone. *Clinical & experimental metastasis* **17**, 163-170 (1999).
195. Papatheodorou, I.*, et al.* A metadata approach for clinical data management in translational genomics studies in breast cancer. *BMC medical genomics* **2**, 66 (2009).
196. Weigelt, B.*, et al.* Breast cancer molecular profiling with single sample predictors: a retrospective analysis. *The lancet oncology* **11**, 339-349 (2010).
197. Gazinska, P.*, et al.* Comparison of basal-like triple-negative breast cancer defined by morphology, immunohistochemistry and transcriptional profiles. *Modern pathology : an official journal of the United States and Canadian Academy of Pathology, Inc* **26**, 955-966 (2013).
198. Ritsma, L.*, et al.* Intravital microscopy through an abdominal imaging window reveals a pre-micrometastasis stage during liver metastasis. *Science translational medicine* **4**, 158ra145 (2012).
199. Hothorn T HK, v.d.W.M., Zeileis A Implementing a Class of Permutation Tests: The coin Package. *Journal of Statistical Software; 28: 1-23.* (2008).
200. Hothorn T HK, v.d.W.M., Zeileis A A Lego System for Conditional Inference. *The American Statistician; 60: 257-263* (2006).
201. Kim, S.*, et al.* CD117(+) CD3(-) CD56(-) OX40Lhigh cells express IL-22 and display an LTi phenotype in human secondary lymphoid tissues. *European journal of immunology* **41**, 1563-1572 (2011).
202. Withers, D.R.*, et al.* Cutting edge: lymphoid tissue inducer cells maintain memory CD4 T cells within secondary lymphoid tissue. *Journal of immunology* **189**, 2094-2098 (2012).
203. Thelen, M. & Stein, J.V. How chemokines invite leukocytes to dance. *Nature immunology* **9**, 953-959 (2008).
204. Sorlie, T.*, et al.* Gene expression patterns of breast carcinomas distinguish tumor subclasses with clinical implications. *Proceedings of the National Academy of Sciences of the United States of America* **98**, 10869-10874 (2001).

205. Perou, C.M., *et al.* Molecular portraits of human breast tumours. *Nature* **406**, 747-752 (2000).
206. Schutyser, E., Struyf, S. & Van Damme, J. The CC chemokine CCL20 and its receptor CCR6. *Cytokine & growth factor reviews* **14**, 409-426 (2003).
207. de Rinaldis, E., *et al.* Integrated genomic analysis of triple-negative breast cancers reveals novel microRNAs associated with clinical and molecular phenotypes and sheds light on the pathways they control. *BMC genomics* **14**, 643 (2013).
208. Gentleman, R.C., *et al.* Bioconductor: open software development for computational biology and bioinformatics. *Genome biology* **5**, R80 (2004).
209. Schroeder M H-KB, C.A., Sotiriou A, Bontempi G and Quackenbush J. . breastCancerMAINZ: Gene expression dataset published by Schmidt et al. [2008] (MAINZ). R package version 1.0.5. 2011; http://compbio.dfci.harvard.edu/. (2011).
210. Schroeder M H-KB, C.A., Sotiriou A, Bontempi G and Quackenbush J. . breastCancer TRANSBIG: Gene expression dataset published by Desmedt et al. [2007] (TRANSBIG). R package version 1.0.5. 2011; http://compbio.dfci.harvard.edu/. (2011).
211. Schroeder M H-KB, C.A., Sotiriou A, Bontempi G and Quackenbush J. . breastCancerUNT: Gene expression dataset published by Sotiriou et al. [2007] (UNT). R package version 1.0.5. 2011; http://compbio.dfci.harvard.edu/. (2011).
212. Schroeder M H-KB, C.A., Sotiriou A, Bontempi G and Quackenbush J. . breastCancerUPP: Gene expression dataset published by Miller et al. [2005] (UPP). R package version 1.0.5. 2011; http://compbio.dfci.harvard.edu/. (2011).
213. Schroeder M H-KB, C.A., Sotiriou A, Bontempi G and Quackenbush J. breastCancerVDX: Gene expression datasets published by Wang et al. [2005] and Minn et al. [2007] (VDX). R package version 1.0.5. 2011; http://compbio.dfci.harvard.edu/. (2011).
214. Desmedt, C., *et al.* Strong time dependence of the 76-gene prognostic signature for node-negative breast cancer patients in the TRANSBIG multicenter independent validation series. *Clinical cancer research : an official journal of the American Association for Cancer Research* **13**, 3207-3214 (2007).
215. Schmidt, M., *et al.* The humoral immune system has a key prognostic impact in node-negative breast cancer. *Cancer research* **68**, 5405-5413 (2008).
216. Miller, L.D., *et al.* An expression signature for p53 status in human breast cancer predicts mutation status, transcriptional effects, and patient survival. *Proceedings of the National Academy of Sciences of the United States of America* **102**, 13550-13555 (2005).
217. Wang, Y., *et al.* Gene-expression profiles to predict distant metastasis of lymph-node-negative primary breast cancer. *Lancet* **365**, 671-679 (2005).
218. Minn, A.J., *et al.* Lung metastasis genes couple breast tumor size and metastatic spread. *Proceedings of the National Academy of Sciences of the United States of America* **104**, 6740-6745 (2007).

219. Sotiriou, C.*, et al.* Gene expression profiling in breast cancer: understanding the molecular basis of histologic grade to improve prognosis. *Journal of the National Cancer Institute* **98**, 262-272 (2006).
220. Van der Auwera, I.*, et al.* First international consensus on the methodology of lymphangiogenesis quantification in solid human tumours. *British journal of cancer* **95**, 1611-1625 (2006).
221. Breiteneder-Geleff, S.*, et al.* [Podoplanin--a specific marker for lymphatic endothelium expressed in angiosarcoma]. *Verhandlungen der Deutschen Gesellschaft fur Pathologie* **83**, 270-275 (1999).
222. Ji, R.C., Eshita, Y. & Kato, S. Investigation of intratumoural and peritumoural lymphatics expressed by podoplanin and LYVE-1 in the hybridoma-induced tumours. *International journal of experimental pathology* **88**, 257-270 (2007).
223. Raica, M., Cimpean, A.M. & Ribatti, D. The role of podoplanin in tumor progression and metastasis. *Anticancer research* **28**, 2997-3006 (2008).
224. Evangelou, E., Kyzas, P.A. & Trikalinos, T.A. Comparison of the diagnostic accuracy of lymphatic endothelium markers: Bayesian approach. *Modern pathology : an official journal of the United States and Canadian Academy of Pathology, Inc* **18**, 1490-1497 (2005).
225. Van der Auwera, I.*, et al.* Tumor lymphangiogenesis in inflammatory breast carcinoma: a histomorphometric study. *Clinical cancer research : an official journal of the American Association for Cancer Research* **11**, 7637-7642 (2005).
226. Weidner, N. Current pathologic methods for measuring intratumoral microvessel density within breast carcinoma and other solid tumors. *Breast cancer research and treatment* **36**, 169-180 (1995).
227. Randall, T.D., Carragher, D.M. & Rangel-Moreno, J. Development of secondary lymphoid organs. *Annual review of immunology* **26**, 627-650 (2008).
228. Hong, Y.K.*, et al.* Prox1 is a master control gene in the program specifying lymphatic endothelial cell fate. *Developmental dynamics : an official publication of the American Association of Anatomists* **225**, 351-357 (2002).
229. Tran, B.*, et al.* Cancer genomics: technology, discovery, and translation. *Journal of clinical oncology : official journal of the American Society of Clinical Oncology* **30**, 647-660 (2012).
230. Lehmann, B.D.*, et al.* Identification of human triple-negative breast cancer subtypes and preclinical models for selection of targeted therapies. *The Journal of clinical investigation* **121**, 2750-2767 (2011).
231. Hicks, D.G.*, et al.* Breast cancers with brain metastases are more likely to be estrogen receptor negative, express the basal cytokeratin CK5/6, and overexpress HER2 or EGFR. *The American journal of surgical pathology* **30**, 1097-1104 (2006).
232. Irshad, S., Ellis, P. & Tutt, A. Molecular heterogeneity of triple-negative breast cancer and its clinical implications. *Current opinion in oncology* **23**, 566-577 (2011).

233. Cheang, M.C.*, et al.* Basal-like breast cancer defined by five biomarkers has superior prognostic value than triple-negative phenotype. *Clinical cancer research : an official journal of the American Association for Cancer Research* **14**, 1368-1376 (2008).
234. Isaka, N., Padera, T.P., Hagendoorn, J., Fukumura, D. & Jain, R.K. Peritumor lymphatics induced by vascular endothelial growth factor-C exhibit abnormal function. *Cancer research* **64**, 4400-4404 (2004).
235. Denkert, C.*, et al.* Tumor-associated lymphocytes as an independent predictor of response to neoadjuvant chemotherapy in breast cancer. *Journal of clinical oncology : official journal of the American Society of Clinical Oncology* **28**, 105-113 (2010).
236. Kreike, B.*, et al.* Gene expression profiling and histopathological characterization of triple-negative/basal-like breast carcinomas. *Breast cancer research : BCR* **9**, R65 (2007).
237. Pulaski, B.A. & Ostrand-Rosenberg, S. Mouse 4T1 breast tumor model. *Current protocols in immunology / edited by John E. Coligan ... [et al.]* **Chapter 20**, Unit 20 22 (2001).
238. Kaur, P.*, et al.* A mouse model for triple-negative breast cancer tumor-initiating cells (TNBC-TICs) exhibits similar aggressive phenotype to the human disease. *BMC cancer* **12**, 120 (2012).
239. Dexter, D.L.*, et al.* Heterogeneity of tumor cells from a single mouse mammary tumor. *Cancer research* **38**, 3174-3181 (1978).
240. Rankin, W., Grill, V. & Martin, T.J. Parathyroid hormone-related protein and hypercalcemia. *Cancer* **80**, 1564-1571 (1997).
241. Kim, M.Y.*, et al.* Heterogeneity of lymphoid tissue inducer cell populations present in embryonic and adult mouse lymphoid tissues. *Immunology* **124**, 166-174 (2008).
242. Evans, I. & Kim, M.Y. Involvement of lymphoid inducer cells in the development of secondary and tertiary lymphoid structure. *BMB reports* **42**, 189-193 (2009).
243. Bernardo, M.E., Locatelli, F. & Fibbe, W.E. Mesenchymal stromal cells. *Annals of the New York Academy of Sciences* **1176**, 101-117 (2009).
244. Religa, P.*, et al.* Presence of bone marrow-derived circulating progenitor endothelial cells in the newly formed lymphatic vessels. *Blood* **106**, 4184-4190 (2005).
245. Maruyama, K.*, et al.* Inflammation-induced lymphangiogenesis in the cornea arises from CD11b-positive macrophages. *The Journal of clinical investigation* **115**, 2363-2372 (2005).
246. Kerjaschki, D.*, et al.* Lymphatic endothelial progenitor cells contribute to de novo lymphangiogenesis in human renal transplants. *Nature medicine* **12**, 230-234 (2006).
247. Tanigaki, Y.*, et al.* The expression of vascular endothelial growth factor-A and -C, and receptors 1 and 3: correlation with lymph node metastasis and prognosis in tongue squamous cell carcinoma. *International journal of molecular medicine* **14**, 389-395 (2004).
248. Hall, B., Andreeff, M. & Marini, F. The participation of mesenchymal stem cells in tumor stroma formation and their application as targeted-gene delivery vehicles. *Handbook of experimental pharmacology*, 263-283 (2007).

249. Corcione, A.*, et al.* Human mesenchymal stem cells modulate B-cell functions. *Blood* **107**, 367-372 (2006).
250. Di Nicola, M.*, et al.* Human bone marrow stromal cells suppress T-lymphocyte proliferation induced by cellular or nonspecific mitogenic stimuli. *Blood* **99**, 3838-3843 (2002).
251. Zhang, W.*, et al.* Effects of mesenchymal stem cells on differentiation, maturation, and function of human monocyte-derived dendritic cells. *Stem cells and development* **13**, 263-271 (2004).
252. Bassi, E.J., Aita, C.A. & Camara, N.O. Immune regulatory properties of multipotent mesenchymal stromal cells: Where do we stand? *World journal of stem cells* **3**, 1-8 (2011).
253. Shay, J.W. & Wright, W.E. Senescence and immortalization: role of telomeres and telomerase. *Carcinogenesis* **26**, 867-874 (2005).
254. Zimmermann, S.*, et al.* Lack of telomerase activity in human mesenchymal stem cells. *Leukemia* **17**, 1146-1149 (2003).
255. Dominici, M.*, et al.* Minimal criteria for defining multipotent mesenchymal stromal cells. The International Society for Cellular Therapy position statement. *Cytotherapy* **8**, 315-317 (2006).
256. Alimzhanov, M.B.*, et al.* Abnormal development of secondary lymphoid tissues in lymphotoxin beta-deficient mice. *Proceedings of the National Academy of Sciences of the United States of America* **94**, 9302-9307 (1997).
257. Koni, P.A.*, et al.* Distinct roles in lymphoid organogenesis for lymphotoxins alpha and beta revealed in lymphotoxin beta-deficient mice. *Immunity* **6**, 491-500 (1997).
258. Kedrin, D.*, et al.* Intravital imaging of metastatic behavior through a mammary imaging window. *Nature methods* **5**, 1019-1021 (2008).
259. Gunther, K.*, et al.* Prediction of lymph node metastasis in colorectal carcinoma by expressionof chemokine receptor CCR7. *International journal of cancer. Journal international du cancer* **116**, 726-733 (2005).
260. Panse, J.*, et al.* Chemokine CXCL13 is overexpressed in the tumour tissue and in the peripheral blood of breast cancer patients. *British journal of cancer* **99**, 930-938 (2008).
261. Yuvaraj, S.*, et al.* A novel function of CXCL13 to stimulate RANK ligand expression in oral squamous cell carcinoma cells. *Molecular cancer research : MCR* **7**, 1399-1407 (2009).
262. Razis, E.*, et al.* Improved outcome of high-risk early HER2 positive breast cancer with high CXCL13-CXCR5 messenger RNA expression. *Clinical breast cancer* **12**, 183-193 (2012).
263. DeNardo, D.G., Andreu, P. & Coussens, L.M. Interactions between lymphocytes and myeloid cells regulate pro- versus anti-tumor immunity. *Cancer metastasis reviews* **29**, 309-316 (2010).
264. Viola, A., Sarukhan, A., Bronte, V. & Molon, B. The pros and cons of chemokines in tumor immunology. *Trends in immunology* **33**, 496-504 (2012).
265. Qian, B.Z.*, et al.* CCL2 recruits inflammatory monocytes to facilitate breast-tumour metastasis. *Nature* **475**, 222-225 (2011).
266. Molon, B.*, et al.* Chemokine nitration prevents intratumoral infiltration of antigen-specific T cells. *The Journal of experimental medicine* **208**, 1949-1962 (2011).

267. Yau, C.*, et al.* A multigene predictor of metastatic outcome in early stage hormone receptor-negative and triple-negative breast cancer. *Breast cancer research : BCR* **12**, R85 (2010).
268. Sabatier, R.*, et al.* Kinome expression profiling and prognosis of basal breast cancers. *Molecular cancer* **10**, 86 (2011).
269. Ono, M.*, et al.* Tumor-infiltrating lymphocytes are correlated with response to neoadjuvant chemotherapy in triple-negative breast cancer. *Breast cancer research and treatment* **132**, 793-805 (2012).
270. Nieto, M.A. The ins and outs of the epithelial to mesenchymal transition in health and disease. *Annual review of cell and developmental biology* **27**, 347-376 (2011).
271. Mueller, C.G. & Hess, E. Emerging Functions of RANKL in Lymphoid Tissues. *Frontiers in immunology* **3**, 261 (2012).
272. Palafox, M.*, et al.* RANK induces epithelial-mesenchymal transition and stemness in human mammary epithelial cells and promotes tumorigenesis and metastasis. *Cancer research* **72**, 2879-2888 (2012).
273. Gonzalez-Suarez, E.*, et al.* RANK ligand mediates progestin-induced mammary epithelial proliferation and carcinogenesis. *Nature* **468**, 103-107 (2010).
274. Sambandam, Y.*, et al.* CXCL13 activation of c-Myc induces RANK ligand expression in stromal/preosteoblast cells in the oral squamous cell carcinoma tumor-bone microenvironment. *Oncogene* **32**, 97-105 (2013).
275. Lum, L.*, et al.* Evidence for a role of a tumor necrosis factor-alpha (TNF-alpha)-converting enzyme-like protease in shedding of TRANCE, a TNF family member involved in osteoclastogenesis and dendritic cell survival. *The Journal of biological chemistry* **274**, 13613-13618 (1999).
276. Zhang, L.*, et al.* C-Src-mediated RANKL-induced breast cancer cell migration by activation of the ERK and Akt pathway. *Oncology letters* **3**, 395-400 (2012).
277. El-Haibi, C.P., Singh, R., Sharma, P.K., Singh, S. & Lillard, J.W., Jr. CXCL13 mediates prostate cancer cell proliferation through JNK signalling and invasion through ERK activation. *Cell proliferation* **44**, 311-319 (2011).
278. Tan, W.*, et al.* Tumour-infiltrating regulatory T cells stimulate mammary cancer metastasis through RANKL-RANK signalling. *Nature* **470**, 548-553 (2011).
279. Fernandez-Valdivia, R.*, et al.* The RANKL signaling axis is sufficient to elicit ductal side-branching and alveologenesis in the mammary gland of the virgin mouse. *Developmental biology* **328**, 127-139 (2009).
280. Yamada, T.*, et al.* RANKL expression specifically observed in vivo promotes epithelial mesenchymal transition and tumor progression. *The American journal of pathology* **178**, 2845-2856 (2011).
281. Reyes ME, M.H., Zhang D, Reuben JM, Woodward W, Darnay BG, Hortobagyi GH, and Ueno NT. Receptor Activator of Nuclear Factor Kappa B (RANK) as a potential therapeutic target in triple-negative breast cancer *Cancer Research: December 15, 2012; Volume 72, Issue 24, Supplement 3* **doi: 10.1158/0008-5472.SABCS12-P5-03-09** (2012).

282. Martin, T.J. & Mundy, G.R. Bone metastasis: can osteoclasts be excluded? *Nature* **445**, E19; discussion E19-20 (2007).
283. Santini, D.*, et al.* Receptor activator of NF-kB (RANK) expression in primary tumors associates with bone metastasis occurrence in breast cancer patients. *PloS one* **6**, e19234 (2011).
284. Mikami, S.*, et al.* Increased RANKL expression is related to tumour migration and metastasis of renal cell carcinomas. *The Journal of pathology* **218**, 530-539 (2009).
285. Theill, L.E., Boyle, W.J. & Penninger, J.M. RANK-L and RANK: T cells, bone loss, and mammalian evolution. *Annual review of immunology* **20**, 795-823 (2002).
286. Sobacchi, C.*, et al.* Osteoclast-poor human osteopetrosis due to mutations in the gene encoding RANKL. *Nature genetics* **39**, 960-962 (2007).
287. Guerrini, M.M.*, et al.* Human osteoclast-poor osteopetrosis with hypogammaglobulinemia due to TNFRSF11A (RANK) mutations. *American journal of human genetics* **83**, 64-76 (2008).
288. Kong, Y.Y.*, et al.* OPGL is a key regulator of osteoclastogenesis, lymphocyte development and lymph-node organogenesis. *Nature* **397**, 315-323 (1999).
289. McGrath, E.E. OPG/RANKL/RANK pathway as a therapeutic target in cancer. *Journal of thoracic oncology : official publication of the International Association for the Study of Lung Cancer* **6**, 1468-1473 (2011).
290. Lipton, A.*, et al.* Superiority of denosumab to zoledronic acid for prevention of skeletal-related events: a combined analysis of 3 pivotal, randomised, phase 3 trials. *European journal of cancer* **48**, 3082-3092 (2012).
291. Scagliotti, G.V.*, et al.* Overall survival improvement in patients with lung cancer and bone metastases treated with denosumab versus zoledronic acid: subgroup analysis from a randomized phase 3 study. *Journal of thoracic oncology : official publication of the International Association for the Study of Lung Cancer* **7**, 1823-1829 (2012).
292. Quail, D.F. & Joyce, J.A. Microenvironmental regulation of tumor progression and metastasis. *Nature medicine* **19**, 1423-1437 (2013).
293. Magri, G.*, et al.* Innate lymphoid cells integrate stromal and immunological signals to enhance antibody production by splenic marginal zone B cells. *Nature immunology* **15**, 354-364 (2014).
294. Lane, P.J., Gaspal, F.M., McConnell, F.M., Withers, D.R. & Anderson, G. Lymphoid tissue inducer cells: pivotal cells in the evolution of CD4 immunity and tolerance? *Frontiers in immunology* **3**, 24 (2012).
295. Sharpe, A.H. & Freeman, G.J. The B7-CD28 superfamily. *Nature reviews. Immunology* **2**, 116-126 (2002).

Chapter 9: Appendix 1

The following is the work published by during the course of this doctorate. Some of this work is cited in the text.

Breast Cancer Res Treat (2014) 144:331–341
DOI 10.1007/s10549-014-2855-4

CLINICAL TRIAL

Assessment of microtubule-associated protein (MAP)-Tau expression as a predictive and prognostic marker in TACT; a trial assessing substitution of sequential docetaxel for FEC as adjuvant chemotherapy for early breast cancer

S. Irshad · C. Gillett · S. E. Pinder · R. P. A'Hern · M. Dowsett · I. O. Ellis · J. M. S. Bartlett · J. M. Bliss · A. Hanby · S. Johnston · P. Barrett-Lee · P. Ellis · A. Tutt

Received: 19 January 2014 / Accepted: 22 January 2014 / Published online: 12 February 2014

Abstract The TACT trial is the largest study assessing the benefit of taxanes as part of adjuvant therapy for early breast cancer. The goal of this translational study was to clarify the predictive and prognostic value of Tau within the TACT trial. Tissue microarrays (TMA) were available from 3,610 patients. ER, PR, HER2 from the TACT trial and Tau protein expression was determined by immunohistochemistry on duplicate TMAs. Two parallel scoring systems were generated for Tau expression ('dichotomised' vs. 'combined' score). The positivity rate of Tau expression was 50 % in the trial population ($n = 2{,}483$). Tau expression correlated positively with ER ($p < 0.001$) and PR status ($p < 0.001$); but negatively with histological grade ($p < 0.001$) and HER2 status ($p < 0.001$). Analyses with either scoring systems for Tau expression demonstrated no significant interaction between Tau expression and efficacy of docetaxel. Contrary to the hypothesis that taxane benefit would be enriched in Tau negative/low patients, the only groups with a suggestion of a reduced event rate in the taxane group were the HER2-positive, Tau positive subgroups. Tau expression was seen to be a prognostic factor on univariate analysis associated with an improved DFS, independent of the treatment group ($p < 0.001$). It had no prognostic value in ER-negative tumours and the weak prognostic effect of Tau in ER-positive tumours ($p = 0.02$) diminished, when considering ER as an ordinal variable. On multivariable analyses, Tau had no prognostic value in either group. In addition, no significant interaction between Tau expression and benefit from docetaxel in patients within the PR-positive and

Electronic supplementary material The online version of this article (doi:10.1007/s10549-014-2855-4) contains supplementary material, which is available to authorized users.

S. Irshad · A. Tutt (✉)
Breakthrough Breast Cancer Research Unit, Department of Research Oncology, Guy's Hospital, King's College London School of Medicine, London SE1 9RT, UK
e-mail: andrew.tutt@kcl.ac.uk

S. Irshad
e-mail: sheeba.irshad@kcl.ac.uk

C. Gillett · S. E. Pinder
King's Health Partners Cancer Biobank, Guy's Hospital, King's College London School of Medicine, London SE1 9RT, UK

R. P. A'Hern · J. M. Bliss
Clinical Trials and Statistics Unit (ICR-CTSU), Division of Clinical Studies, The Institute of Cancer Research, London SM2 5NG, UK

M. Dowsett
Academic Department of Biochemistry, The Royal Marsden Hospital, Fulham Road, London SW3 6JJ, UK

M. Dowsett
Academic Department of Biochemistry, The Breakthrough Breast Cancer Research Centre, Fulham Road, London SW3 6JJ, UK

I. O. Ellis
Department of Histopathology, Molecular Medical Sciences, Nottingham City Hospital, University of Nottingham, Nottingham, UK

J. M. S. Bartlett
Transformative Pathology, Ontario Institute for Cancer Research, Toronto, ON M5G 0A3, Canada

A. Hanby
Section of Pathology and Tumour Biology, Leeds Institute of Cancer and Pathology (LICAP), St James's University Hospital, Wellcome Trust Brenner Building, Leeds LS9 7TF, UK

negative subsets was seen. This is now the second large adjuvant study, and the first with quantitative analysis of ER and Tau expression, failing to show an association between Tau and taxane benefit with limited utility as a prognostic marker for Tau in ER-positive early breast cancer patients.

Keywords Breast cancer · Clinical trials · TACT · Taxanes · Tau · Predictive biomarker · Prognostic biomarker

Introduction

Taxanes are potent cytotoxic compounds that have become a standard component of many adjuvant and neoadjuvant chemotherapy regimens for early breast cancer [1–5]. Overview analyses have suggested a small but clear incremental benefit for taxane-based therapy [6]. However, the addition of taxanes to cytotoxic regimens has not always demonstrated a consistent improvement in outcomes. Some studies have clearly shown an overall survival (OS) benefit, others an improvement in disease-free survival (DFS) but not OS, while others have shown no benefit [6]. Explanations for the variable evidence of additional therapeutic efficacy may include differences in sequence, duration and choice of control regimen. The UK Taxotere as Adjuvant Chemotherapy Trial (TACT) assessed the benefit of taxanes as part of an adjuvant therapy for early breast cancer patients and did not demonstrate an improvement in DFS, its primary endpoint measure [7, 8]. In the TACT trial treatment duration was similar in the comparator groups. The EBCTCG meta-analyses of adjuvant taxane treatment ($n = 44{,}000$ in 33 studies) confirmed that in trials where more anthracycline was given in the control groups to balance the treatment duration of taxanes, no significant difference in breast cancer mortality in favour of taxanes was observed, but in trials in which four cycles of a taxane were added to a fixed anthracycline-based regimen, breast cancer mortality decreased [9].

In addition to differences in clinical trial design and demographic differences in trial patient populations, the biological heterogeneity between patients' tumours in relation to sensitivity and resistance to microtubule inhibition is likely to be critical in determining taxane benefit. Identification of definitive biomarkers to predict which patients benefit from taxane therapy and, conversely, which can be spared the cytotoxic effects of such treatments would be an important improvement in patient care [10]. Taxanes are known to exert their cytotoxic activity by interfering with spindle microtubule dynamics causing G2-M interphase cell cycle arrest, inducing subsequent apoptosis of tumour cells [3, 11]. Microtubule-associated proteins (MAPs) are endogenous proteins which participate in the organization, stabilization and function of the microtubules [12], and have, therefore, been under investigation as candidate markers to predict response to taxane therapy.

MAP-Tau protein (50–64 KDa) binds to the same pocket as taxanes in microtubules, thus competing for the drug-binding site [13–15]. In vitro experiments with small interfering RNAs have indicated that suppression of Tau increases the sensitivity of breast cancer cells to taxanes [16, 17], however, results from clinical studies evaluating Tau as a predictive biomarker for taxane sensitivity have been conflicting. Early studies of neoadjuvant taxane therapy reported a significant correlation between low Tau protein expression and higher pathological complete response (pCR) rate [16, 18]. Although this association has been supported by other clinical studies in the metastatic setting [19, 20]; no correlation between Tau gene/protein expression levels and efficacy of taxanes was observed in the retrospective subset analyses of the neoadjuvant GeparTrio [21], the adjuvant Hellenic Cooperative Oncology Group (HECOG) [22] or the National Surgical Adjuvant Breast and Bowel Project (NSABP) B-28 trials [23].

Tau mRNA expression is induced by oestrogen, as well as tamoxifen, and correlates with oestrogen receptor (ER) expression [18, 22, 24]. It is possible that greater paclitaxel treatment effects observed in patients with Tau negative, ER-positive tumours who also received hormonal therapy may be skewed by the greater effect of addition of a taxane in those with less endocrine therapy sensitive disease. High Tau mRNA expression was shown to be significantly associated with reduced risk of recurrence (at both 5 and 10 years, $p = 0.005$ and $p = 0.05$, respectively) in patients treated with tamoxifen, indicating a potential predictive value of high Tau expression for endocrine therapy [18]. However, the positive association between Tau and ER expression within ER-positive tumours may explain this observation, addressing this question was one of the motivations of the current study.

As well as linking high Tau expression with endocrine sensitive disease and poorer response to chemotherapy, high Tau expression has been shown to be an independent good prognostic factor in some series [18, 20, 22, 23, 25]. In NSABP B-28 study ($n = 1{,}942$), a positive prognostic effect of high Tau expression was found in patients with ER-positive tumours. However, there were too few

S. Johnston
Department of Medicine, Royal Marsden Hospital, Fulham Road, London SW3 6JJ, UK

P. Barrett-Lee
Academic Breast Unit, Velindre Cancer Center, Velindre NHS Trust, Cardiff CF14 2TL, UK

P. Ellis
Department of Medical Oncology, Guy's & St Thomas' Foundation Trust, London SE1 9RT, UK

($n = 97$) Tau positive patients in the ER-negative group to confidently address this question for this subgroup [23]. In contrast, a more recent study by Baquero et al. [26], reporting on the Yale University breast cancer cohort ($n = 651$) consisting of 57 % ER-negative cases, Tau showed a prognostic value in patients with ER-negative tumours. It is noteworthy that the immunohistochemistry (IHC) staining and scoring procedures were fundamentally different between the two studies. The relationship between ER and Tau in relation to prognosis and taxane treatment benefit prediction thus remains unclear and further study with separate analyses of ER-positive and negative tumours, and quantitative analyses of degree of expression of these biomarkers, are required to explore the Tau and oestrogen association in more detail. The TACT trial translational tissue database provides an appropriate test-bed for assessing biomarkers such as Tau. The goal of this translational study was to clarify the prognostic and predictive value of Tau using tissue specimens from patients enrolled into TACT.

Patients and methods

This study is reported in accordance with REMARK criteria [27], and biomarker analysis was performed in a GCLP-compliant facility.

Patients

A total of 4,162 patients with node-positive or high-risk node-negative operable early breast cancer were randomised within the TACT trial to FEC (fluorouracil 600 mg/m^2, epirubicin 60 mg/m^2 and cyclophosphamide 600 mg/m^2) four cycles followed by docetaxel (100 mg/m^2) four cycles, or control. Control regimens were FEC_{60} for a total of eight cycles or epirubicin (100 mg/m^2) for four cycles followed by classical CMF (cyclophosphamide 600 mg/m^2, methotrexate 40 mg/m^2 and fluorouracil 600 mg/m^2) for four cycles [7].

TMA construction and immunohistochemistry

A representative formalin-fixed, paraffin-embedded (FFPE) block of invasive breast tumour was requested for each patient who consented to its collection for research in a prospectively planned programme for translational biomarker evaluation within the TACT trial cohort 'trans-TACT', as described in [28]. From each FFPE block, four 0.6 mm cores of invasive tumour were selected to create a tissue microarray (TMA). Within the TACT patient population, tumour tissues from 3,610 patients (87 % of total) were available for TMA construction. Each TMA block contained between 100 and 200 cores of tissue, depending upon the array design. Clinical and pathological data [age, histological grade, invasive tumour size, lymph node status, ER and progesterone receptor (PR) status, disease outcome data] were collected within the TACT trial. Central HER2 testing was carried out, as described elsewhere [29]. Sections from duplicate TMA blocks composed of 0.6 mm tumour cores were used to assess Tau protein expression using IHC. The IHC procedure was centralized with sections processed within 5 days.

TMA sections were dewaxed and rehydrated. Antigen retrieval was achieved using the Pascal pressurized retrieval unit with Dako Target Retrieval Solution (pH 6). Sections were transferred to an automated staining system (BioGenex i6000) and the following antibodies applied; Tau (US Biological T1029, 1:50), ER (Labvision SP-1, 1:150), PR (Dako PgR636, 1:400). Following incubation, bound antibody was detected using the Envision/HRP kit (Dako, Denmark) and sections counterstained with haematoxylin.

Assessment of ER, PR and Tau expression

Staining for ER, PR and Tau was performed at Guy's and St Thomas' Hospital on duplicate TMAs and central specialist review was separately undertaken by two of CG, SEP, JB and AH for each marker, without reference to treatment allocation or clinical outcome. ER (by CG and SEP) and PR (by JB and AH) were quantified using the Allred score [30], resulting in a scale of 0–8. For ER and PR, a score of 3 or more was considered positive [30].

For Tau expression (assessed by CG and SEP) both the intensity (negative, weak, moderate or strong) and proportion of invasive tumour cells showing cytoplasmic staining (in 5 % increments) were recorded (Fig. 1). Cores with less than 20 invasive cells were excluded as insufficient for assessment. If there was disagreement between the two observers on intensity score, or if proportion differed by more than 10 %, the cases were jointly re-assessed by CG and SEP and consensus reached. For each marker, the rounded average of the scores from the duplicate TMAs was regarded as the final result. An 'average Allred' score of 1, representing the average of duplicate cores with Allred scores of 0 and 2 was, therefore, obtained for a small number of cases.

Two parallel scoring systems were generated for the Tau expression: a) a 'dichotomised score' of negative versus positive, where Tau positive cases were defined as those demonstrating any expression and b) a 'combined Allred score' summing the intensity and the proportion of cytoplasmic staining, where intensity was scored 0–3, and proportion staining converted into a 0–5 score (0 % = 0, <1 % = 1, 1–10 % = 2, 11–33 % = 3, 34–65 % = 4 and 66–100 % = 5), thus representing Tau as a semi-

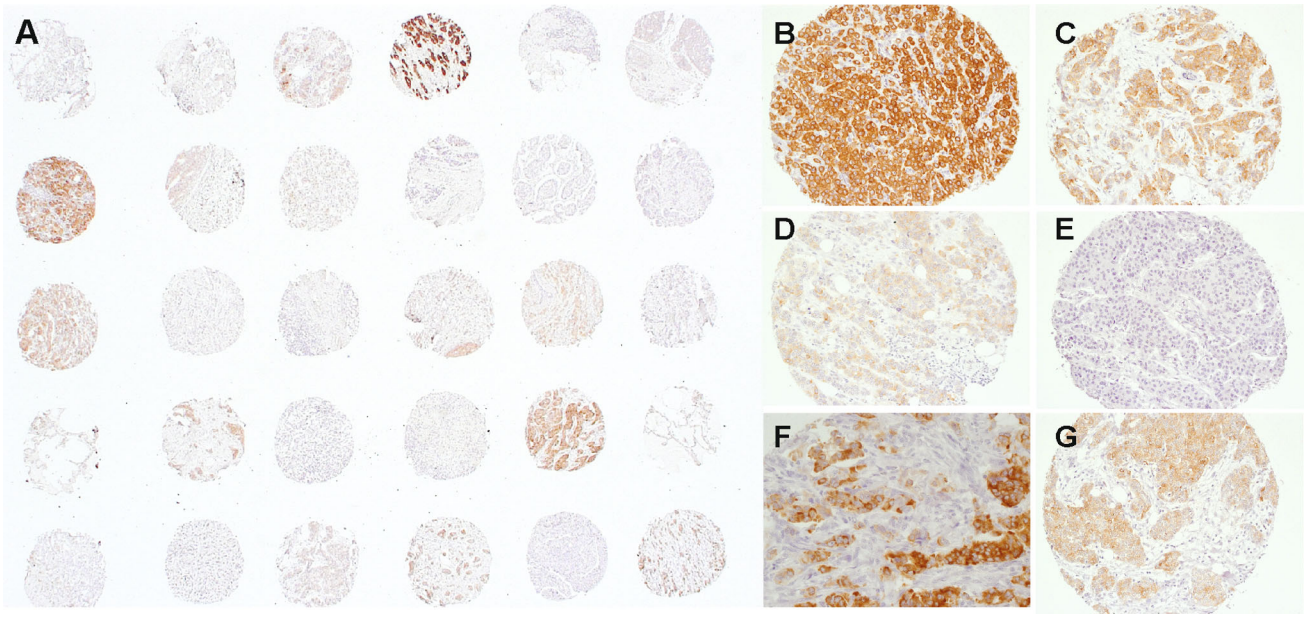

Fig. 1 Representative immunohistochemical staining of Tau expression in tissue microarrays constructed from the TACT trial patient population. **A** Low-power tissue microarray showing variable expression between tumour cores. **B** Strong expression (strong, 100 %). **C** Moderate expression (Moderate, 95 %). **D** Weak expression (Weak, 80 %). **E** No expression (Negative). **F** Intra-tumour variability demonstrating strong and no expression. **G** Intra-tumour variability showing weak and moderate expression

quantitative categorical variable with scores from 0 to 8. For simplicity, when illustrating the distribution of Tau by other characteristics and displaying the results of multivariable analysis, the Tau combined score was classified into three groups: 'negative' with a score of 0; 'intermediate' with a score of 1–6 and 'high' with a score of 7–8.

Statistical analysis

DFS was the primary endpoint of the study, defined as time from randomisation to first invasive relapse, new primary invasive breast cancer (ipsilateral or contralateral), or death from any cause; patients who remained alive and disease free at their date of last follow up being censored at that point. Kaplan–Meier curves were plotted for survival endpoints, and treatment groups compared by use of the log-rank test. Hazard ratios (HRs) (with 95 % CIs) were obtained from Cox proportional hazards regression models with a HR less than 1 favouring the experimental regimen (FEC-T). The proportionality assumption of the Cox model was tested by fitting time-dependent effects (proportional to log (follow up time) for each factor using the TVC command in STATA. Unless stated otherwise, all analyses were unadjusted and stratified by centre's choice of control regimen. All patients as randomised on an intention-to-treat basis were included in a specific analysis, if they had the factors required for that analysis successfully measured. A significance level of $p < 0.05$ was considered significant. This analysis is based on a database snapshot frozen on 25th November 2011 [8]. All analyses were done in STATA 11.2 for windows. The TACT trial is registered as an International Standard Randomised Controlled Trial, number ISRCTN79718493/

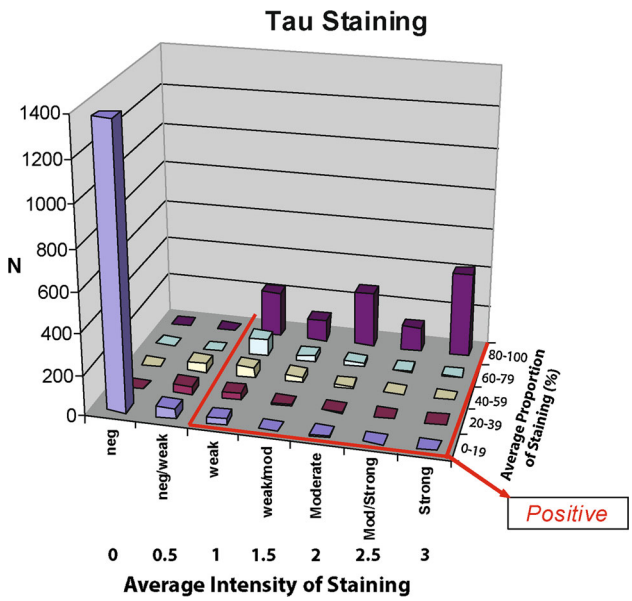

Fig. 2 Relationship between intensity and proportion of Tau staining. The number of cases is depicted along the vertical *y axis*. Subgroups of intensity of staining are depicted along the horizontal *x axis*. The percentage of cell staining within tissue sections is depicted along the *z axis*. Tau positive status in the dichotomized scoring analysis was defined as demonstrating at least weak intensity staining (*red box*)

Table 1 Tau expression correlation with clinical variables

		Tau expression			*p* value
		n (%)			
		Negative/low 1,124	Intermediate 647	High 712	
Age median (range)	2,493	49 (25-70)	49 (25–88)	48 (28–75)	0.06
No. of lymph nodes with metastasis					
0	552	311 (59.6)	101 (19.4)	110 (21.1)	
1–3	1,097	423 (38.6)	308 (28.1)	366 (33.4)	
4+	864	390 (45.1)	238 (27.6)	236 (27.3)	0.002
Invasive tumour size (cm)					
<2	1,599	718 (44.9)	426 (26.6)	455 (28.5)	
2–5	662	293 (44.3)	165 (24.9)	204 (30.8)	
>5	222	113 (50.9)	56 (25.2)	53 (23.9)	0.09
Histological grade					
1	135	30 (22.2)	35 (25.9)	70 (51.9)	
2	916	283 (30.9)	269 (29.4)	364 (39.7)	
3	1,432	811 (56.6)	343 (24)	278 (19.4)	<0.001
ER, Allred score					
0	783	611 (78)	106 (13.5)	66 (8.4)	
1[a]	60	39 (65)	15 (25)	6 (10)	
2	44	27 (61.4)	12 (27.3)	5 (11.4)	
3	77	38 (49.4)	20 (26)	19 (24.7)	
4	130	64 (49.2)	39 (30)	27 (20.8)	
5	173	54 (31.2)	60 (34.7)	59 (34.1)	
6	327	87 (26.6)	119 (36.4)	121 (37)	
7	441	111 (25.2)	138 (31.3)	192 (43.5)	
8	448	93 (20.8)	138 (30.8)	217 (48.4)	<0.001
PR, Allred score					
0	1,026	719 (70.1)	191 (18.6)	116 (11.3)	
1[a]	88	52 (59.1)	24 (27.3)	12 (13.6)	
2	101	46 (45.5)	32 (31.7)	23 (22.8)	
3	105	44 (41.9)	40 (38.1)	21 (20)	
4	176	61 (34.7)	61 (34.7)	54 (30.7)	
5	139	41 (29.5)	60 (43.2)	38 (27.3)	
6	159	33 (20.8)	61 (38.4)	65 (40.9)	
7	236	54 (22.9)	67 (28.4)	115 (48.7)	
8	453	74 (16.3)	111 (24.5)	268 (59.2)	<0.001
HER2 status					
Negative	1,910	781 (40.9)	490 (25.7)	639 (33.5)	
Positive	573	343 (59.9)	157 (27.4)	73 (12.7)	<0.001

[a] The rounded average of the Allred score from the duplicate TMAs was regarded as the definite result for each marker, thus an average Allred score of 1 is obtained for cases with duplicate cores scoring 0 and 2, respectively

CRUK01/001. With 796 events an interaction equivalent to a HR (taxane group: non-taxane group) of 0.76 in patients with Tau negative tumours and 1.08 in patients with Tau positive tumours would be detectable with 80 % power, one-sided 5 % significance level, these levels have been chosen to be compatible with the overall HR of 0.92.

Results

Patient characteristics and Tau expression

Sixty-nine percent ($n = 2,483$) of the tumours from the total of 3,610 cases in the TMAs were assessable for ER,

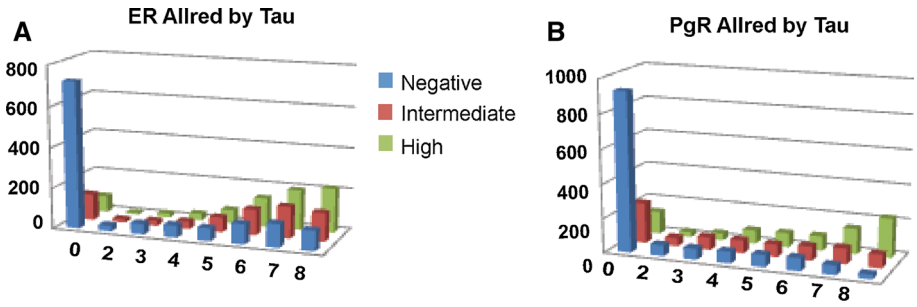

Fig. 3 Tau, ER and PR correlation as semi-quantitative categorical variables. The number of cases is depicted along the vertical *y axis*. **A**, **B** *X axes* represent ER and PR Allred subgroups, respectively. *Z axes* represent the Tau subgroups: *blue* negative; *red* intermediate and *green* high expression

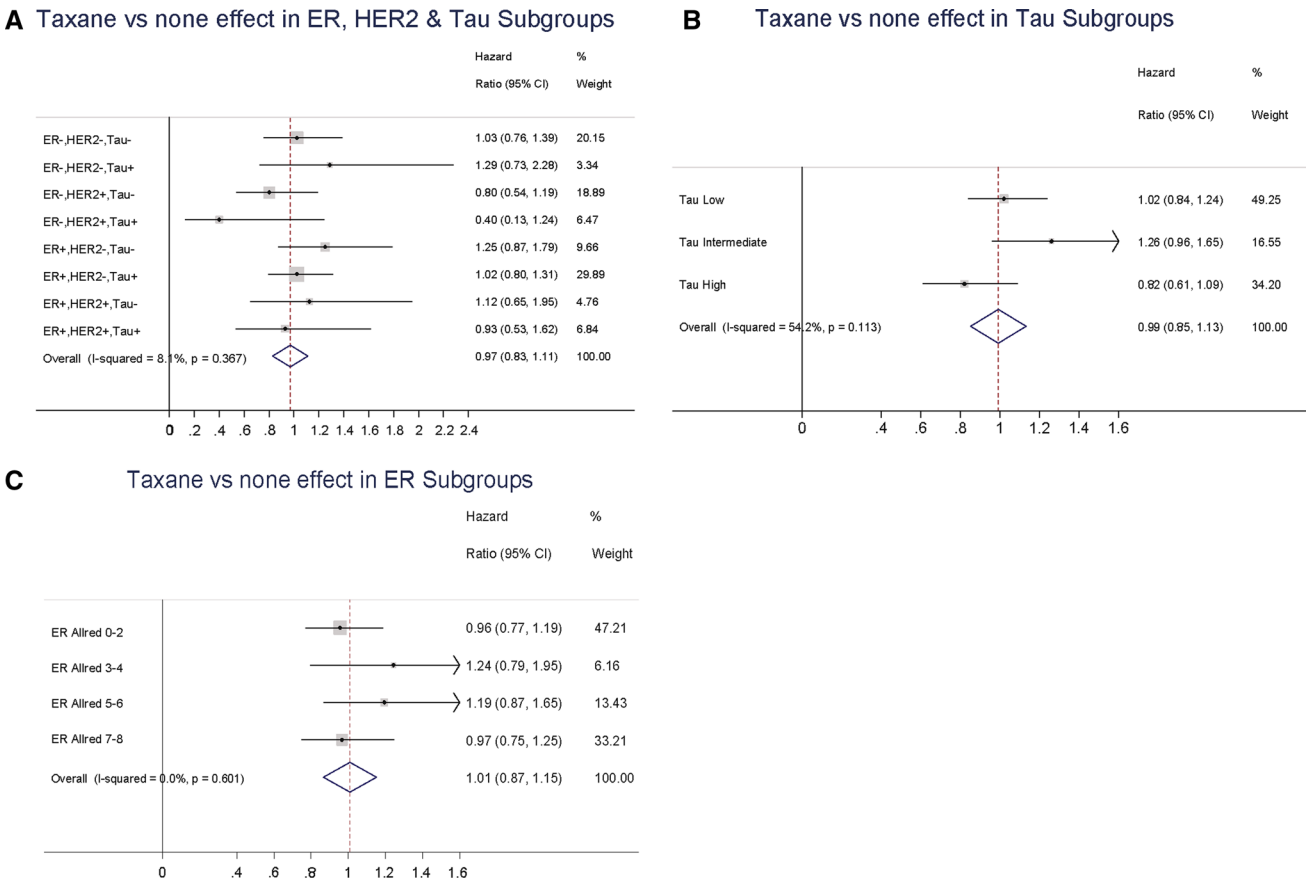

Fig. 4 Tau expression and docetaxel efficacy within breast cancer subgroup. Forest plots reporting on the interaction between Tau expression and efficacy of docetaxel. **A** by dichotomized cut off for Tau, ER and HER2. **B** By 'combined' score for Tau. **C** By Allred scores for ER. The *solid squares* are centred on the point estimate, and the *horizontal line* through each *square* represents the 95 % CI. The size of each *square* represents the weight of the study in the subgroup analysis. The *centre* of the *diamond* represents the summary estimate of the effect size, and the *horizontal tips* represent the 95 % CI. The *solid vertical line* corresponds to no effect, and the *dashed vertical line* corresponds to the summary estimate. *CI* confidence interval

PR, HER2 and Tau. Biomarker assessable patients showed very similar patient characteristics to the overall trial population (Supplementary Table 1). The median follow up time was 8.2 years. A very strong association was observed between the intensity and the proportion of Tau staining ($p < 0.001$) (Fig. 2). Tau positive status, defined as demonstrating at least weak intensity staining was assigned to 50 % of cases in the dichotomized scoring analysis ($n = 1{,}242$). The combined scoring system yielded the three Tau groups as described: negative—45 % 281 ($n = 1{,}124$) of the whole population, intermediate—26 % 282 ($n = 647$), and high—29 % ($n = 712$). Tau

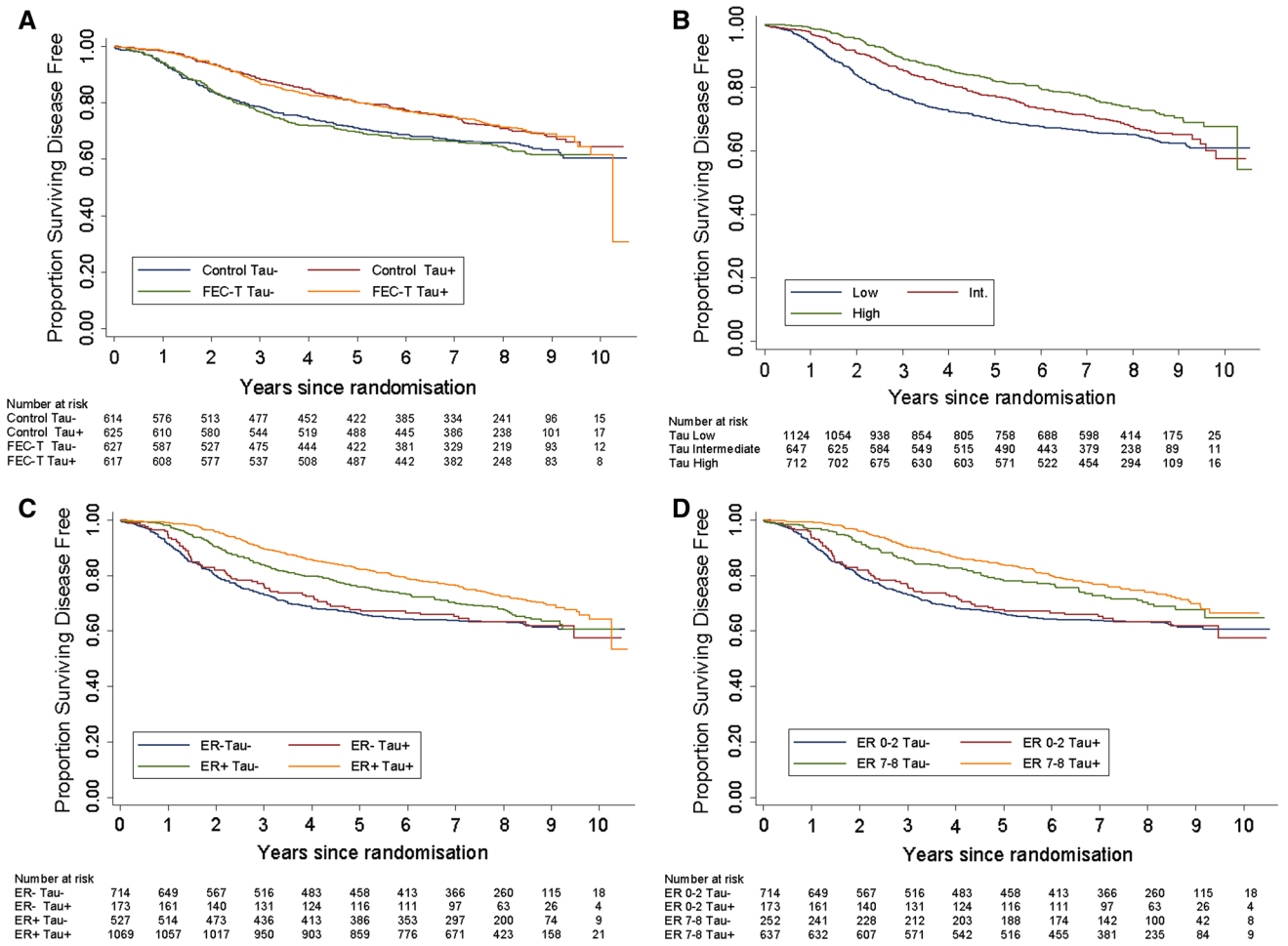

Fig. 5 Univariate analyses of disease-free survival (DFS). Kaplan–Meier curves are shown. **A** DFS according to dichotomized Tau status and treatment subgroups: *Blue line* control/Tau negative, *green line* FEC-T/Tau negative, *red line* control/Tau positive and *orange line* FEC-T/Tau positive. **B** DFS according to combined Tau status: *Blue line* low Tau, *red line* intermediate Tau, *green line* high Tau. **C** DFS according to dichotomized ER and Tau subgroups: *blue line* ER and Tau negative, *green line* ER positive and Tau negative, *red line* ER negative and Tau positive and *orange line* ER and Tau positive. **D** DFS according to ER Allred scoring and dichotomized Tau subgroups. Cases with negative and high Allred ER scores only are depicted: *blue line* ER 0–2 and Tau negative, *green line* ER 7–8 and Tau negative, *red line* ER 0–2 and Tau positive; *orange line* ER 7–8 and Tau positive. Control = 8*FEC60 or 4*E-4*CMF. *DFS* disease-free survival

positive status correlated positively with ER status ($p < 0.001$) and PR status ($p < 0.001$) (Table 1; Fig. 3A, B, respectively). In contrast, Tau positive status correlated negatively with histological grade ($p < 0.001$) (from the local histopathology reports) and central HER2 status ($p < 0.001$). Tau expression did not show a significant correlation with age or tumour size but was weakly correlated with nodal status (Table 1).

Tau expression as a predictive biomarker for taxane benefit

Exploratory analysis of the main TACT trial suggested benefit from docetaxel might be related to ER negativity and HER2 positivity, with a suggestion of docetaxel benefit in node-positive patients with ER-negative/HER2-positive disease (HR 0.7 (95 % CI 0.49–1.00)). Dichotomised cut-offs for Tau and ER status (i.e. positive or negative) demonstrated no significant interaction between Tau expression and efficacy of docetaxel (Fig. 4A). Although not statistically significant, patients with ER-negative/HER2-positive/Tau positive tumours appeared to exhibit an association with greater taxane benefit; contrary to the preclinical hypothesis that Tau expression induced resistance to taxanes and that taxane benefit would be enriched in Tau negative patients. These results were further validated using the 'combined' and the 'Allred' scores for Tau and ER, respectively, confirming no role of Tau as a predictive marker for taxane benefit (Fig. 4B, C).

Tau expression as a prognostic biomarker

In agreement with the NSABP B-28 trial analysis, Tau expression (both dichotomised and combined scoring) was seen to be a prognostic factor on univariate analysis associated with an improved DFS, independent of the treatment groups ($p < 0.001$, Fig. 5A, B). Among patients with ER-positive tumours ($n = 1{,}596$), patients with Tau positive disease ($n = 1{,}069$) had an improved DFS (Fig. 5C) compared with Tau negative tumours ($p = 0.02$). Among the patients with ER-negative cancers ($n = 887$), Tau expression had no prognostic value (Fig. 5C). Tau may appear to be prognostic in ER-positive patients due to its association with degrees of ER positivity, rather than being a truly independent factor. To test this we used quantitative ER in the analysis, the weak prognostic effect of Tau did not remain in the proportional hazards model when considering ER as an ordinal variable, however, there was some evidence of a prognostic effect with regard to events occurring early in follow up (Fig. 5D and see multivariable analysis (Table 2).

Tau and PR expression

Like Tau, PR is an ER-regulated gene and, as studies indicate Tau expression is perhaps a reflection of ER downstream function, we therefore, hypothesized that Tau expression would correlate strongly with PR expression. As described, central PR status correlated positively with Tau expression (Table 1). Dichotomised cut-offs for Tau and PR status (i.e. positive or negative), demonstrated no significant interaction between Tau expression and efficacy of docetaxel in patients within the PR-positive and negative subsets (Fig. 6A). No prognostic effect of Tau was observed amongst PR subgroups (Fig. 6B).

Table 2 Multivariable Analysis for ER-positive and ER-negative cancers

	ER positive		ER negative	
	$n = 1{,}596$		$n = 887$	
	HR (95 % CI)	P value	HR (95 % CI)	p value
Lymph node status				
Negative versus positive	1.77 (1.58–1.97)	<0.001	1.85 (1.66–2.06)	<0.001
Invasive tumour size (cm)				
<2	1.00		1.00	
2–5	0.65 (0.51–0.83)	0.001	0.88 (0.67–1.15)	0.35
>5	1.32 (1.01-1.72)	0.042	1.44 (1.02-2.03)	0.037
Age				
<40	1.00		1.00	
40–49	0.69 (0.53–0.9)	0.006	1.14 (0.84–1.55)	0.41
50–59	0.73 (0.56–0.95)	0.021	0.89 (0.65–1.22)	0.48
60+	0.9 (0.63–1.27)	0.54	0.8 (0.52–1.25)	0.33
Histological grade				
1	1.00		1.00	
2	1.17 (0.78–1.77)	0.44	2.19 (0.3–16.07)	0.44
3	1.89 (1.26–2.86)	0.002	2.66 (0.37–19.15)	0.33
Taxane versus none	1.11 (0.93-1.34)	0.25	0.87 (0.7-1.09)	0.22
HER2				
Pos. versus neg.	1.08 (0.86–1.37)	0.49	1 (0.79–1.27)	0.99
ER, Allred score				
Ordinal (3–8)	0.93 (0.81–1.06)	0.26		
PR, Allred score				
Ordinal (0–8)	0.93 (0.86-1.01)	0.08	0.87 (0.69-1.08)	0.2
Tau				
Negative/low	1.00		1.00	
Intermediate	1.02 (0.81–1.29)	0.84	0.98 (0.71–1.36)	0.92
High	0.94 (0.73–1.19)	0.59	1.07 (0.72–1.57)	0.75

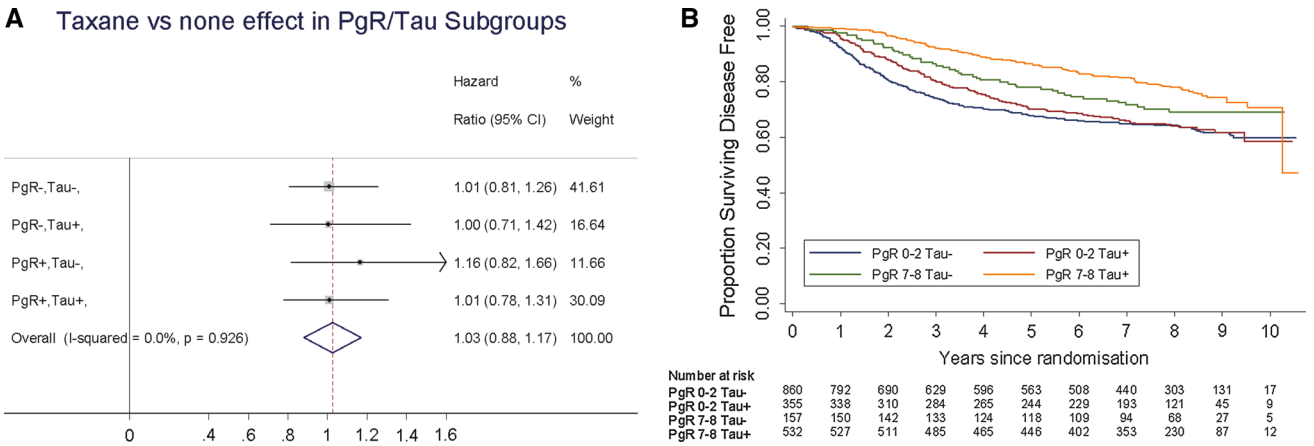

Fig. 6 Tau and PR expression. **A** Forest plots reporting on the interaction between Tau and PR expression. **B** Kaplan–Meier curve reporting on the DFS according to PR Allred scoring and dichotomized Tau subgroups. Cases with negative and high Allred PR scores only are depicted: *blue line* PR 0–2 and Tau negative, *green line* PR 7–8 and Tau negative, *red line* PR 0–2 and Tau positive and *orange line* PR 7–8 and Tau positive. *DFS* disease-free survival

Multivariable analyses

Multivariable analyses were performed separately for ER-positive and ER-negative cancers (Table 2). Tau had no prognostic value in either of these groups when proportional hazards throughout follow up were assumed. Investigation of time-dependent effects in the multivariable model suggested that high Tau expression may be associated with a time-dependent effect relative to the low-expression category. In the ER-positive group, the risk of an event in the high Tau category relative to the low category is approximately a half in the first 2 years, but this effect has largely disappeared in 5 years; this can be seen in the early separation of Tau negative vs Tau positive curves in Fig. 5C, D, the curves separate within the first 2 years, but thereafter, the risk of an event is similar in both groups.

Discussion

In this study, we investigated the predictive and prognostic value of Tau in patients enrolled into the TACT trial examining the role of taxane benefit as adjuvant therapy in early breast cancer. Clinical studies evaluating Tau as a biomarker for prognostic and treatment predictive effects have been conflicting; this may relate to their design. Although dichotomization of quantitative variables is a common approach in clinical research, it may be seen as introducing an extreme form of rounding, with an inevitable loss of information and power [31]. There is a risk of underestimating the extent of variation in outcome between groups, as individuals close to, but on opposite sides of, the cut-point are characterized as being very different rather than very similar. Dichotomization has also been shown to increase the probability of false positive results [32]. Within our study analyses using both dichotomized and ordinal parameters for Tau, ER and PR analyses were, therefore, performed.

We observed no evidence for a role of Tau as a predictive marker of taxane benefit. Contrary to the hypothesis that taxane benefit would be enriched in Tau negative tumours, the only group with (non-significantly) reduced event rate in the taxane group were the HER2- and Tau positive subgroup. This is now the second large adjuvant study which, despite our studies use of both dichotomized and ordinal parameters, fails to show an association between Tau and response to taxane therapy; suggesting that measurement of Tau does not aid in clinical decision making to select optimal use of taxanes. Thus, the preclinical observations that high Tau expression confers selective resistance to paclitaxel in breast cancer cell lines remains largely unsubstantiated in clinical trials [16, 17]. In clinical studies, it is likely that other molecular mechanisms relating to chemotherapy resistance override the importance of Tau as a predictive biomarker for response to taxane therapy. Mechanisms of resistance are complex and are likely to be multiple, it may, therefore, be difficult to detect individual molecular markers that predict cytotoxicity from microtubule stabilizing agents like taxanes from amongst the competing mechanisms. In addition, because of the high level of biological, molecular and genetic heterogeneity in breast cancer, the use of a single marker is unlikely to be sufficiently specific and reliable. It is also worth noting that low Tau expression is closely associated with ER negativity, high histological grade and

HER2 positivity, which might explain the earlier observations that low Tau was associated with higher pCR rates in a group with the worst prognosis.

Within our study, Tau expression was seen to be a prognostic factor associated with improved DFS, when all breast cancer patients are analysed together on univariate analysis. Tau is an ER-regulated gene with expression induced by both oestrogen and tamoxifen in vitro. The improved DFS amongst the Tau positive (i.e. high expression) patients in the trial population is likely to be a surrogate for endocrine sensitive, ER-positive tumours in which the relative sensitivity or resistance between individual chemotherapy agents is of limited relevance. Stratification by ER status confirmed that Tau expression had no prognostic value in ER-negative tumours. The good prognostic effect seen among patients with ER-positive cancers, however, was weakened, when applying ER as an ordinal variable and where the added effect of Tau is minor compared with the prognostic effect of quantitative ER in a group of patients treated with appropriate endocrine therapy. Multivariable analyses performed separately for ER-positive and ER-negative cancers also indicated that Tau had limited prognostic value in either of these groups beyond possibly identifying a subgroup of ER-positive patients with good prognosis during early follow up. PR, another oestrogen-regulated gene, approached statistical significance in the ER-positive group. Importantly, our conclusions apply to an essentially higher risk patient population who had been selected for chemotherapy and randomization to a taxane-based regimen in the TACT trial.

Disparities between RNA and protein expression, as well as the techniques used to assess these parameters [18, 22, 23, 26] may also have contributed to lack of agreement between studies. In separate clinical studies, RT-PCR and different immunohistochemistry approaches have been used to assess Tau expression. Tau has six isoforms that are spliced from a single gene and in vitro studies indicate that expression of Tau protein isoforms less than 70 kDa have the most influence on sensitivity to taxanes [24] Therefore, analysis of Tau mRNA expression may not be an appropriate for examining the utility of Tau as a predictor of taxane sensitivity. Furthermore, the status of the expression of different Tau protein isoforms is important in determining sensitivity to taxanes, but immunohistochemistry cannot, at present, be used to identify separate isoforms [24]. The antibody used in our and other studies [16, 20], recognizes both non-phosphorylated and phosphorylated forms of Tau proteins (45–68 kD). There may be value in the examination of individual Tau isoform expression in breast cancer tissues to further inform how Tau may be related to other aspects of the biology to response to taxanes.

Identification of robust biomarkers capable of identifying women with a high likelihood of response to taxanes would represent a significant advance in breast cancer research. When Tau was first proposed as a potential biomarker to discriminate between taxane sensitivity and resistance, there was great optimism that it may offer clinical utility in improving patient care. This report from the adjuvant taxane trial TACT, along with those from the GeparTrio, NSABP and HECOG trials confirms that there is no clinical application for Tau and demonstrates again the perils of relying on a single biomarker to report the complexity of drug resistance in relation to clinical outcome. This is disappointing, but recent advances in genomic and proteomic technologies are likely to drive the development of novel multi-component companion diagnostic biomarkers for the taxane class of drugs and may prove to be more fruitful in the future.

Acknowledgments The TACT trial is jointly funded by Cancer Research UK (CRUK/01/001) and educational Grants from Aventis, Roche and Pfizer. Storage, construction of microarrays and tissue HER2 testing were funded by an educational grant from Roche. We would like to thank all the patients who agreed to enter the TACT trial and donate their tumour tissue for TransTACT. This work was supported by the Experimental Cancer Medicine Centre Initiative, which is jointly funded by Cancer Research UK, the National Institute for Health Research in England and the Departments of Health for Scotland, Wales and Northern Ireland. We acknowledge support from the NIHR RM/ICR Biomedical Research Centre. Patient tissue samples were provided by Guy's and St Thomas' Breast Tissue and Data Bank, which is supported by the Department of Health via the National Institute for Health Research and comprehensive Biomedical Research Centre award. The views expressed are those of the author(s) and not necessarily those of the NHS, the NIHR or the Department of Health. We would like to acknowledge the funding to Dr Sheeba Irshad from Breakthrough Breast Cancer and the Sarah Greene Tribute Fund. Professor Andrew Tutt is funded by the Research Oncology and Breakthrough Breast Cancer funds.

Conflict of interest No conflicts of interest.

Ethical standards The experiments comply with the current laws of the United Kingdom.

References

1. De Laurentiis M, Cancello G, D'Agostino D, Giuliano M, Giordano A, Montagna E, Lauria R, Forestieri V, Esposito A, Silvestro L et al (2008) Taxane-based combinations as adjuvant chemotherapy of early breast cancer: a meta-analysis of randomized trials. J Clin Oncol 26(1):44–53
2. Bria E, Nistico C, Cuppone F, Carlini P, Ciccarese M, Milella M, Natoli G, Terzoli E, Cognetti F, Giannarelli D (2006) Benefit of taxanes as adjuvant chemotherapy for early breast cancer: pooled analysis of 15,500 patients. Cancer 106(11):2337–2344

3. Nowak AK, Wilcken NR, Stockler MR, Hamilton A, Ghersi D (2004) Systematic review of taxane-containing versus non-taxane-containing regimens for adjuvant and neoadjuvant treatment of early breast cancer. Lancet Oncol 5(6):372–380
4. Trudeau M, Charbonneau F, Gelmon K, Laing K, Latreille J, Mackey J, McLeod D, Pritchard K, Provencher L, Verma S (2005) Selection of adjuvant chemotherapy for treatment of node-positive breast cancer. Lancet Oncol 6(11):886–898
5. Trudeau M, Sinclair SE, Clemons M (2005) Neoadjuvant taxanes in the treatment of non-metastatic breast cancer: a systematic review. Cancer Treat Rev 31(4):283–302
6. Early Breast Cancer Trialists' Collaborative G, Peto R, Davies C, Godwin J, Gray R, Pan HC, Clarke M, Cutter D, Darby S, McGale P et al (2012) Comparisons between different polychemotherapy regimens for early breast cancer: meta-analyses of long-term outcome among 100,000 women in 123 randomised trials. Lancet 379(9814):432–444
7. Ellis P, Barrett-Lee P, Johnson L, Cameron D, Wardley A, O'Reilly S, Verrill M, Smith I, Yarnold J, Coleman R et al (2009) Sequential docetaxel as adjuvant chemotherapy for early breast cancer (TACT): an open-label, phase III, randomised controlled trial. Lancet 373(9676):1681–1692
8. Bliss JM, Ellis P, Kilburn L, Bartlett J, Bloomfield D, Cameron D, Canney P, Coleman RE, Dowsett M, Earl H, Verril M, Wardley A, Yarnold J, Ahern R, Atkins N, Fletcher M, McLinden M, Barrett-Lee P (2012) Mature analysis of UK Taxotere as Adjuvant Chemotherapy (TACT) trial (CRUK 01/001); effects of treatment and characterisation of patterns of breast cancer relapse. Cancer Res 72(24):1–608
9. Palmieri C, Jones A (2012) The 2011 EBCTCG polychemotherapy overview. Lancet 379(9814):390–392
10. Esteva FJ, Valero V, Pusztai L, Boehnke-Michaud L, Buzdar AU, Hortobagyi GN (2001) Chemotherapy of metastatic breast cancer: what to expect in 2001 and beyond. Oncologist 6(2):133–146
11. Crown J, O'Leary M, Ooi WS (2004) Docetaxel and paclitaxel in the treatment of breast cancer: a review of clinical experience. Oncologist 9(Suppl 2):24–32
12. Felgner H, Frank R, Biernat J, Mandelkow EM, Mandelkow E, Ludin B, Matus A, Schliwa M (1997) Domains of neuronal microtubule-associated proteins and flexural rigidity of microtubules. J Cell Biol 138(5):1067–1075
13. Kar S, Fan J, Smith MJ, Goedert M, Amos LA (2003) Repeat motifs of tau bind to the insides of microtubules in the absence of taxol. EMBO J 22(1):70–77
14. Cassimeris L, Spittle C (2001) Regulation of microtubule-associated proteins. Int Rev Cytol 210:163–226
15. Weingarten MD, Lockwood AH, Hwo SY, Kirschner MW (1975) A protein factor essential for microtubule assembly. Proc Natl Acad Sci USA 72(5):1858–1862
16. Rouzier R, Rajan R, Wagner P, Hess KR, Gold DL, Stec J, Ayers M, Ross JS, Zhang P, Buchholz TA et al (2005) Microtubule-associated protein tau: a marker of paclitaxel sensitivity in breast cancer. Proc Natl Acad Sci USA 102(23):8315–8320
17. Wagner P, Wang B, Clark E, Lee H, Rouzier R, Pusztai L (2005) Microtubule Associated Protein (MAP)-Tau: a novel mediator of paclitaxel sensitivity in vitro and in vivo. Cell Cycle 4(9):1149–1152
18. Andre F, Hatzis C, Anderson K, Sotiriou C, Mazouni C, Mejia J, Wang B, Hortobagyi GN, Symmans WF, Pusztai L (2007) Microtubule-associated protein-tau is a bifunctional predictor of endocrine sensitivity and chemotherapy resistance in estrogen receptor-positive breast cancer. Clin Cancer Res 13(7):2061–2067
19. Tanaka S, Nohara T, Iwamoto M, Sumiyoshi K, Kimura K, Takahashi Y, Tanigawa N (2009) Tau expression and efficacy of paclitaxel treatment in metastatic breast cancer. Cancer Chemother Pharmacol 64(2):341–346
20. Shao YY, Kuo KT, Hu FC, Lu YS, Huang CS, Liau JY, Lee WC, Hsu C, Kuo WH, Chang KJ et al (2010) Predictive and prognostic values of tau and ERCC1 in advanced breast cancer patients treated with paclitaxel and cisplatin. Jpn J Clin Oncol 40(4):286–293
21. Rody A, Karn T, Gatje R, Ahr A, Solbach C, Kourtis K, Munnes M, Loibl S, Kissler S, Ruckhaberle E et al (2007) Gene expression profiling of breast cancer patients treated with docetaxel, doxorubicin, and cyclophosphamide within the GEPARTRIO trial: HER-2, but not topoisomerase II alpha and microtubule-associated protein tau, is highly predictive of tumor response. Breast 16(1):86–93
22. Pentheroudakis G, Kalogeras KT, Wirtz RM, Grimani I, Zografos G, Gogas H, Stropp U, Pectasides D, Skarlos D, Hennig G et al (2009) Gene expression of estrogen receptor, progesterone receptor and microtubule-associated protein Tau in high-risk early breast cancer: a quest for molecular predictors of treatment benefit in the context of a Hellenic Cooperative Oncology Group trial. Breast Cancer Res Treat 116(1):131–143
23. Pusztai L, Jeong JH, Gong Y, Ross JS, Kim C, Paik S, Rouzier R, Andre F, Hortobagyi GN, Wolmark N et al (2009) Evaluation of microtubule-associated protein-Tau expression as a prognostic and predictive marker in the NSABP-B 28 randomized clinical trial. J Clin Oncol 27(26):4287–4292
24. Ikeda H, Taira N, Hara F, Fujita T, Yamamoto H, Soh J, Toyooka S, Nogami T, Shien T, Doihara H et al (2010) The estrogen receptor influences microtubule-associated protein tau (MAPT) expression and the selective estrogen receptor inhibitor fulvestrant downregulates MAPT and increases the sensitivity to taxane in breast cancer cells. Breast Cancer Res 12(3):R43
25. Dumontet C, Krajewska M, Treilleux I, Mackey JR, Martin M, Rupin M, Lafanechere L, Reed JC (2010) BCIRG 001 molecular analysis: prognostic factors in node-positive breast cancer patients receiving adjuvant chemotherapy. Clin Cancer Res 16(15):3988–3997
26. Baquero MT, Lostritto K, Gustavson MD, Bassi KA, Appia F, Camp RL, Molinaro AM, Harris LN, Rimm DL (2011) Evaluation of prognostic and predictive value of microtubule associated protein tau in two independent cohorts. Breast Cancer Res 13(5):R85
27. McShane LM, Altman DG, Sauerbrei W, Taube SE, Gion M, Clark GM (2005) Statistics Subcommittee of the NCIEWGoCD: reporting recommendations for tumour MARKer prognostic studies (REMARK). Br J Cancer 93(4):387–391
28. Bartlett JM, A'Hern R, Piper T, Ellis IO, Dowsett M, Mallon EA, Cameron DA, Johnston S, Bliss JM, Ellis P et al (2013) Phosphorylation of AKT pathway proteins is not predictive of benefit of taxane therapy in early breast cancer. Breast Cancer Res Treat 138(3):773–781
29. Bartlett JM, Ellis IO, Dowsett M, Mallon EA, Cameron DA, Johnston S, Hall E, A'Hern R, Peckitt C, Bliss JM et al (2007) Human epidermal growth factor receptor 2 status correlates with lymph node involvement in patients with estrogen receptor (ER) negative, but with grade in those with ER-positive early-stage breast cancer suitable for cytotoxic chemotherapy. J Clin Oncol 25(28):4423–4430
30. Harvey JM, Clark GM, Osborne CK, Allred DC (1999) Estrogen receptor status by immunohistochemistry is superior to the ligand-binding assay for predicting response to adjuvant endocrine therapy in breast cancer. J Clin Oncol 17(5):1474–1481
31. MacCallum RC, Zhang S, Preacher KJ, Rucker DD (2002) On the practice of dichotomization of quantitative variables. Psychol Methods 7(1):19–40
32. Austin PC, Brunner LJ (2004) Inflation of the type I error rate when a continuous confounding variable is categorized in logistic regression analyses. Stat Med 23(7):1159–1178

Oncogene (2013) **32,** 2712–2714

www.nature.com/onc

COMMENTARY

BRCA1 mutations and luminal-basal transformation

T Ng[1,2], S Irshad[1,2] and J Stebbing[3]

The multifunctional roles of BRCA1 include its ability to regulate transcriptional processes that control differentiation at multiple levels, as well as functioning as a tumor suppressor. Data herein demonstrate that germline mutations in *Brca1* impair luminal cell lineage and mammary development, with its deficiency converting ER-positive luminal tumors into basal-like cancers. Heterozygous mutations in *Brca1* lead to downregulation of a number of luminal differentiation genes, explaining how it suppresses basal-like tumors, also highlighting its importance outside of its known highly publicized role in DNA repair.

Oncogene (2013) **32,** 2712–2714; doi:10.1038/onc.2012.379; published online 27 August 2012

In this issue of *Oncogene*, Bai *et al.*[1] describe studies that show germline mutation of *Brca1* in p18-deficient mice blocks the increase of luminal progenitor cells, impairs luminal gene expression and promotes malignant transformation of mammary tumors (schematic, Figure 1).

In several human solid tumors, including breast and ovarian cancers, the tumor-promoting effect of a loss of tumor-suppressing function of BRCA1, due to mutations, may be contingent on additional genetic changes within the cell-cycle pathways.[2] Recently, there have been genetic data to support the notion that human BRCA1 breast cancers may be derived from mammary epithelial luminal progenitors.[3] Bai *et al.*[1] now show that a haploid loss of *Brca1*, when coupled to the deletion of p18 (INK4c), a cyclin-dependent kinase (CDK) inhibitor, can promote an expansion of luminal progenitors and malignant transformation, giving rise to ER-negative tumor cells that are of luminal epithelial origin.

p18 is a CDK inhibitor, which is a downstream target of GATA3, and restrains mammary luminal progenitor cell proliferation and tumorigenesis.[4] Given the literature that describes the physical and functional linkage of BRCA1 to important transcriptional regulators, such as p53, c-Myc and p300,[5] it is of interest to map out a more comprehensive picture of the transcriptional feedback-control network that exists between BRCA1 and various cell-cycle regulators. Indeed, Bai *et al.*[1] demonstrate that haploid loss of *Brca1* in primary mammary epithelial cells increased p18 mRNA level and that knockdown of *Brca1* in three different cell lines led to an average of 1.3- and 1.5-fold increase in p18 mRNA and protein levels, respectively. Moreover, p18 is not the only cell-cycle regulator that is upregulated. Previously, BRCA1 overexpression has been shown to cause cell-cycle arrest by a mechanism that requires p21WAF1, another CDK inhibitor.[2] In the present study,[1] p21 mRNA level was not altered in *Brca1* + / − mammary glands at 3 months of age, but increased by 2.9- and 3.1-fold in p18 − / − and p18 − / − ; *Brca1* + /– glands, respectively. p16INK4a mRNA levels were increased 1.7-fold in *Brca1* + / − , and 1.4- and 3.9-fold in p18 − / − and p18 − / − ;*Brca1* + /– glands, respectively. In aggregate, these new data strongly suggest a concerted but complex regulatory feedback between BRCA1 and a network of cell-cycle regulators on one hand, as well as among the different CDK inhibitors within the network. The precise identities of the transcriptional regulators that potentially mediate this feedback control, in response to BRCA1 loss or mutation, are currently unclear. One possible candidate mechanism may involve changes in the promoter methylation status of these CDK-inhibitor genes (for example, Taghavi *et al.*[6]).

The question that has not yet been addressed by the current study is whether the loss of BRCA1 function, for example, through the *Brca1*^{C61G} mutation,[7] known to impair the ubiquitin ligase activity of BRCA1 result in a similar increase in the levels of p18, along with a malignant transformation of mammary tumors in p18-deficient mice? Mechanistically, do these functionally impaired mutants of BRCA1 differ from the wild-type protein in terms of their ability to physically interact with important transcriptional regulators, such as p53, c-Myc and p300, and thereby the ability to regulate the transcription of downstream targets, for example, of luminal differentiation genes such as *Foxa1*.[1]

A major clinical implication of the current study is to support the notion that CDK inhibition may be a useful therapeutic approach particularly for BRCA1-deficient cancers, because, for example, tumor cells that lack BRCA1 (or ATM) are particularly sensitive to CDK inhibitors, especially CDK2 blockade.[8] However, the expression levels of multiple, rather than a single, CDK inhibitors may be altered in BRCA1-deficient tumors and thus broad-spectrum CDK inhibitors may be required. Herein rests a drug-development paradox in that early pan-CDK inhibitors have evolved to specific second- and third-generation drugs with higher selectivity. Despite this, CDK inhibitors have not yet achieved their desired results in clinical trials, and perhaps the multiple CDK variants with their cell cycle and transcriptional regulatory roles are too complex to target.

Finally, in terms of companion diagnostics for such therapeutic approaches, we need to focus our research efforts on finding assays that can identify rare (∼5%) non-hereditary BRCA1-deficient breast cancers. In the absence of a known mutation, assays that can be applied to patient samples to probe the function of BRCA1 are rare. Recently, the first images that quantify the extent of BRCA1 sumoylation in cells have been published,[9] and can potentially serve as a surrogate measurement of BRCA1 function during DNA repair. SUMOylation, independently of mutation status, may stimulate E3 ubiquitin ligase activity of BRCA1, perhaps by inducing a conformational change

[1]Richard Dimbleby Department of Cancer Research, Randall Division and Division of Cancer Studies, Kings College London, Guy's Medical School Campus, London, UK; [2]Breakthrough Breast Cancer Research Unit, Research Oncology, King's College London, Guy's Medical School Campus, London, UK and [3]Department of Medical Oncology, Imperial College, Hammersmith Campus, London, UK. Correspondence: Professor J Stebbing, Department of Medical Oncology, Imperial College, Hammersmith Campus, W12 0NN, London, UK. E-mail: j.stebbing@imperial.ac.uk
Received 8 June 2012; revised 2 July 2012; accepted 4 July 2012; published online 27 August 2012

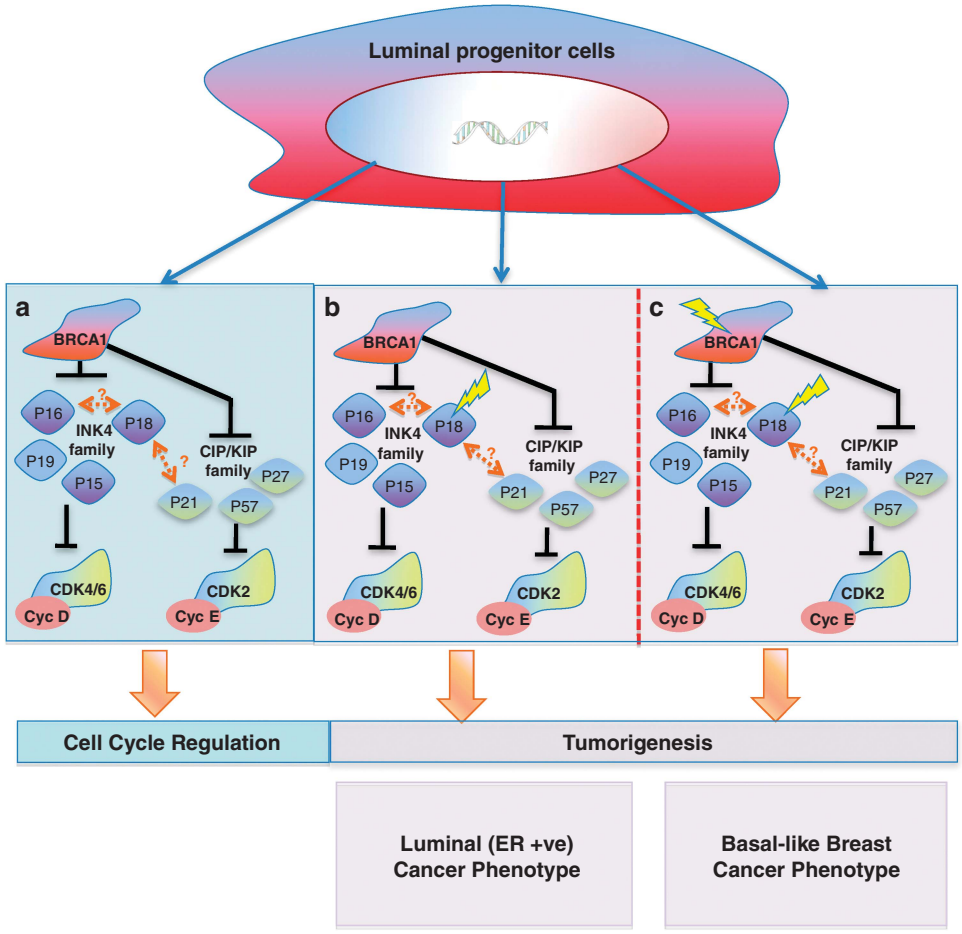

Figure 1. Functional role of BRCA1 in mammary luminal progenitor cell differentiation. (**a**) Several groups demonstrate the role of BRCA1 in mammary epithelial cell differentiation,[12–16] and in this issue of oncogene, Bai *et al.*[1] report on the predominant expression of BRCA1 in luminal epithelium. BRCA1 negatively regulates CDK inhibitors (INK4 and CIP/KIP family), which restrain mammary luminal progenitor cell proliferation and tumorigenesis.[4] Although the cross-talk between BRCA1 and various cell-cycle regulators remains to be fully elucidated, data presented by Bai *et al.*[1] strongly suggests the existence of a complex transcriptional regulatory feedback mechanisms between BRCA1 and a network of cell-cycle regulators, and among the different CDK inhibitors within the network. (**b**) p18 deficiency has been shown to increase luminal progenitor cell proliferation, leading to luminal ER-positive tumor development.[4] (**c**) Bai *et al.*[1] demonstrate that germline mutations in BRCA1 impair luminal progenitor cell differentiation and, when combined with loss of p18 (INK4C), can promote basal-like tumor formation, giving rise to ER-negative tumor cells that are of luminal epithelial origin.

and/or affecting protein–protein interaction, providing insights into how BRCA1 is both regulated and modified.

There is clearly a heterogeneity that we do not yet understand and the 'BRCAness' of breast cancer subtypes is probably a spectrum, with basal-like tumors at one end, which probably best resemble BRCA1-mutant cancers. Results of clinical trials in these patients, including those of the PARP inhibitors, have probably been disturbed by noise from nonbasal-like tumors, but patient numbers dictate that we cannot be too selective.

The present paper[1] has highlighted the importance of studying the function of BRCA1 outside the DNA-repair context, such as transcriptional regulation of cell-cycle control genes and more recently its interaction with a cytoskeleton protein complex, ezrin–radixin–moesin, which affects breast cancer cell spreading and motility.[10] It also utilizes a new mouse model that harbors a germline mutation of *Brca1*, with broad applicability to both luminal and basal-like breast tumors. Overall, these findings will hopefully yield new approaches that are based on the concept of synthetic lethality[11] to target BRCA-deficient tumors.

CONFLICT OF INTEREST

The authors declare no conflict of interest.

REFERENCES

1 Bai F, Smith MD, Chan HL, Pei X-H. Germline mutation of *Brca1* alters the fate of mammary luminal cells and causes luminal-to-basal mammary tumor transformation. *Oncogene* 2013; **32**: 2715–2725.
2 Somasundaram K, Zhang H, Zeng Y-X, Houvras Y, Peng Y, Zhang H *et al.* Arrest of the cell cycle by the tumour-suppressor BRCA1 requires the CDK-inhibitor p21WAF1/CiPI. *Nature* 1997; **389**: 187–190.
3 Molyneux G, Geyer FC, Magnay FA, McCarthy A, Kendrick H, Natrajan R *et al.* BRCA1 basal-like breast cancers originate from luminal epithelial progenitors and not from basal stem cells. *Cell Stem Cell* 2010; **7**: 403–417.
4 Pei X-H, Bai F, Smith MD, Usary J, Fan C, Pai S-Y *et al.* CDK inhibitor p18INK4c is a downstream target of gata3 and restrains mammary luminal progenitor cell proliferation and tumorigenesis. *Cancer Cell* 2009; **15**: 389–401.
5 Chen Y, Lee W-H, Chew HK. Emerging roles of BRCA1 in transcriptional regulation and DNA repair. *J Cell Physiol* 1999; **181**: 385–392.
6 Taghavi N, Biramijamal F, Sotoudeh M, Khademi H, Malekzadeh R, Moaven O *et al.* p16INK4a hypermethylation and p53, p16 and MDM2 protein expression in esophageal squamous cell carcinoma. *BMC Cancer* 2010; **10**: 138.
7 Drost R, Bouwman P, Rottenberg S, Boon U, Schut E, Klarenbeek S *et al.* BRCA1 ring function is essential for tumor suppression but dispensable for therapy resistance. *Cancer Cell* 2011; **20**: 797–809.
8 Deans AJ, Khanna KK, McNees CJ, Mercurio C, Heierhorst J, McArthur GA. Cyclin-dependent kinase 2 functions in normal dna repair and is a therapeutic target in BRCA1-deficient cancers. *Cancer Res* 2006; **66**: 8219–8226.

9 Morris JR, Boutell C, Keppler M, Densham R, Weekes D, Alamshah A *et al.* The SUMO modification pathway is involved in the BRCA1 response to genotoxic stress. *Nature* 2009; **462**: 886–890.
10 Coene ED, Gadelha C, White N, Malhas A, Thomas B, Shaw M *et al.* A novel role for BRCA1 in regulating breast cancer cell spreading and motility. *J Cell Biol* 2011; **192**: 497–512.
11 Turner NC, Lord CJ, Iorns E, Brough R, Swift S, Elliott R *et al.* A synthetic lethal siRNA screen identifying genes mediating sensitivity to a PARP inhibitor. *EMBO J* 2008; **27**: 1368–1377.
12 Furuta S, Jiang X, Gu B, Cheng E, Chen PL, Lee WH. Depletion of BRCA1 impairs differentiation but enhances proliferation of mammary epithelial cells. *Proc Natl Acad Sci USA* 2005; **102**: 9176–9181.
13 Marquis ST, Rajan JV, Wynshaw-Boris A, Xu J, Yin GY, Abel KJ *et al.* The developmental pattern of Brca1 expression implies a role in differentiation of the breast and other tissues. *Nat Genet* 1995; **11**: 17–26.
14 Rajan JV, Wang M, Marquis ST, Chodosh LA. Brca2 is coordinately regulated with Brca1 during proliferation and differentiation in mammary epithelial cells. *Proc Natl Acad Sci USA* 1996; **93**: 13078–13083.
15 Lane TF, Deng C, Elson A, Lyu MS, Kozak CA, Leder P. Expression of Brca1 is associated with terminal differentiation of ectodermally and mesodermally derived tissues in mice. *Genes Dev* 1995; **9**: 2712–2722.
16 Kubista M, Rosner M, Kubista E, Bernaschek G, Hengstschlager M. Brca1 regulates *in vitro* differentiation of mammary epithelial cells. *Oncogene* 2002; **21**: 4747–4756.

BJR

Received:
9 January 2014

Accepted:
3 March 2014

doi: 10.1259/bjr.20140065

Cite this article as:
Chowdhury R, Ganeshan B, Irshad S, Lawler K, Eisenblätter M, Milewicz H, et al. The use of molecular imaging combined with genomic techniques to understand the heterogeneity in cancer metastasis. Br J Radiol 2014;87:20140065.

REVIEW ARTICLE

The use of molecular imaging combined with genomic techniques to understand the heterogeneity in cancer metastasis

[1,2]R CHOWDHURY, MRCP(UK), BSc (Hons), [3]B GANESHAN, PhD, BEng Biomedical Engineering, [4]S IRSHAD, MRCP(UK), BSc, [1,5]K LAWLER, PhD, [1,6]M EISENBLÄTTER, MD, [7]H MILEWICZ, PhD, [8]M RODRIGUEZ-JUSTO, MB ChB, FRCPath, [3]K MILES, MD, FRCR, [2,9]P ELLIS, MD, FRACP, [3]A GROVES, MD, FRCR, [10,11]S PUNWANI, FRCR, PhD and [1,4,7,9]T NG, FMedSci, PhD

[1]Richard Dimbleby Department of Cancer Research, Randall Division of Cell and Molecular Biophysics, King's College London, London, UK
[2]Department of Medical Oncology, Guy's and St Thomas' NHS Foundation Trust, London, UK
[3]Institute of Nuclear Medicine, University College London Hospital, London, UK
[4]Breakthrough Breast Cancer Research Unit, Research Oncology, King's College London, Guy's Hospital, London, UK
[5]Institute for Mathematical and Molecular Biomedicine, Kings College London, Guy's Medical School Campus, London, UK
[6]Division of Imaging Sciences and Biomedical Engineering, School of Medicine, King's College London, The Rayne Institute/St Thomas' Hospital, London, UK
[7]UCL Cancer Institute, University College London, London, UK
[8]Department of Research Pathology, Faculty of Biomedical Sciences, University College London Medical School and University College London Hospitals, London, UK
[9]Division of Cancer Studies, King's College London, Guy's Medical School Campus, London, UK
[10]Division of Imaging, University College London Hospital, London, UK
[11]Centre of Medical Imaging, University College London Hospital, London, UK

Address correspondence to: Professor Tony Ng
E-mail: *tony.ng@kcl.ac.uk*

Ruhe Chowdhury, Balaji Ganeshan and Sheeba Irshad have contributed equally to this article.

ABSTRACT

Tumour heterogeneity has, in recent times, come to play a vital role in how we understand and treat cancers; however, the clinical translation of this has lagged behind advances in research. Although significant advancements in oncological management have been made, personalized care remains an elusive goal. Inter- and intratumour heterogeneity, particularly in the clinical setting, has been difficult to quantify and therefore to treat. The histological quantification of heterogeneity of tumours can be a logistical and clinical challenge. The ability to examine not just the whole tumour but also all the molecular variations of metastatic disease in a patient is obviously difficult with current histological techniques. Advances in imaging techniques and novel applications, alongside our understanding of tumour heterogeneity, have opened up a plethora of non-invasive biomarker potential to examine tumours, their heterogeneity and the clinical translation. This review will focus on how various imaging methods that allow for quantification of metastatic tumour heterogeneity, along with the potential of developing imaging, integrated with other *in vitro* diagnostic approaches such as genomics and exosome analyses, have the potential role as a non-invasive biomarker for guiding the treatment algorithm.

Although continual improvements in diagnosis, surgical techniques and radiation oncology have together provided improved survival for many forms of human cancers, a majority of deaths from cancer are caused by the development and continuous growth of metastases that are resistant to conventional therapies. Similarly, although the use of systemic non-targeted and targeted adjuvant therapies has helped to prevent the spread of tumour cells from the primary site and is now a standard practice for many tumour types, the emergence of resistant disease continues to be a significant cause of patient mortality. These features provide an insight into the dynamic nature of the signalling network within the tumour cells,[1] and human cancers are now being increasingly recognized as heterogeneous, characterized by distinct pathological, genomic, clinical and therapeutic features.

Nearly 150 years after the original theory of tumours originating from immature cells by Virchow,[2] innovative technological approaches unequivocally demonstrate the cellular

heterogeneity of tumours, composed of distinct subpopulations of cancer cells within ("intra") and between ("inter") tumours of individual patients. These subpopulations are characterized by specific genetic and morphological profiles, representing the clonal selection and evolution of that tumour.[3,4] This heterogeneity provides a powerful internal mechanism through which tumour cells can ultimately escape environmental stresses, including oncological therapies, posing a considerable challenge for translational researchers.

There is considerable evidence that the tumour microenvironment actively contributes to tumour heterogeneity.[5] Arguably the best example of this is the "pre-metastatic niche", defined as the creation of an ideal thriving environment for the primary tumour to "seed" to. Through the secretion of cytokines, chemokines and growth factors, the primary tumour "primes" a distal site to become an ideal niche/target organ, favourable for future metastatic colonization.[6] Although in some cases the target organ is already primed for metastatic spread and many organs may have "seeding" of cells, only a few will take "root".[7] Increasing understanding of tumour heterogeneity demands an effort from researchers to establish and understand pre-metastatic changes within distant organs and their major drivers.

This new paradigm of cancer heterogeneity has yet to be fully assimilated into everyday patient management. It has been well documented with certain cancers that imaging signals can show phenotypic tumour heterogeneity and have clinical implications; for example, in radio-iodine imaging of metastatic thyroid cancer, some metastatic lesions may not take up radio-iodine and therefore will be unaffected by radio-iodine therapy. However, for the majority of tumours, biopsies remain the standard of care for assessing tumour biology but cannot be expected to represent the entirety of a tumour in this tumour heterogenic era.[4] Many physicians advocate the re-biopsy of metastatic disease at re-presentation for histological analysis and comparison with the primary, in an attempt to improve the choice of therapy upon relapse, having taken into account, for instance, intertumoral heterogeneity between the primary and metastatic disease.[8] Repeated biopsy of tumour tissue is invasive, may be practically difficult, has resource implications and is clearly confounded by intratumoral heterogeneity. These shortcomings give huge potential to the recent advances in molecular imaging, which have the ability to visualize and quantify heterogeneity of tumour receptor expression, metabolism, apoptosis, blood flow or structure, non-invasively over time, *i.e.* at baseline and to assess response to treatment.

Owing to space constraints, we can only select a subset of imaging techniques for illustration purposes; a more comprehensive précis of the different image modalities has been reviewed elsewhere.[8]

VARIOUS IMAGING MODALITIES AND METHODS THAT CAN HELP TO MAP THE HETEROGENEITY IN TUMOUR METASTASIS

The development of metastasis is multifactorial and is dependent on the complex interaction between host factors and the tumour biology. This process is highly selective, and the metastatic lesion represents the end point of many sequential events that only a few cells can survive. Recent advances in next generation sequencing (NGS) have increased the understanding of (1) the clonal heterogeneity between primary and metastatic tumours and (2) the degree of genetic heterogeneity of metastatic tumours. For example, a study comparing sequences of primary tumours and metastases in lobular breast cancers revealed multiple mutations present only in metastases and several other mutations with increased frequency in metastatic sites.[9] Similarly, a number of studies report on the discordance in oestrogen receptor, progesterone receptor and human epidermal growth factor receptor 2 (HER2) expression between different metastatic sites.[10] As pointed out, histological analyses with repeated invasive biopsies have limitations. For instance, when different metastatic deposits are heterogeneous with respect to receptor expression and/or cellularity[11] and are not all subjected to biopsy, then a clinical decision based on *in vitro* analysis of the biopsied material may be prone to undersampling error. However, recent advances in imaging techniques, image acquisition and image analysis have been used to measure quantitative imaging biomarkers that may be able to address the complexities of tumour heterogeneity better than a standard histological biopsy. Here, we critically appraise these strategies specifically in the context of heterogeneous metastatic disease.

^{18}F-fludeoxyglucose–positron emission tomography/CT

Although CT is the imaging modality most widely used for tumour assessment, it provides very little in the way of distinct tumour activity information. The addition of positron emission tomography (PET) to CT can add such further information, and ^{18}F-fludeoxyglucose (^{18}F-FDG) is the most commonly used PET radiotracer, although there are many other radiotracers that examine different aspects of tumour biology. The ability of ^{18}F-FDG-PET to detect cancer is based on elevated aerobic glycolysis in the malignant tissue in comparison with the normal tissue—also known as the Warburg[12] effect. Although primarily reporting on tumour cell activity, ^{18}F-FDG-PET has been shown to also inform on tumour heterogeneity. A retrospective study using ^{18}F-FDG-PET/CT to monitor response among lesions in patients with bone-dominant metastatic breast cancer treated with systemic therapies reported that lesions showed heterogeneous metabolic response amongst responding and non-responding bony and non-bony lesions.[13]

Novel utilization of ^{18}F-FDG-PET/CT in recent years, such as texture analysis on CT imaging, has been shown to reflect tumour heterogeneity and associated prognosis. This has been examined in multiple tumour types, including lung,[14–16] colorectal[17–19] and oesophageal[20] cancers. There are a number of ways to extract texture elements in images. One such CT textural analysis methodology utilizes a two-step filtration–histogram technique. The first stage uses a Laplacian of gaussian spatial band-pass filter to selectively extract and enhance features of different sizes corresponding to fine, medium and coarse texture scales, allowing detection of spatial differences within a tissue (arising from the different band of spatial frequencies employed). The Laplacian detects intensity changes (or edges) within an image, which have been first smoothened by the gaussian distribution, based on the spatial scale filter (SSF) value. A lower SSF value (*e.g.* 2 mm) extracts and enhances features of a "finer" texture scale, whereas an

SSF value of 3, 4 or 5 mm extracts and enhances features of a "medium" texture scale and a higher SSF value (*e.g.* 6 mm) extracts and enhances features of a "coarser" texture scale, as shown in Figures 1 and 2. These novel texture analyses have also been applied to other imaging modalities, *e.g.* MRI,[21,22] and will be discussed later (section on Simultaneous positron emission tomography/MR and textural analysis).

Generation of these texture parameters provides vital information on the image features themselves (reviewed in Miles et al[23]). Standard deviation (SD) increases approximately in proportion to the square root of the number of features highlighted and their mean intensity difference compared with background (*i.e.* dark and bright features are both positive). Skewness is related to the average brightness of the highlighted features (predominantly bright features give positive values, while predominantly dark objects give negative values), which tends to zero with increasing number of features highlighted and moves away from zero with intensity variation in highlighted features. Kurtosis is related inversely to the number of features highlighted (whether bright or dark) and increases by intensity variations in highlighted features. By quantifying these different image features (size, concentration and density variation of the features highlighted by the filter) within a lesion (representing the different aspects of tissue heterogeneity), computed image texture analysis algorithms have the potential to provide additional morphological information relating to tumour heterogeneity. The intratumoral variability assessed by this technique is at a scale where the measured heterogeneity is likely to reflect tumour *vs* stroma and/or tumour *vs* necrosis. These features could feasibly correlate with a metastatic phenotype, but more work is required in this area to understand the associations between tumour–stromal relationships and gene expression and/or metastatic potential (see section Molecular imaging of metastatic potential). Yet, the prognostic application of CT textural analysis has been validated in various tumours types, with coarser tumours pertaining to a poorer prognosis[24] (Figure 3). In fact, overall survival (OS), progression-free survival (PFS) and local progression-free survival were all lower in individuals with high primary tumour coarseness.[25] Analysis of tumour texture in pre- and post-chemotherapy treatment in colorectal patients, to examine response and prognosis, has revealed that tumours that respond to treatment have lower initial tumour coarseness.[18] In addition to its correlation with survival, there is also limited pre-clinical literature which suggests that the application of these texture techniques can

Figure 1. (a) Conventional hepatic CT image. (b–d) Corresponding images selectively display (b) fine, (c) medium and (d) coarse texture obtained by using values for image filtration [spatial scale filter value (or sigma)] of 0.5 [width, 2 pixels (1.68 mm)], 1.5 [width, 6 pixels (5.04 mm)] and 2.5 [width, 12 pixels (10.08 mm)], respectively. Images should be viewed in the online format. Reproduced from Miles et al[18] with permission from the Radiological Society of North America.

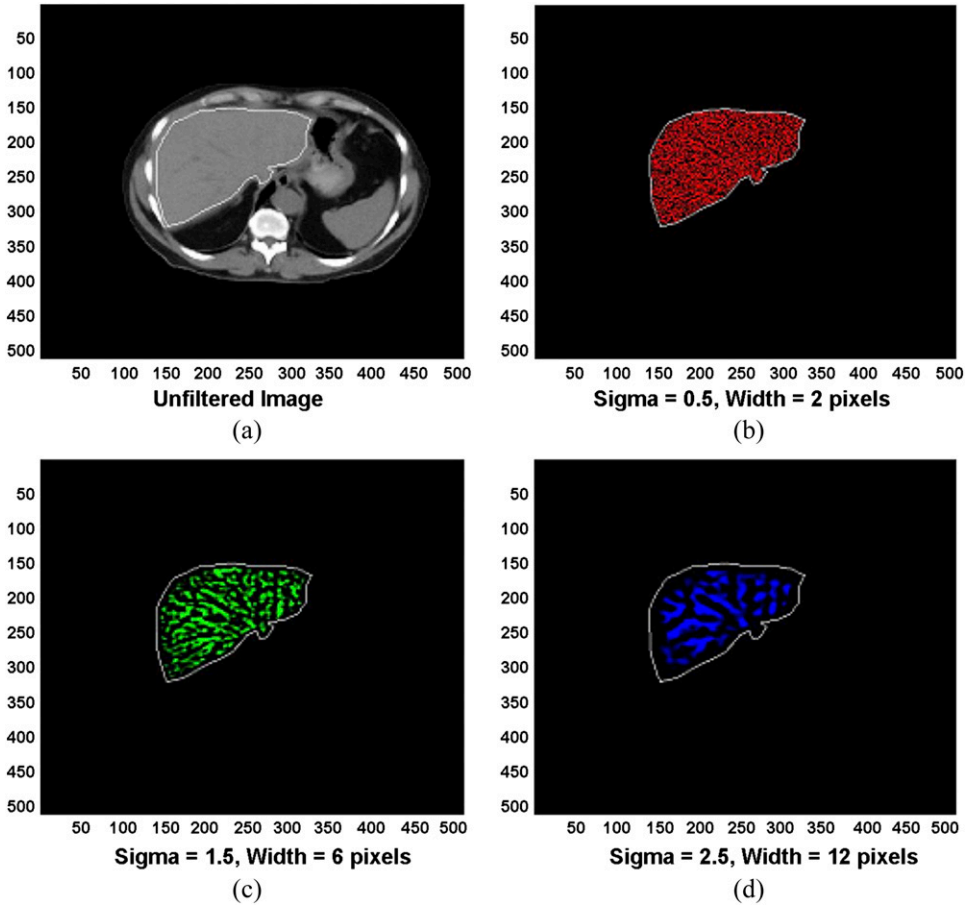

Figure 2. (a) A conventional CT (from a positron emission tomography/CT) image of a patient with a lung lesion and (b–d) corresponding images selectively displaying fine, medium and coarse texture obtained from TexRAD CT texture analysis (image heterogeneity) commercial research software (www.texrad.com, Radstock, UK). Images should be viewed in the online format.

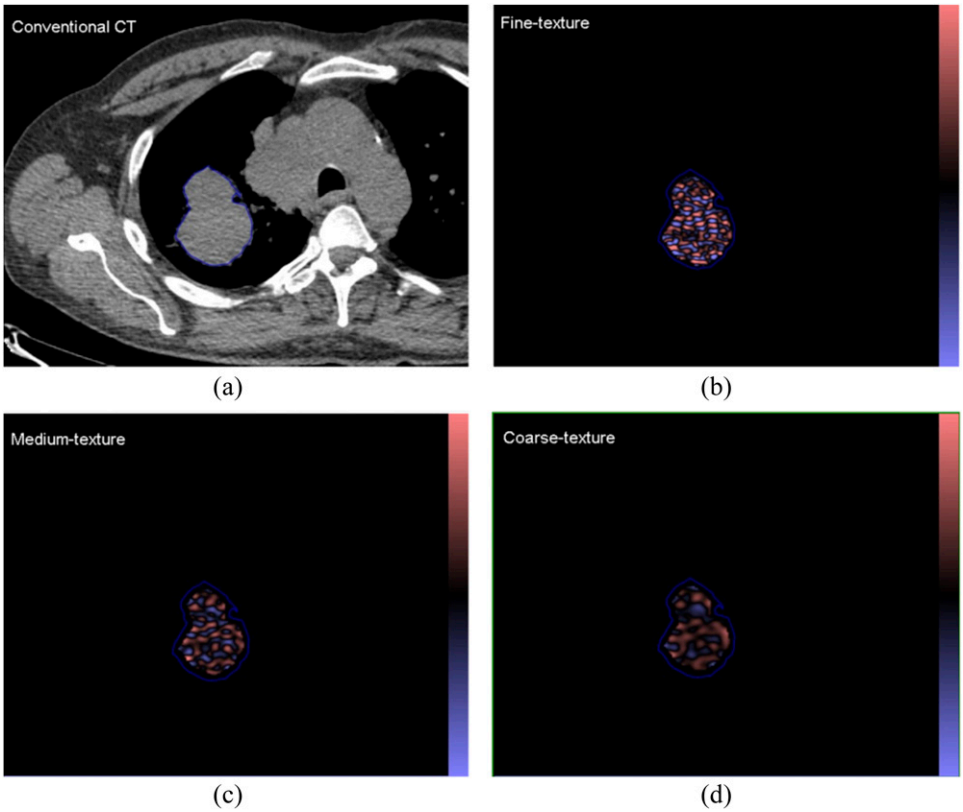

be used to analyse the surface heterogeneity of the primary tumour, and may yield non-invasive image parameters that may distinguish between metastatic and non-metastatic tumour phenotypes,[26] with exciting translational potential which needs further investigation.

PET texture analysis (PTA) can be conducted on the standardized uptake value (SUV) images used to measure the maximum SUV. The SUV images (individual pixel values) with initial units of uptake in Bq ml^{-1} can be converted (scaled) to SUV calibrated by patient weight and actual tracer activity (taking into consideration the initial tracer activity, amount of decay between the tracer measured time and scan time with respect to the half-life period of ^{18}F-FDG) with final units of uptake in g ml^{-1}. The tumour heterogeneity can be measured only on the SUV image without image filtration, using the histogram characteristics as described above in the section ^{18}F-fludeoxyglucose–positron emission tomography/CT. Image filtration is not appropriate owing to the inherently poor resolution of PET (SUV) data. A recent study in non-small-cell lung cancer (NSCLC) using PET/CT image data sets has shown the ability of PTA to be a prognostic marker of survival.[27] Other groups have shown that intra-tumour heterogeneity on PET via texture analysis predicts response to radiochemotherapy in oesophageal cancer (entropy, size, local and global heterogeneity and homogeneity, SUV),[28] and lung cancer (coarseness, contrast, busyness, complexity).[25] Given the poorer spatial resolution of PET compared with CT, the biophysical basis of metabolic textural features is not intuitive and requires further exploration.

Non-^{18}F-fludeoxyglucose–positron emission tomography for imaging the metastatic potential of primary tumours and/or detecting tumour metastases

^{18}F-fluoro-3′-deoxy-3′-L-fluorothymidine–positron emission tomography

^{18}F-fluorothymidine (FLT) is a tracer used to examine cell proliferation. Pyrimidine analogue thymidine is incorporated in DNA, during the S phase of the cell cycle, where proliferating cells synthesize DNA. ^{18}F-FLT is taken up by the cell and is phosphorylated by thymidine kinase 1. Thymidine kinase 1 activity is the highest during the cell division process in cells and takes place at a greater rate in malignant cells.[29] Given the dependence of this radiotracer on thymidine kinase 1 activity, there can be issues when used in conjunction with certain cytotoxic drugs, which arrest cells in S phase,[30] such as 5-fluorouracil. Various studies have been carried out on correlating imaging with histological findings and on immunostaining with Ki-67 to assess tumour proliferation rate. These studies have shown good correlation between the histological tumour proliferation rate and the ^{18}F-FLT-PET image.[31] Although ^{18}F-FLT-PET is an excellent tool for measuring tumour proliferation, there are several theoretical limitations to its use in detecting micrometastatic disease in patients with cancer. While an increase in proliferation is important for the initiation and maintenance of primary tumours, growth inhibition could ultimately be crucial for survival of carcinoma cells in the circulation. Mechanistically, this apparent paradox is

Figure 3. Kaplan–Meier plots demonstrating differences in patients with high and low primary tumour ^{18}F-fludeoxyglucose–positron emission tomography coarseness (a–c), contrast (d–f) and busyness (g–i). Differences in overall survival (OS) (a, d and g), progression-free survival (PFS) (b, e and h) and local progression-free survival (LPFS) (c, f and i) are demonstrated. Cum, cumulative. Reproduced from Cook et al[25] with permission from SN Turiel & Associates, Inc. © by the Society of Nuclear Medicine and Molecular Imaging, Inc.

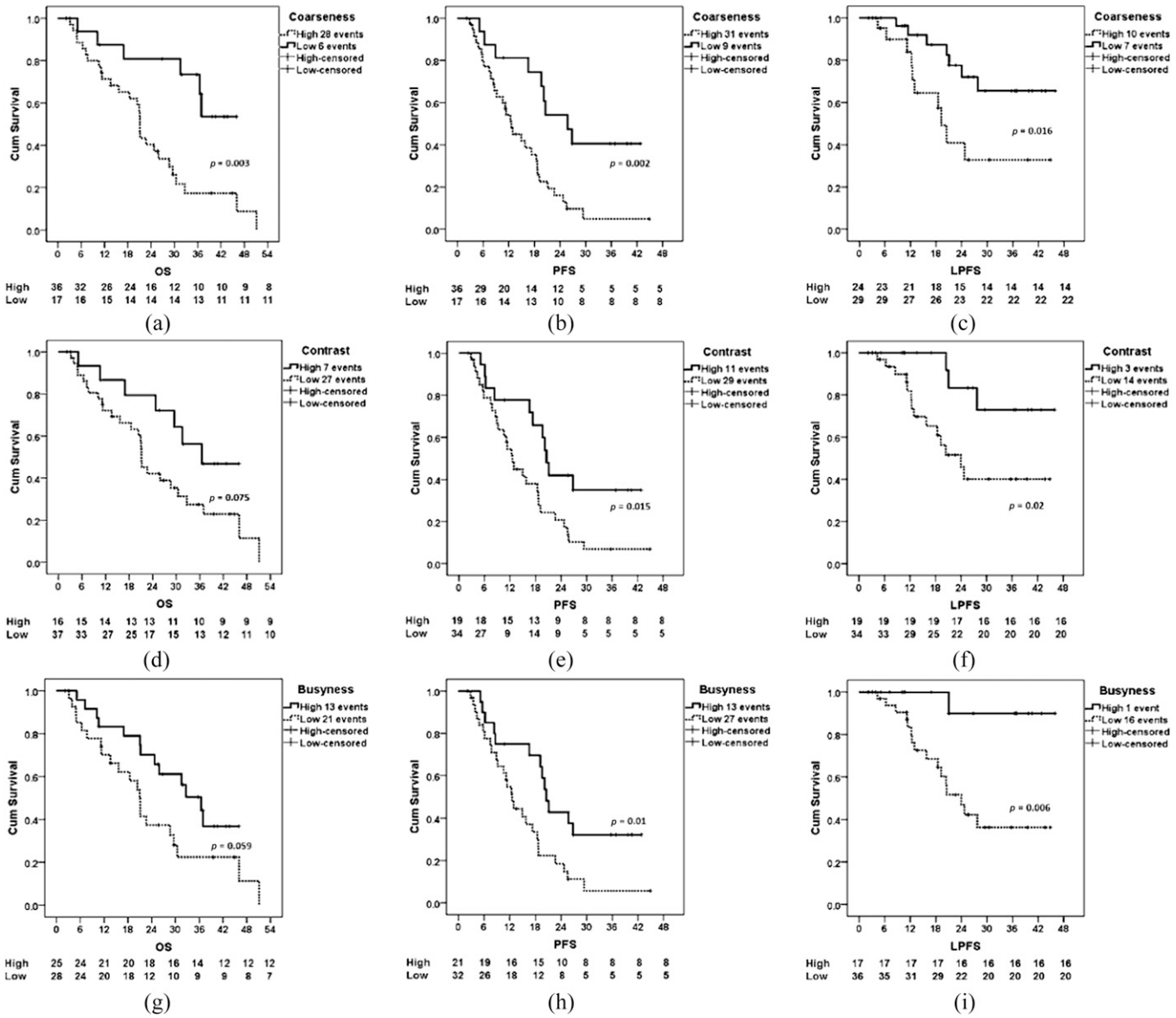

because of the dual function of cell cycle regulators, such as the well-known tumour suppressor gene p53[32] and transcription factor YB-1,[33] which also impact on the cell motility machinery. Additionally, metastatic cells in the target organ can enter into dormancy (*i.e.* a lag in tumour growth),[34] thus the sensitivity of detecting tumour metastases is somewhat limited.[35,36]

^{11}C-choline and ^{18}F-fluorocholine–positron emission tomography

Some tumours have low glucose metabolism, and therefore standard FDG-PET imaging has difficulties in the assessment of disease and treatment response. In prostate cancers, choline-PET imaging has been especially useful for restaging. Choline- and fluorocholine-based tracers used in PET scanning utilize the principle that choline is an essential component of the phospholipid portion of the cell membrane. It is particularly of benefit in a selected group of individuals rather than as a staging method for all; namely, patients with minimal recurrent prostate-specific antigen (PSA) levels of $\geq$1 ng ml^{-1}, those with short PSA doubling time (less than 3 months to a maximum of 6 months), and those with initial high recurrence risk tumour stage.[37,38]

Simultaneous positron emission tomography/MR

As discussed earlier in this review, PET image analysis traditionally focuses on the region of interest. The addition of MR to PET imaging can further add heterogeneity information regarding the

Figure 4. Produced from an imaging unit at the Institute of Nuclear Medicine, University College London, UK. Simultaneous ^{18}F-fludeoxyglucose–positron emission tomography (PET)/MRI-acquired image of a patient with a sigmoid tumour. Fused axial T_2 and PET (a), PET alone (b), MRI apparent diffusion coefficient map (c) and representative subtracted image from a dynamic contrast-enhanced MRI series (d); showing increased metabolism, cellularity and vascularity. Images should be viewed in the online format.

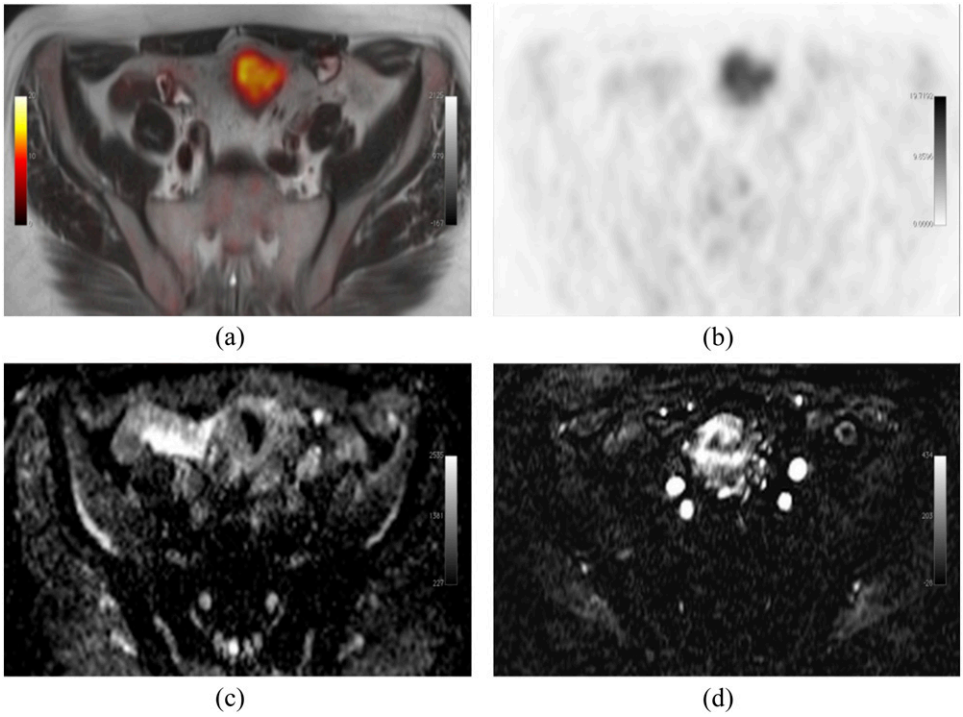

tumour phenotype that is gathered from radionuclide-based studies.[39] Dynamic contrast-enhanced (DCE) imaging differs from traditional MRI through the ability to acquire multiple images, before, during and after contrast injection (Figure 4). In the context of PET/MR, this imaging technique allows dynamic imaging of tumours to take place, with detailed imaging of tumour vascularity[40] through the concomitant evaluation of $\alpha_v\beta_3$ expression and high glucose metabolism within tumours that can show perfusion heterogeneity.[41] This form of imaging has also played a role in treatment assessment with vascular endothelial growth factor (VEGF) inhibitor use, which we discuss later on in further detail in this review (see section Molecular imaging of metastatic potential).

Ongoing developments in the combination of PET/MR with nanoparticle imaging have had further implications in the assessment of tumour heterogeneity.[42] Given the above discussion on specific (FDG- and non-FDG-based) PET tracers that are potentially of use in mapping the heterogeneity of different tumour types, the combination of specific-tracer PET/MR holds particular interest in imaging molecular heterogeneity.

The combination of microstructural and vascular information afforded by MRI with specific metabolic PET tracers can now be achieved in a clinic with whole-body PET/MR scanners.[43] Multiparametric imaging has well-recognized utility for microstructural and vascular tissue characterization and is rapidly establishing an expanding niche in the localization and management of prostate cancer.[44,45] Yet, in general, it remains more difficult to assess metabolic activity with MRI than with PET; MR spectroscopy (MRS) is inconsistently used in clinics, as it requires significant expertise in acquisition and processing of the MR signal; whilst hyperpolarized (HP) MRI in addition requires significant investment in infrastructure. Studies validating the use of whole-body PET/MR compared with PET/CT have repeatedly shown increased sensitivity in early tumour detection, and using diffusion weighting on top of PET/MR can also detect treatment response at varying levels within metastases.[46–50]

Multiparametric PET/MR performed by our group demonstrates the ability to assess glycolysis, cellularity and water content and intralesional heterogeneity (via texture analysis) within a single examination (Figure 5). In general, we found that tumours with more heterogeneous water distribution (*i.e.* higher SD and proportion of positive pixels) were more cellular (*i.e.* lower mean apparent diffusion coefficient) and glycolytic (*i.e.* higher SUV_{mean}). Foci of high cellularity also correspond to areas of increased glycolysis. Textural filters applied to the fractional water images revealed features of around 3- to 4-mm bright objects, which may be associated with pockets of water content and tended to be higher within tumours having adverse biology (restricted diffusion and increased glucose uptake). Multiparametric PET/MRI data sets evaluating tissue microstructure, metabolism and heterogeneity are likely to contain prognostic information/relate to metastatic potential; both hypotheses require further work to validate.

Furthermore, simultaneous PET/MRI offers the opportunity in the clinic to combine tissue characterization multiparametric

Figure 5. Multiparametric positron emission tomography (PET)/MRI of a rectal cancer. (a) High ^{18}F-fludeoxyglucose uptake on fused PET/T_2 MRI, with (b) a correspondingly patchy reduced apparent diffusion coefficient (ADC) in keeping with pockets of high cellularity within the tumour and (c) a fractional water image derived from source fat and water Dixon images of the same tumour confirms that areas of increased cellularity correlate with relatively increased water content (white arrows). (d) Application of a medium coarse textural filter highlights 3- to 4-mm bright objects on the fractional water image (medium texture map). Images should be viewed in the online format. (www.texrad.com, Radstock, UK.)

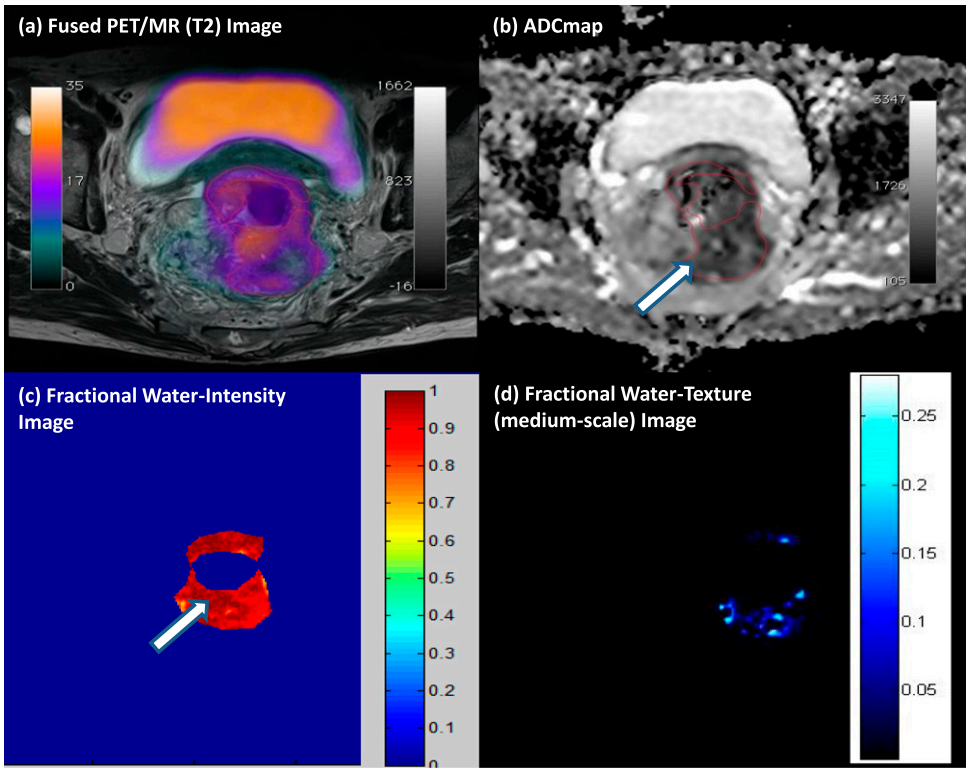

MRI with specific molecular PET imaging, with the potential to assess dynamic biological relationships through multimodal imaging of, for example, tumour cellularity/cell turnover [diffusion-weighted imaging (DWI) or FLT-PET], hypoxia (blood oxygen level-dependent MRI or ^{18}F-fluoromisonidazole PET ligand), vascularity (DCE/MRI or α-V-β-3 PET ligand) and glycolysis (^{18}F-FDG-PET ligand or glucose chemical exchange saturation transfer MRI).[51] Spatial heterogeneity of PET-MRI signals among metastases is often evident.[11] Elucidating the mechanisms leading to heterogeneous multimodal metastatic phenotypes and the consequent therapeutic implications remains the remit of future research.

Imaging the link between metabolism and tumour signalling pathways that are associated with metastasis: hyperpolarized MRI

^{13}C-MRS has been used in the investigation of metabolic processes *in vivo* for many years.[52] Its limitations relate to the difficulty in the signal intensity of the proteins in question, mainly down to the physics of MRI and its use of the apparent diffusion coefficient of water. Hyperpolarization with the dynamic nuclear polarization technique can yield >10 000-fold signal increases in MR-active nuclei, allowing the detection of ^{13}C-labelled substrates *in vivo* and also imaging of tissue distribution, in the absence of any background signal from non-polarized material. Pyruvate is a molecule involved in major metabolic and catabolic pathways in mammalian cells (Krebs cycle) and depending on anaerobic or aerobic metabolism can have various end products. 1-^{13}C-pyruvate imaging can therefore detect lactate, alanine and carbon dioxide.[53,54] The imaging data generated by this technique in a transgenic mouse model of prostate adenocarcinoma were shown to correlate with the histological grading of tumours and have been used to identify tumour necrosis and metastatic lymph nodes. The NCT01229618 clinical trial is examining the role of 1-^{13}C-pyruvate imaging in patients with prostate cancer.[55] HP ^{13}C MR spectroscopic imaging, measuring the HP lactate-to-pyruvate ratios, can be used to monitor the heterogeneity in a major signalling pathway within cancers, namely the PI3K/AKT/mTOR pathway and its response to molecule-targeted therapeutics, such as Everolimus,[56] and potentially inhibitors of other signalling pathways, *e.g.* hypoxia-inducible factor-1 and MYC, which are known to predispose tumour cells to metastasize under both normoxic and hypoxic conditions.[57–59]

Nanoparticle-based imaging

Nanoparticles are small, 1–100 nm, structures that in recent years have been explored in their capacity for imaging, drug delivery and monitoring of treatment outcome.[60] Nanoparticles may be organic based (liposomes, polymeric nanoparticles, micelles, dendrimers and solid lipid nanoparticles), inorganic based (iron oxide

nanoparticles, gold nanoparticles, semiconductor nanocrystals, ceramic nanoparticles and carbon nanotubes) or a hybrid of both. Nanoparticles have large surface to volume ratios contributing to their high loading capacity. As drug delivery systems, nanoparticles have been shown to improve drug solubility, prolong blood circulation half-life and control drug release.[61] One of the major advantages with nanoparticle technology is that drug delivery and imaging probes can be combined into one delivery system.

Gold nanoparticles have high density and extinction coefficients and can be applied as contrast agents for CT, dark field imaging and photoacoustic imaging. The shape of gold nanoparticles can facilitate them to strongly absorb light in the near-infrared range, converting this energy into heat for photothermal therapy. Iron oxide-based nanoparticles are magnetic and therefore used as contrast agents to produce hypodense regions on T_2/T_2 weighted MR images.

Nanoparticles have also been used as a predictive tool in functional imaging. Superparamagnetic iron oxide nanoparticles (SPIONs), specifically reporting on tumour vasculature, have recently been used in predicting the likelihood of brain metastases in melanomas.[62,63] Various imaging nanoparticles are currently undergoing human clinical trials; for example, ^{124}I-labelled cRGDY silica nanoparticles in melanoma (NCT01266096), ^{99m}TC-sulphur colloid nanoparticles in sentinel node mapping in breast cancers (NCT00438477) and ultrasmall (U)SPION in pre-operative pancreatic cancers (NCT00920023). All of the above are a mixture of imaging modalities, CT, MRI and single photon emission CT (SPECT), showing that nanoparticle imaging is not exclusive to one imaging modality. A specific application of these (U)SPIOs to characterize the heterogeneity of macrophage infiltration in the tumour microenvironment will be described in section Application of an integrated imaging–genomic approach to stratify cancer treatment—requirements for clinical translation.

Imaging tumour heterogeneity at a cellular level: intra-operative optical imaging

The basis of radio-guided surgery involves the deployment of a radiolabelled tumour tracer pre-operatively and the use of a detection probe intra-operatively. Intra-operative use of a gamma probe has been shown to reveal small (<10 mm) lesions within the abdomen that can be missed on traditional whole-body functional imaging. This technique has been shown to individualize surgical procedures intra-operatively, resulting in improved complete resection rates with subsequent effects on reducing recurrence rates.[64–67] Moreover, to facilitate the visualization of cancer cells at a higher resolution, intra-operative tumour imaging has been successfully conducted with near-infrared dye-labelled molecule-targeted antibodies against various tumour cell targets, *e.g.* folate receptor, VEGF (bevacizumab) and HER2 (trastuzumab).[68,69] The first-in-man ovarian cancer surgery was performed with an optical detection device that has a corresponding resolution varying between 150 and 30 μm.[69] It allows for individual cellular clusters to be visualized and dissected. Further genomic investigations of these cellular clusters is likely to add further details to the degree of cell-to-cell tumour heterogeneity and its role in promoting resistance within an evolving tumour genome.

MOLECULAR IMAGING OF METASTATIC POTENTIAL

Early identification of patients at high risk of metastatic disease is arguably the most important task for improving cancer mortality. The pre-metastatic niche hypothesis comprises the creation of a supportive environment for circulating tumour cells to "seed" to.[70] This dynamic process is thought to involve both chemokine secretion at the primary tumour site and subsequent activation of immune cells in the target tissue of metastasis. In response to tumour-secreted factors (TSFs), intra- and extramedullary haematopoiesis and consecutive immune cell differentiations are altered in order to promote the survival and outgrowth of disseminated tumour cells. Certain organs carry a greater susceptibility to specific tumours; for example, bone metastases are prevalent in breast and prostate cancers, whereas are rarer in others, such as ovarian. The understanding of tumour heterogeneity should allow us to not only assess the primary tumour at a molecular level but also examine distant organs for pre-metastatic changes.

Although targeted SPECT and PET probes mostly address surface markers or metabolic features of the primary tumour cells themselves, the same principles can be used for visualization of metastasis-associated changes of tissue composition or intercellular communication. Using a PET imaging probe for vascular cell adhesion molecule-1 (VLA-4), reportedly highly expressed in bone marrow-derived cells that have been implicated in establishing the pre-metastatic niche,[71] Shokeen et al[72] reported using imaging combined with immunohistochemistry, an enrichment of these haematopoietic progenitor cells (HPCs) at the sites of metastasis. Besides the HPCs, tumour-associated macrophage (TAM) accumulation in the tumour microenvironment has been linked to increased tumour invasiveness and therefore metastasis[5] In primary tumours, visualization of TAM by MRI is established and frequently performed using macromolecular substances that are taken up by the target cells via phagocytosis, such as (U)SPIONs,[73] as mentioned earlier in this review. Nevertheless, the limited sensitivity of MRI (compared with the extremely high sensitivity of PET microdosing), combined with the high background activity of phagocytic cells in typical target organs of metastasis, would, however, probably hinder the use of such techniques in imaging of pre-metastatic tissue priming.

Another aspect of the promoting effect of TAM on tumour metastasis is through enhanced angiogenesis, partly through an increase in VEGF secretion by macrophages.[74–77] VEGF is an important signalling pathway in vasculogenesis and angiogenesis, and therefore plays a vital role in tumour growth, survival and metastases. In oncology, there have been multiple anti-VEGF therapies, of various forms, monoclonal antibodies (bevacizumab) and small tyrosine kinase inhibitors (pazopanib). The use of DCE/MR in vascular imaging has already been discussed in the assessment of angiogenesis. The lack of an appropriate biomarker for VEGF inhibitors has been a particular issue in the clinical setting. VEGF inhibitors are used widely in various tumour types, such as breast,[78] colon,[79] ovarian,[80] renal cell[81] and hepatocellular;[82] however, treatment response can be very difficult to assess, especially in the maintenance setting. DCE/MRI allows non-invasive

quantification of tumour microvasculature through dynamic imaging of enhancement and washout of injected contrast material. The vascular configuration in tumours promotes an initial faster and greater accumulation of contrast within the interstitial space and favours more rapid removal of contrast from the interstitium, as the concentration of contrast in the blood falls owing to renal excretion. These features can be fitted to pharmacokinetic models, and the derived variables have been directly related to VEGF modulation of vascular permeability.[83,84]

Imaging of mediators of inflammation, such as tumour necrosis factors or interleukin-1α, has been performed successfully in clinical and experimental imaging of inflammation.[85,86] However, given the high background activity and relatively low specific accumulation of the respective tracers at the target site where there is a significant degree of inflammation, it is not hopeful that the subtle potential changes in pre-metastatic tissue could specifically be picked up using these or comparable approaches. It has recently been established that, in pre-metastatic lung tissue of tumour-bearing animals, the vessel permeability is locally altered in response to TSFs,[87] resembling local inflammation. This permeability as well as the accompanied increase in extravascular cellularity (*e.g.* inflammatory cell content in the extravascular compartment) could in theory be visualized using established imaging approaches such as MRI.[88,89] It would be of interest to see changes in tissue architecture and other MRI-based assessment of features, such as collagen content, consecutive mechanical characteristics, vessel architecture etc., that are revealed during the establishment of metastasis.

Moreover, further investigation of the cellular composition of the pre-metastatic niche and the main regulating factors is strongly required.[90] It would potentially enable the use of specific MRI approaches for tissue characterization as well as an armament of specific probes for radionuclide and optical imaging of already established disease-associated target molecules and cells.[91] In this context, exosomes are 40- to 100-nm-diameter membrane vesicles of endocytic origin that have been demonstrated to contain mRNA, miRNA and proteins, and are gaining increasing interest in terms of their translational research potential in cancer.[92–96] They are released into the extracellular space from various cell types and body fluids and mediate intercellular transfer of RNAs and proteins. As such, exosome analysis is ideally suited for monitoring the evolving tumour longitudinally, in terms of its whole transcriptome, miRNome and proteome profiles.[92,97] Exosomes have been shown to have an important role in intercellular communication, and they are involved in stimulation of the secretion of growth factors, cytokines. There is growing evidence that exosomes are generally involved in the manipulation of the pre-metastatic niche.[96,98,99] Imaging the transfer of exosomes secreted by tumour cells into host cells in a cancer mouse model suggests that the tumour-derived exosomes contribute to the formation of a niche to promote tumour growth and metastasis.[100] A number of current studies have shown that there is a correlation between exosomes and metastasis in different types of cancers. The detection and quantification of exosomes carrying tumour-relative antigens in melanoma patients may represent a potential tool for cancer screening and prediction of metastatic risk.[101] Tumour-derived microvesicles from patients with head and neck cancer induce apoptosis of activated $CD8^+$ T cells that correlated with disease activity and the presence of lymph node metastases.[102] Furthermore, exosomes adapt to hypoxia in the local tumour microenvironment during cancer progression and thus reflect the hypoxic state of cancer cells. Under hypoxic conditions, a change of the protein cargo of exosomes secreted by tumour cells was observed that modulates the microenvironment and promotes angiogenesis and metastasis.[95] In highly aggressive brain tumours, the analysis of exosomes from patient samples reveals the enrichment in exosomes of hypoxia-regulated mRNAs and proteins.[103] In addition to the *in vitro* analysis of plasma/serum exosomes, the effect of the exosomes on pulmonary vascular permeability[96] can be assessed by the aforementioned MR-based whole-body imaging techniques.

Clinically, exosomes are increasing in prominence for their diagnostic/predictive potential in cancers. For example, the tumour suppressor gene phosphatase and tensin homolog is only expressed in exosomes that circulate in the blood of patients with prostate cancer, but it is not detected in exosomes from normal subjects, and might be thus a potential biomarker for prostate cancer.[104] In another study, potential diagnostic markers for human NSCLC were identified by proteomic analysis of purified microvesicles from pleural effusion in patients with NSCLC.[102] Micro-RNA and protein profiling of brain metastasis cell-derived exosomes *vs* non-brain metastasis revealed changes in specific miRNA and proteins which may contribute to the discovery of new biomarkers for brain metastasis.[105] Similarly, proteome profiling of exosomes from human primary and metastatic colorectal cancer reveal different expression of key metastatic factors.[106] These examples demonstrate the increasing importance of exosomes in the identification of

Figure 6. Intertumour heterogeneity of gene expression profiles associated with cellular processes and disease progression. Unsupervised hierarchical clustering showing pair-wise correlations of a panel of gene signature scores across primary breast tumour tissue samples (234 patients). Representative signatures are indicated for each cluster: T-cells, B-cells and dendritic cells, Immune1*, Motility, stem-cell-like, tumour growth factor β (TGFβ) response, RAS*, Stroma2*, GGI*, Gene70*, MYC* (*signature curated by Ignatiadis et al[112]). Recent studies report expression-based prognostic and predictive stratification of primary breast tumours, which are phenotypically similar according to current clinical methods.[111,113,114] Images should be viewed in the online format.

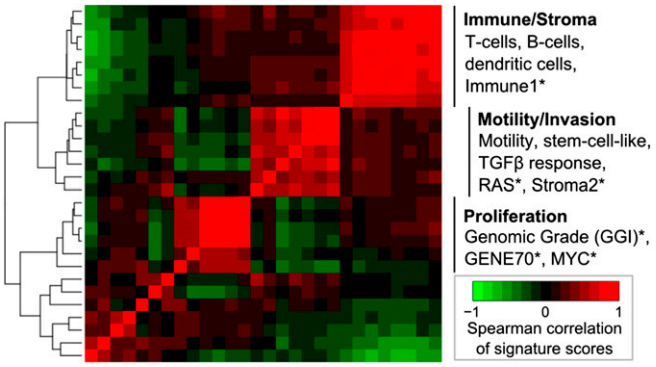

Figure 7. Schematic of potential future trial design, incorporating functional imaging and tissue samples to further biomarker research.

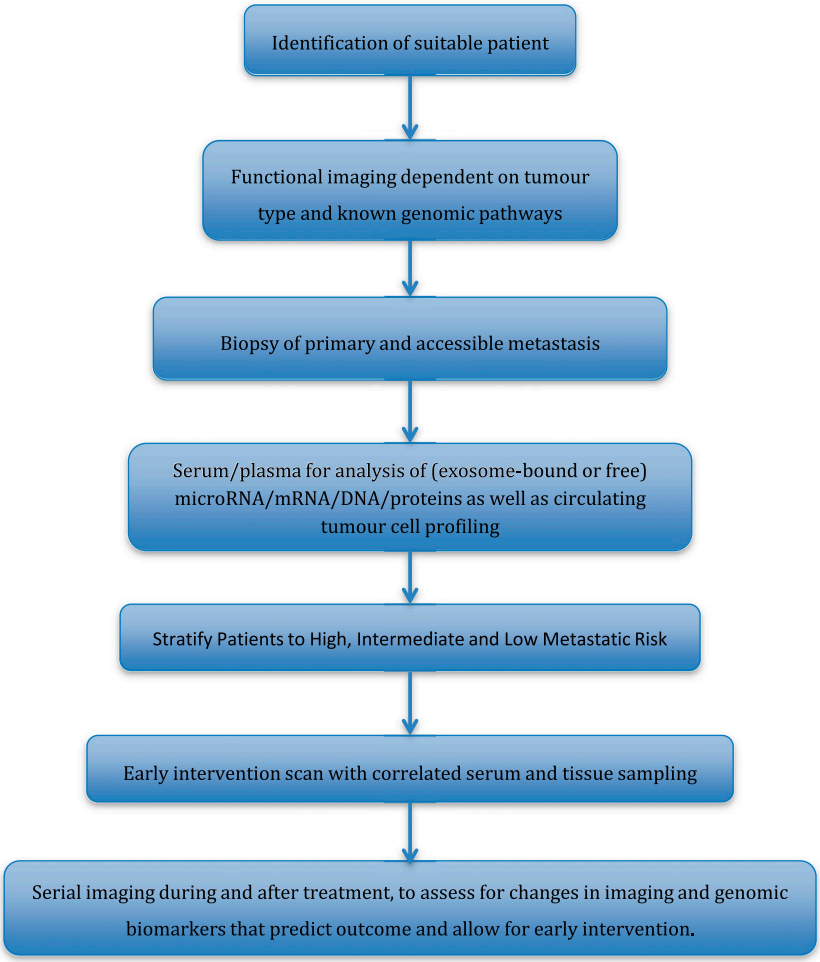

novel biomarkers in metastatic cancers, although imaging in patients is still a little way off clinical application.[107]

APPLICATION OF AN INTEGRATED IMAGING–GENOMIC APPROACH TO STRATIFY CANCER TREATMENT—REQUIREMENTS FOR CLINICAL TRANSLATION

Much energy has been expended recently in establishing the role of imaging biomarkers for evaluating treatment response in cancers. An ongoing collaborative effort by the American College of Radiology Imaging Network (ACRIN), Philadelphia, PA, Cancer and Leukaemia Group B, Chicago, IL, and the National Cancer Institute, Bethesda, MD, Specialized Programs of Research Excellence recently conducted the largest multicentre imaging trial (ACRIN 6657) as part of the I-SPY1 trial (Investigation of Serial Studies to Predict Your Therapeutic Response With Imaging and Molecular Analysis). ACRIN 6657 utilizes MRI to measure treatment response in patients receiving neoadjuvant chemotherapy.[108] Volumetric estimates of the tumour size, based on functional criteria applied to contrast-enhanced images, were seen to have greater sensitivity than linear tumour diameter measurements for predicting pathologically complete responses in patients completing neoadjuvant chemotherapy. The greatest difference in predictive ability occurred at the early time points, providing "proof of concept" that imaging parameters can serve as non-invasive predictive biomarkers of early treatment response. Its subsequent I-SPY2 clinical trial platform targeting the rapid focused clinical development of paired oncologic therapies and biomarkers now uses MR volumes to provide information about response to chemotherapy between regimens—information that cannot otherwise be obtained without surgical resection.[109] Additionally, its sub-study, ACRIN 6698, combines both DCE and DWI MRI data to generate novel imaging biomarkers that may correlate with treatment response,[110] and its results are eagerly awaited. Integration of these imaging biomarkers with genomic profiles of tumours are likely to prove essential for future clinical translation.

Transcriptomic analyses of primary solid tumours have revealed differential activation of gene expression signatures relating to cellular processes, including proliferation, cell migration and immune response (Figure 6) with the potential for prognostic and predictive stratification of tumours, which are phenotypically similar by current clinical methods.[111,112,115] Meanwhile, putative associations between clinical imaging traits and gene expression profiles have been reported in solid tumours. Exploratory studies have reported correlations between selected image traits and the

expression of individual genes or larger modules of co-expressed genes[113,116] reviewed in Rutman and Kuo.[117] Genomic copy number and other genomic aberrations exhibit variation between tumours from different patients[118,119] and between subclones within a primary tumour[4,120] Lesional and temporal variations in HER2 amplification and specific HER2 insertional mutations (such as $HER2^{YVMA}$), for example, could have clinical implications for HER2-targeted treatment and monitoring in the metastatic setting.[121,122] PET imaging using tracer-linked trastuzumab has been used to identify HER2-positive tumour and metastatic sites,[123,124] indicating the potential for non-invasive monitoring of HER2-positive lesions. In the treatment–response setting, early metabolic response to trastuzumab (less than 48 h post treatment) was detected in a pre-clinical study using optical metabolic imaging but not FDG-PET.[125] Many more genomic aberrations have been catalogued as part of large-cohort studies of primary solid tumours, revealing both recurrent mutations (*e.g.* p53, PIK3CA[119,126]) and recurrent dysregulation associated with a diversity of less frequent underlying genomic or transcriptional variation.[121,127] Detection of intertumoral, interlesional and temporal variations may prove to be critical for describing and monitoring disease progression but would require methods for non-invasive detection. Non-invasive imaging, coupled to more advanced analyses, may in the future yield parameters that oncologists can monitor longitudinally, in conjunction with high-coverage NGS of plasma-derived DNA to monitor the evolution of tumour genomic profiles under treatment pressure.[128] Some initial results have shown that there may be a correlation between some of these mutations (codons 12, 13 and 61 of KRAS, for instance) and various PET/CT-based parameters in colorectal cancers.[129]

TRANSLATION OF IMAGING TECHNOLOGIES IN ONCOLOGICAL TRIALS

Given the lack of measurable biomarkers through patient sampling, the advances in molecular imaging provide an impetus for testing functional imaging as a cancer biomarker, in a way that is complementary to tissue- and blood-based biomarkers. Despite these rapid advances, the translation of such techniques into clinics continues to lag behind. Incorporation of functional imaging to evaluate tumour responses should play an important role in designing future trials (Figure 7). Strategically planned biomarker evaluations with access to functional imaging in early phase trials (Phase I/II) will allow for efficient Phase III clinical trial designs, increasing the chances of positive Phase III biomarker-driven trial results. Functional imaging can not only provide information on the treatment response but can also monitor mutational pathways and the various molecular pathway pressures on an individual tumour, allowing a more robust stratification of treatment pathways. A major setback for targeted therapy has been the duration of tumour response, as many patients go on to have progressive disease after a relatively short response period. At present, although we understand a small fraction of these tumour escape pathways, we are unable to respond in a clinical setting to early mutational changes. Functional imaging information can help identify and assess high-/at-risk patients non-invasively, allowing for implementation of appropriate management plans governed by their personal escape pathway and thereby improving patient outcome.

At present robust large patient trials examining the methods we have discussed in this review are lacking. However, a few large trials are currently incorporating functional imaging within their remit. The NeoPHOEBE trial is a Phase II trial examining the application of FDG-PET as a biomarker of early response in the neoadjuvant setting in the treatment of HER2-positive breast cancer. Similarly, the FOCUS4 trial, currently recruiting, is a molecularly stratified randomized trial for patients with inoperable or metastatic colorectal cancer. It contains five arms [v-raf murine sarcoma viral oncogene homolog B (BRAF), PI3KCA, RAS, no mutation and non-classified] of randomization with prior histological analysis of patient pathology determining treatment. Despite the optimism behind these trials, the need for robust validation is crucial in order to offer patients lasting results.

The role of clinical trials should not be purely to review efficacy of treatment but also to aid the development of new research. To this end, the acquisition of patient samples at each step of the treatment paradigm plays a vital role in developing the translational application of research. As previously discussed, the role of exosomes in cancers is developing in prominence and understanding alongside the emerging role of circulating tumour cells and their reflection of the primary and metastatic tumour.

The integration of functional imaging, patient sampling and drug development together with wider research is likely to play a key role in fully understanding the nature of heterogeneity and ultimately how to control its effects to clinical advantage.

CONCLUSION

In this review, we have discussed the novel application of current imaging techniques in the assessment of heterogeneity especially in the context of examining metastasis and predicting metastatic potential. Although we have access to and are developing new tracers and new imaging techniques, there is a significant need for large patient trials and applications to fully determine their specific validity in the personalized patient treatment paradigm.

CONFLICTS OF INTEREST

B. Ganeshan and K.A. Miles are shareholders in TexRAD Ltd, a company developing and marketing the commercial (research) texture analysis software.

FUNDING

This work was supported by KCL Breakthrough Breast Cancer Research Unit/Sarah Green Fellowship funding (SI) and an endowment fund from Dimbleby Cancer Care to King's College London (TN). KL and ME were supported by the KCL-UCL Comprehensive Cancer Imaging Centre funding [CR-UK & EPSRC, in association with the MRC and DoH (England)]. HM was supported by an FP7-HEALTH-2010 European Union grant entitled "IMAGINT" (grant no. 259881). This work was undertaken at UCLH/UCL, which received a proportion of the funding from the UK's Department of Health's NIHR Biomedical Research Centre's funding scheme. Further funding was received from other NIHR sources.

REFERENCES

1. Fruhwirth GO, Fernandes LP, Weitsman G, Patel G, Kelleher M, Lawler K, et al. How Förster resonance energy transfer imaging improves the understanding of protein interaction networks in cancer biology. *Chemphyschem* 2011; **12**: 442–61.
2. Virchow R. *Die cellular pathologie in ihrer begründung auf physiologische und pathologische gewebelehre*. Berlin, Germany: August Hirschwald; 1858.
3. Navin N, Kendall J, Troge J, Andrews P, Rodgers L, McIndoo J, et al. Tumour evolution inferred by single-cell sequencing. *Nature* 2011; **472**: 90–4. doi: 10.1038/nature09807
4. Gerlinger M, Rowan AJ, Horswell S, Larkin J, Endesfelder D, Gronroos E, et al. Intratumor heterogeneity and branched evolution revealed by multiregion sequencing. *N Engl J Med* 2012; **366**: 883–92. doi: 10.1056/NEJMoa1113205
5. Quail DF, Joyce JA. Microenvironmental regulation of tumor progression and metastasis. *Nat Med* 2013; **19**: 1423–37.
6. Psaila B, Lyden D. The metastatic niche: adapting the foreign soil. *Nat Rev Cancer* 2009; **9**: 285–93.
7. Hüsemann Y, Geigl JB, Schubert F, Musiani P, Meyer M, Burghart E, et al. Systemic spread is an early step in breast cancer. *Cancer Cell* 2008; **13**: 58–68.
8. Patel GS, Kiuchi T, Lawler K, Ofo E, Fruhwirth GO, Kelleher M, et al. The challenges of integrating molecular imaging into the optimization of cancer therapy. *Integr Biol (Camb)* 2011; **3**: 603–31. doi: 10.1039/c0ib00131g
9. Shah SP, Morin RD, Khattra J, Prentice L, Pugh T, Burleigh A, et al. Mutational evolution in a lobular breast tumour profiled at single nucleotide resolution. *Nature* 2009; **461**: 809–13. doi: 10.1038/nature08489
10. Hoefnagel LD, van der Groep P, van de Vijver MJ, Boers JE, Wesseling P, Wesseling J, et al. Discordance in ERα, PR and HER2 receptor status across different distant breast cancer metastases within the same patient. *Ann Oncol* 2013; **24**: 3017–23.
11. Gaertner FC, Fürst S, Schwaiger M. PET/MR: a paradigm shift. *Cancer Imaging* 2013; **13**: 36–52.
12. Warburg O. On the origin of cancer cells. *Science* 1956; **123**: 309–14.
13. Huyge V, Garcia C, Alexiou J, Ameye L, Vanderlinden B, Lemort M, et al. Heterogeneity of metabolic response to systemic therapy in metastatic breast cancer patients. *Clin Oncol (R Coll Radiol)* 2010; **22**: 818–27. doi: 10.1016/j.clon.2010.05.021
14. Ganeshan B, Goh V, Mandeville HC, Ng QS, Hoskin PJ, Miles KA. Non–small cell lung cancer: histopathologic correlates for texture parameters at CT. *Radiology* 2013; **266**: 326–36.
15. Ganeshan B, Panayiotou E, Burnand K, Dizdarevic S, Miles K. Tumour heterogeneity in non-small cell lung carcinoma assessed by CT texture analysis: a potential marker of survival. *Eur Radiol* 2012; **22**: 796–802. doi: 10.1007/s00330-011-2319-8
16. Ganeshan B, Abaleke S, Young RCD, Chatwin CR, Miles KA. Texture analysis of non-small cell lung cancer on unenhanced computed tomography: initial evidence for a relationship with tumour glucose metabolism and stage. *Cancer Imaging* 2010; **10**: 137–43.
17. Ganeshan B, Miles KA, Young RCD, Chatwin CR. Hepatic enhancement in colorectal cancer: texture analysis correlates with hepatic hemodynamics and patient survival. *Acad Radiol* 2007; **14**: 1520–30. doi: 10.1016/j.acra.2007.06.028
18. Miles KA, Ganeshan B, Griffiths MR, Young RC, Chatwin CR. Colorectal cancer: texture analysis of portal phase hepatic CT images as a potential marker of survival. *Radiology* 2009; **250**: 444–52. doi: 10.1148/radiol.2502071879
19. Ganeshan B, Miles KA, Young RC, Chatwin CR. In search of biologic correlates for liver texture on portal-phase CT. *Acad Radiol* 2007; **14**: 1058–68. doi: 10.1016/j.acra.2007.05.023
20. Cheng NM, Dean Fang YH, Chang JT, Huang CG, Tsan DL, Ng SH, et al. Textural features of pretreatment 18F-FDG PET/CT images: prognostic significance in patients with advanced T-stage oropharyngeal squamous cell carcinoma. *J Nucl Med* 2013; **54**: 1703–9.
21. Brown R, Zlatescu M, Sijben A, Roldan G, Easaw J, Forsyth P, et al. The use of magnetic resonance imaging to noninvasively detect genetic signatures in oligodendroglioma. *Clin Cancer Res* 2008; **14**: 2357–62. doi: 10.1158/1078-0432.CCR-07-1964
22. Foroutan P, Kreahling JM, Morse DL, Grove O, Lloyd MC, Reed D, et al. Diffusion MRI and novel texture analysis in osteosarcoma xenotransplants predicts response to anti-checkpoint therapy. *PLoS One* 2013; **8**: e82875.
23. Miles KA, Ganeshan B, Hayball MP. CT texture analysis using the filtration-histogram method: what do the measurements mean? *Cancer Imaging* 2013; **13**: 400–6. doi: 10.1102/1470-7330.2013.9045
24. Ganeshan B, Skogen K, Pressney I, Coutroubis D, Miles K. Tumour heterogeneity in oesophageal cancer assessed by CT texture analysis: preliminary evidence of an association with tumour metabolism, stage, and survival. *Clin Radiol* 2012; **67**: 157–64.
25. Cook GJ, Yip C, Siddique M, Goh V, Chicklore S, Roy A, et al. Are pretreatment 18F-FDG PET tumor textural features in non-small cell lung cancer associated with response and survival after chemoradiotherapy? *J Nucl Med* 2013; **54**: 19–26. doi: 10.2967/jnumed.112.107375
26. Fan X, River JN, Zamora M, Tarlo K, Kellar K, Rinker-Schaeffer C, et al. Differentiation of nonmetastatic and metastatic rodent prostate tumors with high spectral and spatial resolution MRI. *Magn Reson Med* 2001; **45**: 1046–55.
27. Win T, Miles KA, Janes SM, Ganeshan B, Shastry M, Endozo R, et al. Tumor heterogeneity and permeability as measured on the CT component of PET/CT predict survival in patients with non-small cell lung cancer. *Clin Cancer Res* 2013; **19**: 3591–9. doi: 10.1158/1078-0432.CCR-12-1307
28. Tixier F, Hatt M, Le Rest CC, Le Pogam A, Corcos L, Visvikis D. Reproducibility of tumor uptake heterogeneity characterization through textural feature analysis in 18F-FDG PET. *J Nucl Med* 2012; **53**: 693–700.
29. Boothman DA, Davis TW, Sahijdak WM. Enhanced expression of thymidine kinase in human cells following ionizing radiation. *Int J Radiat Oncol Biol Phys* 1994; **30**: 391–8.
30. Mirjolet JF, Barberi-Heyob M, Merlin JL, Marchal S, Etienne MC, Milano G, et al. Thymidylate synthase expression and activity: relation to S-phase parameters and 5-fluorouracil sensitivity. *Br J Cancer* 1998; **78**: 62–8.
31. Francis DL, Freeman A, Visvikis D, Costa DC, Luthra SK, Novelli M, et al. In vivo imaging of cellular proliferation in colorectal cancer using positron emission tomography. *Gut* 2003; **52**: 1602–6.
32. Roger L, Gadea G, Roux P. Control of cell migration: a tumour suppressor function for p53? *Biol Cell* 2006; **98**: 141–52.

33. Evdokimova V, Tognon C, Ng T, Sorensen PH. Reduced proliferation and enhanced migration: two sides of the same coin? Molecular mechanisms of metastatic progression by YB-1. *Cell Cycle* 2009; **8**: 2901–6.
34. Giancotti FG. Mechanisms governing metastatic dormancy and reactivation. *Cell* 2013; **155**: 750–64.
35. Troost EGC, Vogel WV, Merkx MA, Slootweg PJ, Marres HA, Peeters WJ, et al. 18F-FLT PET does not discriminate between reactive and metastatic lymph nodes in primary head and neck cancer patients. *J Nucl Med* 2007; **48**: 726–35. doi: 10.2967/jnumed.106.037473
36. Troost EG, Bussink J, Oyen WJ, Kaanders JH. 18F-FDG and 18F-FLT do not discriminate between reactive and metastatic lymph nodes in oral cancer. *J Nucl Med* 2009; **50**: 490–1. doi: 10.2967/jnumed.108.055962
37. Umbehr MH, Müntener M, Hany T, Sulser T, Bachmann LM. The role of 11C-choline and 18F-fluorocholine positron emission tomography (PET) and PET/CT in prostate cancer: a systematic review and meta-analysis. *Eur Urol* 2013; **64**: 106–17. doi: 10.1016/j.eururo.2013.04.019
38. Yang Z, Sun Y, Zhang Y, Xue J, Wang M, Shi W, et al. Can fluorine-18 fluoroestradiol positron emission tomography–computed tomography demonstrate the heterogeneity of breast cancer in vivo? *Clin Breast Cancer* 2013; **13**: 359–63.
39. Judenhofer MS, Wehrl HF, Newport DF, Catana C, Siegel SB, Becker M, et al. Simultaneous PET-MRI: a new approach for functional and morphological imaging. *Nat Med* 2008; **14**: 459–65.
40. Choyke PL, Dwyer AJ, Knopp MV. Functional tumor imaging with dynamic contrast-enhanced magnetic resonance imaging. *J Magn Reson Imaging* 2003; **17**: 509–20.
41. Metz S, Ganter C, Lorenzen S, van Marwick S, Herrmann K, Lordick F, et al. Phenotyping of tumor biology in patients by multimodality multiparametric imaging: relationship of microcirculation, alphavbeta3 expression, and glucose metabolism. *J Nucl Med* 2010; **51**: 1691–8.
42. Glaus C, Rossin R, Welch MJ, Bao G. In vivo evaluation of (64)Cu-labeled magnetic nanoparticles as a dual-modality PET/MR imaging agent. *Bioconjug Chem* 2010; **21**: 715–22.
43. Fraioli F, Punwani S. Clinical and research applications of simultaneous positron emission tomography and MRI. *Br J Radiol* 2014; **87**: 20130464. doi: 10.1259/bjr.20130464
44. Langer DL, van der Kwast TH, Evans AJ, Trachtenberg J, Wilson BC, Haider MA. Prostate cancer detection with multi-parametric MRI: logistic regression analysis of quantitative T2, diffusion-weighted imaging, and dynamic contrast-enhanced MRI. *J Magn Reson Imaging* 2009; **30**: 327–34.
45. Panebianco V, Barchetti F, Sciarra A, Musio D, Forte V, Gentile V, et al. Prostate cancer recurrence after radical prostatectomy: the role of 3-T diffusion imaging in multi-parametric magnetic resonance imaging. *Eur Radiol* 2013; **23**: 1745–52.
46. Reiner CS, Stolzmann P, Husmann L, Burger IA, Hüllner MW, Schaefer NG, et al. Protocol requirements and diagnostic value of PET/MR imaging for liver metastasis detection. *Eur J Nucl Med Mol Imaging* 2014; **41**: 649–58. doi: 10.1007/s00259-013-2654-x
47. Antoch G, Bockisch A. Combined PET/MRI: a new dimension in whole-body oncology imaging? *Eur J Nucl Med Mol Imaging* 2009; **36**(Suppl. 1): S113–20. doi: 10.1007/s00259-008-0951-6
48. Wiesmüller M, Quick HH, Navalpakkam B, Lell MM, Uder M, Ritt P, et al. Comparison of lesion detection and quantitation of tracer uptake between PET from a simultaneously acquiring whole-body PET/MR hybrid scanner and PET from PET/CT. *Eur J Nucl Med Mol Imaging* 2013; **40**: 12–21. doi: 10.1007/s00259-012-2249-y
49. Chandarana H, Heacock L, Rakheja R, DeMello LR, Bonavita J, Block TK, et al. Pulmonary nodules in patients with primary malignancy: comparison of hybrid PET/MR and PET/CT imaging. *Radiology* 2013; **268**: 874–81. doi: 10.1148/radiol.13130620
50. Ohno Y, Koyama H, Yoshikawa T, Matsumoto K, Aoyama N, Onishi Y, et al. Diffusion-weighted MRI versus 18F-FDG PET/CT: performance as predictors of tumor treatment response and patient survival in patients with non-small cell lung cancer receiving chemoradiotherapy. *AJR Am J Roentgenol* 2012; **198**: 75–82.
51. Walker-Samuel S, Ramasawmy R, Torrealdea F, Rega M, Rajkumar V, Johnson SP, et al. In vivo imaging of glucose uptake and metabolism in tumors. *Nat Med* 2013; **19**: 1067–72.
52. Golman K. Molecular imaging using hyperpolarized 13C. *Br J Radiol* 2003; 76(Suppl. 2): S118–27.
53. Brindle KM, Bohndiek SE, Gallagher FA, Kettunen MI. Tumor imaging using hyperpolarized 13C magnetic resonance spectroscopy. *Magn Reson Med* 2011; **66**: 505–19.
54. Day SE, Kettunen MI, Gallagher FA, Hu DE, Lerche M, Wolber J, et al. Detecting tumor response to treatment using hyperpolarized 13C magnetic resonance imaging and spectroscopy. *Nat Med* 2007; **13**: 1382–7.
55. Nelson SJ, Kurhanewicz J, Vigneron DB, Larson PE, Harzstark AL, Ferrone M, et al. Metabolic imaging of patients with prostate cancer using hyperpolarized [1-^{13}C]pyruvate. *Sci Transl Med* 2013; **5**: 198ra108. doi: 10.1126/scitranslmed.3006070
56. Chaumeil MM, Ozawa T, Park I, Scott K, James CD, Nelson SJ, et al. Hyperpolarized 13C MR spectroscopic imaging can be used to monitor Everolimus treatment in vivo in an orthotopic rodent model of glioblastoma. *Neuroimage* 2012; **59**: 193–201.
57. Dafni H, Larson PE, Hu S, Yoshihara HA, Ward CS, Venkatesh HS, et al. Hyperpolarized 13C spectroscopic imaging informs on hypoxia-inducible factor-1 and myc activity downstream of platelet-derived growth factor receptor. *Cancer Res* 2010; **70**: 7400–10.
58. Hu S, Balakrishnan A, Bok RA, Anderton B, Larson PE, Nelson SJ, et al. 13C-pyruvate imaging reveals alterations in glycolysis that precede c-Myc-induced tumor formation and regression. *Cell Metab* 2011; **14**: 131–42. doi: 10.1016/j.cmet.2011.04.012
59. Wolfer A, Ramaswamy S. MYC and metastasis. *Cancer Res* 2011; **71**: 2034–7.
60. Berry CC, Curtis ASG. Functionalisation of magnetic nanoparticles for applications in biomedicine. *J Phys D: Appl Phys* 2003; **36**: R198–206.
61. Farokhzad OC, Langer R. Impact of nanotechnology on drug delivery. *ACS Nano* 2009; **3**: 16–20.
62. Sundstrøm T, Daphu I, Wendelbo I, Hodneland E, Lundervold A, Immervoll H, et al. Automated tracking of nanoparticle-labeled melanoma cells improves the predictive power of a brain metastasis model. *Cancer Res* 2013; **73**: 2445–56.
63. Weinstein JS, Varallyay CG, Dosa E, Gahramanov S, Hamilton B, Rooney WD, et al. Superparamagnetic iron oxide nanoparticles: diagnostic magnetic resonance imaging and potential therapeutic applications in neurooncology and central nervous system inflammatory pathologies, a review. *J Cereb Blood Flow Metab* 2010; **30**: 15–35.
64. Sarikaya I, Povoski SP, Al-Saif OH, Kocak E, Bloomston M, Marsh S, et al. Combined use of preoperative 18F FDG-PET imaging and intraoperative gamma probe detection for accurate assessment of tumor recurrence

in patients with colorectal cancer. *World J Surg Oncol* 2007; **5**: 80.
65. Epenetos AA, Kosmas C. Monoclonal antibodies for imaging and therapy. *Br J Cancer* 1989; **59**: 152–5.
66. Nieroda CA, Mojzisik C, Sardi A, Ferrara PJ, Hinkle G, Thurston MO, et al. Radioimmunoguided surgery in primary colon cancer. *Cancer Detect Prev* 1990; **14**: 651–6.
67. Nieroda CA, Mojzisik C, Hinkle G, Thurston MO, Martin EW. Radioimmunoguided surgery (RIGS) in recurrent colorectal cancer. *Cancer Detect Prev* 1991; **15**: 225–9.
68. Terwisscha van Scheltinga AG, van Dam GM, Nagengast WB, Ntziachristos V, Hollema H, Herek JL, et al. Intraoperative near-infrared fluorescence tumor imaging with vascular endothelial growth factor and human epidermal growth factor receptor 2 targeting antibodies. *J Nucl Med* 2011; **52**: 1778–85.
69. Van Dam GM, Themelis G, Crane LM, Harlaar NJ, Pleijhuis RG, Kelder W, et al. Intraoperative tumor-specific fluorescence imaging in ovarian cancer by folate receptor-α targeting: first in-human results. *Nat Med* 2011; **17**: 1315–19.
70. Kaplan RN, Rafii S, Lyden D. Preparing the "soil": the premetastatic niche. *Cancer Res* 2006; **66**: 11089–93.
71. Kaplan RN, Riba RD, Zacharoulis S, Bramley AH, Vincent L, Costa C, et al. VEGFR1-positive haematopoietic bone marrow progenitors initiate the pre-metastatic niche. *Nature* 2005; **438**: 820–7. doi: 10.1038/nature04186
72. Shokeen M, Zheleznyak A, Wilson JM, Jiang M, Liu R, Ferdani R, et al. Molecular imaging of very late antigen-4 (α4β1 integrin) in the premetastatic niche. *J Nucl Med* 2012; **53**: 779–86. doi: 10.2967/jnumed.111.100073
73. Daldrup-Link H, Coussens LM. MR imaging of tumor-associated macrophages. *Oncoimmunology* 2012; **1**: 507–9.
74. Lohela M, Bry M, Tammela T, Alitalo K. VEGFs and receptors involved in angiogenesis versus lymphangiogenesis. *Curr Opin Cell Biol* 2009; **21**: 154–65.
75. Obeid E, Nanda R, Fu YX, Olopade OI. The role of tumor-associated macrophages in breast cancer progression (review). *Int J Oncol* 2013; **43**: 5–12.
76. Pollard JW. Macrophages define the invasive microenvironment in breast cancer. *J Leukoc Biol* 2008; **84**: 623–30.
77. Tartour E, Pere H, Maillere B, Terme M, Merillon N, Taieb J, et al. Angiogenesis and immunity: a bidirectional link potentially relevant for the monitoring of antiangiogenic therapy and the development of novel therapeutic combination with immunotherapy. *Cancer Metastasis Rev* 2011; **30**: 83–95.
78. Miles DW, Chan A, Dirix LY, Cortés J, Pivot X, Tomczak P, et al. Phase III study of bevacizumab plus docetaxel compared with placebo plus docetaxel for the first-line treatment of human epidermal growth factor receptor 2-negative metastatic breast cancer. *J Clin Oncol* 2010; **28**: 3239–47.
79. Saltz LB, Clarke S, Díaz-Rubio E, Scheithauer W, Figer A, Wong R, et al. Bevacizumab in combination with oxaliplatin-based chemotherapy as first-line therapy in metastatic colorectal cancer: a randomized phase III study. *J Clin Oncol* 2008; **26**: 2013–19. doi: 10.1200/JCO.2007.14.9930
80. Burger RA, Sill MW, Monk BJ, Greer BE, Sorosky JI. Phase II trial of bevacizumab in persistent or recurrent epithelial ovarian cancer or primary peritoneal cancer: a Gynecologic Oncology Group Study. *J Clin Oncol* 2007; **25**: 5165–71.
81. Motzer RJ, Hutson TE, Tomczak P, Michaelson MD, Bukowski RM, Rixe O, et al. Sunitinib versus interferon alfa in metastatic renal-cell carcinoma. *N Engl J Med* 2007; **356**: 115–24. doi: 10.1056/NEJMoa065044
82. Llovet JM, Ricci S, Mazzaferro V, Hilgard P, Gane E, Blanc JF, et al. Sorafenib in advanced hepatocellular carcinoma. *N Engl J Med* 2008; **359**: 378–90.
83. Hirashima Y, Yamada Y, Tateishi U, Kato K, Miyake M, Horita Y, et al. Pharmacokinetic parameters from 3-Tesla DCE-MRI as surrogate biomarkers of antitumor effects of bevacizumab plus FOLFIRI in colorectal cancer with liver metastasis. *Int J Cancer* 2012; **130**: 2359–65.
84. Kelly RJ, Rajan A, Force J, Lopez-Chavez A, Keen C, Cao L, et al. Evaluation of KRAS mutations, angiogenic biomarkers, and DCE-MRI in patients with advanced non-small-cell lung cancer receiving sorafenib. *Clin Cancer Res* 2011; **17**: 1190–9. doi: 10.1158/1078-0432.CCR-10-2331
85. Barrera P, van der Laken CJ, Boerman OC, Oyen WJ, van de Ven MT, van Lent PL, et al. Radiolabelled interleukin-1 receptor antagonist for detection of synovitis in patients with rheumatoid arthritis. *Rheumatology* 2000; **39**: 870–4.
86. Barrera P, Oyen WJ, Boerman OC, van Riel PL. Scintigraphic detection of tumour necrosis factor in patients with rheumatoid arthritis. *Ann Rheum Dis* 2003; **62**: 825–8.
87. Hiratsuka S, Ishibashi S, Tomita T, Watanabe A, Akashi-Takamura S, Murakami M, et al. Primary tumours modulate innate immune signalling to create pre-metastatic vascular hyperpermeability foci. *Nat Commun* 2013; **4**: 1853.
88. Kiessling F, Farhan N, Lichy MP, Vosseler S, Heilmann M, Krix M, et al. Dynamic contrast-enhanced magnetic resonance imaging rapidly indicates vessel regression in human squamous cell carcinomas grown in nude mice caused by VEGF receptor 2 blockade with DC101. *Neoplasia* 2004; **6**: 213–23.
89. Ehling J, Lammers T, Kiessling F. Non-invasive imaging for studying anti-angiogenic therapy effects. *Thromb Haemost* 2013; **109**: 375–90. doi: 10.1160/TH12-10-0721
90. Rafii S, Lyden D. S100 chemokines mediate bookmarking of premetastatic niches. *Nat Cell Biol* 2006; **8**: 1321–3.
91. Weissleder R, Pittet MJ. Imaging in the era of molecular oncology. *Nature* 2008; **452**: 580–9.
92. Soekmadji C, Russell PJ, Nelson CC. Exosomes in prostate cancer: putting together the pieces of a puzzle. *Cancers (Basel)* 2013; **5**: 1522–44.
93. Lorentzen E, Conti E. The exosome and the proteasome: nano-compartments for degradation. *Cell* 2006; **125**: 651–4. doi: 10.1016/j.cell.2006.05.002
94. Makino DL, Halbach F, Conti E. The RNA exosome and proteasome: common principles of degradation control. *Nat Rev Mol Cell Biol* 2013; **14**: 654–60.
95. Park JE, Tan HS, Datta A, Lai RC, Zhang H, Meng W, et al. Hypoxic tumor cell modulates its microenvironment to enhance angiogenic and metastatic potential by secretion of proteins and exosomes. *Mol Cell Proteomics* 2010; **9**: 1085–99. doi: 10.1074/mcp.M900381-MCP200
96. Peinado H, Alečković M, Lavotshkin S, Matei I, Costa-Silva B, Moreno-Bueno G, et al. Melanoma exosomes educate bone marrow progenitor cells toward a pro-metastatic phenotype through MET. *Nat Med* 2012; **18**: 883–91.
97. Xiao D, Ohlendorf J, Chen Y, Taylor DD, Rai SN, Waigel S, et al. Identifying mRNA, microRNA and protein profiles of melanoma exosomes. *PLoS One* 2012; **7**: e46874.
98. Rana S, Malinowska K, Zöller M. Exosomal tumor microRNA modulates premetastatic organ cells. *Neoplasia* 2013; **15**: 281–95.
99. Kahlert C, Kalluri R. Exosomes in tumor microenvironment influence cancer progression and metastasis. *J Mol Med (Berl)* 2013; **91**: 431–7.
100. Suetsugu A, Honma K, Saji S, Moriwaki H, Ochiya T, Hoffman RM. Imaging exosome transfer from breast cancer cells to stroma at metastatic sites in orthotopic

nude-mouse models. *Adv Drug Deliv Rev* 2013; **65**: 383–90. doi: 10.1016/j.addr.2012.08.007

101. Logozzi M, De Milito A, Lugini L, Borghi M, Calabrò L, Spada M, et al. High levels of exosomes expressing CD63 and caveolin-1 in plasma of melanoma patients. *PLoS One* 2009; **4**: e5219.
102. Bergmann C, Strauss L, Wieckowski E, Czystowska M, Albers A, Wang Y, et al. Tumor-derived microvesicles in sera of patients with head and neck cancer and their role in tumor progression. *Head Neck* 2009; **31**: 371–80.
103. Kucharzewska P, Christianson HC, Welch JE, Svensson KJ, Fredlund E, Ringnér M, et al. Exosomes reflect the hypoxic status of glioma cells and mediate hypoxia-dependent activation of vascular cells during tumor development. *Proc Natl Acad Sci U S A* 2013; **110**: 7312–17.
104. Gabriel K, Ingram A, Austin R, Kapoor A, Tang D, Majeed F, et al. Regulation of the tumor suppressor PTEN through exosomes: a diagnostic potential for prostate cancer. *PLoS One* 2013; **8**: e70047. doi: 10.1371/journal.pone.0070047
105. Camacho L, Guerrero P, Marchetti D. MicroRNA and protein profiling of brain metastasis competent cell-derived exosomes. *PLoS One* 2013; **8**: e73790. doi: 10.1371/journal.pone.0073790
106. Ji H, Greening DW, Barnes TW, Lim JW, Tauro BJ, Rai A, et al. Proteome profiling of exosomes derived from human primary and metastatic colorectal cancer cells reveal differential expression of key metastatic factors and signal transduction components. *Proteomics* 2013; **13**: 1672–86.
107. Matusiak N, van Waarde A, Bischoff R, Oltenfreiter R, van de Wiele C, Dierckx RA, et al. Probes for non-invasive matrix metalloproteinase-targeted imaging with PET and SPECT. *Curr Pharm Des* 2013; **19**: 4647–72.
108. Hylton NM, Blume JD, Bernreuter WK, Pisano ED, Rosen MA, Morris EA, et al. Locally advanced breast cancer: MR imaging for prediction of response to neoadjuvant chemotherapy—results from ACRIN 6657/I-SPY TRIAL. *Radiology* 2012; **263**: 663–72.
109. Barker AD, Sigman CC, Kelloff GJ, Hylton NM, Berry DA, Esserman LJ. I-SPY 2: an adaptive breast cancer trial design in the setting of neoadjuvant chemotherapy. *Clin Pharmacol Ther* 2009; **86**: 97–100. doi: 10.1038/clpt.2009.68
110. Hylton N, Partridge S, Rosen M, Kim E, L'Heureux D, Esseman L. OT2-03-06: ACRIN 6698 MR Imaging Biomarkers for Assessment of Breast Cancer Response to Neoadjuvant Chemotherapy: A Sub-Study of the I-SPY 2 TRIAL (Investigation of Serial Studies To Predict Your Therapeutic Response with Imaging And moLecular Analysis). *Cancer Res* 2012; **71**(Suppl.).
111. Teschendorff AE, Miremadi A, Pinder SE, Ellis IO, Caldas C. An immune response gene expression module identifies a good prognosis subtype in estrogen receptor negative breast cancer. *Genome Biol* 2007; **8**: R157.
112. Ignatiadis M, Singhal SK, Desmedt C, Haibe-Kains B, Criscitiello C, Andre F, et al. Gene modules and response to neoadjuvant chemotherapy in breast cancer subtypes: a pooled analysis. *J Clin Oncol* 2012; **30**: 1996–2004. doi: 10.1200/JCO.2011.39.5624
113. Lee JD, Yun M, Lee JM, Choi Y, Choi YH, Kim JS, et al. Analysis of gene expression profiles of hepatocellular carcinomas with regard to 18F-fluorodeoxyglucose uptake pattern on positron emission tomography. *Eur J Nucl Med Mol Imaging* 2004; **31**: 1621–30.
114. Ignatius MS, Chen E, Elpek NM, Fuller AZ, Tenente IM, Clagg R, et al. In vivo imaging of tumor-propagating cells, regional tumor heterogeneity, and dynamic cell movements in embryonal rhabdomyosarcoma. *Cancer Cell* 2012; **21**: 680–93.
115. Karn T, Pusztai L, Holtrich U, Iwamoto T, Shiang CY, Schmidt M, et al. Homogeneous datasets of triple negative breast cancers enable the identification of novel prognostic and predictive signatures. *PLoS One* 2011; **6**: e28403.
116. Segal E, Sirlin CB, Ooi C, Adler AS, Gollub J, Chen X, et al. Decoding global gene expression programs in liver cancer by noninvasive imaging. *Nat Biotechnol* 2007; **25**: 675–80. doi: 10.1038/nbt1306
117. Rutman AM, Kuo MD. Radiogenomics: creating a link between molecular diagnostics and diagnostic imaging. *Eur J Radiol* 2009; **70**: 232–41.
118. Greenman C, Stephens P, Smith R, Dalgliesh GL, Hunter C, Bignell G, et al. Patterns of somatic mutation in human cancer genomes. *Nature* 2007; **446**: 153–8.
119. Koboldt DC, Fulton RS, McLellan MD, Schmidt H, Kalicki-Veizer J, McMichael JF, et al. Comprehensive molecular portraits of human breast tumours. *Nature* 2012; **490**: 61–70.
120. Nik-Zainal S, Van Loo P, Wedge DC, Alexandrov LB, Greenman CD, Lau KW, et al. The life history of 21 breast cancers. *Cell* 2012; **149**: 994–1007.
121. Arcila ME, Chaft JE, Nafa K, Roy-Chowdhuri S, Lau C, Zaidinski M, et al. Prevalence, clinicopathologic associations, and molecular spectrum of ERBB2 (HER2) tyrosine kinase mutations in lung adenocarcinomas. *Clin Cancer Res* 2012; **18**: 4910–18.
122. Perera SA, Li D, Shimamura T, Raso MG, Ji H, Chen L, et al. HER2YVMA drives rapid development of adenosquamous lung tumors in mice that are sensitive to BIBW2992 and rapamycin combination therapy. *Proc Natl Acad Sci U S A* 2009; **106**: 474–9. doi: 10.1073/pnas.0808930106
123. Dijkers EC, Oude Munnink TH, Kosterink JG, Brouwers AH, Jager PL, de Jong JR, et al. Biodistribution of 89Zr-trastuzumab and PET imaging of HER2-positive lesions in patients with metastatic breast cancer. *Clin Pharmacol Ther* 2010; **87**: 586–92. doi: 10.1038/clpt.2010.12
124. Tamura K, Kurihara H, Yonemori K, Tsuda H, Suzuki J, Kono Y, et al. 64Cu-DOTA-trastuzumab PET imaging in patients with HER2-positive breast cancer. *J Nucl Med* 2013; **54**: 1869–75. doi: 10.2967/jnumed.112.118612
125. Walsh AJ, Cook RS, Manning HC, Hicks DJ, Lafontant A, Arteaga CL, et al. Optical metabolic imaging identifies glycolytic levels, subtypes, and early-treatment response in breast cancer. *Cancer Res* 2013; **73**: 6164–74.
126. Stransky N, Egloff AM, Tward AD, Kostic AD, Cibulskis K, Sivachenko A, et al. The mutational landscape of head and neck squamous cell carcinoma. *Science* 2011; **333**: 1157–60. doi: 10.1126/science.1208130
127. Hofree M, Shen JP, Carter H, Gross A, Ideker T. Network-based stratification of tumor mutations. *Nat Methods* 2013; **10**: 1108–15.
128. Diaz LA, Williams RT, Wu J, Kinde I, Hecht JR, Berlin J, et al. The molecular evolution of acquired resistance to targeted EGFR blockade in colorectal cancers. *Nature* 2012; **486**: 537–40. doi: 10.1038/nature11219
129. Miles KA, Ganeshan B, Rodriguez-Justo M, Goh VJ, Ziauddin Z, Engledow A, et al. Multifunctional imaging signature for V-KI-RAS2 Kirsten rat sarcoma viral oncogene homolog (KRAS) mutations in colorectal cancer. *J Nucl Med* 2014; **55**: 386–91. doi: 10.2967/jnumed.113.120485

Breast Cancer RESEARCH

REVIEW

Genomic scars as biomarkers of homologous recombination deficiency and drug response in breast and ovarian cancers

Johnathan A Watkins, Sheeba Irshad, Anita Grigoriadis* and Andrew NJ Tutt

Abstract

Poly (ADP-ribose) polymerase (PARP) inhibitors and platinum-based chemotherapies have been found to be particularly effective in tumors that harbor deleterious germline or somatic mutations in the *BRCA1* or *BRCA2* genes, the products of which contribute to the conservative homologous recombination repair of DNA double-strand breaks. Nonetheless, several setbacks in clinical trial settings have highlighted some of the issues surrounding the investigation of PARP inhibitors, especially the identification of patients who stand to benefit from such drugs. One potential approach to finding this patient subpopulation is to examine the tumor DNA for evidence of a homologous recombination defect. However, although the genomes of many breast and ovarian cancers are replete with aberrations, the presence of numerous factors able to shape the genomic landscape means that only some of the observed DNA abnormalities are the outcome of a cancer cell's inability to faithfully repair DNA double-strand breaks. Consequently, recently developed methods for comprehensively capturing the diverse ways in which homologous recombination deficiencies may arise beyond *BRCA1/2* mutation have used DNA microarray and sequencing data to account for potentially confounding features in the genome. Scores capturing telomeric allelic imbalance, loss of heterozygosity (LOH) and large scale transition score, as well as the total number of coding mutations are measures that summarize the total burden of certain forms of genomic abnormality. By contrast, other studies have comprehensively catalogued different types of mutational pattern and their relative contributions to a given tumor sample. Although at least one study to explore the use of the LOH scar in a prospective clinical trial of a PARP inhibitor in ovarian cancer is under way, limitations that result in a relatively low positive predictive value for these biomarkers remain. Tumors whose genome has undergone one or more events that restore high-fidelity homologous recombination are likely to be misclassified as double-strand break repair-deficient and thereby sensitive to PARP inhibitors and DNA damaging chemotherapies as a result of prior repair deficiency and its genomic scarring. Therefore, we propose that integration of a genomic scar-based biomarker with a marker of resistance in a high genomic scarring burden context may improve the performance of any companion diagnostic for PARP inhibitors.

Introduction

Cancer is a disease of the genome. In certain types of cancers, a handful of mutations drive and accompany carcinogenesis; in others, tumor growth unfolds in the context of widespread genomic turmoil [1]. The latter scenario is the consequence of the tumor securing a mutator phenotype in which one or more of the mechanisms that preserve genomic integrity are undermined. The resultant increase in the rate of spontaneous change to the genome, a phenomenon termed 'genomic instability', furnishes the genetic variation that is grist to the mill of natural selection [2]. Immune responses, anti-growth signaling, and competition for space and resources all contribute to the selection of cancer cell clones with the fitness advantage to proliferate and dominate the tumor landscape [3].

Unearthing the information buried within cancer genomes will have two consequences for the management of cancer in the clinic. On the one hand, identification of the genetic abnormalities that direct the acquisition of malignant features other than the mutator phenotype may

* Correspondence: anita.grigoriadis@kcl.ac.uk
Breakthrough Breast Cancer Research Unit, Guy's Hospital, Kings College London, Kings Health Partners AHSC, 3rd Floor, Bermondsey Wing Guy's Hospital, Great Maze Pond, London SE1 9RT, UK

enable the selection of therapies that disrupt the relevant oncogenic pathway. On the other hand, tracing scars in a patient's tumor genome back to particular drivers of the mutator phenotype that caused them will enable the selection of treatments that target these origins. In this review, we will focus on the latter application and, in particular, on how the genomic scars that are carved out by a deficiency in a DNA repair process known as homologous recombination (HR) may be measured and used as biomarkers or companion diagnostics for response to platinum-based chemotherapies and synthetic lethal agents such as the poly (ADP-ribose) polymerase (PARP) inhibitors.

The need for a companion diagnostic based on homologous recombination deficiency

Familial mutations in one copy of either the *BRCA1* or *BRCA2* gene predispose patients to female breast (85% lifetime risk), ovarian (10% to 40%), male breast, pancreatic, or prostate cancer [4]. The majority of breast tumors that develop in carriers of *BRCA1* mutations - the products of which are involved in HR - are triple-negative breast cancers (TNBCs) overlapping with the gene expression-defined subtype of breast cancer known as 'basal-like breast cancer', whereas *BRCA2* mutation-associated breast cancers have a less restricted immunohistochemical phenotype [5-7]. As a result of the BRCA1/2-related deficiency in HR, precancerous cells within at-risk organs are unable to reliably repair DNA double-strand breaks [8], resulting in genomic instability that eventually leads to cancer. These tumors are intrinsically sensitive to DNA damage response inhibitors, such as the PARP inhibitors, whose putative efficacy leverages upon a synthetic lethal effect [9] in which cell death results from mutations in two or more genes but not in each gene individually (reviewed in [10]). This phenomenon is well illustrated by PARP inhibition in BRCA1/2-deficient cells whereby PARP-dependent base excision repair and replication fork maintenance functions become critical to cell viability.

Elegant preclinical work by Bryant and colleagues [11] and Farmer and colleagues [12] demonstrating the increased sensitivity of BRCA1/2-deficient cells to PARP inhibition and the subsequent resistance to PARP inhibition on restoration of BRCA2 functionality provided the impetus for the use of PARP inhibitors in patients with BRCA1/2-associated cancers and subsequently in sporadic cancers that display 'BRCAness' (that is, have defective HR without germline *BRCA1/2* mutations) [13]. BRCAness can be explained by epigenetic silencing of *BRCA1/2* or the inactivation of several other HR-associated genes such as *PTEN*, *ATM*, *ATR*, *AURA*, *PALB2*, *BRIP*, and *RAD51* and the *FANC* family of genes [14-18]. These have been associated with several malignancies, including TNBC and sporadic high-grade serous ovarian cancer (HGSC).

Despite the early success of PARP inhibitors in demonstrating efficacy and a favorable toxicity profile in the treatment of previously heavily treated hereditary BRCA1/2-related breast and ovarian cancers [19-22], trials that expanded to include patients without *BRCA1/2* mutations were less successful. Clinical features considered surrogates for BRCAness within these trials (for example, TNBC or HGSC) might not have been sufficiently specific in predicting response to PARP inhibitors. Indeed, 50% of HGSCs are thought to be HR-deficient [23].

Recent recognition that iniparib (also known as BSI-201 or SAR240550) from BiPar/Sanofi (formerly Sanofi-Aventis, Paris, France) was erroneously considered a PARP inhibitor during its clinical evaluation within a phase III trial [24,25], and new phase I and II data reporting on the anti-tumor activity of various potent PARP inhibitors such as niraparib (MK4827) [26], BMN673 [27], and rucaparib [28] in *BRCA1/2*-mutated tumors and sporadic HGSC, non-small-cell lung cancer, prostate cancer, and pancreatic cancer, have renewed enthusiasm for PARP inhibitor drug development. Therefore, the challenge remains to develop an efficient and coordinated strategy to identify effective biomarkers such that the patients who are more likely to respond to drugs like the PARP inhibitors may be identified. The complexity of the crosstalk between DNA repair pathways suggests that assays that detect the status of multiple DNA repair pathways could prove critical for PARP inhibitor biomarker development.

Genomic aberrations in cancer

The majority of TNBCs and HGSCs exhibit a high burden of genomic aberration. High-throughput genomic technology such as next-generation sequencing and DNA microarrays have made it possible to construct comprehensive catalogues that illustrate the complexity of such changes in those cancers. Commonly used classifications of genomic aberrations address the size and type of variation in DNA sequence (Figure 1). Mutations encompass substitutions, insertions, and deletions (collectively termed 'indels') that affect one or a few nucleotide bases. Depending on the location of the mutation, either the amount (mutation in a regulatory region) or the sequence (non-synonymous coding mutation) of a gene product may be affected; in either case, the impact on a protein's function is the primary interest. Conversely, the significance of mutations irrespective of their genomic location lies with the processes by which they were generated [29,30]. Structural aberrations are operationally defined as acquired changes that exceed 1 Kbp in size. In general, two fundamental types are discernible: (a) regional copy number aberrations (CNAs), which are delineated by a gain or loss in the number of copies of a defined, subchromosomal region of DNA; and (b) structural rearrangements, which are defined by a change to the precise location or orientation of a given sequence of DNA.

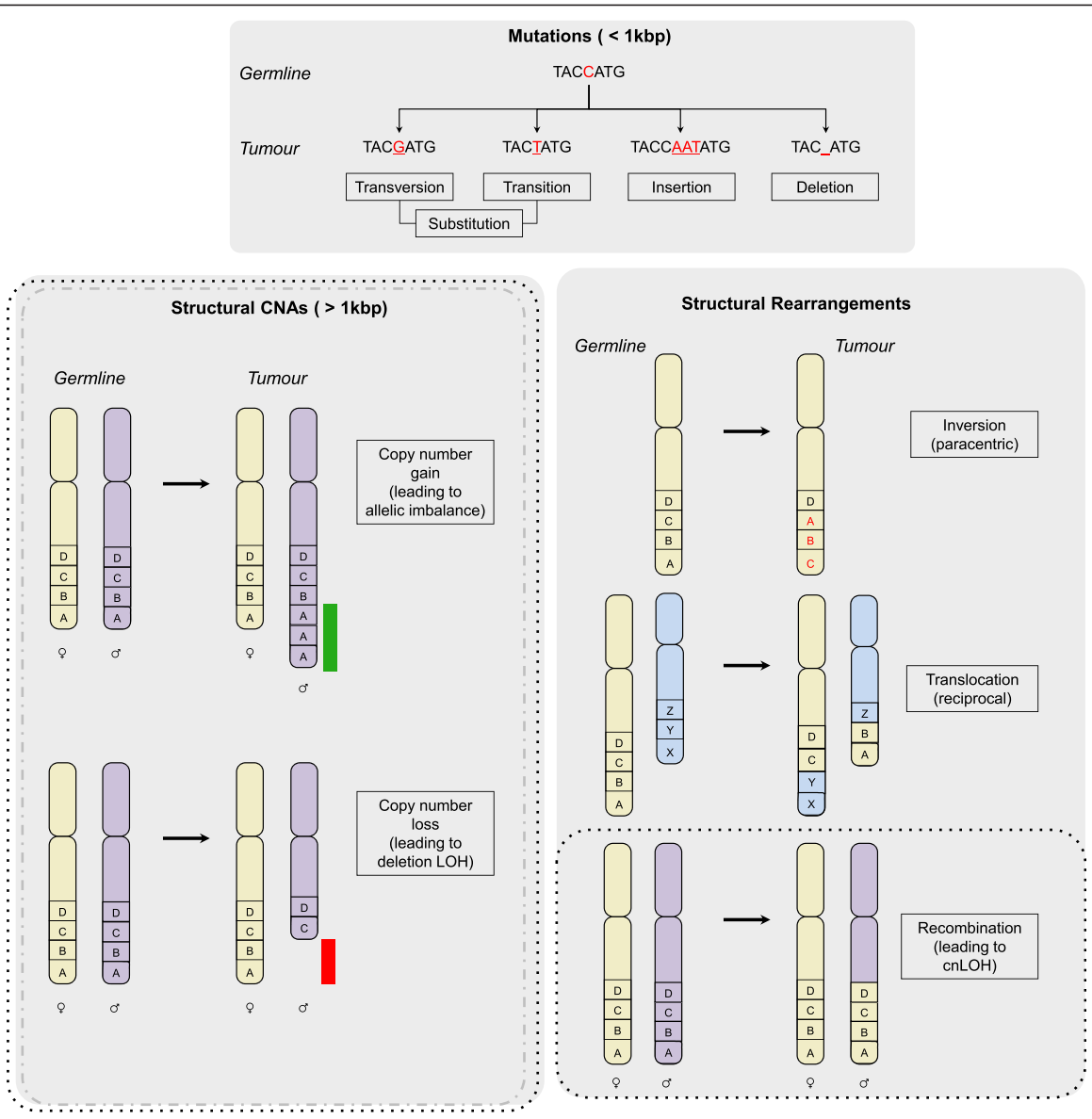

Figure 1 Genomic aberrations in cancer. Three classes of genomic aberration that develop in cancer cells are depicted: mutations of less than 1 Kbp in length (top box), structural copy number aberrations (CNAs) (bottom left box), and structural rearrangements (bottom right box). The initial state in the germline is shown followed by the corresponding change in the tumor. Mutations that affect regions of less than 1 Kbp are of three basic types: substitutions, of which there are transversions and transitions; insertions; and deletions. Insertions and deletions are often collectively termed 'indels'. Structural CNAs are typically greater than 1 Kbp in size. One of the basic types is copy number gain. The two homologous chromosomes are shown with a gain of two further copies of region A on the paternal chromosome leading to an imbalance in the allelic ratio (1:3, maternal: paternal). The gained region is highlighted by the green bar adjacent to paternal region A. Copy number loss of regions A and B on the paternal chromosome is shown with a red bar highlighting the deleted regions. Three of the commonest types of structural rearrangement are shown, with the letters A to D and X to Z depicting defined chromosomal segments. An inversion on the same chromosome results in a change to the orientation of DNA sequences on the same chromosome either paracentrically (without crossing the centromere) or pericentrically (crossing the centromere). The inverted sequences in the tumor are shown in red. Translocations can be reciprocal or non-reciprocal and typically occur between non-homologous chromosomes (the green and blue chromosomes are non-homologous). A reciprocal translocation is shown with regions A and B exchanged for regions X and Y. Recombinations typically occur between sister chromatids where they are conservative, but can occur between homologous chromosomes (the green and purple chromosomes are homologous with green being the maternal, and purple the paternal) where recombinations at a heterozygous allelic locus can lead to cnLOH. The dotted boxes indicate where these aberrations are detectable by single-nucleotide polymorphism microarrays, whereas the grey dashed line encompasses those that can also be captured by array comparative genomic hybridization (aCGH), which does not distinguish between alleles. All forms of aberration may be interrogated by using sequencing. A, adenine; C, cytosine; cnLOH, copy number-neutral loss of heterozygosity; G, guanine; LOH, loss of heterozygosity; T, thymine.

Of these, translocations (exchange of material between non-homologous regions of DNA), inversions (a change to the orientation of a defined sequence of DNA), and recombinations (most often used to express the exchange of material between homologous regions of DNA) are the most frequently described [31]. The potential outcome of this latter structural rearrangement is that of regional loss of heterozygosity (LOH), in which one of the parental copies of a heterozygous region of DNA is lost and the other retained. LOH that occurs as a result of a copy number loss is generally termed a 'deletion LOH', whereas LOH generated by an isolated recombinational event is called 'copy number-neutral LOH'. Both copy number-neutral LOH and CNAs that lead to an imbalance in the ratio of parental alleles from the normal 1:1 constitute regions of allelic imbalance. When the rate of one or more of these structural changes increases, a cell is said to exhibit 'structural chromosomal instability' [32]. CNAs and LOH can also be created by alterations in the number of whole chromosomes as a result of errors in the segregation of chromosomes during mitosis. Elevation in the incidence of such events is termed 'numerical chromosomal instability' [32].

Genomic scars as reporters of homologous recombination deficiency and drug response

A genomic scar can be defined as a genomic aberration with a known origin. Recent attempts at developing an assay that acknowledges the different means by which defects in HR may occur besides *BRCA1/2* dysfunction have centered around the measurement of such scars (Table 1) [29,33-35]. The major challenge in this endeavor has been to distinguish HR defect (HRD)-related genomic aberrations from the wide-ranging complexity inherent to cancer genomes. Indeed, the role played by BRCA1 in other DNA repair mechanisms such as mismatch repair and its role at stalled replication forks may obfuscate any HRD-related signal [36,37]. On the other hand, spontaneous, chance events and mutagen-induced changes have no definitive root in defective HR and yet the scars of these events may confound the quantification of a bona fide HRD. Furthermore, numerical chromosomal instability and one-off events such as whole-genome duplications and a newly described phenomenon known as 'chromothripsis' can all prevent the accurate measurement of HRD-related scars [32]. Chromothripsis, which is a single chromosomal shattering event followed by reconstitution of the genomic fragments, results in localized, complex rearrangements that, even if they have a basis in a targetable HR deficiency, can result in an overestimate of the gravity, and hence exploitability, of the defect [38,39]. In contrast, events that spatially overlap in such a way that only the effects of one are countable can lead to an underestimate of the extent of genomic instability [29]. In cases in which matched genomic germline data are unavailable, germline copy number variants and germline runs of homozygosity can confound CNA- and LOH-based measures of scarring, respectively.

On account of these issues, recent research has taken advantage of the allelic information and mutational context afforded by advances in single-nucleotide polymorphism (SNP) microarray and high-throughput sequencing technologies, respectively, and several measures of scarring believed to report an HRD have been developed.

Structural chromosomal instability scars from microarrays

By training a classifier on bacterial artificial chromosome and oligonucleotide array comparative genomic hybridization (aCGH) data from *BRCA1/2* germline mutation status-annotated breast cancer data sets, several studies have demonstrated the utility of genome-wide information in identifying HR-defective tumors, which they also linked to better platinum response rates [40-42]. In general, these studies found that *BRCA1* and *BRCA2* germline-mutated cancers harbored a greater number of break points and hence copy number changes. In two studies of independent TNBC cohorts, these aCGH classifiers exhibited a sensitivity of approximately 80% in defining samples with *BRCA1* mutation [40,42]. However, in comparison with newer SNP microarray technology, aCGH presents a number of limitations, which make it more difficult to discriminate between HRD-related genomic changes and the many confounding alterations that can affect the genome, leading to poorer specificity. Specifically, the information from SNP microarray platforms makes it possible to distinguish between inherited copy number changes due to normal cell contamination and acquired DNA repair defect-related changes in cancer cells, an ability that is notably absent from aCGH analyses. Moreover, as one study described below demonstrates, the capacity to estimate tumor ploidy status from SNP microarray data - again a feature absent from aCGH data - may have implications for predicting platinum treatment outcome [35].

Capitalizing on these advantages, Birkbak and colleagues [33] used SNP microarray data to test their hypothesis that the aberrant chromosomal structures formed as a result of defective HR are likely to be resolved with allelic imbalance extending from the double-strand break point to the subtelomeres of a chromosome. By scoring tumors for the frequency with which these types of genomic segment occurred, they extracted a telomeric allelic imbalance score (N_{tAi}) (Figure 2 and Table 1) [33], which ranges from 0 to 46, with 2 being the maximum permissible contribution by each chromosome. High levels of N_{tAi} were shown to predict sensitivity to platinum agents in breast cancer cell lines, HGSCs and TNBCs. Moreover, tumors with mutation, promoter methylation, or low levels of mRNA for either *BRCA1* or *BRCA2* were demonstrated to have a higher burden of N_{tAi} than tumors without *BRCA1/2* deficiency.

Table 1 Genomic scars of homologous recombination deficiency and relationships to drug response

Input	Name	Demonstrated objective(s)	Output	Data sets used (sample size)	References
Segmented allele-specific copy number from SNP microarray data	Telomeric allelic imbalance score (N_{tAi})	1. Indicate sensitivity to platinum drugs	Integer between 0 and 46 per sample	Breast cancer cell lines (10 + 24)	[33,43]
		2. Indicate BRCA1/2 dysfunction		Cisplatin-1 TNBC trial (27)	
				Cisplatin-2 TNBC trial (37)	
				TCGA HGSCs (218)	
	Homologous recombination defect (HRD) score	1. Indicate HR dysfunction	Integer from 0 upper sample	MDACC ovarian cancers (152)	[32,42,43]
		2. Indicate sensitivity to platinum drugs		UPMC ovarian cancers (152)	
				TCGA ovarian cancers (435)	
				Cancer cell lines (57)	
				Cisplatin-1 TNBC trial (27)	
				Cisplatin-2 TNBC trial (37)	
				PreECOG TNBC/BRCA1/2 trial (80)	
	Large-scale transition (LST) score	1. Indicate HR dysfunction	Integer from 0 upper sample	BLBC discovery set (65)	[35,43]
		2. Indicate sensitivity to platinum drugs		BLBC validation set (55)	
				BLBC cell lines (17)	
				Cisplatin-1 TNBC trial (27)	
				Cisplatin-2 TNBC trial (37)	
	LOH clustering	1. Indicate sensitivity to platinum drugs	Three clusters of tumors: HiA,	Boston HGSCs (47)	[34]
		2. Indicate BRCA1/2 dysfunction	HiB, and Lo	Boston TNBCs (50)	
		3. Provide prognostic information		AOCS HGSCs (85)	
				TCGA HGSCs (116)	
Single-nucleotide variant calls from exome sequencing data	Total number of somatic, synonymous, and non-synonymous coding mutations (Nmut)	1. Indicate sensitivity to platinum drugs	Integer from 0 upper sample	TCGA HGSCs (316)	[44]
		2. Indicate BRCA1/2 dysfunction			
		3. Provide prognostic information			
Mutational catalogue from whole-genome sequencing data	Mutational signature 3/Mutational signature D	Indicate BRCA1/2 dysfunction	Proportion of mutational spectrum contributed by mutational signature 3 per sample	Initial breast cancer data set (21)	[1,45]
				Larger breast cancer data set (879)	

AOCS, Australian Ovarian Cancer Study; BLBC, basal-like breast cancer; HGSC, high-grade serous ovarian cancer; HR, homologous recombination; LOH, loss of heterozygosity; MDACC, MD Anderson Cancer Center; Nmut, number of coding mutation; SNP, single-nucleotide polymorphism; TCGA, The Cancer Genome Atlas; TNBC, triple-negative breast cancer; UPMC, University of Pittsburgh Medical Center.

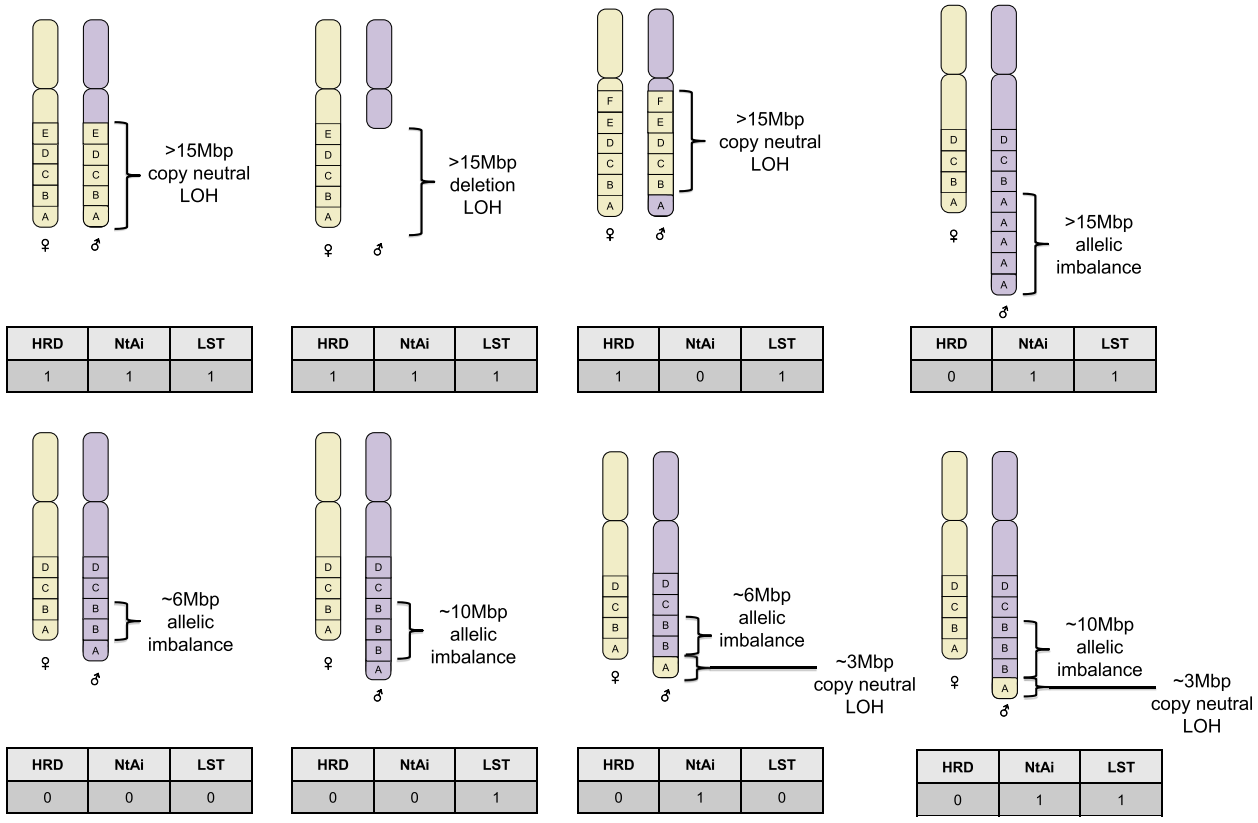

Figure 2 Scoring by genomic scars of homologous recombination deficiency and drug response. Eight examples of various forms of structural copy number aberrations and rearrangements are given, whereby each box, lettered A to F, represents a genomic segment of approximately 3 Mbp in length. Below the chromosomes, the three genomic scars - homologous recombination defect (HRD), telomeric allelic imbalance score (NtAi), and large-scale transition (LST) - are listed along with the respective integer count for the scar (0 = not seen, 1 = detected once). LOH, loss of heterozygosity.

In contrast, Wang and colleagues [34] discovered that clustering HGSCs according to significantly frequent regions of LOH produces three platinum response-linked groups of tumors: one harboring comparatively little LOH (Lo cluster) and two possessing high levels of LOH: the HiA and HiB clusters, distinguished by the presence and absence of 13q chromosomal loss and more frequent LOH on 5q and 17, respectively (Table 1). When the platinum response data available for three independent HGSC data sets were used, patients in the HiA cluster were found to have lower rates of resistance. In contrast, the rate of resistance was higher for the HiB and Lo clusters. Application of this LOH clustering approach to a high-grade breast cancer data set separated tumors into a Lo cluster comprising HER2- and hormone receptor-positive cancers and a Hi cluster comprising TNBCs and *BRCA1*-associated tumors. However, the relevance of the HiA-versus-HiB distinction to TNBC has yet to be investigated.

Leveraging on the known association between *BRCA1/2* deficiency and response to DNA damage-inducing drugs [21,43], Abkevich and colleagues [29], of Myriad Genetics Inc. (Salt Lake City, UT, USA), developed an HRD score defined as the number of subchromosomal segments (excluding chromosome 17) with LOH of a size exceeding 15 Mbp but shorter than the length of a complete chromosome (Figure 2 and Table 1). The objective of this score was to provide a comprehensive means of assessing defects in HR beyond sequencing of *BRCA1* and *BRCA2*. To evaluate the correlation between HRD score and HR deficiency, three independent HGSC cohorts along with 57 cancer cell lines were assessed for bi-allelic functional inactivation of *BRCA1*, *BRCA2*, or *RAD51C* through the integration of mutation, methylation, expression, and LOH data. The presence of bi-allelic inactivation of these genes was taken as a surrogate for HR deficiency. In all data sets, HRD score was elevated in HR-deficient samples, which stood in contrast to measures of whole chromosomal LOH and LOH of regions of less than 15 Mbp in length, suggesting that the maximum and minimum size thresholds employed were able to filter out aberrations because of numerical chromosomal instability and short non-HRD-related aberrations, respectively. Furthermore, in the phase II PrECOG 0105 study of gemcitabine and carboplatin plus iniparib (BSI-201) as neoadjuvant therapy for TNBC and BRCA1/2 mutation-associated breast cancer, 70% of patients with an HRD score of more than 9 responded compared with 20%

of patients with an HRD score of less than 10, indicating that HRD score was significantly correlated with pathologic response. This association remained significant when patients with known *BRCA1* or *BRCA2* were excluded from the analysis [44]. Besides breast and ovarian cancers, HRD scores above 9 were characteristic for HR deficiency and were also observed in esophagus, lung, and prostate tumors as well as gastric, colon, and brain cell lines, advancing the case that HRD score has general applicability to distinct cancer types.

A separate signature of chromosomal instability, termed 'large-scale transitions' (LSTs), was established by using basal-like breast cancer and cell line data sets in which samples with *BRCA1* promoter methylation or *BRCA1/2* mutation (germline or somatic) were considered BRCA1/2-inactive [35]. For this genomic scar, copy number variant regions shorter than 3 Mb are first filtered and smoothed. This is followed by a count of the number of break points that occur between regions of at least 10 Mb in length for each chromosomal arm of a sample, with the sample's LST score being the sum of these counts (Figure 2 and Table 1). After genomic ploidy was estimated on the basis of SNP-based microarray data, near-diploid tumors were classified as *BRCA1/2*-deficient if the number of LSTs exceeded 15. In near-tetraploid tumors, an LST cutoff value of 20 was used to segregate tumors into *BRCA1/2*-intact and *BRCA1/2*-deficient. The LST measure of HRD-related genomic scarring and its associated cutoff were found to significantly indicate *BRCA1/2* deficiency in an independent validation data set of basal-like breast cancers as well as basal-like breast cancer cell lines.

Recently, it has been shown that HRD, N_{tAi}, and LST are highly correlated with each other and with *BRCA1/2* deficiency (*BRCA1* promoter methylation, germline, or somatic) in a breast cancer cohort that encompassed all the molecularly defined subtypes. Among TNBCs, all three scores were associated with cisplatin sensitivity [45]. Furthermore, the arithmetic mean of the three scores was even more strongly associated with *BRCA1/2* deficiency and therapeutic response.

Sequencing-based mutational signatures

The advent of massively parallel sequencing has enabled the mutational effects of a diverse range of etiological drivers to be unraveled. By finding the total number of somatic synonymous and non-synonymous mutations (Nmut) in the exome of each ovarian tumor in a cohort of 316, Birkbak and colleagues [46] found Nmut to be higher among patients who responded well to chemotherapy (platinum agent with or without taxane) than among those who failed to respond (Table 1). Moreover, higher Nmut was observed in patients with germline or somatic *BRCA1/2* mutation. Interestingly, within the 70 ovarian tumors harboring either germline or somatic *BRCA1/2* mutation, cases that were considered chemotherapy-sensitive possessed a higher mutational burden than cases that were considered resistant, whereas in the wild-type *BRCA1/2* population, this association was not observed.

In contrast to the integer scores that Nmut and three of the SNP microarray-based scars provide, several sequence-based studies have concentrated on examining the specific type and pattern of mutations that certain genomic events leave in their wake. In the first study to use mutational context to mathematically extract signatures of mutational processes, Nik-Zainal and colleagues [47] catalogued somatically acquired mutational signatures in 21 deep-sequenced breast cancers (Table 1). These included eight TNBCs, of which five possessed germline mutation and heterozygous loss of *BRCA1*, and four non-TNBC tumors with *BRCA2* germline mutation and heterozygous loss. Interrogating the bases either side of each substitution to give a trinucleotide sequence context comprising 96 possible combinations followed by non-negative matrix factorization, the authors were able to decompose the spectrum of sequence contexts into five signatures ('signatures A-E') each believed to represent the scar of a distinct mutational process [1]. Hierarchical clustering of the relative contributions of these signatures to the mutational catalogue of each breast cancer revealed 'signature A' and 'signature D', representing a lesser and greater proportion of the total signature contribution, respectively, in *BRCA1/2*-associated tumors than in *BRCA1/2* wild-type tumors. Whereas 'signature A' exhibited enrichment for C > T conversions at XpCpG trinucleotides, 'signature D' displayed a relatively even distribution of mutations across the 96 trinucleotides. During investigation of the patterns of indels in the 21 tumors, two further hallmarks of *BRCA1*/2 mutation were ascertained. The first was the observation that the size of indels was typically greater in *BRCA1/2*-inactivated cancers. The second hallmark required the authors to examine whether the sequences flanking each indel were either short tandem repeats or short homologous sequences. *BRCA1/2*-inactivated tumors were differentiated from *BRCA1/2*-intact tumors by having a greater frequency of short homologous sequences adjoining indels. This observation is congruent with the notion of error-prone non-homologous end joining compensating for defective HR since such short homology-flanked indels would facilitate the joining of two non-homologous sequences through processes such as micro-homology single-strand annealing.

Following this seminal work, the repertoire of mutational signatures across 30 different cancer types was examined, and a further 16 substitution-based mutational signatures were identified (Table 1) [1]. The *BRCA1/2* defect-associated mutational signature D was relabeled 'signature 3' and was seen to be exclusively over-represented in breast, ovarian, and pancreatic cancers for which germline

mutations to *BRCA1/2* have been reported to elevate the risk. Among breast tumors in the study, 'signature 3' was found to be operative in 255 out of 879 cases, which exceeds the estimated 5% to 10% of breast cancers accounted for by *BRCA1/2*-mutated tumors [48], supporting the case that 'signature 3' captures the effects of HR deficiencies attributable to a variety of means of *BRCA1/2* inactivation as well as abnormalities in the function of other genes associated with HR.

The companion diagnostic challenge

The development of biomarkers that accurately and robustly predict treatment outcome is a key part of the drive toward personalized medicine. Already one prospective clinical trial is under way to establish HRD score for selecting appropriate patients with ovarian cancer for treatment with the PARP inhibitor, rucaparib (ClinicalTrials.gov ID: NCT01891344), and equivalent studies will be carried out as exploratory analyses in TNBCs or *BRCA1/2*-related breast cancers. Moreover, despite the sensitivity with which the genomic scars discussed predict inactivation of genes involved in HR, limitations exist to the application of these assays as a companion diagnostic for drugs that target HRDs. Unlike gene expression, which is liable to the influence of many confounding variables, genomic scars offer a comparatively stable readout of a tumor's lifetime DNA damage repair competency, including the impact of HR inactivation where constructed to do so. Consequently, similar to other biomarkers such as estrogen receptor testing as a companion diagnostic for hormonal therapy,

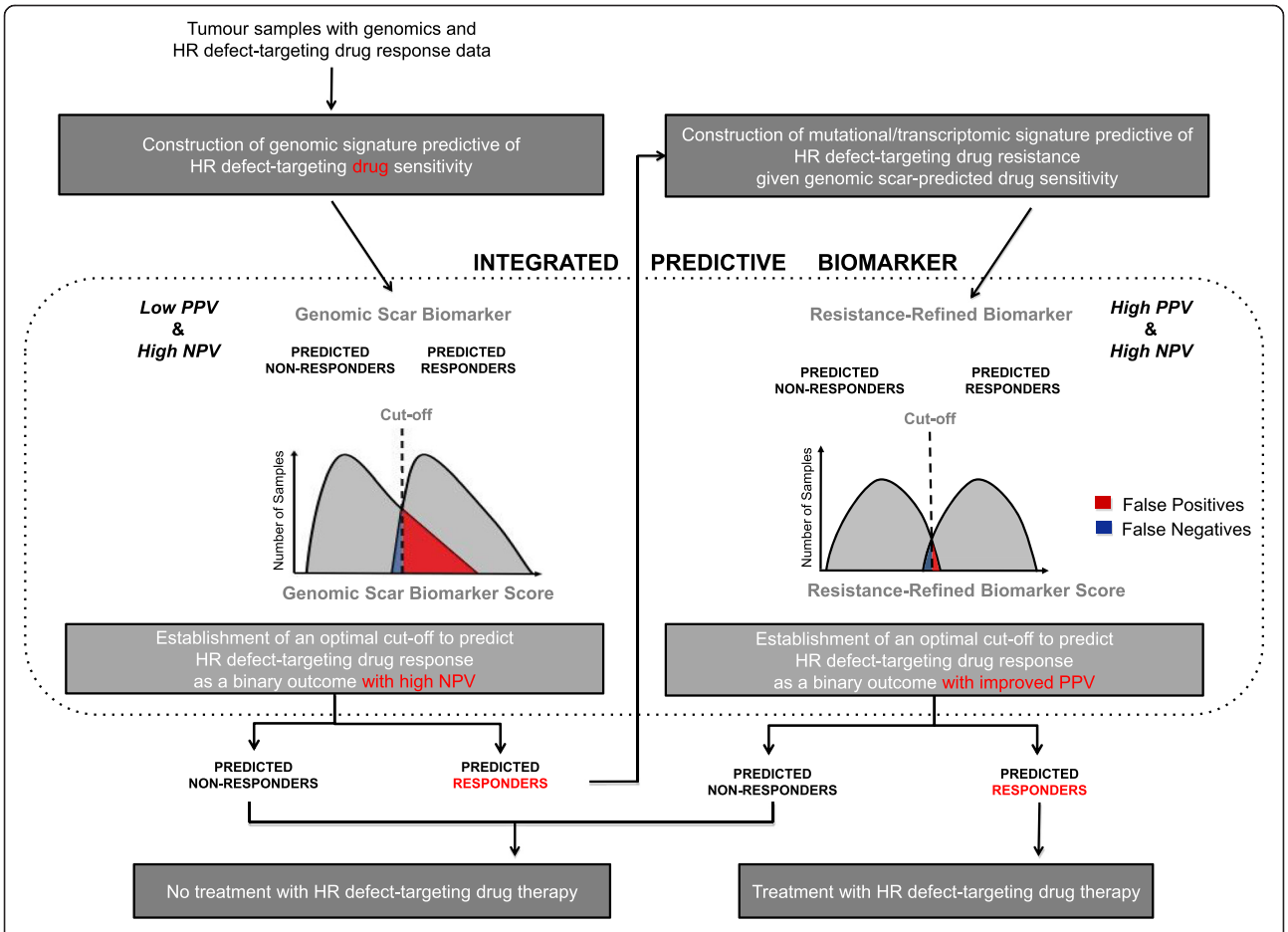

Figure 3 Workflow for the development of an integrated predictive biomarker of response to homologous recombination (HR) defect directed therapy. The workflow begins with genomics data - either sequence or single-nucleotide polymorphism microarray data - for tumor samples that have been annotated with patient response data to a given HR targeting drug therapy. After development of a genomic scar measure and a cutoff with high negative predictive value (NPV) were shown to identify non-responders but likely poor positive predictive value (PPV) due to inclusion of patients who have developed resistance (for example, 53BP1 loss) subsequent to development of the genomic scar, two groups can be identified: those predicted not to respond and those predicted to respond accepting a poor PPV. Patients in the former group should not be treated with the drug, whereas for patients in the predicted responder group, gene expression or mutation data are collected. Within the latter group, a biomarker excluding those with acquired resistance is constructed that is highly specific for response to the drug, better dichotomizing patients into those who do and those who do not benefit. By combining the genomic scar biomarker with the resistance-refined biomarker, the resultant two-step companion diagnostic should possess both high NPV and high PPV.

genomic scars are likely to prove to be high-negative predictive value (NPV) biomarkers of response to HR deficiency-targeting drugs, meaning that the great majority of patients who test negative for the biomarker will not benefit from the therapy. However, the relative stability of genomic scars is also their weakness. By chronicling the past but not documenting the present, genomic scar measures report whether or not a defect in HR has been operative at some point in tumorigenesis and not whether it remains operative at the point of treatment. A variety of mechanisms could restore HR or compensate for its loss in the aftermath of genomic scarring. Loss of *53BP1* [49] and reversion mutations to *BRCA1* and *BRCA2* [50-53] have both been demonstrated to confer resistance to platinum agents and PARP inhibitors through the restoration of HR. Pathways that operate independently of repair processes, such as drug catabolism and transporter activity, may also grant resistance [54]. To add further complexity to the issue, one study has found that upregulated activity of the c-MYC oncoprotein induces resistance to cisplatin mediated by regulation of PARP1-interacting genes [55]. Consequently, genomic scarring measures are likely to have relatively low positive predictive values (PPVs) with the consequence that a substantial number of patients who would not benefit from platinum-based agents and PARP inhibitors would be predicted to do so. Thus, although the argument for using genomic scars as a companion diagnostic may be sustainable on the basis that platinum-based agents either are the standard of care (in ovarian cancer) or have a toxicity profile at least comparable to that of standard alternatives (in breast cancer), the development of a biomarker that possesses both high NPV and PPV represents an optimal and achievable objective.

To address this, the development of a genomic scar-based predictive biomarker could be followed by the construction of a second biomarker by using only the population for which the genomic scar predicts drug efficacy (Figure 3). By looking within a genomic scar-predicted responder population, the signal from resistance mechanisms that specifically operate within a HR-deficient setting should be stronger than if the population was taken as a whole. Mutational data could reveal reversions in a suite of HR-related genes, whereas transcriptional data might uncover the elevated expression of genes that compensate for HR impairment. Coupling the high-NPV genomic scar biomarker with a high-PPV post-genomic scar biomarker into an integrated biomarker would thus capture the best of both approaches (Figure 3).

Conclusions

Although targeting DNA repair deficiencies in cancer has been a mainstay of the therapeutic oncology armamentarium for decades, this has been more through serendipity and observation of average effects in populations than by mechanistic DNA repair activity-informed design. Consequently, the approach has lacked a personalized medicine companion diagnostic strategy. Consistent with the requirement of the US Food and Drug Administration for every new drug to be accompanied to market by a biomarker that predicts its effectiveness, the rapidity with which PARP inhibitors and now genomic scars have been brought from concept to clinical trial reflects the current interest in selecting patients for whom administration of a drug that impacts the DNA damage response is predicted to be clinically beneficial. However, therapies directed at HRDs are not the only examples of therapy that could be individualized by using genomic scar-based biomarkers. Any flaw in the genomic maintenance machinery that (a) can be capitalized on therapeutically and (b) leaves an imprint in the genome that is detectable through current techniques and technologies is ripe for the development of a genomic scar to predict drug response. In compiling a list of 21 validated mutational signatures, researchers have already taken the first steps toward the goal of constructing a repertoire of integrated predictive biomarkers [1]. One example outside the context of HR deficiency is that of Alexandrov and colleagues' 'Signature 6' [1], which was found to be associated with a defect in DNA mismatch repair. Such a signature may in turn predict the effectiveness of drugs like methotrexate, which has been shown to be selectively effective in mismatch repair-deficient cancer cells [56]. The next steps therefore will require the characterization of the etiologies behind every one of these signatures and, in the case of SNP microarray-based scars, the expansion of our understanding of the interaction between the scar repertoire and the presence of other targetable deficiencies in the DNA maintenance machinery.

Note: This article is part of a series on *'Recent advances in breast cancer treatment'*, edited by Jenny Chang. Other articles in this series can be found at http://breast-cancer-research.com/series/treatment.

Abbreviations

aCGH: array comparative genomic hybridization; CNA: Copy number aberration; HGSC: High-grade serous ovarian cancer; HR: Homologous recombination; HRD: Homologous recombination defect; LOH: Loss of heterozygosity; LST: Large-scale transition; Nmut: Number of coding mutation; NPV: Negative predictive value; N_{tAi}: telomeric allelic imbalance score; PARP: Poly (ADP-ribose) polymerase; PPV: Positive predictive value; SNP: Single-nucleotide polymorphism; TNBC: Triple-negative breast cancer.

Competing interests

The authors declare that they have no competing interests.

Acknowledgments

AG, SI, and ANJT are supported by Breakthrough Breast Cancer at its Research Unit at Guy's Hospital, King's College London. This research was supported by the National Institute for Health Research (NIHR) Biomedical Research Centre at Guy's

and St Thomas' NHS Foundation Trust and King's College London. The views expressed are those of the authors and not necessarily those of the NHS, the NIHR, the Department of Health, or Breakthrough Breast Cancer.

Published: 03 Jun 2014

References

1. Alexandrov LB, Nik-Zainal S, Wedge DC, Aparicio SA, Behjati S, Biankin AV, Bignell GR, Bolli N, Borg A, Børresen-Dale AL, Boyault S, Burkhardt B, Butler AP, Caldas C, Davies HR, Desmedt C, Eils R, Eyfjörd JE, Foekens JA, Greaves M, Hosoda F, Hutter B, Ilicic T, Imbeaud S, Imielinski M, Jäger N, Jones DT, Jones D, Knappskog S, Kool M, *et al*: **Signatures of mutational processes in human cancer.** *Nature* 2013, **500:**415–421.
2. Merlo LM, Pepper JW, Reid BJ, Maley CC: **Cancer as an evolutionary and ecological process.** *Nat Rev Cancer* 2006, **6:**924–935.
3. Greaves M, Maley CC: **Clonal evolution in cancer.** *Nature* 2012, **481:**306–313.
4. Levy-Lahad E, Friedman E: **Cancer risks among BRCA1 and BRCA2 mutation carriers.** *Br J Cancer* 2007, **96:**11–15.
5. Carey L, Winer E, Viale G, Cameron D, Gianni L: **Triple-negative breast cancer: disease entity or title of convenience?** *Nat Rev Clin Oncol* 2010, **7:**683–692.
6. Mavaddat N, Barrowdale D, Andrulis IL, Domchek SM, Eccles D, Nevanlinna H, Ramus SJ, Spurdle A, Robson M, Sherman M, Mulligan AM, Couch FJ, Engel C, McGuffog L, Healey S, Sinilnikova OM, Southey MC, Terry MB, Goldgar D, O'Malley F, John EM, Janavicius R, Tihomirova L, Hansen TV, Nielsen FC, Osorio A, Stavropoulou A, Benítez J, Manoukian S, Peissel B, *et al*: **Pathology of breast and ovarian cancers among BRCA1 and BRCA2 mutation carriers: results from the Consortium of Investigators of Modifiers of BRCA1/2 (CIMBA).** *Cancer Epidemiol Biomarkers Prev* 2012, **21:**134–147.
7. Turner NC, Reis-Filho JS: **Tackling the diversity of triple-negative breast cancer.** *Clin Cancer Res* 2013, **19:**6380–6388.
8. Li ML, Greenberg RA: **Links between genome integrity and BRCA1 tumor suppression.** *Trends Biochem Sci* 2012, **37:**418–424.
9. Glendenning J, Tutt A: **PARP inhibitors - current status and the walk towards early breast cancer.** *Breast* 2011, **20**(suppl 3):S12–S19.
10. Kaelin WG Jr: **The concept of synthetic lethality in the context of anticancer therapy.** *Nat Rev Cancer* 2005, **5:**689–698.
11. Bryant HE, Schultz N, Thomas HD, Parker KM, Flower D, Lopez E, Kyle S, Meuth M, Curtin NJ, Helleday T: **Specific killing of BRCA2-deficient tumours with inhibitors of poly(ADP-ribose) polymerase.** *Nature* 2005, **434:**913–917.
12. Farmer H, McCabe N, Lord CJ, Tutt AN, Johnson DA, Richardson TB, Santarosa M, Dillon KJ, Hickson I, Knights C, Martin NM, Jackson SP, Smith GC, Ashworth A: **Targeting the DNA repair defect in BRCA mutant cells as a therapeutic strategy.** *Nature* 2005, **434:**917–921.
13. Turner N, Tutt A, Ashworth A: **Hallmarks of 'BRCAness' in sporadic cancers.** *Nat Rev Cancer* 2004, **4:**814–819.
14. Beger C, Pierce LN, Kruger M, Marcusson EG, Robbins JM, Welcsh P, Welch PJ, Welte K, King MC, Barber JR, Wong-Staal F: **Identification of Id4 as a regulator of BRCA1 expression by using a ribozyme-library-based inverse genomics approach.** *Proc Natl Acad Sci U S A* 2001, **98:**130–135.
15. Esteller M, Silva JM, Dominguez G, Bonilla F, Matias-Guiu X, Lerma E, Bussaglia E, Prat J, Harkes IC, Repasky EA, Gabrielson E, Schutte M, Baylin SB, Herman JG: **Promoter hypermethylation and BRCA1 inactivation in sporadic breast and ovarian tumors.** *J Natl Cancer Inst* 2000, **92:**564–569.
16. Saal LH, Gruvberger-Saal SK, Persson C, Lövgren K, Jumppanen M, Staaf J, Jönsson G, Pires MM, Maurer M, Holm K, Koujak S, Subramaniyam S, Vallon-Christersson J, Olsson H, Su T, Memeo L, Ludwig T, Ethier SP, Krogh M, Szabolcs M, Murty VV, Isola J, Hibshoosh H, Parsons R, Borg A: **Recurrent gross mutations of the PTEN tumor suppressor gene in breast cancers with deficient DSB repair.** *Nat Genet* 2008, **40:**102–107.
17. Sourisseau T, Maniotis D, McCarthy A, Tang C, Lord CJ, Ashworth A, Linardopoulos S: **Aurora-A expressing tumour cells are deficient for homology-directed DNA double strand-break repair and sensitive to PARP inhibition.** *EMBO Mol Med* 2010, **2:**130–142.
18. Turner NC, Reis-Filho JS, Russell AM, Springall RJ, Ryder K, Steele D, Savage K, Gillett CE, Schmitt FC, Ashworth A, Tutt AN: **BRCA1 dysfunction in sporadic basal-like breast cancer.** *Oncogene* 2007, **26:**2126–2132.
19. Tutt A, Robson M, Garber JE, Domchek SM, Audeh MW, Weitzel JN, Friedlander M, Arun B, Loman N, Schmutzler RK, Wardley A, Mitchell G, Earl H, Wickens M, Carmichael J: **Oral poly(ADP-ribose) polymerase inhibitor olaparib in patients with BRCA1 or BRCA2 mutations and advanced breast cancer: a proof-of-concept trial.** *Lancet* 2010, **376:**235–244.
20. Gelmon KA, Tischkowitz M, Mackay H, Swenerton K, Robidoux A, Tonkin K, Hirte H, Huntsman D, Clemons M, Gilks B, Yerushalmi R, Macpherson E, Carmichael J, Oza A: **Olaparib in patients with recurrent high-grade serous or poorly differentiated ovarian carcinoma or triple-negative breast cancer: a phase 2, multicentre, open-label, non-randomised study.** *Lancet Oncol* 2011, **12:**852–861.
21. Fong PC, Boss DS, Yap TA, Tutt A, Wu P, Mergui-Roelvink M, Mortimer P, Swaisland H, Lau A, O'Connor MJ, Ashworth A, Carmichael J, Kaye SB, Schellens JH, de Bono JS: **Inhibition of poly(ADP-ribose) polymerase in tumors from BRCA mutation carriers.** *N Engl J Med* 2009, **361:**123–134.
22. Audeh MW, Carmichael J, Penson RT, Friedlander M, Powell B, Bell-McGuinn KM, Scott C, Weitzel JN, Oaknin A, Loman N, Lu K, Schmutzler RK, Matulonis U, Wickens M, Tutt A: **Oral poly(ADP-ribose) polymerase inhibitor olaparib in patients with BRCA1 or BRCA2 mutations and recurrent ovarian cancer: a proof-of-concept trial.** *Lancet* 2010, **376:**245–251.
23. Cancer Genome Atlas Research N: **Integrated genomic analyses of ovarian carcinoma.** *Nature* 2011, **474:**609–615.
24. Patel AG, De Lorenzo SB, Flatten KS, Poirier GG, Kaufmann SH: **Failure of iniparib to inhibit poly(ADP-Ribose) polymerase in vitro.** *Clin Cancer Res* 2012, **18:**1655–1662.
25. O'Shaughnessy J, Danso MA, Rugo HS, Miller K, Yardley DA, Carlson RW, Finn WS, Freese E, Gupta S, Blackwood-Chirchir A, Winer EP: **A randomized phase III study of iniparib (BSI-201) in combination with gemcitabine/carboplatin (G/C) in metastatic triple-negative breast cancer (TNBC).** *J Clin Oncol* 2013, **29**. abstract 1007.
26. Sandhu SK, Schelman WR, Wilding G, Moreno V, Baird RD, Miranda S, Hylands L, Riisnaes R, Forster M, Omlin A, Kreischer N, Thway K, Gevensleben H, Sun L, Loughney J, Chatterjee M, Toniatti C, Carpenter CL, Iannone R, Kaye SB, de Bono JS, Wenham RM: **The poly(ADP-ribose) polymerase inhibitor niraparib (MK4827) in BRCA mutation carriers and patients with sporadic cancer: a phase 1 dose-escalation trial.** *Lancet Oncol* 2013, **14:**882–892.
27. de Bono JS, Mina LA, Gonzalez M, Curtin NJ, Wang E, Henshaw JW, Chadha M, Sachdev JC, Matei D, Jameson GS, Ong M, Basu B, Wainberg ZA, Byers LA, Chugh R, Dorr A, Kaye SB, Ramanthan RK: **First-in human trial of novel oral PARP inhibitor BMN673 in patients with solid tumors.** *J Clin Oncol* 2013, **31**. abstract 2580.
28. Kristeleit R, Shapiro G, LoRusso P, Infante JR, Flynn M, Patel MR, Tolaney SM, Hilton JF, Calvert AH, Giordano H, Isaacson JD, Borrow J, Allen AR, Jaw-Tsai SS, Burris HA: **A phase I dose-escalation and PK study of continuous oral rucaparib in patients with advanced solid tumors.** *J Clin Oncol* 2013, **31**. abstract 2585.
29. Abkevich V, Timms KM, Hennessy BT, Potter J, Carey MS, Meyer LA, Smith-McCune K, Broaddus R, Lu KH, Chen J, Tran TV, Williams D, Iliev D, Jammulapati S, FitzGerald LM, Krivak T, DeLoia JA, Gutin A, Mills GB, Lanchbury JS: **Patterns of genomic loss of heterozygosity predict homologous recombination repair defects in epithelial ovarian cancer.** *Br J Cancer* 2012, **107:**1776–1782.
30. Nik-Zainal S, Alexandrov LB, Wedge DC, Van Loo P, Greenman CD, Raine K, Jones D, Hinton J, Marshall J, Stebbings LA, Menzies A, Martin S, Leung K, Chen L, Leroy C, Ramakrishna M, Rance R, Lau KW, Mudie LJ, Varela I, McBride DJ, Bignell GR, Cooke SL, Shlien A, Gamble J, Whitmore I, Maddison M, Tarpey PS, Davies HR, Papaemmanuil E, *et al*: **Mutational processes molding the genomes of 21 breast cancers.** *Cell* 2012, **149:**979–993.
31. Campbell PJ, Stephens PJ, Pleasance ED, O'Meara S, Li H, Santarius T, Stebbings LA, Leroy C, Edkins S, Hardy C, Teague JW, Menzies A, Goodhead I, Turner DJ, Clee CM, Quail MA, Cox A, Brown C, Durbin R, Hurles ME, Edwards PA, Bignell GR, Stratton MR, Futreal PA: **Identification of somatically acquired rearrangements in cancer using genome-wide massively parallel paired-end sequencing.** *Nat Genet* 2008, **40:**722–729.
32. Geigl JB, Obenauf AC, Schwarzbraun T, Speicher MR: **Defining 'chromosomal instability'.** *Trends Genet* 2008, **24:**64–69.
33. Birkbak NJ, Wang ZC, Kim JY, Eklund AC, Li Q, Tian R, Bowman-Colin C, Li Y, Greene-Colozzi A, Iglehart JD, Tung N, Ryan PD, Garber JE, Silver DP, Szallasi Z, Richardson AL: **Telomeric allelic imbalance indicates defective DNA repair and sensitivity to DNA-damaging agents.** *Cancer Discov* 2012, **2:**366–375.
34. Wang ZC, Birkbak NJ, Culhane AC, Drapkin R, Fatima A, Tian R, Schwede M, Alsop K, Daniels KE, Piao H, Liu J, Etemadmoghadam D, Miron A, Salvesen HB, Mitchell G, DeFazio A, Quackenbush J, Berkowitz RS, Iglehart JD, Bowtell DD, Australian Ovarian Cancer Study Group, Matulonis UA: **Profiles of genomic**

instability in high-grade serous ovarian cancer predict treatment outcome. *Clin Cancer Res* 2012, **18:**5806–5815.

35. Popova T, Manié E, Rieunier G, Caux-Moncoutier V, Tirapo C, Dubois T, Delattre O, Sigal-Zafrani B, Bollet M, Longy M, Houdayer C, Sastre-Garau X, Vincent-Salomon A, Stoppa-Lyonnet D, Stern MH: **Ploidy and large-scale genomic instability consistently identify basal-like breast carcinomas with BRCA1/2 inactivation.** *Cancer Res* 2012, **72:**5454–5462.
36. Pathania S, Nguyen J, Hill SJ, Scully R, Adelmant GO, Marto JA, Feunteun J, Livingston DM: **BRCA1 is required for postreplication repair after UV-induced DNA damage.** *Mol Cell* 2011, **44:**235–251.
37. Wang Q, Zhang H, Guerrette S, Chen J, Mazurek A, Wilson T, Slupianek A, Skorski T, Fishel R, Greene MI: **Adenosine nucleotide modulates the physical interaction between hMSH2 and BRCA1.** *Oncogene* 2001, **20:**4640–4649.
38. Schepeler T, Lamy P, Hvidberg V, Laurberg JR, Fristrup N, Reinert T, Bartkova J, Tropia L, Bartek J, Halazonetis TD, Pan CC, Borre M, Dyrskjøt L, Orntoft TF: **A high resolution genomic portrait of bladder cancer: correlation between genomic aberrations and the DNA damage response.** *Oncogene* 2013, **32:**3577–3586.
39. Stephens PJ, Greenman CD, Fu B, Yang F, Bignell GR, Mudie LJ, Pleasance ED, Lau KW, Beare D, Stebbings LA, McLaren S, Lin ML, McBride DJ, Varela I, Nik-Zainal S, Leroy C, Jia M, Menzies A, Butler AP, Teague JW, Quail MA, Burton J, Swerdlow H, Carter NP, Morsberger LA, Iacobuzio-Donahue C, Follows GA, Green AR, Flanagan AM, Stratton MR, *et al*: **Massive genomic rearrangement acquired in a single catastrophic event during cancer development.** *Cell* 2011, **144:**27–40.
40. Lips EH, Mulder L, Hannemann J, Laddach N, Vrancken Peeters MT, van de Vijver MJ, Wesseling J, Nederlof PM, Rodenhuis S: **Indicators of homologous recombination deficiency in breast cancer and association with response to neoadjuvant chemotherapy.** *Ann Oncol* 2011, **22:**870–876.
41. Schouten PC, van Dyk E, Braaf LM, Mulder L, Lips EH, de Ronde JJ, Holtman L, Wesseling J, Hauptmann M, Wessels LF, Linn SC, Nederlof PM: **Platform comparisons for identification of breast cancers with a BRCA-like copy number profile.** *Breast Cancer Res Treat* 2013, **139:**317–327.
42. Vollebergh MA, Lips EH, Nederlof PM, Wessels LF, Schmidt MK, van Beers EH, Cornelissen S, Holtkamp M, Froklage FE, de Vries EG, Schrama JG, Wesseling J, van de Vijver MJ, van Tinteren H, de Bruin M, Hauptmann M, Rodenhuis S, Linn SC: **An aCGH classifier derived from BRCA1-mutated breast cancer and benefit of high-dose platinum-based chemotherapy in HER2-negative breast cancer patients.** *Ann Oncol* 2011, **22:**1561–1570.
43. Rottenberg S, Jaspers JE, Kersbergen A, van der Burg E, Nygren AO, Zander SA, Derksen PW, de Bruin M, Zevenhoven J, Lau A, Boulter R, Cranston A, O'Connor MJ, Martin NM, Borst P, Jonkers J: **High sensitivity of BRCA1-deficient mammary tumors to the PARP inhibitor AZD2281 alone and in combination with platinum drugs.** *Proc Natl Acad Sci U S A* 2008, **105:**17079–17084.
44. Telli ML, Jensen KC, Abkevich V, Hartman AR, Vinayak S, Lanchbury J, Gutin A, Timms K, Ford JM: **Homologous recombination deficiency (HRD) score predicts pathologic response following neoadjuvant platinum-based therapy in triple-negative and BRCA1/2 mutation-associated breast cancer (BC).** *San Antonio Breast Cancer Symposium* 2012, **72**. abstract PD09-04.
45. Timms KM, Abkevich V, Neff C, Morris B, Potter J, Tran TV, Chen J, Sangale Z, Tikishville E, Zharkikh A, Perry M, Gutin A, LAnchbury JS: **Association between BRCA1/2 status and DNA-based assays for homologous recombination deficiency in breast cancer.** *San Antonio Breast Cancer Symposium* 2013. abstract P6-05-10.
46. Birkbak NJ, Kochupurakkal B, Izarzugaza JM, Eklund AC, Li Y, Liu J, Szallasi Z, Matulonis UA, Richardson AL, Iglehart JD, Wang ZC: **Tumor mutation burden forecasts outcome in ovarian cancer with BRCA1 or BRCA2 mutations.** *PloS One* 2013, **8:**e80023.
47. Nik-Zainal S, Van Loo P, Wedge DC, Alexandrov LB, Greenman CD, Lau KW, Raine K, Jones D, Marshall J, Ramakrishna M, Shlien A, Cooke SL, Hinton J, Menzies A, Stebbings LA, Leroy C, Jia M, Rance R, Mudie LJ, Gamble SJ, Stephens PJ, McLaren S, Tarpey PS, Papaemmanuil E, Davies HR, Varela I, McBride DJ, Bignell GR, Leung K, Butler AP, *et al*: **The life history of 21 breast cancers.** *Cell* 2012, **149:**994–1007.
48. Campeau PM, Foulkes WD, Tischkowitz MD: **Hereditary breast cancer: new genetic developments, new therapeutic avenues.** *Hum Genet* 2008, **124:**31–42.
49. Jaspers JE, Kersbergen A, Boon U, Sol W, van Deemter L, Zander SA, Drost R, Wientjens E, Ji J, Aly A, Doroshow JH, Cranston A, Martin NM, Lau A, O'Connor MJ, Ganesan S, Borst P, Jonkers J, Rottenberg S: **Loss of 53BP1 causes PARP inhibitor resistance in Brca1-mutated mouse mammary tumors.** *Cancer Discov* 2013, **3:**68–81.
50. Edwards SL, Brough R, Lord CJ, Natrajan R, Vatcheva R, Levine DA, Boyd J, Reis-Filho JS, Ashworth A: **Resistance to therapy caused by intragenic deletion in BRCA2.** *Nature* 2008, **451:**1111–1115.
51. Norquist B, Wurz KA, Pennil CC, Garcia R, Gross J, Sakai W, Karlan BY, Taniguchi T, Swisher EM: **Secondary somatic mutations restoring BRCA1/2 predict chemotherapy resistance in hereditary ovarian carcinomas.** *J Clin Oncol* 2011, **29:**3008–3015.
52. Sakai W, Swisher EM, Karlan BY, Agarwal MK, Higgins J, Friedman C, Villegas E, Jacquemont C, Farrugia DJ, Couch FJ, Urban N, Taniguchi T: **Secondary mutations as a mechanism of cisplatin resistance in BRCA2-mutated cancers.** *Nature* 2008, **451:**1116–1120.
53. Swisher EM, Sakai W, Karlan BY, Wurz K, Urban N, Taniguchi T: **Secondary BRCA1 mutations in BRCA1-mutated ovarian carcinomas with platinum resistance.** *Cancer Res* 2008, **68:**2581–2586.
54. Burger H, Loos WJ, Eechoute K, Verweij J, Mathijssen RH, Wiemer EA: **Drug transporters of platinum-based anticancer agents and their clinical significance.** *Drug Resist Updat* 2011, **14:**22–34.
55. Pyndiah S, Tanida S, Ahmed KM, Cassimere EK, Choe C, Sakamuro D: **c-MYC suppresses BIN1 to release poly(ADP-ribose) polymerase 1: a mechanism by which cancer cells acquire cisplatin resistance.** *Sci Signal* 2011, **4:**ra19.
56. Martin SA, McCarthy A, Barber LJ, Burgess DJ, Parry S, Lord CJ, Ashworth A: **Methotrexate induces oxidative DNA damage and is selectively lethal to tumour cells with defects in the DNA mismatch repair gene MSH2.** *EMBO Mol Med* 2009, **1:**323–337.

10.1186/bcr3670
Cite this article as: Watkins *et al.*: Genomic scars as biomarkers of homologous recombination deficiency and drug response in breast and ovarian cancers. *Breast Cancer Research* 2014, 16:211

Review Article · Übersichtsarbeit

Breast Care

Breast Care 2012;7:273–280
DOI: 10.1159/000341529

Published online: August 13, 2012

Profiling the Immune Stromal Interface in Breast Cancer and Its Potential for Clinical Impact

Sheeba Irshad[a] Anita Grigoriadis[a] Katherine Lawler[b] Tony Ng[b] Andrew Tutt[a]

[a]Breakthrough Breast Cancer Research Unit, Guy's Hospital, Kings College London; Kings Health Partners AHSC,
[b]Richard Dimbleby Department of Cancer Research, Randall Division and Division of Cancer Studies, Kings College London, Guy's Medical School Campus, London, UK

Keywords
Genomic biomarkers · Immune stromal interface · Breast cancer

Schlüsselwörter
Genom-Biomarker · Immun-stromale Wechselwirkung · Mammakarzinom

Summary
Advances in DNA sequencing technologies, as well as refined bioinformatics methods for interpretation of complex datasets, have provided the opportunity to comprehensively assess gene expression in tumours and their surrounding microenvironment. More recently, these advances have highlighted the interplay between the immune effector mechanisms and breast cancer cell biology, emphasizing the long-recognized link between immunity and cancer. Studying immune-associated genes has not only resulted in further stratification within the broad pathological types of breast cancers, but also provided further biological insights into the complex heterogeneity within breast cancer subgroups. On the basis that anti-cancer therapies can modify the host-tumour interaction, investigators have focused their attention on the predictive value of immune parameters as markers of therapeutic anti-tumour response. We discuss the current status of immune signatures in breast cancer and some of the fundamental limitations that need to be overcome to move these discoveries into clinic.

Zusammenfassung
Fortschritte in der DNA-Sequenzierungstechnologie sowie verfeinerte Bioinformatik-Methoden zur Interpretation komplexer Datensätze haben die umfassende Bestimmung der Genexpression in Tumoren und der sie umgebende Mikroumwelt möglich gemacht. In jüngster Vergangenheit haben diese Fortschritte das Zusammenspiel zwischen Immuneffektormechanismen und der Mammakarzinom-Zellbiologie hervorgehoben und damit die seit langem akzeptierte Verbindung zwischen Immunität und Krebs betont. Die Erforschung von Genen des Immunsystems hat nicht nur die Stratifizierung der vielfältigen pathologischen Formen des Mammakarzinoms erweitert, sondern auch neue zelluläre Einblicke in die komplexe Heterogenität des Mammakarzinoms gegeben. In Anlehnung an die Tatsache, dass antitumoröse Therapien die Wirt-Tumor-Interaktion modifizieren können, haben Forscher den Fokus ihrer Aufmerksamkeit auf den prädiktiven Wert von Immunparametern als Marker des Ansprechens auf die Krebstherapie gerichtet. Wir diskutieren den aktuellen Stand auf dem Gebiet der Immunsignaturen beim Mammakarzinom sowie einige der fundamentalen Limitationen, die es zu überwinden gilt, um diese Entdeckungen in die Klinik zu überführen.

Introduction

A decade from the first draft of the human genome sequence [1, 2], our increasing understanding of the genetic aberrations that drive human malignancies has provided an impetus towards achieving more personalized cancer care. Genome sequence analysis (genomics) is beginning to reveal how DNA sequences vary from individual to individual: epidemiological genome-wide association studies have identified a number of single nucleotide polymorphisms (SNPs) related to disease susceptibility and breast cancer survival [3–5], and within the tumour a catalogue of sequence polymorphisms

KARGER
Fax +49 761 4 52 07 14
Information@Karger.de
www.karger.com

1661-3791/12/0074-0273$38.00/0

Accessible online at:
www.karger.com/brc

Professor Andrew Tutt, M.D.
Research Oncology
3rd Floor Bermondsey Wing, Guys Hospital
Great Maze Pond, London SE1 9RT, UK
Tel. +44 207 1889881
breakthroughunit@kcl.ac.uk

and chromosomal aberrations exhibit variations between individuals [6, 7]. Additionally, recent advances in mRNA and microRNA gene expression profiling (transcriptomics) in tumours have helped identify prognostic and predictive biomarkers in many types of human malignancies [8–10]. No cancer type has seen as much attention to the layers of its genomic background as breast cancer, and early work by Perou et al. [11] showed that transcriptional data generated using microarrays could stratify patients into distinct molecular 'intrinsic subtypes' relating to tumour biology and behaviour. 5 groups were identified and named Luminal A, Luminal B, Basal-like, Normal-like and the HER2-enriched subgroups. This classification has since seen further adaptation and evolved to include a 6th subgroup based on the low expression level of tight junction (claudin) genes – *the claudin-low group* [12–14]. These seminal publications resulted in an explosion of interest in the field of cancer genomics with countless publications attempting to unravel the complexities of both the inter-patient and intra-tumour heterogeneity of breast tumours at DNA copy number, sequence and transcriptional levels [15–17].

In parallel, recent years have seen a growing appreciation of the concept of 'cancer immunoediting' describing the integration of the immune system's dual but opposing impacts: host-protection and tumour promotion [18]. Cancer immunoediting consists of 3 successive steps whereby immune cells in the tumour microenvironment are thought to interact intimately and actively with the transformed cells [18–20]. In the 'elimination' phase, various components of the immune response work together to destroy developing tumours long before they become clinically apparent. During the 'equilibrium' phase, a balance is established between the tumour and the immune system, shaping each other reciprocally. Finally, the immune system contributes to the selection of tumour variants that enter the 'escape' phase, in which their outgrowth is no longer blocked by immunity resulting in clinically apparent disease [18–22]. The cells playing a key role in this process have been identified in both the innate (e.g. natural killer cells, natural killer T-cells, macrophages and dendritic cells) and the adaptive (e.g. $CD4^+$ T helper type 1 (T_H1) and $CD8^+$ T-cells) immune 'arms'. While the exact interplay between these components remains to be fully elucidated, the extensive transcriptomics information of breast cancers has provided novel insights into the interaction between the immune and breast cancer cell biology. Figure 1 gives a schematic illustration of the development of immunological gene expression signatures, and highlights that the relevance of early transcriptomics discoveries for identification of immune predictive and prognostic biomarkers is only now being fully appreciated. There remain some fundamental limitations, however, that need to be overcome to move these exciting discoveries from the bench to the bedside.

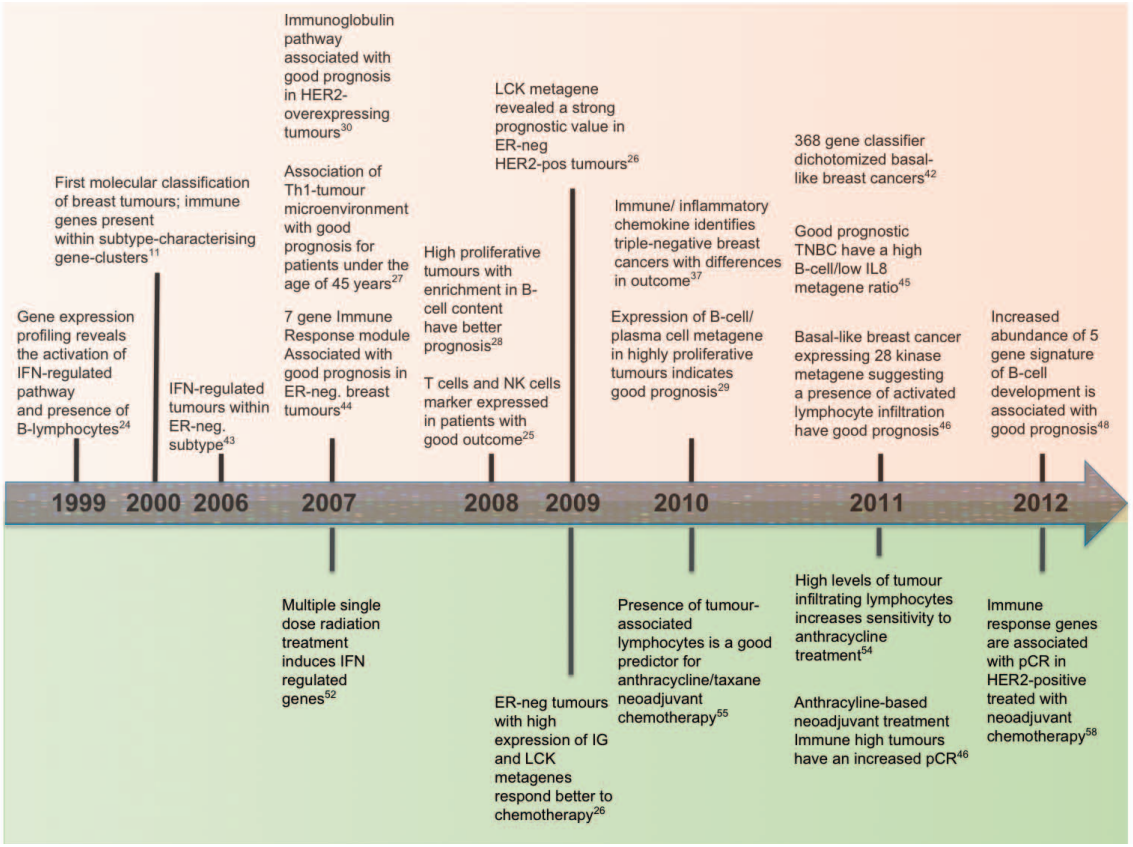

Fig. 1. Prognostics.

Immune Signatures in Breast Cancers

The presence of a prognostic impact of lymphocyte infiltration in breast cancer has long been debated and remains controversial. Several lines of evidence support the hypothesis that lymphocytic infiltration is a marker of host anti-tumour immune response. Even the first applications of microarray analysis to whole tumour sections revealed variations in the expression of several genes associated with immune cells; including for example, the interferon-regulated genes [23, 24], B-lymphocyte markers [24], as well as T-lymphocyte-associated genes [23]. Laser-captured microdissection of stromal components identified a good-outcome signature of 26 genes enriched for elements of the T_H1 immune response [25]. Rody et al. [26] identified 7 clusters of immune system-related metagenes by large-scale microarray analysis and demonstrated an association with different immunological cell types. A strong positive prognostic value for the T-cell surrogate marker (lymphocyte-specific kinase (LCK) metagene) was observed among all oestrogen receptor (ER)-negative tumours and amongst ER-positive tumours with HER2 overexpression, whereas an IgG metagene as a marker for B-cells had no significant prognostic value. Another earlier study reported that increased expression of T_H1-associated genes was protective in breast cancer patients, but only in patients under 45 years of age [27]. The importance of subtle variations in the expression levels of immune cell-associated genes within breast tumours is evident. Schmidt et al. [28] demonstrated that the IgG metagene outperformed the T-cell metagene as a favourable prognostic factor in highly proliferating specimens, while a further study reported that among ER-negative and ER-positive highly proliferative cancers, a subset of tumours with high expression of a B-cell/plasma cell metagene carries a favourable prognosis [29]. In HER2-overexpressing breast cancers, the expression of genes associated with the immunoglobulin pathway correlated with tumour-infiltrating lymphocytes and predicted favourable clinical outcome among highly proliferating tumours [30]. These immunoglobulin genes are likely to be co-regulated, and therefore the prominence of an immunoglobulin pathway does not necessarily imply that the lymphocytic infiltrate is composed mostly of a particular immune cell subset such as B cells. Interestingly, in ovarian cancer, the causal nature of relationship between the strong association of T-cell infiltrate with good patient outcome has been debated: it may be due to the T-cell infiltrate effectively eliminating tumour cells, or might reflect indolent tumour cell biology characterized by slower growth, thus increasing the opportunity for immune cell infiltration into the tumour microenvironment [31]. However, this is challenged by the observation that highly proliferating tumours are more likely to be associated with higher T-cell infiltrates [32], possibly due to mitotically active cancers exhibiting high genomic instability [33]. It can therefore be hypothesized that a higher mutational rate is likely to generate neo-antigens with higher immunogenicity [34]. Similarly, other studies have reported that p53 abnormalities and increased immune cell infiltrates are significantly more common in high-grade serous ovarian cancers with germline and somatic mutations in *BRCA1* or *BRCA2,* compared with tumours lacking *BRCA* abnormalities [35, 36]. In ER-negative breast cancers, a clear anti-correlation between proliferation genes and an immune signature of 14 genes involved in proinflammatory cytokine/chemokine signalling has been observed [37]; on the other hand, the observed correlation between tumour growth and immune microenvironment [28] raises the possibility that a slow growing tumour is associated with a different tumour-host interaction (e.g. a humoral response to the tumour and its antigens) than a fast growing one. Studies report the enhancement of metastatic potency of breast cancer cell lines enriched with stromal cells [38], lending support to the concept of a symbiotic relationship between tumours and its microenvironment. In contrast, highly proliferative tumour cells may produce different signals which will in turn influence the microenvironment down a different path. Thus, the proliferation rate of a tumour [39] might be a surrogate indicator of the tumour's stromal environment as well as the intrinsic properties within the tumour cell that influence that environment. Unravelling the complexity of this association would be valuable information for targeted therapeutic strategies with potential to target both tumour cells and their interface with an immunologically active and cytokine-rich stroma and might shed further light on the signals influencing tumour growth and its microenvironment.

There has been an increasing focus on the potential for immune-related features for further stratification of breast cancers, alongside proliferation and associated gene expression signatures (genomic grade index [40], 70-gene signature [41] and 76-gene signature [42]) which appear to be successful in particular for stratifying ER-positive tumours where cell proliferation is a key element for outcome prediction. Using a test-and-validation strategy on a comprehensive collection of breast tumours, Hu et al. [43] were the first to report that interferon (IFN)-γ and regulators of STAT1-based immunity may have an anti-tumour effect. IFNs are a family of structurally related cytokines and possess a wide range of immune properties including antiviral activity, promotion of antigen presentation as well as inhibition of cell growth and proliferation. This study provided the first suggestion that the expression of multiple immune-related genes had an influence on the outcome of breast cancers of non-ER-positive type. It was shortly followed by a publication interrogating 3 publicly available microarray data sets, comprising 186 adjuvant therapy-naïve ER-negative breast cancers, and thereby identifying 7 immune-responsive genes capable of specifying tumours with reduced risk for distant metastasis [44]. Interestingly, a correlation between the so-called immune response (IR+) module and the previously determined IFN-regulated cluster was observed. The small overlap of genes (including *STAT1*)

and the difference in their clinico-pathological features (IFN-expressing tumours encompassed more cases with positive lymph node metastasis) strengthened the IR+ module as a key gene signature for subtype classification. Focusing on basal-like breast cancers – the majority of which are ER-negative tumours – revealed a positive relation to outcome with the presence of either a module encompassing 28 kinases or a gene signature derived from medullary breast cancers [45, 46]. Medullary breast carcinomas are highly proliferative breast cancers showing increased lymphocytic infiltration and having an overall good prognosis. Genes involved in the IL15 and IL12 pathway appear to be the main players in the medullary breast cancer signature and indicated a better prognosis [45]. In agreement with this immunological pathway was the expression pattern of the kinome-gene module in basal-like breast cancers, which also pointed to an activation of T_H1-biased lymphocytic infiltration in good prognostic cancers [46]. Characterisation of a comprehensive transcriptomic dataset of triple-negative breast tumours, by definition also ER-negative and with significant clinically and biologically overlap to the basal-like subtype, could further dissect their tumour-host interaction. A specific relationship between individual components of an immune response such as the ratio of a high B-cell content to a low IL8 expression seem to infer a positive prognosis for triple-negative breast cancers [47]. A positive association of lymphocytic infiltration and outcome in ER-negative breast tumours has recurrently and robustly been observed and triggered expectation for the development of new therapies based on immune response manipulation for breast cancer subtypes.

However, the fine print within the bulk of observations should not be overlooked, and novel insights into tumour immunology need to be cautiously evaluated. Recently, Ascierto et al. [48] identified among 299 immune function genes, a 5-gene signature *(IGKC, GBP1, STAT1, IGLL5* and *OCLN)* involved in B-cell development with a high predictive accuracy for relapse-free survival of 85%. At the same time, genes involved in primary immunodeficiency signalling, T-cell apoptosis, CTLA4 signalling and production of nitric oxide and reactive oxygen species were also up-regulated in the tumour specimens of patients who were subsequently free of relapse. The authors offer an explanation for this paradoxically concurrent expression of immune effector and suppressor genes whereby tumour-derived factors (e.g. GM-CSF, VEGF and MCP-1) facilitate the expression of immune suppressor genes as well as acting as chemo-attractants for immune cells. Surgical intervention may then disturb this carefully balanced system between immune suppressor and effector genes, leading to the different expression ratio between these 2 sides. It is also possible that the immune activation of cancer cells initiates a positive feedback loop whereby the cancer cells not only invite immune cells to the tumour microenvironment but they are also more sensitive to pre-inflammatory factors secreted by immune cells.

Nonetheless, recent genomic studies have evidently indicated that the expression of genes related to immune response provide important prognostic information in ER-negative, HER2-overexpressing or highly proliferating ER-positive breast cancers. The value of molecular signatures such as the Food and Drug Administration (FDA)-approved 70-gene MammaPrint® (Agendia, Amsterdam, The Netherlands) prognostic panel and Oncotype DX® (Genomic Health, Redwood City, CA, USA) in defining the role of chemotherapy in an intermediate prognostic risk group defined by a 21-gene panel, are currently tested in the context of the prospective randomized phase III trials, MINDACT and TAILORx, respectively. However, since this first generation of gene signatures has largely been focused on hormone receptor-positive disease and only partly includes immune-related genes [49, 50], the integration of these elements into prognostic and predictive models for further breast cancer subgroups is the next step to assess validity and optimize efficacy.

Predictive Immune Biomarkers in Breast Cancer

The development of predictive immune signatures to help guide the use of anti-tumour therapy is still in its infancy. However, on the basis that anti-cancer therapies can modify the host-tumour interaction, cancer genomic experts have focused their attention on the predictive value of immune parameters as markers of therapeutic anti-tumour response. Gianni et al. [51] have shown that immune-related genes, such as *CD3,* are linked to response to chemotherapy in a cohort of 89 breast cancers, of which 11 had a pathological complete response (pCR). More recently, Sabatier et al. [46] investigated the link between an immune cell-derived 28-kinase metagene and response to anthracycline-based neoadjuvant chemotherapy for basal-like breast cancers. 'Immune-High' patients experienced more pCR (59%) than 'Immune-Low' patients (43%), and although this was not significant ($p = 0.29$), similar trends have been observed with modest predictive value for neoadjuvant chemotherapies: high expression of both IgG and LCK metagenes in ER-negative breast carcinomas [26], and a high B-cell/low IL8 ratio for triple-negative breast cancers [47]. Similarly, gene expression profiling of breast tumour cell lines and mouse models exposed to single-dose (10 Gy) versus fractionated (2 Gy × 5) radiation have revealed that only the fractionated regimen induced an interferon-related gene signature, including *STAT1* [52]. Taken together, these model systems illustrate that chemotherapeutic agents may restore the immunological equilibrium not only due to the 'debulking' of the tumour mass but also due to direct or indirect effects on the immune system. In fact, anthracycline-based chemotherapies have been shown to induce a vigorous infiltration of anticancer immune effectors in mice [53]. A recent clustering analysis of the neoadjuvant (EORTC) cohort defined an 8-gene lymphocyte mRNA expression signature

(including *CD19, CD3D, CD48, GZMB, LCK, MS4A1, PRF1 and SELL*) to examine the association between tumour-infiltrating lymphocytes (TIL) and short-term response to neoadjuvant chemotherapy in ER-negative tumours (n = 113) [54]. TIL-enriched tumours significantly predicted anthracycline sensitivity with an odds ratio of 6.3 for HER2-positive and triple-negative tumour phenotypes. Additionally, Denkert et al. [55] reported a significant relationship between TIL (identified by a combination of H and E assessment, and expression analysis of several TIL genes by polymerase chain reaction) and pathologic response to neoadjuvant anthracycline/taxane therapy in a large group of 1,058 patients (one fourth of whom were ER-negative).

Several studies have suggested possible mechanisms of tumour-immune interaction in response to chemotherapy. Appropriate preclinical models have shown that 2 receptors present on dendritic cells, namely TLR4 (a toll-like receptor) and *P2RX7* (a purinergic receptor), are essential for their cross-talk with a dying cell. They recognise 2 soluble molecules released from the dying tumour cells, HMGB1 and ATP, respectively. In the absence of TLR4 or P2RX7, the immune system fails to mount an antitumor immune response after chemotherapy [56, 57]. A loss-of-function polymorphism of the TLR4 is an independent predictive biomarker for response to anthracycline chemotherapy in breast cancer patients [56]. Similarly, anthracycline-treated individuals with breast cancer carrying a loss-of-function allele of P2RX7 developed metastatic disease more rapidly than individuals bearing the normal allele [57]. A comprehensive analysis of publicly available gene expression studies evaluating anthracycline with or without taxane-based neoadjuvant chemotherapy has reported that high immune module scores were associated with increased probability of achieving pCR in all breast cancer subtypes with varying degree of significance [58]. Although the data with regards to predictive immune response gene sets is still very sparse, the above data provide preliminary validation of the concept that selective immune defects can influence the efficacy of anticancer chemotherapies. Hence studies exploring the possibility of predicting therapeutic outcome by assessing dynamic variables such as changes in the frequency, composition, activation status and repertoire of TIL, the expression of immune-relevant metagenes (in repeated lymph node biopsies), or the generation of tumour-specific antibodies (in patient sera) after chemotherapy need to be encouraged.

Discussion

While multigene prognostic and predictive gene signatures were once expected to replace clinicopathological parameters for therapy decision-making, a complete transition has not yet taken place. This is partly due to inherent problems of technical robustness and experimental as well as analytical standardization [14]. Likewise, the inherent complexity of immune gene signatures (fig. 2 A), heterogeneous assay protocols between laboratories, and the use of different statistical strategies are proving to be rate-limiting steps for the development of immune-related biomarkers for clinical application. The high data variability and poor reproducibility complicate meta-analyses comparing results across laboratories, however, efforts are being made internationally to minimize these obstacles. For example, 2 large immunological consortia (the Cancer Immunotherapy Consortium (CIC) in the US and the Association of Cancer Immunoguiding Program (CIP) in Europe) have recently addressed the issue of immune assay harmonization across laboratories with the objective of accelerating immune biomarker identification and drug development [59].

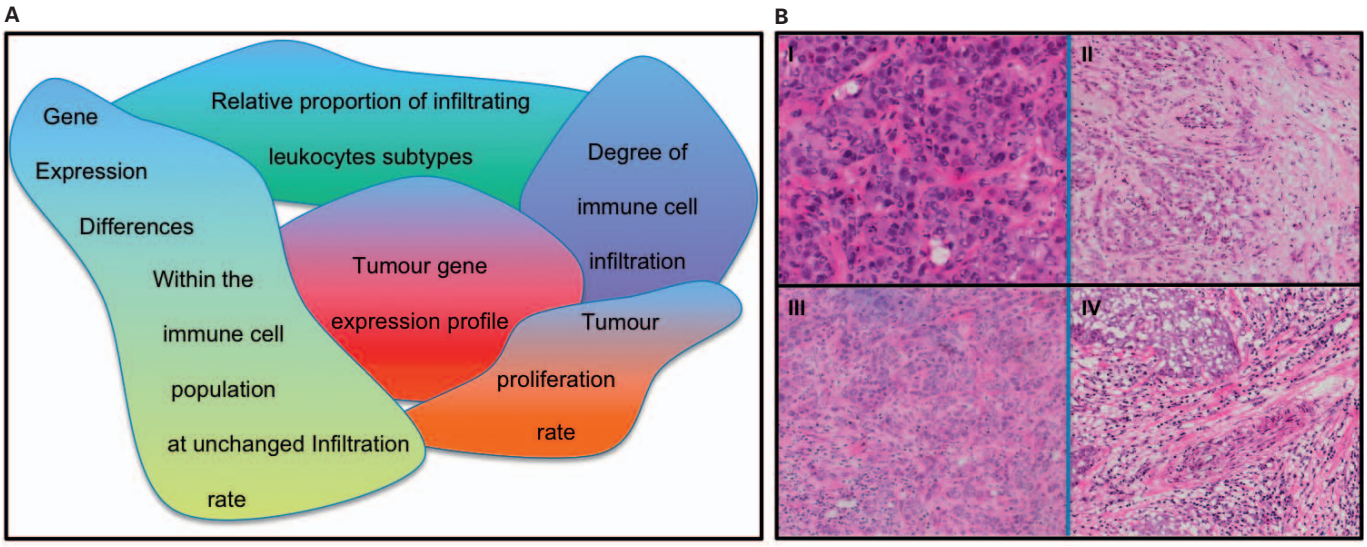

Fig 2. A Inherent complexities of interpreting immune gene signatures. **B** Triple-negative tumours show a different degree of lymphocytic contents: I minimal non-malignant (stromal and lymphocytic) enrichment; II small presence (< 10%); III moderate presence (10–30%), and IV strong enrichment (> 30%) (images courtesy of Patrycja Gazinska).

More specifically, Rody et al. [26] have argued that the level of lymphocytic infiltration has a greater effect on the tumour gene expression profile than the differences in a mixture of distinct types of immune cells. Although immune gene signatures appear to be highly sensitive to the composition of tumour cell content, it may be difficult to detect differences in immune cell composition in a background of differential infiltration levels between tumour samples. Enrichment of samples to > 70% malignant epithelium has become standard for expression profiling experiments and should help to minimize this obstacle for many tumour samples. In triple-negative breast cancer specimens, however, where the lymphocytic cells are intertwined with cancerous cells (fig. 2 B), this is not always feasible.

The dynamic plasticity of the tumour microenvironment itself adds further complexity to the task of translating immune cancer genomics into cancer therapies. Possible alteration of immune milieu within the tumour due to surgical or chemotherapeutic interventions means that the composition of the profiled tumour sample might not resemble the true immune microenvironment. Recent evidence indicates that T-cells alter their end-stage commitment in response to microenvironmental cues, for example shifting from a T_H17 commitment to a T_H1-, T_H2- or T-reg-specific pattern [60], with shift patterns ultimately determining the functional role of these immune cells. Similarly, molecular variations between tumour samples may be occurring at the protein and protein-protein interaction level, for example mediated by post-translational modifications, thus hampering the identification of transcriptomic-based immune gene signatures as robust fingerprints for prediction of survival or treatment response.

Lastly, although gene expression profiling of the primary tumour and its microenvironment are likely to help drive various tumour immunology hypotheses, one important consideration in the development of cancer immunotherapy is tissue source for utilization into biomarker assays. Applying microarray-based expression profiling on peripheral blood mononuclear cell (PBMC) from patient blood samples may represent a useful tool in the identification of immune signatures associated with cancer immunotherapy. Although little is known about PBMC gene expression immune signatures in cancers, several studies in the autoimmune literature have demonstrated utility of PBMC expression arrays to help identify predictors of response to therapy and prognosis [61–63]. More importantly, validation of immune signatures on a large scale is much more feasible on blood-based technologies, and PBMC-based biomarkers of immune response in patients receiving cancer immunotherapy [64] need to be further explored as means to guide therapy and prognosis.

Conclusion

In conclusion, recent genomic approaches provide an opportunity to evaluate the tumour microenvironment (including stromal, endothelial and immune cells) and offer the possibility of identifying cytokines and signalling molecules that are important for limiting pro-tumourigenic responses and enhancing anti-tumour immune responses. Whilst the majority of the ER-positive breast cancer prognostic signatures are associated with proliferation signals, genes related to immune response appear to provide important prognostic information in other breast cancer subtypes (e.g. ER-negative, HER2-overexpressing or highly proliferating ER-positive breast cancers). Moreover, accumulating evidence indicates that chemotherapy can stimulate anticancer immune responses, and immune-related genes are linked to chemotherapy response and patient outcome. Large-scale studies exploring the composition, intra- and peritumoural distribution, architecture, and functional articulation of the immune infiltrate along with its context are needed to fully comprehend the immune readouts in breast cancer. As massive amounts of biological and immunological data are generated, technological and advances in the biostatistical analysis of genomics represent a remarkable opportunity to fine-tune breast cancer classification, prognosis and treatment prediction.

Acknowledgement

We would like to acknowledge the funding to Dr. Sheeba Irshad, Dr. Anita Grigoriadis and Professor Tutt from the Breakthrough Breast Cancer and the Sarah Greene Tribute Funds. Dr. Katherine Lawler is funded by the Comprehensive Cancer Imaging Centre (CCIC) and Professor Ng from the Dimbleby Cancer Care and the Breakthrough Breast Cancer Funds.

Disclosure Statement

The authors declare no conflict of interest.

References

1 Lander ES, Linton LM, Birren B, Nusbaum C, Zody MC, Baldwin J, Devon K, Dewar K, Doyle M, FitzHugh W, Funke R, et al.: Initial sequencing and analysis of the human genome. Nature 2001;409:860–921.
2 Venter JC, Adams MD, Myers EW, Li PW, Mural RJ, Sutton GG, Smith HO, Yandell M, Evans CA, Holt RA, Gocayne JD, et al.: The sequence of the human genome. Science 2001;291:1304–1351.
3 Campa D, Kaaks R, Le Marchand L, Haiman CA, Travis RC, Berg CD, Buring JE, Chanock SJ, Diver WR, Dostal L, Fournier A, et al.: Interactions between genetic variants and breast cancer risk factors in the breast and prostate cancer cohort consortium. J Natl Cancer Inst 2011;103:1252–1263.
4 Garcia-Closas M, Hall P, Nevanlinna H, Pooley K, Morrison J, Richesson DA, Bojesen SE, Nordestgaard BG, Axelsson CK, Arias JI, Milne RL, et al.: Heterogeneity of breast cancer associations with five susceptibility loci by clinical and pathological characteristics. PLoS Genet 2008;4:e1000054.
5 Peng R, Wang S, Shi Y, Liu D, Teng X, Qin T, Zeng Y, Yuan Z: Patients 35 years old or younger

with operable breast cancer are more at risk for relapse and survival: a retrospective matched case-control study. Breast 2011;20:568–573.
6 Kwei KA, Kung Y, Salari K, Holcomb IN, Pollack JR: Genomic instability in breast cancer: pathogenesis and clinical implications. Mol Oncol 2010;4:255–266.
7 Stephens PJ, McBride DJ, Lin ML, Varela I, Pleasance ED, Simpson JT, Stebbings LA, Leroy C, Edkins S, Mudie LJ, Greenman CD, et al.: Complex landscapes of somatic rearrangement in human breast cancer genomes. Nature 2009;462:1005–1010.
8 Iorio MV, Croce CM: MicroRNA involvement in human cancer. Carcinogenesis 2012;Epub ahead of print.
9 Nambiar PR, Gupta RR, Misra V: An 'omics' based survey of human colon cancer. Mutat Res 2010;693:3–18.
10 Tran B, Dancey JE, Kamel-Reid S, McPherson JD, Bedard PL, Brown AM, Zhang T, Shaw P, Onetto N, Stein L, Hudson TJ, et al.: Cancer genomics: technology, discovery, and translation. J Clin Oncol 2012;30:647–660.
11 Perou CM, Sorlie T, Eisen MB, van de Rijn M, Jeffrey SS, Rees CA, Pollack JR, Ross DT, Johnsen H, Akslen LA, Fluge O, et al.: Molecular portraits of human breast tumours. Nature 2000;406:747–752.
12 Prat A, Parker JS, Karginova O, Fan C, Livasy C, Herschkowitz JI, He X, Perou CM: Phenotypic and molecular characterization of the claudin-low intrinsic subtype of breast cancer. Breast Cancer Res 2010;12:R68.
13 Sotiriou C, Pusztai L: Gene-expression signatures in breast cancer. N Engl J Med 2009;360:790–800.
14 Weigelt B, Mackay A, A'Hern R, Natrajan R, Tan DS, Dowsett M, Ashworth A, Reis-Filho JS: Breast cancer molecular profiling with single sample predictors: a retrospective analysis. Lancet Oncol 2010;11:339–349.
15 Curtis C, Shah SP, Chin SF, Turashvili G, Rueda OM, Dunning MJ, Speed D, Lynch AG, Samarajiwa S, Yuan Y, Graf S, et al.: The genomic and transcriptomic architecture of 2,000 breast tumours reveals novel subgroups. Nature 2012;486:346–352.
16 Gerlinger M, Rowan AJ, Horswell S, Larkin J, Endesfelder D, Gronroos E, Martinez P, Matthews N, Stewart A, Tarpey P, Varela I, et al.: Intratumor heterogeneity and branched evolution revealed by multiregion sequencing. N Engl J Med 2012;366:883–892.
17 Shah SP, Roth A, Goya R, Oloumi A, Ha G, Zhao Y, Turashvili G, Ding J, Tse K, Haffari G, Bashashati A, et al.: The clonal and mutational evolution spectrum of primary triple-negative breast cancers. Nature 2012;486:395–399.
18 Dunn GP, Bruce AT, Ikeda H, Old LJ, Schreiber RD: Cancer immunoediting: from immunosurveillance to tumor escape. Nat Immunol 2002;3:991–998.
19 Koebel CM, Vermi W, Swann JB, Zerafa N, Rodig SJ, Old LJ, Smyth MJ, Schreiber RD: Adaptive immunity maintains occult cancer in an equilibrium state. Nature 2007;450:903–907.
20 Mantovani A, Allavena P, Sica A, Balkwill F: Cancer-related inflammation. Nature 2008;454:436–444.
21 Kraman M, Bambrough PJ, Arnold JN, Roberts EW, Magiera L, Jones JO, Gopinathan A, Tuveson DA, Fearon DT: Suppression of antitumor immunity by stromal cells expressing fibroblast activation protein-alpha. Science 2010;330:827–830.
22 Teng MW, Swann JB, Koebel CM, Schreiber RD, Smyth MJ: Immune-mediated dormancy: an equilibrium with cancer. J Leukoc Biol 2008;84:988–993.
23 Huang E, Cheng SH, Dressman H, Pittman J, Tsou MH, Horng CF, Bild A, Iversen ES, Liao M, Chen CM, West M, et al.: Gene expression predictors of breast cancer outcomes. Lancet 2003;361:1590–1596.
24 Perou CM, Jeffrey SS, van de Rijn M, Rees CA, Eisen MB, Ross DT, Pergamenschikov A, Williams CF, Zhu SX, Lee JC, Lashkari D, et al.: Distinctive gene expression patterns in human mammary epithelial cells and breast cancers. Proc Natl Acad Sci U S A 1999;96:9212–9217.
25 Finak G, Bertos N, Pepin F, Sadekova S, Souleimanova M, Zhao H, Chen H, Omeroglu G, Meterissian S, Omeroglu A, Hallett M, et al.: Stromal gene expression predicts clinical outcome in breast cancer. Nat Med 2008;14:518–527.
26 Rody A, Holtrich U, Pusztai L, Liedtke C, Gaetje R, Ruckhaeberle E, Solbach C, Hanker L, Ahr A, Metzler D, Engels K, et al.: T-cell metagene predicts a favorable prognosis in estrogen receptor-negative and HER2-positive breast cancers. Breast Cancer Res 2009;11:R15.
27 Hsu SD, Anders CK, Acharya CR, Zhang Y, Wang Y, Foekens JA, Blackwell KL, Drake CG, Morse MA, Febbo PG: Immune signatures hold prognostic import across solids tumors. J Clin Oncol 2007;25:21041.
28 Schmidt M, Bohm D, von Torne C, Steiner E, Puhl A, Pilch H, Lehr HA, Hengstler JG, Kolbl H, Gehrmann M: The humoral immune system has a key prognostic impact in node-negative breast cancer. Cancer Res 2008;68:5405–5413.
29 Bianchini G, Qi Y, Alvarez RH, Iwamoto T, Coutant C, Ibrahim NK, Valero V, Cristofanilli M, Green MC, Radvanyi L, Hatzis C, et al.: Molecular anatomy of breast cancer stroma and its prognostic value in estrogen receptor-positive and -negative cancers. J Clin Oncol 2010;28:4316–4323.
30 Alexe G, Dalgin GS, Scanfeld D, Tamayo P, Mesirov JP, DeLisi C, Harris L, Barnard N, Martel M, Levine AJ, Ganesan S, et al.: High expression of lymphocyte-associated genes in node-negative HER2+ breast cancers correlates with lower recurrence rates. Cancer Res 2007;67:10669–10676.
31 Kandalaft LE, Coukos G: The microenvironment of ovarian cancer: lessons on immune mediated tumor rejection or tolerance; in Wang E, Marincola FM (eds): Signatures of Rejection, 1st ed.Springer, New York, NY, 2010.
32 Adams SF, Levine DA, Cadungog MG, Hammond R, Facciabene A, Olvera N, Rubin SC, Boyd J, Gimotty PA, Coukos G: Intraepithelial t cells and tumor proliferation: impact on the benefit from surgical cytoreduction in advanced serous ovarian cancer. Cancer 2009;115:2891–2902.
33 Belgen H, Einhorn N, Sjovall K, Roschkes A, Ghadimis BM, McShane LM, Nilsson B, Shah K, Ried T, Auer G: Prognostic significance of cell cycle proteins and genomic instability in borderline, early and advanced stage ovarian carcinomas. Int J Gynecol Cancer 2000;10:477–487.
34 Duesberg P, Stindl R, Hehlmann R: Explaining the high mutation rates of cancer cells to drug and multidrug resistance by chromosome reassortments that are catalyzed by aneuploidy. Proc Natl Acad Sci U S A 2000;97:14295–14300.
35 McAlpine JN, Porter H, Kobel M, Nelson BH, Prentice LM, Kalloger SE, Senz J, Milne K, Ding J, Shah SP, Huntsman DG, et al.: BRCA1 and BRCA2 mutations correlate with tp53 abnormalities and presence of immune cell infiltrates in ovarian high-grade serous carcinoma. Mod Pathol 2012;25:740–750.
36 Shah CA, Allison KH, Garcia RL, Gray HJ, Goff BA, Swisher EM: Intratumoral t cells, tumor-associated macrophages, and regulatory t cells: association with p53 mutations, circulating tumor DNA and survival in women with ovarian cancer. Gynecol Oncol 2008;109:215–219.
37 Yau C, Esserman L, Moore DH, Waldman F, Sninsky J, Benz CC: A multigene predictor of metastatic outcome in early stage hormone receptor-negative and triple-negative breast cancer. Breast Cancer Res 2010;12:R85.
38 Karnoub AE, Dash AB, Vo AP, Sullivan A, Brooks MW, Bell GW, Richardson AL, Polyak K, Tubo R, Weinberg RA: Mesenchymal stem cells within tumour stroma promote breast cancer metastasis. Nature 2007;449:557–563.
39 Beresford MJ, Wilson GD, Makris A: Measuring proliferation in breast cancer: practicalities and applications. Breast Cancer Res 2006;8:216.
40 Sotiriou C, Wirapati P, Loi S, Harris A, Fox S, Smeds J, Nordgren H, Farmer P, Praz V, Haibe-Kains B, Desmedt C, et al.: Gene expression profiling in breast cancer: understanding the molecular basis of histologic grade to improve prognosis. J Natl Cancer Inst 2006;98:262–272.
41 Van 't Veer LJ, Dai H, van de Vijver MJ, He YD, Hart AA, Mao M, Peterse HL, van der Kooy K, Marton MJ, Witteveen AT, Schreiber GJ, et al.: Gene expression profiling predicts clinical outcome of breast cancer. Nature 2002;415:530–536.
42 Wang Y, Klijn JG, Zhang Y, Sieuwerts AM, Look MP, Yang F, Talantov D, Timmermans M, Meijer-van Gelder ME, Yu J, Jatkoe T, et al.: Gene-expression profiles to predict distant metastasis of lymph-node-negative primary breast cancer. Lancet 2005;365:671–679.
43 Hu Z, Fan C, Oh DS, Marron JS, He X, Qaqish BF, Livasy C, Carey LA, Reynolds E, Dressler L, Nobel A, et al.: The molecular portraits of breast tumors are conserved across microarray platforms. BMC Genomics 2006;7:96.
44 Teschendorff AE, Miremadi A, Pinder SE, Ellis IO, Caldas C: An immune response gene expression module identifies a good prognosis subtype in estrogen receptor negative breast cancer. Genome Biol 2007;8:R157.
45 Sabatier R, Finetti P, Cervera N, Lambaudie E, Esterni B, Mamessier E, Tallet A, Chabannon C, Extra JM, Jacquemier J, Viens P, et al.: A gene expression signature identifies two prognostic subgroups of basal breast cancer. Breast Cancer Res Treat 2011;126:407–420.
46 Sabatier R, Finetti P, Mamessier E, Raynaud S, Cervera N, Lambaudie E, Jacquemier J, Viens P, Birnbaum D, Bertucci F: Kinome expression profiling and prognosis of basal breast cancers. Mol Cancer 2011;10:86.
47 Rody A, Karn T, Liedtke C, Pusztai L, Ruckhaeberle E, Hanker L, Gaetje R, Solbach C, Ahr A, Metzler D, Schmidt M, et al.: A clinically relevant gene signature in triple negative and basal-like breast cancer. Breast Cancer Res 2011;13:R97.
48 Ascierto ML, Kmieciak M, Idowu MO, Manjili R, Zhao Y, Grimes M, Dumur C, Wang E, Ramakrishnan V, Wang XY, Bear HD, et al.: A signature of immune function genes associated with recurrence-free survival in breast cancer patients. Breast Cancer Res Treat 2012;131:871–880.

49 Cronin M, Sangli C, Liu ML, Pho M, Dutta D, Nguyen A, Jeong J, Wu J, Langone KC, Watson D: Analytical validation of the oncotype DX genomic diagnostic test for recurrence prognosis and therapeutic response prediction in node-negative, estrogen receptor-positive breast cancer. Clin Chem 2007;53:1084–1091.
50 Knauer M, Mook S, Rutgers EJ, Bender RA, Hauptmann M, van de Vijver MJ, Koornstra RH, Bueno-de-Mesquita JM, Linn SC, van 't Veer LJ: The predictive value of the 70-gene signature for adjuvant chemotherapy in early breast cancer. Breast Cancer Res Treat 2010;120:655–661.
51 Gianni L, Baselga J, Eiermann W, Guillem Porta V, Semiglazov V, Lluch A, Zambetti M, Sabadell D, Raab G, Llombart Cussac A, Bozhok A, et al.: Feasibility and tolerability of sequential doxorubicin/paclitaxel followed by cyclophosphamide, methotrexate, and fluorouracil and its effects on tumor response as preoperative therapy. Clin Cancer Res 2005;11:8715–8721.
52 Tsai MH, Cook JA, Chandramouli GV, DeGraff W, Yan H, Zhao S, Coleman CN, Mitchell JB, Chuang EY: Gene expression profiling of breast, prostate, and glioma cells following single versus fractionated doses of radiation. Cancer Res 2007;67:3845–3852.
53 Ma Y, Aymeric L, Locher C, Mattarollo SR, Delahaye NF, Pereira P, Boucontet L, Apetoh L, Ghiringhelli F, Casares N, Lasarte JJ, et al.: Contribution of IL-17-producing gamma delta t cells to the efficacy of anticancer chemotherapy. J Exp Med 2011;208:491–503.
54 West NR, Milne K, Truong PT, Macpherson N, Nelson BH, Watson PH: Tumor-infiltrating lymphocytes predict response to anthracycline-based chemotherapy in estrogen receptor-negative breast cancer. Breast Cancer Res 2011;13:R126.
55 Denkert C, Loibl S, Noske A, Roller M, Muller BM, Komor M, Budczies J, Darb-Esfahani S, Kronenwett R, Hanusch C, von Torne C, et al.: Tumor-associated lymphocytes as an independent predictor of response to neoadjuvant chemotherapy in breast cancer. J Clin Oncol 2010;28:105–113.
56 Apetoh L, Ghiringhelli F, Tesniere A, Obeid M, Ortiz C, Criollo A, Mignot G, Maiuri MC, Ullrich E, Saulnier P, Yang H, et al.: Toll-like receptor 4-dependent contribution of the immune system to anticancer chemotherapy and radiotherapy. Nat Med 2007;13:1050–1059.
57 Ghiringhelli F, Apetoh L, Tesniere A, Aymeric L, Ma Y, Ortiz C, Vermaelen K, Panaretakis T, Mignot G, Ullrich E, Perfettini JL, et al.: Activation of the NLRP3 inflammasome in dendritic cells induces IL-1beta-dependent adaptive immunity against tumors. Nat Med 2009;15:1170–1178.
58 Ignatiadis M, Singhal SK, Desmedt C, Haibe-Kains B, Criscitiello C, Andre F, Loi S, Piccart M, Michiels S, Sotiriou C: Gene modules and response to neoadjuvant chemotherapy in breast cancer subtypes: a pooled analysis. J Clin Oncol 2012;30:1996–2004.
59 Van der Burg SH, Kalos M, Gouttefangeas C, Janetzki S, Ottensmeier C, Welters MJ, Romero P, Britten CM, Hoos A: Harmonization of immune biomarker assays for clinical studies. Sci Transl Med 2011;3:108ps144.
60 O'Shea JJ, Paul WE: Mechanisms underlying lineage commitment and plasticity of helper CD4+ T cells. Science 2010;327:1098–1102.
61 Emamian ES, Leon JM, Lessard CJ, Grandits M, Baechler EC, Gaffney PM, Segal B, Rhodus NL, Moser KL: Peripheral blood gene expression profiling in Sjogren's syndrome. Genes Immun 2009;10:285–296.
62 Julia A, Erra A, Palacio C, Tomas C, Sans X, Barcelo P, Marsal S: An eight-gene blood expression profile predicts the response to infliximab in rheumatoid arthritis. PLoS One 2009;4:e7556.
63 McKinney EF, Lyons PA, Carr EJ, Hollis JL, Jayne DR, Willcocks LC, Koukoulaki M, Brazma A, Jovanovic V, Kemeny DM, Pollard AJ, et al.: A CD8+ T cell transcription signature predicts prognosis in autoimmune disease. Nat Med 2010;16:586–591, p. 581 following p. 591.
64 Baine MJ, Chakraborty S, Smith LM, Mallya K, Sasson AR, Brand RE, Batra SK: Transcriptional profiling of peripheral blood mononuclear cells in pancreatic cancer patients identifies novel genes with potential diagnostic utility. PLoS One 2011;6:e17014.

Treatment of Metastatic Triple-Negative Breast Cancer

Jennifer Glendenning, Sheeba Irshad & Andrew Tutt

Current Breast Cancer Reports

ISSN 1943-4588

Curr Breast Cancer Rep
DOI 10.1007/s12609-011-0062-4

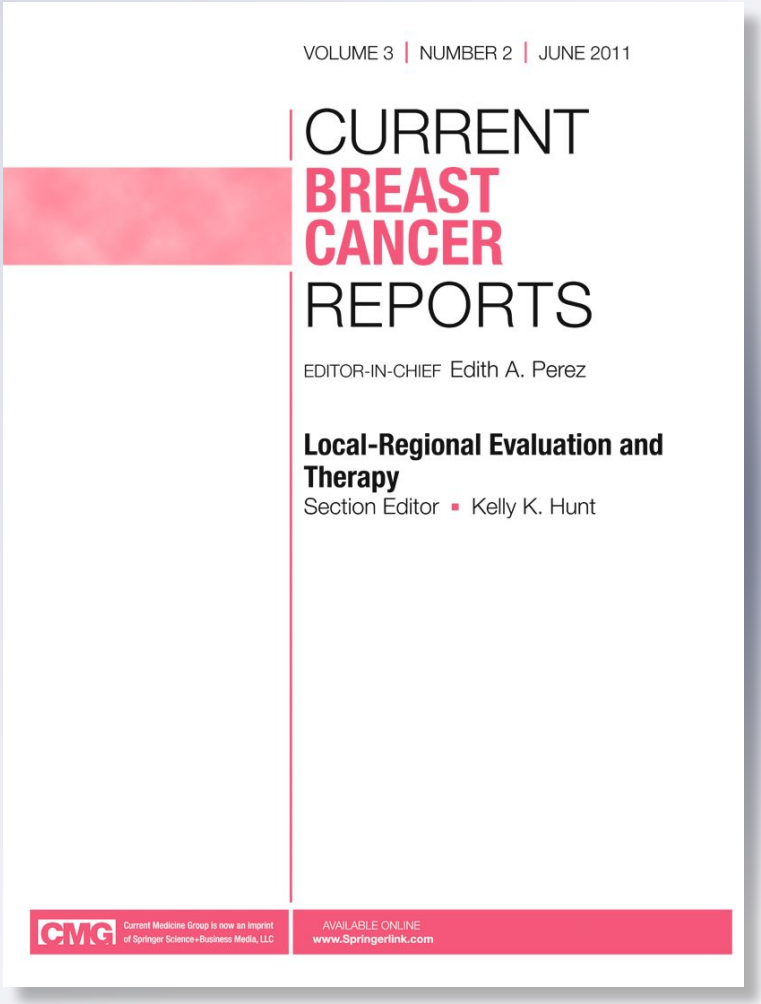

Springer

Curr Breast Cancer Rep
DOI 10.1007/s12609-011-0062-4

SYSTEMIC THERAPY (J O'SHAUGHNESSY, SECTION EDITOR)

Treatment of Metastatic Triple-Negative Breast Cancer

Jennifer Glendenning · Sheeba Irshad · Andrew Tutt

Abstract The triple-negative breast cancer (TNBC) phenotype, defined as the lack of estrogen and progesterone hormone receptors and the HER2 receptor, represents approximately 15% to 20% of all breast cancer cases. Challenges faced in management of these patients arise from the heterogeneity of TNBC and the absence of well-defined molecular targets. Subgroups derive significant benefit from cytotoxics however, patients with TNBC have higher rates of distant recurrence and a poorer prognosis than women with other breast cancer subtypes overall. Currently, cytotoxic chemotherapy is the only systemic treatment option at all stages of disease, and rational drug selection based on tumor biology remains an aspiration. In the context of relapse, the most efficacious regimens remain undefined and the typical clinical picture is one of rapid disease progression and little durable benefit to therapy. This article reviews current approaches in metastatic TNBC and considers novel therapies in development that may improve the outlook for those with this disease.

Keywords Triple negative breast cancer · Metastasis · Targeted therapy · Epidermal growth factor receptor · PARP inhibitor · Platinum · Angiogenesis

J. Glendenning · S. Irshad · A. Tutt
Breakthrough Breast Cancer Research Unit, Guy's Hospital, London, UK

J. Glendenning · S. Irshad · A. Tutt
Kings College London, Kings Health Partners AHSC, London, UK

J. Glendenning · S. Irshad · A. Tutt (✉)
Research Oncology, Guys Hospital,
3rd Floor Bermondsey Wing, Great Maze Pond,
London SE1 9RT, UK
e-mail: andrew.tutt@kcl.ac.uk

Published online: 14 January 2012

Introduction

Triple-negative breast cancer (TNBC) describes the 15% to 20% of breast cancers that are negative for estrogen and progesterone hormone receptors and the human epidermal growth factor receptor 2 (HER2). Challenges faced in management of these patients arise from the heterogeneity of TNBC and the absence of well-defined molecular targets. Subgroups derive significant benefit from cytotoxics with achievement of pathological complete response (pCR) in the neoadjuvant setting predicting excellent long-term outcome [1]. However, patients with TNBC have higher rates of distant recurrence and a poorer prognosis overall than women with other breast cancer subtypes [2]. Currently cytotoxic chemotherapy is the only systemic treatment option at all stages of disease, and rational drug selection based on tumor biology remains an aspiration. In the context of relapse, the most efficacious regimens remain undefined and the typical clinical picture is one of rapid disease progression and little durable benefit to therapy [3••]. In this article, we review current approaches in metastatic TNBC and consider novel therapies in development that may improve the outlook for those with this disease.

The Metastatic Triple-Negative Challenge

The approach to the patient with relapsed or metastatic TNBC shares the goal common to all settings of incurable advanced cancer relapse, namely improving both quantity and quality of life. Improvements in breast cancer survival are not solely attributable to better systemic therapy for early breast cancer. Through the early and late 1990s, cohort studies in metastatic breast cancer have demonstrated improvements in survival of nearly 30% reflecting use of

newer cytotoxics and targeted therapies in this setting [4]. However these gains appear limited to the hormone and/or HER2-positive breast cancer populations that have benefited from targeted therapies such aromatase inhibitors or trastuzumab [5]. Additionally, population-based studies report patterns of metastasis that differ in TNBC from that seen in the receptor-positive tumors. Relapses occur early, peaking at 2 to 3 years after diagnosis but subsequently decline and plateau with little risk of relapse and death after 5 years [2, 6]. Emerging data suggests that even small, node-negative, early TNBC may have disproportionately greater loco-regional and distant relapse risk than comparable tumors of other biological subtypes [7, 8]. Distant relapse is more likely to be visceral, with particular predilection for lung and brain [1], the latter being present in 14% to 25% of patients at first metastatic diagnosis and in nearly half prior to death [3••, 9]. Median duration of disease control on first- to third-line systemic therapy is brief (only 13, 9, and 4 weeks, respectively), and the median overall survival of only 13 months reflects the aggressive tempo of progression [3••].

Gene expression profiling has led to the identification of at least five breast cancer subtypes [10, 11]. Although molecular subtyping cannot yet guide rational treatment selection in routine clinical practice, it is helping to unravel the heterogeneity within TNBC. Approximately 80% of TNBCs are "basal-like" (BL), sharing features with tumors arising in *BRCA1* carriers [12], and its detection can be enhanced by use of additional immunohistochemical tests demonstrating CK5/6 and/or epidermal growth factor receptor (EGFR) positivity [13]. pCR rates following neoadjuvant taxane/anthracycline chemotherapy are usually greatest in the BL subgroup, and these patients have an excellent long-term prognosis [14]. However, the overall poor prognosis associated with TNBC is predominately driven by those within the BL subpopulation who have significant residual disease despite neoadjuvant chemotherapy [1, 11] and relative chemo-insensitivity in these patients is evident from the poor survival patterns following metastatic relapse [3••]. Next-generation sequencing indicates that a metastatic tumor derives from a selected subset of cells from the primary tumor that contain pre-existing mutations and that they also develop a small number of de novo mutations [15••]. Pragmatically, significant residual disease indicates high-risk of early relapse, but in the absence of a maintenance therapy strategy this prognostic insight does not translate into a means of improving outcomes. "Post-neoadjuvant" novel targeted therapy or alternative chemotherapy trials might well be focused on this very high-risk early TNBC population, but better understanding of the biology of residual disease and the heterogeneity of response to standard chemotherapy is required to develop treatment strategies that can positively impact on outcomes.

Rational Approaches in Relapsed TNBC

There is no global consensus regarding the optimal strategy for the treatment of metastatic breast cancer, and regional differences in availability and regulatory approval of newer agents further diversifies treatment patterns. In the context of adjuvant anthracycline therapy, recent cytotoxic guidelines recommend taxane-based first-line therapy (level 1 evidence) for metastatic TNBC, but there is no standard approach for subsequent lines of treatment [16]. Capecitabine is commonly prescribed following prior anthracycline and taxane exposure [17]. However, although this is a regulatory-approved standard of care and some patients derive benefit [18], analysis of a TNBC subset treated with this agent in the control arm of prospective trials provides little evidence supporting significant delay in progression in this population [19].

The relative efficacy of anthracycline and taxanes with regard to other cytotoxics in TNBC is controversial. For example, retrospective analysis of MA5 (adjuvant cyclophosphamide/methotrexate/5-FU [CMF] versus cyclophosphamide/epirubicin/5-FU [CEF]) suggested BL-breast cancers may not derive particular benefit from anthracyclines [20]. However, significant activity of classical CMF has been reported within the TNBC subset [21, 22], and lower cyclophosphamide exposure in the CEF arm potentially confounds attribution of differences. Furthermore, data from a meta-analysis of anthracycline versus nonanthracycline regimens in early breast cancer suggests benefits to anthracyclines in the TNBC subset [23]. There is a significant body of data from adjuvant trials incorporating taxanes suggesting that their addition to anthracycline- or anthracycline/cyclophosphamide-containing regimens particularly benefits node-positive disease [24–27], and in a neoadjuvant setting single-agent taxanes may be more active than anthracyclines in BL-breast cancer [28]. However, preclinical [29] and some clinical data in *BRCA1*-associated tumors indicate that these may be less taxane sensitive [30, 31]. Application of a *BRCA1*-associated defective DNA repair gene expression signature appears to differentiate sporadic TNBCs that are sensitive to anthracyclines and resistant to taxane-based chemotherapy [32], and a paclitaxel response metagene has been proposed as a paclitaxel-specific predictor of pCR in TNBC [33]. However, no validated signatures are yet available that can predict response to initial or subsequent chemotherapy or relapse risk overall.

Exploiting an Impaired DNA Damage Response

Gene expression microarray confirms molecular similarity between BL-TNBC and >90% of *BRCA1*-associated breast

cancer [34, 35]. Through the homologous recombination (HR) pathway, *BRCA1* plays an important role in DNA double-strand break (DSB) repair, contributing to the maintenance of genome stability. Disrupted HR arising as a result of either germline or functional inactivation would be expected to confer particular sensitivity to DNA damaging cytotoxics. Furthermore, tumors deficient in one DNA repair pathway will be more dependent on alternative DNA repair pathways, providing an opportunity for targeted therapy. Poly-ADP ribose polymerases (PARPs) are a family of enzymes that catalyze polymerization of poly-ADP ribose chains on target proteins, thereby modifying their action [36]. Nuclear PARPs have a key role in maintaining genomic integrity, in particular single-strand DNA break (SSB) repair through the base excision repair (BER) pathway. In the context of PARP inhibition, SSBs degenerate into DSBs, requiring repair through HR or alternative more error-prone DSB repair pathways. A BRCA-like phenotype can be found in over 50% of TNBC, and the mechanisms accounting for this include impairment of DNA damage induced by RAD51 protein focus induction, BRCA1-like array comparative genomic hybridization, and promoter methylation or reduced mRNA expression [37•, 38]. This overlap between *BRCA1*-associated tumors and sporadic TNBC is guiding investigational approaches in both early and advanced disease settings, where the focus has centered on the role of platinum and PARP inhibition.

Platinum

An observational study in 101 *BRCA1* carriers reported greater pCR following neoadjuvant cisplatin than other regimens (pCR 83% following cisplatin monotherapy compared to 22%, 21%, 8%, and 7% for AC, FAC, AT, or CMF, respectively) [30]. Platinum sensitivity is further supported by a small prospective study in 25 *BRCA1* carriers that reported 72% pCR following 4 cycles of cisplatin 75 mg/m^2 [39]. Using the same regimen in sporadic TNBC, 22% (6 of 28) achieved pCR and a further 50% achieved good pathological response (defined by Miller-Payne score of 3–5) [40]. Of six patients achieving pCR, two were subsequently found to be germline *BRCA* carriers, and both promotor methylation and low BRCA1 expression correlated with platinum response, supporting overlap between germline *BRCA1* carriers and at least a subset of those with sporadic TNBC. To date, no validated tests can predict platinum sensitivity in sporadic TNBC, but a *BRCA1*-like comparative genomic hybridization profile may discriminate a highly platinum sensitive subset [41]. In metastatic disease, retrospective data from several groups also support potentially greater platinum sensitivity and benefit over conventional regimens in the TNBC subtype [42–44]. The TBCRC009 prospective trial reported overall response rates (RR) of 30.2% (95% CI, 22.1%–39.4%) following first-line or second-line platinum using either cisplatin 75 mg/m^2 or carboplatin AUC6 selected according to investigator discretion [45]. Exploratory subgroup analysis of RR favored cisplatin over carboplatin (RR of 37% and 23%, respectively); however, this study cannot address questions regarding the optimal platinum agent. Both agents exceeded previous reports in comparable populations treated with cisplatin± cetuximab (RR of 10% and 20%, respectively) [46], and carboplatin with cetuximab (RR of 18%) [47]. The UK TNT trial (NCT00532727, Table 1) prospectively compares carboplatin AUC6 with docetaxel 100 mg/m^2. Powered to detect a 15% improvement in RR with carboplatin, this study will provide the first randomized data specifically evaluating platinum against an accepted standard in the relapsed TNBC and *BRCA1*-associated disease setting. Importantly, the study design integrates exploratory biological substudies that seek to identify predictive biomarkers of response.

PARP Inhibitors

PARP inhibitors (PARPi) are thought to exert their anticancer effects through at least two distinct but potentially complementary effects. Firstly through a *synthetic lethal* effect, whereby an accumulation of PARPi-induced SSBs increase DSBs, causing subsequent death in tumor cells deficient in HR, and secondly *sensitizing* tumor cells by exploiting a postulated differential reliance on the BER pathway for repair of therapeutic damage between malignant and normal tissues [48–50]. Early phase testing provided clinical proof of concept with sustained responses observed in *BRCA1/2* carriers, including>50% of patients with TNBC [51•].

PARP1 levels are commonly increased in TNBC and the BL subtype, and high levels adversely correlate with outcome. It is uncertain whether this reflects high rates of tumor proliferation or is secondary to the profound underlying DNA damage seen in TNBC, but it supports the premised importance of the BER pathway in breast cancer and a potential therapeutic role for PARPi [52–54]. In sporadic TNBC, the greatest body of clinical data comes from chemotherapy combinations with the agent iniparib (BSI-201). This agent initially described as a PARPi by BIPAR sciences is now thought to have substantially lower activity against PARP 1 [55] and is no longer described as a PARPi by Sanofi-Aventis. In metastatic TNBC, a randomised phase 2 study (n=123) compared gemcitabine 1000 mg/m^2 and carboplatin AUC 2 (days 1 and 8) (GC) alone or in combination with iniparib (5.6 mg/kg on days 1, 4, 8, and 11) given until disease progression, after which cross-over was permitted [56•]. The addition of iniparib improved clinical benefit rate from 34% to 56% (P=0.01), overall RR from 32% to 52% (P=0.02), and median progression-free

Table 1 Current active trials with focus in metastatic triple-negative breast cancer subset

NTN	Phase (accrual target #)	Primary endpoint	Therapeutic target	Targeted agent	Cytotoxic	TE	Study completion date
NCT00532727	3 (400)	ORR			Docetaxel vs carboplatin	Yes	Jan 2014
NCT01207102	2 (70)	PFS			Abraxane/carboplatin		Dec 2014
NCT01287624	3	PFS			Gemcitabine/cisplatin vs gemcitabine/taxol		Jan 2014
NCT 01238952	1 (35)	MTD			Carboplatin /NK012		July 2011
NCT00951054	2 (61)	ORR			NK012		Nov 2012
NCT01251874[a]	1 (42)	Tolerability	PARP1 / PARP2	Veliparib	Carboplatin	Yes	Nov 2012
NCT01104259	1 (36)	DLT	PARP1 / PARP2	Veliparib	Cisplatin/vinorelbine	Yes	May 2012
NCT00647062[a]	1 (101)	Safety+ biochemical changes	PARP1 / PARP2	Olaparib	Carboplatin	Yes	Dec 2009
NCT01173497	2 (40)	TTP	PARP1 / PARP2	Iniparib	Irinotecan		Jan 2013
NCT01176669	2 (60)	PFS	VEGFR-2	Aptinib	N/A		May 2012
NCT00472693	2 (37)	PFS	VEGF-A	Bevacizumab	Abraxane		Dec 2011
NCT00479674	2 (70)	PFS	VEGF-A	Bevacizumab	Abraxane/carboplatin		May 2015
NCT00691379	1/2 (46)	ORR	VEGF-A	Bevacizumab	Paclitaxel/carboplatin		Dec 2011
NCT01069796	2 (62)	ORR	VEGF-A	Bevacizumab	Paclitaxel/capecitabine		Dec 2015
NCT01207102	2 (70)_	PFS	VEGF-A	Bevacizumab	Gemcitabine/carboplatin		Dec 2014
NCT00608972	2 (50)	PFS	VEGF-A	Bevacizumab	Liposomal doxorubicin / carboplatin		Jun 2014
NCT01094184	4 (50)	Safety	VEGF-A	Bevacizumab	Taxane (investigator's choice)		April 2013
NCT00733408	2 (63)	PFS	VEGF-A+EGFR	Bevacizumab+ erlotinib	Paclitaxel albumin stabilised nanoparticles	Yes	Apr 2014
NCT00633464	2 (80)	ORR	EGFR	Cetuximab	Ixabepilone		May 2011
NCT01009983	2 (32)	ORR	EGFR	Panitumomab	Carboplatin/paclitaxel	Yes	June 2016
NCT00597597	2 (43)	PFS	EGFR	Erlotinib	N/A		April 2011
NCT01272141	2 (43)	ORR	EGFR+mTOR	Lapatinib+ everolimus	N/A		Feb 2013
NCT00998036	1 (18)	MTD	EGFR+mTOR	Erlotinib+ temsirolimus	Cisplatin		Sept 2014
NCT01186991	rPh2 (180)	PFS	VEGF-A+MET	Bevacizumab± metMAb	Paclitaxel		Apr 2014
NCT01147484	2 (38)	ORR	Met, VEGFR2	Foretinib	N/A	Yes	May 2013
NCT01127763	2 (28)	ORR/toxicity	mTOR	Everolimus (Rad001)	Carboplatin		May 2015
NCT01111825[a]	1/2 (60)	MTD/ ORR	mTor+multitargeted TKI (EGFR, HER2, HER4)	Temsirolimus+ neratinib	N/A	Yes	Apr 2013
NCT01333137	2 (140)	PFS	Cdk 4 D1, Cdk1 B, and Cdk9 T inhibitor	± PF276-00	Gemcitabine/carboplatin		Sep 2012
NCT01333423	1 (40)	DLT	CDK 2,7 & 9 inhibitor	Seliciclib	Liposomal doxorubicin		May 2014
NCT01307891	2 (60)	ORR	Death receptor 5	Tigituzumab	Abraxane	Yes	Oct 2014
NCT01151449	2 (50)	ORR	Gamma secretase	R04929096	N/A	Yes	Mar 2011
NCT01194908	2 (39)	MTD	Methylated estrogen receptor	Decitabine, LBH589 and Tamoxifen	N/A	Yes	Nov 2012

[a] Trial has planned subset analysis of triple-negative breast cancer

DLT dose-limiting toxicity, *PFS* progression-free survival, *MTD* maximum tolerated dose, *ORR* overall response rate, *TE* translational endpoints

survival (PFS) from 3.6 to 5.9 months (hazard ratio [HR] for progression 0.59; $P=0.01$). Although not powered to detect a survival benefit, a significant improvement in median overall survival (OS) from 7.7 to 12.4 months was observed (HR for death 0.57; $P=0.01$). A subsequent phase 3 study using the same study arms with cross-over permitted at centrally confirmed progression supports the favorable safety profile observed in phase 2 and provides further evidence

of activity for the addition of iniparib to GC with improved PFS (5.1 vs 4.1 months; HR 0.79 (95% CI, 0.65–0.98]; P= 0.027) [57•]. However, this study failed to meet the prespecified effect size for the co-primary PFS and OS endpoints (HR of 0.66 and 0.65, respectively) and exploratory analysis showed differences significant only in the second- or third-line setting. A potentially confounding enrichment for patients with shorter progression-free interval in the experimental arm was noted, and data are lacking on *BRCA* carrier status and potential for enrichment in either arm. Evaluation of gene expression signatures and central pathology review is awaited to facilitate understanding of these data. In line with the change in description by the sponsor, the activity of iniparib against PARP1 has recently been questioned, with a preclinical pharmacodynamic study showing absence of inhibition of poly-ADP ribose on target proteins, but the suggestion that that iniparib might suppress genes functioning in telomere maintenance pathways with PARP5/6 postulated as potential targets [55].

It is important to note that as iniparib is now thought to have very little PARP 1 inhibitory activity, questions regarding the role of potent PARPi in combination with chemotherapy in TNBC remain untested by any randomized phase 3 trial, and available efficacy and tolerability data are limited. Veliparib (ABT 888) in combination with temozolomide appears to be a tolerable where temozolomide dose is reduced, but a small single-arm study showed little initial evidence of efficacy in patients with sporadic TNBC [58]. The combination of olaparib with weekly paclitaxel for relapsed TNBC was evaluated in a single-arm initial safety cohort report. Synergistic toxicity with non–DNA-damaging taxane therapy was not predicted from this combination, but dose-limiting myelosuppression impervious to the addition of G-CSF prophylaxis and dose reduction following protocol amendment necessitated early closure of the trial. However, this combination achieved RR of 33% and 40% in the two cohorts, supporting the premise that the addition of PARPi to chemotherapy may improve response in the sporadic TNBC population [59]. Ongoing trials testing PARPi in advanced TNBC are included in Table 1.

Minor Groove Binders

A novel class of anticancer agents, DNA minor groove binders (MGBs) have recently been shown to be potent inducer of apoptosis in in vitro and in vivo preclinical tumor models. Moreover, brostallicin, a second-generation MGB, has been reported to retain sensitivity in chemo-resistant DNA mismatch repair-deficient cells [60–62] and demonstrated synergy in combination with cisplatin [63–65], suggesting its potential value in cancer treatment. Its unique mechanism of action and the promising results from phase 1 and phase 2 clinical trials [65–67] involving more than 230 patients led to a phase 2 study of brostallicin (NCT01091454, currently suspended) in combination with cisplatin in patients with refractory metastatic TNBC. Others agents examined in early phase analysis have shown some activity in HER2-positive and BRCA1/2 mutation-associated breast cancer, but not particular efficacy in unselected TNBC [68].

Targeting Angiogenesis

Angiogenesis plays an essential role in breast cancer development, invasion, and metastasis, and elevated levels of vascular endothelial growth factor (VEGF) correlate with poor outcome [69]. VEGF can be targeted by the monoclonal antibody bevacizumab, preventing its interaction with the VEGF receptor. VEGF is more commonly overexpressed in TNBC than other breast cancer subtypes [69]. In unselected metastatic breast cancer, three randomised phase 3 trials have demonstrated improvements in PFS and ORR in combination with taxane, anthracycline, or capecitabine chemotherapy agents [70–72]. Although no statistically significant benefit was seen, pooled OS data from these trials indicates an early benefit at 1 year (1-year survival control arm, 76.5%; bevacizumab/chemotherapy arm, 81.6%; P=0.003) [73] and suggests maximum benefit in TNBC, where PFS increased from 5.4 to 8.1 months with the addition of bevacizumab (stratified HR 0.68; 95% CI, 0.56–0.83, log rank P<0.001) [74].

Therapy-associated toxicity, such as hemorrhage risk, is of concern, particularly in the metastatic setting where impact of therapy on quality of life is an important consideration. Meta-analysis based on 16 randomized control trials, demonstrated that the addition of bevacizumab is associated with an increased risk of fatal adverse events, with an RR of 1.33 (incidence 2.9% vs 2.2%) [75]. Although risk appears greatest in tumors of pulmonary origin, metastatic TNBC characterized by pulmonary and cerebral disease is theoretically a breast cancer population at greater potential risk of complications from bevacizumab-associated haemorrhage. Following concerns regarding the balance of safety and efficacy, in December 2010 the FDA withdrew its licence in unselected metastatic breast cancer, but further evaluation in TNBC continues (Table 1) [76].

Antitubulin Agents

Two novel mitotic inhibitors, ixabepilone and eribulin, may be of benefit in taxane-resistant metastatic TNBC. Ixabepilone binds the beta-tubulin subunit, stabilizing microtubules and causing extended cell cycle arrest and apoptosis with

lower susceptibility to taxane resistance mechanisms, in particular β-tubulin III isoform over-expression [77]. Two randomized phase 3 studies have investigated capecitabine± ixebepilone in anthracycline and taxane pretreated breast cancer. Pooled analysis of the 443 patients with metastatic TNBC found improved ORR (31% vs 15%) and PFS (4.2 vs 1.7 months; HR 0.63 [95% CI, 0.52–0.77]), a trend toward OS (10.3 vs 9.0 months, respectively; HR 0.87 [95% CI, 0.71–1.07]) with the addition of ixabepilone [19]. Toxicity was considered acceptable with the most common adverse toxicities, comprising reversible peripheral neuropathy and neutropenia. The randomised phase 2 trial (NCT00633464, Table 1) will provide further data for ixepebilone in metastatic TNBC.

Eribulin is a non-taxane microtubule inhibitory agent with preclinical activity in paclitaxel-resistant cell lines [78]. The randomized phase 3 Eribulin Monotherapy versus Treatment of Physician's Choice in Patients with Metastatic Breast Cancer (EMBRACE) study compared eribulin monotherapy with investigator's choice in 762 patients with heavily pretreated metastatic breast cancer, including 19% with TNBC [79]. This is the first agent to demonstrate an OS benefit in unselected metastatic breast cancer (median OS 13.1 vs 10.6 months, HR 0.81 [95% CI, 0.66–0.99]) and had a toxicity profile no worse than the comparator arm. Eribulin has both FDA and European Medicines Agency (EMEA) approval for use in anthracycline- and taxane-pretreated breast cancer where patients have received at least two agents in the metastatic setting, but it requires further investigation to explore specific efficacy in TNBC. No trials are currently proposed in the metastatic setting, but using a 2-year DFS primary endpoint, NCT01401959 will evaluate adjuvant eribulin following failure to achieve pCR following neoadjuvant therapy in triple-negative, hormone receptor-positive/HER2-negative, and HER2-positive cohorts.

EGFR Inhibitors and Other Kinase Inhibitors

The epidermal growth factor receptor (EGFR) is strongly expressed in TNBCs, especially in the sporadic and BRCA-associated BL-subgroups, and this is associated with an inferior outcome [13, 80, 81]. Preclinical studies have shown synergy of anti-EGFR compounds and agents causing DNA damage [82]. The claudin low molecular subgroup is characterized by the low to absent expression of luminal differentiation markers, high enrichment for epithelial-to-mesenchymal transition (EMT) markers, immune response genes, and cancer stem cell-like features in addition to hormone and HER2 negativity [83]. EMT plays a major role in invasion and metastasis of TNBC [84, 85], which can be reversed in vitro by the EGFR inhibitor, erlotinib [86]. In metaplastic cancer, a rare but typical TN subgroup, EGFR gene amplification has been shown to be present in approximately 25% of cases [87]. These studies, along with others, have provided the impetus for a series of clinical trials evaluating EGFR inhibitors for patients with TNBC, alone and in combination with chemotherapeutics.

A phase 2 study, TBCRC-001, randomized patients with significantly pretreated metastatic TNBC to receive cetuximab 250 mg/m^2 either alone or in combination with weekly carboplatin AUC2. The cetuximab-alone arm showed a modest 6% response compared with a response rate of 18% in the combination arm [47]. In the randomized phase 2 BALI-1 trial, the addition of cetuximab to cisplatin was associated with an increase in the RR to 20% from 10% for the cisplatin-alone arm but did not achieve statistical significance (P=0.11) [46]. Subset analysis from another phase 2 study conducted by the US Oncology Group (225200 trial) showed a higher RR but no improvement in PFS with the addition of cetuximab (250 mg/m^2) to irinotecan (90 mg/m^2), carboplatin (AUC2) than to the same chemotherapy alone in patients with TNBC [88]. In phase 2 evaluation, the EGFR inhibitor gefitinib failed to show single-agent efficacy in ER-negative disease [89], and in the neoadjuvant setting the benefit of erlotinib appears limited to the ER-positive group only [90]. None of these cited trials required EGFR positivity as an eligibility criterion, and recent evidence indicates discrepancy between EGFR positive immunostaining and the presence of EGFR mutations in TNBC. Trials evaluating other EGFR inhibitors in TNBC are ongoing (Table 1), but to date a role in unselected TNBC appears limited, indicating the need for EGFR expression testing and identification of appropriate companion diagnostic in future studies [91].

Although a proportion of high-expressing EGFR tumors promote cell proliferation via the activation of the RAS/MAPK/MAPK kinase, a number of other tumor-promoting mechanisms that impact EGFR and downstream pathways are seen in TNBC, and rationally designed clinical trials targeting multiple pathways may be required to achieve synergistic efficacy [92–96]. In TBCRC001 trial, serial biopsies of tumors prior to and following cetuximab therapy demonstrated that whereas the majority of the patients had tumors with EGFR pathway activation by gene expression array, cetuximab was only effective in 25% of cases, and all clinical benefit was seen in this group [47]. The approach of using multityrosine kinase inhibitors, such has dasatinib or sunitinib, is being evaluated in TNBC. A phase 2 study of dasatinib, an orally bioavailable multi-tyrosine kinase inhibitor of *src* and *abl,* in patients with advanced TNBC reported a modest (< 5%) response [97]. The main targets of dasatinib are yet to be fully validated, although an ongoing study (NCT00780676) is evaluating a predictive gene signature for as a single agent in different breast cancer subtypes.

Sunitinib, a multi-tyrosine kinase inhibitor with antiangiogenic properties was reported a response rate of 15% in a subset with TNBC [98]. However phase 3 evaluations of sunitinib as monotherapy and in combination with chemothrapy were all negative in patients with advanced HER2-negative breast cancer [99, 100]. An ongoing adjuvant study evaluating sunitinib in combination with carboplatin and paclitaxel in TNBC is awaited (NCT00887575).

Recent interest has also focused on targeting the c-MET oncogene, which encodes the tyrosine kinase receptor for hepatocyte growth factor in BL breast carcinoma [52, 101, 102]. MET appears to be a key regulator of EGFR tyrosine kinase inhibitor resistance in cancer due to trans-phosphorylation via an MET/Src-mediated signaling pathway; thus, clinical benefit is likely to require simultaneous inhibition of EGFR and MET signals [103]. In TNBC, a high prevalence of loss of the tumor suppressor protein tyrosine phosphatase PTPN12, which interacts with another tyrosine kinase, platelet-derived growth factor receptor-b (PDGFR-b), has been reported. Dual blockade with lapatinib and sunitinib slows the growth of xenografted TNBC tumors in preclinical evaluation [94]. Additionally, preclinical data demonstrate that inhibition of the mitogen-activated protein kinase (MEK), a component of the MAPK pathway, in TNBC cells leads to constitutive activation of the phosphatidylinositol b-kinase (P13K) pathway, with increased activation of the downstream targets AKT and mTOR [104]. Combined inhibition of MEK and P13K pathways have been shown to result in increased cellular effect in TN cells, suggesting combined inhibition may be a rational approach for a future clinical trial [96]. Loss of the tumor suppressor phosphatase and tensin homolog on chromosome 10 (PTEN) appears frequently in patients with TNBC, and a significant negative correlation has been seen between low PTEN expression and activation of a downstream P13K targets, mTOR and AKT [105]. Two randomized trials evaluating the role of an oral mTOR inhibitor, everolimus (RAD001), in patients with either metastatic (NCT00827567) or locally advanced TNBC (NCT00930930) are ongoing.

High throughput tumor profiling technologies have identified a number of new targets that are beyond the scope of this review; however, some of the more promising targets are summarized in Table 2. Identification of predictive biomarkers and simultaneous blockade of multiple signalling pathways is likely to be required for optimal therapeutic benefit in patients with TN disease.

Opportunities to Do Better

Management of those with metastatic TNBC requires an integrated approach. There are no data from any RCTs to support a specific follow-up strategy for breast cancer [106], but it is possible that patients with TNBC may benefit from follow-up better related to the clinical behavior associated with this biological subtype. The characteristic rapid tempo of progression may detrimentally impact fitness for therapy and clinical trial eligibility. The majority of TNBC relapses occur in the first 3 years [3••]; therefore, in individuals predicted to be at high risk of relapse, such those with significant residual disease after neoadjuvant therapy, it

Table 2 Other targets in triple-negative breast cancer

Target	Rationale in TNBC	Drug development
Androgen receptor	Between 10% and 35% of TNBC express the androgen receptor [113, 114].	Ongoing phase 2 trial using bicalutamide, an antiandrogen, in the treatment of androgen-positive TNBC (NCT00468715)
		Ongoing phase 1/2 using abiraterone (NCT00755885) in ER-positive or ER-negative and androgen receptor-positive tumors
Fibroblast growth receptor 2 (FGFR2)	Amplified in up to 4% of TNBC [115]	Phase 2 of an FGFR inhibitor (TKI258) reported antitumor activity in this heavily pretreated breast cancer population [116]
Heat shock protein (HSP)-90	PU-H71, novel purine scaffold HSP-90 inhibitor, has shown preclinical activity in TNBC [117]	The first-in-human phase 1 trial of PU-H71 in patients with advanced malignancies has recently been initiated (NCT01393509)
Tumor necrosis factor-related apoptosis-inducing ligand (TRAIL)	TRAIL functions as a metastasis suppressor by activating pro-apoptotic TRAIL receptors and a subset of TNBCs; those with mesenchymal features have been reported to be sensitive to TRAIL-mediated apoptosis [118]	

TNBC triple-negative breast cancer

may be appropriate to maintain active oncologic follow-up in the highest risk period.

Patients with TNBC are at particular risk of pulmonary and central nervous system metastasis [1]. Survival following diagnosis of cerebral metastasis (CM) differs according to breast cancer subtype and is poorest in those with TNBC [107, 108]. A study reported the brain to be the first site or only site of metastasis in 32% of patients with TNBC, with 35% of immunohistochemistry-defined BL-breast cancer subset having CM [109]. Survival reflected clinical parameters relating to underlying fitness, age, and systemic disease control but not biological markers (CK5/6, EGFR, c-kit) differentiating between basal and non-BL breast cancer subtypes. The propensity for CM in TNBC requires further investigation to understand the driving biology and facilitate identification of those at highest risk with a view to preventive or early detection screening and intervention activities. Unlike other breast cancer subtypes, those with TNBC derive little benefit from systemic therapy after diagnosis of CM, likely reflecting both poor patient fitness and activity of systemic therapy in the context of pretreated advanced disease [108]. Proactive use of CNS imaging to screen the brain at time of metastatic presentation remains untested but approaches directed at those with significant residual disease after neoadjuvant chemotherapy who have the highest risk might include trials incorporating CNS screening and/or prophylaxis with a rational comparable to small cell lung carcinoma. In patients with TNBC brain metastasis, NCT01173497 will evaluate iniparib+irinotecan following and in place of radiotherapy (Table 1).

Tumors arising in *BRCA1* carriers are typically of TN phenotype and although early evidence of activity of potent PARPi [51•, 110, 111] and of platinum salts [30] is most apparent in BRCA-associated cancers, genetic testing is currently routinely performed to guide primary cancer risk-reduction strategies but not systemic therapy selection or clinical trial entry. Diagnostic *BRCA* testing is generally offered to "high-risk" sporadic subpopulations, including those diagnosed at younger age, with bilateral presentation, or developing second primary cancers in addition to those with a significant family history. Definitions of "low age" vary, but expanding access to genetic testing to include all women with TNBC diagnosed younger than 50 years of age has been estimated to be both cost-effective and reduce subsequent breast and ovarian cancer risks by 23% and 41%, respectively [112].

Conclusions

Metastatic TNBC remains a heterogeneous disease characterized by rapid progression and poorer survival outcomes when compared with other breast cancer subtypes, and effective therapy remains an area of significant unmet need. Diagnosis does not describe a single disease entity but a collection of molecular subtypes currently unified by absence of predictive markers for endocrine and anti-HER2 therapy. Better characterization of molecular determinants of chemo-sensitivity and resistance and identification of targeted agents with associated positive companion diagnostics will be required to improve outcomes. In the current setting of modest activity of standard therapy for advanced TNBC, patients should be encouraged to participate in clinical trials. Optimal evaluation of current agents and those in development will require an integrated and co-operative approach to TNBC-specific clinical trial design, thus permitting rapid accrual and trial evolution in this breast cancer subtype.

Disclosure J. Glendenning: none; S. Irshad: none; A. Tutt has been a consultant for Sanofi-Aventis, Clovis, Pfizer, and Eisai; has received a grant from Sanofi-Aventis; has received honoraria from AstraZeneca; has had travel expenses covered by Sanofi-Aventis, AstraZeneca, and Roche; and has patents from the Institute of Cancer Research London relating to PARP inhibition in *BRCA1*- and *BRCA2*-associated cancers.

References

Papers of particular interest, published recently, have been highlighted as:
- • Of importance
- •• Of major importance

1. Liedtke C. Mazouni c, Hess KR, Andre F, Tordai A, Mejia JA, et al. Response to Neoadjuvant Therapy and Long-Term Survival in Patients with Triple-Negative Breast Cancer J Clin Oncol. 2008;26(8):1275–81.
2. Dent RA, Trudeau M, Pritchard KI, Wedad MH, Kahn HK, Sawka CA, et al. Triple-negative breast cancer: clinical features and patterns of recurrence. Clin Cancer Res. 2007;13:4429–34.
3. •• Kassam F, Enright K, Dent RA, Dranitsaris G, Myers J, Flynn C, et al. Survival outcomes for patients with metastatic triple-negative breast cancer: implications for clinical practice and trial design. Clin Breast Cancer. 2009;9(1):29–33. *This article reports the clinical picture of rapid disease progression and little durable benefit to therapy on diagnosis of metastatic triple-negative breast cancer.*
4. Chia SK, Speers CH, D'yachkova Y, Kang A, Malfair-Taylor S, Barnett J, et al. The imact of new chemotherapeutic and hormone agents on survival in a population-based cohort of women with metastatic breast cancer. Cancer. 2007;110(5):973–9.
5. Shigematsu H, Kawaguchi H, Nakamure Y, Tanaka K, Shiotani S, Koga C, et al. Significant surival improvment of patients with recurrrent breast cancer in the periods 2001-2008 and 1992-2000. BMC Cancer. 2011;31(11).
6. Esserman L, Moore D, Tsing P, Chu P, Yau C, Ozanne E, et al. Biologic markers determine both the risk and the timing of

recurrence in breast cancer. Breast Cancer Res Treat. 2011;129 (2):607–16.
7. Abdulkarim BS, Cuartero J, Hanson J, Deschenes J, Lesniak D, Sabri S. Increased risk of locoregional recurrence for women with T1-2N0 triple-negative breast cancer treated with modified radical mastectomy without adjuvant radiation therapy compared with breast-conserving therapy. J Clin Oncol. 2011;29(21):2852–8.
8. Kaplan HG, Malmgren JA, Atwood M. T1N0 triple negative breast cancer: risk of recurrence and adjuvant chemotherapy. The Breast Journal. 2009;15(5):454–60.
9. Lin N, Claus E, Sohl J, Razzak AR, Arnaout A, Winer EP. Sites of distant recurrence and clinical outcomes in patients with metastatic triple-negative breast cancer: high incidence of central nervous systemic metastasis. Cancer. 2008;113 (10):2638–45.
10. Sorlie T, Perou CM, Tibshirani R, Aas T, Geisler S, Johnsen H, et al. Gene expression patterns of breast carcinomas distinguish tumour subclasses with clinical implications. Proceeding of the National Academy of Sciences of the United States of America. 2001;98(19):10869-74.
11. Cheang MCU, Voduc D, Bajdik C, Leung S, McKinney S, Chia SK, et al. Basal-like breast cancer defined by five biomarkers has superior prognostic value than the triple-negative phenotype. Clinical Cancer Research. 2008;14(15):1368–76.
12. Reis-Filho JS, Tutt ANJ. Triple negative tumours: a critical review. Histopathology. 2008;52(1):108–18.
13. Nielsen TO, Forrest DH, Karaca G, Hu Z, Hernandez-Boussard T, Livasy C, et al. Immunohistochemical and clinical characterisation of the basal-like subtype of invasive breast carcinoma. Clinical Cancer Research. 2004;10:5367–74.
14. Rouzier R, Perou CM, Symmans WF, Ibrahim N, Cristofanilli M, Andersone K, et al. Breast cancer molecular subtypes respond differently to preoperative chemotherapy. Clinical Cancer Research. 2005;11(16):5678–85.
15. •• Ding L, Ellis MJ, Li S, Larson DE, Chen K, Wallis JW, et al. Genome remodelling in a basal-like breast cancer metastasis and xenograft. Nature. 2010;464(7291):999–1005. *This article reviews next-generation sequencing genomic analysis of a primary basal-like breast cancer tumor, a brain metastasis, and a first-passage xenograft derived from the primary tumor and suggests that the metastatic tumor forms from a selected subset of cells from the primary tumor that contain pre-existing mutations and also develops a small number of de novo mutations*.
16. Cardoso F, Senkus-Konefka E, Fallowfield L, Costa A, Castiglione M. Locally recurrent or metastatic breast cancer: ESMO Clinical Practice Guidelines for diagnosis, treatment and follow-up. Ann Oncol. 2010;21 Suppl 5:v15–9.
17. Kilburn LS, JL, Bliss JM, Tutt AN on behalf of the TNT Trial Management Group. . Treatment options for locally advanced or metastatic triple negative breast cancer: A survey of current UK practice. . The Breast. 2009;18(Suppl 1): S65 (Abstract 0186).
18. Kotsori A, Dolly S, Sheri A, Parton M, Shaunak N, Ashley S, et al. Is capecitabine efficacious in triple negative metastatic breast cancer? Oncology. 2010;79(5–6):331–6.
19. Rugo HS, Roche H, Thomas ES, K B, Chung HC, Lerzo GL, et al. Ixabepilone plus capecitabine in patients with triple negative tumours: A pooled analysis of patients from two large phase III clinical studies. San Antonio Breast Cancer Symposium. 2008: abstract 3057.
20. Cheang M, Chia SK, Tu D, Jiang S, Shepherd LE, Pritchard KI, et al. Anthracyclines in basal breast cancer: The NCIC-CTG trial MA5 comparing adjuvant CMF to CEF. J Clin Oncol. 2009;27 (15S):ASCO Meeting Abstract 519.
21. Colleoni M, Cole BF, Viale G, Regan MM, Price KN, Maiorano E, et al. Classical cyclophosphamide, methotrexate, and fluorouracil chemotherapy is more effective in triple-negative, node-negative breast cancer: results from two randomized trials of adjuvant chemoendocrine therapy for node-negative breast cancer. J Clin Oncol. 2010;28(18):2966–73.
22. Falo C, Moreno A, Varela M, Lloveras B, Figueras A, Escobedo A. HER-2/neu status and response to CMF: retrospective study in a series of operable breast cancer treated with primary CMF chemotherapy. J Cancer Res Clin Oncol. 2007;133(7):423–9.
23. Di Leo A IJ, Piette F. A meta-analysis of phase III trials evaluating the predictive value of HER2 and topoisomerase II alpha in early breast cancer patients treated with CMF or anthracycline-based adjuvant therapy. Breast Cancer Res Treat 2008;107: Abstract 705.
24. Roche H, Fumoleau P, Spielmann M, Canon JL, Delozier T, Serin D, et al. Sequential adjuvant epirubicin-based and docetaxel chemotherapy for node-positive breast cancer patients: the FNCLCC PACS 01 Trial. J Clin Oncol. 2006;24(36):5664–71.
25. Hugh J, Hanson J, Cheang MC, Nielsen TO, Perou CM, Dumontet C, et al. Breast cancer subtypes and response to docetaxel in node-positive breast cancer: use of an immunohistochemical definition in the BCIRG 001 trial. J Clin Oncol. 2009;27(8):1168–76.
26. Hayes DF, Thor AD, Dressler LG, Weaver D, Edgerton S, Cowan D, et al. HER2 and response to paclitaxel in node-positive breast cancer. N Engl J Med. 2007;357(15):1496–506.
27. Martin M, Segui MA, Anton A, Ruiz A, Ramos M, Adrover E, et al. Adjuvant docetaxel for high-risk, node-negative breast cancer. N Engl J Med. 2010;363(23):2200–10.
28. Martin M RA, Lopez Garcia-Asenjo, Cheang. M.C, Oliva. B, Garcia Saenz. J, He X, Caldes T, Diaz-Rubio. E, Perou. C.M. Molecular and genomic predictors of response to single-agent doxorubicin (ADR) versus single-agent docetaxel (DOC) in primary breast cancer (PBC). J Clin Oncol. 2010;28:15s (suppl; abstr 502).
29. Quinn JE, Kennedy RD, Mullan PB, Gilmore PM, Carty M, Johnston PG, et al. BRCA1 functions as a differential modulator of chemotherapy-induced apoptosis. Cancer Res. 2003;63 (19):6221–8.
30. Byrski T, Gronwald J, Huzarski T, Grzybowska E, Budryk M, Stawicka M, et al. Pathologic complete response rates in young women with BRCA1-positive breast cancers after neoadjuvant chemotherapy. J Clin Oncol. 2010;28(3):375–9.
31. Delaloge S, Bidard F, El Masmoudi Y, de Paillerets BB, Caron O, Bourgier C, et al. BRCA1 germ-line mutation: Predictive of sensitivity to anthracyclin alkylating agents regimens but not to taxanes? J Clin Oncol. 2008;26(15s):ASCO Meeting Abstract 574.
32. Rodriguez A, Makris A, Wu M, Rimawi M, Froehlich A, Dave B, et al. DNA repair signature is associated with anthracycline response in triple negative breast cancer patients. Breast Cancer Res Treat. 2010;123(1):189–96.
33. Juul N, Szallasi Z, Eklund AC, Li Q, Burrell RA, Gerlinger M, et al. Assessment of an RNA interference screen-derived mitotic and ceramide pathway metagene as a predictor of response to neoadjuvant paclitaxel for primary triple-negative breast cancer: a retrospective analysis of five clinical trials. The Lancet Oncology. 2010;11(4):358–65.
34. Foulkes WD, Stefansson IM, Chappuis PO, Begin LR, Goffin JR, Wong N, et al. Germline BRCA1 mutations and a basal epithelial phenotype in breast cancer. J Nat Cancer Inst. 2003;95(19):1482–5.
35. Sorlie T, Tibshirani R, Parker J, Hastie T, Marron JS, Nobel A, et al. Repeated observation of breast tumor subtypes in independent gene expression data sets. Proc Natl Acad Sci U S A. 2003;100 (14):8418–23.
36. Schreiber V, Dantzer Fo, Ame J-C, de Murcia G. Poly(ADP-ribose): novel functions for an old molecule. Nat Rev Mol Cell Biol. 2006;7(7):517–28.

37. • Graeser M, McCarthy A, Lord CJ, Savage K, Hills M, Salter J, et al. A marker of homologous recombination predicts pathological complete response to neoadjuvant chemotherapy in primary breast cancer. Clinical Cancer Research. 2010;16(24):6159–68. *This study raises the possibility of functional analysis of DNA repair competance in relation to therapy response in neoadjuvant models of breast cancer.*
38. Lips EH, Mulder L, Hannemann J, Laddach N, Vrancken Peeters MTFD, van de Vijver MJ, et al. Indicators of homologous recombination deficiency in breast cancer and association with response to neoadjuvant chemotherapy. Ann Oncol. 2011;22 (4):870–6.
39. Gronwald J, Byrski T, Huzarski T, Dent RA, Bielicka V, Zuziak D, et al. Neoadjuvant therapy with cisplatin in BRCA1-positive breast cancer patients. J Clin Oncol. 2009;27(15s):Abstract 502.
40. Silver DP, Richardson AL, Eklund AC, Wang ZC, Szallasi Z, Li Q, et al. Efficacy of neoadjuvant cisplatin in triple-negative breast cancer. J Clin Oncol. 2010;28(7):1145–53.
41. Vollebergh MA, Lips EH, Nederlof PM, Wessels LFA, Schmidt MK, van Beers EH, et al. An aCGH classifier derived from BRCA1-mutated breast cancer and benefit of high-dose platinum-based chemotherapy in HER2-negative breast cancer patients. Ann Oncol. 2011;22(7):1561–70.
42. Sirohi B, Arnedos M, Popat S, Ashley S, Nerurkar A, Walsh G, et al. Platinum-based chemotherapy in triple-negative breast cancer. Ann Oncol. 2008;19(11):1847–52.
43. Staudacher L, Cottu PH, Dieras V, Vincent-Salomon A, Guilhaume MN, Escalup L, et al. Platinum-based chemotherapy in metastatic triple-negative breast cancer: the Institut Curie experience. Ann Oncol. 2011;22(4):848–56.
44. Villarreal-Garza CM, Clemons M, Kassam F, Enright K, Verma S, Myers JA, et al. Platinum-based chemotherapy in triple-negative breast cancer. J Clin Oncol. 2011;29(15s):ASCO Meeting Abstract 1090.
45. Isakoff SJ, Goss PE, Mayer EL, Traina TA, Carey LA, Krag K, et al. TBCRC009: A multicenter phase II study of cisplatin or carboplatin for metastatic triple-negative breast cancer and evaluation of p63/p73 as a biomarker of response. J Clin Oncol. 2011;29(15s):ASCO Meeting Abstract 1025.
46. Baselga J, Gomez P, Awada a, Greil R, Braga S, Climent MA, et al. The addition of cetuximab to cisplatin increases overall response rate (ORR) and Progression Free Survival (PFS) in metastatic triple negative breast cancer (TNBC): results of a randmomised phase II study (BALI-1). Ann Oncol. 2010;21: viii96-viii121.
47. Carey LA, Rugo HS, Marcom PK, Irvin W, Ferraro M, Burrows E, et al. TBCRC 001: EGFR inhibition with cetuximab added to carboplatin in metastatic triple-negative (basal-like) breast cancer. J Clin Oncol. 2008;26(15s):ASCO Meeting Abstract 1009.
48. Farmer H, McCabe N, Lord C, Tutt A, Johnson D, Richardson T, et al. Targeting the DNA repair defect in BRCA mutant cells as a therapeutic strategy. Nature. 2005;434:917–21.
49. Bryant H, Schultz N, Thomas H, Parker K, Flower D, Lopez E, et al. Specific killing of BRCA2-deficient tumours with inhibitors of poly(ADP-ribose) polymerase. Nature. 2005;434:913–7.
50. Donawho CK, Luo Y. ABT-888, an orally active Poly(ADP-Ribose) Polymerase Inhibitor that potentiates DNA-damaging agents in preclinical tumour models. Clinical Cancer Research. 2007;13(9):2728–37.
51. • Tutt AN, Robson M, Garber JE, Domchek SM, Audeh W, Weitzel JN, et al. Oral poly(ADO-ribose) polymerase inihibitor in patients with BRCA1 or BRCA2 mutations and advanced breast cancer: a proof-of-concept trial. Lancet. 2010;376 (9737):235–44. *This is a proof-of-concept phase 2 trial showing synthetic lethal effect of potent PARP inhibition in BRCA1 and BRCA2 mutation-associated metastatic breast cancer.*
52. Goncalves A, Finetti P, Sabatier R, Gilabert M, Adelaide J, Borg J, et al. Poly(ADP-ribose) polymerase-1 mRNA expression in human breast cancer: a meta-analysis. Breast Cancer Res Treat. 2010;127(1):273–81.
53. Cotter MB, Pierce A, McGowan PM, Madden SF, Flanagan L, Quinn C, et al. PARP1 in triple-negative breast cancer: Expression and therapeutic potential. J Clin Oncol. 2011;29(15s):ASCO Meeting Abstract 1061.
54. Ossovskaya V, Koo IC, Kaldjian EP, Alvares C, Sherman BM. Upregulation of poly(ADP-ribose) polymerase-1 (PARP1) in triple-negative breast cancer and other primary human tumor types. Genes and cancer. 2010;1(8):812–21.
55. Jiuping Ji MPL, Mitsutaka Kadota, Yiping Zhang1, Ralph E. Parchment1, Joseph E. Tomaszewski3, James H. Doroshow. Pharmacodynamic and pathway analysis of three presumed inhibitors of poly (ADP-ribose) polymerase: ABT-888, AZD2281, and BSI201 Proc AACR. 2011;Abstract 4527.
56. • O'Shaughnessy J, Osborne C, Pippen JE, Yoffe M, Patt D, Rocha C, et al. Iniparib plus Chemotherapy in Metastatic Triple-Negative Breast Cancer. New Engl J Med. 2011;354 (3):205–14. *This article contains phase 2 data providing evidence of progression-free and overal survival advantage to the addition of iniparib to gemcitabine and carboplatin in metastatic triple-negative breast cancer.*
57. • O'Shaughnessy J, Schwartzberg LS, Danso MA, Rugo HS, Miller K, Yardley DA, et al. A randomized phase III study of iniparib (BSI-201) in combination with gemcitabine/carboplatin (G/C) in metastatic triple-negative breast cancer (TNBC). ASCO Meeting Abstracts 2011 June 9, 2011 29 (15_suppl):1007. *This is an important follow-up of a phase 3 trial of similar design with significant weakening of effect of iniparib in the design used.*
58. Isakoff SJ, Overmoyer B, Tung NM, Gelman RS, Giranda VL, Bernhard KM, et al. A phase II trial of the PARP inhibitor veliparib (ABT-888) and temozolamide for metastatic breast cancer. J Clin Oncol. 2010;28(15s):ASCO Meeting Abstract 1019.
59. Dent RA, Lindeman GJ, Clemons M, Wildiers H, Chan A, McCarthy A, et al. Safety and efficacy of the oral PARP inhibitor olaparib (AZD2281) in combination with paclitaxel for the first- or second-line treatment of patients with metastatic triple-negative breast cancer: Results from the safety cohort of a phase I/II multicenter trial. J Clin Oncol. 2010;28(15s):ASCO Meeting Abstract 1018.
60. Geroni C, Marchini S, Cozzi P, Galliera E, Ragg E, Colombo T, et al. Brostallicin, a novel anticancer agent whose activity is enhanced upon binding to glutathione. Cancer Res. 2002;62 (8):2332–6.
61. Fedier A, Fowst C, Tursi J, Geroni C, Haller U, Marchini S, et al. Brostallicin (PNU-166196)–a new DNA minor groove binder that retains sensitivity in DNA mismatch repair-deficient tumour cells. Br J Cancer. 2003;89(8):1559–65.
62. Fedier A, Fink D. Mutations in DNA mismatch repair genes: implications for DNA damage signaling and drug sensitivity (review). Int J Oncol. 2004;24(4):1039–47.
63. Sabatino MA, Colombo T, Geroni C, Marchini S, Broggini M. Enhancement of in vivo antitumor activity of classical anticancer agents by combination with the new, glutathione-interacting DNA minor groove-binder, brostallicin. Clin Cancer Res. 2003;9(14):5402–8.
64. Lorusso D, Mainenti S, Pietragalla A, Ferrandina G, Foco G, Masciullo V, et al. Brostallicin (PNU-166196), a new minor groove DNA binder: preclinical and clinical activity. Expert Opin Investig Drugs. 2009;18(12):1939–46.
65. Caponigro F, Lorusso D, Fornari G, Barone C, Merlano M, Airoldi M, et al. Phase I dose-escalation study of brostallicin, a minor groove binder, in combination with cisplatin in patients with

advanced solid tumors. Cancer Chemother Pharmacol. 2010;66 (2):389–94.
66. Ten Tije AJ, Verweij J, Sparreboom A, Van Der Gaast A, Fowst C, Fiorentini F, et al. Phase I and pharmacokinetic study of brostallicin (PNU-166196), a new DNA minor-groove binder, administered intravenously every 3 weeks to adult patients with metastatic cancer. Clin Cancer Res. 2003;9(8):2957–64.
67. Lockhart AC, Howard M, Hande KR, Roth BJ, Berlin JD, Vreeland F, et al. A phase I dose-escalation and pharmacokinetic study of brostallicin (PNU-166196A), a novel DNA minor groove binder, in adult patients with advanced solid tumors. Clin Cancer Res. 2004;10(2):468–75.
68. Tedesco KL, Blum JL, Goncalves A, Lubinski J, Osborne CRC, Lardelli P, et al. Final results of a phase II trial of trabectedin (T) in triple-negative, HER2-positive, and BRCA1/2 germ-line-mutated metastatic breast cancer (MBC) patients (pts). J Clin Oncol. 2011;29(15s):ASCO Meeting Abstract 1125.
69. Linderholm BK, Hellborg H, Johansson U, Elmberger G, Skoog L, LehtiÃ¶ J, et al. Significantly higher levels of vascular endothelial growth factor (VEGF) and shorter survival times for patients with primary operable triple-negative breast cancer. Ann Oncol. 2009;20(10):1639–46.
70. Miller K, Wang M, Gralow J, Dickler M, Cobleigh M, Perez EA, et al. Paclitaxel plus bevacisumab versus paclitaxel alone for metastatic breast cancer. N Eng J Med. 2007;357 (26):2666–76.
71. Miles DW, Chan A, Dirix LY, Cortes J, Pivot X, Tomczak P, et al. Phase III study of bevacizumab plus docetaxel compared with placebo plus docetaxel for the first-line treatment of human epidermal growth factor receptor 2-negative metastatic breast cancer. J Clin Oncol. 2010;28(20):3239–47.
72. Robert NJ, Dieras V, Glaspy J, Brufsky AM, Bondarenko I, Lipatov ON, et al. RIBBON-1: Randomized, double-blind, placebo-controlled, phase III trial of chemotherapy with or without bevacizumab for first-line treatment of human epidermal growth factor receptor 2-negative, locally recurrent or metastatic breast cancer. J Clin Oncol. 2011;29(10):1252–60.
73. O'Shaughnessy J, Miles D, Gray RJ, Dieras V, Perez EA, Zon R, et al. A meta-analysis of overall survival data from three randomized trials of bevacizumab (BV) and first-line chemotherapy as treatment for patients with metastatic breast cancer (MBC). J Clin Oncol. 2010;28(15s):ASCO Meeting Abstract 1005.
74. O'Shaughnessy J, Dieras V, Glaspy J, Brufsky A, Miller K, Miles D, et al. Comparison of Subgroup Analysis of PFS from three phase III studies of Bevacisumab in combination with chemotherapy in patients with HER2-negative metastatic breast cancer. Cancer Research. 2009;69(24):supplement 3.
75. Ranpura V, Hapani S, Wu S. Treatment-related mortality with bevacisumab in cancer patents: a metanalysis. JAMA. 2011;305 (5):487–94.
76. http://www.fda.gov/Drugs/DrugSafety/PostmarketDrugSafetyInformationforPatientsandProviders/ucm193900.htm. Accessed 29 June 2011.
77. Pivot XB, Li RK, Thomas ES, Chung H-C, Fein LE, Chan VF, et al. Activity of ixabepilone in oestrogen receptor-negative and oestrogen receptor-progesterone receptor-human epidermal growth factor receptor 2-negative metastatic breast cancer. Eur J Cancer. 2009;45(17):2940–6.
78. Kuznetsov G, TenDyke K, Yu MJ. Anti-proliferative effects of halichondrin B analog eribulin mesylate (E7389) against paclitaxel-resistant human cancer cells in vitro. Proc Am Assoc Cancer Res. 2007;48:abst C58.
79. Cortes J, O'Shaughnessy J, Loesch D, Blum JL, Vahdat LT, Petrakova K, et al. Eribulin monotherapy versus treatment of physicians choice in patients with metastatic breast cancer (EMBRACE): a phase 3 open-label randomised study. Lancet. 2011;377:914–23.
80. Rakha EA, El-Sayed ME, Green AR, Lee AHS, Robertson JF, Ellis IO. Prognostic markers in triple-negative breast cancer. Cancer. 2007;109(1):25–32.
81. Viale G, Rotmensz N, Maisonneuve P, Bottiglieri L, Montagna E, Luini A, et al. Invasive ductal carcinoma of the breast with the 'triple-negative' phenotype: prognostic implications of EGFR immunoreactivity. Breast Cancer Res Treat. 2009;116 (2):317–28.
82. Corkery B, Crown J, Clynes M, O'Donovan N. Epidermal growth factor receptor as a potential therapeutic target in triple-negative breast cancer. Ann Oncol. 2009;20(5):862–7.
83. Prat A, Parker J, Karginova O, Fan C, Livasy C, Herschkowitz J, et al. Phenotypic and molecular characterization of the claudin-low intrinsic subtype of breast cancer. Breast Cancer Res. 2010;12(5):R68.
84. Vincent-Salomon A, Thiery JP. Host microenvironment in breast cancer development: epithelial-mesenchymal transition in breast cancer development. Breast Cancer Res. 2003;5(2):101–6.
85. Sarrio D, Rodriguez-Pinilla SM, Hardisson D, Cano A, Moreno-Bueno G, Palacios J. Epithelial-mesenchymal transition in breast cancer relates to the basal-like phenotype. Cancer Res. 2008;68 (4):989–97.
86. Ueno NT, Zhang D. Targeting EGFR in triple negative breast cancer. J Cancer. 2011;2:324–8.
87. Reis-Filho JS, Milanezi F, Carvalho S, Simpson PT, Steele D, Savage K, et al. Metaplastic breast carcinomas exhibit EGFR, but not HER2, gene amplification and overexpression: immunohistochemical and chromogenic insitu hybridization analysis. Breast Cancer Res. 2005;7(6):R1028–35.
88. O'Shaughnessy J, Weckstein DJ, Vukelja SJ, McKintyre K, Krekow L, Holmes FA, et al. Preliminary results of a randomized phase II study of weekly irinotecan/carboplatin with or without cetuximab in patients with metastatic breast cancer (abstract 308). Breast Cancer Res Treat. 2007;106(supl 1):S32.
89. Green MD, Francis PA, Gebski V, Harvey V, Karapetis C, Chan A, et al. Gefitinib treatment in hormone-resistant and hormone receptor-negative advanced breast cancer. Ann Oncol. 2009;20 (11):1813–7.
90. Guix M, de Matos Granja N, Meszoely I, Adkins TB, Wieman BM, Frierson KE, et al. Short preoperative treatment with erlotinib inhibits tumor cell proliferation in hormone receptor-positive breast cancers. J Clin Oncol. 2008;26(6):897–906.
91. Teng YH-F, Tan W-J, Thike A-A, Cheok P-Y, Tse GM-K, Wong N-S, et al. Mutations in the epidermal growth factor receptor (EGFR) gene in triple negative breast cancer: possible implications for targeted therapy. Breast Cancer Research. 2011;13(2):R35.
92. Hynes NE, Lane HA. ERBB receptors and cancer: the complexity of targeted inhibitors. Nat Rev Cancer. 2005;5(5):341–54.
93. Hoadley K, Weigman V, Fan C, Sawyer L, He X, Troester M, et al. EGFR associated expression profiles vary with breast tumor subtype. BMC Genomics. 2007;8(1):258.
94. Sun T, Aceto N, Meerbrey Kristen L, Kessler Jessica D, Zhou C, Migliaccio I, et al. Activation of Multiple Proto-oncogenic Tyrosine Kinases in Breast Cancer via Loss of the PTPN12 Phosphatase. Cell. 2011 2011/03/04;144(5):703-18.
95. Toft DJ, Cryns VL. Minireview: Basal-like breast cancer: from molecular profiles to targeted therapies. Mol Endocrinol. 2011;25 (2):199–211.
96. Mirzoeva OK, Das D, Heiser LM, Bhattacharya S, Siwak D, Gendelman R, et al. Basal subtype and MAPK/ERK kinase (MEK)-phosphoinositide 3-kinase feedback signaling determine susceptibility of breast cancer cells to MEK inhibition. Cancer Res. 2009;69(2):565–72.
97. Finn R, Dering J, Ginther C, Wilson C, Glaspy P, Tchekmedyian N, et al. Dasatinib, an orally active small molecule inhibitor of both the src and abl kinases, selectively inhibits growth of basal-

type/"triple-negative" breast cancer cell lines growing in vitro. Breast Cancer Res Treat. 2007;105(3):319–26.
98. Burstein HJ, Elias AD, Rugo HS, Cobleigh MA, Wolff AC, Eisenberg PD, et al. Phase II study of sunitinib malate, an oral multitargeted tyrosine kinase inhibitor, in patients with metastatic breast cancer previously treated with an anthracycline and a taxane. J Clin Oncol. 2008;26(11):1810–6.
99. Barrios C, Liu M-C, Lee S, Vanlemmens L, Ferrero J-M, Tabei T, et al. Phase III randomized trial of sunitinib versus capecitabine in patients with previously treated HER2-negative advanced breast cancer. Breast Cancer Res Treat. 2010;121(1):121–31.
100. Crown J, Dieras V, Staroslawska E, Yardley DA, Davidson N, Bachelot TD, et al. Phase III trial of sunitinib (SU) in combination with capecitabine (C) versus C in previously treated advanced breast cancer (ABC). J Clin Oncol. 2010;28(18S):ASCO Meeting Abstract LBA1011.
101. Garcia S, Dales JP, Charafe-Jauffret E, Carpentier-Meunier S, Andrac-Meyer L, Jacquemier J, et al. Poor prognosis in breast carcinomas correlates with increased expression of targetable CD146 and c-Met and with proteomic basal-like phenotype. Hum Pathol. 2007;38(6):830–41.
102. Ponzo MG, Park M. The Met receptor tyrosine kinase and basal breast cancer. Cell Cycle. 2010;9(6):1043–50.
103. Mueller KL, Hunter LA, Ethier SP, Boerner JL. Met and c-Src cooperate to compensate for loss of epidermal growth factor receptor kinase activity in breast cancer cells. Cancer Res. 2008;68(9):3314–22.
104. Sebolt-Leopold JS. MEK inhibitors: a therapeutic approach to targeting the Ras-MAP kinase pathway in tumors. Curr Pharm Des. 2004;10(16):1907–14.
105. Lopez-Knowles E, O'Toole SA, McNeil CM, Millar EK, Qiu MR, Crea P, et al. PI3K pathway activation in breast cancer is associated with the basal-like phenotype and cancer-specific mortality. Int J Cancer. 2010;126(5):1121–31.
106. Kataja V, Castiglione M, Group ObotEGW. Primary breast cancer: ESMO Clinical Recommendations for diagnosis, treatment and follow-up. Ann Oncol. 2009;20(suppl 4):iv10-iv4
107. Anders CK, Deal AM, Miller CR, Khorram C, Meng H, Burrows E, et al. The prognostic contribution of clinical breast cancer subtype, age, and race among patients with breast cancer brain metastases. Cancer. 2011;117(8):1602–11.
108. Niwinska A, Murawska M, Pogoda K. Breast cancer brain metastases: differences in survival depending on biological subtype, RPA RTOG prognostic class and systemic treatment after whole-brain radiotherapy (WBRT). Ann Oncol. 2010;21(5):942–8.
109. Niwinska A, Olszewski W, Murawska M, Pogoda K. Triple-negative breast cancer with brain metastases: a comparison between basal-like and non-basal-like biological subtypes. J Neuro Oncol. 2011;105(3):547–53.
110. Fong PC, Boss DS, A YT, Tutt AN, Wu P, Mergui-Roelvink M, et al. Inhibition of Poly(ADP-Ribose) Polymerase in Tumours from BRCA Mutation Carrier. N Eng J Med. 2009;361(2):123-34.
111. Audeh MW, Carmichael J, Penson RT, Friedlander M, Powell B, Bell-McGuinn KM, et al. Oral poly(ADP-ribose) polymerase inhibitor olaparib in patients with BRCA1 or BRCA2 mutations and recurrent ovarian cancer: a proof-of-concept trial. Lancet. 2010;376(9737):245–51.
112. Kwon JS, Gutierrez-Barrera AM, Young D, Sun CC, Daniels MS, Lu KH, et al. Expanding the criteria for BRCA mutation testing in breast cancer survivors. J Clin Oncol. 2010;28(27):4214–20.
113. Gonzalez L, Zambrano A, Lazaro-Trueba I, Lopez E, Gonzalez JJ, Martin-Perez J, et al. Activation of the unliganded estrogen receptor by prolactin in breast cancer cells. Oncogene. 2009;28 (10):1298–308.
114. Niemeier LA, Dabbs DJ, Beriwal S, Striebel JM, Bhargava R. Androgen receptor in breast cancer: expression in estrogen receptor-positive tumors and in estrogen receptor-negative tumors with apocrine differentiation. Mod Pathol. 2010;23(2):205–12.
115. Turner N, Lambros MB, Horlings HM, Pearson A, Sharpe R, Natrajan R, et al. Integrative molecular profiling of triple negative breast cancers identifies amplicon drivers and potential therapeutic targets. Oncogene. 2010;29(14):2013–23.
116. Andre. F BTD, Campone. M, F. Dalenc, J. M. Perez-Garcia, S. A. Hurvitz, N. C. Turner, H. S. Rugo, M. M. Shi, Y. Zhang, A. C. M. Kay, A. J. Yovine, J. Baselga; . A multicenter, open-label phase II trial of dovitinib, an FGFR1 inhibitor, in FGFR1 amplified and non-amplified metastatic breast cancer. J Clin Oncol. 2011;29 (15s):ASCO Meeting Abstract 508.
117. Caldas-Lopes E, Cerchietti L, Ahn JH, Clement CC, Robles AI, Rodina A, et al. Hsp90 inhibitor PU-H71, a multimodal inhibitor of malignancy, induces complete responses in triple-negative breast cancer models. Proc Natl Acad Sci U S A. 2009;106(20):8368–73.
118. Rahman M, Davis SR, Pumphrey JG, Bao J, Nau MM, Meltzer PS, et al. TRAIL induces apoptosis in triple-negative breast cancer cells with a mesenchymal phenotype. Breast Cancer Res Treat. 2009;113(2):217–30.

Molecular heterogeneity of triple-negative breast cancer and its clinical implications

Sheeba Irshad[a], Paul Ellis[b] and Andrew Tutt[a,b]

[a]Breakthrough Breast Cancer Research Unit, Research Oncology, Kings College London School of Medicine, Kings Health Partners AHSC and [b]Integrated Cancer Centre, Guy's Hospital, Kings Health Partners AHSC, London, UK

Correspondence to A. Tutt, Breakthrough Breast Cancer Research Unit, Research Oncology, 3rd Floor Bermondsey Wing, Guy's Hospital Campus, Kings College London School of Medicine, Kings Health Partners AHSC, London SE1 9RT, UK
E-mail: andrew.tutt@icr.ac.uk

Current Opinion in Oncology 2011, 23:566–577

Purpose of review

Triple-negative breast cancer (TNBC) is defined by a lack of expression of hormone receptors, oestrogen and progesterone, as well as human epidermal factor receptor 2. This review focuses on the increasing understanding of the molecular heterogeneity of TNBC subtypes and the therapeutic implications of this subclassification.

Recent findings

Emerging evidence clearly indicates that TNBC is a heterogeneous disease with varying prognosis according to clinical, pathological and genetic factors. Some distinct histological special types within this clinically defined collection of entities have been shown to have a particularly good prognosis (e.g. medullary carcinomas), and others very poor outcome (e.g. metaplastic carcinomas), whereas the broader immunohistochemically defined 'core-basal-like' or gene expression defined 'basal' groups generally have a poor prognosis. This molecular subclassification has implicated several biological processes as potential therapeutic targets: the DNA damage response, drivers of deregulated proliferation, angiogenesis, epithelial–mesenchymal transition and immune deregulation.

Summary

Molecular stratification of these prognostic groups has been critical in identifying novel therapeutic targets for future drug development. The development of poly-(ADP)ribose polymerase inhibitors for *BRCA1*-mutation carriers with TNBC has led the ongoing efforts to translate fundamental biological insights into improved therapies for a difficult-to-treat breast cancer subgroup.

Keywords

basal-like breast cancer, heterogeneity, target identification, triple-negative breast cancer

Curr Opin Oncol 23:566–577

1040-8746

Introduction

Breast cancer is recognized as a heterogeneous disease with subgroups that exhibit substantial differences in terms of presentation, morphology, molecular profile and response to therapy. A clinical shorthand classification divides breast cancer into three major subtypes based on the expression of oestrogen (ER), progesterone (PgR) hormone receptors, human epidermal factor receptor 2 (HER2) and grade or Ki67 staining: luminal (ER/PgR-positive disease) divided into low (A) and high proliferation (B) forms, HER2-amplified tumours and triple-negative breast cancers (TNBCs) [1]. TNBC describes a subset of breast cancers that lack expression of oestrogen and PgR as defined by immunohistochemistry (IHC), as well as HER2 overexpression or gene amplification of HER2 by IHC or in-situ hybridization, respectively. Given that no targeted therapies are licensed for treatment, TNBC represents a significant clinical challenge. Advances in molecular profiling studies suggest that TNBC encompasses several biological entities. This review will focus on this molecular heterogeneity and the therapeutic implications of this subclassification.

Triple-negative breast cancer

TNBC is currently a diagnosis of exclusion accounting for approximately 15–20% of all breast cancer diagnoses, depending on the thresholds used to define oestrogen and PgR positivity on IHC and the methods used for HER2 assessment [2–4]. Although the ASCO–CAP guidelines for IHC testing recommend that oestrogen and progesterone assays be considered positive if at least 1% of the tumour cells are positive, there is considerable variation in the IHC cut-offs used worldwide. In 2000, the Stanford group classified breast cancer into four subtypes based on gene-expression profile: Luminal (A and B),

HER2-enriched, normal-like and basal-like [5]. The latter group is dominated by the TNBC phenotype and some investigators have suggested that the TNBC and basal-like phenotypes are effectively synonymous [6]. A diagnosis of TNBC requires low or absent levels of the expression of only three genes using primarily protein-based assays (IHC), whereas rigorous definition of basal-like breast cancer (BLBC) depends on assessment of mRNA expression from around 500 genes [7]. Many researchers have proposed IHC-based surrogates to define the genomic BLBC subtype, with the addition of positive detection of one or more of the following: basal cytokeratins (CK5/6, CK14 and CK17); epidermal growth factor receptor (EGFR); and C-kit to define a basal-like phenotype [8,9]. The use of oestrogen and progesterone negative with EGFR and/or CK5/6 positivity had 76% sensitivity and 100% specificity for the identification of BLBCs defined by microarray expression profiling analysis [10]. At present, evaluation of these basal markers has not been standardized for routine clinical practice.

Although 40–80% of TNBCs are basal-like, many are nonbasal-like and biologically distinct [6,11–15]. Up to 44% of TNBCs can be completely negative for all measured basal markers [16]. Similarly, up to 45% of BLBC are not triple negative with 15–45% oestrogen-positive tumours and between 6 and 35% of HER2-positive tumours showing a basal-like gene-expression profile [7,8,17,18]. Although these recent advances in molecular profiling studies have led to a great deal of interest in exploring the heterogeneity of TNBCs, it has in fact been evident in clinical practice for a number of years.

Although most TNBCs are reported to be invasive ductal carcinomas, a number of other histological types (e.g. metaplastic, medullary, secretory, myoepithelial and adenoid cystic tumours) can also exhibit a TNBC phenotype. Stratification of TNBC into these specific histological subtypes has important prognostic implications, with some nonductal invasive TNBCs being reported as having a more favourable prognosis [3,11,19]. Adenoid cystic, secretory and classical medullary carcinomas have excellent prognosis [20–22]. In contrast, metaplastic TNBCs have been reported to be resistant to cytotoxic agents [23]. Similarly, although TNBCs, especially the BLBC subtype, are typically reported as high-grade tumours with high mitotic indices, presence of central tumour necrosis (and/or fibrosis), pushing borders of invasion and stromal lymphocytic infiltrates, up to 10% of TNBCs have been shown to be grade 1, highlighting the importance of an accurate morphological diagnosis [4,9,17,24,25].

TNBCs, especially BLBCs, are more prevalent amongst young African, African-American and Latino women

Key points

- Triple-negative breast cancer (TNBC) is a heterogeneous disease with varying prognosis according to clinical, pathological and genetic factors.
- Molecular stratification of these varying prognostic groups is crucial to optimize current systemic therapy and identify novel therapeutic targets for future drug development.
- Some of the biological processes currently being investigated as potential targets in this group of breast cancer patients include the DNA damage response, drivers of deregulated proliferation, angiogenesis, epithelial–mesenchymal transition and immune deregulation.
- Translation of the biological insight has resulted in the development of PARP inhibitors for *BRCA1* mutation carriers with TNBC and possibly for a subgroup of sporadic TNBCs with dysfunctional homologous recombination DNA repair.
- Other novel targeted therapies under investigation for treatment in TNBC include antiangiogenic agents and EGFR, MET and SRC kinase targeted agents.

[3,26,27] and are known to be associated with an aggressive clinical course reflected in higher rates of central nervous system and lung metastases [7,28,29]. Cheang *et al.* [12] reported that patients with BL-TNBC had a significantly decreased overall survival (OS) compared with patients with non-BLBC. Several studies also demonstrate that a subgroup of TNBC patients display remarkable sensitivity to chemotherapeutic agents. Between 17 and 58% of patients with TNBC have been shown to achieve pathological complete response (pCR) after anthracycline/platinum-based neoadjuvant chemotherapy, and these patients have an excellent prognosis [30–32]. In comparison, those who fail to achieve pCR have an exceptionally poor outcome [33]. Molecular heterogeneity within TNBC explains this paradox of high rates of pCR and poor OS in TNBC when taken as a whole. Poor survival for the group taken overall being driven by the group of patients with more chemotherapy-resistant disease reflected in those with significant residual disease after neoadjuvant chemotherapy.

Molecular and biological heterogeneity of triple-negative breast cancer

Gene expression profiling identifies several different molecular subtypes within TNBC, with 40–80% being represented by BLBCs and the rest including normal-like, claudin-low, interferon-rich, molecular apocrine and HER2-enriched TNBCs [34,35]. Although this molecular stratification of TNBC and heterogeneity within BLBC is still controversial and requires further research,

Figure 1 Pathway dysfunctions implicated in the pathogenesis of subgroups within triple-negative breast cancer

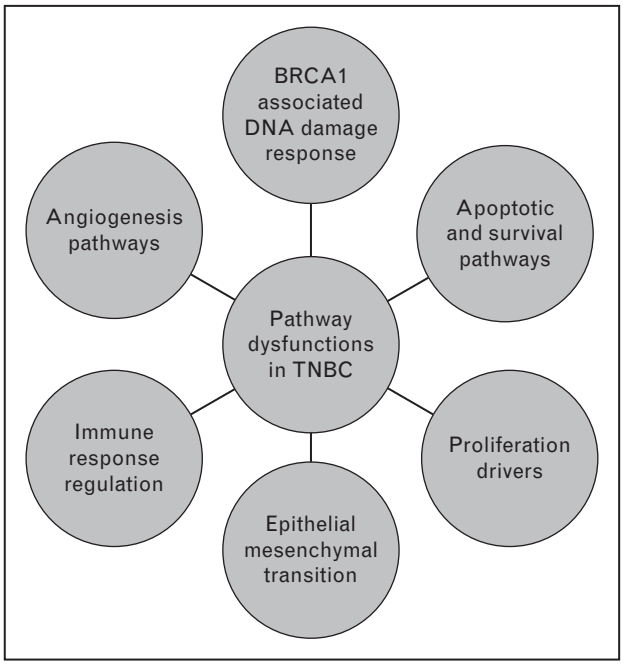

increasing evidence supports the existence of claudin-low and interferon-rich TNBC subgroups. Furthermore, rapid advancement in next-generation sequencing technologies has given an insight into some of the genetic events associated with tumour progression and metastasis. Ding *et al.* [36••] report on a primary BLBC tumour, a brain metastasis and a first-passage xenograft derived from the primary tumour and suggest that the metastatic tumour forms from a selected subset of cells from the primary tumour that contain preexisting mutations, and also develops a small number of *de novo* mutations. Understanding the biological effects of this molecular heterogeneity is fundamental for individualizing cancer therapy. A number of pathway dysfunctions have been implicated in the pathogenesis of TNBC subgroups (see Fig. 1).

BRCA1 pathway and BRCAness

Increasing evidence suggests a link between the BRCA1-associated DNA damage response and BLBC [37,38]. More than 75% of *BRCA1* mutated (but not *BRCA2*) tumours have a triple-negative phenotype, a basal-like phenotype or both [39–42]. Like sporadic BLBCs, BRCA1 tumours are characterized by high tumour grade, mitotic indices and chromosomal instability, reflecting aberrant DNA repair pathways that are common to both subtypes of cancer [43]. Both subtypes frequently express basal cytokeratins (particularly CK 5/6, 14 and 17), myoepithelial markers [caveolins (Cav) 1 and 2, c-kit and P-cadherin] and high levels of EGFR expression [6,11,15,17,44]. BRCA1 tumours have been shown to segregate together with sporadic BLBCs in hierarchical clustering analysis [45]. This association between tumours has been termed 'BRCAness' [37].

Mechanisms accounting for the BRCA-like phenotype in sporadic BLBCs have been extensively investigated. Somatic mutations of *BRCA1* and *BRCA2* genes are very rare in sporadic cancers, although loss of heterozygosity (LOH) of the genomic regions encompassing these genes is not uncommon [45,46]. Despite the lack of somatic *BRCA1* mutations in BLBCs, studies demonstrate that the BRCA1 pathway is dysfunctional in many sporadic BLBCs [38,39,47]. Sporadic BLBCs have reduced BRCA1 protein expression [48–50]. Promoter methylation may contribute to this reduced BRCA1 expression occurring in 10–15% of sporadic breast cancers overall and up to 40–50% of TNBC [51,52,53•]. High levels of a regulator protein Id4 have also been reported to down-regulate BRCA1 expression [54]. Regardless of the underlying biological mechanisms, the BRCAness of tumours has been muted as a promising therapeutic target in some sporadic breast cancer subgroups. Recent evidence suggests that functional assays for BRCA1-dependent homologous recombination based on the quantification of anthracycline and cyclophosphamide chemotherapy-induced RAD51 focus formation may be possible and may correlate with the TNBC phenotype and those tumours with high pathological response to these agents [55•,56•].

Apoptotic and proliferation pathway abnormalities

Distinctive patterns of apoptotic and proliferation gene abnormalities are frequently observed in TNBCs [44,57]. p53 mutations – impairing DNA damage-induced checkpoint activation and apoptosis, thereby promoting genome instability – are frequently observed in BLBCs, with one series reporting a prevalence as high as 82% [2]. The pattern of p53 mutations observed in BLBCs is similar to that of BRCA1-mutated tumours and differs from that observed in sporadic breast carcinomas of luminal phenotype [38]. A recent study demonstrated that p53 protein expression was able to subdivide triple-negative tumours in two prognostic subgroups: basal-like (p53-positive) and normal breast-like (p53-negative) tumours [58]. p53-positive tumours appear to exhibit a higher rate of pCR (22%) when compared with both p53-negative triple-negative (10%) and non-triple-negative tumours (4%) [59].

Up to 57% of BLBCs are found to have high levels of EGFR expression, and for a proportion this promotes cell proliferation via the activation of the RAS/MAPK/

MAPK-kinase pathway [60,61]. However, other cell proliferation promoting mechanisms are seen in triple-negative disease. Decreased expression and LOH of the tumour-suppressor gene *Rb1* correlates with a worse prognosis than those without *Rb1* LOH [62]. Sun *et al.* [63••] report the loss of the protein tyrosine phosphatase PTPN12 in a large proportion (60%) of TNBC and that PTPN12 acts as a growth suppressor by antagonizing key EGFR and HER2 tyrosine kinase pathways. Similarly, a small heat-shock protein α-basic-crystallin is expressed in about half of all BLBCs and its overexpression can induce EGF-independent cell growth, migration and invasion, along with constitutive activation of the MAP-kinase pathway downstream of EGFR [64]. α-Basic-crystallin expression has also been shown to be significantly associated with brain metastases amongst BLBCs [65] and resistance of tumours to neoadjuvant chemotherapy explaining its association with poor survival in patients [66].

The c-MET oncogene, encoding the tyrosine kinase receptor for hepatocyte growth factor, is implicated in the initiation and progression of BLBC [67,68,69•]. The overexpression of this receptor in BLBCs correlates with high expression levels of the transcription factor Y-box binding protein-1 (YB-1) known to interact with the EGFR-enhancer region. In this context, resistance to the EGFR inhibitor can occur because EGFR is transphosphorylated via a Met/Src-mediated signalling pathway. Accordingly, future clinical trials may need to be designed to impair cell proliferation by combined neutralization of EGFR and c-Met signals [70].

TNBCs also appear to demonstrate higher levels of AKT activation [71]. The PI3K/AKT pathway activation triggers cell proliferation and highly aggressive TNBC, for example, the metaplastic subgroup more frequently shows PI3K pathway aberrations compared with other BLBCs [72]. A number of mechanisms are known to be involved in PI3K/AKT pathway activation (see Fig. 2). In one series, low pTEN expression was reported in 65.5% of patients with TNBCs [73•]. Interestingly, pTEN inactivation has also recently been linked to chromosome instability due to defects in RAD51-mediated DNA double strand break repair [74]. The biological events triggered by AKT activation and/or AKT itself may prove to be a treatment target.

Angiogenesis

Increased levels of vascular endothelial growth factor (VEGF) have also been reported in patients with TNBCs, implicating the VEGF pathway in its aetiology [75]. This is supported further by histological examination of BLBC demonstrating the presence of glomeruloid microvascular proliferation [40], VEGF-2 being a prognostic factor amongst patients with TNBC [76•] and breast tumours with p53 mutations having higher VEGF levels [77].

Epithelial–mesenchymal transition-associated pathways

A putative subtype of breast cancer has recently been described based on unsupervised clustering of gene expression and termed 'claudin-low' [78]. These comprise only 5–10% of breast cancers and have a triple negative and basal-like phenotype [79•]. Clustering analysis shows that although similar to basal-like, claudin-low are a distinct subtype with an enriched stem-cell

Figure 2 Mechanisms for PI3k/AKT pathway activation

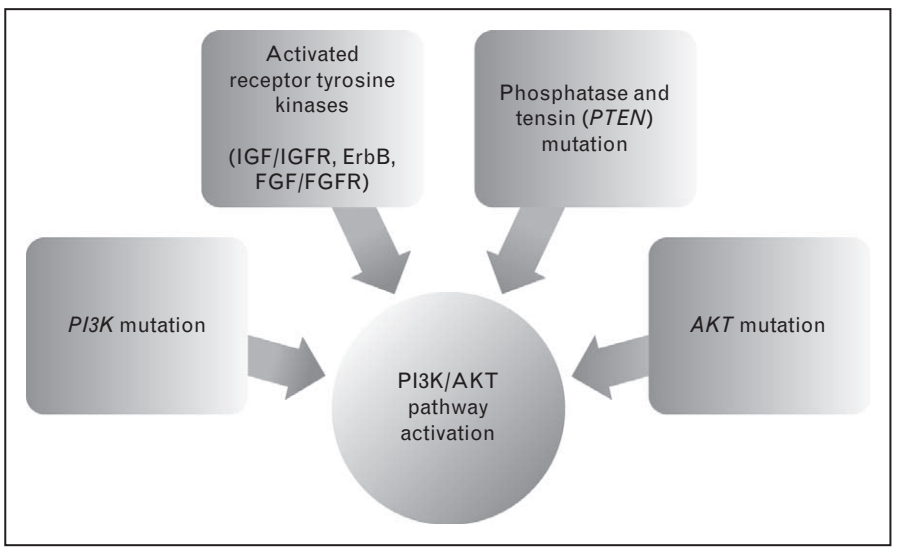

(tumour-initiating cell) signature [34]. Claudin-low tumours show features of a process called epithelial-to-mesenchymal transition (EMT), such as upregulation of a mesenchymal marker, vimentin, and downregulation of epithelial markers such as E-cadherin [80,81]. Most of these tumours are characterized by a high grade with minimal differentiation and a high immune cell infiltrate [78], and are often associated with increased invasiveness and metastatic potential, and a poorer prognosis [82,83]. Metaplastic carcinomas appear to be similar to the claudin-low subtype, demonstrating gene-expression patterns consistent with EMT, such as downregulation of cell-adhesion molecules, as well as high expression of stem-cell markers [84]. Furthermore, those BLBCs showing EMT features, such as overexpression of Src family tyrosine kinase LYN, an EMT mediator, are associated with poor survival [85•].

Expression of EMT-associated transcription factors (FOXC2, Snail and Slug) seen in claudin-low and some BLBC subgroups has been shown to be achieved through activation of TGFb, Wnt and Notch pathway [81,86,87•]. A subset of TNBC cell lines with mesenchymal phenotype has been shown to be highly sensitive to tumour necrosis factor-related apoptosis-inducing ligand (TRAIL) inducing apoptosis in these cell lines [88]. The mechanism underlying the differential TRAIL sensitivity of the mesenchymal TNBC cell lines is unknown, but data indicate that TRAIL-R2 (DR2) is the predominant death-inducing receptor in the TRAIL-sensitive triple-negative cell lines.

Immune-related triple-negative breast cancer

The interferon-rich subgroup encompasses TNBC tumours with a considerably better prognosis. They express high levels of genes related to inflammatory cells and/or interferon pathways [89,90]. A German group recently evaluated 28 breast cancer datasets and, showing a high B-cell (immune system) and low IL-8 (inflammation) metagene expression, identified a subset of TNBC patients (32% of all tumours) with a favourable prognosis and a 5-year event-free survival of 84% [91•]. Conversely, studies have shown that high levels of IL-8 expression are associated with a higher invasiveness potential of cancer cells [92]. Additionally, a number of recent studies suggest that activated tumour-associated macrophages (TAMs) are responsible for the secretion of proangiogenic cytokines which stimulate neovascularization [93–95] and BLBCs have significantly higher percentage of alternatively activated (M2) macrophages as compared to the luminal A subtype [96]. The investigators concluded that the M2 macrophage phenotype is associated with aggressive histopathologic features and poor clinical outcome. Thus, developing strategies to antagonize these chemokines and immune cell functions may provide an opportunity to interfere with metastasis, which is the main cause of death in most patients.

Therapeutic implications of biological heterogeneity

The generally poor prognosis of patients with TNBC and/or BLBC and their tendency to relapse with distant metastases indicate a need for more effective systemic therapies for this disease.

Cytotoxic chemotherapy agent selection

Cytotoxic chemotherapy is the mainstay of systemic treatment. The strong evidence of defective DNA repair mechanisms and rapid proliferation rates in TNBCs likely underpins the high de-novo response in many TNBCs to chemotherapy agents [97]. More specifically, studies have demonstrated that the activity of conventional anthracycline–taxane-based regimens given in a neoadjuvant setting is particularly high in BLBCs [98]. Dysfunctional BRCA1 pathway in TNBC, BLBC and BRCA1 associated tumours sensitizes these tumours to DNA-damaging agents, renewing interest in exploring platinum agents in these patients [99]. Platinum agents produce DNA cross-links which lead to DNA double-strand breaks, repaired by the BRCA1/2-mediated homologous recombination repair mechanisms [100•]. Consequently, BRCA1-defective cell lines have been shown to be two-fold to three-fold more sensitive to cisplatin compared with BRCA1 competent cell lines [101]. Recently, a molecular pathway by which platinum agents may induce cell death selectively in TNBC has been discovered [102]. Approximately one-third of TNBCs express the p53 family members ΔNp63 and TAp73 forming an apoptosis inhibitory complex in the proliferating cells. Cisplatin-induced DNA damage results in activation of the c-ABL tyrosine kinase and phosphorylation of TAp73, disrupting the complex which triggers apoptosis [102]. A number of small clinical trials have reported on the use of platinum drugs within the TNBC population (see Table 1) [30,103–115,116•,117•]. In a retrospective study of neoadjuvant therapy for breast cancer in *BRCA1*-mutation carriers, the use of cisplatin resulted in higher rates of pCR compared to other regimens [103]. The neoadjuvant response rates to platinum-based chemotherapy have been reported to be higher for patients with TNBCs compared to other tumour types (88 vs. 51%). In the advanced setting, response rates were also higher for patients with TNBCs (41 vs. 31%), along with a trend for superior survival in this group [30]. Randomized trials are currently addressing the activity of platinum compounds in comparison with conventional agents in patients with TNBC and subpopulations within TNBC (NCT00532727 and NCT00861705 [118,119].

Table 1 Clinical evidence to date for platinum agents in TNBC

Level of evidence	TNBC study population	Results
Retrospective studies		
Byrski *et al.* [103]	Neoadjuvant, $n=101$ Retrospective analysis of BRCA1 carriers treated with neoadjuvant chemotherapy with cisplatin delivered in single prospective protocol	pCR 83% following four cycles of single-agent cisplatin compared to 22, 21, 8 and 7% for AC, FAC, AT or CMF, respectively
Sirohi *et al.* [30]	Neoadjuvant $n=17$, adjuvant $n=11$, metastatic $n=34$ Retrospective analysis of patients receiving platinum-based chemotherapy	Neoadjuvant therapy clinical RR rates higher for patients with TNBC Neoadjuvant: clinical CR 88% in TNBC compared to 51% in other tumour types ($P=0.005$) Advanced: TNBC vs. non-TNBC: ORR 41 vs. 31% ($P=0.3$), PFS 6 vs. 4 months ($P=0.05$)
Staudacher *et al.* [104]	Advanced $n=143$ (93 TNBC) Retrospective analysis of patients receiving platinum-based chemotherapy	ORR: TNBC vs. non-TNBC: 33.3 vs. 22% ($P=0.1$) No significant differences in OS and PFS seen
Kim *et al.* [105]	Advanced $n=158$ (62 TNBC) Retrospective comparison between TNBC and non-TNBC patients receiving platinum containing chemotherapy	Similar benefits between TNBC and non-TNBC groups TNBC vs. non-TNBC: ORR: 27.6 vs. 22.8%, Median PFS 4.1 vs. 4.6 months, Median OS 10.8 vs. 10.8 months
Villarreal-Garza *et al.* [106]	Advanced $n=113$ Retrospective comparison of patients receiving platinum-based chemotherapy to conventional chemotherapy	Longer OS in the patients treated with platinum chemotherapy (18 vs. 13 months, $P=0.025$)
Phase II non-randomized controlled trials		
Gronwald *et al.* [107]	Neoadjuvant $n=25$ Four cycles of cisplatin 75 mg/m^2 to BRCA1 carrier patients	pCR – 72%
Isakoff *et al.* [108]	Advanced $n=86$ Single-agent cisplatin 75 mg/m^2 or carboplatin AUC6 selected according to investigator discretion	First-line or second-line single-agent platinum active and well tolerated with durable complete and partial responses Clinical benefit (CB) rate for platinum chemotherapy (CR + PR + SD >6 months) 34%
Frasci *et al.* [109]	Neoadjuvant $n=74$ Weekly cisplatin–epirubicin-paclitaxel + G-CSF	pCR 62%, ORR 98.3%, Median DFS 76% (5 years)
Ryan *et al.* [110]	Neoadjuvant $n=51$ Cisplatin + bevacizumab	pCR 16%, ORR 80%
Silver *et al.* [111]	Neoadjuvant $n=88$ Four cycles of cisplatin at 75 mg/m^2	pCR 21%, ORR 64%
Wang *et al.* [112]	Advanced $n=45$ Gemcitabine + cisplatin	ORR 62.2%, Median PFS 6.2 months
Phase II randomized controlled trials		
Baselga *et al.* [113]	Advanced $n=173$ Cisplatin ± cetuximab	Cisplatin + cetuximab vs. Cisplatin alone ORR: 20.0 vs. 10.3% Median PFS: 3.7 vs. 1.5 months
Carey *et al.* [114]	Advanced $n=102$ Cetuximab ± carboplatin	Cetuximab + carboplatin vs. cetuximab alone with addition of carboplatin at progression ORR: 18 vs. 6% CB: 27 vs. 10%
Bhattacharyya *et al.* [115]	Advanced $n=126$ Cyclophosphamide and methotrexate (CM) ± weekly cisplatin 20 mg/m^2	CM + cisplatin vs. CM alone CB: 90 vs. 63% Median PFS: 10 vs. 7 months Median OS: 16 vs. 12 months
O'Shaughnessy *et al.* [116•]	Advanced Gemcitabine and carboplatin (GC) ± iniparib (GCI)	GC vs. GCI ORR: 32–52% CB: 34 vs. 56% Median PFS: 3.6 vs. 5.9 months
Phase III randomized controlled trial		
O'Shaughnessy *et al.* [117•]	Advanced $n=258$ Gemcitabine and carboplatin (GC) ± iniparib (GCI)	GC vs. GCI: Median PFS: 4.1 vs. 5.1 months Median OS: 11.1 vs. 11.8 months

ORR, objective response rate; OS, overall survival; pCR, pathological complete response; PFS, progression-free survival; PR, progesterone; RR, response rate; TNBC, triple-negative breast cancer.

Table 2 Newer cytotoxic agents under investigation for TNBC subgroups

Cytotoxic agent	Mechanism of action	Evidence in triple-negative disease
Trabectedin	Binds to the minor groove of DNA	Significant sensitivity of mammalian cell lines deficient in the homologous recombination [105] Failed to show efficacy as a single agent in TNBC in a nonrandomized phase II trial [120]
Ixabepilone	An epothilone B analogue binds to β-tubulin causing microtubule stabilization and mitotic arrest	Two phase III studies report higher objective response rates (ORR) and PFS in TNBC patients receiving ixabepilone plus capecitabine compared with capecitabine alone, with a trend towards improved OS for patients treated with the combination arm [121,122] Two adjuvant studies commenced early-stage TNBC

PFS, progression-free survival; TNBC, triple-negative breast cancer.

Newer cytotoxic agents have been investigated and have shown some limited activity in those with heavily pretreated advanced TNBC (see Table 2) [120–122].

Targeted therapies

Owing to the heterogeneity of TNBC discussed above, a number of novel therapeutic targets are being evaluated in clinical studies. Unfortunately, many have failed to show efficacy as single agents or in combination with chemotherapy in patients with triple-negative disease. This is likely to reflect the lack of predictive biomarkers available to optimally select the group of TNBC patients mostly likely to respond. However, a few of these targeted agents are rapidly moving forward through the drug development phases and warrant further discussion.

Poly-(ADP)ribose polymerase inhibitors

Poly-(ADP)ribose polymerases (PARPs) are a family of nuclear enzymes that play a key role in DNA repair mechanisms, particularly the base excision repair (BER) pathway [123]. Loss of PARP1 function leads to increased dependence on BRCA1 and BRCA2 DNA repair function, resulting in a 'synthetic lethality' effect – the phenomenon whereby a mutation in either of the two genes individually has no effect but combining the mutations leads to cell death [124,125]. Although the majority of sporadic TNBCs lack BRCA mutations, the overlap of sporadic subsets with BRCA-associated breast cancer (concept of 'BRCAness') provides the rationale for investigating PARP inhibitors in the TNBC patient population.

There are currently at least eight PARP inhibitors in clinical trial development exploring indications reliant on both synthetic lethality targeting and chemotherapy/radiotherapy potentiation. The majority of the available clinical data for the TNBC population involve the drugs iniparib (BSI-201) and olaparib (AZD2281). A phase I trial of olaparib demonstrated a 47% objective response rate (ORR) and 63% clinical benefit rate (defined as radiological or tumour marker response or stable disease for at least 4 months) amongst patients with BRCA-mutated tumours [126]. Subsequently, two multicentre proof-of-principle phase II studies confirmed the therapeutic efficacy of olaparib in *BRCA1* and *BRCA2*-mutant carriers in breast and ovarian cancers [127••,128]. A small, single-arm study of another oral PARP inhibitor, veliparib, in combination with temozolamide in unselected advanced breast cancer patients reported negative results; however, activity with a clinical benefit rate of 62% was seen in the subset limited to *BRCA*-mutation carriers [129]. In 2009, iniparib became the first agent in the class to enter phase III assessment following promising results from a randomized phase II study investigating its combination with gemcitabine plus carboplatin in patients with TNBC [116•]. This study reported that the combination significantly improved median OS (12.3 vs. 7.7 months, $P = 0.01$) and progression-free survival (PFS) (5.9 vs. 3.6 months, $P = 0.01$). A phase III trial with identical treatment arms was recently reported failing to meet the stringent prespecified criteria for significance targeting a hazard ratio of 0.66 and 0.65 for the dual primary endpoints of OS and PFS. Despite this, inaparib continued to show a significant signal of efficacy [117•]. The formal publication of the results is awaited, but the failure of the phase III trial despite the clear demonstration of tumour activity with this agent may have roots in several aspects of the trial design and highlights the need to optimize dose and patient selection with a companion diagnostic in this highly heterogeneous subgroup of patients. Furthermore, it is becoming clear that this agent may not have its effect through a classic PARP1 inhibition pathway and further exploration of its mechanism of action is warranted.

Angiogenesis inhibitors

Bevacizumab, a humanized anti-VEGF monoclonal antibody, has been the most studied and has demonstrated activity when added to chemotherapy in both neoadjuvant and metastatic first/second-line treatments of TNBC (see Table 3) [110,130–135]. Subset analyses have suggested a greater degree of efficacy in TNBC patients, but it is not clear that this is biologically driven or due to a higher event rate in this population. The results of the BEATRICE trial assessing the role of bevacizumab in combination with chemotherapy in the adjuvant setting are eagerly awaited

Table 3 Bevacizumab in patients with TNBC

	Trial	Description	Results	Subgroup analysis for TNBC [119]
First-line metastatic	E2100	Bevacizumab in combination with paclitaxel	Bevacizumab combination arm significantly prolonged PFS (11.8 vs. 5.9 months, HR 0.60, $P<0.001$) and increased the ORR (36.9 vs. 21.2%, $P<0.001$). OS was similar [130]	Combination arm increased median PFS from 4.7 to 10.2 months (HR 0.045, 95% CI 0.33–0.61)
	AVADO	Bevacizumab in combination with docetaxel	High-dose bevacizumab combination arm (15 mg) significantly prolonged PFS (1 vs. 8.1 months, $P<0.001$) and increased RR to 64% from 46% ($P<0.001$) [131]	Combination arm increased median PFS from 6 to 8.1 months HR = 0.60, 95% CI 0.39–0.92)
	RIBBON-1	Bevacizumab in combination with chemotherapy [capecitabine/or taxane + anthracycline (T + Anth)]	Capecitabine + bevacizumab arm – PFS 8.6 vs 5.7 months, RR 35.4 vs. 23.6% T+Anth arm 9.2 vs. 8 months, RR 51.3 vs. 37.9% [132]	Capecitabine + bevacizumab arm – PFS improved from 4.2 to 6.1 months (HR = 0.72, 95% CI 0.49–1.06); T+Anth + Bevacizumab arm – PFS improved from 8.2 to 14.5 months (HR = 0.78, 95% CI 0.53–1.15)
Second-line metastatic	RIBBON-2	The addition of bevacizumab to chemotherapy	PFS increased from 5.1 to 7.2 months (HR 0.78 $P=0.0072$), and the study demonstrated that ORR increased by 10% ($P=0.0193$) in the bevacizumab arm [133]	
Neoadjuvant	Neoadjuvant cisplatin and bevacizumab	Single-arm phase II neoadjuvant trial for patients with operable TNBC	Reported pathological complete response in 15% treated with four cycles of cisplatin in combination with bevacizumab (three cycles), but toxicity limited completion of neoadjuvant therapy in 11% of patients [110]	
Adjuvant	BEATRICE	A randomized phase III trial testing chemotherapy with and without bevacizumab for patients with triple-negative disease [134]	*Accrual complete – Results pending*	

CI, confidence interval; HR, hazard ratio; RR, response rate; TNBC, triple-negative breast cancer.

[134]. Ongoing studies with other antiangiogenic agents aim to further elucidate the role of these agents in the TNBC population.

Epidermal growth factor receptor inhibitors and other kinase inhibitors

Given the high expression of EGFR in TNBC and BLBC, EGFR monoclonal antibodies have emerged as a possible therapeutic option [10,136]. In preclinical studies, EGFR inhibition can potentiate cisplatin-induced apoptosis in cultured BLBC cells [137]. The data so far suggest that EGFR inhibitors have low efficacy in patients with TNBC when used alone but may improve the efficacy of other agents (see Table 4) [113,114,138]. The lack of single-agent activity may be because the expression of the receptor is not itself a driver but reflects the cell of origin or alternatively that there is constitutive activation of signalling pathways downstream of EGFR in TNBC. For

Table 4 EGFR inhibitors in patients with TNBC

	Description	Results
Carey *et al.* [114]	TBCRC 001: Randomized phase II study comparing cetuximab monotherapy at 250 mg/m^2 with cetuximab combined with weekly carboplatin at AUC 2 in patients with metastatic TNBC.	Reported a modest 6% single-agent RR and 10% clinical benefit rate compared with 18 and 27%, respectively, in the combination arm.
O'Shaughnessy *et al.* [138]	Randomized phase II study of weekly irinotecan (90 mg/m^2) and carboplatin (AUC 2), with or without cetuximab (250 mg/m^2) in patients with metastatic breast cancer.	A subset analysis of those with TNBC showed an ORR rate (49% vs. 30%) but no change in PFS (4.7 vs. 5.1 months) after irinotecan, carboplatin and cetuximab compared to irinotecan and carboplatin alone.
Baselga *et al.* [113]	BALI-study: randomized phase II Trial with cisplatin with or without cetuximab.	Cisplatin/cetuximab combination arm 20% ORR vs. 10.3% for cisplatin alone ($P=0.11$), PFS 3.7 vs. 1.5 months ($P=0.032$).

EGFR, epidermal growth factor receptor; ORR, objective response rate; RR, response rate; TNBC, triple-negative breast cancer.

example, upregulation of MEK/MAPK, PI3K/AKT/mTOR and Src family kinases and loss of PTEN may confer resistance to anti-EGFR therapies [63••,64,87•, 139]. In fact, MEK inhibitors in TNBC cell lines have been shown to lead to activation of the P13K/AKT/mTOR pathway, but combined inhibition of MEK and P13K pathways results in synergistic efficacy [140]. Recently, the authors reporting the frequent loss of PTPN12 in TNBC also demonstrated that PTPN12 interacts with and represses PDGFR-b as well as EGFR phosphorylation, and combined inhibition of EGFR and PDGFR-b with lapatinib and sunitinib slowed the growth of xenografted TNBC-tumours [63••]. Preclinical data have previously suggested that BLBCs may be particularly sensitive to dasatinib, a multityrosine kinase inhibitor of *src* and *abl* [141]. Despite these promising laboratory data, a phase II study evaluating single-agent dasatinib in patients with advanced TNBC reported a modest (<5%) response [142]. Collectively, these results suggest that simultaneous inhibition of these multiply activated signalling pathways may be required.

Conclusion

Although TNBCs as a whole are considered biologically aggressive with a poor prognosis, many are potentially curable with conventional local-regional and chemotherapy treatment, reflecting their heterogeneity. Advances in gene expression profiling coupled with the knowledge of special morphological types of breast cancer may help further clarify a group of low-risk TNBC patients within this high-risk, poor prognosis population. A better understanding of the range of genetic abnormalities seen in TNBCs and BLBCs has revealed potential therapeutic targets, many of which are being evaluated in clinical trials. The correlative biology studies allied to these trials will be crucial if we are to unravel this heterogeneity with positive biomarkers and refine the maximum benefit populations for promising agents such as PARP inhibitors within this group of breast cancers.

Acknowledgements

Authors acknowledge the funding to S.I., P.E., and A.T. from Breakthrough Breast Cancer and the Sarah Greene Tribute Fund.

Conflicts of interest

There are no conflicts of interest.

References and recommended reading

Papers of particular interest, published within the annual period of review, have been highlighted as:

- • of special interest
- •• of outstanding interest

Additional references related to this topic can also be found in the Current World Literature section in this issue (pp. 700–701).

1 Goldhirsch A, Wood WC, Coates AS, *et al.* Strategies for subtypes – dealing with the diversity of breast cancer: highlights of the St Gallen International Expert Consensus on the Primary Therapy of Early Breast Cancer 2011. Ann Oncol 2011; 22:1736–1747.

2 Sorlie T, Perou CM, Tibshirani R, *et al.* Gene expression patterns of breast carcinomas distinguish tumor subclasses with clinical implications. Proc Natl Acad Sci USA 2001; 98:10869–10874.

3 Reis-Filho JS, Tutt AN. Triple negative tumours: a critical review. Histopathology 2008; 52:108–118.

4 Viale G, Rotmensz N, Maisonneuve P, *et al.* Invasive ductal carcinoma of the breast with the 'triple-negative' phenotype: prognostic implications of EGFR immunoreactivity. Breast Cancer Res Treat 2009; 116:317–328.

5 Perou CM, Sorlie T, Eisen MB, *et al.* Molecular portraits of human breast tumours. Nature 2000; 406:747–752.

6 Kreike B, van Kouwenhove M, Horlings H, *et al.* Gene expression profiling and histopathological characterization of triple-negative/basal-like breast carcinomas. Breast Cancer Res 2007; 9:R65.

7 Rakha EA, Elsheikh SE, Aleskandarany MA, *et al.* Triple-negative breast cancer: distinguishing between basal and nonbasal subtypes. Clin Cancer Res 2009; 15:2302–2310.

8 Rakha EA, Tan DS, Foulkes WD, *et al.* Are triple-negative tumours and basal-like breast cancer synonymous? Breast Cancer Res 2007; 9:404–405.

9 Livasy CA, Karaca G, Nanda R, *et al.* Phenotypic evaluation of the basal-like subtype of invasive breast carcinoma. Mod Pathol 2006; 19:264–271.

10 Nielsen TO, Hsu FD, Jensen K, *et al.* Immunohistochemical and clinical characterization of the basal-like subtype of invasive breast carcinoma. Clin Cancer Res 2004; 10:5367–5374.

11 Rakha EA, El-Sayed ME, Green AR, *et al.* Prognostic markers in triple-negative breast cancer. Cancer 2007; 109:25–32.

12 Cheang MC, Voduc D, Bajdik C, *et al.* Basal-like breast cancer defined by five biomarkers has superior prognostic value than triple-negative phenotype. Clin Cancer Res 2008; 14:1368–1376.

13 Carey LA, Perou CM, Livasy CA, *et al.* Race, breast cancer subtypes, and survival in the Carolina Breast Cancer Study. JAMA 2006; 295:2492–2502.

14 Sasa M, Bando Y, Takahashi M, *et al.* Screening for basal marker expression is necessary for decision of therapeutic strategy for triple-negative breast cancer. J Surg Oncol 2008; 97:30–34.

15 Dabbs DJ, Chivukula M, Carter G, Bhargava R. Basal phenotype of ductal carcinoma in situ: recognition and immunohistologic profile. Mod Pathol 2006; 19:1506–1511.

16 Diallo-Danebrock R, Ting E, Gluz O, *et al.* Protein expression profiling in high-risk breast cancer patients treated with high-dose or conventional dose-dense chemotherapy. Clin Cancer Res 2007; 13:488–497.

17 Tan DS, Marchio C, Jones RL, *et al.* Triple negative breast cancer: molecular profiling and prognostic impact in adjuvant anthracycline-treated patients. Breast Cancer Res Treat 2008; 111:27–44.

18 Banerjee S, Reis-Filho JS, Ashley S, *et al.* Basal-like breast carcinomas: clinical outcome and response to chemotherapy. J Clin Pathol 2006; 59:729–735.

19 Weigelt B, Kreike B, Reis-Filho JS. Metaplastic breast carcinomas are basal-like breast cancers: a genomic profiling analysis. Breast Cancer Res Treat 2009; 117:273–280.

20 Azoulay S, Lae M, Freneaux P, *et al.* KIT is highly expressed in adenoid cystic carcinoma of the breast, a basal-like carcinoma associated with a favorable outcome. Mod Pathol 2005; 18:1623–1631.

21 Marchio C, Iravani M, Natrajan R, *et al.* Mixed micropapillary-ductal carcinomas of the breast: a genomic and immunohistochemical analysis of morphologically distinct components. J Pathol 2009; 218:301–315.

22 Vincent-Salomon A, Gruel N, Lucchesi C, *et al.* Identification of typical medullary breast carcinoma as a genomic sub-group of basal-like carcinomas, a heterogeneous new molecular entity. Breast Cancer Res 2007; 9:R24.

23 Hennessy BT, Giordano S, Broglio K, *et al.* Biphasic metaplastic sarcomatoid carcinoma of the breast. Ann Oncol 2006; 17:605–613.

24 Dent R, Trudeau M, Pritchard KI, *et al.* Triple-negative breast cancer: clinical features and patterns of recurrence. Clin Cancer Res 2007; 13:4429–4434.

25 Fulford LG, Easton DF, Reis-Filho JS, *et al.* Specific morphological features predictive for the basal phenotype in grade 3 invasive ductal carcinoma of breast. Histopathology 2006; 49:22–34.

26 Vona-Davis L, Rose DP, Hazard H, *et al.* Triple-negative breast cancer and obesity in a rural Appalachian population. Cancer Epidemiol Biomarkers Prev 2008; 17:3319–3324.

27 Kang SP, Martel M, Harris LN. Triple negative breast cancer: current understanding of biology and treatment options. Curr Opin Obstet Gynecol 2008; 20:40–46.

28 Hicks DG, Short SM, Prescott NL, *et al.* Breast cancers with brain metastases are more likely to be estrogen receptor negative, express the basal cytokeratin CK5/6, and overexpress HER2 or EGFR. Am J Surg Pathol 2006; 30:1097–1104.

29 Tsuda H, Takarabe T, Hasegawa F, *et al.* Large, central acellular zones indicating myoepithelial tumor differentiation in high-grade invasive ductal carcinomas as markers of predisposition to lung and brain metastases. Am J Surg Pathol 2000; 24:197–202.

30 Sirohi B, Arnedos M, Popat S, *et al.* Platinum-based chemotherapy in triple-negative breast cancer. Ann Oncol 2008; 19:1847–1852.

31 Sanchez-Munoz A, Garcia-Tapiador AM, Martinez-Ortega E, *et al.* Tumour molecular subtyping according to hormone receptors and HER2 status defines different pathological complete response to neoadjuvant chemotherapy in patients with locally advanced breast cancer. Clin Transl Oncol 2008; 10:646–653.

32 Keam B, Im SA, Han SW, *et al.* Modified FOLFOX-6 chemotherapy in advanced gastric cancer: Results of phase II study and comprehensive analysis of polymorphisms as a predictive and prognostic marker. BMC Cancer 2008; 8:148.

33 Carey LA, Dees EC, Sawyer L, *et al.* The triple negative paradox: primary tumor chemosensitivity of breast cancer subtypes. Clin Cancer Res 2007; 13:2329–2334.

34 Perou CM. Molecular stratification of triple-negative breast cancers. Oncologist 2010; 15 (Suppl. 5):39–48.

35 Constantinidou A, Jones RL, Reis-Filho JS. Beyond triple-negative breast cancer: the need to define new subtypes. Expert Rev Anticancer Ther 2010; 10:1197–1213.

36 •• Ding L, Ellis MJ, Li S, *et al.* Genome remodelling in a basal-like breast cancer metastasis and xenograft. Nature 2010; 464:999–1005.
Report on a primary BLBC tumour, a brain metastasis and a first-passage xenograft derived from the primary tumour and suggestion that the metastatic tumour forms from a selected subset of cells from the primary tumour that contain preexisting mutations, and also develops a small number of de-novo mutations.

37 Turner N, Tutt A, Ashworth A. Hallmarks of 'BRCAness' in sporadic cancers. Nat Rev Cancer 2004; 4:814–819.

38 Turner NC, Reis-Filho JS. Basal-like breast cancer and the BRCA1 phenotype. Oncogene 2006; 25:5846–5853.

39 Foulkes WD, Brunet JS, Stefansson IM, *et al.* The prognostic implication of the basal-like (cyclin E high/p27 low/p53^{+}/glomeruloid-microvascular-proliferation+) phenotype of BRCA1-related breast cancer. Cancer Res 2004; 64:830–835.

40 Foulkes WD, Stefansson IM, Chappuis PO, *et al.* Germline BRCA1 mutations and a basal epithelial phenotype in breast cancer. J Natl Cancer Inst 2003; 95:1482–1485.

41 Palacios J, Honrado E, Osorio A, *et al.* Phenotypic characterization of BRCA1 and BRCA2 tumors based in a tissue microarray study with 37 immunohistochemical markers. Breast Cancer Res Treat 2005; 90:5–14.

42 Stefansson OA, Jonasson JG, Johannsson OT, *et al.* Genomic profiling of breast tumours in relation to BRCA abnormalities and phenotypes. Breast Cancer Res 2009; 11:R47.

43 Consortium BL. Pathology of familial breast cancer: differences between breast cancers in carriers of BRCA1 or BRCA2 mutations and sporadic cases. Breast Cancer Linkage Consortium. Lancet 1997; 349:1505–1510.

44 Korsching E, Packeisen J, Agelopoulos K, *et al.* Cytogenetic alterations and cytokeratin expression patterns in breast cancer: integrating a new model of breast differentiation into cytogenetic pathways of breast carcinogenesis. Lab Invest 2002; 82:1525–1533.

45 Futreal PA, Liu Q, Shattuck-Eidens D, *et al.* BRCA1 mutations in primary breast and ovarian carcinomas. Science 1994; 266:120–122.

46 Lancaster JM, Cochran CJ, Brownlee HA, *et al.* Detection of BRCA1 mutations in women with early-onset ovarian cancer by use of the protein truncation test. J Natl Cancer Inst 1996; 88:552–554.

47 Rakha EA, El-Sheikh SE, Kandil MA, *et al.* Expression of BRCA1 protein in breast cancer and its prognostic significance. Hum Pathol 2008; 39:857–865.

48 Sourvinos G, Spandidos DA. Decreased BRCA1 expression levels may arrest the cell cycle through activation of p53 checkpoint in human sporadic breast tumors. Biochem Biophys Res Commun 1998; 245:75–80.

49 Thompson ME, Jensen RA, Obermiller PS, *et al.* Decreased expression of BRCA1 accelerates growth and is often present during sporadic breast cancer progression. Nat Genet 1995; 9:444–450.

50 Yoshikawa K, Honda K, Inamoto T, *et al.* Reduction of BRCA1 protein expression in Japanese sporadic breast carcinomas and its frequent loss in BRCA1-associated cases. Clin Cancer Res 1999; 5:1249–1261.

51 Esteller M, Sparks A, Toyota M, *et al.* Analysis of adenomatous polyposis coli promoter hypermethylation in human cancer. Cancer Res 2000; 60:4366–4371.

52 Baldwin RL, Nemeth E, Tran H, *et al.* BRCA1 promoter region hypermethylation in ovarian carcinoma: a population-based study. Cancer Res 2000; 60:5329–5333.

53 • Grushko TA, Nwachukwu N, Charoenthammaraksa S, *et al.*; The University of Chicago, Chicago, IL; Lineberger Comprehensive Cancer Center, Chapel Hill, NC. Evaluation of BRCA1 inactivation by promoter methylation as a marker of triple-negative and basal-like breast cancers. J Clin Oncol 2010; 28(Suppl.):abstract 10510.
The authors suggest BRCA1 inactivation via promoter methylation occurs in almost half of both TNBC and BLBC, suggesting that this epigenetic event drives breast tumour progression toward the TN and BL phenotypes.

54 Beger C, Pierce LN, Kruger M, *et al.* Identification of Id4 as a regulator of BRCA1 expression by using a ribozyme-library-based inverse genomics approach. Proc Natl Acad Sci USA 2001; 98:130–135.

55 • Graeser M, McCarthy A, Lord CJ, *et al.* A marker of homologous recombination predicts pathologic complete response to neoadjuvant chemotherapy in primary breast cancer. Clin Cancer Res 2010; 16:6159–6168.
This study suggests the possibility of a functional assay for homologous recombination in breast cancer biopsy material that might help select patients for trials of HR targeting agents like PARP inhibitors.

56 • Asakawa H, Koizumi H, Koike A, *et al.* Prediction of breast cancer sensitivity to neoadjuvant chemotherapy based on status of DNA damage repair proteins. Breast Cancer Res 2010; 12:R17.
This study suggest the possibility of a functional assay for homologous recombination in breast cancer biopsy material that might help select patients for trials of HR targeting agents like PARP inhibitors.

57 Abd El-Rehim DM, Ball G, Pinder SE, *et al.* High-throughput protein expression analysis using tissue microarray technology of a large well characterised series identifies biologically distinct classes of breast cancer confirming recent cDNA expression analyses. Int J Cancer 2005; 116:340–350.

58 Biganzoli E, Coradini D, Ambrogi F, *et al.* p53 status identifies two subgroups of triple-negative breast cancers with distinct biological features. Jpn J Clin Oncol 2011; 41:172–179.

59 Bidard FC, Matthieu MC, Chollet P, *et al.* p53 status and efficacy of primary anthracyclines/alkylating agent-based regimen according to breast cancer molecular classes. Ann Oncol 2008; 19:1261–1265.

60 Hynes NE, Lane HA. ERBB receptors and cancer: the complexity of targeted inhibitors. Nat Rev Cancer 2005; 5:341–354.

61 Hoadley KA, Weigman VJ, Fan C, *et al.* EGFR associated expression profiles vary with breast tumor subtype. BMC Genomics 2007; 8:258.

62 Herschkowitz JI, He X, Fan C, Perou CM. The functional loss of the retinoblastoma tumour suppressor is a common event in basal-like and luminal B breast carcinomas. Breast Cancer Res 2008; 10:R75.

63 •• Sun T, Aceto N, Meerbrey KL, *et al.* Activation of multiple proto-oncogenic tyrosine kinases in breast cancer via loss of the PTPN12 phosphatase. Cell 2011; 144:703–718.
This study identifies a new tumour suppressor phosphatase whose loss may drive a high proportion of TNBCs.

64 Moyano JV, Evans JR, Chen F, *et al.* AlphaB-crystallin is a novel oncoprotein that predicts poor clinical outcome in breast cancer. J Clin Invest 2006; 116:261–270.

65 Kennecke HF, Voduc D, Leung S, *et al.* α-basic-crystallin expression in basal-like breast cancer and its association with brain metastasis. J Clin Oncol 2009; 27:15s.

66 Ivanov O, Chen F, Wiley EL, *et al.* AlphaB-crystallin is a novel predictor of resistance to neoadjuvant chemotherapy in breast cancer. Breast Cancer Res Treat 2008; 111:411–417.

67 Goncalves A, Charafe-Jauffret E, Bertucci F, *et al.* Protein profiling of human breast tumor cells identifies novel biomarkers associated with molecular subtypes. Mol Cell Proteomics 2008; 7:1420–1433.

68 Garcia S, Dales JP, Charafe-Jauffret E, *et al.* Poor prognosis in breast carcinomas correlates with increased expression of targetable CD146 and c-Met and with proteomic basal-like phenotype. Hum Pathol 2007; 38:830–841.

69 • Ponzo MG, Park M. The met receptor tyrosine kinase and basal breast cancer. Cell Cycle 2010; 9: 1043–1050.
The c-Met oncogene is implicated in the initiation and progression of BLBC.

70 Mueller KL, Hunter LA, Ethier SP, Boerner JL. Met and c-Src cooperate to compensate for loss of epidermal growth factor receptor kinase activity in breast cancer cells. Cancer Res 2008; 68:3314–3322.

71 Umemura S, Yoshida S, Ohta Y, *et al.* Increased phosphorylation of Akt in triple-negative breast cancers. Cancer Sci 2007; 98:1889–1892.

72 Moulder SL. Does the PI3K pathway play a role in basal breast cancer? Clin Breast Cancer 2010; 10:S66–S71.

73 • Lopez-Knowles E, O'Toole SA, McNeil CM, *et al.* PI3K pathway activation in breast cancer is associated with the basal-like phenotype and cancer-specific mortality. Int J Cancer 2010; 126:1121–1131.
More than 70% of breast cancers have an alteration in at least one component of the PI3K pathway and this might be exploited to therapeutic advantage especially in 'basal-like' cancers.

74 Shen WH, Balajee AS, Wang J, *et al.* Essential role for nuclear PTEN in maintaining chromosomal integrity. Cell 2007; 128:157–170.

75 Linderholm BK, Hellborg H, Johansson U, *et al.* Significantly higher levels of vascular endothelial growth factor (VEGF) and shorter survival times for patients with primary operable triple-negative breast cancer. Ann Oncol 2009; 20:1639–1646.

76 • Ryden L, Jirstrom K, Haglund M, *et al.* Epidermal growth factor receptor and vascular endothelial growth factor receptor 2 are specific biomarkers in triple-negative breast cancer. Results from a controlled randomized trial with long-term follow-up. Breast Cancer Res Treat 2010; 120:491–498.
High VEGFR2 expression significantly correlated to decreased breast cancer specific survival in TNBC patients.

77 Linderholm BK, Lindahl T, Holmberg L, *et al.* The expression of vascular endothelial growth factor correlates with mutant p53 and poor prognosis in human breast cancer. Cancer Res 2001; 61:2256–2260.

78 Herschkowitz JI, Simin K, Weigman VJ, *et al.* Identification of conserved gene expression features between murine mammary carcinoma models and human breast tumors. Genome Biol 2007; 8:R76.

79 • Prat A, Parker JS, Karginova O, *et al.* Phenotypic and molecular characterization of the claudin-low intrinsic subtype of breast cancer. Breast Cancer Res 2010; 12:R68.
Claudin-low tumours are characterized by the low to absent expression of luminal differentiation markers, high enrichment for epithelial-to-mesenchymal transition markers, immune response genes and cancer stem cell-like features.

80 Vincent-Salomon A, Thiery JP. Host microenvironment in breast cancer development: epithelial-mesenchymal transition in breast cancer development. Breast Cancer Res 2003; 5:101–106.

81 Sarrio D, Rodriguez-Pinilla SM, Hardisson D, *et al.* Epithelial–mesenchymal transition in breast cancer relates to the basal-like phenotype. Cancer Res 2008; 68:989–997.

82 Gordon LA, Mulligan KT, Maxwell-Jones H, *et al.* Breast cell invasive potential relates to the myoepithelial phenotype. Int J Cancer 2003; 106:8–16.

83 Jones C, Mackay A, Grigoriadis A, *et al.* Expression profiling of purified normal human luminal and myoepithelial breast cells: identification of novel prognostic markers for breast cancer. Cancer Res 2004; 64:3037–3045.

84 Hennessy BT, Gonzalez-Angulo AM, Stemke-Hale K, *et al.* Characterization of a naturally occurring breast cancer subset enriched in epithelial-to-mesenchymal transition and stem cell characteristics. Cancer Res 2009; 69:4116–4124.

85 • Choi YL, Bocanegra M, Kwon MJ, *et al.* LYN is a mediator of epithelial–mesenchymal transition and a target of dasatinib in breast cancer. Cancer Res 2010; 70:2296–2306.
BLBC showing EMT features, such as overexpression of Src family tyrosine kinase LYN, an EMT mediator, are associated with poor survival.

86 Storci G, Sansone P, Trere D, *et al.* The basal-like breast carcinoma phenotype is regulated by SLUG gene expression. J Pathol 2008; 214:25–37.

87 • Toft DJ, Cryns VL. Minireview: basal-like breast cancer: from molecular profiles to targeted therapies. Mol Endocrinol 2011; 25:199–211.
This study reviews ongoing efforts to translate insights from molecular profiles into improved therapies for women with BLBC.

88 Rahman M, Davis SR, Pumphrey JG, *et al.* TRAIL induces apoptosis in triple-negative breast cancer cells with a mesenchymal phenotype. Breast Cancer Res Treat 2009; 113:217–230.

89 Desmedt C, Haibe-Kains B, Wirapati P, *et al.* Biological processes associated with breast cancer clinical outcome depend on the molecular subtypes. Clin Cancer Res 2008; 14:5158–5165.

90 Teschendorff AE, Miremadi A, Pinder SE, *et al.* An immune response gene expression module identifies a good prognosis subtype in estrogen receptor negative breast cancer. Genome Biol 2007; 8:R157.

91 • Rody A, Kam T, Liedtke C, *et al.* Identification of a clinically relevant gene signature in triple negative and basal-like breast cancer. 33rd Annual San Antonio Breast Cancer Symposium. 2010; Abstract S5-5. Presented 11 December 2010.
Evaluated 28 breast cancer datasets and, showing a high B-cell (immune system) and low IL-8 (inflammation) metagene expression, identified a subset of TNBC patients (32% of all tumours) with a favourable prognosis and a 5-year event-free survival of 84%.

92 Freund A, Chauveau C, Brouillet JP, *et al.* IL-8 expression and its possible relationship with estrogen-receptor-negative status of breast cancer cells. Oncogene 2003; 22:256–265.

93 Lin EY, Pollard JW. Macrophages: modulators of breast cancer progression. Novartis Found Symp 2004; 256:158–168; discussion 168–172, 259–169.

94 Luo Y, Zhou H, Krueger J, *et al.* Targeting tumor-associated macrophages as a novel strategy against breast cancer. J Clin Invest 2006; 116:2132–2141.

95 Solinas G, Germano G, Mantovani A, Allavena P. Tumor-associated macrophages (TAM) as major players of the cancer-related inflammation. J Leukoc Biol 2009; 86:1065–1073.

96 Khramtsova G, Liao C, Khramtsov A, *et al.* The M2/alternatively activated macrophage phenotype correlates with aggressive histopathologic features and poor clinical outcome in early stage breast cancer. Cancer Res 2009; 69 (Suppl. 3).

97 Carey L, Winer E, Viale G, *et al.* Triple-negative breast cancer: disease entity or title of convenience? Nat Rev Clin Oncol 2010; 7:683–692.

98 Rouzier R, Perou CM, Symmans WF, *et al.* Breast cancer molecular subtypes respond differently to preoperative chemotherapy. Clin Cancer Res 2005; 11:5678–5685.

99 Kennedy RD, Quinn JE, Mullan PB, *et al.* The role of BRCA1 in the cellular response to chemotherapy. J Natl Cancer Inst 2004; 96:1659–1668.

100 • Isakoff SJ. Triple-negative breast cancer: role of specific chemotherapy agents. Cancer J 2010; 16:53–61.
This study reviews the role of specific chemotherapy agents in the treatment of TNBC.

101 Tassone P, Tagliaferri P, Perricelli A, *et al.* BRCA1 expression modulates chemosensitivity of BRCA1-defective HCC1937 human breast cancer cells. Br J Cancer 2003; 88:1285–1291.

102 Leong CO, Vidnovic N, DeYoung MP, *et al.* The p63/p73 network mediates chemosensitivity to cisplatin in a biologically defined subset of primary breast cancers. J Clin Invest 2007; 117:1370–1380.

103 Byrski T, Huzarski T, Dent R, *et al.* Response to neoadjuvant therapy with cisplatin in BRCA1-positive breast cancer patients. Breast Cancer Res Treat 2009; 115:359–363.

104 Staudacher L, Cottu PH, Diéras V, *et al.* Platinum-based chemotherapy in metastatic triple-negative breast cancer: the Institut Curie experience. Ann Oncol 2011; 22:848–856. doi: 10.1093/annonc/mdq461.

105 Kim T, Lee H, Han S, *et al.* The comparison of the benefits obtained from platinum-containing chemotherapy between triple-negative and nontriple-negative metastatic breast cancer J Clin Oncol 2010; 28(Suppl.):abstract 1071.

106 Villarreal-Garza CM, Clemons M, Kassam F, *et al.* Platinum-based chemotherapy in triple-negative breast cancer. ASCO Meeting Abstracts 2011; 29:1090.

107 Gronwald J, Byrski T, Huzarski T, *et al.* Neoadjuvant therapy with cisplatin in BRCA1-positive breast cancer patients. J Clin Oncol 2009; 27:abstract 502.

108 Isakoff SJ, Goss PE, Mayer EL, *et al.* TBCRC009: A multicenter phase II study of cisplatin or carboplatin for metastatic triple-negative breast cancer and evaluation of p63/p73 as a biomarker of response. ASCO Meeting Abstracts 2011; 29:1025.

109 Frasci G, Comella P, Rinaldo M, *et al.* Preoperative weekly cisplatin–epirubicin–paclitaxel with G-CSF support in triple-negative large operable breast cancer. Ann Oncol 2009; 20:1185–1192.

110 Ryan PT, Isakoff NM, Golshan SJ, *et al.* Neoadjuvant cisplatin and bevacizumab in triple negative breast cancer (TNBC): safety and efficacy. J Clin Oncol 2009; 27:15s.

111 Silver DP, Richardson AL, Eklund AC, *et al.* Efficacy of neoadjuvant cisplatin in triple-negative breast cancer. J Clin Oncol 2010; 28:1145–1153.

112 Wang Z, Hu X, Chen L, *et al.* Efficacy of gemcitabine and cisplatin (GP) as first-line combination therapy in patients with triple-negative metastatic breast cancer: preliminary results report of a phase II trial. J Clin Oncol 2010; 28 (Suppl):abstract 1100.

113 Baselga J, Gomez P, Awada A, *et al.* The addition of cetuximab to cisplatin increases overall response rate (ORR) and progression free survival (PFS) in metastatic triple negative breast cancer (TNBC): results of a randmomised phase II study (BALI-1). Ann Oncol 2010; 21:viii96–viii121.

114 Carey LA, Rugo HS, Marcom PK, *et al.* TBCRC 001: EGFR inhibition with cetuximab added to carboplatin in metastatic triple-negative (basal-like) breast cancer. J Clin Oncol 2008; 26:abstr 1009.

115 Bhattacharyya GS, Basu S, Agarwal V, *et al.* Single institute phase II study of weekly cisplatinum and metronomic dosing of cyclophosphamide and methotrexate in second line metastatic breast cancer triple-negative 41LBA. ECCO 15 – ESMO 2009; 34.

116 O'Shaughnessy J, Osborne C, Pippen JE, *et al.* Iniparib plus chemotherapy in • metastatic triple-negative breast cancer. N Engl J Med 2011; 364:205–214.
The addition of iniparib to chemotherapy improved the clinical benefit and survival of patients with metastatic triple-negative breast cancer without significantly increased toxic effects.

117 O'Shaughnessy J, Schwartzberg LS, Danso MA, *et al.* A randomized phase III • study of iniparib (BSI-201) in combination with gemcitabine/carboplatin (G/C) in metastatic triple-negative breast cancer (TNBC). J Clin Oncol 2011; 29(Suppl):abstract 1007.
The trial did not meet the prespecified criteria for significance for primary endpoints of OS and PFS but continued to show a significant signal of efficacy.

118 Trials C. Triple negative breast cancer trial (TNT). [Assessed 09 May 2011].

119 Paclitaxel with or without carboplatin and/or bevacizumab followed by doxorubicin and cyclophosphamide in treating patients with breast cancer that can be removed by surgery. http://clinicaltrials.gov/ct2/show/NCT00861705?term=NEOADJUVANT+CALGB+TRIPLE+NEGATIVE&rank=1. [Accessed 9 May 2011].

120 Tedesco KL, Blum JL, Goncalves A, *et al.* Final results of a phase II trial of trabectedin (T) in triple-negative, HER2-positive, and BRCA1/2 germ-line-mutated metastatic breast cancer (MBC) patients (pts). ASCO Meeting Abstracts 2011; 29:1125.

121 Thomas ES, Gomez HL, Li RK, *et al.* Ixabepilone plus capecitabine for metastatic breast cancer progressing after anthracycline and taxane treatment. J Clin Oncol 2007; 25:5210–5217. Doi:10.1200/JCO.2007.12.6557.

122 Sparano JA, Vrdoljak E, Rixe O, *et al.* Randomized phase III trial of ixabepilone plus capecitabine versus capecitabine in patients with metastatic breast cancer previously treated with an anthracycline and a taxane. J Clin Oncol 2010; 28:3256–3263. doi:10.1200/JCO.2009.24.4244.

123 Ashworth A. A synthetic lethal therapeutic approach: poly(ADP) ribose polymerase inhibitors for the treatment of cancers deficient in DNA double-strand break repair. J Clin Oncol 2008; 26:3785–3790.

124 Bryant HE, Schultz N, Thomas HD, *et al.* Specific killing of BRCA2-deficient tumours with inhibitors of poly(ADP-ribose) polymerase. Nature 2005; 434:913–917.

125 Farmer H, McCabe N, Lord CJ, *et al.* Targeting the DNA repair defect in BRCA mutant cells as a therapeutic strategy. Nature 2005; 434:917–921.

126 Fong PC, Boss DS, Yap TA, *et al.* Inhibition of poly(ADP-ribose) polymerase in tumors from BRCA mutation carriers. N Engl J Med 2009; 361:123–134.

127 Tutt A, Robson M, Garber JE, *et al.* Oral poly(ADP-ribose) polymerase •• inhibitor olaparib in patients with BRCA1 or BRCA2 mutations and advanced breast cancer: a proof-of-concept trial. Lancet 2010; 376:235–244.
Positive proof of concept for PARP inhibition in BRCA-deficient breast cancers.

128 Audeh MW, Carmichael J, Penson RT, *et al.* Oral poly(ADP-ribose) polymerase inhibitor olaparib in patients with BRCA1 or BRCA2 mutations and recurrent ovarian cancer: a proof-of-concept trial. Lancet 2010; 376:245–251.

129 Isakoff BO, Tung NM, Gelman RS, *et al.* A phase II trial of the PARP inhibitor veliparib (ABT888) and temozolomide for metastatic breast cancer. J Clin Oncol 2010; 28:abstr 1019.

130 Miller K, Wang M, Gralow J, *et al.* Paclitaxel plus bevacizumab versus paclitaxel alone for metastatic breast cancer. N Engl J Med 2007; 357:2666–2676.

131 Miles DW, Chan A, Dirix LY, *et al.* Phase III study of bevacizumab plus docetaxel compared with placebo plus docetaxel for the first-line treatment of human epidermal growth factor receptor 2-negative metastatic breast cancer. J Clin Oncol 2010; 28:3239–3247.

132 O'Shaughnessy JA, Brufsky AM. RiBBON 1 and RiBBON 2: phase III trials of bevacizumab with standard chemotherapy for metastatic breast cancer. Clin Breast Cancer 2008; 8:370–373.

133 Brufsky AB, Smirnov I, Hurvitz VS, *et al.* RIBBON-2: a randomized, double-blind, placebo-controlled, phase III trial evaluating the efficacy and safety of bevacizumab in combination with chemotherapy for second-line treatment of HER2-negative metastatic breast cancer. Cancer Res 2009; 69:495S–496S.

134 BEATRICE Study: a study of avastin (bevacizumab) adjuvant therapy in triple negative breast cancer. 2011. http://clinicaltrials.gov/ct2/show/NCT00528567.

135 Greenberg S, Rugo HS. Challenging clinical scenarios: treatment of patients with triple-negative or basal-like metastatic breast cancer. Clin Breast Cancer 2010; 10 (Suppl. 2):S20–S29.

136 Shien T, Tashiro T, Omatsu M, *et al.* Frequent overexpression of epidermal growth factor receptor (EGFR) in mammary high grade ductal carcinomas with myoepithelial differentiation. J Clin Pathol 2005; 58:1299–1304.

137 Oliveras-Ferraros C, Vazquez-Martin A, Lopez-Bonet E, *et al.* Growth and molecular interactions of the anti-EGFR antibody cetuximab and the DNA cross-linking agent cisplatin in gefitinib-resistant MDA-MB-468 cells: new prospects in the treatment of triple-negative/basal-like breast cancer. Int J Oncol 2008; 33:1165–1176.

138 O'Shaughnessy J, Weckstein DJ, Vukelja SJ, *et al.* Preliminary results of a randomized phase II study of weekly irinotecan/carboplatin with or without cetuximab in patients with metastatic breast cancer. Breast Cancer Res Treat 2007; 106:abstract 308.

139 Marty B, Maire V, Gravier E, *et al.* Frequent PTEN genomic alterations and activated phosphatidylinositol 3-kinase pathway in basal-like breast cancer cells. Breast Cancer Res 2008; 10:R101.

140 Mirzoeva OK, Das D, Heiser LM, *et al.* Basal subtype and MAPK/ERK kinase (MEK)-phosphoinositide 3-kinase feedback signaling determine susceptibility of breast cancer cells to MEK inhibition. Cancer Res 2009; 69:565–572.

141 Finn RS, Dering J, Ginther C, *et al.* Dasatinib, an orally active small molecule inhibitor of both the src and abl kinases, selectively inhibits growth of basal-type/'triple-negative' breast cancer cell lines growing in vitro. Breast Cancer Res Treat 2007; 105:319–326.

142 Finn RS, Bengala C, Ibrahim N, *et al.* Phase II trial of dasatinib in triple-negative breast cancer: results of study CA180059. San Antonio Breast Cancer Symposium. 2008; a3118.

EXPERT REVIEWS

Therapeutic potential of PARP inhibitors for metastatic breast cancer

Expert Rev. Anticancer Ther. 11(8), 1243–1251 (2011)

Sheeba Irshad[1], Alan Ashworth[1] and Andrew Tutt[†1]

[1]*Breakthrough Breast Cancer Unit Research Oncology, 3rd Floor Bermondsey Wing, Guy's Hospital Campus, Kings College London School of Medicine, London, SE1 9RT, UK*
[†]*Author for correspondence: andrew.tutt@icr.ac.uk*

Increasing understanding of the cellular aberrations inherent to cancer cells has allowed the development of therapies to target biological pathways, an important step towards individualization of breast cancer therapy. The clinical development of poly(ADP-ribose) polymerase (PARP) inhibitors, with their novel and selective mechanism of action, are an example of this strategy. PARP plays a key role in DNA repair mechanisms, particularly the base excision repair pathway. Initially developed as inhibitors able to enhance the cytotoxicity of radiation and certain DNA-damaging agents, they have more recently been shown to have single-agent activity in certain tumors. Inhibition of PARP in a DNA repair-defective tumor can lead to gross genomic instability and cell death by exploiting the paradigm of synthetic lethality. Several studies have evaluated the role of PARP inhibitors for treatment of breast cancer, particularly in the context of *BRCA*-mutated and triple-negative breast cancers. In addition, inhibition of PARPs repair functions for chemotherapy-induced DNA lesions has been shown to potentiate the effect of some chemotherapy regimens. This article discusses the current understanding of PARP inhibition as a treatment for metastatic breast cancer, evidence from clinical trials and addresses its future implications.

KEYWORDS: basal-like • breast cancer • *BRCA1* • *BRCA2* • DNA repair • homologous repair • PARP inhibitors • triple-negative breast cancer

Breast cancer is the most common malignancy in women, accounting for 27% of all female cancers. An estimated 1 million cases of breast cancer are diagnosed annually worldwide and approximately 400,000 patients die from the disease every year [1]. It is estimated that the lifetime risk of developing breast cancer is one in nine for women in the UK. Although the survival rates from breast cancer have improved within the last three decades, the burden of metastatic disease remains high. Breast cancer is seen as a heterogeneous disease with subgroups that exhibit substantial differences in biological behavior. These subgroups, while themselves controversial, include: Luminal (A or B), Normal breast-like, Her2 and Basal-like [2]. The latter is most consistently associated with an unfavorable prognosis and limited therapeutic options. In recent years breast cancer research has made extraordinary progress in understanding special types that include HER2-positive and hereditary breast cancers. Owing to this better understanding of the function of the hereditary breast cancer-susceptibility genes *BRCA1* and *BRCA2*, a class of agents called poly(ADP-ribose) polymerase (PARP) inhibitors have found a new therapeutic niche by exploiting DNA-repair defects in these tumor cells. Perhaps of broader significance is the emerging evidence that these agents, both alone and in combination with chemotherapy, may have a role in some sporadic tumors. This article discusses the evidence available to date for the use of PARP inhibitors in metastatic breast cancer and its future implications.

Breast cancer & PARP in DNA repair

DNA is constantly challenged, both by exogenous (e.g., ultraviolet or ionizing radiation and genotoxic chemicals) and endogenous stresses (e.g., cellular metabolism and free-radical generation) [3]. The major forms of DNA damage include single-strand breaks (SSBs), double-strand breaks (DSBs) and alteration of bases. SSBs are the most common DNA aberrations with approximately 10,000 spontaneous SSBs occurring in each cell every day [4]. DSBs are

 10.1586/ERA.11.52 ISSN 1473-7140

most cytotoxic to cells as the complementary strand is not available as a template for DNA repair, and the presence of even a small number of DSBs can be lethal. Unrepaired and aberrantly repaired DNA damage can lead to mutagenesis and thus predispose to cancer. To minimize the impact of these threats and maintain genomic integrity, cells have evolved various lesion-specific DNA repair mechanisms. These include homologous recombination (HR), nonhomologous end joining (NHEJ), base-excision repair (BER), nucleotide-excision repair (NER) and mismatch repair (MMR) pathways [5]. Although the dominant pathway for DSB repair is NHEJ, a high-fidelity HR mechanism predominates during the late S-phase, when a sister chromatid is available to serve as a template for resolving the DSB. Key components of this pathway are the tumor-suppressor gene products *BRCA1* and *BRCA2* that are both necessary for efficient and accurate homologous recombination repair of DNA DSBs and stalled replication forks [6]. *BRCA1* is important at a number of points in the upstream sensing and signaling that leads to the recruitment of DNA-repair proteins to sites of DNA damage, whereas *BRCA2* is crucial for catalyzing the formation of RAD51 filaments on ssDNA at the damaged sites [7,8].

Alterations of a single DNA strand, including SSBs, are mainly repaired using the intact complementary strand as a template by BER [5]. PARP is the critical component of this repair pathway. The PARP family was first described in 1963 [9]. A family of 17 PARPs have currently been identified. Although the role of the most abundant nuclear enzymes PARP1 and PARP2 in DNA repair is well established, other family members such as PARP3 and PARP5 (tankyrase) have more recently also been implicated in maintaining genomic stability [10]. PARP1 is a molecular sensor of DNA strand breaks, the catalytic activity of which is stimulated more than 500-fold on binding to DNA breaks [11]. This results in the formation of large branched chains of poly-ADP ribose from its substrate nicotinamide adenine dinucleotide (NAD^+) [10]. This ribosylation results in the recruitment of a number of protein targets that are involved in the cellular response to DNA damage and DNA metabolism. PARP2, in common with PARP1, is activated by DNA strand interruptions and is also required for efficient repair of ssDNA lesions [12–14]. Any unrepaired SSBs during DNA replication are converted into DSBs at replication forks, resulting in increased HR activity capable of the error-free repair of these lesions [15,16].

More recent studies have demonstrated that PARP1/2 activity does not solely contribute to BER [17]. PARP activation appears to have a broader role in DNA-damage repair and replication fork restart, chromatin remodeling and gene transcription [18–20]. In contrast to its role in genome maintenance and thus as a survival factor, PARP1 has also been shown to promote cell death in the presence of extensive DNA damage via its capacity to deplete cellular energy pools culminating in cell dysfunction and necrosis [21,22]. It is therefore not surprising that the PARP family has become an attractive target for drug development and its pharmacological inhibition is likely to provide significant benefits in a number of disorders.

PARP inhibition & synthetic lethality

Studies demonstrating a dramatic reduction in the repair of DNA strand breaks following PARP inhibition and increased HR activity acting as a very efficient error-free rescue mechanism have provided the basis for investigating the potential for 'synthetic lethality' to induce selective cytotoxicity for cancer therapy [15,16,23,24]. Synthetic lethality is the phenomenon whereby a mutation in either of the two genes individually has no effect, but combining the mutations leads to cell death. This effect was first described in 1946 and studied in genetically tractable organisms such as *Drosophila* and yeast [25]. In 1997, Hartwell *et al.* made the first suggestion that synthetic lethality could be applied to streamline anticancer drug discovery [26].

Poly(ADP-ribose) polymerase inhibitors first entered clinical trials in cancer patients as agents able to enhance the cytotoxic effects of ionizing radiation and DNA-damaging chemotherapy drugs. Many commonly used chemotherapeutic agents, such as alkylating agents and camptothecins damage DNA by causing single-strand breaks or lesions that lead to their formation [27]. In 2005, two simultaneous papers reported the single-agent activity of PARP inhibitors in *BRCA1* or *BRCA2* deficient and matched control cell lines [28,29]. Both these studies demonstrated that inhibition of PARP in tumor cells with deficient HR repair generates unrepaired DNA single-strand breaks, resulting in the accumulation of DNA DSBs and collapsed replication forks [28,29]. In this setting, cancer cells with *BRCA1* or *BRCA2* dysfunction are selectively sensitized to PARP inhibition, which leads to chromosomal instability, cell-cycle arrest and apoptosis. Importantly, cell lines retaining a single wild-type gene copy, a model for normal tissues in a *BRCA1* or *BRCA2* carrier, were not sensitized. Taken together, these preclinical studies clearly provided the impetus to explore the use of PARP inhibitors in the treatment of *BRCA*-mutated tumors and classes of sporadic tumor, which share loss of homologous recombination function or upregulation of PARP-dependant functions. There are currently at least eight PARP inhibitors in clinical trial development exploring indications reliant on both synthetic lethality targeting and chemotherapy and radiation therapy potentiation. In order to establish appropriate inhibitory doses for this novel target, the PARP inhibitor ABT-888 (veliparib) represented one of the first compounds in oncology to undergo a Phase 0 evaluation in humans, resulting in pivotal single-agent pharmocokinetic and pharmacodynamic data being available prior to Phase I initiation [30]. A detailed discussion of the individual PARP inhibitors in development is beyond the scope of this article, but the reader should refer to the following citations [31–33].

Rationale for & results of PARP inhibition in germline *BRCA*-mutated breast cancer

Hereditary forms of breast cancer constitute 5–7% of breast cancer cases overall and are associated with germline mutations in the *BRCA1* [34] or *BRCA2* [35] tumor-suppressor genes. Inheritance of one mutated *BRCA1* or *BRCA2* allele leads to a lifetime risk of breast cancer that is as high as 80% [36]. Impairment of HR

function in these cells forces the repair of DSBs via error-prone NHEJ repair, predisposing the genome to genetic aberrations that drive carcinogenesis [37–39]. This tumor-specific defect also causes the cancer cells to be selectively sensitized to inhibitors of other DNA-repair pathways, which include PARP-dependent base excision repair [28,29]. Nonmalignant normal tissue cells within *BRCA* mutation carriers should be relatively unaffected, because these cells are heterozygous for the mutation retaining a functional *BRCA1* and *BRCA2* gene product.

Fong *et al.* reported the 'first in man' Phase I trial investigating the role of a selective and potent PARP inhibitor, olaparib (previously known as KU-0059436 and AZD2281), including *BRCA1* and *BRCA2* mutation carriers with advanced tumors in an expansion cohort [40]. A total of 60 patients were enrolled, 15% of whom had breast cancer. Olaparib was administered orally and the maximum tolerated dose (MTD) was established at 400 mg twice daily given continuously in a 28-day cycle. Dose-limiting toxicities were myelosuppression and CNS side effects, such as grade 3 somnolence. After demonstration of an initial signal of efficacy in a *BRCA1* carrier, an expansion cohort of *BRCA1* and *BRCA2* carriers was recruited. In this group of 19 patients dominated by those with ovarian cancer, there was a 47% response rate and a 63% clinical benefit rate (defined as radiological or tumor marker response or stable disease for at least 4 months). Designed alongside the Phase I and started before the expansion cohort, two multicenter proof-of-principle Phase II studies in *BRCA1* and *BRCA2*-associated breast and ovarian cancer, respectively (ICEBERG1 and ICEBERG2), had been initiated after establishment of MTD in Phase I. Both studies confirmed the therapeutic efficacy of olaparib in *BRCA1* and *BRCA2* mutation carriers with breast or ovarian cancer [41,42]. Updated results of the breast cancer study have recently been published (ICEBERG 1 study) [41]. This study recruited a total of 54 breast cancer patients with advanced heavily pretreated disease to two nonrandomized sequential dose cohorts of 100 mg twice daily (a previously established pharmacodynamically active dose) and 400 mg twice daily (previously established MTD) of olaparib. Of the 27 patients in the 400-mg cohort, 18 were carriers of *BRCA1* mutations and nine had *BRCA2* mutations. In the 100-mg cohort, 15 patients were carriers of *BRCA1* mutations, 11 had *BRCA2* mutations and one carried mutations in both *BRCA1* and *BRCA2*. Both dose levels demonstrated clinical activity; however, 400 mg twice daily appeared to be more efficacious with improved outcomes. The study reported an overall response rate (ORR) of 41% (11 out of 27) with one complete response (CR) and ten partial responses (PRs), and a median progression-free survival (PFS) of 5.7 months at 400 mg twice daily in contrast to an ORR of 22% (six out of 27) with six PRs and a median PFS of 3.8 months at the lower dose level [41]. Overall, olaparib was well tolerated with G1/2 fatigue being the most common adverse event in the cohort given 400 mg twice daily (41%; n = 11).

Interestingly, the results of the Phase I trial had reported significant PARP inhibition with olaparib in normal and tumor tissues from doses ≥60 mg, resulting in downstream DNA replication fork arrest (demonstrated by an increase in γH2AX foci in plucked eyebrow hair follicles) [40]. These findings raise two main considerations for future studies:

- The inferior anti-tumor activity seen in the 100-mg twice daily cohort may indicate that target inhibition achieved within the tumor differs from that achieved in surrogate tissues, such as hair follicle cells;
- While these DNA strand breaks may be repaired when pharmacological inhibition is removed, they raise concerns over the potential consequences of continuous dosing over a long period or combination with chemotherapy induced DNA damage if there is accumulation of mutations within normal tissues.

Nonetheless, the olaparib ICEBERG studies have provided proof of concept for PARP inhibition hypothesis in cancers that harbor defects in HR repair pathways across different tumor primary sites of origin.

As reflected by the number of PARP inhibitor-related abstracts reported at ASCO 2010, the aforementioned studies have supported the continued enrollment of patients into clinical trials evaluating the role of PARP inhibitors in combination with chemotherapy [43–47]. Schelman *et al.* reported the promising anti-tumor activity of an orally administered PARP1/2 inhibitor, MK-4827, in both BRCA-deficient and sporadic cancers [44]. Similarly, Isakoff *et al.* reported the activity of a combination of the PARP inhibitor, Veliparib (ABT888) with temozolamide in patients with metastatic breast cancer [45]. Of note, activity appeared restricted to the *BRCA1*/2 carrier subpopulation in this small Phase II trial. Recent clinical trials evaluating the chemotherapy sensitivities for standard regimens in patients with *BRCA1*/2 mutation are likely to provide important information for establishing adequate standard treatment controls and projected study accrual targets and feasibility for PARP inhibitor versus best standard chemotherapy trials [48,49].

Rationale for & results of PARP inhibition in basal-like & triple-negative breast cancers

Emerging evidence suggests that there is a potential therapeutic role for PARP inhibition in a wider subgroup of sporadic breast cancers that may have defective HR DNA repair pathways. Breast cancers arising in germ-line carriers of *BRCA1* mutation, in particular those diagnosed before the age of 50 years, have been shown to have a characteristic phenotype that differentiates these from sporadic cancers [50–52]. Morphological and immunohistochemical studies have clearly shown that there is an association between tumors derived from *BRCA1* germline mutation carriers and those of sporadic basal-like tumors [53]. At least 80–90% of *BRCA1*-related breast cancers are basal-like [54]. Interestingly, *BRCA2* mutation carriers do not share a predisposition for the basal-like phenotype but are most commonly luminal ER-positive cancers [55]. The clinical outcomes for women with sporadic basal-like breast cancer compared with those with *BRCA1*-related cancers are broadly similar; notably early relapse (within 5 years), similar pattern of metastatic spread with a proclivity to develop metastatic deposits in the brain and lungs, and a poorer prognosis

compared with luminal-type breast cancers, particularly if the disease is not chemotherapy sensitive [56,57]. Morphologically, both *BRCA1*-mutated germline tumors and basal-like tumors have a high histological grade, high mitotic indices, pushing borders, conspicuous lymphocytic infiltrate and medullary/atypical medullary features [58]. *BRCA1* tumors have been shown to consistently segregate together with sporadic basal-like breast cancers in hierarchical clustering analysis [54]. This association between tumors is termed 'BRCAness', whereby some sporadic cancers share characteristics with *BRCA1* cancers. Profound genomic instability seems characteristic of both *BRCA1*-related breast cancer and sporadic basal-like breast cancer, which may reflect aberrant DNA-repair pathways that are common to both subtypes of cancer [59].

Mechanisms accounting for the BRCA-like phenotype in sporadic tumors have been under intensive investigation. Somatic mutations of *BRCA1* and *BRCA2* genes are very rare in sporadic cancers, although loss of heterozygosity of the genomic regions encompassing these genes is not uncommon [60,61]. *BRCA1* mRNA levels have been shown to be reduced or undetectable in certain sporadic breast carcinomas and breast cancer cell lines [62–65]. Promoter methylation may contribute to this reduced *BRCA1* expression and has been implicated in up to 10–15% of sporadic breast cancers and up to 40–50% of so-called triple-negative (ER-, PR- and Her2-negative) breast cancer [66–68]. However, this is unlikely to be the sole mechanism, and overexpression of regulatory proteins such as Id4 has also been reported as downregulating *BRCA1* expression [69]. The role of epigenetic silencing in disrupting *BRCA2* protein function is less clear [70]. However, it has been demonstrated that the *BRCA2* gene is negatively regulated by protein interactions with gene products of the *EMSY* gene, which has been reported as being amplified in 13% of sporadic breast tumors. Thus, both genetic and epigenetic mechanisms can create the BRCAness phenotype in some sporadic breast cancers, and these may therefore benefit from the therapeutic approach of synthetic lethality with PARP inhibition. Likewise, the observation that cells deficient in other crucial homologous recombination proteins are sensitive to PARP inhibition provides the rationale for testing PARP inhibitors in other cancers; for example, recently it has been shown that PTEN-deficient cells are exquisitely sensitive to PARP inhibition [71]. This is particularly exciting considering the high incidence of PTEN inactivation in human tumors.

Although one of the most consistently identified types of breast cancer on gene-expression profiling, identification of sporadic breast tumors with basal-like phenotype with a convenient and universally agreed immunohistochemical method remains a challenge. Approximately 15% of sporadic invasive breast cancers are basal-like [72,73]. Basal-like breast cancers when identified using gene-expression arrays are characterized, among others, by the expression of genes associated with proliferation markers expressed in normal basal/myothelial cells and by low-level expression of hormone receptor- and HER2-related genes [74]. Identification of BRCAness within a tumor is difficult for a number of reasons: multiple genes are involved in the HR pathway, *BRCA1* and *BRCA2* are large genes, and somatic mutations do not seem limited to particular nucleotides or hot spots [75]. The search for readily applicable functional assays for homologous recombination is critical for optimal implementation of these agents in a clinical setting. Studies recently reported the strategy of using epigenetic inactivation of the *BRCA1* gene by CpG island hypermethylation as a potential predictive biomarker for the application of PARP inhibitors to sporadic *BRCA1*-hypermethylated tumors [76,77]. Veeck *et al.* report that 36.7% (25 out of 68 tumors) of triple-negative noninherited breast cancer tumors had *BRCA1* methylation [76]. Nevertheless, this study examined the effect of *BRCA1* promoter methylation state on PARP inhibitor sensitivity on a single cell line with a *BRCA1*-methylated promoter, and hence additional work is required to demonstrate that this is indeed generally predictive of response to PARP inhibitors [78]. Graeser and colleagues have recently reported the possibility of the assessment of HR function by quantification of RAD51 damage response competent proliferating cells following standard anthracycline and cyclophosphamide neoadjuvant breast cancer chemotherapy [79].

Owing to the lack of general acceptance of gene-expression profiling methodologies for identifying basal-like breast cancer in clinical samples, the so-called triple-negative (ER, PR and HER2) breast cancer – identified by immunohistochemistry and FISH – has become a commonly used proxy that identifies the majority of subtype [80]. It is worth noting that although the term 'basal-like' is often used synonymously with the term 'triple-negative', basal-like subtype is a large but incompletely overlapping subset of the triple-negative breast cancer category. Approximately 15% of the triple-negative breast cancers are not basal-like [81]. Despite this, most current clinical trials exploring the role of PARP inhibitors in sporadic breast cancers select patients according to this immunohistochemical surrogate of basal-like breast cancer [82]. In 2009, a small-molecule intravenous agent, claiming to be a PARP1 inhibitor, called BSI-201, or iniparib, became the first in its class to enter Phase III assessment. A Phase II study had previously investigated gemcitabine plus carboplatin with or without BSI-201 in patients with advanced triple-negative breast cancer. A total of 120 triple-negative breast cancer patients received gemcitabine 1000 mg/m^2 plus carboplatin AUC2 on days 1 and 8, with or without intravenous BSI-201 at 5.6 mg/kg on a twice-weekly schedule (days 1, 4, 8 and 11). Recently published final analysis reported that the combination of BSI-201 to gemcitabine/carboplatin significantly improved median overall survival compared with patients receiving gemcitabine/carboplatin alone (12.3 vs 7.7 months; p = 0.01) [83]. Statistically significant improvements in median PFS (5.9 vs 3.6 months; p = 0.01) and ORR (52 vs 32%; p = 0.02) were reported in favor of the experimental arm. The addition of BSI-201 to gemcitabine/carboplatin did not appear to potentiate toxicities seen with gemcitabine/carboplatin alone. Currently the results await confirmation by a Phase III trial of similar design in the same population. Some regard the target dose of carboplatin at AUC2 day 1 and day 8 an inadequate breast cancer control regimen in this study. It is, however, noteworthy that Phase II trials in unselected breast cancer patients have shown similar response rates with carboplatin

AUC4/5 given every 3 weeks as with AUC2 given every other week with gemcitabine [84–86]. Indeed, the overall response rate of 32% and the PFS of 3.6 months following the gemcitabine/carboplatin control arm would be regarded as consistent with the results of more standard chemotherapy drugs used in the population treated [83]. Despite the current uncertainties, this phase II study has supported the design and enrollment of patients into clinical trials evaluating the role of potent PARP inhibitors in combination with chemotherapy in both early and advanced sporadic triple-negative breast tumors. A press release by the sponsor has indicated the trial failed to meet its prespecified end points and the activity of the agent against PARP1 has been questioned. Further data have emerged while this review has been in process (see [87]).

Despite synergism between PARP inhibition and cytotoxic agents being intensely investigated, the optimal PARP inhibitor–chemotherapy drug combination for investigation in TNBC remains to be established. A common theme emerging from Phase I combination studies of a range of potent PARP inhibitors has been that myelosupression is a common dose-limiting toxicity [43,47,88]. Dent *et al.* evaluated the tolerability of olaparib combined with weekly paclitaxel in patients with metastatic TNBC. Although the combination was well tolerated, acceptable dose intensity could not be maintained due to neutropenia, despite secondary prophylaxis with GCSF [89]. The iniparib combination study reported by O'Shaughnessy and discussed earlier did not report any increase in normal tissue toxicity. Although an intermittent PARP inhibitor dosing regimen, reduction in chemotherapy dose intensity, or differences in intracellular or cell type-specific PARP inhibitor pharmacokinetics or target pharmacodynamics may have provided protection from enhanced myelosupression reported in other combination trials. It seems likely that iniparib's reported lack of activity against PARP1 is the main explanation here [90]. Thus, target inhibition, optimal relative dose level and scheduling of PARP inhibitor and chemotherapeutic agent will require careful consideration in future PARP inhibitor and chemotherapy clinical trial design. If studies are to be designed in adjuvant and neoadjuvant settings, these will need to characterize possible long-term effects of these agents on marrow toxicity and induction of malignancy, especially when combined with DNA-damaging agents.

Expert commentary & five-year view

The management of patients with both localized and advanced breast cancer continues to evolve. PARP inhibitors are a novel class of drugs that target DNA breakage repair mechanisms, and preliminary studies have shown them to have excellent anti-tumor activity with an acceptable toxicity profile as single agents and for some agents in combination with chemotherapy. They represent a significant advance in breast cancer research, translating knowledge of gene function into clinical practice by adding a potential targeted therapy option for BRCA deficiency-associated breast cancers that are not usually amenable to anti-HER2-directed therapies. Perhaps more broadly applicable is the clinical synergy reported in combination studies of PARP inhibitor and cytotoxic agents in some sporadic triple-negative breast cancers, a subgroup for which, at present, there is no targeted treatment.

Larger studies are needed to address a wide variety of clinical questions in an effort to refine a putative role for PARP inhibitors in patients with breast cancer. The implementation of these randomized Phase II/III trials in the *BRCA1* and *BRCA2* carrier community may present some challenges. Together with the small proportion of breast cancer patients likely to be eligible, the general lack of availability of rapid turnaround genetic counseling and testing for *BRCA1* and *BRCA2* mutation poses a serious threat for the recruitment of patients with a known genetic breast cancer diagnosis. As previously demonstrated, collaboration in international intergroups is likely to be a prerequisite for accrual of adequate patient numbers [41,42]. A recent report of a study conducted in sporadic as well as *BRCA1*/2-mutated TNBC or high-grade serous ovarian cancers provided the tantalizing possibility of a role for single-agent PARP inhibition in high-grade sporadic serous ovarian cancer but provided less reassurance for a role for single-agent PARP inhibitor therapy in sporadic TNBC [91]. The lack of activity of olaparib in the TNBC group should be interpreted with caution, not only because of the small number of patients evaluated and their extensive prior treatments, but also owing to the fact that TNBC comprises a heterogeneous group of diseases where representation of a PARP inhibitor-sensitive BRCAness subgroup may be low in a very small unselected population. Identification of a convenient and accurate biomarker to identify PARP-inhibitor sensitive non-*BRCA*-mutant HR-deficient cancers is crucial for future clinical development of BRCAness targeting approaches in sporadic cancers.

A recent study has shown that hypoxia-induced HR defects can yield a BRCAness phenotype. It is known that the ability to repair DNA damage by the HR pathway is impaired in hypoxic cells. Chan *et al.* demonstrated both *in vitro* and *in vivo* that hypoxic cells can be selectively killed by PARP inhibition [92]. These results therefore expand the possibilities of PARP inhibitors in the clinic and support a novel treatment strategy by specifically targeting hypoxic tumor cells that are resistant to radiotherapy or chemotherapy.

In addition, not all patients with the *BRCA1* and *BRCA2* mutations responded to PARP inhibitors in the Phase II studies, and it is imperative that further research investigates the basis for this difference in response. Although no clinical studies have reported mechanisms of resistance in patients treated with PARP inhibitors, acquired resistance is a common feature of molecular targeted agents following prolonged drug exposure. Evidence in platinum-refractory patients with *BRCA* mutations has suggested the selection for intragenic 'reversion mutations', whereby patients have an additional mutation that restores the open reading frame of the gene and homologous recombination functionality [93–95]. Since platinum salts are thought to exert their *BRCA1*/2-selective effects by a similar mechanism to PARP inhibitors, it is not surprising that this model of acquiring 'reversion mutations' is supported by studies of PARP inhibitor-resistant clones that acquired the ability to form RAD51 foci after PARP inhibitor treatment [93]. It is likely, however, that other resistance mechanisms independent of restoration of *BRCA1*/2 function may also be relevant [96]. Liu *et al.* report

the upregulation of RAD51-based recombination by a resistant cell line with functional HR to compensate for the loss of base excision repair [97]. Another study reports the development of drug resistance following long-term treatment with a PARP inhibitor, caused by upregulation of p-glycoprotein efflux pumps [98]. Examining clinical samples from patients on PARP inhibitors trials prior to and following the development of resistance should be explored.

Although there remain several unresolved issues, PARP inhibitors are, both as single agents and in combination, undoubtedly making progress towards personalizing treatment in breast cancer. They will also bring the welcome challenge of discovering and implementing a rapid access companion diagnostic necessary to select patients who will most benefit.

Financial & competing interests disclosure

Alan Ashworth and Andrew Tutt may benefit financially from the development of PARP inhibitors through patents held jointly with AstraZeneca through the Institute of Cancer Research 'rewards to inventors' scheme. Andrew Tutt has acted as an unpaid or paid consultant and/or received honoraria for Pfizer, Eisai, sanofi-aventis, AstraZeneca and Clovis Inc. and has received research funding from sanofi-aventis. The authors have no other relevant affiliations or financial involvement with any organization or entity with a financial interest in or financial conflict with the subject matter or materials discussed in the manuscript apart from those disclosed.

No writing assistance was utilized in the production of this manuscript.

Key issues

- Genomic instability due to defects in DNA-repair pathways is a common characteristic of many tumors.
- Poly(ADP-ribose) polymerase (PARP)1 is involved in modification of DNA and recruitment of DNA-repair effectors in both ssDNA and replication fork-associated damage.
- If PARP1 is inhibited, unrepaired damage and arrested DNA replication forks require *BRCA1* and *BRCA2* for repair, and the combined loss of function in selected tumor cells is associated with cell death, leading to single-agent effectiveness.
- Combinations of PARP1 inhibitors and certain DNA-damaging agents in appropriate selected tumors, such as *BRCA1*/*BRCA2* function-deficient sporadic carriers, may be both synergistic and tumor selective.

References

1 Jemal A, Siegel R, Ward E, Hao Y, Xu J, Thun MJ. Cancer statistics, 2009. *CA Cancer J. Clin.* 59(4), 225–249 (2009).

2 Weigelt B, Mackay A, A'Hern R *et al.* Breast cancer molecular profiling with single sample predictors: a retrospective analysis. *Lancet Oncol.* 11(4), 339–349 (2010).

3 Aguilera A, Gomez-Gonzalez B. Genome instability: a mechanistic view of its causes and consequences. *Nat. Rev. Genet.* 9(3), 204–217 (2008).

4 Norbury CJ, Hickson ID. Cellular responses to DNA damage. *Annu. Rev. Pharmacol. Toxicol.* 41, 367–401 (2001).

5 Hoeijmakers JH. Genome maintenance mechanisms for preventing cancer. *Nature* 411(6835), 366–374 (2001).

6 Gudmundsdottir K, Ashworth A. The roles of *BRCA1* and *BRCA2* and associated proteins in the maintenance of genomic stability. *Oncogene*, 25(43), 5864–5874 (2006).

7 Greenberg RA, Sobhian B, Pathania S, Cantor SB, Nakatani Y, Livingston DM. Multifactorial contributions to an acute DNA damage response by *BRCA1*/BARD1-containing complexes. *Genes. Dev.* 20(1), 34–46 (2006).

8 Yang H, Li Q, Fan J, Holloman WK, Pavletich NP. The *BRCA2* homologue *Brh2* nucleates RAD51 filament formation at a dsDNA–ssDNA junction. *Nature* 433(7026), 653–657 (2005).

9 Chambon P, Weill JD, Mandel P. Nicotinamide mononucleotide activation of new DNA-dependent polyadenylic acid synthesizing nuclear enzyme. *Biochem. Biophys. Res. Comm.* 11, 39–43 (1963).

10 Otto H, Reche PA, Bazan F *et al. In silico* characterization of the family of PARP-like poly(ADP-ribosyl)transferases (pARTs). *BMC Genomics* 6, 139 (2005).

11 Schreiber V, Dantzer F, Ame JC, de Murcia G. Poly(ADP-ribose): novel functions for an old molecule. *Nat. Rev. Mol. Cell. Biol.* 7(7), 517–528 (2006).

12 Ame JC, Rolli V, Schreiber V *et al.* PARP-2, a novel mammalian DNA damage-dependent poly(ADP-ribose) polymerase. *J. Biol. Chem.* 274(25), 17860–17868 (1999).

13 Menissier de Murcia J, Ricoul M, Tartier L *et al.* Functional interaction between PARP-1 and PARP-2 in chromosome stability and embryonic development in mouse. *EMBO J.* 22(9), 2255–2263 (2003).

14 Schreiber V, Ame JC, Dolle P *et al.* Poly(ADP-ribose) polymerase-2 (PARP-2) is required for efficient base excision DNA repair in association with PARP-1 and XRCC1. *J. Biol. Chem.* 277(25), 23028–23036 (2002).

15 D'Amours D, Desnoyers S, D'Silva I, Poirier GG. Poly(ADP-ribosyl)ation reactions in the regulation of nuclear functions. *Biochem. J.* 342 (Pt 2), 249–268 (1999).

16 de Murcia JM, Niedergang C, Trucco C *et al.* Requirement of poly(ADP-ribose) polymerase in recovery from DNA damage in mice and in cells. *Proc. Natl Acad. Sci. USA* 94(14), 7303–7307 (1997).

17 Ferraris DV. Evolution of poly(ADP-ribose) polymerase-1 (PARP-1) inhibitors. From concept to clinic. *J. Med. Chem.* 53(12), 4561–4584 (2010).

18 Bryant HE, Petermann E, Schultz N *et al.* PARP is activated at stalled forks to mediate Mre11-dependent replication restart and recombination. *EMBO J.* 28(17), 2601–2615 (2009).

19 Audebert M, Salles B, Calsou P. Effect of double-strand break DNA sequence on the PARP-1 NHEJ pathway. *Biochem. Biophys. Res. Comm.* 369(3), 982–988 (2008).

20 Heitz F, Harter P, Ewald-Riegler N, Papsdorf M, Kommoss S, du Bois A. Poly(ADP-ribosyl)ation polymerases: mechanism and new target of anticancer therapy. *Expert Rev. Anticancer Ther.* 10(7), 1125–1136 (2010).

21 Moroni F, Meli E, Peruginelli F *et al.* Poly(ADP-ribose) polymerase inhibitors attenuate necrotic but not apoptotic neuronal death in experimental models of cerebral ischemia. *Cell Death Differ.* 8(9), 921–932 (2001).

22 Virag L, Szabo C. The therapeutic potential of poly(ADP-ribose) polymerase inhibitors. *Pharmacol. Rev.* 54(3), 375–429 (2002).

23 Molinete M, Vermeulen W, Burkle A *et al.* Overproduction of the poly(ADP-ribose) polymerase DNA-binding domain blocks alkylation-induced DNA repair synthesis in mammalian cells. *EMBO J.* 12(5), 2109–2117 (1993).

24 Lindahl T, Satoh MS, Poirier GG, Klungland A. Post-translational modification of poly(ADP-ribose) polymerase induced by DNA strand breaks. *Trends Biochem. Sci.* 20(10), 405–411 (1995).

25 Dobzhansky T. Genetics of natural populations. Xiii. Recombination and variability in populations of *Drosophila pseudoobscura*. *Genetics* 31(3), 269–290 (1946).

26 Hartwell LH, Szankasi P, Roberts CJ, Murray AW, Friend SH. Integrating genetic approaches into the discovery of anticancer drugs. *Science* 278(5340), 1064–1068 (1997).

27 Canan Koch SS, Thoresen LH, Tikhe JG *et al.* Novel tricyclic poly(ADP-ribose) polymerase-1 inhibitors with potent anticancer chemopotentiating activity: design, synthesis, and X-ray cocrystal structure. *J. Med. Chem.* 45(23), 4961–4974 (2002).

28 Farmer H, McCabe N, Lord CJ *et al.* Targeting the DNA repair defect in *BRCA* mutant cells as a therapeutic strategy. *Nature* 434(7035), 917–921 (2005).

29 Bryant HE, Schultz N, Thomas HD *et al.* Specific killing of *BRCA2*-deficient tumours with inhibitors of poly(ADP-ribose) polymerase. *Nature* 434(7035), 913–917 (2005).

30 Kummar S, Kinders R, Gutierrez ME *et al.* Phase 0 clinical trial of the poly (ADP-ribose) polymerase inhibitor ABT-888 in patients with advanced malignancies. *J. Clin. Oncol.* 27(16), 2705–2711 (2009).

31 Underhill C, Toulmonde M, Bonnefoi H. A review of PARP inhibitors: from bench to bedside. *Ann. Oncol.* 22(2), 268–279 (2010).

32 Sandhu SK, Yap TA, de Bono JS. Poly(ADP-ribose) polymerase inhibitors in cancer treatment: a clinical perspective. *Eur. J. Cancer* 46(1), 9–20 (2010).

33 Amir E, Seruga B, Serrano R, Ocana A. Targeting DNA repair in breast cancer: a clinical and translational update. *Cancer Treat. Rev.* 36(7), 557–565 (2010).

34 Moynahan ME, Chiu JW, Koller BH, Jasin M. *BRCA1* controls homology-directed DNA repair. *Mol. Cell* 4(4), 511–518 (1999).

35 Moynahan ME, Pierce AJ, Jasin M. *BRCA2* is required for homology-directed repair of chromosomal breaks. *Mol. Cell* 7(2), 263–272 (2001).

36 Moynahan ME. The cancer connection: *BRCA1* and *BRCA2* tumor suppression in mice and humans. *Oncogene* 21(58), 8994–9007 (2002).

37 Tirkkonen M, Johannsson O, Agnarsson BA *et al.* Distinct somatic genetic changes associated with tumor progression in carriers of *BRCA1* and *BRCA2* germ-line mutations. *Cancer Res.* 57(7), 1222–1227 (1997).

38 Tirkkonen M, Kainu T, Loman N *et al.* Somatic genetic alterations in *BRCA2*-associated and sporadic male breast cancer. *Genes Chromosomes Cancer* 24(1), 56–61 (1999).

39 Liu X, Holstege H, van der Gulden H *et al.* Somatic loss of *BRCA1* and *p53* in mice induces mammary tumors with features of human *BRCA1*-mutated basal-like breast cancer. *Proc. Natl Acad. Sci. USA* 104(29), 12111–12116 (2007).

40 Fong PC, Boss DS, Yap TA *et al.* Inhibition of poly(ADP-ribose) polymerase in tumors from *BRCA* mutation carriers. *N. Engl. J. Med.* 361(2), 123–134 (2009).

41 Tutt A, Robson M, Garber JE *et al.* Oral poly(ADP-ribose) polymerase inhibitor olaparib in patients with *BRCA1* or *BRCA2* mutations and advanced breast cancer: a proof-of-concept trial. *Lancet* 376(9737), 235–244 (2010).

42 Audeh MW, Carmichael J, Penson RT *et al.* Oral poly(ADP-ribose) polymerase inhibitor olaparib in patients with *BRCA1* or *BRCA2* mutations and recurrent ovarian cancer: a proof-of-concept trial. *Lancet* 376(9737), 245–251 (2010).

43 Giaccone GR, Kelly A, Gutierrez RJ *et al.* A Phase I combination study of olaparib (AZD2281; KU-0059436) and cisplatin (C) plus gemcitabine (G) in adults with solid tumors. *J. Clin. Oncol.* 28(Suppl. 15S) (2010) (Abstract 3027).

44 Sandhu SK, Wenham RM, McFadden WR *et al.* First-in-human trial of a poly(ADP-ribose) polymerase (PARP) inhibitor MK-4827 in advanced cancer patients (pts) with anti-tumor activity in BRCA-deficient and sporadic ovarian cancers. *J. Clin. Oncol.* 28(Suppl. 15s) (2010) (Abstract 3001).

45 Isakoff SJ, Tung NM, Gelman RS *et al.* A Phase II trial of the PARP inhibitor veliparib (ABT888) and temozolomide for metastatic breast cancer. *J. Clin. Oncol.* 28(Suppl. 15S) (2010) (Abstract 1019).

46 Tan AR, Stein MN, Moss RA *et al.* Preliminary results of a Phase I trial of ABT-888, a poly(ADP-ribose) polymerase (PARP) inhibitor, in combination with cyclophosphamide. *J. Clin. Oncol.* 28(Suppl. 15S) (2010) (Abstract 3000).

47 Ji JJ, Chen AP, Zhang Y *et al.* SAIC-Frederick, Bethesda, MD. Pharmacodynamic response in Phase I combination study of ABT-888 and topotecan in adults with refractory solid tumors and lymphomas. *J. Clin. Oncol.* 28(Suppl. 15S) (2010) (Abstract 2514).

48 Kriege M, Seynaeve C, Meijers-Heijboer H *et al.* Sensitivity to first-line chemotherapy for metastatic breast cancer in *BRCA1* and *BRCA2* mutation carriers. *J. Clin. Oncol.* 27(23), 3764–3771 (2009).

49 Seynaeve C AJ, Hooning M, Van Deurzen CH *et al.* Activity of taxane chemotherapy for metastatic breast cancer (MBC) in *BRCA1* and *BRCA2* mutation carriers compared to sporadic BC patients. *J. Clin. Oncol.* 28(Suppl. 15S) (2010) (Abstract 1020).

50 Vaziri SA, Krumroy LM, Elson P *et al.* Breast tumor immunophenotype of *BRCA1*-mutation carriers is influenced by age at diagnosis. *Clin. Cancer Res.* 7(7), 1937–1945 (2001).

51 Foulkes WD, Brunet JS, Stefansson IM *et al.* The prognostic implication of the basal-like (cyclin E high/p27 low/p53+/glomeruloid-microvascular-proliferation+) phenotype of *BRCA1*-related breast cancer. *Cancer Res.* 64(3), 830–835 (2004).

52 Eerola H, Heikkila P, Tamminen A, Aittomaki K, Blomqvist C, Nevanlinna H. Relationship of patients' age to histopathological features of breast tumours in *BRCA1* and *BRCA2* and mutation-negative breast cancer families. *Breast Cancer Res.* 7(4), R465–R469 (2005).

53 Foulkes WD, Stefansson IM, Chappuis PO *et al.* Germline *BRCA1* mutations and a basal epithelial phenotype in breast cancer. *J. Natl Cancer Inst.* 95(19), 1482–1485 (2003).

54 Sorlie T, Tibshirani R, Parker J *et al.* Repeated observation of breast tumor subtypes in independent gene expression data sets. *Proc. Natl Acad. Sci. USA* 100(14), 8418–8423 (2003).

55 Honrado E, Benitez J, Palacios J. Histopathology of *BRCA1*- and *BRCA2*-associated breast cancer. *Crit. Rev. Oncol. Hematol*. 59(1), 27–39 (2006).

56 Kriege M, Seynaeve C, Meijers-Heijboer H *et al.* Distant disease-free interval, site of first relapse and post-relapse survival in *BRCA1*- and *BRCA2*-associated compared to sporadic breast cancer patients. *Breast Cancer Res. Treat*. 111(2), 303–311 (2008).

57 Luck AA, Evans AJ, Green AR, Rakha EA, Paish C, Ellis IO. The influence of basal phenotype on the metastatic pattern of breast cancer. *Clin. Oncol. (R. Coll. Radiol.)* 20(1), 40–45 (2008).

58 Turner NC, Reis-Filho JS. Basal-like breast cancer and the *BRCA1* phenotype. *Oncogene* 25(43), 5846–5853 (2006).

59 Turner N, Tutt A, Ashworth A. Hallmarks of 'BRCAness' in sporadic cancers. *Nat. Rev. Cancer* 4(10), 814–819 (2004).

60 Futreal PA, Liu Q, Shattuck-Eidens D *et al.* *BRCA1* mutations in primary breast and ovarian carcinomas. *Science* 266(5182), 120–122 (1994).

61 Lancaster JM, Wooster R, Mangion J *et al.* *BRCA2* mutations in primary breast and ovarian cancers. *Nat Genet.* 13(2), 238–240 (1996).

62 Sourvinos G, Spandidos DA. Decreased *BRCA1* expression levels may arrest the cell cycle through activation of p53 checkpoint in human sporadic breast tumors. *Biochem. Biophys. Res. Comm.* 245(1), 75–80 (1998).

63 Thompson ME, Jensen RA, Obermiller PS, Page DL, Holt JT. Decreased expression of *BRCA1* accelerates growth and is often present during sporadic breast cancer progression. *Nat. Genet.* 9(4), 444–450 (1995).

64 Wilson CA, Ramos L, Villasenor MR *et al.* Localization of human *BRCA1* and its loss in high-grade, non-inherited breast carcinomas. *Nat. Genet.* 21(2), 236–240 (1999).

65 Yoshikawa K, Honda K, Inamoto T *et al.* Reduction of *BRCA1* protein expression in Japanese sporadic breast carcinomas and its frequent loss in *BRCA1*-associated cases. *Clin. Cancer Res*. 5(6), 1249–1261 (1999).

66 Esteller M, Tortola S, Toyota M *et al.* Hypermethylation-associated inactivation of p14(ARF) is independent of p16(INK4a) methylation and *p53* mutational status. *Cancer Res*. 60(1), 129–133 (2000).

67 Baldwin RL, Nemeth E, Tran H *et al.* *BRCA1* promoter region hypermethylation in ovarian carcinoma: a population-based study. *Cancer Res.* 60(19), 5329–5333 (2000).

68 Grushko TA, Charoenthammaraksa S, Huo D *et al.* Evaluation of *BRCA1* inactivation by promoter methylation as a marker of triple-negative and basal-like breast cancers. *J. Clin. Oncol.* 28(Suppl. 15S) (2010) (Abstract 10510), (2010) (Abstract 10510).

69 Beger C, Pierce LN, Kruger M *et al.* Identification of Id4 as a regulator of *BRCA1* expression by using a ribozyme-library-based inverse genomics approach. *Proc. Natl Acad. Sci. USA* 98(1), 130–135 (2001).

70 Collins N, Wooster R, Stratton MR. Absence of methylation of CpG dinucleotides within the promoter of the breast cancer susceptibility gene *BRCA2* in normal tissues and in breast and ovarian cancers. *Br. J. Cancer* 76(9), 1150–1156 (1997).

71 Mendes-Pereira AM, Martin SA, Brough R *et al.* Synthetic lethal targeting of PTEN mutant cells with PARP inhibitors. *EMBO Mol. Med.* 1(6–7), 315–322 (2009).

72 Nielsen TO, Hsu FD, Jensen K *et al.* Immunohistochemical and clinical characterization of the basal-like subtype of invasive breast carcinoma. *Clin. Cancer Res.* 10(16), 5367–5374 (2004).

73 Abd El-Rehim DM, Ball G, Pinder SE *et al.* High-throughput protein expression analysis using tissue microarray technology of a large well-characterised series identifies biologically distinct classes of breast cancer confirming recent cDNA expression analyses. *Int. J. Cancer* 116(3), 340–350 (2005).

74 Perou CM, Sorlie T, Eisen MB *et al.* Molecular portraits of human breast tumours. *Nature* 406(6797), 747–752 (2000).

75 Bast RC Jr, Mills GB. Personalizing therapy for ovarian cancer: BRCAness and beyond. *J. Clin. Oncol.* 28(22), 3545–3548 (2010).

76 Veeck J, Ropero S, Setien F *et al.* *BRCA1* CpG Island hypermethylation predicts sensitivity to poly(adenosine diphosphate)-ribose polymerase inhibitors. *J. Clin. Oncol.* 28(29), e563–e564 (2010).

77 Grushko TA, Charoenthammaraksa S, Huo D *et al.* Evaluation of *BRCA1* inactivation by promoter methylation as a marker of triple-negative and basal-like breast cancers. *J. Clin. Oncol.* 28(15s), (2010) (Abstract 10510).

78 Yap TA, de Bono JS, Kaye SB *et al.* Reply to Veeck *et al. J. Clin. Oncol.* 28(29) e565–e566 (2010).

79 Graeser MK, McCarthy A, Lord CJ *et al.* A marker of homologous recombination predicts pathological complete response to neoadjuvant chemotherapy in primary breast cancer. *Clin. Cancer Res.* 16(24), 6159–6168 (2010).

80 Kreike B, van Kouwenhove M, Horlings H *et al.* Gene expression profiling and histopathological characterization of triple-negative/basal-like breast carcinomas. *Breast Cancer Res.* 9(5), R65 (2007).

81 Nofech-Mozes S, Trudeau M, Kahn HK *et al.* Patterns of recurrence in the basal and non-basal subtypes of triple-negative breast cancers. *Breast Cancer Res. Treat* 118(1), 131–137 (2009).

82 Sorlie T, Perou CM, Tibshirani R *et al.* Gene expression patterns of breast carcinomas distinguish tumor subclasses with clinical implications. *Proc. Natl Acad. Sci. USA* 98(19), 10869–10874 (2001).

83 O'Shaughnessy J, Osborne C, Pippen JE *et al.* Iniparib plus chemotherapy in metastatic triple-negative breast cancer. *N. Engl. J. Med.* 364(3), 205–214 (2011).

84 Yardley DA, Burris HA 3rd, Simons L *et al.* A Phase II trial of gemcitabine/carboplatin with or without trastuzumab in the first-line treatment of patients with metastatic breast cancer. *Clin. Breast. Cancer* 8(5), 425–431 (2008).

85 Chan D, Yeo WL, Tiemsim Cordero M *et al.* Phase II study of gemcitabine and carboplatin in metastatic breast cancers with prior exposure to anthracyclines and taxanes. *Invest. New Drugs* 28(6), 859–865 (2010).

86 Laessig D, Stemmler HJ, Vehling-Kaiser U *et al.* Gemcitabine and carboplatin in intensively pretreated patients with metastatic breast cancer. *Oncology* 73(5–6), 407–414 (2007).

87 O'Shaughnessy J, Schwartzberg LS, Danso MA *et al.* A randomized phase III study of iniparib (BSI-201) in combination with gemcitabine/carboplatin (G/C) in metastatic triple-negative breast cancer (TNBC). *J. Clin. Oncol.* 29(Suppl.) (2011) (Abstract 1007).

88 Plummer RL, Evans P, Steven J *et al.* First and final report of a phase II study of the poly(ADP-ribose) polymerase (PARP) inhibitor, AG014699, in combination with temozolomide (TMZ) in patients with metastatic malignant melanoma (MM). *J. Clin. Oncol. 2006 ASCO Ann. Meeting Proc. Part I*, 24(18S), 8013 (2006).

89 Dent R, Wildiers H, Chan A *et al.* Safety and efficacy of the oral PARP inhibitor olaparib (AZD2281) in combination with paclitaxel for the first- or second-line treatment of patients with metastatic triple-negative breast cancer: Results from the safety cohort of a Phase I/II multicenter trial. *J. Clin. Oncol.* 28(Suppl. 15S) (2010) (Abstract 1018).

90 Jiuping J, Maxwell PL, Mitsutaka K *et al.* Pharmacodynamic and pathway analysis of three presumed inhibitors of poly (ADP-ribose) polymerase: ABT-888, AZD2281, and BSI201. *Proc. AACR* (2011) (Abstract 4527).

91 Gelmon K. Can we define tumors that will respond PARP inhibitors? A Phase II correlative study of olaparib in advanced serous ovarian cancer and triple-negative breast cancer. *J. Clin. Oncol.* 28, 233S (2010).

92 Chan N, Pires IM, Bencokova Z *et al.* Contextual synthetic lethality of cancer cell kill based on the tumor microenvironment. *Cancer Res.* 70(20), 8045–8054 (2010).

93 Edwards SL, Brough R, Lord CJ *et al.* Resistance to therapy caused by intragenic deletion in *BRCA2*. *Nature* 451(7182), 1111–1115 (2008).

94 Sakai W, Swisher EM, Karlan BY *et al.* Secondary mutations as a mechanism of cisplatin resistance in *BRCA2*-mutated cancers. *Nature* 451(7182), 1116–1120 (2008).

95 Swisher EM, Sakai W, Karlan BY, Wurz K, Urban N, Taniguchi T. Secondary *BRCA1* mutations in *BRCA1*-mutated ovarian carcinomas with platinum resistance. *Cancer Res.* 68(8), 2581–2586 (2008).

96 Evers B, Helleday T, Jonkers J. Targeting homologous recombination repair defects in cancer. *Trends Pharmacol. Sci.* 31(8), 372–380 (2010).

97 Liu X, Han EK, Anderson M *et al.* Acquired resistance to combination treatment with temozolomide and ABT-888 is mediated by both base excision repair and homologous recombination DNA repair pathways. *Mol. Cancer Res.* 7(10), 1686–1692 (2009).

98 Rottenberg S, Jaspers JE, Kersbergen A *et al.* High sensitivity of *BRCA1*-deficient mammary tumors to the PARP inhibitor AZD2281 alone and in combination with platinum drugs. *Proc. Natl Acad. Sci. USA* 105(44), 17079–17084 (2008).